University of Alberta

The paragenesis and geochemistry of the Bellekeno Ag-Pb-Zn vein,

Keno Hill district, Yukon, Canada

by

Jos James Hantelmann

A thesis submitted to the Faculty of Graduate Studies and Research

in partial fulfillment of the requirements for the degree of

Masters of Science

Department of Earth and Atmospheric Sciences

Fall convocation 2013

Edmonton, Alberta

Abstract

The Keno Hill district Ag-Pb-Zn deposit occurs within the Tombstone-Tungsten Belt, Yukon. Vein mineralization, dominated by siderite, sphalerite, and galena, is spatially associated with, but paragenetically later than, intrusion-related gold mineralization. A direct genetic link between the Keno Hill mineralization and the Roop Lakes stock cannot be demonstrated; however the age of Keno Hill mineralization and spatial geochemical variations of mineral chemistry suggests that some genetic or temporal relationship exists.

Twelve distinct mineral assemblages record 5 different fluid compositions defining a cooling trend from >300˚C to <160˚C (Th). Fluids evolved and variably mixed; decreasing temperature and dilution appear to be the principal controls on silver and base-metal mineralization. Moderately saline fluids (<20 wt % NaCl equiv.) could be derived from either magmatic or formation waters, with some of the dissolved components derived from the surrounding country rock. A late stage, lower temperature fluid is of meteoric origin.

Preface

The author is responsible for collecting all samples, sample selection for all analyses, and completing all preliminary sample preparation for all analyses in this study. Preliminary sample preparation typically involves mineral separation, and grinding. Additional samples and their analytical results from the Keno Hill district and region from other studies and authors are referenced throughout this report.

Thin sections and fluid inclusion wafers were prepared at the University of Alberta, Vancouver Petrographics Ltd., and Vancouver GeoTech Labs.

Electron Microprobe work was completed at the University of Alberta by the author, equipment calibration was complete by Sergei Matveev.

X-Ray Diffraction analyses were completed at the University of Alberta by Diane Caird.

Fluid inclusion analyses were completed by author at the University of Alberta.

The author completed some second stage sample preparation of carbonate minerals for carbon and oxygen analyses, however most second stage sample preparation was complete at the respective laboratories. Carbon and oxygen isotopes were determined at the University of Alberta, Stable Isotope Laboratory by Olga Levner and Dr. Karlis in 2009 and 2010; and at the University of Western Ontario, Laboratory for Stable Isotope Science by Li Huang, Kim Law, and Fred Longstaffe in January 2012. Sulfur isotopes were determined at the University of Calgary, Isotope Science Laboratory by Jesusa Pontoy in August 2010.

All stages of Pb isotope sample preparation were completed by the author, analyses were completed at the University of Alberta by Andy DuFrane and the author.

Acknowledgments

I would like to thank my supervisor, Dr. Sarah Gleeson, firstly for giving me the opportunity to conduct this work, and then for her immeasurable guidance, patience, and challenges throughout the development and preparation of this research project. Thanks also to Dr. Jeremy Richards, for providing access to his Microthermometry laboratory, as well as for his constructive reviews which greatly improved the quality of this manuscript.

Additionally, I owe many thanks to following, for their contributions in the form of explaining analytical techniques, showing how the laboratory equipment work, and/or completing various lab work, all of whom were crucial to the advancement of this project: from the University of Alberta, Sergei Matveev (Electron Microprobe Laboratory, manager and technician), Diane Caird (X-ray Diffraction Laboratory, technician), Dr. Andy DuFrane (MC-ICP-MS Laboratory, manager), Dr. Karlis Muehlenbachs, and Olga Levner (Stable Isotope Laboratory, technician); from the University of Western Ontario, Fred Longstaffe, Li Huang, and Kim Law (Stable Isotope Laboratory); and from the University of Calgary, Jesusa Pontoy (Isotope Science Laboratory).

This research was generously funded by: Alexco Resources Corporation (TSX-V: AXR); the Yukon Geological Survey (YGS); and the Natural Sciences and Engineering Research Council (NSERC).

I am grateful to Alexco Resources Corp. and staff for their provision of room and board during the summer of 2009, access to the entire property, rock samples, digital data, and countless discussions on the project. Al McOnie (AXR), Stan Dodd (AXR), Dick Lippoth (AXR), Don Murphy (YGS), Venessa Bennett (YGS), and Simon Craggs (University of New Brunswick, Ph.D. student) were valuable at the early stages of this project by way of helping me understanding the Keno Hill deposit, and key underlying geological questions.

Special thanks to family, especially my wife and son, for their patience and support throughout the years I have dedicated to this project.

Table of Contents

Appendices

List of Tables

List of Figures

List of Symbols and Abbreviations

Element symbols are also used throughout the text.

Measurements

μm	micrometer		
mm	millimeter	˚C	degree Celsius
cm	centimeter	%	percent
m	meter	‰	per mil
masl	meters above sea level	kV	kilovolt
wt	weight	nA	nano amp
t	ton (metric)	Ma	million years
ppm	parts per million	N.D.	no data
n	mean	B.D.	below detection limit
σ	standard deviation	N/A	not applicable
SE	standard error	~	approximately
R^2	coefficient of determination		

Mineral textures and Lithological units

V	vein	GSch	graphitic schist
B	breccia	PhSch	phyllitic schist
b	banded	PhQtzt	phyllitic quartzite
c	coarse	Pht	phyllite
clr	clear	LS	limestone
cld	cloudy	Qtzt	quartzite
d	dark	F1	foliation, earliest/first phase
e	euhedral		
f	fine		
l	layered	HS	hand sample
m	massive	TS	thin-section
z	zoned	PPL	plane polarized light
Tr	trace	RL	reflected light
		XP	crossed polars

Minerals

Most abbreviations are derived from Whitney and Evans (2010), and those accepted by the Geological Association of Canada.

Ab	albite	$NaAlSi_3O_8$
Aca	acanthite	Ag_2S
Ag	silver	Ag
An	anorthite	$CaAl_2Si_2O_8$
Ang	anglesite	$PbSO_4$
Ank	ankerite	$(Ca,Mg,Fe)CO_3$
Andr	andorite	$AgPbSb_3S_6$
Apy	arsenopyrite	FeAsS
Au	gold	Au
Boul	boulangerite	$Pb_5Sb_4S_{11}$
Brt	barite	$BaSO_4$
Cal	calcite	$CaCO_3$
Ccp	chalcopyrite	$CuFeS_2$
Cer	cerussite	$PbCO_3$
Cob	cobaltite	CoAsS
Cnt	cerianite	CeO2
Cst	cassiterite	SnO_2
Dol	dolomite	$CaMg(CO_3)_2$
Fah	fahlore	$(Cu,Ag)_{10}(Fe,Zn)_2(As,Sb)_4S_{13}$
Frb	freibergite	$Ag_6(Cu_4Fe_2)(Sb_4S_{13-X})$
Ger	gersdorffite	NiAsS
Gn	galena	PbS
Goe	goethite	FeO – OH
Gr	graphite	C
Hal	halloysite	$Al_2Si_2O_5(OH)_4$-$2H_2O$
Hem	hematite	Fe_2O_3
Ilt-2M2	illite-2M2	$(K,H)Al_2(Si_3Al)O_{10}(OH)_2$-$xH_2O$
Jam	jamesonite	$FePb_4Sb_6S_{14}$
Kln	kaolinite	$Al_2Si_2O_5(OH)_4$
Kut	kutnohorite	$Ca(Mn,Mg)(CO_3)_2$
Mag	magnetite	Fe_3O_4
Mil	millerite	NiS
Mnz	monazite	$(Ce,La,Y,Th)PO_4$
Mrc	marcasite	FeS_2
Ms-2M1	muscovite-2M1	$KAl_3Si_3O_{10}(OH)_2$
Ms-2M2	muscovite-2M2	$(K,Na)Al_2(Si,Al)_4O_{10}(OH)_2$
Ms-3T	muscovite-3T	$(K,Na)(Al,Mg,Fe)_2Si_{3.1}Al_{0.9}O_{10}(OH)_2$
Orp	orpiment	As_2S_3

Phl	phlogopite	$KMg_3Si_3AlO_{10}(F,OH)_2$
Po	pyrrhotite	$Fe_{1-x}S$
Plb	polybasite	$Cu(Cu,Ag)_6Ag_9Sb_2S_{11}$
Prt	proustite	Ag_3AsS
Py	pyrite	FeS_2
Pyr	pyrargyrite	Ag_3SbS_3
Qz	quartz	SiO_2
Rbc	rhomboclase	$(H_3O)Fe(SO_4)_2(H_2O)_3$
Rea	realgar	AsS
Rds	rhodochrosite	$MnCO_3$
Rt	rutile	TiO_2
Sch	scheelite	$CaWO_4$
Sd	siderite	$(Fe, Mn)CO_3$
Sp	sphalerite	$(Zn,Fe)S$
Stb	stibnite	Sb_2S_3
Stn	stephanite	Ag_5SbS_4
Szm	szomolnokite	$Fe(SO_4)(H_2O)$
Tnt	tennantite	$Cu_6(Cu_4(Fe,Zn)_2)As_4S_{13}$
Ttr	tetrahedrite	$Cu_6(Cu_4(Fe,Zn)_2)Sb_4S_{13}$
Ag-Ttr	argentotetrahedrite	$Ag_{10}(Fe,Zn)_2Sb_4S_{13}$
Val	valentinite	Sb_2O_3
Zrn	zircon	$ZrSiO_4$

1.0 Introduction and Objectives

A series of silver-lead-zinc-bearing veins, collectively referred to as the Keno Hill district, were first discovered in central Yukon in the early 1900's. By 1913 a number of mining companies were selectively mining silver-rich ore-shoots throughout the area. The Yukon Minfile database reports that between 1921 and 1988, approximately 6,769 t silver, 273, 662 t lead, and 153,198 t zinc were produced.

Keno Hill has been described as a sediment-hosted Ag-Pb-Zn vein type deposit, and likened to other Ag-bearing deposits such as at Coeur d'Alene, USA and those in the Kokanee Range, Canada (Beaudoin and Sangster, 1992). However, there are mineralogical and geochemical characteristics of the Keno Hill mineralization that are reminiscent of many Ag-bearing epithermal and other hydrothermal polymetallic vein deposits (e.g. So and Yun, 1992; Konstantinov et al., 1993; Plumlee and Whitehouse-Veaux, 1994; Schalamuk and Logan, 1994; Mulshaw et al., 1997; Borisenko et al., 1999; Borisenko et al., 2000; Liu et al., 2001; Anikina et al., 2010; Pavlova and Borovikov, 2010). More recently, in the Yukon, a genetic relationship between Ag-Pb-Zn and intrusion-related gold (IRG) mineralization has been postulated (Poulsen et al., 1997; Marsh et al., 2003; Hart et al., 2004a; Mair et al., 2006). However, conclusive evidence for a genetic link between IRG, epithermal, or sediment-hosted vein deposits and Keno Hill remains elusive; also the source(s) of metals, and conditions related to ore-deposition of the Keno Hill Ag-Pb-Zn veins are poorly defined.

The aims of this study were to: 1) determine the hydrothermal mineral paragenesis and develop a classification scheme for the distinct mineral assemblages, 2) identify the source(s) of the ore-related elements and associated hydrothermal fluids, and 3) determine the mechanism(s) that controlled the deposition of the ore-bearing mineral assemblages.

In order to address the genesis of the Keno Hill Ag-bearing veins, a detailed study was carried out on the Bellekeno vein, which is currently being mined by Alexco Resources Corp. This provided an excellent opportunity to collect a relatively continuous and complete spectrum of samples from a single mineralized structure. Additional samples were obtained from other veins throughout the district (i.e. Silver King, Tick, Pool, Bermingham, Eagle, Onek, Wernecke, Lucky Queen, K-structure, Keno 700, Porcupine, Homestake, Alice, Try Again) for comparison with the Bellekeno samples, providing some insight of the geochemical variation of the veins on a district wide scale.

2.0 Location and Geologic Setting

The Keno Hill district is located in central Yukon Territory, Canada (NTS map sheet 105M), in the northwestern Selwyn Basin (Figure 2-1). The Selwyn Basin comprises Proterozoic to Paleozoic miogeoclinal slope-to-basin strata; a succession of clastic and carbonaceous sediments deposited in an epicratoic rift basin off the ancestral North American continental margin (Gabrielse, 1967; Abbott, et al., 1986; Gabrielse and Yorath, 1991; Gordey and Anderson, 1993; Mair et al., 2006). Episodic passive continental rifting in the Selwyn Basin during Cambrian to Late Devonian is evident from three episodes of alkali-rich to ultrapotassic intrusive (dikes and sills) and volcanic rocks (Goodfellow et al., 1995). Numerous stratiform sediment-hosted and sedimentary exhalative Zn-Pb-Ag deposits are found within the Selwyn Basin (McLaren and Godwin, 1978; Gordey and Anderson, 1993) and are temporally and spatially associated with the Proterozoic to Paleozoic rifting and volcanism (Goodfellow et al., 1995; Lund, 2008).

Northward foreland convergence of the outboard allochthonous Yukon-Tanana terrane resulted in extensive compressional deformation of the Selwyn Basin sediments during the Late Jurassic to Early Cretaceous (Tempelman-Kluit, 1979; Monger et al. 1982; Poulton and Tempelman-Kluit, 1982; Gordey and Anderson, 1993; Mair et al., 2006). Subsequently, the Tombstone-Tungsten Belt (TTB), a series of compositionally diverse felsic to intermediate calc-alkaline and alkaline intrusions were emplaced during the Late Cretaceous (approximately 90 to 96 Ma) within the Selwyn Basin, and form a linear belt, extending from Alaska to the Northwest Territories (Mortensen et al., 1995; Murphy, 1997; Mortensen et al., 2000). Based on lithological and spatial characteristics, the TTB is sub-divided into 3 groups within the Selwyn Basin, from northwest to southeast: the Tombstone (92 to 90 Ma), Mayo (95 to 92 Ma), and Tungsten (97 to 94 Ma) plutonic suites; where the intrusions trend from being relatively oxidized (or least reduced) and metaluminous in the northwest to reduced and peraluminous in the southeast (Hart et al., 2004).

A metallogenic belt of gold deposits that ranges from central Alaska to the Northwest Territories is referred to as the Tintina Gold Province (Thompson et al., 1999; Lang and Baker, 2001; Hart et al., 2002; Goldfarb et al., 2007; Hart, 2007). In the Yukon Territory, IRG deposits within the Tintina Gold Province are both spatially and temporally related to the TTB, although more notably with the Tombstone and Mayo Plutonic Suites (Poulsen et al., 1997; Thompson et al., 1999; Mair et al., 2000; Baker and Lang, 2001; Hart et al., 2002; Marsh et al., 2003; Hart, 2007). Although various styles of mineralization and metallogenic associations are included in the IRG deposit classification, they are typically characterized by sheeted quartz veins containing variable to trace, native gold, arsenopyrite, pyrite, pyrrhotite, scheelite, molybdenite, galena, chalcopyrite, bismuthinite, and stibnite; and lesser gangue comprised of K-feldspar, biotite, muscovite, carbonate, tourmaline, and albite. Silver-lead-zinc mineralization similar to and including the Keno Hill type may represent a later and lower temperature hydrothermal paragenetic stage and occurs peripheral to IRG deposits in the TTB (Lang and Baker, 2001; Hart et al., 2004b; Mair et al., 2006; Hart, 2007) (Figure 2-2).

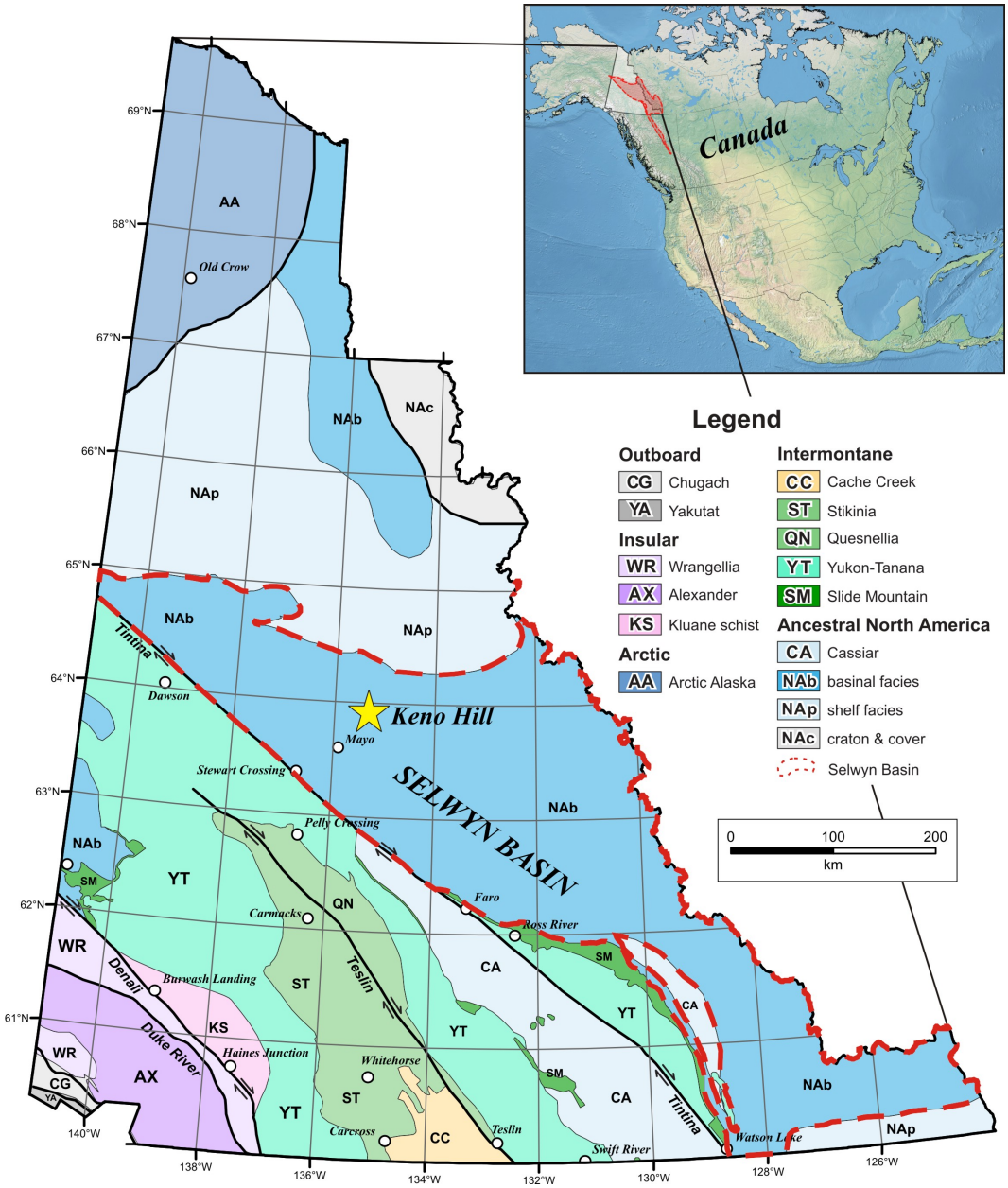

Figure 2-1. Yukon Terrane map; modified from Yukon Geological Survey (2011). The limit of the Selwyn Basin, defined by the broken red line, primarily occurs within the Yukon; the complete boundary of the Selwyn Basin is shown in the in-set map of Canada.

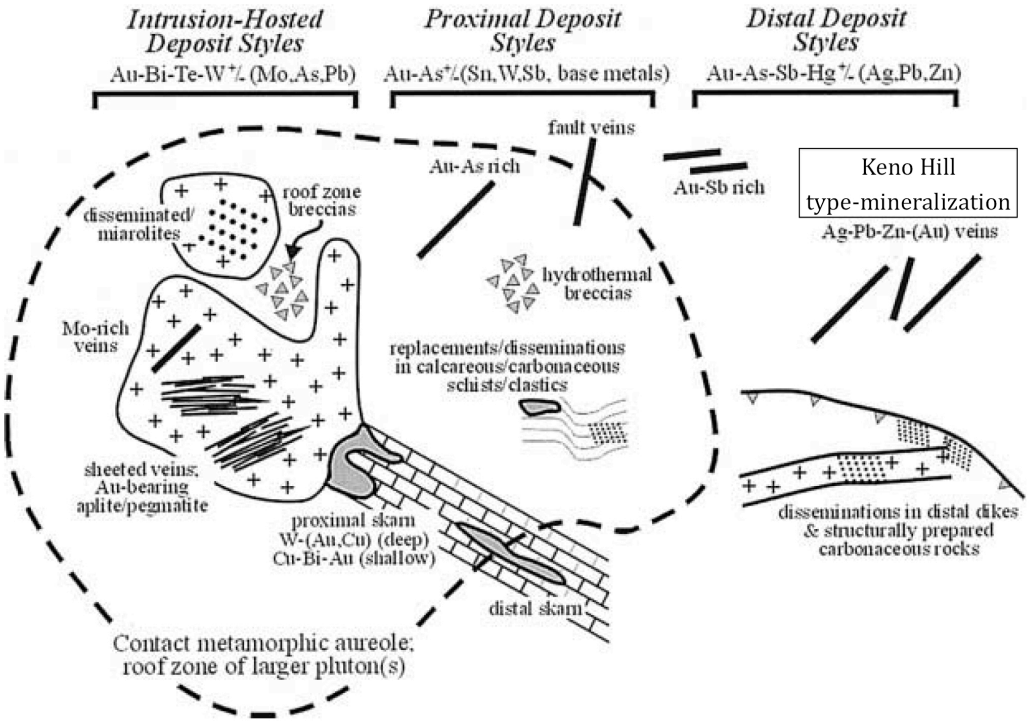

Figure 2-2. Schematic model of intrusion-related gold mineralization styles and metallurgical assemblages from Lang and Baker (2001). Note the outer-most zone of Ag-Pb-Zn mineralization may be spatially associated with IRG mineralization forming late in the paragenesis after Au-mineralization and at lower hydrothermal fluid temperatures.

A temporally restricted period of felsic magmatism occurred from the Late Cretaceous to early Paleogene (64 to 67 Ma), the McQuesten intrusions; compositionally they are predominantly monzogranite and peraluminous (Murphy, 1997).

Also since the Late Cretaceous, the transcurrent, northwest-southeast striking, strike-slip Tintina fault system has accommodated approximately 450 to 900 km of dextral displacement (Tempelman-Kluit, 1979; Gabrielse, 1985; Price and Carmichael, 1986; Mortensen et al., 2000; Wyld et al., 2006; Saltus, 2007), juxtaposing the Yukon Tanana terrane against the southwest of the Selwyn Basin in central Yukon. The Tintina fault likely formed in response to a north-south oriented compressional stress field associated with the northward movement of the Kula plate (Engebretson et al. 1985; Hart et al. 2004b; Doubrovine and Tarduno, 2008). Intrusion-related gold mineralization in the TTB occurred within an east-west compressional and north-south extensional stress regime that may have formed in a transitional tectonic stress field, post-dating Early Cretaceous northeast-southwest oriented compression, but prior to the development of the Tintina fault system during the Late Cretaceous and Tertiary (Stephens et al., 2004). The apparent association of paragenetically later Ag-Pb-Zn mineralization with IRG systems (e.g.

Mair et al., 2006) suggests that this polymetallic mineralizing event may have occurred within similar, or later, fault structures than the IRG mineralization; there is however, little to no published information on the relationship of the Keno Hill structures with the regional stress regime.

2.2 Local Geology

The following synopsis includes only the stratigraphic units exposed in the Keno Hill district, primarily derived from the detailed and comprehensive reports by Murphy (1997), Roots (1997), Mair et al. (2006), and references therein (Figure 2-3).

The oldest rocks in the Keno Hill district are the Precambrian to Early Cambrian Hyland Group, which regionally comprise a succession of fine to coarse grained metamorphosed clastic and carbonate rocks. In the Keno Hill district, the dominant unit of this age has been mapped as a quartz-muscovite schist (Alexco Resources Corp., internal and public reports). The Devonian to Mississippian Earn Group is comprised of fine to coarse sediments, varying from shale and phyllite to conglomerate, and limestone. The Mississippian Keno Hill quartzite, which is the most important host rock of the Keno Hill Ag-Pb-Zn veins, is comprised of predominantly massive quartzite, variably phyllitic and/or carbonaceous, inter-bedded with phyllitic to graphitic schist, and localized limestone beds. The Keno Hill quartzite may be up to 2 kilometers thick; however the complex structural deformation precludes an accurate measurement of the thickness. Historic reports (e.g. Boyle, 1965; Poulton and Tempelman-Kluit, 1982) on the local geology, informally divided the lithology into 3 sub-units: the Lower Schist, Central Quartzite, and Upper Schist, which may persist into some current literature; these units correspond to the Earn Group, Keno Hill quartzite, and Hyland Group rocks, respectively (e.g. Poulton and Tempelman-Kluit, 1982; Murphy, 1997).

A series of intermediate to mafic dikes or sills intrude the Hyland Group, Earn Group, and the Keno Hill quartzite. These units may be over 100 meters thick, and vary from laterally extensive layers several kilometers in length to discontinuous lenses. Diabase sills, with a U-Pb age date of 232 ± 1.5 Ma from zircon and baddelyite (Mortensen and Thompson, 1990), within the Keno Hill quartzite in the Ogilvie Mountains are inferred to be of similar age as the intermediate and mafic dikes and sills in the Keno Hill district.

The Late Jurassic to Early Cretaceous north-south compressional deformation is responsible for two prominent detachment thrust faults, the Tombstone and Robert Service Thrusts, both of which generally strike east-west and are gently dipping to the south and characterized by a high degree of shear strain: predominantly northwest- to lesser northeast-verging tight to isoclinal folds, pervasive axial-planar foliation, and asymmetric boudinage. This area of structurally complex deformation, referred to as the Tombstone Strain Zone, hosts the Keno Hill Ag-Pb-Zn vein deposits, and has resulted in highly foliated Hyland Group, Earn Group, and Keno Hill quartzite rocks in the district. The Robert Service Thrust displaces the stratigraphically older Precambrian Hyland Group on top of the Keno Hill quartzite. In the hanging-wall of the Tombstone Thrust, the Earn Group, the Keno Hill quartzite, and the Paleozoic mafic dikes/sills have been thrust above Proterozoic to Triassic sediments, and stratigraphically lower Hyland Group rocks. The most

extensive deformation of the Tombstone Strain Zone is generally restricted to the hanging wall sheet of the Tombstone Thrust and the lower part of the Hyland Group in the Robert Service Thrust sheet, where original bedding has generally been transposed parallel to the axial planar foliation, and where metamorphic grade extends up to middle greenschist facies. A broad west to southwest plunging fold structure, the McQuesten antiform, with an inferred reverse fault (south-side up) occupying the axial-plane, post-dates the Tombstone Strain Zone deformation and is age bracketed from approximately Late Jurassic to Cretaceous (Murphy, 1997). The limited number of studies of this structurally complex area have different structural conclusions concerning the stratigraphic units and their structural position.

The Roop Lakes stock/Mayo Lake Batholith, has a U-Pb age of 92.8 ± 0.5 Ma from titanite (Roots, 1997), is the most prominent intrusive body in the Keno Hill district, and is located approximately 20 kilometers east-southeast of Keno City (Figure 2-3). This intrusion is considered to be part of the Mayo Plutonic Suite of the TTB, emplaced during the Late Cretaceous, and is syenite to granodiorite with biotite, hornblende, and pyroxene (Murphy, 1997; Hart et al., 2004a). Additional and smaller intrusive bodies including aplite and/or quartz-feldspar porphyry dikes and sills are reported throughout the district by previous exploration and mining companies. For example, two aplitic dikes, with a U-Pb age of 93 ± 1.7 Ma from zircon (Tupper and Bennett, 2010), within the Keno Hill district are indistinguishable in age from the Roop Lakes stock and TTB/Mayo Plutonic suite.

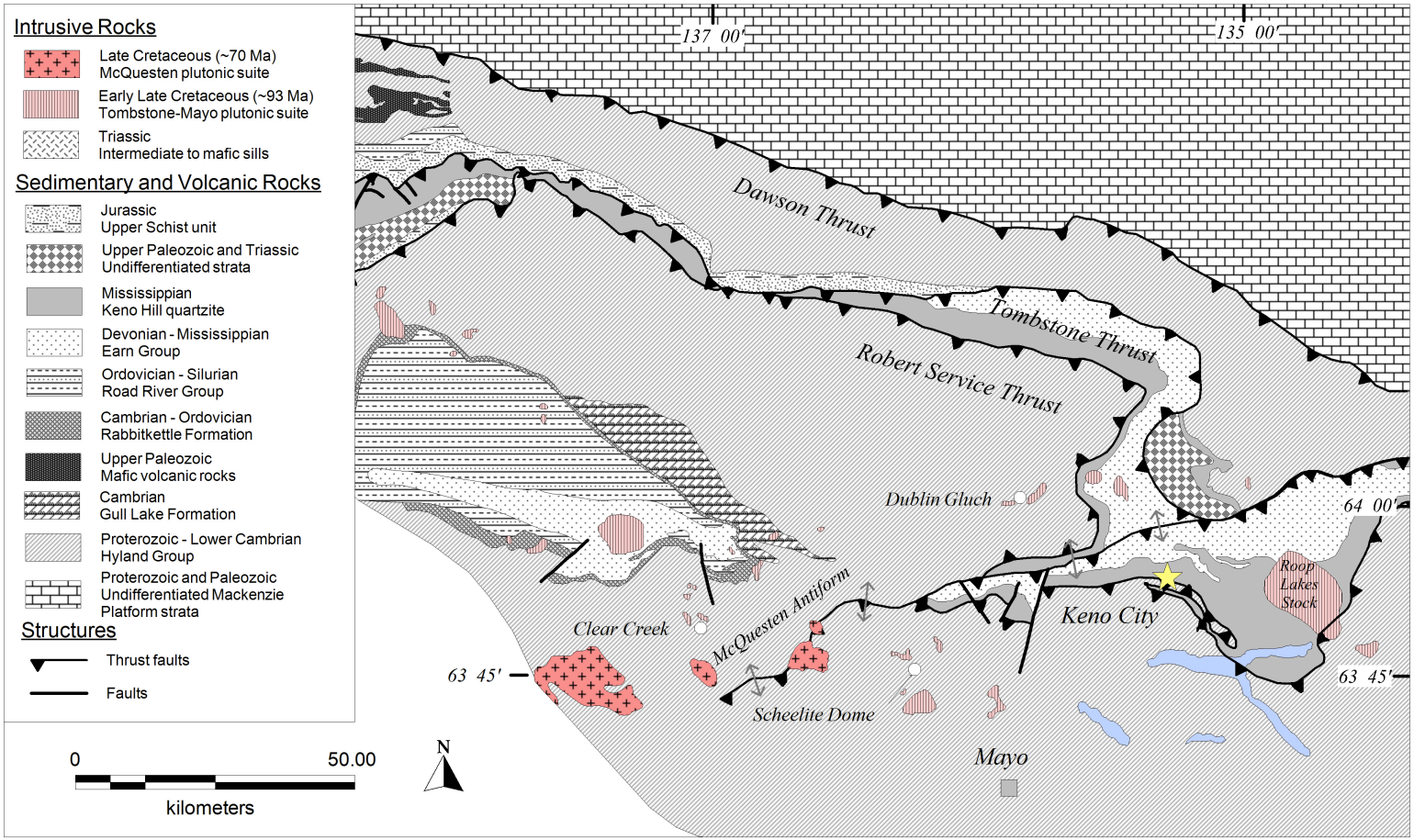

Figure 2-3. Regional geology of the northwest Selwyn Basin, re-drawn after Murphy (1997). Note intrusion-related gold deposits Dublin Gulch, Scheelite Dome, and Clear Creek also identified. The Roop Lakes stock, part of the Mayo plutonic suite may play a role in the genesis of the Keno Hill mineralization.

2.3 Keno Hill Mineralization and Fault Structures

The Ag-Pb-Zn deposits occur as a series of veins and breccias occurring within a northeast-southwest trending area at least 20 kilometers long, and up to 6 kilometers wide (Figure 2-4) on Galena, Keno, and Sourdough Hills. Keno Hill mineralization has been commonly referred to as vein-faults since early mapping by McTaggart (1960), based on the relative coeval relationship between faulting or fault-related brecciation and mineralization. Boyle (1965) documented three phases of hypogene mineralization, followed by a supergene stage, and included 3 distinct faulting events.

The strike of veins varies from north to east-northeast, with bends and/or jogs along vein strike resulting in locally anastomosing vein geometry, and steep dips to the southeast. Boyle (1965) classified the veins as either longitudinal or transverse, based on their orientation. Longitudinal veins trend northeast to east-northeast and are considered to be the older of the two types. Transverse veins trend north to north-northeast, and appear to bridge between, or connect, longitudinal veins. Vein minerals associated with the transverse type are observed cementing later fractures within longitudinal veins. Vein widths vary considerably, up to 15 meters (Boyle, 1965), but are typically less than 1 to 2 meters. Fault displacement within and following the trend of the veins appears to be either syn- to post-genetic with respect to vein mineralization based on cemented breccias, and localized areas of shearing fault planes associated with little vein growth, and strained crystals. The vein-faults have accommodated sinistral strike-slip and normal dip-slip displacement (McTaggart, 1960; Boyle, 1965; Lynch, 1989b). The effects of host rock lithology on rheological mechanics was recognized as an important control on vein growth and dilation zones by Boyle (1965), which may be a key factor responsible for permitting hydrothermal fluid flow and related mineralization. Numerous later stage northwest- to northeast-striking faults with normal and/or apparent dextral displacement, generally post-date the Ag-Pb-Zn mineralization (Boyle, 1965; Murphy, 1997). However the presence of minor, late stage minerals (i.e. galena) within some northwest-striking fault structures suggest that these late faults may have developed near the end of the hydrothermal mineralization, or alternatively these minerals may have been re-mobilized. Additionally, minor post-mineralization movement along foliation has also been observed locally, with apparent dip-slip displacement less than a centimeter.

Demonstrating a direct link between the Keno Hill veins and the Roop Lakes stock is difficult since there is no metallogenic association, and the veins occur outside the metamorphic contact aureole of the pluton. However, Lynch (1989) inferred a genetic relationship based on east to west lateral changes of hydrothermal fluid chemistry and vein mineral assemblages away from the Roop Lakes stock. Sinclair et al. (1980) suggested an age of 87 ± 3 Ma for the Keno Hill mineralization based on whole rock K-Ar analyses of impure quartzite wall-rock samples adjacent to and containing the Ag-Pb-Zn vein-type mineralization, which further supports at least a temporal relationship of the veins with the TTB/Mayo Plutonic Suite.

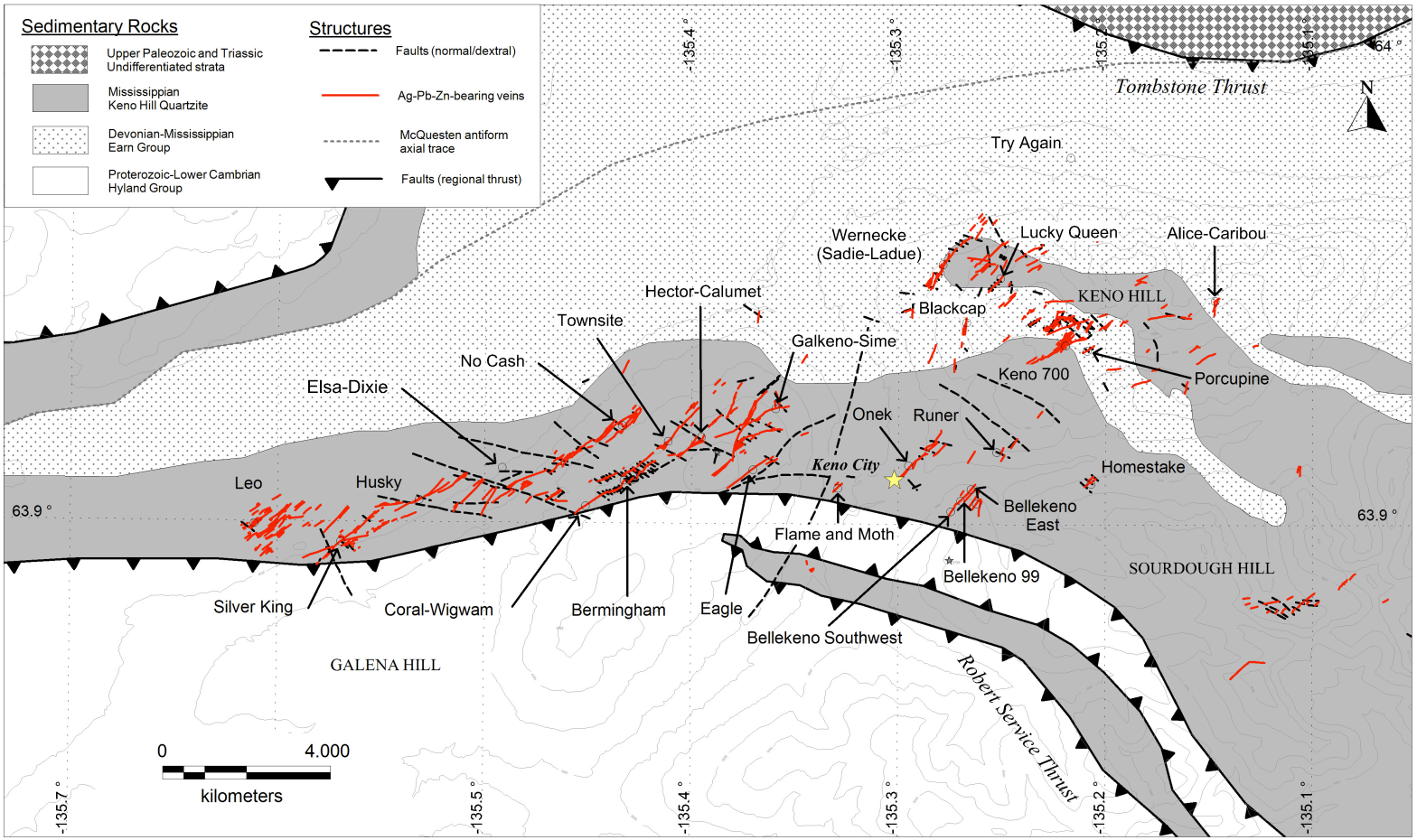

Figure 2-4. Local geology, from Alexco Resource Corp., Ag-Pb-Zn-bearing veins-breccias-faults predominantly cemented by siderite or quartz (red lines), and post-mineralization dextral and/or normal faults (dashed-black lines); with regional geology from Murphy (1997). Note that most Ag-Pb-Zn veins are primarily hosted within the Keno Hill quartzite.

3.0 Sampling and Analytical Techniques

Over 300 samples were collected during the 2009 summer field season, mostly from drill core but also include approximately 50 surface samples. Mineral assemblages and the hydrothermal paragenesis were described from over 100 hand samples, and 80 thin sections.

3.1 Electron Microprobe Analytical (EMPA) Techniques

Mineral chemistry was determined using Cameca SX100 Electron Microprobe (EMPA), operated at 20 kV accelerating voltage, 20 nA probe current, and 1 micron beam diameter for sulfide minerals; and 15 kV accelerating voltage, 15 nA probe current, and 5 microns beam diameter for carbonate minerals; count times varied from 10 to 50 seconds depending the element analyzed. The University of Alberta, Electron Microprobe Laboratory manager and technician, Sergei Matveev, completed the calibration using natural and synthetic standards from the University of Alberta collection and Smithsonian Institute (Jarosewich, 2002). Data reduction was performed using the PAP correction (Pouchou and Pichoir, 1985). Microprobe data is reported in weight percent (wt %); carbonate mineral chemistry CO_2 content is based on 6 oxygen calculations. The author carried out the data point selection. Accuracy is dependent on the quality of the calibration, which was not determined during this study; however the accuracy is typically better than ± 5 %. Precision is quantified statistically from analysed data counts, also not determined during this study; however best theoretical precision is generally 0.2 %.

Electron Microprobe mineral chemistry data were not collected on the minerals in all stages. Silicate minerals were not examined in this study due to their volumetrically minor abundance in association with the Ag-Pb-Zn-bearing mineral assemblages.

3.2 X-Ray Diffraction

A total of 36 wall rock samples from across the district were analyzed, and from a variety of different hydrothermal vein assemblages/stages. Samples generally greater than 2 grams were ground to a fine powder, and sieved to pass 50 μm; prepared by the author. The University of Alberta, X-Ray Diffraction Laboratory manager and technician, Diane Caird, completed the analyses. The powdered samples were then mounted into holders; smaller samples were mounted on zero-background plates and analyzed by a Rigaku Geigerflex Powder Diffractometer, equipped with a cobalt tube, graphite monochromator and scintillation detector. Routine search/match is run on a separate computer using JADE 9.1 software and the ICDD and ICSD databases. The Rigaku Ultima IV comes with Cross Beam Optics and includes the Scintillation Detector with graphite monochromator, or the D/Tex ultra high-speed position sensitive system with Kß filter to remove unwanted K-beta peaks.

3.3 Fluid Inclusions

Over 250 fluid inclusions in quartz, siderite, sphalerite, and calcite from 38 chips were analysed. Microthermometry measurements were completed by the author using a Linkam THMSG600 heating-freezing stage in Dr. Jeremy Richard's Fluid Inclusion Laboratory at the University of Alberta. The author and co-students completed the equipment calibration using natural pure H_2O and CO_2 fluid inclusions (AR305, AR308, AR116-2). The freezing (pure CO_2 = -56.6˚C) and melting (pure H_2O = 0.0˚C) point temperatures were determined to have an accuracy and precision of ± 0.1˚C. Heating experiments were conducted first in anticipation that subsequent freezing experiments could potentially alter or stretch the fluid inclusion due to the expansion of ice (Lawler and Crawford, 1983); temperature measurements >160˚C have an accuracy and precision of ± 2˚C, determined from repeat analyses of fluid inclusions with homogenization temperatures of 163˚C and approximately 376˚C.

3.4 Carbon and Oxygen Isotopes

A total of 46 carbonate samples were analyzed for their $\delta^{13}C$ and $\delta^{18}O$ values. The siderite (n=34) and calcite (n=10) samples are from various locations throughout the district, with the majority from the Bellekeno vein. Two limestone (n=2) samples were collected from an outcrop on Sourdough Hill.

All samples were hand sorted, pulverized, and sieved to passing 50 μm by the author at the University of Alberta. A second stage of sample preparation, a method similar to that described by McCrea (1950), involves reacting the pulverized sample with phosphoric acid under vacuum conditions at 25˚C for 24 hours, and 50˚C for 7 days, for calcite and siderite, respectively; and then cryogenically distilling the evolved CO_2 gas into a sample tube. The author completed the second stage of sample preparation for all calcite, limestone, and 8 of the siderite samples, which were analyzed at the University of Alberta, Stable Isotope Laboratory by Olga Levner and Dr. Karlis Muehlenbachs using a Finningan Mat 252 mass spectrometer. National Bureau Standards (NBS-18, NBS-19, and NBS-20) were inserted into the sample stream to determine the precision and accuracy of ± 0.1 ‰ (1σ) for both $\delta^{13}C$ and $\delta^{18}O$. The remaining 26 siderite samples were sent to University of Western Ontario, Department of Earth Science, Laboratory for Stable Isotope Science. Samples were prepared (second stage) by reacting approximately 2 to 15 mg of sample with phosphoric acid at 90˚C for 5 hours, and analyzed by Li Huang, Kim Law, and Fred Longstaffe using a Thermo Finnigan Delta^{PLUS}XL mass spectrometer. National Bureau Standards (NBS-18, NBS-19) and were inserted into the sample stream to determine both precision and accuracy (1σ = 0.1 ‰ and 0.3 ‰, for $\delta^{13}C$ and $\delta^{18}O$ respectively, n=7). Results are reported in per mil notation (‰), $\delta^{13}C$ in reference to the Pee Dee Belemnite (PDB), and $\delta^{18}O$ in reference to Standard Mean Ocean Water (SMOW) (Hut, 1987). The siderite-phosphoric acid fractionation factor has been applied according to Rosenbaum and Sheppard (1986).

3.5 Sulfur Isotopes

A total of 70 sulfide minerals: arsenopyrite (n=1), pyrite (n=15), galena (n=28), and sphalerite (n=26) were analyzed for their $\delta^{34}S$ values. Most samples were collected from various paragenetic stages of the Bellekeno vein, with few samples from other veins within the district. However, some stages lack data because they either contain little to no sulfides (i.e. stages 1, 2, 6, 10, 11, and 12), or because individual sulfide phases could not be isolated due to the complex mineral intergrowths (i.e. stage 9).

Sulfide minerals were hand sorted, pulverized, with a mortar and pestle, and sieved to pass 50 μm by the author at the University of Alberta. All sulfide samples were analyzed at the University of Calgary, Department of Physics and Astronomy, Isotope Science Laboratory by Jesusa Pontoy using a Thermo Finnigan Delta^{PLUS}XL mass spectrometer. Samples were weighed to approximately 100 to 400 mg, packed into high purity tin cups, and then delivered by the A200S auto sampler of a Continuous Flow-Isotope Ratio Mass Spectrometer (CF-EA-IRMS), into a quartz tube combustion reactor. The temperature of the column was maintained at 1020˚C, where 'flash-combustion' was achieved by pulses of O_2 gas injected at the time of the sample entry. The resulting gas is then transported in a UHP helium carrier flow (approximately 90 ml/min) through a GC column delivered to the mass spectrometer analyzer. International Atomic Energy Agency standards (IAEA CO-1, IAEA CO-8, IAEA CO-9) were used to determine both precision and accuracy (1σ = 0.3 ‰, n=10). $\delta^{34}S$ values are reported in per mil notation (‰), in reference to the Canyon Diablo Troilite (CDT).

3.6 Lead Isotopes

A total of 18 samples of galena were analyzed to determine their $^{206}Pb/^{204}Pb$, $^{207}Pb/^{204}Pb$, and $^{208}Pb/^{204}Pb$ isotope ratios. Most samples are from the Bellekeno vein, with a few samples from other veins in the eastern part of the district.

Galena samples were hand sorted, then approximately 1 to 5 mg of galena were dissolved in a 1.5 mL solution of 2% HNO_3 at 50˚C for approximately 24 hours. This solution was then diluted until the solution contained approximately 50 ppb Pb. Sample preparation was complete by the author. Andy DuFrane and the author performed the analyses using a multi-collector inductively coupled plasma mass spectrometer (MC-ICP-MS) at the University of Alberta, MC-ICP-MS Laboratory. This analytical method has been described in detail and evaluated by White et al. (2000). National Bureau Standard NBS-981 was inserted into the sample stream to determine both precision and accuracy (1σ = 0.0261, n=6, mean = 36.72 for $^{208}Pb/^{204}Pb$; 1σ = 0.0077, n=6, mean = 15.499 for $^{207}Pb/^{204}Pb$; and 1σ = 0.0068, n=6, mean = 16.947 for $^{206}Pb/^{204}Pb$).

4.0 Results

Most of the samples examined in this study are from Bellekeno vein in the southeast end of the district (Figure 2-4). The Bellekeno vein strikes northeast to southwest for nearly 1 kilometer, with a vein width varying from centimeters to over 6 meters, and is divided into 3 mineralized zones: East, 99 (Central), and Southwest. Lode mineralization and barren zones are strongly influenced by the host lithology and vein orientation (e. g. Boyle, 1965). Samples from Bellekeno include all 3 zones, and vary in elevation from 965 to 1045 meters above sea level (masl). Additional samples, including both drill-core and surface, from veins throughout the Keno Hill district were analysed to provide some district scale spatial context.

4.1 Hydrothermal Paragenesis, Mineralogy and Geochemistry

The mineral assemblages and paragenetic sequence presented here are largely based on observations from a detailed examination of the southwestern zone of the Bellekeno vein. The hydrothermal mineral assemblage classification was applied to facies logging in the field and using drill-core photos. Mineral chemistry data (from EMPA analyses) are summarized in Table 4-1 and Table 4-2, for carbonates and sulfides, respectively; only some relatively major chemical differences are discussed below. The complete table of all EMPA mineral chemistry data (1,377 data points for sulfides, oxides, and sulfates; and carbonates) are in Appendix III (A) and (B).

The Keno Hill hydrothermal vein-breccia mineralization has been grouped into 12 discrete and sequential stages (Figure 4-1) based on the distinct mineral assemblages, textures, and geochemistry observed in this study. These 12 stages are described in detail below. Most of the stages/mineral assemblages defined below appear to correlate well with samples from other veins, suggesting that the paragenetic sequence is broadly consistent throughout the district. Considering that all or most paragenetic stages are rarely observed in a single vein cross-cut, the schematic sketch of the Bellekeno vein cross-cut (Figure 4-2) is a limited representation exhibiting nearly all the observed paragenetic stages (1 through 8) and a variety mineralization textures, and also includes major assay values for the observed stages. The petrographic descriptions of 78 samples can be found in Appendix II.

Vein and breccia growth is complex and highly variable within each stage/mineral assemblage and throughout a single vein structure, resulting in highly localized differences and considerable variation in the relative mineral abundances, textures, and cross-cutting relationships. Extrapolating any mineral assemblage or paragenetic stage for more than a few meters in any direction requires care. The absence of one or more mineral assemblages in any given vein cross-cut view is not uncommon and generally appears to be the result of a lack of mineralization (i.e. not all hydrothermal stages precipitated consistently throughout veins or the district). With the exception of oxidation and weathering of minerals in the upper parts of the veins, secondary replacement, dissolution, and/or leaching of particular minerals or stages appear to be relatively unimportant as these textures are relatively uncommon or spatially limited. Also, stages dominated by the relatively soft sphalerite, may commonly be affected by later stage mineralization and/or subsequent fault displacement. Minor post-vein mineralization displacement along

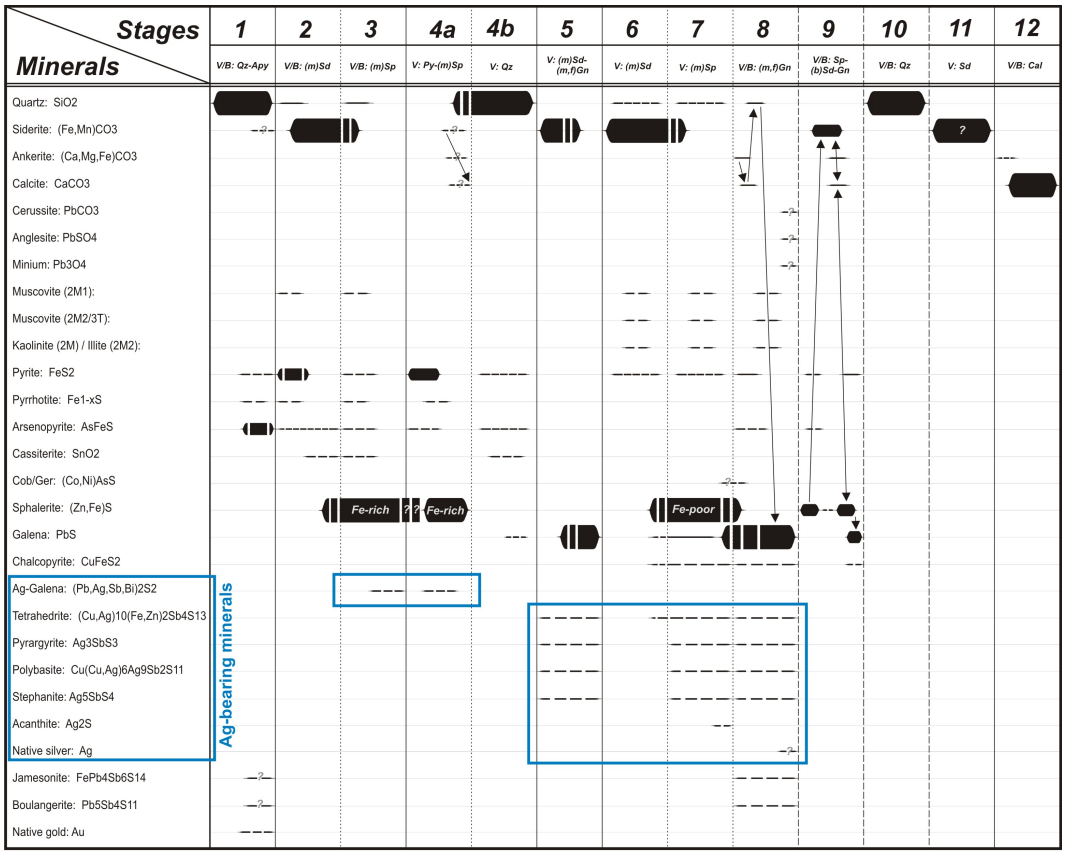

Figure 4-1. Keno Hill vein and breccia hydrothermal mineral paragenesis of hypogene stages associated with Ag-Pb-Zn mineralization. Mineral abbreviations used are summarized in Appendix I. The paragenesis is principally determined from observations of the Bellekeno vein. The minerals and stages with Ag-bearing minerals are highlighted within the blue squares.

the foliation planes in the host lithology is apparent (Figure 4-3 A). Vein growth may be either symmetrical or asymmetrical to irregular; where individual stages vary from macroscopic and massive to microscopic or crustified zones. Mineral assemblage boundaries vary from gradational/transitional or intergrown, to sharp/abrupt and distinct, to irregular; furthermore, boundary types are not spatially consistent. For example, a particular stage may have a sharp cross-cutting boundary with an earlier stage in one area of the vein; and alternatively, the same stages may have an intergrown transition in another area of the vein. Remnant vugs may be present in any stage, however many of which have been in-filled by later stage minerals; as opposed to a particular mineral that has co-precipitated with the surrounding host mineral/assemblage. For example, a later stage mineral such as galena that does not sequentially follow or transition from stage 1 quartz, may in-fill remnant vugs from stage 1.

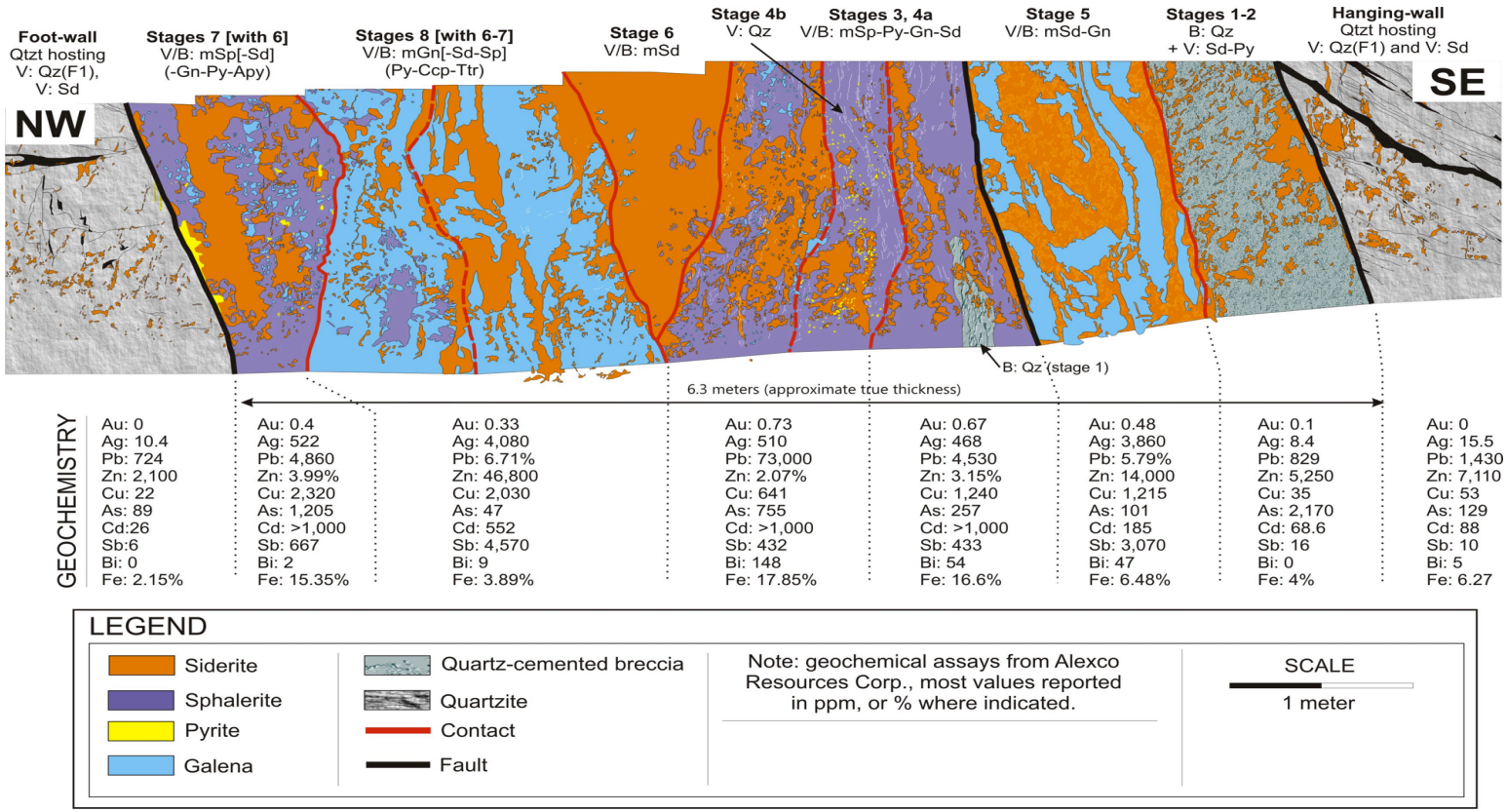

Figure 4-2. Schematic drawing of Bellekeno vein (Southwest zone) cross-cut level 750 (approximatly 990 masl), facing northeast rib. Only major (to moderately) abundant vein/breccia-filling minerals are represented or listed. Abreviations are as follows: B = breccia, V = vein, m = massive, Apy = arsenopyrite, Ccp = chalcopyrite, Ttr = tetrahedrite, Gn = galena, Py = pyrite, Sd = siderite, Sp = sphalerite, Qz = quartz, Qtzt = quartzite. V: Qz(F1) are quartz veins parallel foliation. Black lines define faults with apparent displacement and/or contain fault gouge. Red lines (solid or dashed) define contacts between hydrothermal stages. Geochemical assays from Alexco Resources Corp.; values are reported in parts per million (ppm), except were indicated as %.

Stage 1

Breccias, veins (up to few meters wide), and veinlets are comprised of predominantly quartz, intergrown with lesser pyrite and arsenopyrite (Figure 4-3 B, C). Quartz is commonly massive, milky white to clear, and anhedral to subhedral (mostly with grain sizes of 250 μm to >4 mm). Locally massive arsenopyrite and lesser pyrite occur as anhedral to euhedral clusters (<500 μm to <1 mm) within quartz. Sphalerite is translucent yellow to orange-brown, and anhedral. Native gold is reported to be associated with this stage (Stage 2 from Boyle, 1965; jamesonite-boulangerite zone from Lynch, 1989), but gold was not observed in this study.

Stage 1 is commonly absent in most veins examined; it appears to be better developed in the eastern part of the district (i.e. Homestake vein). Lynch (1989) referred to these veins as part of the jamesonite-boulangerite zone; however, we consider that the presence of minor siderite, sphalerite, galena, boulangerite and jamesonite reflect later stage mineralization (from stages 6 to 8 described below) associated with brecciation or infilling remnant vugs after stage 1 (Figure 4-4 A).

Stage 2

This stage is dominated by breccias, veins, and veinlets of siderite, variably intergrown with pyrite, and associated with minor arsenopyrite and cassiterite (Figure 4-3 B to F; Figure 4-4 B to D). Stage 2 is frequently the earliest hydrothermal stage observed in contact with the host rocks (i.e. stage 1 absent). Minor early quartz and muscovite may be present, commonly as crusts or rims around wall-rock clasts; or quartz may be more locally abundant and intergrown with siderite. Siderite is predominant, cementing breccias, veins, and veinlets. Two texturally distinct types of siderite are apparent. Type I is fine grained (<250 μm), pale brown to cream or cloudy, and generally pre-dates type II. The cloudy texture appears to be a result of abundant microscopic fluid and/or mineral inclusions (<5 μm). Type II siderite is variably translucent, light brown, subhedral to euhedral, with variable grain sizes (500 μm to >1cm). In a few samples, minor ankerite is precipitated late in stage 2. Pyrite (with lesser arsenopyrite and cassiterite) occurs as individual anhedral to euhedral crystals or clusters (<500 μm). A genetic relationship between pyrite (and arsenopyrite) with quartzite and phyllite is suggested by their frequent spatial proximity or intergrown nature. Some muscovite may be hydrothermal in origin, occurring as subhedral to euhedral clusters filling vugs, alternatively in some areas it appears to be recrystallizing from the very fine and opaque phyllosilicate minerals that constitute the phyllitic and schistose host rock units.

The mineral chemistry of stage 2 siderite is consistent throughout the paragenesis (Table 4-1). The chemical formula of the Bellekeno siderite can generally be expressed as $Fe_{0.75}Mn_{0.25}CO_3$; however, the composition may fluctuate within a single crystal, where either Mn and/or Fe can vary by several wt %, with Mg and Ca varying by only a fraction of a wt %. The variation between Fe, Mn, Mg, and Ca defines chemically zoned crystal structure, whereby the edges of many crystals are commonly associated with a relative decrease in Mn, accompanied by an increase in Mg, Ca, or Fe.

District-wide variations of the siderite composition are apparent (Figure 4-5; Table 4-1; and section 5.4 Keno Hill District Spatial Zonation); the most pronounced differences are defined by a relative increase in the Mn and Mg associated with a decrease in Fe content to the north and west of the Bellekeno vein (e.g. Alice, Keno 700, Porcupine, Pool, and Silver King). One exception is at Wernecke, where the relative increase in Mg is associated with a decrease in Mn, and the Fe content is similar to that of Bellekeno.

Vein									
Mineral	**Stage**	**n =**	**Total**	**CO_2**	**MgO**	**CaO**	**MnO**	**FeO**	**SrO**
Bellekeno									
Siderite	2	121	99.98	38.2	1.22	0.51	15.70	44.26	0.03
Siderite	6	68	99.99	39.4	1.05	0.43	14.64	44.34	0.04
Siderite	9	70	99.98	38.2	1.03	0.87	15.66	44.13	0.05
Ankerite	2 to 11	53	99.99	44.1	9.78	31.24	4.71	9.98	0.12
Calcite	11	32	99.98	43.2	0.24	52.55	2.49	1.33	0.08
Alice									
Siderite	6 ?	13	99.99	38.4	3.83	0.50	24.95	32.20	0.03
Wernecke									
Siderite	6 ?	12	100.00	39.4	5.10	0.92	10.70	43.78	0.04
Keno 700/Porcupine									
Siderite	2 to 6	53	99.98	38.9	2.60	0.59	17.15	40.56	0.06
Ankerite	9 to 11	5	99.97	45.9	10.08	31.76	2.28	9.53	0.14
Calcite	11	6	99.98	44.6	0.29	53.51	0.20	1.18	0.10
Silver King/Pool									
Siderite	2 to 9	20	99.99	38.3	3.65	1.69	19.32	36.89	0.02
Ankerite	9 ?	15	99.98	43.7	11.25	30.94	5.04	8.91	0.05
Calcite	11	7	99.99	43.4	0.23	52.97	2.06	1.28	0.02
Detection Limits					0.10	0.10	0.58	0.52	0.05

Table 4-1. Summary of average carbonate gangue mineral chemistry (wt %) from EMPA analyses, from Keno Hill district veins. Notations: number of samples (n).

Stage 3

Minor early quartz is present, partly intergrown with sphalerite, which cements breccias, veins, veinlets, as well as vug-fills within stage 2 siderite (Figure 4-3 E; Figure 4-4 B). Sphalerite is mostly dark purple in hand sample, dark red to brown and opaque in thin section, with an anhedral to euhedral habit, and occurs as fine blebs (<50 μm) to coarse irregular masses millimeters to meters wide. Mineral inclusions (<10 μm) of chalcopyrite (i.e. 'chalcopyrite-disease') and pyrrhotite are common, but not ubiquitous. Locally, sphalerite and siderite may be intergrown, this nature suggesting a continuous transition between stages 2 and 3. Minor pyrite, arsenopyrite, cassiterite, galena, and muscovite may be intergrown with sphalerite. Pyrite and lesser arsenopyrite are anhedral to euhedral (<250 μm), may form crystal clusters (<2 mm). Cassiterite is anhedral to subhedral, occurring as blebs (<50 μm) commonly associated with pyrite and arsenopyrite. Galena is anhedral to euhedral (<500 μm) within pyrite, sphalerite, or siderite, and infilling microscopic veinlets and breccias.

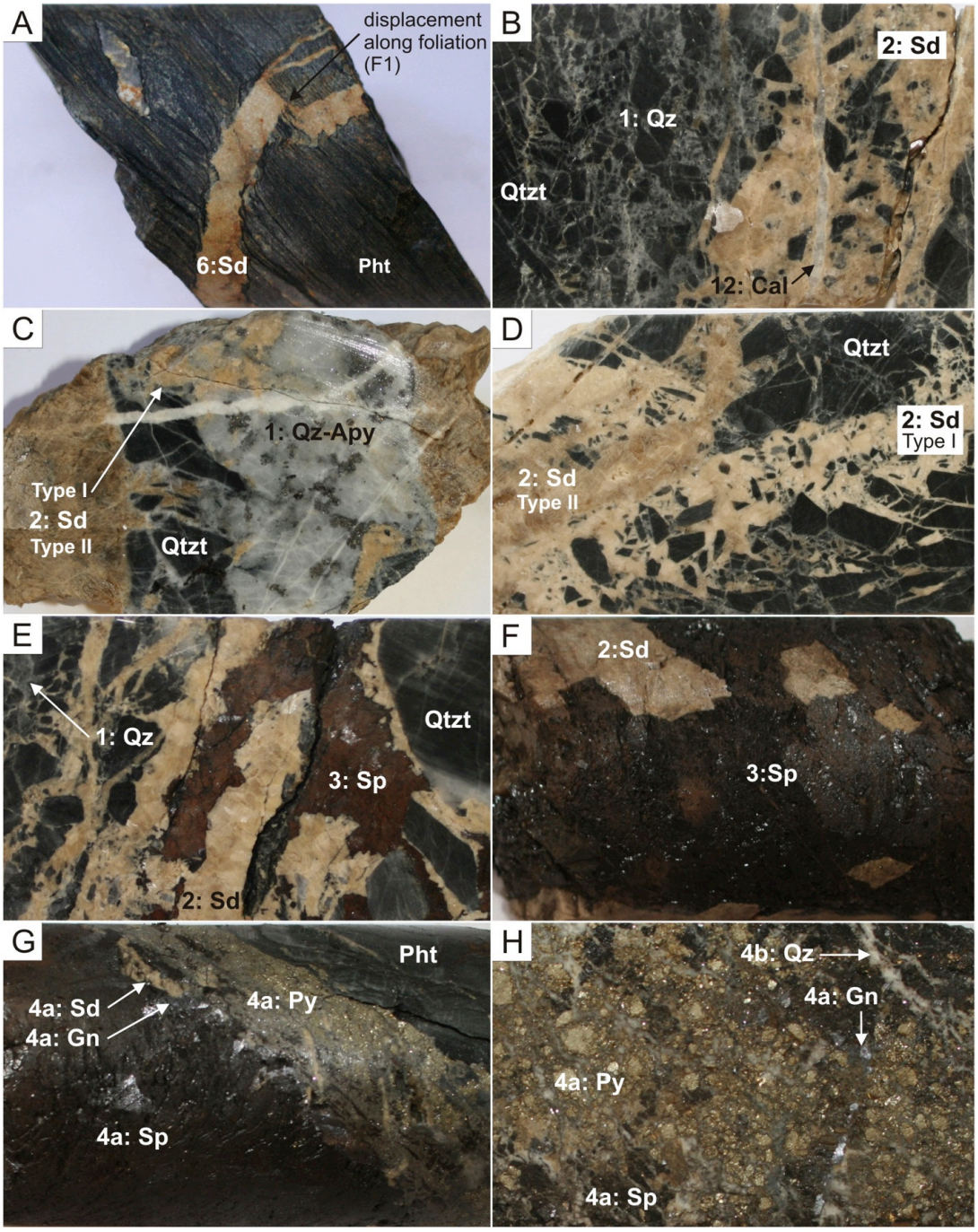

Figure 4-3 (A-H). Photographs of drill-core samples; field of view for all frames is approximately 101.2 mm x 63.5 mm. Mineral abbreviations are summarized in Appendix I, numbers preceding mineral abbreviations indicate paragenetic stages. A) K09-199: 66.9 m. B) BKUD09-172: 11.7 m. C) BKUD09-157: 101.9 m. D) BKUD09-140: 10.4 m. E) BKUD09-144: 36.4 m. F) BKUD09-146: 46.5 m. G) BKUD09-143: 51.2 m. H) BKUD09-153: 87 m.

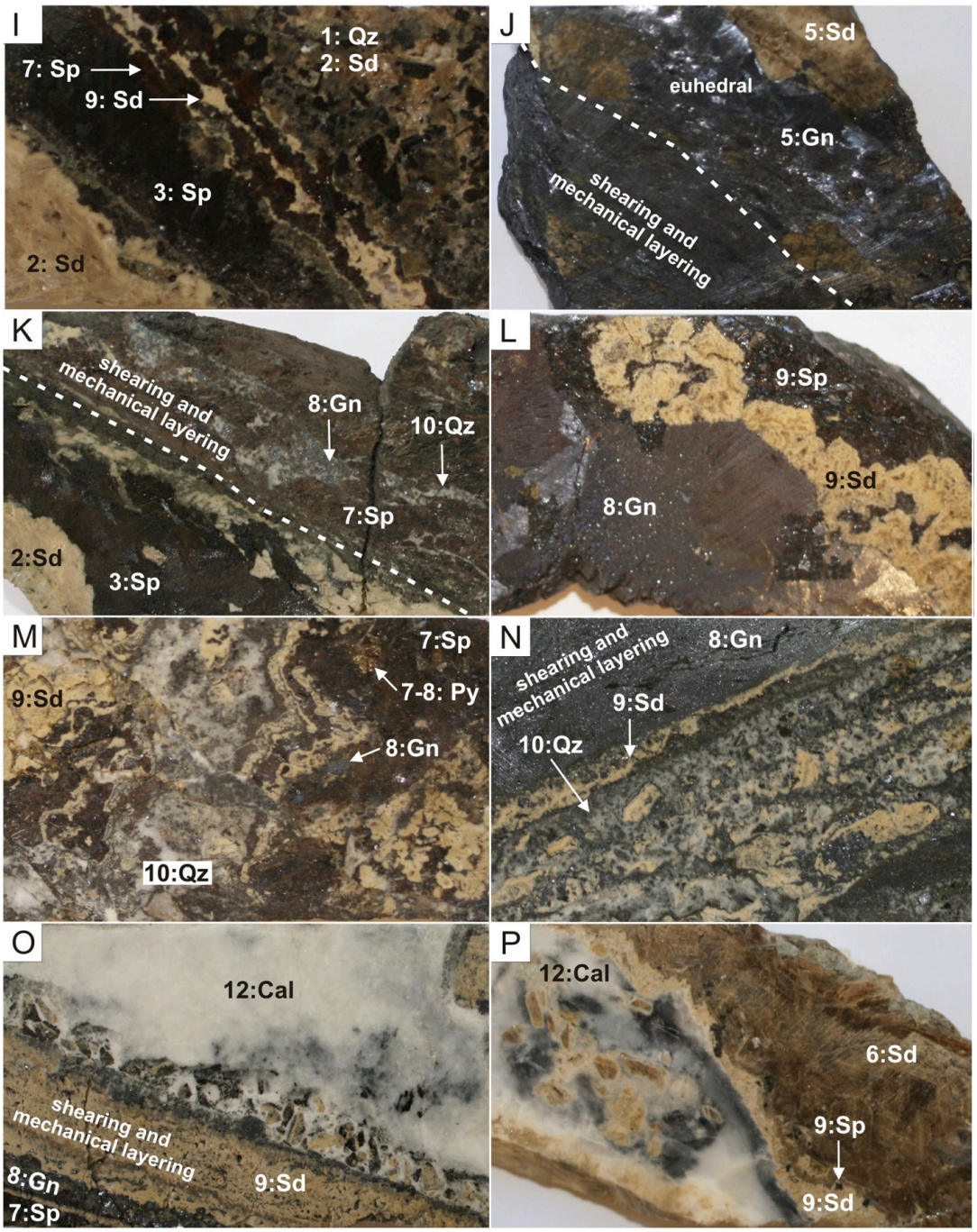

Figure 4-3 (I-P). Photographs of drill-core samples; field of view for all frames is approximately 101.2 mm x 63.5 mm. Mineral abbreviations are summarized in Appendix I, numbers preceding mineral abbreviations indicate paragenetic stages. I) BKUD09-146: 46.3 m. J) BKUD09-153: 88.6 m. K) K09-197: 193.6 m. L) BKUD09-143: 52.8 m. M) BKUD09-143: 52.7 m. N) BKUD09-160: 54.1 m. O) BKUD09-160: 56.5 m. P) BKUD09-153: 84 m.

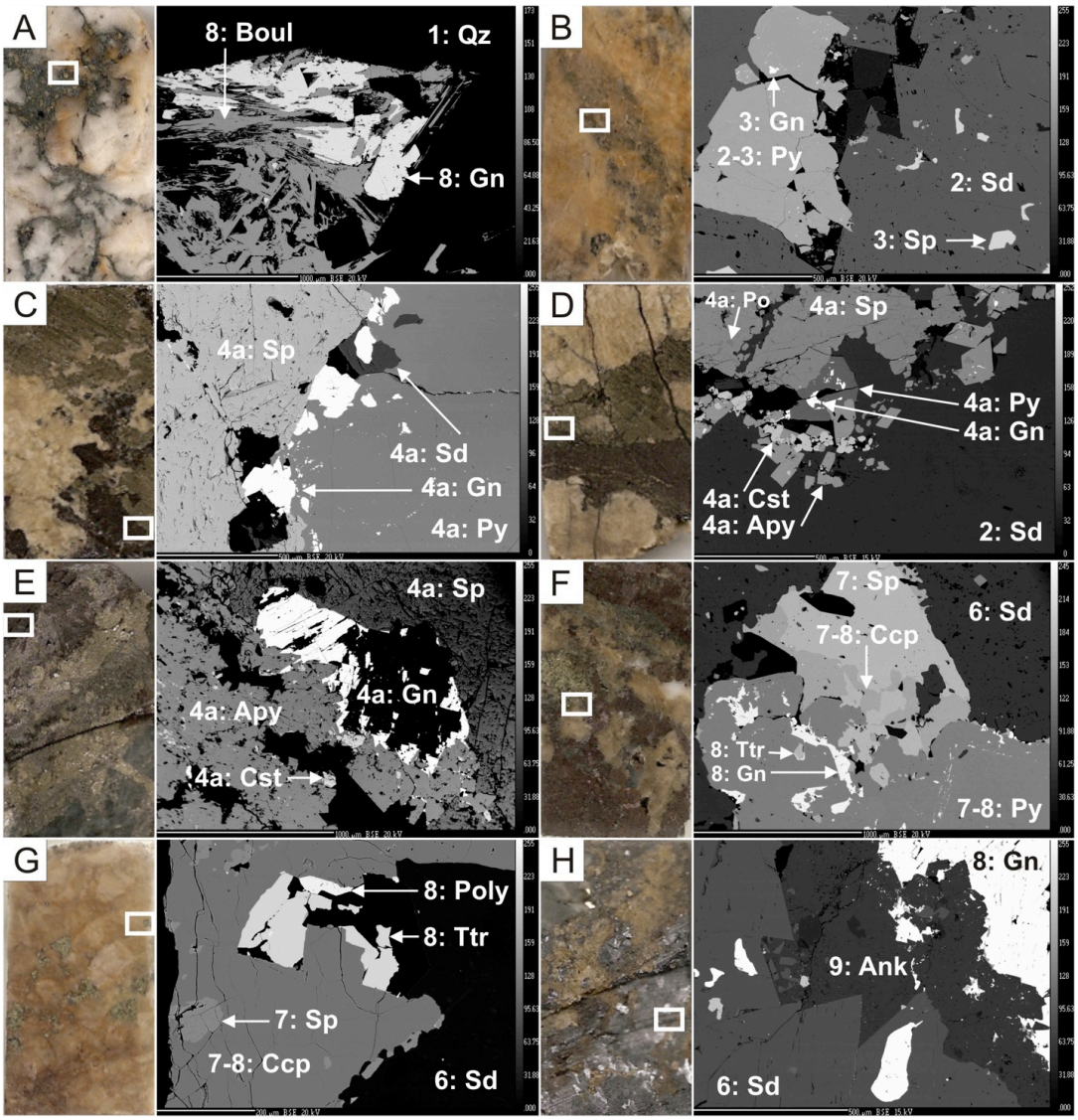

Figure 4-4 (A-H). Sample off-cuts (each approximately 20 mm by 35 mm) at left, with white or black rectangles inset defining detail from electron microprobe photomicrographs at right. Mineral abbreviations are summarized in Appendix I, numbers preceding mineral abbreviations indicate paragenetic stages. A) HOM-53-1, point 2. B) K07-95: 402.1 m, point 4. C) BKUD09-134: 42.4 m, point 6. D) BKUD09-134: 45 m, point 2. E) BKUD09-146: 46.5 m, point 4. F) BKUD09-139: 8.3 m, point 10. G) K07-86: 223.3 m, point 1. H) BKUD09-171: 32.8 m, point 10.

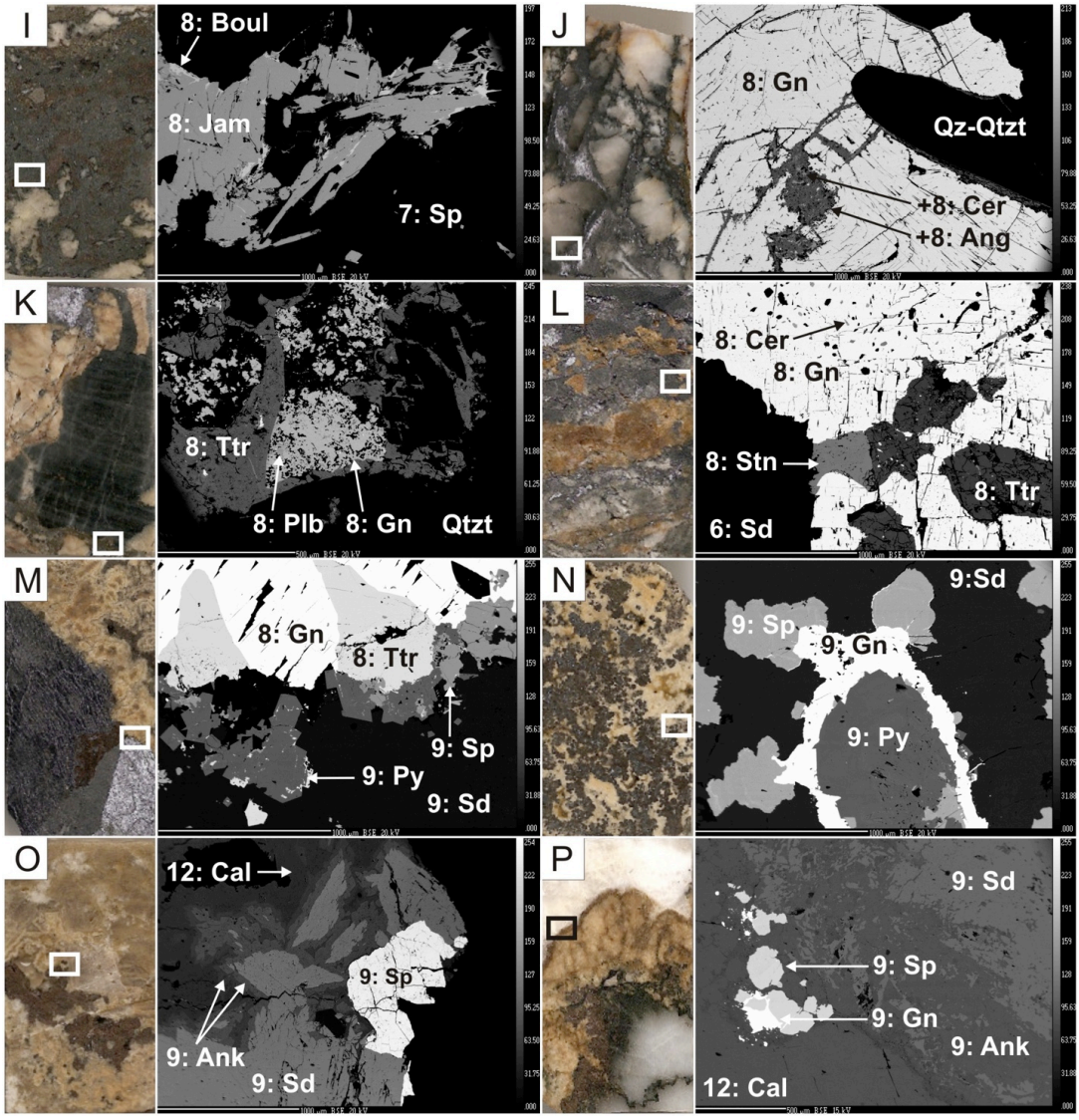

Figure 4-4 (I-P). Sample off-cuts (each approximately 20 mm by 35 mm) at left, with white or black rectangles inset defining detail from electron microprobe photomicrographs at right. Mineral abbreviations are summarized in Appendix I, numbers preceding mineral abbreviations indicate paragenetic stages. I) BRM-44: surface, point 2. J) Try Again: surface, point 5. K) K06-2: 167.2 m, point 7. L) K08-161: 229.8 m, point 3. M) BKUD09-143: 52.8 m, point 3. N) BKUD09-163: 14.8 m, point 5. O) BKUD09-157: 100.5 m, point 8. P) K07-87: 106.7 m, point 2.

The opaque nature of the sphalerite may be attributed to the relatively high Fe-content, averaging 7.47 ± 4 wt % (Table 4-2). Cadmium is a consistently minor constituent within sphalerite averaging 0.57 ± 0.5 wt %. The relatively low Cu-content in sphalerite may be an effect of most Cu being precipitated as chalcopyrite mineral inclusions. The chemistry of stage 3 galena is distinct from later stages (i.e. 5 and 8), based on the Ag content, which averages 0.46 wt %, ranging from below the detection limit up to 1.08 wt %.

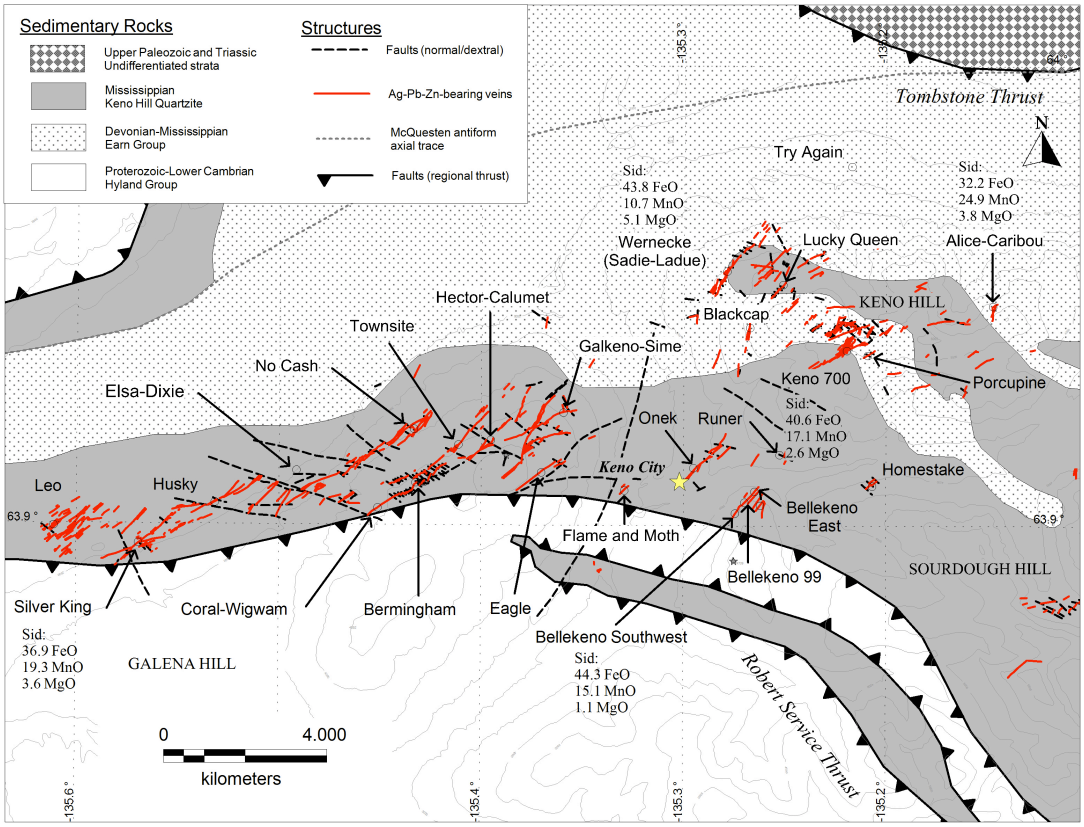

Figure 4-5. Keno Hill district siderite mineral chemistry, wt % FeO, MnO, and MgO. Note that FeO content generally decrease to the west and north is associated with an increase in MnO and MgO. The Wernecke samples are unique in that they exhibit the most pronounced increase in MgO.

Stage 4a

Early pyrite is followed by more abundant sphalerite, occurring as veins and veinlets which commonly exhibit symmetrical growth and cross-cut stages 2, 3, or the host-rock with sharp contacts (Figure 4-3 G, H; Figure 4-4 C to E). Pyrite is anhedral to euhedral occurring as clusters (<4 mm). Stage 4a sphalerite is texturally similar to that of stage 3; and generally post-dates, or is partly intergrown with the earlier pyrite of this stage. Tupper and Bennett (2010) report Au-enriched pyrite associated with a suite of minerals that appear to be similar to this stage. Variable arsenopyrite, with minor cassiterite and galena may be present.

The sphalerite and galena mineral chemistry of this stage are generally similar to that of stage 3 both in terms of textures and chemical composition. Sphalerite Fe-content averages 8.90 wt % with low average Cu-concentrations. Galena is again Ag-bearing and is slightly more enriched than in stage 3, Ag averages 1.10 wt %, varying from below the detection limit up to 2.89 wt %. Unique to this stage, some galena also contains minor Bi, ranging from below the detection limit up to 3.54 wt %.

Stage 4b

This stage is composed of veins and veinlets comprising of predominantly quartz, with lesser pyrite, arsenopyrite, cassiterite, and galena (Figure 4-3 H). Quartz is subhedral to euhedral, with a grain size of 250 μm to 2 mm. Pyrite and arsenopyrite are anhedral to euhedral (<50 μm). Cassiterite is similar to that in stage 4a. Galena is anhedral, and occurs as fine mineral inclusions or blebs (<100 μm). This stage is volumetrically insignificant, and is generally only observed cross-cutting stage 4a. This close spatial association suggests a temporal relationship between these 2 stages. Equally, this association may be the results of a rheological effect, where the relatively soft sphalerite may have localized these veins.

Stage 5

The nature of this stage could not be well constrained using the samples of this study. Siderite is the earliest mineral observed and is texturally similar to type II siderite in stage 2. Galena post-dates siderite and is subhedral to euhedral, forming irregular masses millimeter to meters in width, occurring as veins and vug-fills. Galena is commonly sheared and/or brecciated; where high strain has been accommodated by the galena, it has a fine grain size and is anhedral with a banded texture defining shear planes (Figure 4-3 J). Sphalerite is absent from this stage.

No stage 5 minerals were analyzed using EMPA. Equally, no silver-bearing minerals were identified in this stage; however based on geochemical assays, a similar array of sulfosalts as described in stage 8 are expected because similar concentrations of Ag, Sb, and Cu (note the assay values from this stage in Figure 4-2) are present in stage 5.

Stage 6

This stage is dominated by type II siderite which forms irregular masses, millimeters to meters wide and has a coarse grain size (<1 cm) and (Figure 4-3 P; Figure 4-4 F, G, H, I, K, L, O). Siderite may be coated by a thin layer (125 μm thick) of anhedral to subhedral, type I siderite. Quartz is subhedral to euhedral (<500 μm), variably present and intergrown with siderite, and generally more abundant than quartz in stage 2. The chemical composition of stage 6 siderite is similar to that of stage 2 siderite (see above).

Stage 7

Stage 7 is dominated by sphalerite, distinct from that of stage 3 and 4a based on appearance, mineral chemistry (below), and associated minerals. Sphalerite is reddish to honey brown, and variably translucent to opaque in thin section, with oscillatory zoning defined by alternating light and dark colour bands (Figure 4-3 I, K, M; Figure 4-4 F, G, I). It is anhedral to euhedral, and occurs as pockets to irregular masses micrometers to meters wide, or as vug-fill blebs within earlier stages. This sphalerite commonly lacks mineral inclusions (i.e. no “chalcopyrite disease”) as compared to stage 3 and 4a sphalerite. Quartz, siderite, pyrite, galena, chalcopyrite, Ag/Cu-tetrahedrite, polybasite, pyrargyrite, and acanthite, although minor, are commonly intergrown with sphalerite. Chalcopyrite is anhedral, and occurs as

Mineral	Stage	n =	Total	S	Fe	Cu	Zn	As	Ag	Cd	Sn	Sb	Pb
Arsenopyrite	most 2 to 4b	79	99.91	21.86	35.33	B.D.	B.D.	42.53	B.D.	B.D.	B.D.	B.D.	B.D.
Pyrite	throughout	218	100.04	52.96	46.58	B.D.	B.D.	0.67	B.D.	B.D.	B.D.	B.D.	B.D.
Pyrrhotite	most 2 to 4a	8	99.63	40.13	59.07	B.D.	0.55	B.D.	B.D.	B.D.	B.D.	B.D.	B.D.
Cassiterite	most 2 to 4b, minor 6 to 8	29	79.71	B.D.	0.39	B.D.	0.06	B.D.	B.D.	B.D.	79.35	B.D.	B.D.
Sphalerite	3	99	99.22	33.39	7.47	728 ppm	57.77	B.D.	B.D.	0.57	B.D.	B.D.	B.D.
Galena	3	15	100.36	14.10	0.36	B.D.	0.48	B.D.	0.52	B.D.	B.D.	B.D.	85.14
Sphalerite	4a	52	98.64	32.50	8.90	0.10	56.58	B.D.	B.D.	0.71	B.D.	B.D.	B.D.
Galena	4a	62	99.25	13.32	0.55	B.D.	0.15	B.D.	1.06	B.D.	B.D.	B.D.	84.34
Sphalerite	7	229	99.55	33.15	4.29	0.16	61.43	B.D.	B.D.	0.49	B.D.	B.D.	B.D.
Chalcopyrite	most 7 to 8	38	98.19	34.70	29.01	33.58	0.15	B.D.	0.63	B.D.	B.D.	B.D.	B.D.
Galena	mostly 8 (and 5)	232	100.59	13.50	775 ppm	B.D.	806 ppm	B.D.	0.12	B.D.	B.D.	B.D.	87.47
Boulangerite	6 to 8	21	100.26	18.61	B.D.	B.D.	B.D.	0.16	B.D.	B.D.	B.D.	26.03	55.30
Jamesonite	6 to 8	9	99.84	21.34	2.55	B.D.	B.D.	0.12	B.D.	B.D.	0.12	35.63	40.03
Tetrahedrite	6 to 8, minor 9	135	100.68	22.09	4.08	20.77	2.08	0.23	23.45	1.53	B.D.	26.69	B.D.
Pyrargyrite	6 to 8, or later ?	3	101.83	17.09	B.D.	0.73	0.14	0.14	58.37	3.02	B.D.	22.36	B.D.
Stephanite	6 to 8, or later ?	5	99.55	14.34	B.D.	0.16	0.11	B.D.	70.67	5.93	B.D.	8.36	B.D.
Polybasite	6 to 8, or later ?	3	102.04	13.32	0.12	3.59	B.D.	B.D.	72.47	1.40	B.D.	11.16	B.D.
Andorite (?)	6 to 8	1	99.92	18.80	B.D.	B.D.	B.D.	0.10	24.41	0.74	B.D.	27.27	29.04
Unknown (?)	6 to 8	1	97.27	30.84	24.22	29.38	B.D.	B.D.	10.53	1.28	B.D.	1.30	B.D.
Valentinite	6 to 8	5	83.65	0.12	0.11	B.D.	0.28	2.80	B.D.	B.D.	0.38	79.13	B.D.
Cobaltite-Gersdorffite	6 to 8 ?	3	98.31	19.43	7.82	B.D.	B.D.	44.02	B.D.	B.D.	B.D.	B.D.	B.D.
Cerussite	6 or later than 8?	4	80.07	B.D.	0.24	0.13	B.D.	3.51	B.D.	B.D.	B.D.	B.D.	75.99
Anglesite	later than 8?	15	75.39	7.83	B.D.	B.D.	0.40	0.10	B.D.	B.D.	B.D.	B.D.	67.07
Sphalerite	9	49	100.33	33.49	4.34	0.67	60.62	B.D.	0.28	0.54	0.25	B.D.	B.D.
Galena	9	11	99.00	13.67	B.D.	B.D.	B.D.	B.D.	0.19	B.D.	B.D.	B.D.	85.48
Detection Limit (ppm)				4260	730	530	700	650	1050	1960	1130	3550	20900

Table 4-2. Summary of average sulfide and ore-bearing oxides/carbonates mineral chemistry (wt %), from EMPA analyses from Keno Hill district veins (combined). Values are reported in wt. %, unless otherwise noted as ppm. Notations: number of samples analyzed (n), below detection limit (B.D.).

Mineral	Stage	n =	Total	Bi	Ni	Co	Mo
Arsenopyrite	most 2 to 4b	79	99.91	B.D.	286 ppm	652 ppm	B.D.
Pyrite	throughout	218	100.04	B.D.	B.D.	406 ppm	B.D.
Pyrrhotite	most 2 to 4a	8	99.63	B.D.	0.13	B.D.	645 ppm
Cassiterite	most 2 to 4b, minor 6 to 8	29	79.71	B.D.	B.D.	B.D.	B.D.
Sphalerite	3	99	99.22	B.D.	B.D.	B.D.	253 ppm
Galena	3	15	100.36	B.D.	B.D.	B.D.	B.D.
Sphalerite	4a	52	98.64	B.D.	B.D.	B.D.	B.D.
Galena	4a	62	99.25	0.58	B.D.	B.D.	B.D.
Sphalerite	7	229	99.55	B.D.	B.D.	B.D.	277 ppm
Chalcopyrite	most 7 to 8	38	98.19	B.D.	B.D.	B.D.	B.D.
Galena	mostly 8 (and 5)	232	100.59	B.D.	B.D.	B.D.	B.D.
Boulangerite	6 to 8	21	100.26	B.D.	B.D.	B.D.	196 ppm
Jamesonite	6 to 8	9	99.84	B.D.	B.D.	B.D.	195 ppm
Tetrahedrite	6 to 8, minor 9	135	100.68	B.D.	B.D.	B.D.	B.D.
Pyrargyrite	6 to 8, or later ?	3	101.83	B.D.	B.D.	B.D.	582 ppm
Stephanite	6 to 8, or later ?	5	99.55	B.D.	B.D.	B.D.	B.D.
Polybasite	6 to 8, or later ?	3	102.04	B.D.	B.D.	B.D.	B.D.
Andorite (?)	6 to 8	1	99.92	B.D.	B.D.	B.D.	B.D.
Unknown (?)	6 to 8	1	97.27	B.D.	B.D.	B.D.	B.D.
Valentinite	6 to 8	5	83.65	B.D.	B.D.	B.D.	B.D.
Cobaltite-Gersdorffite	6 to 8 ?	3	98.31	B.D.	18.89	7.99	B.D.
Cerussite	6 or later than 8?	4	80.07	B.D.	B.D.	B.D.	399 ppm
Anglesite	later than 8?	15	75.39	B.D.	B.D.	B.D.	832 ppm
Sphalerite	9	49	100.33	B.D.	B.D.	B.D.	371 ppm
Galena	9	11	99.00	B.D.	B.D.	B.D.	B.D.
Detection Limit (ppm)				410	*200*	280	170

Table 4-2 (continued). Summary of average sulfide and ore-bearing oxides/carbonates mineral chemistry (wt %), from EMPA analyses from Keno Hill district veins (combined). Values are reported in wt. %, unless otherwise noted as ppm. Notations: number of samples analyzed (n), below detection limit (B.D.).

irregular blebs and pockets (<500 μm). Pyrite is anhedral to subhedral (<2 mm) and forms clusters micrometers to centimeters wide. Galena is anhedral (<300 μm) and is generally contained within the sphalerite. The most common sulfosalts are Ag/Cu-tetrahedrite, with lesser polybasite, pyrargyrite, and boulangerite occurring as inclusions (<250 μm), which may form clusters (<1.5 mm). Acanthite is rare, only observed in one sample as a small irregular-shaped inclusion (<25 μm) in sphalerite and spatially associated with other sulfosalts. Overall these sulfosalts are intergrown with or post-date sphalerite (Figure 4-6) and pyrite, but generally pre-date chalcopyrite.

The mineral chemistry of stage 7 sphalerite is distinct from that of stages 3 and 4a primarily based on the Fe-content, which is on average lower, approximately 4.30 ± 4 wt % (Table 4-2; Appendix III B). The Cu-content of sphalerite averages 0.18 wt %, some samples contain >1 wt %. There may be minor Sn and Sb present, with one anomalously high value containing 2.87 wt % Sb from the Wernecke area.

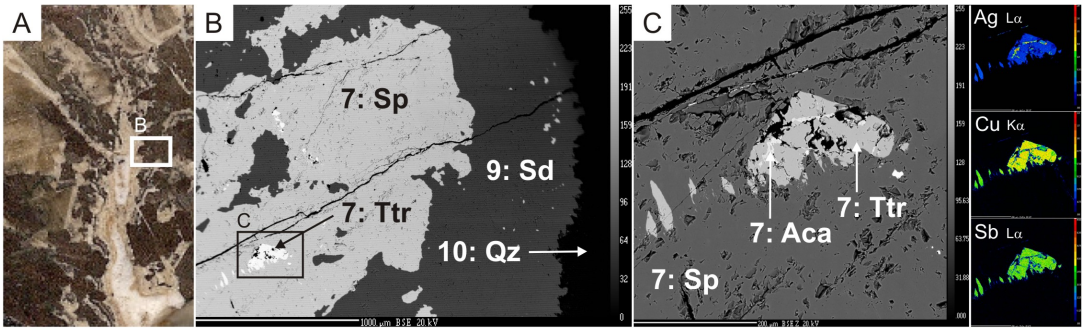

Figure 4-6. Sample BKUD09-158: 36.5 m. A) Thin-section off-cut showing stages 6 (darker) siderite (Sd), 7 sphalerite (Sp), 9 (lighter) siderite cross-cutting earlier stages, 10 quartz (Qz) infilling after stage 9. B) and C) Electron microprobe photomicrographs showing tetrahedrite (Ttr) and acanthite (Aca), with other unidentified sulfosalts within sphalerite. Electron microprobe maps at right show variable Ag-, Cu-, and Sb-content. Ag within tetrahedrite varies from 21 to 26 wt %, and Cu from 18 to 21 wt %, Sb-content is generally consistent at around 27 wt %.

Stage 8

Minor quartz is common early during this stage, occurring as anhedral to euhedral grains (500 μm to >2 mm), with clear cores and cloudy outer zones. Pyrite may be paragenetically early, and intergrown with galena; it is also often spatially associated with quartzite clasts. Pyrite and lesser amounts of arsenopyrite are anhedral to subhedral (<250 μm to <1 mm), and form clusters (<1 cm). In one sample chalcopyrite is the dominant early mineral. Minor/trace cobaltite-gersdorffite was identified from the EMPA, which appears to be associated with the early stage 8 quartz. Galena is predominantly euhedral (generally >1mm) forming irregular masses millimeters to meters wide, infilling massive veins and breccias or vugs within earlier stages (Figure 4-3 K to O; Figure 4-4 F to M). Shearing (syn- and/or post-mineralization) is apparent from strained or misshaped galena crystals, which are texturally fine grained and exhibit a banded texture defined by the mechanical or shear-related layering of siderite, sphalerite, and/or pyrite from earlier stages. The presence of sphalerite and siderite within this stage suggests a

transitional nature from stages 6 and 7; although stage 8 may also clearly cross-cut most of the earlier stages.

Sulfosalts and other Ag-bearing minerals are most commonly associated and either intergrown with stage 8 galena-pyrite, and stage 7 sphalerite, or post-date these phases in micro-fractures (Figure 4-6). Tetrahedrite (argentotetrahedrite) is the most frequently observed Ag-bearing mineral, and has grain sizes ranging from <125 μm to <1 mm. Minor chalcopyrite, pyrite, galena, pyrargyrite, polybasite, stephanite, acanthite and native silver occur as inclusions (<50 μm) or clusters (<500 μm) associated with or post-dating galena, Ag/Cu-tetrahedrite, chalcopyrite, and (stage 7) sphalerite. Where present boulangerite and jamesonite occur as anhedral masses (<100 μm), or euhedral laths (>1mm) and may be associated with galena. One sample from the Bermingham vein contains minor valentinite, occurring as blebs (<50 μm) intergrown with boulangerite. Native silver occurs rarely as irregular masses (<500 μm). Small inclusions (<20 μm) of an Ag-Sb-Pb mineral (similar to andorite, however more Ag- and Pb-rich, and Sb-poor), and an unknown Cu-Ag-Fe bearing (Sb absent) mineral may be associated with the above sulfosalts. A few samples contain late minor anglesite, cerussite, or lead-oxides infilling fractures within, or forming as a rim of alteration, around galena.

Stage 8 galena is relatively Ag- and Sb-poor, containing an average of 0.13 wt % Ag, and 0.20 wt % Sb; which is distinct from stages 3 and 4a galena (Table 4-2; Appendix III B). Only a few samples contain more than 0.5 wt % Ag or Sb, many of these anomalous samples are spatially associated with Ag-bearing sulfosalts. There is considerable variation of tetrahedrite chemistry in terms of Ag- and Cu-content, ranging from 11.54 to 40.87 wt % and 9.30 to 29.50 wt %, respectively, throughout the district and at the vein scale (Figure 4-7). The Sb-content is relatively consistent, averaging 26.68 wt %. Both Cu- and Ag-rich tetrahedrite may be present within a single sample; however the Cu- and Ag-content does not generally vary by more than 10 wt % in a single sample. Although there is a wide range of tetrahedrite composition in any given vein and individual sample, there is a broad trend of increasingly Ag-rich tetrahedrite from the southeast to the north and west. Also from observations of the Bellekeno vein alone, there is a generalized vertical trend to more Cu-rich tetrahedrite with increasing depth (Figure 4-8).

Stage 9

Stage 9, although volumetrically insignificant, when present it follows or is partly intergrown with stage 8 and comprises variably irregular, complex and repetitive alternating to oscillatory banded sequences defined by a series of mineral composition and textures. Each individual sequence is typically defined by early sphalerite with variably minor to absent pyrite, galena, and mica/muscovite, and post-dated by multiple bands of siderite with lesser ankerite and possibly calcite. This general sequence may repeat multiple times, but is largely dominated by siderite (Figure 4-3 I, L to P; Figure 4-4 N to P).

Where present, sphalerite is euhedral and occurs as irregular masses with oscillatory zoning of light and dark brown colour bands, similar to that of stage 7. Minor chalcopyrite, pyrrhotite, and pyrite mineral inclusions (<250 μm) may be contained within sphalerite. Pyrite may also occur as anhedral masses (<375 μm)

between sphalerite and a later phase of galena. Galena when present is subhedral to euhedral, and occurs as irregular clusters intergrown with or infilling after sphalerite. Minor galena, pyrite, and tetrahedrite may occur as inclusions (<50 μm) in the sphalerite.

The carbonate gangue of this stage is volumetrically dominant, and forms a banded texture defined by repetitive and alternating bands (generally <2 mm thick) of type I siderite and ankerite layers with a bladed crystal habit; and fewer layers of type II siderite which are commonly late in each sequence. Minor early pyrite and arsenopyrite are subhedral to euhedral (<1 mm), and occur as clusters precipitated prior to and partly intergrown with the banded siderite. Sphalerite may be present as mineral inclusions (<30 μm) within the type I siderite layers, or larger pockets (<1 mm) after the type II siderite layers; and are inferred to reflect the beginning of a subsequent sequence.

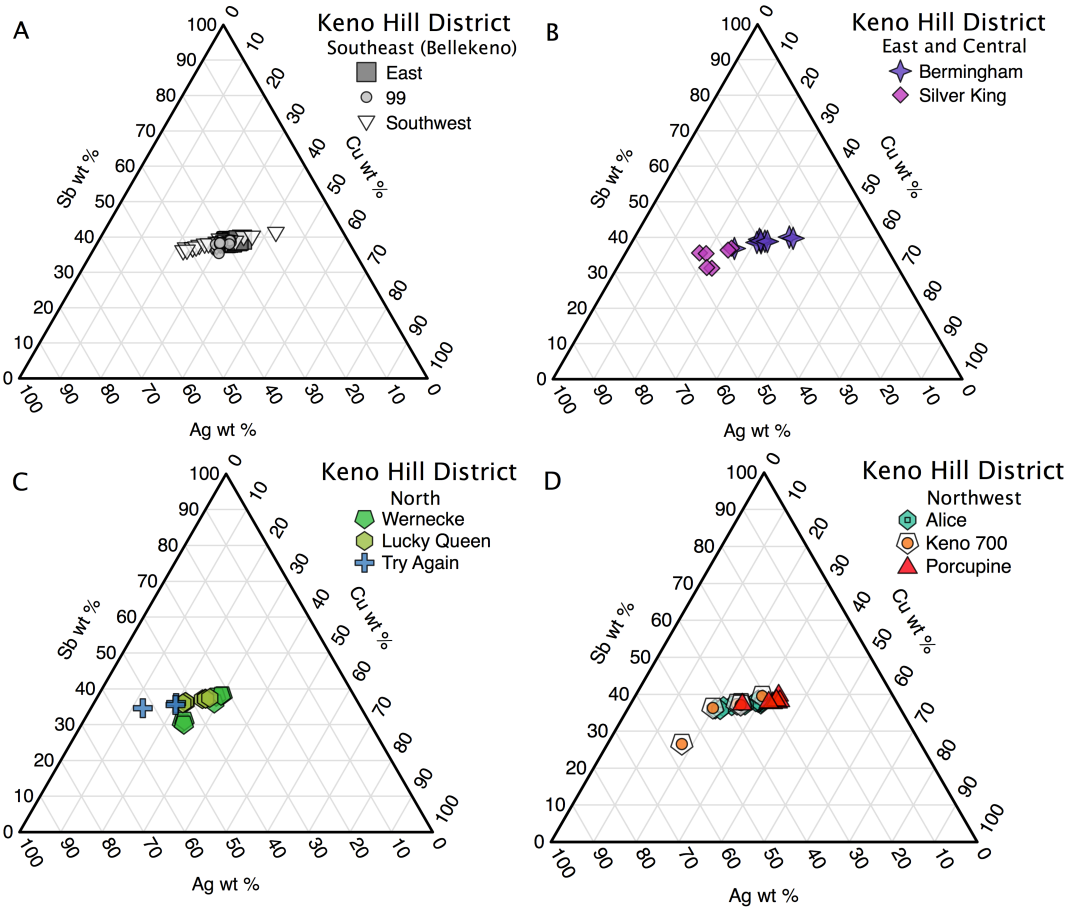

Figure 4-7. Sb-Cu-Ag ternary diagram from the Keno Hill district vein tetrahedrite, showing relative wt % Sb- Cu- and Ag-contents, normalized by Sb+Cu+Ag. A) Southwest (all Bellekeno); B) East and Central; C) North; and D) Northwest.

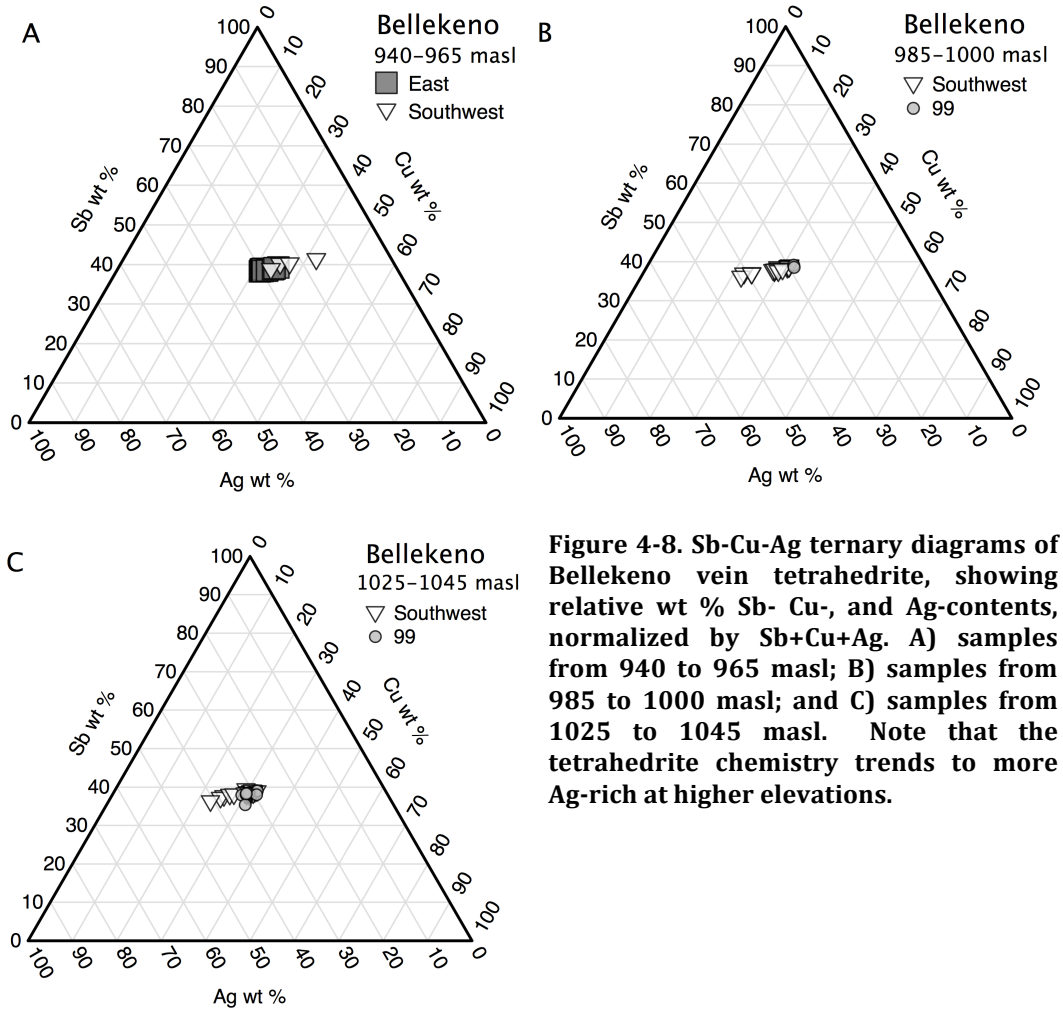

Figure 4-8. Sb-Cu-Ag ternary diagrams of Bellekeno vein tetrahedrite, showing relative wt % Sb- Cu-, and Ag-contents, normalized by Sb+Cu+Ag. A) samples from 940 to 965 masl; B) samples from 985 to 1000 masl; and C) samples from 1025 to 1045 masl. Note that the tetrahedrite chemistry trends to more Ag-rich at higher elevations.

The mineral chemistry of stage 9 siderite is again similar to that of stages 2 and 6. The chemical composition of ankerite (Table 4-1) is highly variable, due to cation exchange between Mg, Mn, and Fe, with less variation in Ca. Magnesium contents vary from 3.80 to 15.78 wt %; Mn contents vary from 1.13 to 13.58 wt %; and Fe contents vary from 4.35 to 14.48 wt %. Calcium is more consistent averaging approximately 31.21 ± 4 wt %. Sphalerite compositions are broadly similar to those of stage 7 in terms of Fe, Cu, Cd, Ag, Sn, and Sb (Table 4-2). Most samples have Ag content <0.28 wt %, with a few anomalously high areas containing >1 wt % Ag. Although only minor constituents, both Sn and Sb are also on average relatively higher than in stage 7, with 0.25 wt % and 0.18 wt %, respectively. There is one anomalously high value of 2.52 wt % Sn, and a few anomalously higher Sb values approximately >1 wt %; all these samples are from the Bellekeno vein. The galena mineral chemistry here is only based on 2 samples analyzed; however it appears to be similar to that of stage 8, with a slight decrease in average Fe, Cu, Sb and Ag concentrations.

Stage 10

Stage 10 is dominated by quartz veins or cemented to clast-encrusted breccias, with variable siderite, ankerite, and calcite (Figure 4-3 M, N). Breccias are generally small (less than few centimeters wide) and clast-supported. Quartz is anhedral to euhedral (<2 mm); individual crystal cores may be clear but outer growth zones are more common cloudy or milky to opaque white. Carbonate textures are similar to those described in stage 9 and likely reflects the transitional nature from stages 9 to 12. No mineral chemistry was analyzed from this stage.

Stage 11

This stage does not appear to be common and was only recognized in two samples as small veins and breccias cemented by siderite, post-dating but partly intergrown with stage 10 quartz. Siderite textures are similar to type I (see stage 2). No mineral chemistry was analyzed from this stage.

Stage 12

The last stage of hydrothermal mineralization is dominated by calcite-cemented veins and breccias, and/or infilling vugs in earlier stages (Figure 4-3 O, P; Figure 4-3 O, P). Calcite is anhedral to euhedral variably clear to cloudy in appearance, with a grain size <1 mm. Minor siderite, ankerite, and quartz occur as thin rims and may be paragenetically early during this stage, or may represent brief and sequential transitions from stages 9, 10, and 11.

The calcite mineral chemistry (Table 4-1) is consistent on a district wide scale, with only minor variations of cation exchange between Ca and Mn or Fe. The Ca content averages approximately 52.74 ± 4 wt %; with Mn and Fe ranging from below the detection limit up to 4.40 wt % and 0.56 to 2.09 wt %, respectively. The Mg content is consistently low, averaging 0.24 wt %.

Other

There is a mineral assemblage of predominantly pyrite, cementing veins and breccias. This pyrite-rich stage was only observed in the Tick (500 meters southeast of Husky) and Leo veins and does not correlate to any of the 12 stages discussed above. Limited observations of this mineral assemblage precluded the relative temporal relationship; however, it is inferred to be paragenetically late (possibly post-dating stage 12).

4.2 Alteration: X-Ray Diffraction

Any potentially unique alteration minerals, if present, may be used as an effective method for future exploration to locate the specific mineral assemblages. Most of the lithologic units hosting the Keno Hill vein mineralization are relatively unaltered (i.e. Keno Hill quartzite), although minor silicification or re-crystallization of quartz was observed. Boyle (1965) documented minor sericite/muscovite within the sedimentary units; whereas the mafic dikes/sills may be highly altered by carbonate, sericite, leucoxene, and quartz, which may extend outward for generally <1 meter into the adjacent host-rock. Late stage oxidation is common within all lithology units around veins.

Bulk X-ray diffraction (XRD) analyses were used to identify alteration minerals present within the wall-rock associated with different hydrothermal vein assemblages. A summary of samples and detected minerals are listed in Table 4-3 below; the complete set of XRD data plots are in Appendix V. Most of the XRD analyses of the wall-rock identified minerals that are part of the adjacent hydrothermal vein assemblages as expected. In terms of alteration minerals, this study only identified variations in the presence and composition of clay minerals.

Muscovite was commonly observed within and associated with most vein assemblages, some of which may be of hydrothermal origin based on textural evidence, such as vug filling pockets within vein stages. However some muscovite may have also form by recrystallizing the phyllosilicate grains that constitute the phyllitic and schistose host rock units. Muscovite-2M1 [$KAl_2(Si_3Al)O_{10}(OH,F)_2$] was found in most samples and associated with most stages throughout the hydrothermal paragenesis. Muscovite polytypes 2M2, and 3T with more variable mineral chemistry [$(K,Na)(Al,Mg,Fe)_2(Si,Al)_4O_{10}(OH)_2$], as well as kaolinite [$Al_2(Si_2O_5)(OH)_4$] and illite-2M2 [$(K,H_{30})Al_2(Si(Si_3Al)O_{10}$ $(OH)_2$-XH_2O], are generally associated with later paragenetic stages (i.e. stages 6 to 8). No spatial distribution patterns are apparent in terms of the presence of these different clay minerals, as both are observed throughout the district. Considering that muscovite is likely a major rock-forming mineral in the phyllitic host rock, it is uncertain whether the different muscovite mineral chemistry is due to changes in the hydrothermal fluid or inherited from the country rock.

Only one sample analysed contained sulfate minerals, szomolnokite and rhomboclase, which were associated with an apparent late stage mineral assemblage. One sample contained $CsSbSe_2$ and cerianite, both of which may be of hydrothermal origin, and associated with siderite, muscovite, and quartz. A number of samples contained minerals such as feldspars (i.e. anorthite and albite), and oxides (i.e., rutile), which are likely primary constituents of the sedimentary rock.

A more detailed study of wall-rock alteration would be required to determine the extent to which the hydrothermal fluids affected or penetrated the host rocks, and if such later stage clay minerals can effectively identify the later stages of mineralization most closely associated with Ag-mineralization.

Sample	Vein Location	Stages	Clay Minerals	Other Minerals
SK-003	Silver King	6 to 8 ?	Ms-2M1/3T	Qz
WRN-008	Wernecke	2 or 6 to 8 ?	Ms-2M1	Qz, Gn, Sd, Dol
K06-2: 138.4m	Silver King	6	Kln, Ms-3T	Qz, Rds, Py, Ab
K06-2: 311.5m	Silver King	>12 ?	Ms-2M1	Qz, Py
K06-25: 33.3m	K-Structure	8	Phl, Ms-2M1/3T	Qz
K07-114: 196m	Lucky Queen	2 or 6 to 8, 12 ?	*None*	Qz, Sd, Cal
K07-114: 197m	Lucky Queen	6 to 8	Ms-3T	Qz, Sd
K07-122: 152.6m	Onek	2 to 3	Ms-2M1	Qz, Sd, Py, An
K07-60: 120.1m	Tick (Husky)	>12 ?	Hal	Py, Qz
K07-60: 121.8m	Tick (Husky)	2 or 6 ?	*None*	Qz, Sd, Py
K07-67: 168.2m	Bellekeno-E	2 or 6 ?	Kln, Ilt-2M2	Qz, Sd, Py, Kut
K07-70: 160m	Bellekeno-E	6 to 8 ?	Ms-2M1	Qz, Py, Sd, Gn
K07-76: 115.3m	Bellekeno-E	1, 8 ?	Ms-3T, Kln	Qz, Gn, Sd
K07-88: 63m	Bermingham	2 to 8	Ms-2M1, Kln	Qz, Sd, Py
K08-131: 36m	Leo	>12 ?	Ilt-2M2	Qz, Py, Rbc, Szm
K08-131: 63.4m	Leo	>12 ?	Ilt-2M2, Ms-2M1	Qz
K08-131: 78.5m	Leo	>12 ?	Kln, Ms-2M1	Py, Qz
K08-131: 99m	Leo	>12 ?	Kln, Ms-2M1/3T	Qz, Rt, Py, Dol
K08-155: 115.9m	Onek	1 to 2	Ms-2M1	Qz, Sd
K08-161: 229.7m	Lucky Queen	6 to 8	Ms-2M1	Qz, Cnt, Gn, Sd
K09-187: 195.1m	Bellekeno-E	2 to 3	*None*	Sd, Sp, Qz
K09-199: 52.9m	Keno 700	6 to 7 or 9 ?	Ms-2M1	Sd, Dol, Sp, Qz
K09-200: 75.2m	Keno 700	1, 6 to 8 ?	Ms-2M1	Qz, Cnt, Sd, $CsSbSe_2$, An
K09-200: 88.4m	Keno 700	1, 6, 12	Ms-2M1/3T	Qz, Sd, Py, Cal, Kut
BKUD09-140: 10.4m	Bellekeno-SW	2	Ms-2M1	Qz, Sd
BKUD09-144: 38.5m	Bellekeno-SW	1, 2 or 6, 8, 12	Ms-3T (?)	Qz, Sd, Apy
BKUD09-146: 46.5m	Bellekeno-SW	4a	Ms-3T (?)	Qz, Sd, Apy, Py
BKUD09-150: 60.4m	Bellekeno-SW	2	Ms-2M1	Qz, Py
BKUD09-157: 98.4m	Bellekeno-SW	2 or 6, 12	Ms-2M1/3T	Qz, Sd
BKUD09-158: 35.2m	Bellekeno-SW	1, 2 or 6, 12	Ms-2M2	Qz, Sd, Py
BKUD09-160: 56.5m	Bellekeno-SW	7 to 9, 12	Ms-2M1, Kln	Qz, Py, Rt
BKUD09-161: 20.4m	Bellekeno-SW	1 to 2	Ms-2M1	Qz, Py, Cal, Sd
BKUD09-166: 18.9m	Bellekeno-SW	5 or 6 to 8, 12	Kln-2M	Gn, Sd, Py, Qz, Cal, Kut
BKUD09-173: 31.2m	Bellekeno-99	2 to 3 or 6 to 7 ?	*None*	Qz, Py, Sd
BKUD09-173: 34.4m	Bellekeno-99	2	Ms-2M1	Gn, Sd, Py, Qz, Ab

Table 4-3. Summary of samples analysed by XRD with detected minerals. Notations: mineral abbreviations are summarized in Appendix I. The K-structure vein is located approximately 1 km southeast of the Lucky Queen vein. The Tick vein is located 500 m southeast of the Husky vein.

4.3 Microthermometry

Fluid inclusions were examined to constrain the temperatures and chemistry of fluids throughout the hydrothermal paragenesis. Microthermometric data from this study are primarily from the Bellekeno vein from stages 1, 2, 3, 6, 7, 8, 9, and 12. No data were determined for stages 3 and 4a sphalerite due to its opacity. Stage 10 quartz and stage 11 siderite were not examined based on their relatively spatially restricted extent and cloudy nature. Siderite from stage 5 was also not analysed.

Fluid inclusions were classified as either primary (P) pseudo-secondary (PS), or secondary (S) according criteria established by Roedder (1984). Microthermometric measurements of individual fluid inclusion assemblages (FIA) include liquid-vapour homogenization to liquid ($Th_{(L-V)L}$) and liquid-vapour homogenization to vapour ($Th_{(L-V)V}$), CO_2 homogenization (Th_{CO2}), CO_2 melting (Tm_{CO2}), first ice melting (Te), final ice melting (Tm_{ICE}), and final clathrate melting (Tm_{Cl}). Many Te values were observed to be <21.2°C, an indication that the aqueous salt composition is more complex than just H_2O-NaCl (Shepherd et al., 1985). As these Te measurements were not well constrained in this study due to the small size of the inclusions, fluid salinities are reported in NaCl equivalent weight percent (wt % NaCl equiv.), calculated from Tm and Tm_{Cl} values using the equations from Bodnar (1993) and Diamond (1992), respectively. Where both Tm and Tm_{Cl} were both determined from a single fluid inclusion, Tm_{Cl} was given preference and used to calculate the final reported salinity, as the presence of clathrate indicates that salinity calculated from Tm_{ICE} will be higher than true salinity (Diamond, 1994). Pressure corrections were determined from two independent geothermometers, which confirm an approximately similar or hotter (i.e. up to +55°C hotter) temperature of mineralization compared to the Th measurements of this study, see section 5.2 Depth of Mineralization for further discussion.

Fluid inclusion assemblages (FIA) are defined by fluid inclusions that occur within a single growth zone, with internally consistent liquid to vapour ratios, ranges of Th, and similar fluid compositions for various fluid inclusion sizes and shapes (Goldstein and Reynolds, 1994). The Keno Hill vein mineralization is typically massive in nature and growth zone textures within individual crystals rare (generally limited to stages 7 and 9) as such, in the absence of growth zones, clusters of fluid inclusions were used to characterize FIA. Fluid inclusion data from this study are grouped according to their respective minerals, stages, and veins as summarized in Table 4-4. A complete table of all results (288 fluid inclusions analyzed) can be found in Appendix IV. A histogram of all fluid inclusions Th data is graphically presented in Figure 4-9. The fluid inclusion results discussed below are from the Bellekeno vein, unless otherwise noted.

The focus of this study was on the paragenetic stages most closely associated with the Ag-Pb-Zn mineralization (i.e. stages 2 to 9). The majority of inclusions analysed within siderite, sphalerite and quartz are <5 to 30 μm in size, irregular to negative crystal shaped, and are aqueous containing two-phases, liquid H_2O with a vapour bubble varying from 15 to 30 % by volume, and classified as pseudo-secondary, or tentatively primary. Phase changes were difficult to observe in many inclusions due to their small size, the cloudy nature of the crystals, and the double refraction in carbonate minerals. All fluid inclusions from stage 2 or higher/later are either two-

phase aqueous or aqueous-carbonic, with homogenization by vapour bubble shrinking during heating experiments. Post-mineralization deformation is common throughout the veins, as such careful was given to examine samples or areas within samples that exhibit little later stage deformation effects, and fluid inclusions determined to be secondary in origin were generally avoided. Fluid inclusion data from the Bellekeno vein, and a composite of other Keno Hill district veins are plotted as Th vs. salinity in Figure 4-10 and Figure 4-11, respectively.

Vein	Stage	n	Th (^{o}C) *		Tm (^{o}C)		Tm_{Cl} (^{o}C)	
Mineral			range	mean	range	mean	range	mean
Bellekeno								
Siderite	2	20	249 to 293	270	-10.0 to -5.0	-8.6	3.5	3.5
Quartz	2 to 3	8	265 to 298	280	-10.0 to -8.0	-9.0	4.8 to 50	4.9
Siderite	6	76	214 to 282	254	-16.5 to -6.0	-10.5	-5.0 to 3.0	-1.7
Sphalerite	7	48	210.to 261	233	-16.0 to -6.0	-10.5	2.5 to 5.0	3.7
Quartz	8	19	200 to 263	228	-2.3 to -1.6	-2.0	N.D.	N.D.
Siderite	9	20	190 to 276	238	-8.0 to -1.4	-5.4	N.D.	N.D.
Sphalerite	9	11	145 to 196	169	-5.0 to -1.7	-3.7	N.D.	N.D.
Calcite	12	7	164 to 186	174	-3.9 to -3.0	-3.6	N.D.	N.D.
Homestake								
Quartz *	1	16	282 to 304 *	293 *	-6.0 to -3.2	-4.6	7.9 to 10.2	10.0
Keno 700								
Quartz	1	12	244 to 274	257	-10.0 to -6.3	-8.2	N.D.	N.D.
Siderite	6	6	254 to 261	259	-10.5	-10.5	-4.8 to -2.5	-3.7
Silver King								
Siderite	6	7	274 to 282	277	-10.0	-10.0	-2.5 to -1.0	-1.8
Alice								
Siderite	6	6	232 to 248	241	-10.0 to -9.0	-9.5	N.D.	N.D.
Sphalerite	7	8	239 to 248	246	-5.5 to -4.0	-4.9	N.D.	N.D.
Pool								
Sphalerite	9	8	170 to 206	197	-1.2 to 0.0	-0.7	N.D.	N.D.

Table 4-4. Summary of microthermometric data for quartz, siderite, sphalerite and calcite from the Keno Hill district veins. Notations: number of samples analysed (n), homogenization temperature (Th), all samples homogenized to liquid-phase ($Th_{(L-V)L}$) except for samples with * which homogenized to vapour-phase ($Th_{(L-V)V}$), final ice melting temperature (Tm), final clathrate melting temperature (Tm_{Cl}), no data (N.D.) for Tm_{Cl} signifies that no clathrate was observed. The Homestake vein stage 1 quartz is the only sample with fluid inclusions that exhibit final CO_2 melting temperatures (Tm_{CO2}), summarized in text above.

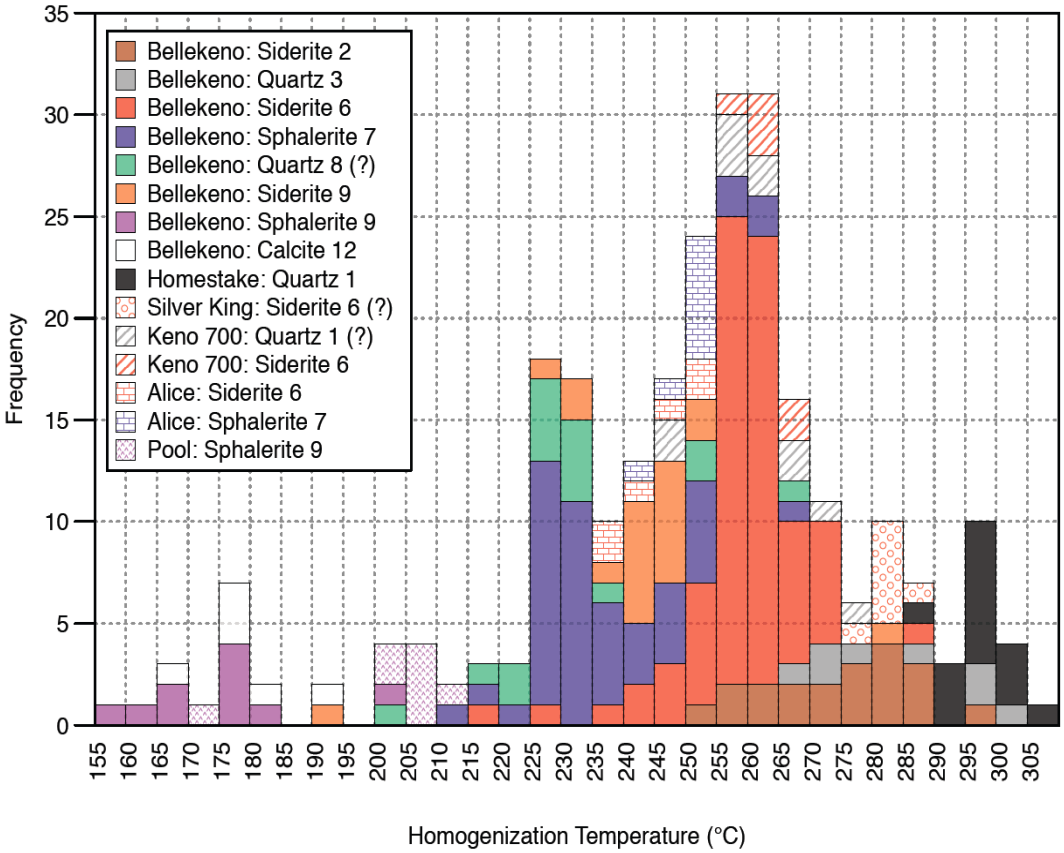

Figure 4-9. Histogram of all Keno Hill district vein fluid inclusion homogenization temperatures (°C), from this study. In the legend, numbers to the right of the minerals indicate respective paragenetic stages. With the exception of the Homestake, stage 1 quartz, which homogenized to vapour, all remaining fluid inclusions homogenized to liquid.

Stage 1: Quartz

Two samples of stage 1 quartz were analysed. One sample from the Homestake vein contained a CO_2-rich fluid inclusion assemblage comprised of liquid H_2O, liquid CO_2, and vapour CO_2 (Figure 4-12 A). All Tm_{CO2} occurred between -56.8 and -57.0°C. Liquid and vapour CO_2 homogenized (Th_{CO2}) between 24.0 and 25.9°C. From the Tm_{CO2} and Th_{CO2} measurements, the presence of <0.05 molar CH_4 may be inferred (Shepherd et al., 1985). Homogenization occurred by CO_2 vapour bubble expansion ($Th_{(L-V)V}$) with an average of 293°C (n=16, 1σ = ±5.3°C). No liquid phase fluid inclusions were observed in this sample. Salinity varied considerably from 0 to 9.2 wt % NaCl equiv. The presence of CH_4 and/or N_2 is indicated by some of the Tm_{Cl} values which are slightly greater than +10°C, and the slightly depressed melting point of solid CO_2 (Shepherd et al., 1985).

A stage 1 quartz sample from the Keno 700 vein contained two-phase aqueous inclusions with an average ($Th_{(L-V)L}$) of 257°C (n=11, 1σ = ±9.3°C), and a salinity of

11.8 wt % NaCl equiv. (n=11, 1σ = ±1.3 wt % NaCl equiv.). These fluid inclusions are interpreted to be either pseudo-secondary or secondary, and some exhibited stretching or necking textures (Figure 4-12 B). This fluid composition is more reminiscent of stages 2 or 6 (see below), and considering that this sample has been cross-cut by siderite cemented veins/breccias of these stages, it is likely that fluids associated with these later stages were trapped in this stage 1 quartz.

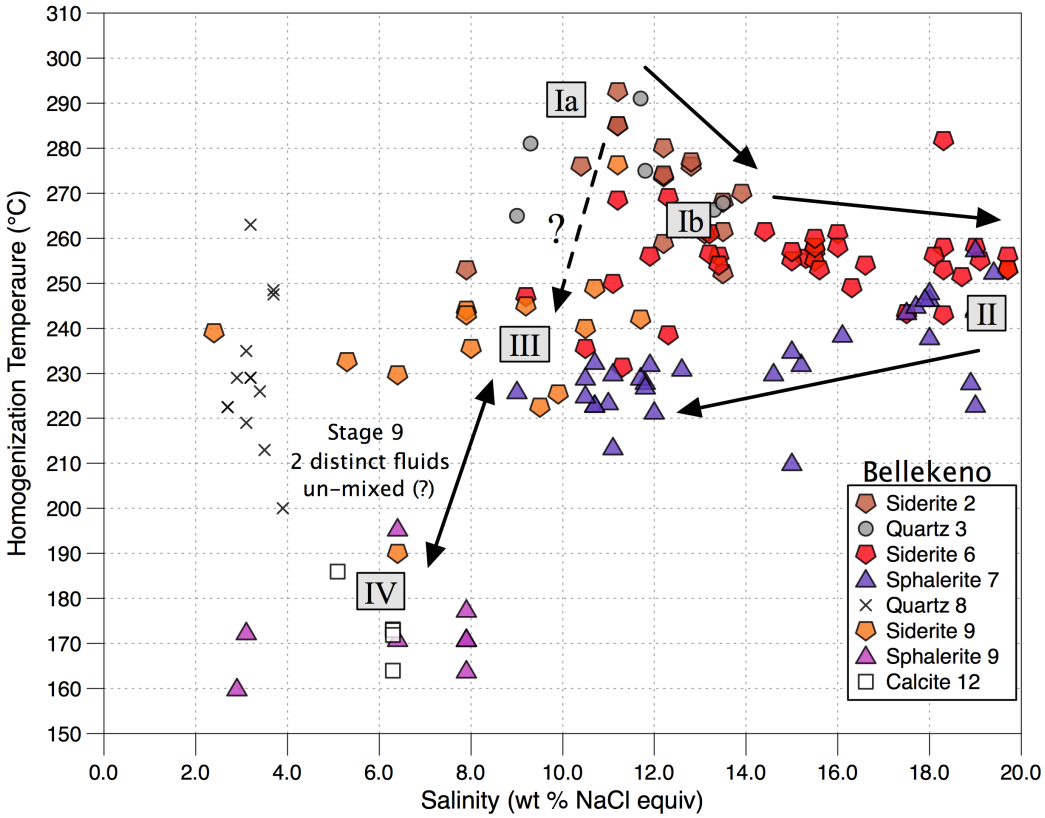

Figure 4-10. Bellekeno vein fluid inclusion plot of homogenization temperatures (°C) vs. salinity (wt % NaCl equiv.) from this study. All samples are aqueous, H_2O-rich, with homogenization to liquid phase.

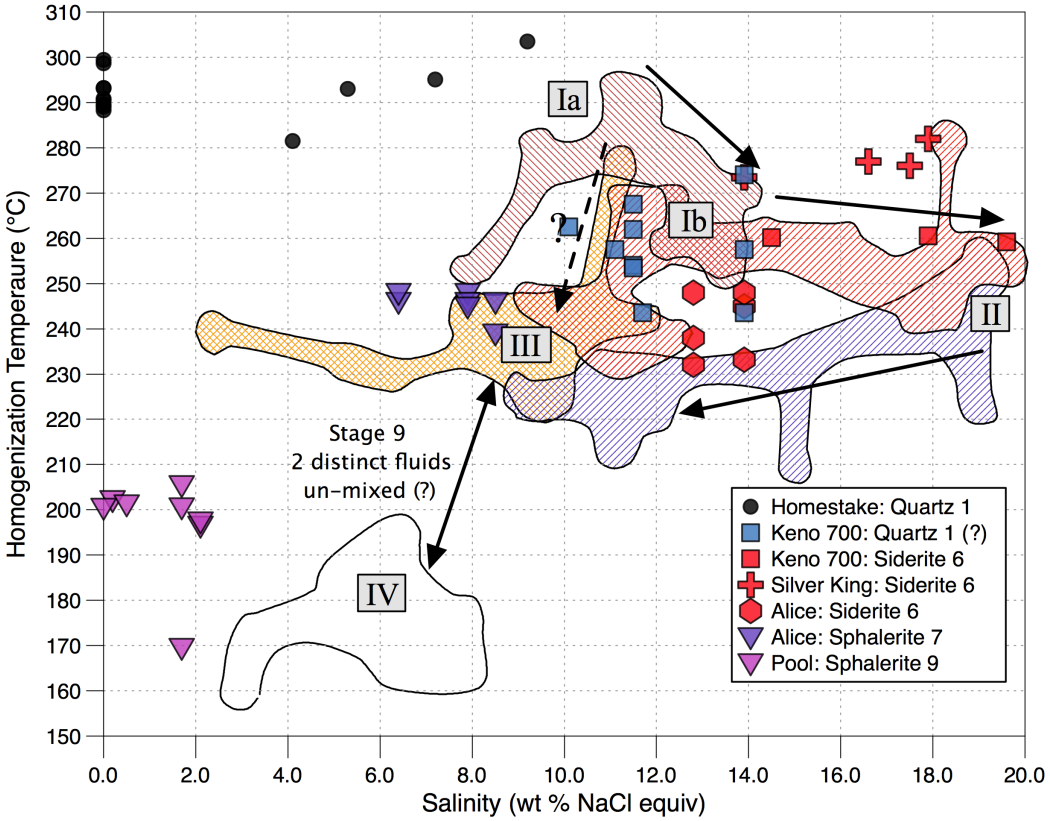

Figure 4-11. Comparison of Keno Hill district veins with Bellekeno vein fluid inclusion plot, homogenization temperature (°C) vs. salinity (wt % NaCl). The Bellekeno vein sample Th and salinity ranges are outlined and hatched in same colour from Figure 4-9 (i.e. Stages: 2 = brown, 6 = red, 7 = purple, 9 (siderite) = orange, and 9 (sphalerite)/12 = grey. All Homestake vein stage 1 quartz samples are CO_2-rich and homogenized to a vapour phase; all remaining fluid inclusion samples are aqueous, H_2O-rich fluid inclusion with homogenization to liquid phase. Stage 1 quartz from the Keno 700 vein fluid inclusions are secondary. Note the different ranges of Th and salinity for some of the other Keno Hill district veins compared to equivalent stages in the Bellekeno vein. As each mineral and stage is interpreted to represent a unique FIA, the fluid mixing model is further supported the range of salinity values particularly for Keno 700 vein, stage 6 siderite, and Alice vein, stage 7 sphalerite.

Stage 2: Siderite

Primary aqueous fluid inclusions in siderite define an approximately linear trend from a ($Th_{(L-V)L}$) and salinity of up to 292°C and 11 wt % NaCl equiv., to 260°C and 14 wt % NaCl equiv. (Figure 4-12 C). Clathrates were identified in some fluid inclusions from one sample (Appendix IV). The higher Th with lower salinity is defined as end-member Ia, and the lower Th with higher salinity is defined as end-member Ib.

Stage 2-3: Quartz

Aqueous fluid inclusions in one sample of quartz partly intergrown with stage 2 siderite, and stage 3 sphalerite, have an average ($Th_{(L-V)L}$) of 280°C (n=8, 1σ = ±13.1°C) and salinity of 12.8 wt % NaCl equiv. (n=6, 1σ = ±1.9 wt % NaCl equiv.) (Figure 4-12 D). Clathrates were identified in this sample. Most of these fluid

inclusion data occur within the range of stage 2 siderite, which supports a transition or continuation of mineralization between stages 2 and 3, as suggested by textural observations.

Stage 6: Siderite

Aqueous fluid inclusions in stage 6 siderite predominantly have a ($Th_{(L-V)L}$) of between 250 and 260°C, and define a range salinity from approximately 13.0 to 19.7 wt % NaCl equiv. (Figure 4-12 E). Clathrates were identified in most of these samples (Appendix IV). The lower salinity range is generally coincident with that of the stage 2 siderite end-member Ib. The higher salinity values are defined as end-member II.

Three stage 6 siderite samples from three different veins in the district were analysed to compare with the Bellekeno data. The FIA from the Keno 700 vein have a range of ($Th_{(L-V)L}$) and salinity that falls within that defined by the Bellekeno stage 6 siderite trend. The fluid inclusions from the Silver King vein sample have a range of salinity that is consistent with that of the Bellekeno stage 6 siderite trend; however the range of ($Th_{(L-V)L}$) from 273 to 282°C is slightly higher than that of the Bellekeno trend, with the exception of one Bellekeno fluid inclusion which has a ($Th_{(L-V)L}$) of 282°C. Conversely, fluid inclusions from the Alice vein, have a consistent salinity with an average of 13.4 wt % NaCl equiv. (n=6, 1σ = ±0.6 wt % NaCl equiv.), but have a range in ($Th_{(L-V)L}$) from 232 to 248°C. The salinities of the Alice fluid inclusion samples are similar to that of the Bellekeno end-member Ib; however the range in Th is generally lower than that of Bellekeno trend (Figure 4-10).

Stage 7: Sphalerite

Aqueous fluid inclusions in stage 7 sphalerite define a linear trend, from a ($Th_{(L-V)L}$) and salinity of approximately 250°C and 19 wt % NaCl to 220°C and 10 wt % NaCl equiv., respectively (Figure 4-12 F). Clathrates were identified in most of these samples. The higher $Th_{(L-V)L}$ and salinity is generally coincident with that of the Bellekeno stage 6 siderite end-member II. The lower $Th_{(L-V)L}$ and salinity is defined as end-member III.

The same Alice vein sample, which contained the stage 6 siderite described above, also contained stage 7 sphalerite. The aqueous fluid inclusions in the Alice stage 7 sphalerite have an average $Th_{(L-V)L}$ of 246°C (n=8, 1σ = ±3.0°C), and salinity of 7.7 wt % NaCl equiv. (n=7, 1σ = ±0.9 wt % NaCl equiv.). There is a distinct shift of the stage 7 sphalerite Alice fluid inclusions to a slightly higher $Th_{(L-V)L}$ and lower salinity compared to that of end-member III, defined by Bellekeno stage 7 sphalerite.

Stage 8: Quartz

All aqueous fluid inclusions within this single stage 8 quartz sample were determined to be of secondary origin; these inclusions occur in a tabular cluster and appear to define healed fracture planes. The salinity was approximately consistent with an average of 3.3 wt % NaCl equiv. (n=16, 1σ = ±0.3 wt % NaCl equiv.), but the FIA have a range of $Th_{(L-V)L}$ from 200 to 263°C.

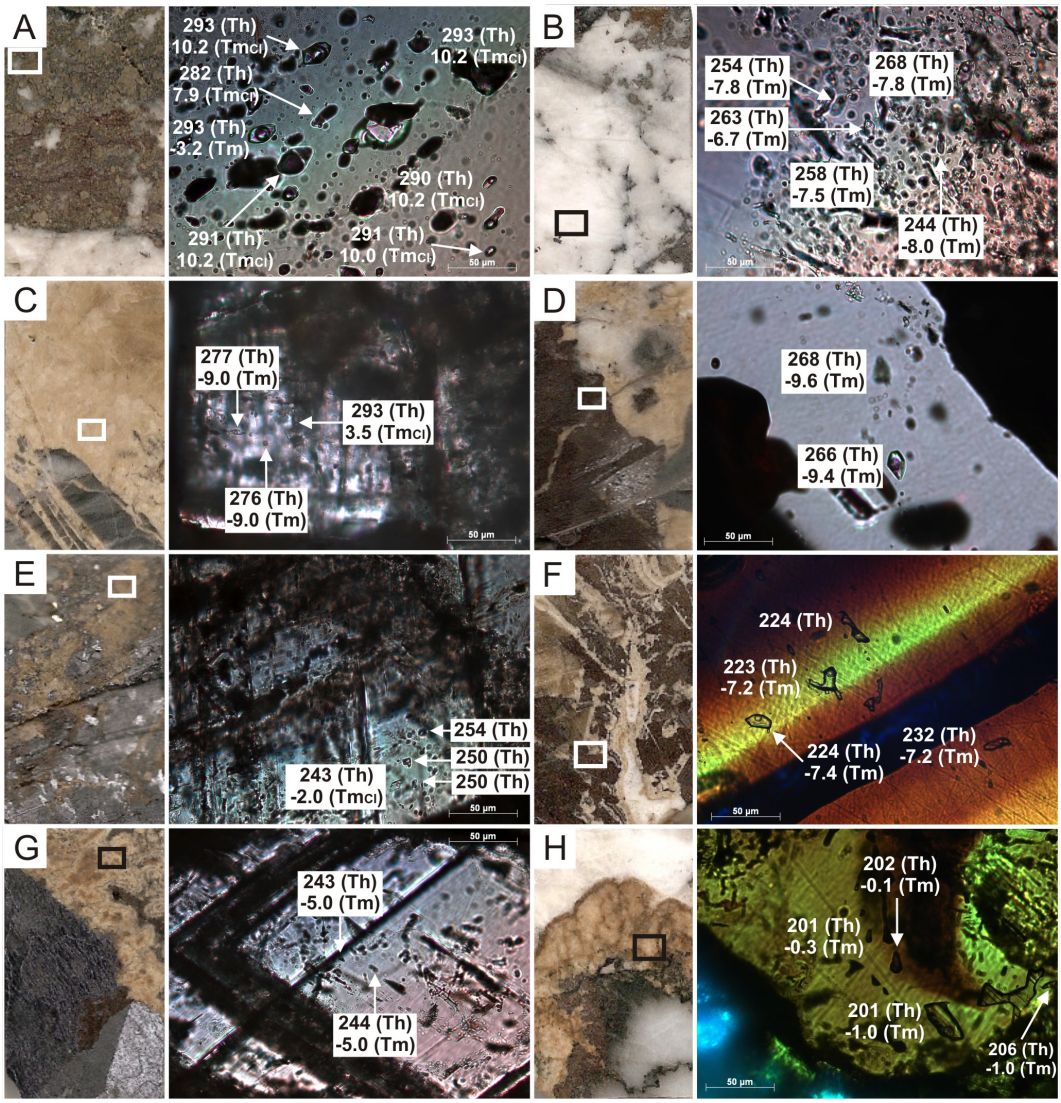

Figure 4-12. Sample off-cuts (each approximately 20 mm by 35 mm) at left, with photomicrographs from transmitting light microscope at right showing select fluid inclusions and their respective Th, Tm, and Tm_{Cl} measurements. Detailed photomicrograph areas shown are indicated by white or black squares on the off-cuts. Data are immediately to the left of the fluid inclusions they represent unless arrows indicate otherwise. A) HOM-053: surface, stage 1 quartz with 3-phase CO_2-rich fluid inclusions, and homogenize to a vapour-phase. B) K08-165: 176.5m, stage 1 quartz. All fluid inclusions analysed are aqueous 2-phase, the cluster of fluid inclusions are collectively interpreted as secondary. C) BKUD09-163: 31.8m, stage 2 siderite with 2-phase aqueous fluid inclusions, clathrate observed in 3 of the 5 inclusions analysed from this sample. D) BKUD09-161: 20m, quartz growth during a transition between stages 2 siderite and stage 3 sphalerite, with 2-phase aqueous fluid inclusions, clathrate observed in 2 of 6 inclusions analysed. E) BKUD09-171: 32.8m, stage 6 siderite with 2-phase aqueous fluid inclusions, clathrate observed in 2 of 14 inclusions from this sample. F) BKUD09-158: 36.5m, stage 7 sphalerite with 2-phase aqueous fluid inclusions, clathrate observed in 4 of 6 inclusions analysed. G) BKUD09-143: 52.8m, stage 9 siderite with 2-phase aqueous fluid inclusions. H) K07-87: 106.7m, stage 9 sphalerite with 2-phase aqueous fluid inclusions.

Stage 9: Siderite and Sphalerite

The aqueous FIA of stage 9 siderite and sphalerite contain different ranges in $Th_{(L-V)L}$ and salinity. The $Th_{(L-V)L}$ and salinity of stage 9 siderite fluid inclusions range from 190 to 276°C and 2.4 to 11.7 wt % NaCl equiv., respectively (Figure 4-12 G, H). The stage 9 sphalerite fluid inclusions have a range of $Th_{(L-V)L}$ and salinity of 145 to 195°C and 2.9 to 7.9 wt % NaCl, respectively. Although there is some scatter of the $Th_{(L-V)L}$ and salinity from the stage 9 siderite fluid inclusions, this range is approximately consistent with the end-member III defined by stage 7 sphalerite. There appears to be a shift to slightly lower fluid salinity and higher Th associated with stage 9 siderite.

One stage 9 sphalerite sample from the Pool vein, has aqueous fluid inclusions with an average $Th_{(L-V)L}$ of 197°C (n=8, 1σ = ±11.3°C), and salinity of 1.3 wt % NaCl equiv. (n=8, 1σ = ±0.9 wt % NaCl equiv.). There is a distinct relative shift to a lower salinity and higher $Th_{(L-V)L}$ of the stage 9 sphalerite Pool fluid inclusions compared to that of the Bellekeno end-member IV.

Stage 12: Calcite

Aqueous fluid inclusions from one calcite sample have a range of $Th_{(L-V)L}$ from 164 to 189°C, and salinity from 5.0 to 6.3 wt % NaCl equiv. This cluster falls within the range of end-member IV.

4.4 Carbon and Oxygen Isotopes

Carbon and oxygen isotopic data from the Keno Hill district are summarized in Table 4-5 and graphically presented in Figure 4-13, including data from Lynch et al. (1990).

The 2 limestone samples have $\delta^{13}C$ and $\delta^{18}O$ values that range from +0.7 to +5.7 ‰, and from +19.6 to +22.2 ‰, respectively.

All siderite isotopic compositions cluster within a range of $\delta^{13}C$ and $\delta^{18}O$ values from -8.4 to -11.9 ‰, and +14.8 to +18.9 ‰, respectively, with an average $\delta^{13}C$ value of -10.8 ‰ (n=34, 1σ= ±0.7), and $\delta^{18}O$ value of +16.6 ‰ (n=34, 1σ= ±0.7). The Bellekeno and Onek samples define a tight cluster of $\delta^{13}C$ and $\delta^{18}O$ values averaging -11.0 ‰ (n=28, 1σ= ±0.4) and +16.4 ‰ (n=28, 1σ= ±0.2), respectively. The C and O isotopic compositions of both stages 2 and 6 are indistinguishable from each other. The larger variability of the $\delta^{18}O$ and $\delta^{13}C$ values are associated with samples from other vein deposits in the district; where a spatial pattern is apparent; additional data from Lynch et al. (1990) further support this observation (Figure 4-14 and Figure 4-15). The more northerly vein mineralization is typically associated with relatively higher siderite $\delta^{13}C$ values, where as the more easterly deposits have higher siderite $\delta^{18}O$ values. Lynch et al. (1990) documented a similar east to west decrease in $\delta^{18}O$ values from siderite throughout the district, see section 5.4 Keno Hill District Spatial Zonation for further discussion.

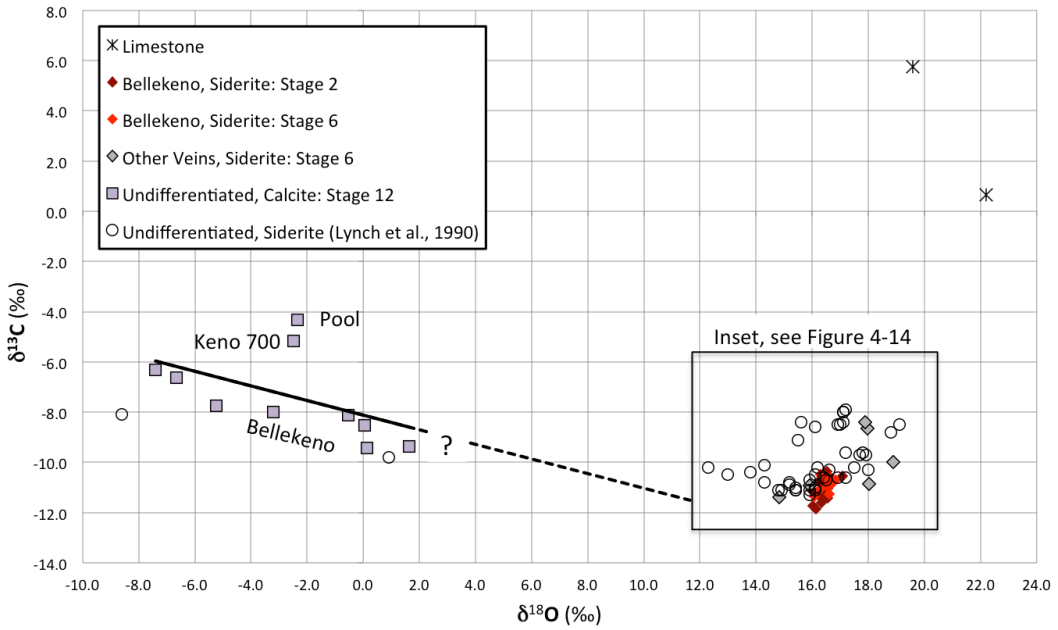

Figure 4-13. Keno Hill district carbon and oxygen isotopic compositions (‰) from limestone, and vein siderite and calcite; including data from Lynch et al. (1990). $\delta^{13}C$ and $\delta^{18}O$ are reported in reference to PDB and SMOW, respectively. The Pool vein is located approximately 500 m southeast of Husky vein.

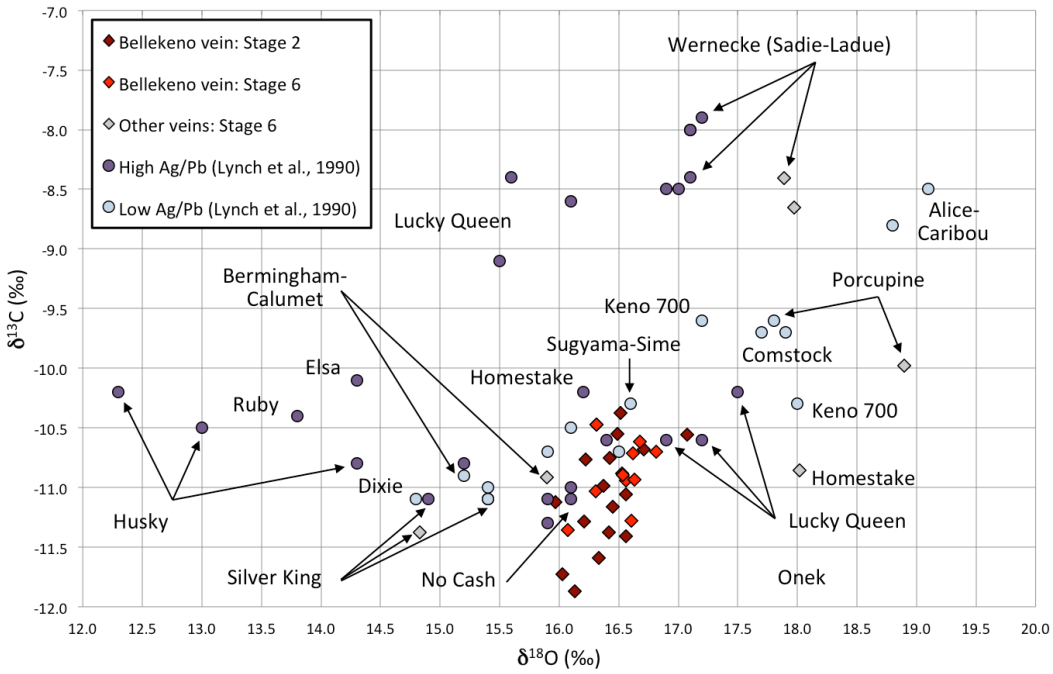

Figure 4-14. Detail from Figure 4-13. Keno Hill district carbon and oxygen isotopic compositions (‰) from vein siderite, including data from Lynch et al. (1990). $\delta^{13}C$ and $\delta^{18}O$ are reported in reference to PDB and SMOW, respectively. Each vein generally has a distinct range of isotopic compositions.

Calcite samples from the Bellekeno vein define a linear trend, one end-member has $\delta^{13}C$ and $\delta^{18}O$ values of -6.3 ‰ and -7.4 ‰, respectively; the other end-member has $\delta^{13}C$ and $\delta^{18}O$ values of -9.4 ‰ and $\delta^{18}O$ of +0.1 ‰, respectively. Two calcite samples, which plot as outliers from the Bellekeno data trend, with relatively higher $\delta^{13}C$ values (approximately +2 ‰) are from other veins (i.e. Pool, and Keno 700) in the Keno Hill district.

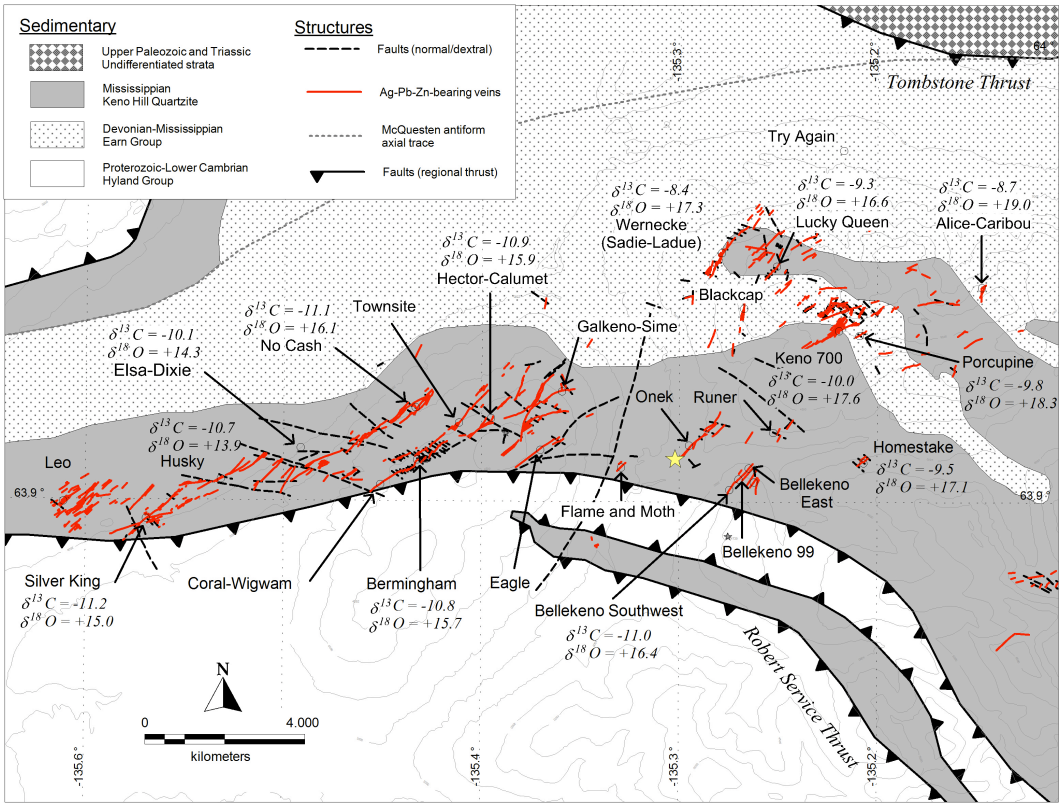

Figure 4-15. Keno Hill district plan of vein siderite samples, with average carbon and oxygen isotopic compositions (‰), including data from Lynch et al. (1990). $\delta^{13}C$ and $\delta^{18}O$ are reported in reference to PDB and SMOW, respectively. Sample locations are approximate. Trends in the isotopic compositions are apparent: more positive $\delta^{13}C$ values to the north, and more negative $\delta^{18}O$ values to the west.

Sample	Vein Location	$\delta^{13}C$ (‰)	$\delta^{18}O$ (‰)
Limestone			
KH-SDH-65: surface	Sourdough Hill	5.8	19.6
KH-SDH-66: surface	Sourdough Hill	0.7	22.2
Stage 2: Siderite			
BKUD09-153: 87.5 m	Bellekeno-SW	-11.3	16.2
BKUD09-134: 45 m	Bellekeno-SW	-11.4	16.6
BKUD09-163: 17 m	Bellekeno-SW	-10.5	16.3
BKUD09-140: 9.9 m	Bellekeno-SW	-11.9	16.1
BKUD09-157: 100.3 m	Bellekeno-SW	-11.2	16.5
K07-66: 146 m	Bellekeno-E	-10.7	16.7
K07-79: 61 m	Bellekeno-E	-10.6	17.1
K07-95: 401 m	Bellekeno-E	-11.1	16.0
K09-197: 193 m	Bellekeno-E	-10.8	16.2
BK-140: 8.8 m	Bellekeno-SW	-11.7	16.0
BK-143: 18 m	Bellekeno-SW	-11.4	16.4
BK-143: 50.5 m	Bellekeno-SW	-10.6	16.5
BK-144: 36.4 m	Bellekeno-SW	-11.1	16.6
BK-157: 100.3 m	Bellekeno-SW	-10.9	16.5
BK-160: 52.1 m	Bellekeno-SW	-10.7	16.4
BK-166: 20.8 m	Bellekeno-SW	-11.6	16.3
K07-122: 163.8 m	Onek	-10.4	16.5
K08-155: 132.5 m	Onek	-11.0	16.4
Stage 6: Siderite			
BKUD09-153: 84 m	Bellekeno-SW	-11.3	16.6
BKUD09-163: 16.95 m	Bellekeno-SW	-11.4	16.1
BK-L750-571: 7 m	Bellekeno-SW	-10.5	16.3
K07-86: 223.2 m	Bellekeno-E	-10.7	16.6
K09-187: 201.2 m	Bellekeno-E	-10.9	16.6
BK-139: 8.3 m	Bellekeno-SW	-10.9	16.6
BK-143: 54 m	Bellekeno-SW	-10.6	16.7
BK-148: 33.5 m	Bellekeno-99	-10.7	16.8
BK-170: 7.6 m	Bellekeno-SW	-11.0	16.3
BK-171: 43.5 m	Bellekeno-99	-10.9	16.5
HOM-051: surface	Homestake	-10.9	18.0
POR-056: surface	Porcupine	-10.0	18.9
WRN-008-1: surface	Wernecke	-8.7	18.0
WRN-008-2: surface	Wernecke	-8.4	17.9
K07-88: 59.6 m	Calumet	-10.9	15.9
K06-2: 167.2 m	Silver King	-11.4	14.8
Stage 12: Calcite			
BKUD09-153: 84 m	Bellekeno-SW	-8.5	0.1
BKUD09-166: 18.6 m	Bellekeno-SW	-8.0	-3.2
BKUD09-165: 48 m	Bellekeno	-9.4	1.6
BKUD09-140: 8.8 m	Bellekeno-SW	-7.8	-5.2
BKUD09-144: 38.5 m	Bellekeno-SW	-6.3	-7.4
BKUD09-153: 63.4 m	Bellekeno-SW	-6.6	-6.7
BKUD09-160: 52.1 m	Bellekeno-SW	-8.1	-0.5
BKUD09-160: 56.5 m	Bellekeno-SW	-9.4	0.1
K09-200: 86.3 m	Keno 700	-5.2	-2.5
K07-87: 106.7 m	Pool (Husky)	-4.3	-2.3

Table 4-5. Summary of carbon and oxygen isotopic compositions (‰) from Keno Hill district carbonates. The Pool vein is approximately 500 m southeast of Husky vein.

4.5 Sulfur Isotopes

Results from this study (Table 4-6), including data from Boyle et al. (1970) are plotted in Figure 4-16. The sulfide $\delta^{34}S$ values from this study range from -11.0 to +7.4 ‰, with an average of 0.2 ‰ (n=70, 1σ = ±1.4). In the Bellekeno vein $\delta^{34}S$ values from pyrite range from -0.3 to +2.4 ‰, with an average of +0.5 ‰ (n=11, 1σ = ±0.7); sphalerite $\delta^{34}S$ values range from +0.1 to +2.9 ‰, with average of +1.1 ‰ (n=22, 1σ = ±0.6); and galena $\delta^{34}S$ values range from -2.0 to -1.2 ‰, with average of -1.6 ‰ (n=18, 1σ = ±0.2).

A spatial trend in $\delta^{34}S$ is apparent throughout the district, and is best represented by galena samples because it was the most thoroughly sampled mineral (Figure 4-17). Sulfur isotope values generally decrease from the southeast (i.e. the Bellekeno area) to the north and west, this trend was also documented by Boyle et al. (1970), and Lynch et al. (1990), see section 5.4 Keno Hill District Spatial Zonation for further discussion.

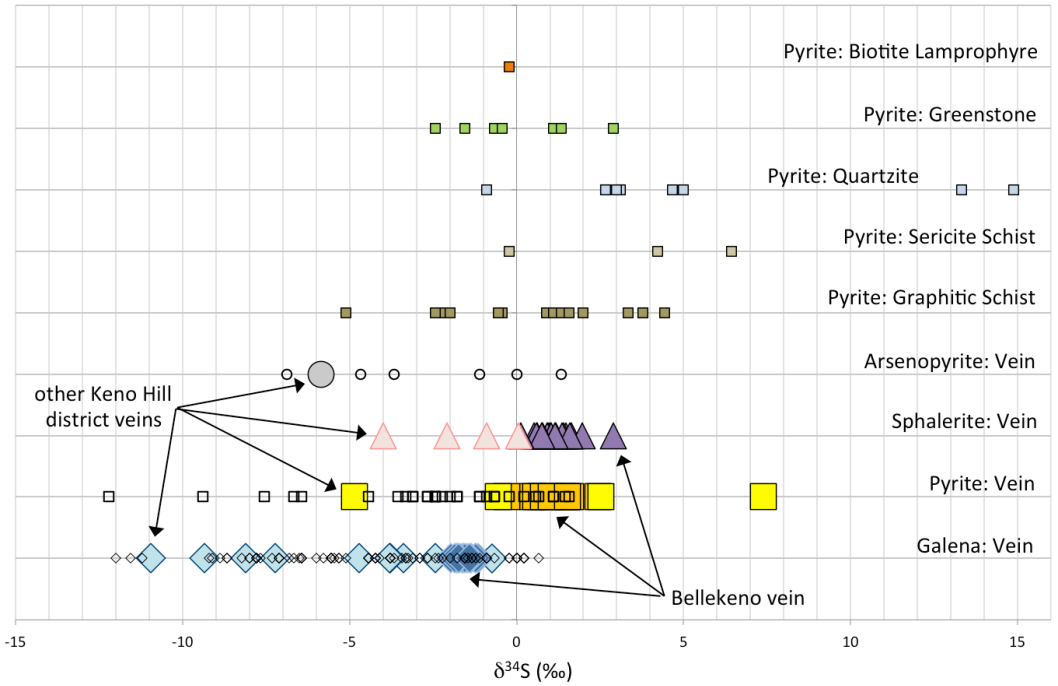

Figure 4-16. Summary of Keno Hill district sulfur isotope data (‰), including results from Boyle et al. (1970) (small symbols), this study (large symbols). $\delta^{34}S$ are reported in reference to CDT. Note that the Bellekeno vein pyrite, sphalerite, and galena define locally restricted ranges of $\delta^{34}S$ values. The other Keno Hill district veins, including undifferentiated vein sulfide data from Boyle et al. (1970), have a wider range of $\delta^{34}S$ values.

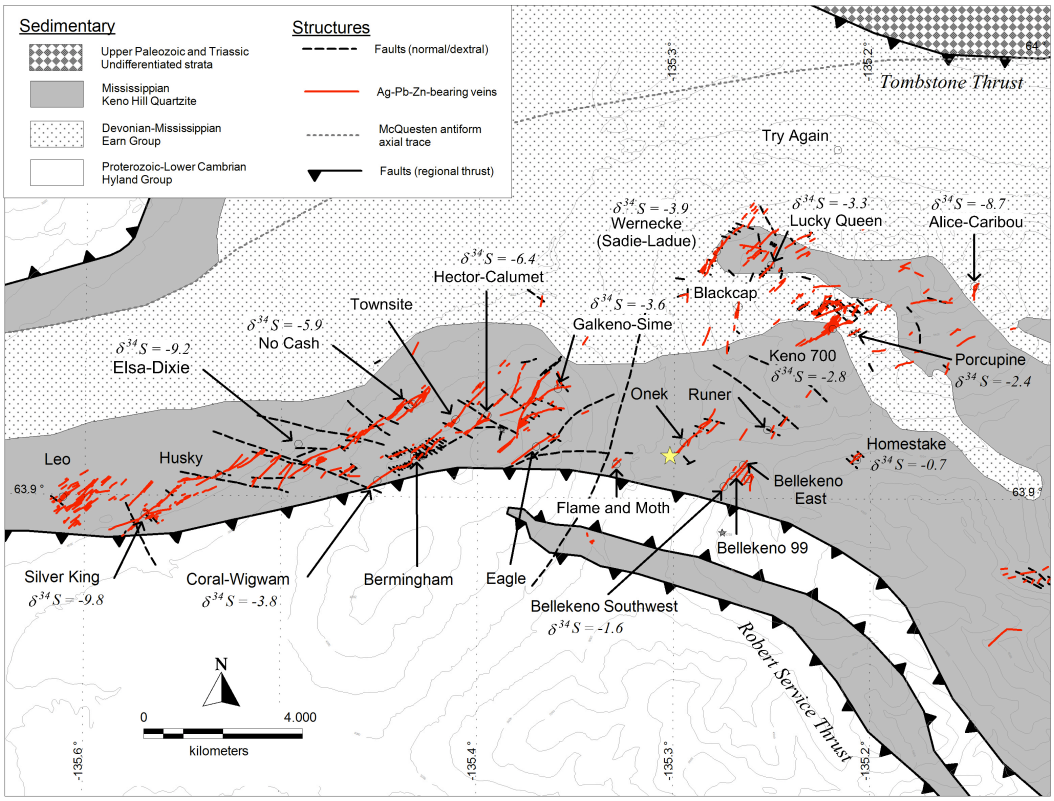

Figure 4-17. Keno Hill district plan of vein galena samples, with average sulfur isotopic compositions (‰), including data from Boyle et al. (1970). $\delta^{34}S$ are reported in reference to CDT. Note that locations are approximate. Trends in the isotopic composition is apparent: $\delta^{34}S$ values decrease to the north and west.

Sulfide geothermometry was calculated for texturally coeval mineral-pairs where available, using the equilibrium isotopic fractionation equations of Ohmoto and Rye (1979) (Figure 4-18). Sphalerite-galena mineral pairs indicate a range of precipitation temperatures between 136 and 361˚C, with an average of 257˚C (n=15, 1σ = 53.4˚C). Although not all sphalerite-galena pairs were closely intergrown, or contemporaneous (i.e. not from paragenetically adjacent stages), Rye and Ohmoto (1974) note that 'geologically reasonable' temperatures may be calculated from sphalerite-galena isotopic fractionation pairs if mineralization has occurred in equilibrium with isotopically homogenous fluid. This is supported by a similar average temperature of 274˚C (n=7, 1σ = 54.4˚C) for only the intergrown sphalerite-galena pairs compared to the average temperature for all samples (text above). Furthermore, an isotopically homogenous $\delta^{34}S$ composition of the hydrothermal fluid, at least at the vein/local scale, is apparent from the consistent $\delta^{34}S_{HS^-}$ values throughout the Bellekeno hydrothermal paragenesis (see section 5.2 Evolution and Conditions of the Keno Hill fluid system). This range of calculated mineralization temperatures is approximately consistent with the fluid inclusion homogenization temperatures from this study (see section 4.3 Microthermometry); where stage 3 appears to have precipitated from 290 to 260°C (from stage 2-3: quartz), and stage 7 from 250 to 220°C. Pyrite-galena and pyrite-sphalerite mineral pairs were evaluated; however consistent or reasonable temperatures were not determined. This discrepancy may be an effect of the chemical process involved with pyrite precipitation, whereby pyrite forms in disequilibrium with the hydrothermal fluid

due to the complex reactions required to form FeS and/or bisulfide (S_2^{2-}) species (Ohmoto and Goldhaber, 1997; Polyakov and Soultanov, 2011).

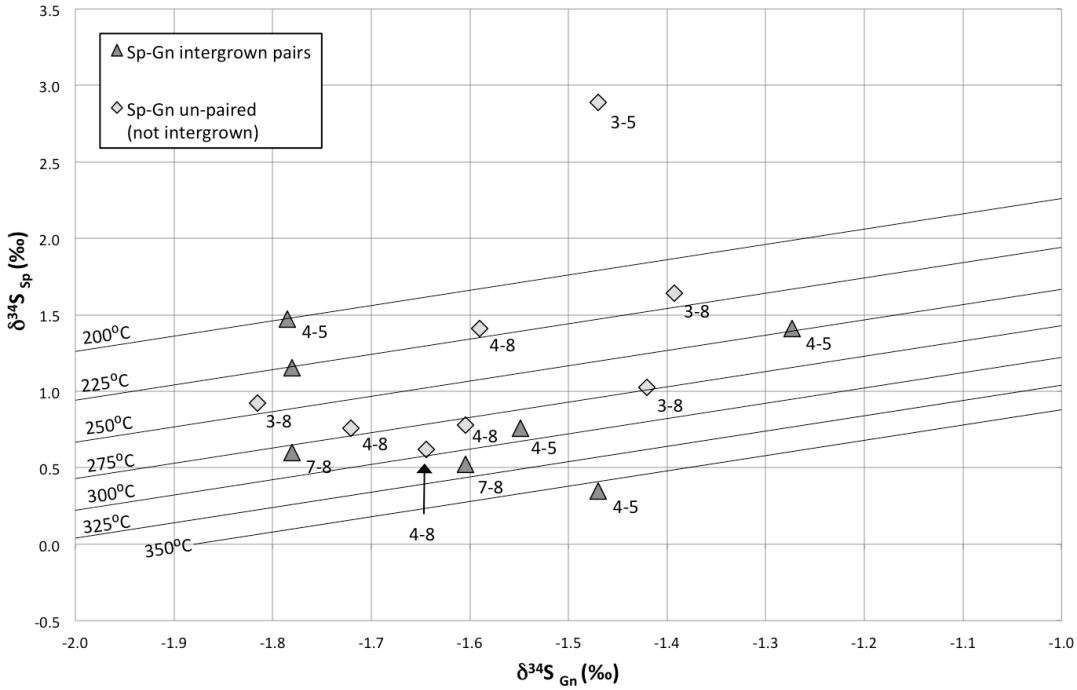

Figure 4-18. Bellekeno vein sulfur isotope geothermometry from sphalerite (Sp) and galena (Gn) mineral pairs. $\delta^{34}S$ are reported in reference to CDT (‰). Text to the lower right of each sample symbol indicates paragenetic stages paired. Isotherm temperatures calculated using isotopic equilibrium equations from Ohmoto and Rye (1979). The average temperature of all Sp-Gn pairs is 257°C (n=15, 1σ = 53.4°C); 274°C (n=7, 1σ = 54.4°C) for only intergrown Sp-Gn pairs (essentially indistinguishable when comparing stages 4-5 and 7-8); and 242°C (n=8, 1σ = 51.1°C) for Sp-Gn samples not intergrown.

Sample	Vein	$\delta^{34}S$ (‰)
Stage 1: Arsenopyrite		
K08-165: 174 m	Keno 700	-5.9
Stage 2: Pyrite		
BKUD-150: 60.4 m	Bellekeno-SW	-0.3
BKUD-163: 27.5 m	Bellekeno-SW	1.5
BKUD-173: 34.4 m	Bellekeno-99	1.5
Stage 3: Sphalerite		
K07-65: 129 m	Bellekeno-E	0.9
K07-66: 142 m	Bellekeno-E	1.6
K07-76: 125 m	Bellekeno-E	1.2
K09-187: 195 m	Bellekeno-E	1.0
BKUD-144: 36.6 m	Bellekeno-SW	2.9
BKUD-148: 33.5 m	Bellekeno-99	1.0
BKUD-153: 87 m	Bellekeno-SW	0.9
BKUD-171: 43.5 m	Bellekeno-99	1.0
K07-122: 159 m	Onek	-0.9
K08-155: 132 m	Onek	-2.1
Stage 4: Pyrite and Sphalerite		
BK-L750-573: 10 m	Bellekeno	0.8
K07-96: 278 m	Bellekeno-E	2.4
K07-96: 278 m	Bellekeno-E	2.0
BKUD-134: 41 m	Bellekeno-SW	0.5
BKUD-134: 41 m	Bellekeno-SW	1.5
BKUD-143: 51.2 m	Bellekeno-SW	0.7
BKUD-143: 51.2 m	Bellekeno-SW	1.4
BKUD-146: 46.6 m	Bellekeno-SW	1.0
BKUD-146: 46.6 m	Bellekeno-SW	1.4
BKUD-150: 63.2 m	Bellekeno-SW	0.6
BKUD-150: 63.2 m	Bellekeno-SW	0.6
BKUD-156: 29 m	Bellekeno-SW	1.1
BKUD-156: 29 m	Bellekeno-SW	1.6
BKUD-161: 20.8 m	Bellekeno-SW	0.8
BKUD-161: 20.8 m	Bellekeno-SW	1.6
BKUD-166: 21.3 m	Bellekeno-SW	1.2
BKUD-166: 21.3 m	Bellekeno-SW	0.8
EAG-047: surface	Eagle	-0.5
EAG-047: surface	Eagle	0.0
K09-201: 238 m	Keno 700	-4.9
K09-201: 238 m	Keno 700	-4.0

Sample	Vein	$\delta^{34}S$ (‰)
Stage 5: Galena		
BKUD-134: 39 m	Bellekeno-SW	-1.8
BKUD-143: 54 m	Bellekeno-SW	-1.3
BKUD-166: 16 m	Bellekeno-SW	-1.5
Stage 7: Sphalerite		
BK-L750-571: 7 m	Bellekeno	0.5
K09-187: 201m	Bellekeno-E	1.2
K09-187: 201 m	Bellekeno-E	0.6
BKUD-139: 8 m	Bellekeno-SW	0.8
BKUD-144: 37 m	Bellekeno-SW	0.3
Stage 8: Galena		
BK-L750-572: 9 m	Bellekeno-SW	-1.6
BK-021: surface	Bellekeno	-1.2
K07-66: 146 m	Bellekeno-E	-1.4
K07-109: 87 m	Bellekeno	-1.2
K09-187: 201 m	Bellekeno-E	-1.8
BKUD-143: 52.8 m	Bellekeno-SW	-1.6
BKUD-144: 37 m	Bellekeno-SW	-1.5
BKUD-150: 64.1 m	Bellekeno-SW	-1.6
BKUD-153: 88.6 m	Bellekeno-SW	-1.8
BKUD-158: 37 m	Bellekeno-SW	-1.4
BKUD-160: 54.1 m	Bellekeno-SW	-2.0
BKUD-163: 16.5 m	Bellekeno-SW	-1.8
BKUD-166: 18.6 m	Bellekeno-SW	-1.7
BKUD-170: 7.6 m	Bellekeno	-1.7
BKUD-171: 32.8 m	Bellekeno-99	-1.4
HOM-051: surface	Homestake	-0.7
POR-056: surface	Porcupine	-2.4
SP-069: surface	Sign Post	-4.7
K06-25: 44 m	K-structure	-3.4
K07-114: 195 m	Lucky Queen	-3.8
K08-161: 231 m	Lucky Queen	-3.8
HEC-034: surface	Hector	-7.2
K07-88: 59 m	Calumet	-8.1
SK-004: surface	Silver King	-9.4
K06-2: 167 m	Silver King	-11.0
Late (?): Pyrite		
K07-60: 120 m	Tick (Husky)	2.5
K08-131: 36 m	Leo	7.4

Table 4-6. Summary of sulfur isotopic compositions (‰) from Keno Hill district sulfides. $\delta^{34}S$ are reported in reference to CDT. The Sign Post and K-structure veins are located approximately 1 km east and southeast of Lucky Queen vein, respectively. The Tick vein is located approximately 500 m southeast of Husky vein.

4.6 Lead Isotopes

The Pb isotopic compositions of Keno Hill district from this study are listed in Table 4-7. The Pb isotope values define a linear trend, with an upper (more radiogenic) end-member with $^{206}Pb/^{204}Pb$ and $^{207}Pb/^{204}Pb$ ratios of 19.25 and 15.69, respectively (Figure 4-19); the lower (more primitive) end-member has $^{206}Pb/^{204}Pb$ and $^{207}Pb/^{204}Pb$ values of 19.09 and 15.65, respectively.

The linear trend of the Pb isotopic ratios appears to define a mixing line, however the sources of each end-member were not determined and remain subject of speculation; see section 5.2 Sources of Oxygen, Carbon, Sulfur, Lead, and Fluid end-members for further discussion on the potential end-member sources. The mixing line in Figure 4-19 is based on a line of best fit for results from this study only, with an R^2 value of 0.81521.

If the more radiogenic spectrum of the mixing line is extrapolated to the shale curve from Godwin and Sinclair (1980), see Table 4-8 for parameters, then a modeled age for the Keno Hill vein mineralization may be determined if the following assumptions are true: 1) the more radiogenic end-member is derived from a sedimentary source; 2) the Pb isotopic composition of the sedimentary reservoir is homogenous and characterized by the point of intersection of the shale curve and the extrapolating the more radiogenic end-member of the mixing line trend; 3) the Pb isotopic composition shale curve is an accurate representation of the inferred sedimentary source. Based on the above assumptions a modeled age of 82 Ma for the Keno Hill vein mineralization is calculated; however considering range of ± 2σ confidence the error of the modeled age is ± 31 Ma. The relatively large range in error and numerous assumptions attached to modeling the age of mineralization suggests that little confidence and weight should be given to this age.

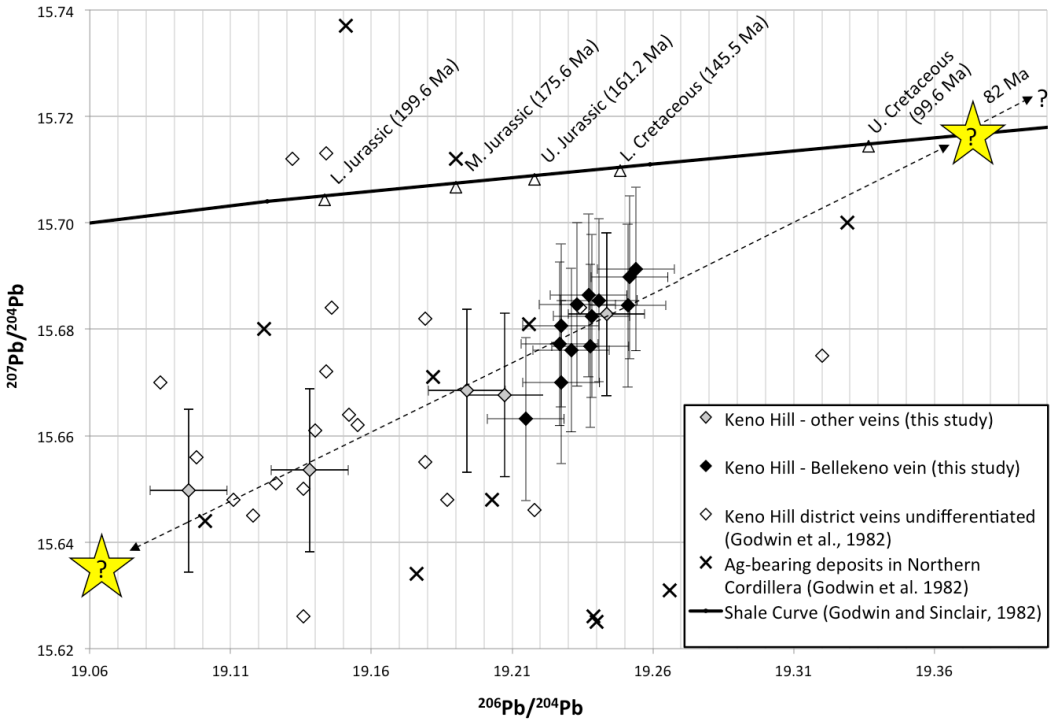

Figure 4-19. Keno Hill district vein galena Pb isotope compositions, $^{206}Pb/^{204}Pb$ vs. $^{207}Pb/^{204}Pb$, with additional data from Godwin et al. (1982), and Godwin and Sinclair (1982). Error bars for results from this study are ± 2σ. See Table 4-8 for shale curve parameters. The shale curve defines the modeled evolution of the Pb isotopic composition from stratiform shale hosted deposits along the eastern margin of the Canadian Cordillera, including the Selwyn Basin. The linear trend line (dashed line) is defined by a line of best-fit through the samples from this study only, with an R^2 value of 0.81521. The linear trend is inferred to define a mixing trend, however end-member sources were not identified in this study. The yellow stars identify the Pb isotopic compositions for inferred end-member sources. Based on the assumptions that the upper and more radiogenic end-member is derived from an isotopically homogenous sedimentary source, in terms of Pb ratios, which coincides with that defined by the shale curve (Godwin and Sinclair, 1982), then a modeled age of 82 ± 31 Ma is calculated.

Sample	Vein Location	$^{208}Pb/^{204}Pb$	2 SE	$^{207}Pb/^{204}Pb$	2 SE	$^{206}Pb/^{204}Pb$	2 SE	$^{207}Pb/^{206}Pb$	2 SE
BKUD09-163: 16.5 m	Bellekeno-SW	39.348	0.004	15.690	0.002	19.252	0.002	0.815	0.00002
BKUD09-160: 54.5 m	Bellekeno-SW	39.373	0.003	15.685	0.001	19.233	0.002	0.816	0.00002
BKUD09-158: 37 m	Bellekeno-SW	39.399	0.004	15.691	0.001	19.254	0.002	0.815	0.00002
BKUD09-171: 32.8 m	Bellekeno-99	39.460	0.004	15.684	0.001	19.251	0.001	0.815	0.00002
BK-021: surface	Bellekeno	39.322	0.004	15.663	0.001	19.215	0.001	0.815	0.00001
BK-L750-572	Bellekeno-SW	39.337	0.003	15.670	0.001	19.227	0.001	0.815	0.00002
K07-66: 146 m	Bellekeno-E	39.394	0.003	15.677	0.001	19.238	0.001	0.815	0.00002
K07-109: 87.8 m	Bellekeno	39.386	0.003	15.676	0.001	19.231	0.001	0.815	0.00002
K09-187:201.2 m	Bellekeno-E	39.355	0.003	15.677	0.001	19.227	0.001	0.815	0.00001
BKUD09-134	Bellekeno-SW	39.361	0.004	15.681	0.002	19.227	0.002	0.815	0.00002
BKUD09-143: 52.8 m	Bellekeno-SW	39.343	0.004	15.682	0.001	19.238	0.002	0.815	0.00002
BKUD09-143: 54 m	Bellekeno-SW	39.331	0.003	15.685	0.001	19.241	0.002	0.815	0.00002
BKUD09-144: 38.5 m	Bellekeno-SW	39.334	0.004	15.686	0.002	19.237	0.002	0.815	0.00002
HOM-051: surface	Homestake	39.126	0.004	15.654	0.001	19.138	0.001	0.818	0.00001
POR-056: surface	Porcupine	39.223	0.003	15.668	0.001	19.207	0.001	0.816	0.00001
K06-25: 44 m	K-Structure	39.247	0.003	15.668	0.001	19.194	0.001	0.816	0.00002
LQ-007: surface	Lucky Queen	39.083	0.003	15.650	0.001	19.095	0.001	0.820	0.00002
K08-161: 229.7 m	Lucky Queen	39.371	0.003	15.683	0.001	19.244	0.001	0.815	0.00002

Table 4-7. Summary of Pb isotopic compositions from Keno Hill district vein galena. The K-structure vein is located approximately 1 km southeast of the Lucky Queen vein. Notations: 2 standard errors (2 SE).

Equations:

$$[^{206}Pb/^{204}Pb]_{t2} = [^{206}Pb/^{204}Pb]_{t1} + \mu(e\ EXP[\lambda_1 t_1] - e\ EXP[\lambda_1 t_2])$$

$$[^{207}Pb/^{204}Pb]_{t2} = [^{207}Pb/^{204}Pb]_{t1} + \mu/137.88(e\ EXP[\lambda_2 t_1] - e\ EXP[\lambda_2 t_2])$$

$$[^{208}Pb/^{204}Pb]_{t2} = [^{208}Pb/^{204}Pb]_{t1} + \omega(e\ EXP[\lambda_3 t_1] - e\ EXP[\lambda_3 t_2])$$

Parameters:		**Source:**
λ_1 =	1.551250E-10	Jaffey et al., 1971
λ_2 =	9.848500E-10	Jaffey et al., 1971
λ_3 =	4.95E-11	LeRoux and Glendenin, 1963
t_1 =	1.89E+09	Godwin et al., 1982 [Basement age]
$[^{206}Pb/^{204}Pb]t_1$ =	15.391	Stacey and Kramers, 1975
$[^{207}Pb/^{204}Pb]t_1$ =	15.246	Stacey and Kramers, 1975
$[^{208}Pb/^{204}Pb]t_1$ =	35.025	Stacey and Kramers, 1975
$\mu(^{238}U/^{204}Pb)$ =	12.159	Goldwin and Sinclair, 1982
$\omega(^{232}Th/^{204}Pb)$ =	49.093	Goldwin and Sinclair, 1982

Table 4-8. Radiogenic Pb decay equations and shale curve parameters from Godwin and Sinclair (1982).

5.0 Discussion

5.1 Structure and Timing of Mineralization

Age of Mineralization

The linear trend of the Keno Hill Pb isotopic compositions (Figure 5-1) may be explained in terms of mixing between 2 main reservoirs, which were not identified in this study and discussed below (see section 5.2 Sources of Oxygen, Carbon, Sulfur, Lead, and Fluid end-members). The modeled age of 82 ± 31 Ma for the Keno Hill mineralization is based on a 3 key and speculative assumptions as outline in section 4.6 Lead Isotopes. Considering that there is a relatively large uncertainty of the modeled age of mineralization determined in this study, this calculated age is unreliable.

The whole-rock K-Ar geochronology method calculated from Sinclair et al. (1980) likely dated the muscovite minerals associated with the various vein assemblages, and is inferred to reflect the age of hydrothermal alteration. Hydrothermal illite could also contribute to the K budget of the whole-rock analyses, however volumetrically illite is not considered to be very important. The age of 87 ± 3 Ma for Ag-Pb-Zn mineralization (Sinclair et al., 1980) indicates a slightly younger age of mineralization compared to that of TTB intrusions, which could be indicating the existence of a prolonged hydrothermal cell associated with TTB magmatism. Alternatively, some of the K in the whole rock analyses of Sinclair et al. (1980) could have been derived from preexisting K-bearing minerals in the host rock, such as contamination from the phyllitic and schistose rock units, affecting their calculated age of mineralization, which could possibly be older than the actual age of hydrothermal mineralization. Furthermore, it is possible that age of mineralization determined by Sinclair et al. (1980) could have been modified or re-set, considering that the temperature of the Keno Hill hydrothermal fluids were also in the same range as the muscovite closing temperature, between 250 to 350°C (e.g. Faure, 1986; McDougall and Harrison, 1988).

The relatively younger calculated age of Ag-Pb-Zn related mineralization is consistent with textural observations, which is paragenetically later than the more intrusion proximal IRG mineralization (Lang and Baker, 2001; Hart et al., 2002; Mair et al., 2006; Hart, 2007; this study). Furthermore, relatively younger and moderately saline fluids (10 to 40 wt % NaCl equiv.) have been observed post-dating IRG mineralization elsewhere (e.g. Baker and Lang, 2001; Lang and Baker, 2001; Baker, 2002), which may be equivalent to fluid end-members I, II, and III from this study. However, the location of the Keno Hill district veins outside the metamorphic contact aureole of the Roop Lakes stock precludes a genetic relationship (Lynch, 1989). Additionally, a separate genetic relationship between TTB magmatism and Ag-Pb-Zn mineralization is implied from the different isotopic Pb compositions from the Keno Hill district vein galena compared to the TTB intrusions. In summary, a direct temporal link between the Roop Lakes stock and the Keno Hill veins cannot be proven, but the veins may be the result of a long-lived hydrothermal system which was driven by the heat from an inferred nearby and buried TTB intrusion.

Table 5-1 summarizes in chronological order the geological events relevant to the Keno Hill district, and the potential timing of the Keno Hill Ag-Pb-Zn hydrothermal mineralization.

Structure

The regional stress regime responsible for the formation and evolution of the fault structures that both host and cross-cut the Keno Hill mineralization remains poorly understood. A relative age of vein mineralization may be inferred based on the cross-cutting nature of the northwest-southeast dextral strike-slip to normal faults in the Keno Hill district, which suggests that they post-date or possibly formed near the end of the Ag-Pb-Zn mineralization. Development of the transcurrent Tintina fault system began during the Late Cretaceous (Tempelman-Kluit, 1979; Price and Carmichael, 1986), and approximately coincides with the modeled age of the Keno Hill mineralization. The sinistral strike-slip to normal northeast-southwest striking Keno Hill veins-faults suggests a north-south oriented principal compressive stress (Murphy, 1997). The later stage northwest-southeast striking, dextral strike-slip faults in the Keno Hill district may also be consistent with a north-south-oriented compressional stress regime. The similar approximate age and orientation of stress fields for both Keno Hill district faults and that of the Tintina fault system also suggests a potential genetic relationship of these structures. This hypothesized structural relationship may be explained in terms of the evolution of strain failure related to the Tintina fault system, where in the Keno Hill district, early antithetic rotation responsible for the northeast-southwest Keno Hill veins-faults, subsequently evolved to a synthetic shearing manifested as the late northwest-southeast oriented faults.

North to northwest-striking faults with sinistral displacement and associated east-striking extensional veins, which formed in response to east-west oriented compression, reportedly control the emplacement of IRG deposits regionally (Stephens et al., 2004). This stress regime contrasts with that of the inferred north-south oriented principal compressive stresses for the Keno Hill district vein-faults. The inconsistencies of the principal tectonic stress orientations associated with IRG and the Keno Hill Ag-Pb-Zn vein mineralization may be explained in terms of different stress regimes active at different times, the re-activation of pre-existing structures, and further supports different ages for these two distinct hydrothermal mineralizing events. Re-activation of pre-existing structures is also consistent with observations in the Keno Hill district as the Ag-Pb-Zn-bearing veins cross-cut and overprint the early quartz-arsenopyrite veins. The similar north-south oriented compressional stresses of the Tintina fault system and inferred for the Keno Hill vein-faults suggests a possible age association with the Keno Hill district Ag-Pb-Zn mineralization.

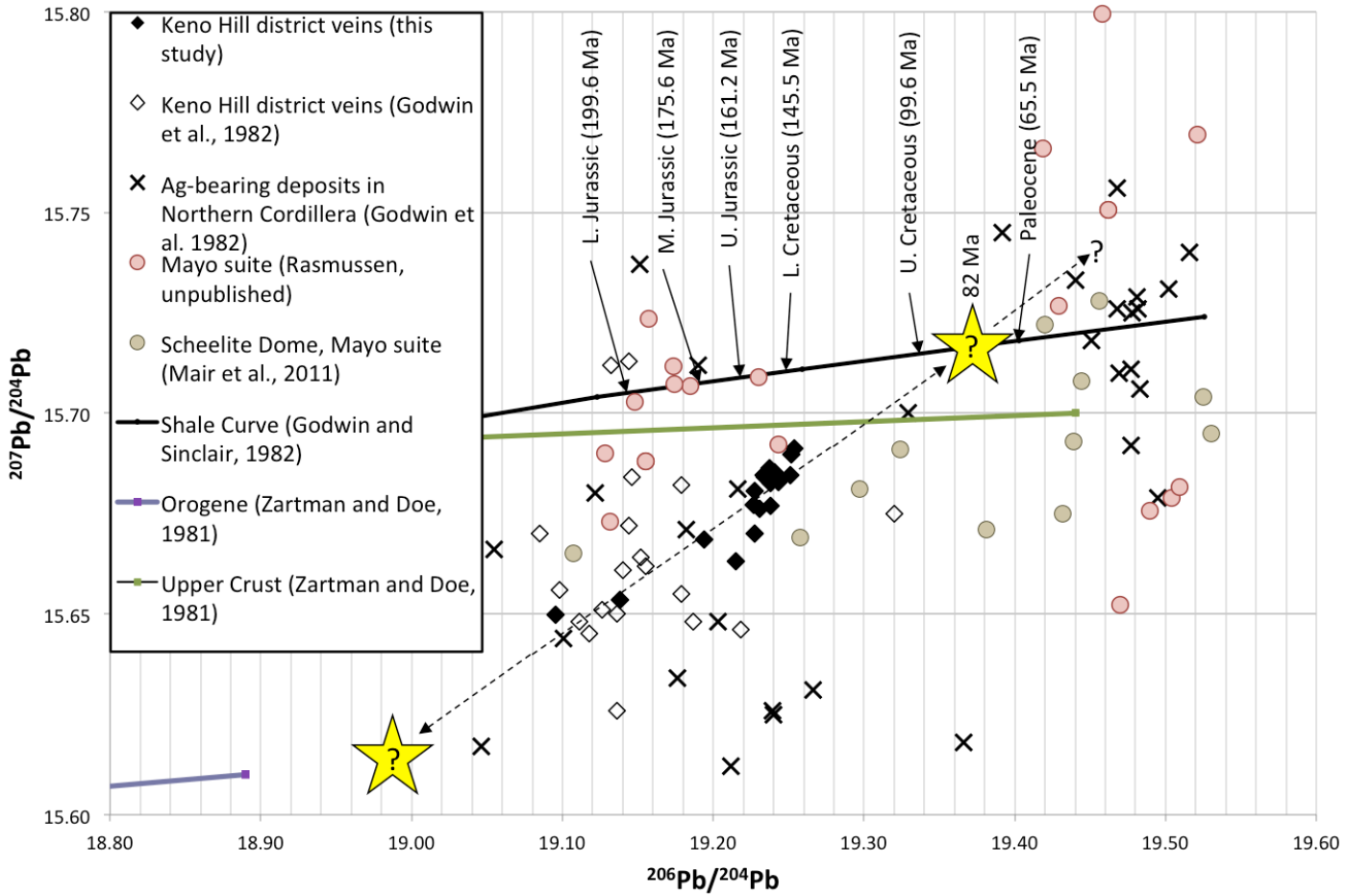

Figure 5-1. Lead isotope ratio composite plot, $^{206}Pb/^{204}Pb$ vs. $^{207}Pb/^{204}Pb$ of the Keno Hill results from this study, including data from Zartman and Doe (1981), the shale curve from Godwin and Sinclair (1982), additional Keno Hill district data from the Godwin et al. (1982), and TTB intrusions from Heffernan (2004), Mair et al. (2011), and Rasmussen pers. comm.

What	Type	Age	Comment
Earn Group	Lithology	Devonian – Mississippian [1]	Keno Hill Ag-Pb-Zn hydrothermal mineralization cross-cuts.
Keno Hill quartzite	Lithology	Mississippian [1]	Keno Hill Ag-Pb-Zn hydrothermal mineralization cross-cuts.
Intermediate to mafic dikes and/or sills	Intrusion	232 ± 1.5 Ma (Triassic) [2]	Keno Hill Ag-Pb-Zn hydrothermal mineralization cross-cuts.
Tombstone Strain Zone	Deformation	142 ± 6 Ma (Late Jurassic - Cretaceous) [1]	Tombstone and Robert Service Thrust faults, and penetrative foliation. Keno Hill Ag-Pb-Zn hydrothermal mineralization cross-cuts.
Keno Hill Ag-Pb-Zn mineralization ?	Hydrothermal mineralization	?	Maximum arguable age of Keno Hill Ag-Pb-Zn hydrothermal mineralization; however likely post-dates the McQuesten antiform.
McQuesten antiform/fault	Deformation	Late Jurassic – Cretaceous [1]	Younger than the Tombstone strain zone, but older than 92.9 ± 3 Ma from the cross-cutting Bos stock. Keno Hill.
Aplitic dikes (Keno Hill district)	Intrusion	93 ± 1.7 Ma (Early Cretaceous) [4]	Tupper and Bennett (2010) suggest that these intrusions post-date Keno Hill Ag-Pb-Zn hydrothermal mineralization; however it is possible that the same fault structure that is hosting the Keno Hill Ag-Pb-Zn hydrothermal mineralization, is cross-cutting the aplitic dikes, and therefore these intrusions are likely relatively older.
Roop Lakes stock	Intrusion	92.8 ± 0.5 Ma (Early Cretaceous) [3]	TTB - Mayo Plutonic Suite. There is no evidence that the Keno Hill Ag-Pb-Zn hydrothermal mineralization cross-cuts this intrusion.
Keno Hill Ag-Pb-Zn mineralization ?	Hydrothermal mineralization	87 ± 3 Ma (?) [5]	Tenuous K-Ar age from Sinclair et al. (1980). Keno Hill Ag-Pb-Zn hydrothermal mineralization may have temporal and genetic relationship with TTB to slightly younger age.
McQuesten Plutonic Suite	Intrusion	64 - 67 Ma (Late Cretaceous) [1]	No known intrusions of this suite in the Keno Hill district.
Keno Hill Ag-Pb-Zn mineralization ?	Hydrothermal mineralization	?	Minimum potential age limit of Keno Hill Ag-Pb-Zn hydrothermal mineralization is not well constrained.
Northwest-southeast (and northeast-southwest) striking faults [6]	Deformation	unknown (Late Cretaceous ?)	Numerous faults with normal and/or dextral displacement cross-cut Keno Hill Ag-Pb-Zn hydrothermal mineralization; could be related to Tintina fault system (?).

Table 5-1. Chronology of geological units and deformation events in the Keno Hill district. Light grey zones define the maximum and minimum potential ages of the Keno Hill Ag-Pb-Zn hydrothermal mineralization, the dark grey zone is the best guess. Sources as they appear in chronological order: [1] Murphy (1997), [2] Mortensen and Thompson (1990), [3] Roots (1997), [4] Tupper and Bennett (2010), [5] Sinclair et al. (1980), and [6] Boyle (1965).

5.2 Evolution and Conditions of the Keno Hill fluid system

The mineral paragenesis and hydrothermal fluid evolution from this study is largely defined by observations from the Bellekeno vein (stages 2 through 12); stage 1 mineralogy and fluid composition has been constrained by the Homestake vein sample, located approximately 2 km to the east of the Bellekeno vein. The paragenetic stages record a progressive cooling of hydrothermal fluid temperatures (Th) from over 300°C in stage 1 to approximately 160°C in stages 9 and 12 (Figure 5-2). Throughout the paragenesis there is a complex variation of fluid salinity and evidence of at least 5 distinct fluid end-members, defined by homogenization temperatures and calculated salinity.

Stage 1 quartz precipitated from a CO_2-rich hydrothermal fluid (vapour) around 300°C, with a salinity of less than 9.2 wt % NaCl equiv. (Figure 5-2). This fluid composition appears to correspond to the type II fluid inclusions from Lynch et al. (1990). The fluid composition, depth of mineralization, and the presence of arsenopyrite and Au of the early stage 1 quartz are similar to the fluids and mineralogy of some IRG and orogenic deposits (e.g. Groves et al., 1998; Sillitoe and Thompson, 1998; Baker and Lang, 2001; Lang and Baker, 2001; Maloof et al., 2001; Baker, 2002; Groves et al., 2003; Marsh et al., 2003; Mair et al., 2006; Mair et al., 2011). Hydrothermal fluids associated with IRG mineralization are commonly CO_2-rich with low salinity, with homogenization temperatures of 250 to 350°C; that have exsolved from intrusions, and primarily precipitate quartz from approximately 2 to 9 kilometers depth in an post-collisional and transitional tectonic setting, and have a distinctive metal zoning (Figure 2-2).

There is a hiatus in mineralization between stages 1 and 2. The presence of minerals such as siderite, sphalerite, galena, jamesonite and boulangerite in stage 1 quartz veins is the result of overprinting and suggest that the fluids that precipitated the minerals of stages 2 to 8 utilized the same vein-fault structures as fluid(s) conduits. Stages 2 though 8 herein are collectively referred to as the "main stages" as these are most closely associated with the Ag-Pb-Zn-mineralization. These paragenetic stages may be divided into 2 broad episodes based on a repetitive sequence of siderite-sphalerite-galena mineralization (stages 2 to 5, and 6 to 8). Although Ag-bearing minerals are primarily associated with galena-rich stages (i.e. 5 and 8), they are also commonly associated with siderite and sphalerite during the second episode (i.e. stages 6 and 7), but not the first episode (i.e. stages 2 and 3 or 4a).

The fluids trapped in stages 2 and 3 delineate a slight cooling trend from 290 to 260°C (Th); this is associated with an increase in fluid salinity from 11 to 14 wt % NaCl equiv., from end-member 1a to 1b (Figure 5-2). The overlap of the fluid inclusion compositions in stage 2 siderite and stage 2-3 quartz is inferred to reflect that the stage 3 sphalerite mineralization is associated with the same fluid (i.e. end-member Ia/b).

There are no fluid inclusion data available from stages 4 and 5; however textural considerations, and the overlap of the temperature and salinity conditions from fluid inclusions in stages 3 and 6, at end-member Ib, suggest a continuation of fluid evolution and mineralization. Significant silver precipitation primarily occurs with stages 5 and 8, but is also associated with stages 6 and 7. The homogenization

temperatures of the stage 6 fluid inclusion assemblages are consistently between 260 and 250°C, with an increase of fluid salinity from 13 to nearly 20 wt % NaCl equiv.

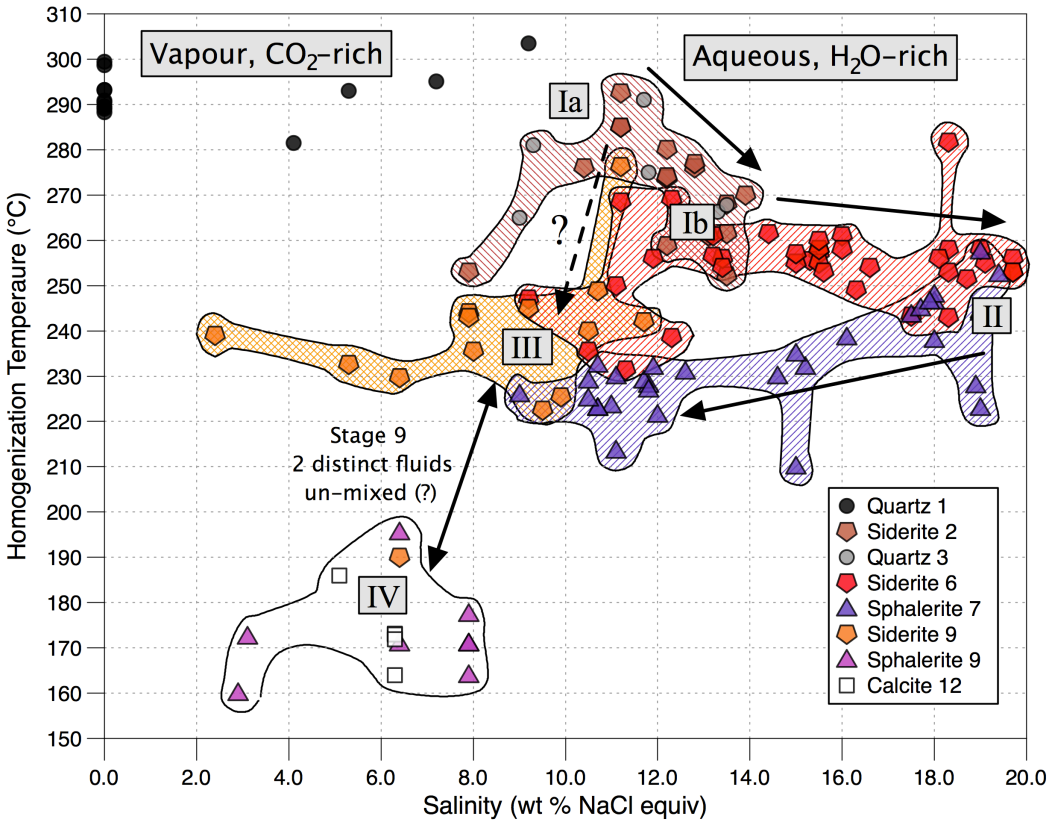

Figure 5-2. Keno Hill hydrothermal vein fluid evolution plot inclusions plot of homogenization temperatures (°C) vs. salinity (wt % NaCl equiv.). Arrows define paragenetic order of mineralization, and inferred mixing trends and evolution of hydrothermal fluids. All stage 1 quartz samples are CO_2-rich with homogenization to vapour phase from the Homestake vein. All aqueous, H_2O-rich fluid inclusion from stages 2, 3, 6, 7, 9, and 12 are from the Bellekeno vein homogenize to liquid phase. Mixing is supported by the range of fluid Th and salinity for individual FIA in stages 6, 7, and 9, are shown in Figures 5-4.

A continuation of mineralization from stages 6 to 7 is inferred based on the intergrown nature of these stages, as well as the overlap of fluid Th and salinity at end-member II. Stage 7 appears to have cooled from 250 to 220°C (Th), and is accompanied by a decrease in fluid salinity from approximately 20 to 10 wt % NaCl equiv. Although no primary fluid inclusions were analysed from stage 8, the temperature of mineralization is inferred to be approximately the same as that for stage 7, based on the intergrown nature of stages 7 and 8, as well as the lower temperatures recorded by the onset of stage 9 mineralization.

The paragenetic evolution of the S isotopic composition for the main stages of the Bellekeno vein is evaluated in terms of $\delta^{34}S_{HS^-}$ values (Figure 5-3), calculated from equilibrium isotopic fractionation factors (Ohmoto and Rye, 1979), at temperatures

of 295˚C for stages 3 and 4, 285˚C for stage 5, 265˚C for stage 7, and 255˚C for stage 8 based on fluid inclusion observations (pressure corrections were applied to the Th measurements, corrected by +25˚C, see section 5.2 Depth of mineralization). An average $\delta^{34}S_{HS^-}$ value of -0.2 ‰ is consistent throughout the hydrothermal paragenesis, which suggests that the S isotopic composition of the hydrothermal fluid(s) was relatively homogenous throughout the main stages of mineralization at the vein scale or at least within the Bellekeno vein. The wide range of $\delta^{34}S$ values throughout the Keno Hill district are discussed below, see section 5.4 Keno Hill District Spatial Zonation. The average $\delta^{34}S$ values for sphalerite have a slightly decreasing trend through the hydrothermal paragenesis; where stage 3 is +1.3 ‰, stage 4a is +1.2 ‰, and stage 7 is +0.7 ‰. This progressive decrease in sphalerite $\delta^{34}S$ values may be explained in terms of decreasing temperature, and/or a small increase in oxidation state or pH. A decrease of fluid temperature throughout the paragenesis is apparent from fluid inclusion observations (i.e. Th). The presence of sulfate minerals at the end of or after stage 8 may be an indication of a shift to higher oxidation state occurred later in the paragenesis; however this may also be explained in terms of an increase in cation and sulfate activity. An increase in pH is consistent with carbonate and base-metal precipitation (Seward and Barnes, 1997). Conversely, from sphalerite-rich stage 7 to galena-rich stage 8 there is a slight positive shift in $\delta^{34}S_{HS^-}$ values, this may be explained in terms of an increase in temperature, or decrease in oxidation state or pH. A decrease in fluid pH is supported by the presence of kaolinite associated with the later stages of mineralization (i.e. later than stage 5). Kaolinite is typically associated with the argillic alteration assemblage of epithermal systems; deposition is associated with fluids at lower temperatures (<250°C) and pH (3 to 4) and is considered to form in response to steam-heated meteoric water (Hawke et al., 1996). Alternatively, it is possible that each of the mixing end-member fluids had a slightly different S isotopic composition.

Stage 9 essentially marks the end of the main stage and significant Ag-Pb-Zn related mineralization. Stage 9 siderite-ankerite precipitated from a fluid approximately corresponding to end-member III, with a Th between 220 and 250°C, and salinity generally between 5 and 12 wt % NaCl equiv. However, sphalerite of the same stage is associated with a fluid temperature (Th) between 160 and 200°C, and salinity between 3 and 8 wt % NaCl equiv., corresponding to end-member IV. Stage 12 calcite also has a similar range of Th and salinity as stage 9 sphalerite; this overlap of fluid compositions suggests that the fluid(s) associated with these minerals/stages were similar. The distinct bimodal distribution of fluid inclusion Th and salinity for both stage 9 siderite and sphalerite suggests that 2 fluids of different composition (and origin?) were both present during stage 9 but did not effectively mix.

Fluid end-member III, with the same approximate salinity as end-member Ia, could be an evolved version of fluid Ia, which may have simply cooled from 290 to 220°C (Th). Evidence for a single evolving fluid (from end-member Ia/b to III) is supported by the overlap of fluid Th and salinity ranges from stage 9 siderite with that of end-members Ia/b, II, and III, suggesting the continual presence or influx of this fluid (end-member 1a) throughout the paragenesis.

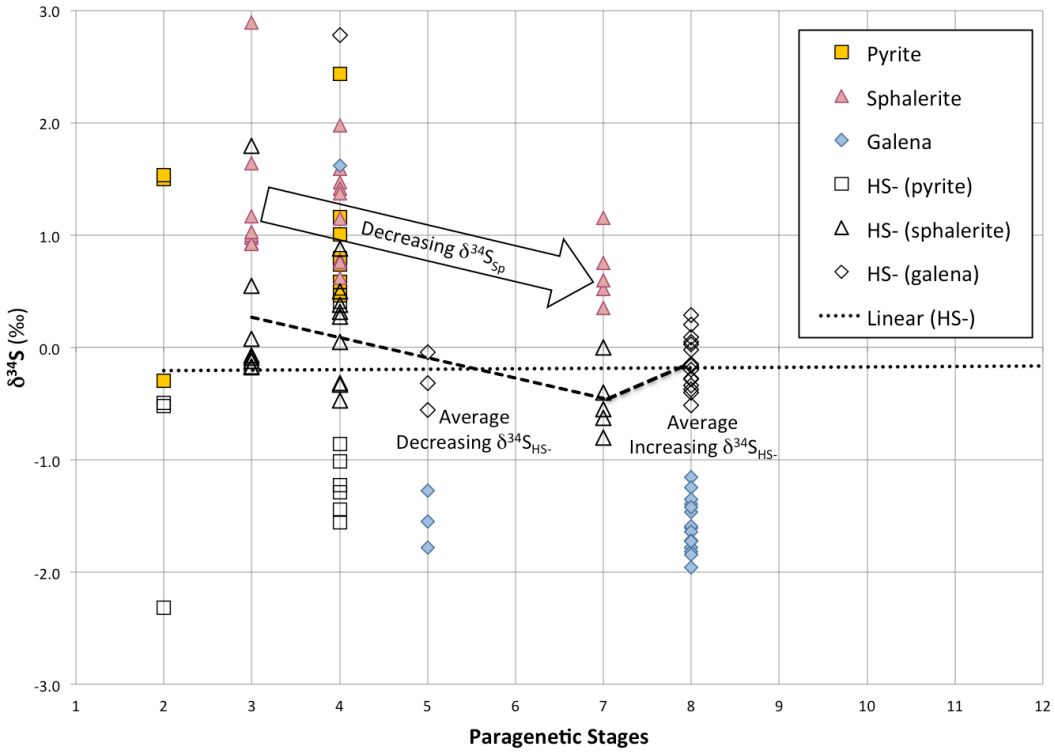

Figure 5-3. Bellekeno vein sulfur isotopic compositions (‰) of sulfides throughout the hydrothermal paragenesis with calculated HS- (open symbols) in equilibrium for each mineral. The line of best-fit for all calculated $\delta^{34}S_{HS-}$ values (thin broken line) has an average of -0.2 ‰ throughout the paragenesis. The average $\delta^{34}S_{HS-}$ from sphalerite and galena defines a decreasing trend up to stage 7, then increases in stage 8 (thick broken line). The $\delta^{34}S$ from stages 3, 4a, and 7 sphalerite also progressively decreases.

Precipitation Mechanisms: Boiling vs. Mixing

From this study, the fluid inclusion data tied to paragenetic stages of the Bellekeno vein suggests that there have been multiple influxes of fluids of different compositions. There are two possibilities to explain the relatively higher fluid salinity observed in stages 6 and 7, defined by end-member II; fluid end-member Ia/b could have boiled, or alternatively end-member II marks the influx of a distinct fluid with a unique fluid composition.

Lynch et al. (1990) inferred that boiling occurred in the system based on: 1) co-existing liquid-rich and vapour-rich fluid inclusions; 2) an increase of fluid salinity associated with a decrease in volatiles; (Hedenquist and Henley, 1985); 3) the shift of siderite $\delta^{18}O$ values to more negative values associated with CO_2 loss (Bottinga, 1968; Drummond and Ohmoto, 1985); and 4) the positive shift of quartz $\delta^{18}O$ values. However their conclusions are based on the changes of the fluid compositions from the early stage 1 quartz to the main stages with siderite. Neither Lynch et al. (1990), nor this study, can show unequivocally that there is a genetic relationship between, or continuity of fluid evolution from stages 1 to 2. Boiling may be inferred from the CO_2-rich vapour phase fluid inclusions from Homestake vein stage 1 quartz; however, no evidence for boiling was observed in any fluid inclusion assemblage in

stage 2 or later in this study. No vapour-rich fluid inclusions were documented in the main stage mineralization and there was no noticeable decrease in volatile content associated with increased fluid salinity, which would otherwise suggest boiling or phase separation had occurred (Hedenquist and Henley, 1985). The presence of CO_2 is apparent based on the formation of clathrates in some fluid inclusions from stages 2, 3, 6, and 7; however there are no trends tying the relative increase in CO_2-content (i.e. higher clathrate melting temperatures) to increased salinity (see fluid inclusion data in Appendix IV). Contrary to the findings by Lynch et al. (1990), the localized shifts in $\delta^{18}O$ and $\delta^{13}C$ values, that were inferred to explain boiling and fluid re-equilibration processes, are not observed in this study. Alternatively, each particular vein appears to have a consistent range of $\delta^{13}C$ and $\delta^{18}O$ values. Therefore we do not consider boiling to be an important process at Keno Hill (at least at the structural levels we have sampled). Additionally, observations by Maloof et al. (2001) at the Dublin Gulch IRG deposit, which hosts a similar suite of hydrothermal mineralization and fluid inclusion compositions, concluded that boiling was unlikely based on a lack textural evidence and the inability of simple adiabatic boiling of a fluid with a fluid composition similar to stage 1 (this study) to produce a fluid with >12 wt. % NaCl equiv. (Hedenquist and Henley, 1985).

The different ranges of Th and salinity for the paragenetic stages 2, 6, 7, 9 and 12 are clear indications that the hydrothermal fluid(s) composition changed over time, and could be explain in terms of evolving fluid compositions, and/or influxes of multiple fluids with different fluid compositions. Although fluid mixing likely occurred in such an environment where multiple fluids with distinct compositions were present, providing direct evidence for the possibility of the fluid mixing hypothesis is difficult and can only be demonstrated in a few FIA, where a continuum of Th and salinity define the proposed mixing trends (see Figure 5-4, and fluid inclusion data in Appendix IV). The linear trends of fluid Th and salinity between end-members Ia/b and II for stage 6 siderite, and between end-member II and III for stage 7 sphalerite are therefore interpreted to represent fluid mixing.

Baker et al. (2006) concluded highly saline brines that post-date IRG mineralization are characterized by higher Fe, Mn, Zn, and Pb concentrations and are strongly controlled by Cl-content. Chloride-complexes are considered important ligands associated with the dissolution and transportation of Pb in solution; an increase in pH, and/or fluid dilution, thereby reducing Cl-concentration, may be responsible for the precipitation of galena (Reed, 1997; Seward and Barns, 1997). Mineralization occurring in response to fluid dilution is consistent with the fluid inclusion observations, whereby a relatively more saline fluid, and likely Pb-bearing, corresponding to end-member II has mixed with a more dilute fluid, end-member III, resulting in the deposition of both stages 7 and 8. This relationship between salinity and base-metal concentration is further supported by a correlation between higher concentrations of Zn and Pb and increased salinity (Cl-content) for some IRG deposit fluids (Baker et al., 2006).

During stage 9, fluid mixing cannot be demonstrated; rather periodic pulses of 2 distinct fluid compositions (i.e. end-members III and IV) are responsible for precipitating either siderite or sphalerite. The complexly banded mineralization texture of stage 9 siderite-ankerite with layers or pockets of sphalerite appears to be

the textural manifestation of this inferred repetitive influx of these 2 different fluids. The end-member III fluid associated with stage 9 siderite may be the evolved and cooler equivalent of end-member Ia.

At least partial fluid mixing between end-member IV and the fluid(s) associated with the main stages (i.e. end-member Ia/Ib, II, or III) is supported by the stage 12 calcite $\delta^{18}O$ trend, which may be extrapolated towards the more enriched $\delta^{18}O$ and negative $\delta^{13}C$ siderite values (Figure 4-13). The large gap of $\delta^{18}O$ calcite values, between 2 and 12 ‰, along this proposed mixing trend may be explained by the dominance of the more negative $\delta^{18}O$ meteoric component (see section 5.2 Sources of Oxygen, Carbon, Sulfur, Lead, and Fluid end-members) and that the 2 fluids were relatively well mixed, preferentially preserving the meteoric fluid isotopic signature.

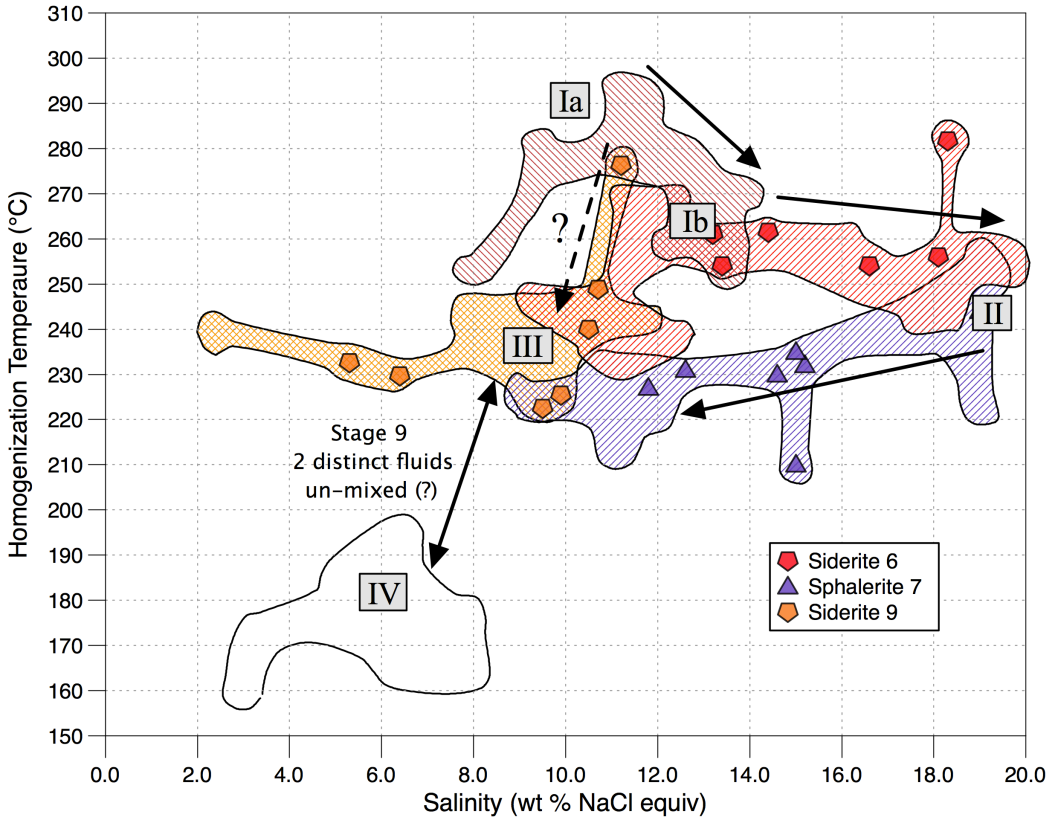

Figure 5-4. Bellekeno vein fluid inclusion assemblages for stages 6, 7 and 9. Fluid mixing is best demonstrated by the ranges of Th and salinity from samples BKUD09-171: 32.8m for stage 6 siderite, and BKUD09-171: 43.5m for stage 7 sphalerite. Stage 9 siderite from a single grown zone in BKUD09-160: 56.5m also show a significant range of Th and salinity within this assemblage, which may also be explained in terms of fluid mixing or the presence of multiple fluids.

Depth of mineralization

Lynch et al. (1990) determined 2 different pressure ranges from fluid inclusions in quartz, either 1514 to 1767 bars or 486 to 675 bars, which appears to correspond to

stage 1 in this study. These pressure estimates were inferred to represent fluctuations between lithostatic and hydrostatic conditions, which correspond to approximately 5 to 7 km depth. The presence of other volatiles, possibly CH_4 (as suggested by this study), indicates that the calculated pressure may be underestimated (Diamond, 1994). The depth of main stage Ag-Pb-Zn associated mineralization (i.e. stages 2 to 8) may be determined by comparing fluid inclusion Th data with the independent estimate of temperature of mineralization of 274°C (n=7, 1σ = 54.4°C) from the sulfur isotope geothermometry (see section 4.5 Sulfur Isotopes). This matter is complicated when considering that the Th data appear to record a temperature range of mineralization of nearly 160°C, with 4 distinct stages of sphalerite mineralization at occurring within 3 different Th ranges. Sphalerite from stages 3 and 4a are inferred to have a similar Th range as stage 2 siderite from 249 to 292°C, with an average of 270°C (n=20, 1σ = 12°C); whereas stage 7 sphalerite has an approximate Th range of 250 to 220°C, with an average of 233°C (n=48, 1σ = 12°C); stage 9 sphalerite is not considered here. Sack (2002) and Sack et al. (2003) determined a range mineralization temperature from tetrahedrite mineral thermometry data between 310 and 250˚C, based on mineral chemistry isotherms of Ag/(Ag+Cu) and Zn/(Zn+Fe) molar ratios (see section 5.4 Keno Hill District Spatial Zonation for further discussion on tetrahedrite mineral chemistry), which further supports the $\delta^{34}S$ geothermometry. If the sulfur isotope geothermometry is representative of the earlier sphalerite mineralization (i.e. stages 3 and 4a), then the pressure correction is essentially negligible and mineralization occurred near the Earth's surface; alternatively the lower Th range exhibited by stage 7 sphalerite (220 and 250°C) corresponds to a pressure correction between approximately 325 and 675 bars, if considering a simple H_2O-NaCl system (Sheppard et al., 1985). The presence of clathrate is apparent in some fluid inclusions from stages 2, 3, 6 and 7, which suggests that between 0.01 and 0.03 molar concentration of CO_2 may be present (Hedenquist and Henley, 1985). The effects of such low concentrations of CO_2 on the pressure correction are not well established however they are expected to be relatively minor and therefore not considered in the pressure estimates of this study. The pressure range determined in this study overlaps with that defined by Lynch et al. (1990) for their type II fluid inclusions. The maximum pressure correction, corresponding to a +25 to +55°C adjustment to the Th measurements, is further supported by the calculated temperature of mineralization from tetrahedrite thermochemistry between 250 and 310°C (Sack et al., 2003). An estimated depth of mineralization between 3.3 and 6.8 km is implied if mineralization occurred under hydrostatic conditions, or 1.2 to 2.5 km if at lithostatic conditions.

Lynch (2009) determined the pressure of mineralization for a sphalerite-pyrite-pyrrhotite-arsenopyrite mineral assemblage (which likely correlates with stages 3 or 4a from this study) of between 1.1 to 1.6 kilobars, corresponding to 10 to 13 kilometers depth, under hydrostatic conditions. This depth of mineralization was shown to be similar to the depth of emplacement of the Roop Lakes stock, which is based on mineral equilibria of contact metamorphic assemblages (Lynch, 2009). However, it is unlikely that hydrostatic conditions will persist to such depths, furthermore, this contrasts with the reported 2 to 8 kilometers depth range of IRG mineralization (e.g. Baker and Lang, 2001; Lang and Baker, 2001; Baker, 2002; Marsh et al., 2003).

Sources of Oxygen, Carbon, Sulfur, Lead, and fluid end-members

The Keno Hill district stage 1 fluid is believed to be similar to the early fluids associated with IRG mineralization; which have been exsolved from ascending TTB intrusions (e.g. Baker and Lang, 2001; Maloof et al., 2001; Baker, 2002; Marsh et al., 2003). Baker and Lang (2001) suggest that the CO_2-content of the TTB magmas may be acquired through crustal assimilation, or alternatively from a mantle source.

Lynch et al. (1990) suggested the hydrothermal fluid that precipitated stage 1 quartz could have boiled and ended up with a fluid composition of end-member Ia; however there is no evidence for boiling at Keno Hill, and such a process could not form a moderately saline fluid of >12 wt. % NaCl equiv. (Hedenquist and Henley, 1985; Maloof et al., 2001). Alternatively, the main stage, moderately saline fluids (i.e. end-members I, II, and III) could be magmatic in origin, meteoric water that has dissolved salt, or formation water. Some IRG deposits in the TTB reportedly exhibit exsolved magmatic fluid that has immiscibly separated to both low-salinity, CO_2-rich, and highly saline H_2O-rich magmatic fluids, depending on the depth of intrusion emplacement (Thompson et al., 1999; Baker and Lang, 2001; Baker, 2002). However, the different isotopic Pb compositions of the Keno Hill vein galenas and the TTB intrusions suggests that the 2 are not related. If the moderately saline fluids in Keno Hill are of magmatic origin, they are associated with a magma that has a more primitive Pb isotopic composition. Baker et al. (2006) report that highly saline fluid inclusions that post-date some IRG mineralization, with higher Fe, Mn, Zn, and Pb concentrations, are of either magmatic or sedimentary basinal origin and likely reflect a separate hydrothermal event than IRG mineralization. It is possible that this later stage saline fluid that post-dating IRG deposits could be related to the moderately saline end-member II defined by this study.

There is evidence that the main stage fluids have partially equilibrated with the country rock based on the C and O isotopic compositions of siderite. The relatively depleted $\delta^{13}C$ values from siderite are consistent with carbon derived from or at least partly equilibrated with reduced organic sources (Ohmoto and Goldhaber, 1997), such as graphite, which is ubiquitous within the Keno Hill quartzite, and is likely the dominant source of carbon (Lynch et al., 1990) of the main stage fluids. Considering the range of primary magmatic water $\delta^{18}O_{SMOW}$ values is typically between +5 and +10 ‰ (Taylor, 1974; Sheppard, 1977), the relatively enriched siderite $\delta^{18}O$ values are interpreted as an indication that the main stage hydrothermal fluids had at least partially derived from, or equilibrated with the surrounding country rocks.

In terms of the isotopic composition of the limestone units in the Keno Hill district; if ancient seawater had a $\delta^{18}O_{SMOW}$ value of around 0 ‰ (Muehlenbachs, 1998), the relatively high $\delta^{18}O$ values of the limestone may be explained in terms of the buffering effects of the surrounding sediments (Taylor, 1974; Sheppard, 1977). Alternatively, Veizer et al. (1999) document variations in $\delta^{18}O$ values of the seawater throughout the historic rock record; they identified Mississippian seawater with a $\delta^{18}O$ value of around +25 ‰, which is nearly consistent with the values documented in this study. The $\delta^{13}C$ values from limestone are relatively enriched compared to average marine limestone, however it still occurs within the

historic range (Schidlowski and Aharon, 1992; Ohmoto and Goldhaber, 1997; Ripperdan, 2001). The isotopic composition of the volumetrically insignificant amount of limestone throughout the district does not appear to have affected the C and O isotopic composition of the hydrothermal carbonates.

As the mineral assemblages of stages 6 and 7 are closely associated with stage 8, the Pb isotopes from galena are inferred to provide some insight into the origin of fluid end-members II and III. The linear trend of the galena Pb isotopic compositions (Figure 5-1) may be explained in terms of a mixing trend between 2 main reservoirs; however neither end-member source was identified in this study. The more radiogenic end-member could be sourced from the regional sediments (see section 4.6 Lead Isotopes), or alternatively, if the mixing line trend is extrapolated further into the radiogenic field then some of the TTB Pb isotopic compositions could define the radiogenic end-member. The Pb isotopic composition of the TTB intrusions in the more radiogenic field are dominated by the Tungsten, Anvil, and Tay River plutonic suites (Rasmussen, unpublished data; Heffernan et al., 2004) which are predominantly located in eastern Yukon and do not likely reflect the more radiogenic end-member source; therefore, a sedimentary source is preferred. The lower and more primitive end-member may be derived from an isotopically homogenous source with $^{207}Pb/^{204}Pb$ and $^{206}Pb/^{204}Pb$ values of at least 15.65 and 19.09, respectively. The less radiogenic Pb values may reflect some mantle contribution as these values may be extrapolated towards the 'orogene trend' from Zartman and Doe (1981), which is based on a calculated mixture of crust and mantle Pb isotopic compositions. This interpretation of a mixed mantle- and sedimentary-derived Pb for the Keno Hill mineralization has also been suggested for the Keno Hill deposit as well as other Ag-Pb-Zn vein deposits (e.g. Beaudoin and Sangster, 1992; Farmer and DePaolo, 1997), and may constitute a common genetic feature for some of these deposits. The more primitive Pb isotopic composition signature suggests that either a deep-seated fluid has indirectly acquired Pb from an intrusion with a mantle component or that the hydrothermal fluids have a magmatic-mantle component from an inferred intrusion. Based on the association between end-members II and III with galena (i.e. stages 5 and 8), it appears that either of these hydrothermal fluid end-members may be at least partially derived from this inferred source with a mantle component.

When the Pb isotopic compositions of the Yukon Ag-bearing deposits are compiled (this study; Godwin et al., 1982) two broad groups of deposits can be defined, which approximately correlate with two groups of mid-Cretaceous intrusive suites (Heffernan et al., 2004; Rasmussen pers. comm.). One group of Ag-bearing deposits, which includes Keno Hill, have less radiogenic ratios with $^{206}Pb/^{204}Pb$ values mostly between 19.08 and 19.26, falling below the shale curve; these values are more similar to the Pb isotopic composition of the Mayo and Tombstone Plutonic suite intrusions. The variability of these intrusive with more primitive isotopic Pb compositions is likely a reflection of the variable contributions from the mantle and crustal components. The other group of Ag-bearing deposits has more radiogenic $^{206}Pb/^{204}Pb$ values of 19.44 and 19.52, and overlaps with the Tungsten, Tay River, and Anvil suite intrusions. The more evolved $^{206}Pb/^{204}Pb$ isotopic composition is consistent with these magmas being of mainly crustal origin (Hart et al., 2004a), and suggests that Pb from some Ag-bearing deposits may have been mostly derived from their associated intrusions (Heffernan et al., 2004). This general correlation suggests

that Ag-bearing deposits in the Selwyn Basin may be broadly associated with regional magmatic events.

From stage 12 calcite the relatively negative $\delta^{18}O$ values, as low as -7.4 ‰, reflect a meteoric fluid component for end-member IV. Lynch (1989) also documented an influx of late meteoric fluid in the west of the district, based on late stage quartz with depleted $\delta^{18}O$ values of -7.1 ‰. The negative $\delta^{13}C$ values from calcite, although not as depleted as in siderite, may reflect a similar source of organically derived carbon for fluid end-member IV.

The source(s) of sulfur cannot be constrained considering the known ranges of $\delta^{34}S$ from potential reservoirs (Seal et al., 2000). Both marine sediments and igneous rocks could be responsible for the observed $\delta^{34}S$ values in the Keno Hill district. Boyle et al. (1970) concluded that the majority of the sulfur is from the sediments based on the average S isotopic composition of various lithological units from the surrounding country rock: sediments (+0.67 ‰), greenstones (+0.08 ‰), and igneous-granite (+0.01 ‰) (Figure 4-16). The wide range of $\delta^{34}S$ from galena is explained in terms of changes in the fluid physiochemical conditions, see section 5.4 Keno Hill District Spatial Zonation.

5.3 Sphalerite and Galena Mineral Chemistry

The shift from sphalerite with higher Fe-content containing pyrrhotite and chalcopyrite mineral inclusions, and co-precipitated with pyrite during stages 3 and 4a, to lower Fe-content with less abundant pyrite and mineral inclusions during stages 7 and 9 is consistent with a temperature decrease and/or an increase in a_{S2} (Scott, 1983; Balabin and Sack, 2000). The Cu-content within Fe-rich sphalerite is lower in stages 3 and 4a compared to stage 7, which is Fe-poor and does not have "chalcopyrite-disease". Higher Cu-content of sphalerite is consistent with higher Fe-content and a higher temperature of mineralization (Hutchison and Scott, 1981). Chalcopyrite inclusions in stage 3 and 4a sphalerite may have formed as a result of Fe and Cu exsolution during re-equilibration at lower temperatures (Mizuta and Scott, 1997); whereby Cu-content originally incorporated in the sphalerite mineral structure is remobilized, and subsequently re-precipitated as chalcopyrite inclusions. Alternatively, chalcopyrite inclusions may form as a result of replacement by Cu reacting with the Fe-content in sphalerite (Barton and Bethke, 1987). Although there is little evidence to preferentially support one hypothesis over the other, the re-equilibration option of stage 3 and 4a sphalerite may be inferred based on the earlier and higher temperature of mineralization, associated with higher Fe-content. The Cu replacement of Fe in sphalerite in stages 3 and 4a is equally plausible, based on the presence of a relatively Cu-enriched fluid(s) during the later stages (i.e. 7 and 8), as evident from the precipitation of Cu-bearing minerals associated with these later stages.

Stages 3 and 4a are inferred to precipitate between 345 and 285°C based on pressure corrected fluid inclusion Th observations. Galenas from stages 3 and 4a may contain up to 2.89 wt % Ag; Bi is generally absent, however a few samples have up to 3.54 wt % and is only present when Ag-content is around 2 wt %; Sb substitution appears to be less important, with averages of less than 0.14 wt %. Stage 8 galena is inferred to precipitate between approximately 305 and 245°C

based on pressure corrected fluid inclusion Th measurements, and contains no Bi and has an average Ag and Sb content of 0.13 wt % and 0.20 wt %, respectively. These observations are consistent with experimental data suggesting that coupled substitution of Ag and Sb or Bi for two Pb increases with increasing temperature (Chutas et al., 2008). Sack et al., (2003) propose that $AgSbS_2$ originally incorporated in galena may be subsequently redistributed out or removed during retrograde exsolution reactions (Sharp and Buseck, 1993; Sack and Goodell; 2002; Chutas et al., 2008). Re-mobilization of Ag from galena does not appear to be an important process because of the consistently lower Ag-content throughout most stage 8 galena, compared to that in stages 3 and 4a. Furthermore, if Ag-remobilization from galena did occur during retrograde reactions, this mechanism had selectively avoided the earlier stages 3 and 4a, which seems unlikely.

5.4 Keno Hill District Spatial Zonation

Lynch (1989) and Lynch et al. (1990) identified lateral spatial variations of O, C, and S isotopic compositions, tetrahedrite mineral chemistry, and 7 zones of mineral assemblages across the district. These zonation patterns are explained in terms of an outward laterally migrating hydrothermal fluid related to the Roop Lakes stock/Mayo Lake pluton, where the f_{S2} and pH decrease from east to west. Results from this study corroborate some of the spatial zonation; including district wide lateral variations in the $\delta^{13}C$ and $\delta^{18}O$ isotopic composition of siderite, as well as vertical variations in the tetrahedrite mineral chemistry recognized in this study. However, 5 of the 7 mineralogical assemblage zones (i.e. 3 to 7) documented by Lynch (1989) are interpreted as different temporal stages in this study, rather than an effect of lateral zonation.

No data presented in this study can directly tie the Keno Hill Ag mineralizing system with Roop Lakes stock/Mayo Lake pluton magmatism. For example, none of the documented Pb isotopic compositions of TTB intrusions correspond to either end-member of the galena Pb isotope mixing trend from this study. However, the district wide trends of the C, O, and S isotopic compositions (Lynch, 1989; Lynch et al. 1990; this study), as well as mineral chemistry zonation (see below) suggest a genetic link between the two.

The district-wide variations of the C and O isotopic compositions of siderite identified in this study are similar to that documented by Lynch et al. (1990), with an increase of $\delta^{13}C$ to the north, on average <+2 ‰, and a decreasing $\delta^{18}O$ trend to the west, by approximately -3 ‰ (Figure 4-15). A shift to more reducing conditions and/or an increase in pH could be responsible for the increasing $\delta^{13}C$ (Ohmoto, 1972). Boiling may cause an increase in pH (Drummond and Ohmoto, 1985); however this interpretation is not supported by the fluid inclusion observations. Alternatively, as graphite may have a reducing effect on fluids (Ohmoto and Kerrick, 1977), the fluid in the northern area may have been locally buffered to a more reduced state compared to that in the Keno Hill quartzite. The Earn Group sediments present in the northern part of the Keno Hill district are primarily comprised of phyllitic shale, and typically contain graphite (more so than the Keno Hill quartzite), which could be responsible for the proposed more reducing conditions. The decreasing $\delta^{18}O$ trend to the west may be explained by the presence

of a fluid with a more negative $\delta^{18}O$ value. The presence of meteoric water with a relatively more negative $\delta^{18}O$ isotopic composition is evident from stage 12 calcite. A greater influx of meteoric fluid in the west is possible (also proposed by Lynch, 1989 and Lynch et al., 1990).

The siderite mineral chemistry is essentially consistent throughout the Bellekeno vein and paragenesis, however varies on a district scale. With the exception of one Wernecke vein sample, there is an overall relative increase of Mn- and Mg-content, associated with a decrease in Fe-content in the siderite to the north and west of the Bellekeno vein (Figure 4-5). These variations in siderite chemistry may be related to changes in the physiochemical fluid conditions (such as oxidation state/pH/temperature?) across the district, a different fluid component influx, or fractional mineralization. Fractional mineralization, whereby some elements are preferentially precipitated early or are subsequently depleted in the fluid, is supported by the sequence of carbonates deposited, typically in the succession of siderite-ankerite-calcite. Furthermore, within siderite, the mineral chemistry commonly becomes relatively Mg, Mn, (and Ca)-enriched towards the crystal edges. These observations suggest that the preferential order of carbonate cations precipitated in the Keno Hill hydrothermal system follows: Fe-Mn-Mg-Ca. Fractional mineralization trends are also observed in variations of the tetrahedrite mineral chemistry (see below).

The $\delta^{34}S$ trend of vein sulfides varies on a district scale, decreasing from east to west, and south to north away from the Roop Lakes stock/Mayo Lake pluton (Figure 4-17). Controls on the S isotopic composition may be explained in terms of the S source (i.e. initial $\delta^{34}S\Sigma_S$) and/or physiochemical changes of the fluid, such as: temperature, pH, and/or f_{O2}. (Rye and Ohmoto, 1974). In the Bellekeno vein, an average $\delta^{34}S_{HS^-}$ of -0.2 ‰ is associated with stage 8 galena; assuming a similar temperature of mineralization of 250˚C in the Silver King area, the $\delta^{34}S_{HS^-}$ would be -9.5 ‰. There are no indications of a fluid with an isotopically lighter $\delta^{34}S$ composition in the west or north (Lynch et al., 1990; Boyle, 1970), and the effects of decreasing fluid temperature alone cannot adequately explain this relatively large negative shift. Alternatively, an increase in oxidation state or pH could explain the observed decreasing $\delta^{34}S$ trend to the west. Furthermore, an increase in fluid oxidation state is supported by the presence of sulfate minerals during later stages in the paragenesis (i.e. stage 8 or later). An increase in pH seems equally plausible and such a change in fluid chemistry is documented as a potential control on carbonate and base-metal precipitation (Seward and Barnes, 1997). An oxidizing effect on the fluid may occur as a result of boiling (Drummond and Ohmoto, 1985), or alternatively by an influx of more oxygenated fluid, such as fresh meteoric water. Again considering that there is no evidence for boiling, and an influx of meteoric water is apparent from stage 12 calcite, the meteoric mixing option is preferred (also proposed by Lynch et al., 1990).

Variations in fluid chemistry throughout the district are also apparent from fluid inclusion observations (Figure 4-11). Stage 6 siderite fluid inclusions from the Silver King vein have a slightly hotter Th, compared to the range for that from the Bellekeno vein samples. Alternatively, stage 6 siderite from the Alice vein has a similar salinity, but a relatively cooler Th, between 250 and 230˚C, compared to most Bellekeno stage 6 siderite samples. Curiously, stage 7 sphalerite fluid

inclusions from the Alice vein (the same sample as the stage 6 siderite) are hotter and less saline than the range defined by the Bellekeno stage 7 sphalerite; these data largely overlap with the range defined by Bellekeno stage 9 siderite. Most of stage 9 sphalerite fluid inclusions from the Pool vein also define a cluster hotter and less saline than the range defined by the Bellekeno samples. These observations suggests that fluid temperatures, remained essentially the same throughout the district, and that a decreasing temperature gradient from east to west is not important. Furthermore, fluid salinity may vary throughout the district, this may be an indication of heterogeneous fluid mixing at the district scale.

The subtle vertical and lateral trends of the tetrahedrite mineral chemistry are apparent at both the vein and district scale, respectively. In the Bellekeno vein, tetrahedrite varies from more Cu-rich at depth to relatively more Ag-rich at higher elevations (Figure 4-8 A, B, and C). Furthermore, throughout the Keno Hill district there is a trend to slightly more Ag-rich tetrahedrite to the north and west of the Bellekeno vein (Figure 5-5), also documented by Lynch (1989). Hackbarth and Petersen (1984) explained the spatial zoning of tetrahedrite mineral chemistry in terms of fractional mineralization, where Cu and As are preferentially precipitated first, closest to the hydrothermal fluid source, and subsequently the relatively Ag- and Sb-enriched residual fluid then precipitates with tetrahedrite later and more distally. Sack et al. (2003) explained the district wide variations of increasing Ag- and Fe-content in tetrahedrite in terms of deposition in 3 different conditions: 1) early and higher temperature of mineralization (>400˚C) for Ag- and Zn-rich tetrahedrite; 2) the majority of the tetrahedrite indicates temperatures of mineralization between 310˚C and 250˚C; and 3) lower temperature (<200˚C) from retrograde mineralization. The later and lower temperature stage of mineralization for Ag- and Fe-rich tetrahedrite is consistent with re-equilibration with sphalerite, where tetrahedrite may exsolved into both Ag-rich and –poor regions. Fluid inclusion analyses from this study support a similar range sulfosalt mineralization temperatures to between 315°C and 245°C, based the range of pressure corrected Th measurements from stages 6 and 7. The different temperatures of tetrahedrite mineralization determined by Sack et al. (2003) compared to this study may be the result of re-equilibration reactions affecting the tetrahedrite mineral chemistry. Both the vertical and lateral zonation of the Ag- and Cu-content of tetrahedrite in the Keno Hill district appear to be consistent with fractional mineralization and evolving fluid chemistry.

In summary, the Keno Hill district Ag-Pb-Zn vein mineralization shows evidence for at least 4 different hydrothermal fluids, which define a paragenetically later and different hydrothermal event than that directly related to IRG mineralization in the TTB. The age of Keno Hill vein mineralization and spatial patters of mineral chemistry continue to suggest that some relationship with TTB magmatism exists. However, the effects of local lithology, and temporal evolution of the involved fluids may explain district wide variations in mineral chemistry. Figure 5-6 summarizes the temporal evolution of the Keno Hill hydrothermal fluid system.

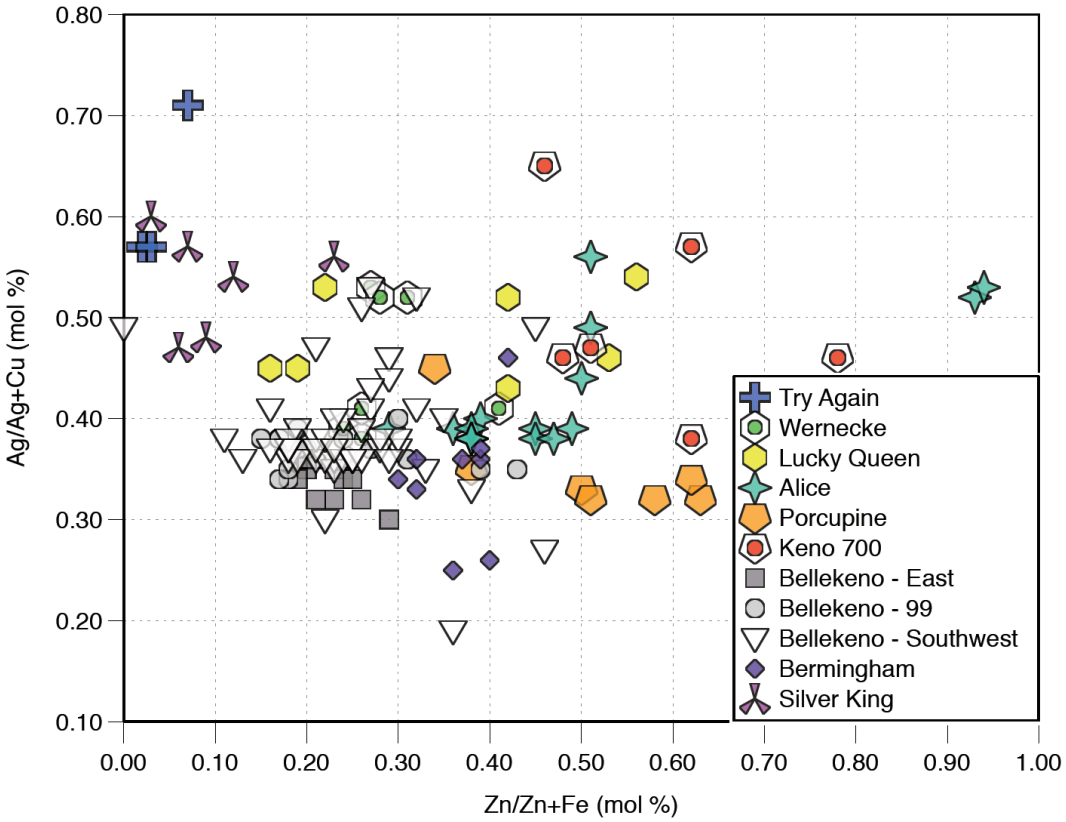

Figure 5-5. Keno Hill district tetrahedrite mineral chemistry, molar Ag/Ag+Cu vs. Zn/Zn+Fe values show spatial variations throughout the district. Relatively Ag-rich tetrahedrite occurs in veins Try Again, Wernecke, and, Lucky Queen are in the north of the district, and also from the Silver King vein in the west of the district. In comparison, the Bellekeno and Bermingham veins located in the southeast and central of the district, respectively, are relatively more Ag-poor tetrahedrite. Refer to Figure 2-4 for vein locations.

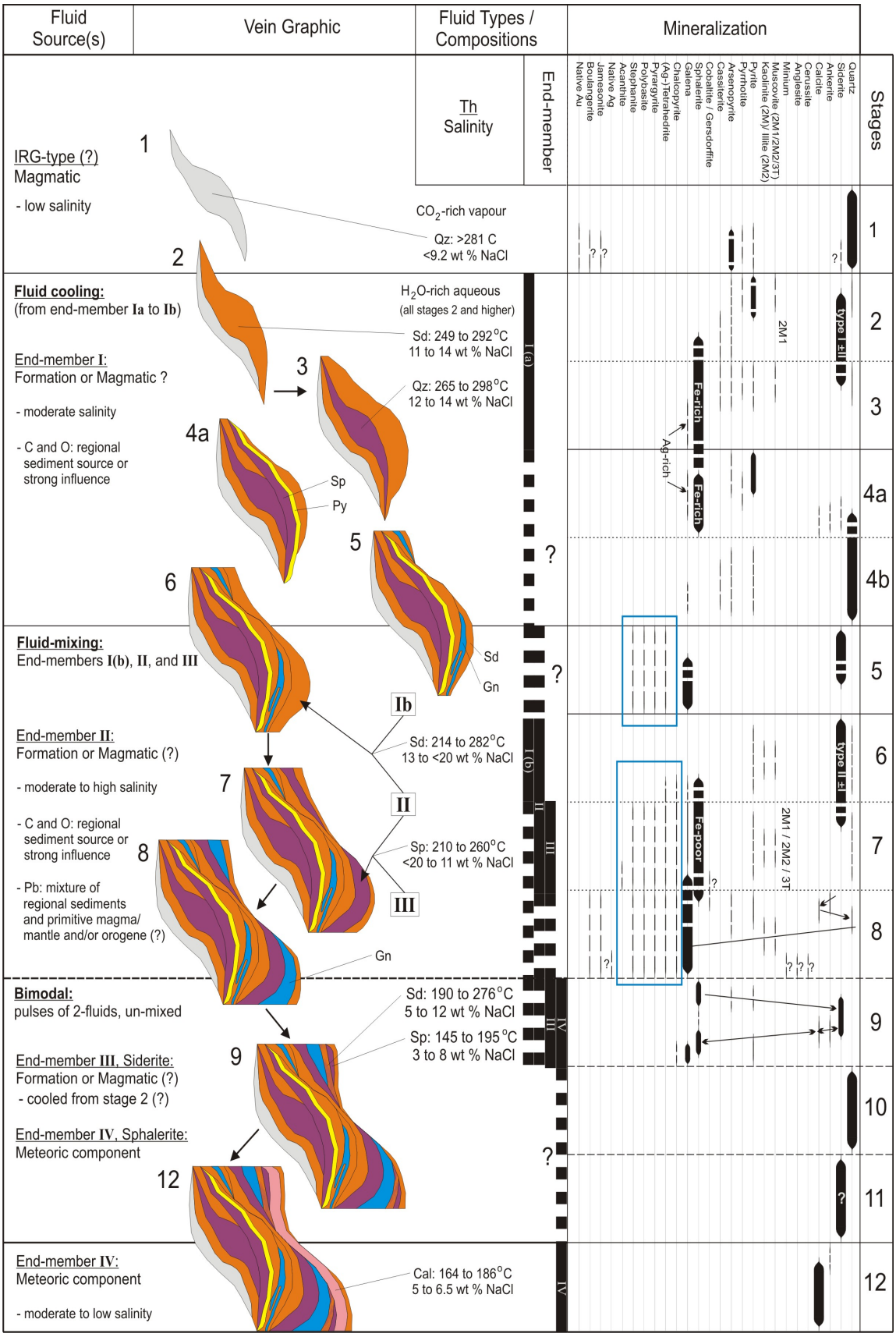
Fluid Source(s)
Vein Graphic
Fluid Types / Compositions
Mineralization
Th Salinity
End-member
Stages
Quartz
Siderite
Ankerite
Calcite
Cerussite
Anglesite
Minium
Muscovite (2M1/2M2/3T)
Kaolinite (2M) / Illite (2M2)
Pyrite
Pyrrhotite
Arsenopyrite
Cassiterite
Cobaltite / Gersdorffite
Sphalerite
Galena
Chalcopyrite
(Ag-)Tetrahedrite
Pyrargyrite
Polybasite
Stephanite
Acanthite
Native Ag
Jamesonite
Boulangerite
Native Au
IRG-type (?)
Magmatic
- low salinity
1
CO2-rich vapour
Qz: >281 C
<9.2 wt % NaCl
2
Fluid cooling:
(from end-member Ia to Ib)
H2O-rich aqueous
(all stages 2 and higher)
Sd: 249 to 292°C
11 to 14 wt % NaCl
End-member I:
Formation or Magmatic ?
- moderate salinity
- C and O: regional sediment source or strong influence
3
Qz: 265 to 298°C
12 to 14 wt % NaCl
4a
Sp
Py
5
6
Fluid-mixing:
End-members I(b), II, and III
Sd
Gn
Ib
End-member II:
Formation or Magmatic (?)
- moderate to high salinity
- C and O: regional sediment source or strong influence
- Pb: mixture of regional sediments and primitive magma/ mantle and/or orogene (?)
Sd: 214 to 282°C
13 to <20 wt % NaCl
7
II
Sp: 210 to 260°C
<20 to 11 wt % NaCl
8
III
Gn
Bimodal:
pulses of 2-fluids, un-mixed
Sd: 190 to 276°C
5 to 12 wt % NaCl
Sp: 145 to 195°C
3 to 8 wt % NaCl
End-member III, Siderite:
Formation or Magmatic (?)
- cooled from stage 2 (?)
9
End-member IV, Sphalerite:
Meteoric component
12
End-member IV:
Meteoric component
- moderate to low salinity
Cal: 164 to 186°C
5 to 6.5 wt % NaCl
I (a)
I (b)
II
III
IV
2M1
type I ±II
Fe-rich
Ag-rich
Fe-rich
type II ±I
2M1 / 2M2 / 3T
Fe-poor
1
2
3
4a
4b
5
6
7
8
9
10
11
12

Figure 5-6. Summary schematic diagram of Keno Hill district showing fluid end-members, evolution, inferred sources, and associated mineralogy. Principal Ag-bearing minerals are highlighted within blue squares in the mineralization column. Vein graphics exhibit a hypothetical evolution of paragenetic vein growth, only principal minerals shown: siderite (Sd) = orange; calcite (Cal) = pink; sphalerite (Sp) = purple; pyrite (Py) = yellow; galena (Gn) = blue. The stage 1 fluid is a vapour-phase, high-temperature (Th >300°C), low-salinity (<9.2 wt % NaCl equiv.), CO_2-rich, and associated with the quartz-aresonopyrite-pyrite assemblage. Stage 1 fluid is reminiscent of intrusion-related gold type fluids, which are are believed to have exsolved from TTB magma. The main stages of mineralization (i.e. 2 to 8) are associated with the most significant Ag-Pb-Zn mineralization; all fluid inclusions are liquid-phase, aqueous H_2O-rich, some of which are CO_2-bearing based on the presence of clathrate. Stages 2 and 3 are associated with a fluid composition between end-members Ia and Ib, Th and salinity ranges from 292 to 249°C, and 11 to 14 wt % NaCl equiv., respectively. The influx of fluid end-member II during stages 6 and 7, has an approximate fluid Th and salinity of 260 to 240°C, and 18 to <20 wt % NaCl equiv. Mixing of end-member II with end-members Ib and III is supported by a range of fluid composition within a single FIA. End-member III appears to be the evolved equivalent from end-member Ia. Based on textural and mineral chemistry relationships stages 5 and 8 are inferred to be associated with stages 6 and 7, and also related to the influx of fluid end-member II. Ag-bearing tetrahedrite and other sulfosalts are largely restricted to stages 5 and 8 deposited with galena. Fluid mixing, and associated dilution is likely responsible for the destabilization of Cl-complexes, which is inferred to be the main control on the aqueous transportation of Pb and Ag, and is the principal mechanism of Ag-mineralization. Two distinct populations of fluid compositions, from both siderite and sphalerite characterize stage 9 fluids. The complexly banded mineral texture unique to stage 9 is believed to exhibit multiple pulses of each of these two fluid types that however did not mix. Stages 9 and 12 fluid characterize end-member IV; Th and salinity ranges from 195 to 145°C, and 3 to 8 wt % NaCl equiv., respectively. A meteoric component for end-member IV is based on the $\delta^{18}O$ values from stage 12 calcite.

8.0 Conclusions

There is conflicting evidence in terms of identifying a relationship between the Keno Hill Ag-Pb-Zn mineralization and the TTB (Mayo plutonic suite) magmatism. Mineral chemistry suggests the hydrothermal fluids associated with Ag-Pb-Zn mineralization has been either derived from a sedimentary source or strongly influenced by the regional sediments, based on C, O, and S isotopic compositions. The Pb isotopic compositions exhibit a mixing trend between an inferred sedimentary reservoir a deep-seated intrusion with a mantle component. The age of the Keno Hill Ag-Pb-Zn mineralization and spatial patterns of mineral chemistry suggests that some genetic or temporal relationship exists. However, some spatial variations throughout the district may also be explained in terms fractional mineralization and physiochemical changes of the hydrothermal fluid influenced by the host lithology and the influx of fluids with different compositions.

The Keno Hill Ag-Pb-Zn vein mineralization and associated gangue mineral assemblages are paragenetically later than IRG-type mineralization, representing a distinct and younger hydrothermal event. Five different fluid end-members, defined by homogenization temperatures and salinity are present throughout the paragenesis.

Within the Bellekeno vein, the main stages of mineralization (stages 2 to 8), define 2 generalized repeating sequences of siderite-sphalerite-galena dominated mineral assemblages. A pressure correction between 325 and 675 bars, corresponding to +25 to +55˚C to the homogenization temperatures is supported by 2 independent geothermometers. Fluid inclusion analyses record the progressive cooling of a hydrothermal system from 290 to 220˚C (homogenization temperature), with fluid salinity ranging between approximately 8 to <20 wt % NaCl equiv., characterized by at least 2 different hydrothermal fluid compositions. Fluid end-member Ia/b appears to have evolved and cooled to a composition defined by end-member III, from 290 to 220°C (homogenization temperature), with a salinity between 8 and 12 wt % NaCl equiv. During stages 6 and 7, the influx of fluid end-member II, having a composition of approximately 250°C (homogenization temperature) and salinity of <20 wt % NaCl equiv., partially mixed with fluid end-members Ia/b and III. Silver-mineralization predominantly occurs with galena-rich mineral assemblages (stages 5 and 8) and are also associated with stages 6 and 7. The effects of decreasing temperature and dilution associated with fluid mixing appear to be the principal mechanisms controlling Ag-Pb-Zn mineralization. The moderately saline hydrothermal fluids from the main stages show evidence of being either derived or at least chemically influenced by the surrounding host rock, and are inferred to be either formation or magmatic in origin. The influx of a late stage fluid with a meteoric component at approximately 160˚C (homogenization temperature) effectively defines the end of the main stage mineralization and does not appear to be associated with any significant Ag-mineralization.

9.0 Bibliography

Abbott, J. G., Gordey, S. P., and Templeman-Kluit, D. J., 1986, Setting of stratiform, sediment hosted lead-zinc deposits in Yukon and northeastern British Columbia: Mineral deposits of the northern Cordillera, Canadian Institute of Mining and Metallurgy (ed. J. A. Morin), Special Volume 37, p. 1-18.

Anderson, R. G., 1987, Plutonic rocks in the Dawson map area, Yukon Territory: Geological Survey of Canada, Paper 87-1A, p. 689-697.

Anikina, E. Y., Gamyanin, G. N., and Bortnikov, N. S., 2010, Sulfur Isotopic Composition of Sulfides at the Mangazeya Silver Desposit, Eastern Sakha-Yakutia, Russia: Geology of Ore Deposits, v. 52, p. 479-495.

Baker, T., 2002, Emplacement depth and carbon dioxide-rich fluid inclusions in intrusion-related gold deposits: Economic Geology, v. 97, p. 1111-1117.

Baker, T., and Lang, J. R., 2001, Fluid inclusion characteristics fo intrusion-related gold mineralization, Tombstone-Tungsten magmatic belt, Yukon Territory, Canada: Mineralium Deposita, v. 36, p. 563-582.

Baker, T., Ebert, S., Rombach, C., and Ryan, C. G., 2006, Chemical Compositions of Fluid Inclusions in Intrusion-Related Gold System, Alaska and Yukon, Using PIXE Microanalysis: Economic Geology, v. 101, p. 311-327.

Balabin, A. I., and Sack, R. O., 2000, Thermodynamics of (Zn,Fe)S sphalerite. A CVM approach with large basis clusters: Mineralogical Magazine, v. 64, p. 923-943.

Barton, P. B., and Bethke, J. P. M., 1987, Chalcopyrite disease in sphalerite: Pathology and epidemiology: American Mineralogist, v. 72, p. 451-467.

Beaudoin, G., and Sangster, D. F., 1992, A Descriptive Model for Silver-Lead-Zinc Veins in Clastic Metasedimentary Terranes: Economic Geology, v. 87, p. 1005-1021.

Becker, M.L., Rasbury, E.T., Meyers, W.J., and Hanson, G.N., 2002, U-Pb calcite age of the Late Permian Castile Formation, Delaware Basin: a constraint on the age of the Permian-Triassic boundary (?): Earth and Planetary Science Letters, v.203, p. 681-689.

Bodnar, R. J., 1993, Revised equation and table for determining the freezing point depression of H_2O-NaCl solutions: Geochimica et Cosmochimica Acta, v. 57, p. 683-684.

Borisenko, A. S., Pavlova, G. G., Borovikov, A. A., and Obolenskiy, A. A., 1999, Ag-Sb Deposits of Yustid Depression, Eastern Russia and Northwest Mongolia: International Geology Review, v. 41, p. 639-664.

Borisenko, A. S., Pavlova, G. G., Borovikov, A. A., Vladimirov, A. G., and Mortsev, N. K., 2000, Silver Deposits of the Pamir Region, Tajikistan: Metallogeny, Mineralogy, and Genesis: International Geology Review, v. 42, p. 702-723.

Boyle, R.W., 1965, Geology, geochemistry, and origin of the lead-zinc-silver deposits of the Keno Hill-Galena Hill area, Yukon Territory (with short descriptions of the tin, tungsten, and gold deposits): Geological Survey of Canada, Bulletin 111, 302 p.

Boyle, R. W., Wanless, R. K., and Stevens, R. D., 1970, Sulfur Isotope Investigation of the Lead-Zinc-Silver-Cadmium Deposit of the Keno Hill-Galena Hill Area, Yukon, Canada: Economic Geology, v. 65, p. 1-10.

Christensen, J.N., Halliday, A.N., Leigh, K.E., Randell, R.N., and Kesler, S.E. 1995, Direct dating of sulfides by Rb-Sr: A critical test using the Polaris Mississippi Valley-type Zn-Pb deposit: Geochimica et Cosmochimica Acta, v. 59, p. 5191-5197.

Chutas, N. I., Kress, V. C., Ghiorso, M. S., and Sack, R. O., 2008, A solution model for high-temperature PbS-$AgSbS_2$-$AgBiS_2$ galena: American Mineralogist, v. 93, p. 1630-1640.

Diamond, L. W., 1992, Stability of CO_2 clathrate hydrate + CO_2 liquid + CO_2 vapour _ aqueous KCl-NaCl solutions: Experimental determination and application to salinity estimates of fluid inclusions: Geochimica et Cosmochimica Acta, v. 56, p. 273-280.

Doubrovine, P. V. and Tarduno, J. A., 2008, A revised kinematic model for the relative motion between Pacific oceanic plates and North America since the Late Cretaceous: Journal of Geophysical Research, v. 113, B12101, 20 p.

Drummond, S. E., and Ohmoto, H., 1985, Chemical Evolution and Mineral Deposition in Boiling Hydrothermal Systems: Economic Geology, v. 80, p. 126-147.

Engebretson, D. C., Cox, A., and Gordon, R. G., 1985, Relative motions between oceanic and continental plates in the Pacific Basin: Geological Society of America, Special Paper, no. 206, v. 59, 59 p.

Farmer, G. L., and DePaolo, D. J., 1997, Sources of Hydrothermal Components: Heavy Isotopes, In: Geochemistry of Hydrothermal Ore Deposits (ed. H. L. Barnes), p. 31-61.

Faure, G., 1986, Principles of isotope geology, 2nd ed.: New York (ed. John Wiley), 589 p.

Gabrielse, H., 1967, Tectonic Evolution of the Northern Canadian Cordillera, Canadian Journal of Earth Sciences, v. 4, p. 271-298.

Gabrielse, H., 1985, Major dextral transcurrent displacements along the northern Rocky Mountain Trench and related lineaments in north-central British Columbia: Geological Society of America Bulletin, v. 96, p. 1-14.

Gabrielse, H, and Yorath, C. J., 1991, Tectonic synthesis, In: Geology of the Cordilleran Orogen of Canada, Ch. 18, (eds. H. Gabrielse and C. J. Yorath), Geological Survey of Canada, no. 4, p. 329-371.

Goldfarb, R. J., Marsh, E. E., Hart, C. J. R., Mair, J. L., Miller, M. L., and Johnson, C., 2007, Geology and Origin of Epigenetic Lode Gold Deposits, Tintina Gold Province, Alaska and Yukon, In: Recent U.S. Geological Survey Studies in the Tintina Gold Province, Alaska, United States, and Yukon, Canada – Results of a 5-Year Project: U. S. Geological Survey, Scientific Investigations Report 2007-5289-A, p. A1-A18.

Goldstein, R. H., and Reynolds, T. J., 1994, Systematics of Fluid Inclusions in Diagenetic Minerals: Society for Sedimentary Geology, SEPM Short Course 31, 199 p.

Goodfellow, W. D., Cecile, M. P., and Leybourne, M. I., 1995, Geochemistry, petrogenesis, and tectonic setting of lower Paleozoic alkalic and potassic volcanic rocks, Northern Canadian Cordilleran Miogeocline, Canadian Journal of Earth Sciences, v. 32, p. 1236-1254.

Godwin, C. I., Sinclair, A. J., and Ryan, B. D., 1982, Lead Isotope Models for the Genesis of Carbonate-Hosted Zn-Pb, Shale-Hosted Ba-Zn-Pb, and Silver-rich Deposits in the Northern Canadian Cordillera: Economic Geology, v. 77, p. 82-94.

Godwin, C. I., and Sinclair, A. J., 1982, Average Lead Isotope Growth Curves for Shale-Hosted Zinc-Lead Deposits, Canadian Cordillera: Economic Geology, v. 77, p. 675-690.

Gordey, S. P., and Anderson, R. G., 1993, Evolution of the Northern Cordilleran Miogeocline, Nahanni Map Area (105I), Yukon and Northwest Territories: Geological Survey of Canada, Memoir 428, 213 p.

Groves, D. I., Goldfarb, R. J., Gebre-Mariam, M., Hagemann, S. G., and Robert, F., 1998, Orogenic gold deposits: A proposed classification in the context of their crustal distribution and relationship to other gold deposit types: Ore Geology Reviews, v. 13, p. 7-27.

Groves, D.I., Goldfarb, R. J., Robert, F., and Hart, C.J.R., 2003, Gold Deposits in Metamorphic Belts: Overview of Current Understanding, Outstanding Problems, Future Research, and Exploration Significance: Economic Geology, v. 98, p. 1-29.

Hackbarth, C. J., and Petersen, U., 1984, A Fractional Crystallization Model for the Deposition of Argentian Tetrahedrite: Economic Geology, v. 79, p. 448-460.

Hart, C. J. R., McCoy, D., Goldfarb, R. J., Smith, M., Roberts, P., Hulstein, R., Bakke, A. A., and Bundtsen, T. K., 2002, Geology, exploration and discovery in the Tintina gold province, Alaska and Yukon: Society of Economic Geologists Special Publication 9: p. 241-274.

Hart, C. J. R., Mair, J. L., Goldfarb, R. J., and Groves, D. I., 2004a, Source and redox controls on metallogenic variations in intrusion-related ore systems, Tombstone-Tungsten Belt, Yukon Territory, Canada, Transactions of the Royal Society of Edinburgh: Earth Sciences, v. 95, p. 339-356.

Hart, C. J. R., Goldfarb, R. J., Lewis, L. L., Mair, J. L., 2004b, The Northern Cordilleran Mid-Cretaceous Plutonic Province: Ilmenite/Magnetite-series Granitoids and Intrusion-related Mineralisation: Resource Geology, v. 54, p. 253-280.

Hart, C. J. R., 2007, Reduced Intrusion-related Gold Systems; In: Mineral deposits of Canada (ed. Goodfellow, W. D.); A Synthesis of Major Deposit Types, District Metallogeny, the Evolution of Geological Provinces, and Exploration Methods; Geological Association of Canada, Mineral Deposits Division, Special Publication No. 5, p. 95-112.

Hawke, M. M., Thompson, A., J. B., and Thompson, J. F. H., 1996, Atlas of Alteration: Geological Association of Canada, Mineral Deposits Division (eds. Thompson, A. J. B., and Thompson, J. F. H.), 118 p.

Hedenquist, J. W., and Henley, R. W., 1985, The importance of CO_2 on freezing point measurements of fluid inclusions; evidence from active geothermal systems and implications for epithermal ore deposition: Economic Geology, v. 80, p. 1379-1406.

Heffernan, R.S., Mortensen, J.K., Gabites, J.E. and Sterenberg, V., 2005, Lead isotope signatures of Tintina Gold Province intrusions and associated mineral deposits from southeastern Yukon and southwestern Northwest Territories: Implications for exploration in the southeastern Tintina Gold Province, In: Yukon Exploration and Geology 2004, D.S. Emond, L.L. Lewis and G.D. Bradshaw (eds.), Yukon Geological Survey, p. 121-128.

Hut, G., 1987, Natural Abundance of the Stable Isotopes of C, O, and H; In: Consultants' Group Meeting on Stable Isotope Reference Samples for Geochemical and Hydrological Investigation, Report to the Director General, International Atomic Energy Agency, Vienna, p. 89-124.

Hutchison, M. N., and Scott, S. D., 1981, Sphalerite Geobarometry in the Cu-Fe-Zn-S System: Economic Geology, v. 76, p. 143-153.

Jaffey, A.H., Flynn, K.F., Glendenin, L.E., Bentley, W.C., and Essling, A.M., 1971, Precision Measurement of Half-lives and Specific Activities of ^{235}U and ^{238}U: Physical Reviews, C, v. 4, p. 1889-1906.

Jarosewich, E., 2002, Smithsonian Microbeam Standards: Journal of Research of the National Institute of Standards and Technology, v. 107, p. 681-685.

Konstantinov, M. M., Rosenblum, I. S., and Strujkov, S. F., 1993, Types of Epithermal

Silver Deposits, Northeastern Russia: Economic Geology, v. 88, p. 1797-1809.
Lang, J. R., and Baker, T., 2001, Intrusion-related gold systems: the present level of understanding: Mineralium Deposita, v. 36, p. 477-489.
Lawler, J. P., and Crawford, M. L., 1983, Stretching of Fluid Inclusions Resulting from a Low-Temperature Microthermometric Technique: Economic Geology, v. 78, p. 527-529.
LeRoux, L.J., and Glendenin, L.L., 1963, Half-life of Thorium-232, in: Proceedings of the National Meeting on Nuclear Energy, Pretoria, South Africa, April, p. 77-78.
Liu, W., Li, X.-J., and Tan, J., 2001, Petrogenetic and Metallogenetic Background of the Dajing Cu-Sn-Ag-Pb-Zn Ore Deposit, Inner Mongolia, and Characteristics of the Mineralizing Fluid: Resource Geology, v. 51, p. 321-331.
Lund, K., 2008, Geometry of the Neoproterozoic and Paleozoic rift margin of western Laurentia: Implications for mineral deposit settings: Geosphere, v. 4, p. 429-444.
Lynch, J.V.G., 1989, Large-scale hydrothermal zoning reflected in the tetrahedrite-freibergite solid solution, Keno Hill Ag-Pb-Zn district, Yukon: Canadian Mineralogist, v. 27, p. 383-400.
Lynch, J.V.G., 1989b, Hydrothermal zoning in the Keno Hill Ag-Pb-Zn Vein System, Yukon; a Study in Structural Geology, Mineralogy, Fluid Inclusions, and Stable Isotope Geochemistry, Ph. D. thesis: University of Alberta, 219 p.
Lynch, J.V.G., Longstaffe, F.J., and Nesbitt, B.E., 1990, Stable isotopic and fluid inclusion indications of large-scale hydrothermal paleoflow, boiling, and fluid mixing in the Keno Hill Ab-Pb-Zn district, Yukon Territory, Canada: Geochimica et Cosmochimica Acta, v. 54, p. 1045-1059.
Lynch, G, 2009, Pressure-depth relationships of the Roop Lakes Stock and Keno Hill Ag-Pb-Zn veins: Yukon Exploration and Geology 2009, p. 229-236.
Mair, J. L., Hart, C. J. R., Goldfarb, R. J., O'Dea, M., and Harris, S., 2000, Geology and metallogenic signature of gold occurrences at Scheelite Dome, Tombstone gold belt, Yukon, In: Yukon Exploration and Geology 1999, (eds. D. S. Edmond, and L. H. Weston), Exploration and Geological Services Division, Yukon, Indian and Northern Affairs Canada, p. 165-176.
Mair, J. L., Goldfarb, R. J., Johnson, C. A., Hart, C. J. R., and Marsh, E. E., 2006, Geochemical Constraints on the Genesis of the Scheelite Dome Intrusion-Related Gold Deposit, Tombstone Gold Belt, Yukon, Canada: Economic Geology, v. 101, p. 523-553.
Mair, J. L., Farmer, G. L., Groves, D. I., Hart, C. J. R., and Goldfarb, R. J., 2011, Petrogenesis of Post collisional Magmatism at Scheelite Dome, Yukon, Canada: Evidence for a Lithospheric Mantle Source for Magmas Associated with Intrusion-Related Gold Systems: Economic Geology, v. 106, p. 451-480.
Maloof, T. L., Baker, T., and Thompson, J. F. H., 2001, The Dublin Gulch intrusion-hosted gold deposit, Tombstone plutonic suite, Yukon Territory, Canada: Mineralium Desposita, v. 36, p. 583-593.
Marsh, E. E., Goldfarb, R. J., Hart, C. J. R., and Johnson, C. A., 2003, Geology and geochemistry of the Clear Creek intrusion-related gold occurrences, Tintina Gold Province, Yukon, Canada: Canadian Journal of Earth Sciences, v. 40, p. 681-699.
McDougall, I., and Harrison, T.M., 1988, Geochronology and thermochronology by the $^{40}Ar/^{39}Ar$ method: Oxford University Press, New York, 212 p.
McTaggart, K. C., 1960, The Geology of Keno and Galena Hills, Yukon Territory (105M): Geological Survey of Canada, Bulletin 58, 37 p.

Mizuta, T., and Scott, S. D., 1997, Kinetics of Iron Depletion near Pyrrhotite and Chalcopyrite Inclusions in Sphalerite: The Sphalerite Speedometer: Economic Geology, v. 92, p. 772-783.

Monger, J. W. H., Price, R. A., and Tempelman-Kluit, D. J., 1982, Tectonic accretion and the origin of the two major metamorphic and plutonic welts in the Canadian Cordillera: Geology, v. 10, p. 70-75.

Mortensen, J. K., and Thompson, R. I., 1990, A U-Pb zircon-baddeleyite age for a differentiated mafic sill in the Ogilvie Mountains, west-central Yukon Territory, In: Radiogenic Age and Isotopic Studies: Report 3, Geological Survey of Canada, Paper 89-2, p. 23-28.

Mortensen, J. K., Murphy, D. C., Harr, C. J. R., and Anderson, R. G., 1995, Timing, tectonic setting and metallogeny of Early and Mid-Cretaceous magmatism in Yukon Territory: Geological Society of America, Abstracts with Programs, v. 27, no. 5, p. 65.

Mortensen, J. K., Hart, C. J. R., Murphy, D. C., and Heffernan, S., 2000, Temporal evolution of early and mid-Cretaceous magmatism in the Tintina Gold belt: British Columbia and Yukon Chamber of Mines, Special Volume 2, p. 49-57.

Muehlenbachs, K., 1998, The oxygen isotopic composition of the oceans, sediments and the seafloor: Chemical Geology, v. 145, p. 263-273.

Mulshaw, S. C., Puig, C., Spiro, B., and Buchanan, D. L., 1997, Genesis of Epizonal Ag Vein Mineralization at San Bartolome in Central Ecuador: Textural Evidence, Fluid Inclusions, and Stable Isotope Geochemistry: Economic Geology, v. 92, p. 210-227.

Murphy, D., 1997, Geology of the McQuesten River Region, Northern McQuesten and Mayo Map Area, Yukon Territory (115P/14, 15, 16; 105M/13, 14): Exploration and Geological Services Division, Yukon, Indian and Northern Affairs Canada, Bulletin 6, 95 p.

Nakai, S., Halliday, A.N., Kesler, S.E., and Jones, H.D., 1990, Rb-Sr dating of sphalerites from Tennessee and the genesis of Mississippi Valley type ore deposits: Nature, v. 346, p. 354-357.

Nakai, S., Halliday, A.N., Kesler, S.E., Jones, H.D., Kyle, J.R., and Lane, T.E., 1993, Rb-Sr dating of sphalerite from Mississippi Valley-type (MVT) ore deposits: Geochimica et Cosmochimica Acta, v. 57, p. 417-427.

Nelson, J., Paradis, S., Christensen, J., and Gabites, J., 2002, Canadian Cordilleran Mississippi Valley-type deposits: A case for Devonian-Mississippian back-arc hydrothermal origin: Economic Geology, v. 97, p. 1013-1036.

Neymark, L.A. and Amelin, Y.V., 2008, Natural radionuclide mobility and its influence on U-Th-Pb dating of secondary minerals from the unsaturated zone at Yucca Mountain, Nevada: Geochimica et Cosmochimica Acta, v. 72, p. 2067-2089.

Ohmoto, H., 1972, Systematics of Sulfur and Carbon Isotopes in Hydrothermal Ore Deposits: Economic Geology, v. 67, p. 551-578.

Ohmoto, H., and Goldhaber, M. B., 1997, Sulfur and Carbon Isotopes, In: Geochemistry of Hydrothermal Ore Deposits (ed. H. L. Barnes), 3rd ed., J. Wiley and Sons, p. 517-611.

Ortega, R., Maire, R., Deves, G., and Quinif, Y., 2005, High-resolution mapping of uranium and other trace elements in recrystallized aragonite-calcite speleothems from caves in the Pyrenees (France): Implication for U-series dating: Earth and Planetary Science Letters, v. 237, p. 911-923.

Pavlova, G. G., and Borovikov, A. A., 2010, Silver-Antimony Deposits of Central Asia: physio-chemical model of formation and sources of mineralization: Australian Journal of Earth Sciences, v. 57, p. 755-775.

Plumlee, G. S., and Whitehouse-Veaux, P. H., 1994, Mineralogy, Paragenesis, and Mineral Zoning of the Bulldog Mountain Vein System, Creed District, Colorado: Economic Geology, v. 89, p. 1883-1905.

Polyakov, V. B., and Soultanov, D. M., 2011, New data on equilibrium iron isotope fractionation among sulfides: Constraints on mechanisms of sulfide formation in hydrothermal and igneous systems: Geochimica et Cosmochimica Acta, v. 75, p. 1957-1974.

Pouchou, J.L. and Pichoir, F., 1985, "PAP" f(rZ) procedure for improved quantitative microanalysis, In: Microbeam Analysis (ed. J.T. Armstrong), p. 104-106.

Poulsen, K. H., Mortensen, J. K., and Murphy, D. C., 1997, Styles of intrusion-related gold mineralization in the Dawson-Mayo area, Yukon Territory: Current Research, Geological Survey of Canada, 1997-A, p. 1-10.

Poulton, T. P. and Tempelman-Kluit, D. J., 1982, Recent discoveries of Jurassic fossils in the Lower Schist Division of central Yukon: Geological Survey of Canada Paper, 1997-A, p. 1-10.

Price, R. A., and Carmichael, D. M., 1986, Geometric test for Late Cretaceous-Paleogene intracontinental transform faulting in the Canadian Cordillera: Geology, v. 14, p. 468-471.

Reed, M. H., 1997, Hydrothermal Alteration and it Relationship to Ore Fluid Composition; In: Geochemistry of Hydrothermal Ore Deposits (ed. H. L. Barnes), 3rd ed. J. Wiley and Sons, p. 303-365.

Ripperdan, R. L., 2001, Stratigraphic Variation in Marine Carbonate Carbon Isotope Ratios; In: Reviews in Mineralogy and Geochemistry (eds. J. W. Valley and D. Cole); Stable Isotope Geochemistry, v. 43, no. 1, p. 633-662.

Roedder, E., 1984, Fluid Inclusions: Mineralogical Society of America, Reviews in Mineralogy, v. 12, 644 p.

Roots, C.F., 1997, Geology of Mayo map area, Yukon Territory (105M): Exploration and Geological Services Division, Yukon, Indian and Northern Affairs Canada, Bulletin 7, 82 p.

Rye, R. O., and Ohmoto, H., 1974. Sulfur and Carbon Isotopes and Ore Genesis, A Review: Economic Geology, v. 69, p. 826-842.

Sack, R. O., 2002, Note on "Large-scale Hydrothermal Zoning Reflected in the Tetrahedrite-Freibergite Solid Solution, Keno Hill Ag-Pb-Zn District, Yukon" by J. V. Gregory Lynch: The Canadian Mineralogist, v. 40, p. 1717-1719.

Sack, R. O., and Goodell, P., 2002, Retrograde reactions involving galena and Ag-sulphosalts in a zoned ore deposit, Julcani, Peru: Mineralogical Magazine, v. 66, p. 1043-1062.

Sack, R. O., Lynch, J. V. G., and Foit, Jr. F., 2003, Fahlore as a petrogenetic indicator: Keno Hill Ag-Pb-Zn District, Yukon, Canada: Mineralogical Magazine, v. 67, p. 1023-1038.

Saltus, R. W., 2007, Matching Magnetic Trends and Patterns Across the Tintina Fault, Alaska and Canada – Evidence for Offset of About 490 Kilometers, In: Recent U.S. Geological Survey Studies in the Tintina Gold Province, Alaska, United States, and Yukon, Canada – Results of a 5-Year Project: U. S. Geological Survey, Scientific Investigations Report 2007-5289-C, p. C1-C7.

Schalamuk, I. B. and Logan, M. A. V., 1994, Polymetallic Ag-Te-bearing Paragenesis of the Cerro Negro District, Famatina Range, La Rioja, Argentina: The Canadian Mineralogist, v. 32, p. 667-679.

Schidlowski, M. and Aharon, P., 1992, Carbon cycle and carbon isotope record, geochemical impact of life over 3.8 Ga Earth history, In: Early Organic Evolution Implications for Mineral and Energy Resources (eds. M. Schidlowski, S. Golbic, M. M. Kimberley, D. M. McKirdy, and P. A. Trudinger), Springer-Verlag, Berlin-Heidelberg, p. 147-175.

Scott, S. D., 1983, Chemical behaviour of sphalerite and arsenopyrite in hydrothermal and metamorphic environments: Mineralogical Magazine, v. 47, p. 427-435.

Seal, R. R., 2006, Sulfur Isotope Geochemistry of Sulfide Minerals: Reviews in Mineralogy and Geochemistry, v. 61, p. 633-677.

Seward, T. M., and Barnes, H. L., 1997, Metal Transport by Hydrothermal Ore Fluids; In: Geochemistry of Hydrothermal Ore Deposits (ed. H. L. Barnes), 3rd ed. J. Wiley and Sons, p. 435-486.

Sharp, T. G., and Buseck, P. R., 1993, The distribution of Au and Sb in galena: Inclusions versus solid solution: American Mineralogist, v. 78, p. 85-95.

Shepherd, T. J., Rankin, A. H., and Alderton, D. H. M., 1985, A Practical Guide to Fluid Inclusion Studies: Glasgow, Blackie and Son, 235 p.

Sheppard, S. M. F., 1977, Identification of the origin of ore-forming solutions by the use of stable isotopes: Geological Society, London, Special Publications, v. 7, p. 25-41.

Sillitoe, R. H., and Thompson, J. F. H., 1998, Intrusion-Related Gold Deposits: Types, Tectono-Magmatic Settings and Difficulties of Distinction from Orogenic Gold Deposits: Resource Geology, v. 48, p. 237-250.

Sinclair, A. J., Tessari, O. J., and Harakal, J. E., 1980, Age of Ag-Pb-Zn mineralization, Keno Hill – Galena Hill area, Yukon Territory: Canadian Journal of Earth Sciences, v. 17, p. 1100-1103.

So, C.-S., and Yun, S.-T., 1992, Geochemistry and Genesis of Hydrothermal Au-Ag-Pb-Zn Deposits in the Hwanggangri Mineralized District, Republic of Korea: Economic Geology, v. 87, p. 2056-2084.

Stacey, J.S., and Kramers, J.D., 1975, Approximation of Terrestrial Lead Isotope Evolution by a Two-stage Model: Earth and Planetary Sciences Letters, V. 26, p. 207-221.

Stephens, J. R., Mair, J. L., Oliver, N. H. S., Hart, C. J. R., and Baker, T., 2004, Structural and mechanical controls on intrusion-related deposits of the Tombstone Gold Belt, Yukon, Canada, with comparisons to other vein-hosted ore-deposit types: Journal of Structural Geology, v. 26, p. 1025-1041.

Taylor, H. P., 1974, The Application of Oxygen and Hydrogen Isotope Studies to Problems of Hydrothermal Alteration and Ore Desposition: Economic Geology, v. 69, p. 843-883.

Tempelman-Kluit, D. J., 1979, Transported cataclasite, ophiolite, and granodiorite in Yukon, evidence of arc-continental collision: Geological Society of Canada, Paper 74-14.

Thompson, J. F. H., Sillitoe, R. H., Baker, T., Lang, J. R., and Mortensen, J. K., 1999, Intrusion-related gold deposits associated with tungsten-tin provinces: Mineralium Deposita, v. 34, p. 323-334.

Tupper, D., and Bennett, V., 2010, Observations of polymetallic Ag-Pb-Zn (+/- Au +/- In) mineralization at the Eagle and Fisher vein-faults, airborne total field

magnetics and identification of Tombstone age-equivalent aplite dykes in the Galena Hill area, Keno City, Yukon: Yukon Exploration and Geology 2009, Yukon Geological Research, p. 305-330.

Veizer, J., Ala, D., Azmy, K., Bruckschen, P., Buhl, D., Bruhn, F., Carden, G. A. F., Diener, A., Ebneth, S., Godderis, Y., Jasper, T., Korte, C., Pawellek, F., Podlaha, O., and Strauss, H., 1999, $^{87}Sr/^{86}Sr$, $\delta^{13}C$ and $\delta^{18}O$ evolution of Phanerozoic seawater: Chemical Geology, v. 161, p. 59-88.

White, W. M., Albarede, F., Telouk P., 2000, High-precision analysis of Pb isotope ratios by multi-collector ICP-MS: Chemical Geology, v. 167, p. 257-270.

Whitney D. L., and Evans, B. W., 2010, Abbreviations for names of rock-forming minerals: American Mineralogist, v. 95, p. 185-187.

Wyld, S. J., Umhoefer, P. J., and Wright, J. E., 2006, Reconstructing northern Cordilleran terranes along known Cretaceous and Cenozoic strike-slip faults: Implications for the Baja British Columbia hypothesis and other models, In: Paleogeography of the North American Cordillera: Evidence For and Against Large-Scale Displacements (eds. J. W. Haggart, R. J. Enkin, and J. W. H. Monger), Geological Association of Canada, Special Paper 46, p. 277-298.

Yang, J.H. and Zhou, X.H., 2001, Rb-Sr, Sm-Nd, and Pb isotope systematics of pyrite: Implications for the age and genesis of lode gold deposits: Geology, v. 29, no. 8, p. 711-714.

Zartman, R. E., and Doe, B. R., 1981, Plumbotectonics – The Model: Tectonophysics, v. 75, p. 135-162.

Appendix I

A. Surface sample locations

Coordinates are in UTM WGS 84, Zone 8.

Sample No.	Easting	Northing	Elevation (masl)	Vein/Zone
Alice	492788	7091200		Alice
Try Again	489373	7094602		Try Again
SK-003	472008	7085477	780	Silver King
LQ-007	487602	7091621	1490	Lucky Queen
WRN-008	486324	7092042	1245	Wernecke
BRM-044	478933	7086935	1320	Bermingham
EAG-047	481803	7087187	1691	Eagle
HOM-053	490232	7086893	1345	Homestake
POR-056	489749	7090016	1627	Porcupine
SP-069	489445	7090637	1262	Sign Post

B. Drill-hole sample locations

Coordinates are in UTM WGS 84, Zone 8. Azimuth is True north, magnetic declination is set at 23.5° East.

Drill-hole No.	Easting	Northing	Elevation (masl)	Azimuth	Dip	Total Depth (m)	Vein/Zone	Samples (down-hole depth in meters)
K06-2	472110.65	7085284.10	817.03	330.0	-70.0	430.00	Silver King	110, 111.5, 138.4, 145.5, 168.3, 167.2, 167.4, 178.2, (311.5, 311.6)
K06-24	488604.42	7090727.27	1616.34	310.0	-50.0	74.60	K-Structure/ Shamrock	22.2, 27.6, 33.3, 40
K06-25	488508.27	7090653.71	1610.53	310.0	-60.0	71.60	K-Structure/ Shamrock	36, (36.3, 36.4), 44.8, (49.2, 49.3)
K07-59	473931.89	7086258.43	773.96	320.0	-70.0	384.01	Husky SW	(287.2, 287.3)
K07-60	475237.59	7086596.97	859.49	319.0	-50.0	250.55	Tick	105.5, 111.4, 117.8, 120.1, 121, (121.8, 121.9), 124.7, 138.2
K07-64	487223.67	7086850.04	1117.85	300.0	-45.0	109.70	Bellekeno - East	38.3, 39.8, 41.2, 42.3, 43.8
K07-65	487224.65	7086849.57	1117.75	300.0	-55.0	199.95	Bellekeno - East	123.9, 124.1, 129.1, 129.5, 129.9
K07-66	487225.44	7086849.35	1117.69	300.0	-70.0	200.25	Bellekeno - East	142.6, 142.9, 143.5, 146.1, 146.5, 146.9
K07-67	487226.40	7086849.10	1117.59	300.0	-80.0	255.73	Bellekeno - East	(160.55, 160.6), 160.7, 168.2
K07-70	487229.45	7086849.69	1117.47	260.0	-60.0	190.80	Bellekeno - East	(144.9, 144.95), 145.2, (145.4, 145.45), 145.8, 146.6, 160
K07-76	487212.90	7086910.70	1090.66	300.0	-90.0	274.01	Bellekeno - East	114.9, 115.3, 125
K07-77	475427.04	7086771.21	833.97	310.0	-65.0	374.14	Tick/Schoolhouse	197
K07-79	487212.18	7086910.71	1090.88	300.0	-45.0	163.37	Bellekeno - East	54.7, (55.8, 55.95), (56.5, 56.6), 58.3, 58.5, (60.6, 60.7), 61.2
K07-86	487294.10	7086815.75	1110.94	270.0	-50.0	249.02	Bellekeno - East	223.5, 224, (227.2, 227.4), 231.1, 231.3),

								231.8
K07-87	475720.28	7087032.21	813.16	335.0	-50.0	199.95	Pool/RCMP	(99.3, 99.4), (106.5, 106.75), 136.6, 139.3, (180.8, 181)
K07-88	479809.18	7087803.53	1282.75	320.0	-60.0	203.30	Townsite/Calumet	55.6, 59.6, 60, (61.5, 61.6), 63
K07-95	487259.08	7086533.80	1188.48	295.0	-55.0	450.20	Bellekeno - East	392.3, 401.45, 401.7, 401.8, 402.1, 402.5,
K07-96	487221.94	7086699.66	1165.34	295.0	-65.0	321.87	Bellekeno - East	270, 274.4, 278.9, 279.1, (282.5, 282.6), (283, 283.1), 283.7
K07-101	486763.87	7086146.89	1357.42	285.0	-68.0	394.11	Bellekeno SW	(369, 369.1)
K07-106	486831.65	7086193.75	1341.72	285.0	-65.0	404.77	Bellekeno SW	(402.1, 402.2)
K07-108	487001.88	7086367.17	1289.64	295.0	-52.0	221.89	Bellekeno - East	335, 336.2, 336.5, 337.4
K07-109	487057.14	7086325.70	1283.63	125.0	-65.0	362.10	Bellekeno	84.1, 87.8, 87.9
K07-112	472214.80	7085402.09	799.87	323.0	-65.0	246.28	Silver King	24.6, 29.5, 34, 44.3
K07-114	487553.96	7091317.54	1590.25	305.0	-70.0	282.85	Lucky Queen	189.4, 196, 196.5, 196.9, 202.4, 202.9
K07-122	485730.68	7087229.54	1041.38	335.0	-58.0	206.65	Onek	151.6, (152.6, 152.7), 153.9, (159.6, 159.7), 160.9, (161.7, 161.8), 163.8, 164, 164.9, 165.1
K08-131	470871.52	7086174.50	685.50	319.5	-50.0	139.60	Leo	36, 43.9, 54.8, 63.4, 64.5, (78.5, 78.6), (86.1, 86.3), 99, 129.5
K08-155	485807.61	7087413.80	1069.31	338.0	-82.0	142.34	Onek	115.9, 116, (121, 121.1), 130.7, 131.8, (132, 132.1), 132.5, 135.1
K08-161	487627.26	7091329.03	1593.60	305.0	-55.0	270.36	Lucky Queen	229.5, (229.7, 229.8), (231.2, 231.3), (231.5, 231.6), 231.8, 251.3
K08-165	489550.32	7090167.95	1653.79	295.0	-60.0	252.37	Keno 700	143, 173.8, 174.8, 176.5, (177.4, 177.6), 182.5
K08-166	487629.37	7091326.81	1594.24	306.0	-63.0	247.80	Lucky Queen	7.5, 222.1, 235.6, 236.1, 236.9, 238.5, 239.5
K09-185	487259.00	7086885.00	1094.00	279.0	-59.0	151.79	Bellekeno - East	128, 129.4, 137

K09-187	487170.00	7086809.83	1142.23	281.0	-85.0	222.50	Bellekeno - East	194, 195.1, (199.4, 199.5), (201.2,201.25), (201.9, 202.05) 204, (204.2, 204.3)
K09-192	487101.27	7086292.66	1277.07	74.0	-52.0	115.82	Bellekeno - Southwest	(67.8, 67.9)
K09-197	487172.90	7086810.19	1142.06	11.0	-78.0	217.90	Bellekeno - East	193.5, 193.7, 194.5, 203.8, 204
K09-199	488937.49	7089879.35	1582.93	315.0	-50.0	131.40	Keno 700	52.6, 52.9, 58.2, 59.5, 61.9, (62.3, 62.5), (63.3, 63.4), 68.8, 91.5
K09-200	488938.05	7089878.81	1583.02	310.0	-70.0	143.76	Keno 700	75.2, 76.4, 80.3, 83.5, 85.7, 86.3, 88.7
K09-201	489029.97	7089782.13	1564.11	323.0	-60.0	253.80	Keno 700	(235.3, 235.4), 236, 237.2, (238, 238.1), (239.1, 239.2)
BKUD09-134	486704.91	7086269.52	993.98	318.4	27.6	52.50	Bellekeno - Southwest	33.5, (39, 39.5), 41.35, 45
BKUD09-136	486564.42	7086194.47	975.38	135.2	27.8	72.40	Bellekeno - Southwest	(65, 65.5), 67.5, 69.5
BKUD09-138	486705.11	7086270.05	992.02	333.2	-11.4	42.00	Bellekeno - Southwest	1.5, 10.5, 22.5, (36.1, 36.2), (36.7, 36.8)
BKUD09-139	486632.32	7086199.63	961.88	93.2	-27.7	18.00	Bellekeno - Southwest	4.8, 8.1, (8.3, 8.4, 8.5), (8.8, 8.9, 9)
BKUD09-140	486632.02	7086200.01	960.87	76.1	-61.1	25.50	Bellekeno - Southwest	8.8, 9.0, 9.5, 9.9, 10.4, 16, 20
BKUD09-143	486705.93	7086270.12	993.16	351.3	9.3	65.50	Bellekeno - Southwest	(18, 18.5), 50.5, 51.2, 52, 52.7, (53.5, 54)
BKUD09-144	486576.46	7086167.18	981.22	119.5	-0.7	46.50	Bellekeno - Southwest	(36.4, 36.5, 36.6), (37, 37.2), 38.5
BKUD09-148	486850.77	7086436.18	1041.31	304.6	-26.7	39.00	Bellekeno - 99	1.7,27, (29.5,29.6), 32.9, (33.5, 33.7)
BKUD09-149	486851.36	7086436.16	1042.85	317.2	22.9	43.00	Bellekeno - 99	5.2, 33.4, 35, 37.8, 38.3
BKUD09-150	486557.60	7086161.16	979.62	137.4	-12.9	81.00	Bellekeno - Southwest	41, 60.4, (61.3,61.4), 63.2, 64.1

BKUD09-151	486883.00	7086477.11	1042.29	290.7	8.3	44.20	Bellekeno - 99	14.4, (29, 29.2), (33.2, 33.3), (34.4, 34.5, 34.6, 34.7)
BKUD09-153	486557.88	7086160.81	979.22	137.8	-30.2	105.00	Bellekeno - Southwest	60.4, (63.4, 63.5, 63.55), 85.8, 86.1, 87, 87.5, 88.6, 88.8
BKUD09-156	486705.77	7086364.00	992.63	166.7	50.2	43.00	Bellekeno - 99	26.5, 29
BKUD09-157	486557.57	7086160.69	979.30	152.7	-26.7	120.00	Bellekeno - Southwest	93.8, 96.3, 98.4, (100.1, 100.3), (100.4, 100.5), (101.4, 101.5), 101.9, (102.1, 102.2)
BKUD09-158	486705.25	7086364.23	992.83	179.0	54.8	55.00	Bellekeno - Southwest	17.1, 35.2, (35.5, 35.6), 35.9, 36, (36.5, 36.6), 37, (45.4, 45.6, 45.7)
BKUD09-160	486599.40	7086185.35	984.09	123.1	-43.2	61.00	Bellekeno - Southwest	29.6, (51.6, 51.9), 52.1, 53.3, 54.1, 54.5, 56.5
BKUD09-161	486599.34	7086185.40	985.21	124.8	5.6	36.00	Bellekeno - Southwest	20, (20.4, 20.45), 20.8, 25.9, 31.3, 34.4
BKUD09-163	486620.83	7086208.83	990.00	141.3	-14.4	35.00	Bellekeno - Southwest	14.8, 16.5, (16.95, 17), (27.5, 27.55), 31.8
BKUD09-165	486759.92	7086410.82	976.24	103.8	-20.1	53.30	Bellekeno - 99	48
BKUD09-166	486621.83	7086209.85	989.58	83.1	-22.0	34.20	Bellekeno - Southwest	(16, 16.1), 17.5, 18.6, 18.9, 20.8, 21.3
BKUD09-169	486652.85	7086242.80	993.80	127.5	29.4	17.00	Bellekeno - Southwest	(6.2, 6.4)
BKUD09-170	486653.56	7086242.32	992.04	122.0	-20.4	16.00	Bellekeno - Southwest	7.6, (11.4, 11.45), (12.7, 12.8)
BKUD09-171	486766.50	7086417.01	977.17	108.4	21.5	48.00	Bellekeno - 99	31, 32.4, 32.8, 35.1, 43.3, 43.5, 44, 44.3
BKUD09-172	486654.32	7086243.60	992.43	91.7	-0.7	20.00	Bellekeno - Southwest	7.8, 11.7, 15.1
BKUD09-173	486766.07	7086417.15	977.67	140.3	-23.4	42.00	Bellekeno - 99	(28.7, 28.8), (31.2, 31.3, 31.35), 34.4, 36

Appendix II

Petrography

The following 78 samples were prepared as thin-sections after initial hand sample descriptions. Some thin-section descriptions have more detailed descriptions because they were also analysed by EMPA, and fluid inclusion studies. Mineral abbreviations used are summarized in the report text. Following the 'Rock Type' category, minerals in bold are volumetrically significant; in minerals within brackets are minor or uncommon, mineral textures precede the mineral abbreviations, and silver bearing minerals are underlined. Arrows (→) used in 'Rock Type' or 'Stages' to indicate transition between paragenetic stages.

Squares within off-cut images indicate areas examined by EMPA. The numbers adjacent to the square identifies to the area examined, and corresponds to the first number after the actual sample number in the EMPA data, the last number in the EMPA data sample number corresponds to each individual sample point analysed. For example: Alice_2-6 identifies data from the Alice sample, in area 2, at point 6. Circles within the off-cut images indicate areas examined by fluid inclusion microthermometry. Individual fluid inclusions analyzed are numbered consequtively. The black or white colours bear no significance, and have only been used for clarity.

Note that the analysed locations identified by the squares and cirles are only approximate; the off-cut image is not an exact representation of either the fluid inclusion wafers or thin sections as the off-cut sample face shows a slightly different plane. Samples that were not used for EMPA or fluid inclusion analyses will have no circles or squares drawn on the off-cut images.

Alice

Location: Alice; Surface

Rock Type: V: (b,cld)**Sd** → (Qz)-(z)**Sp**-Py → **Gn**-Ttr(-Boul-Andr?) (→ Ang)

Stages: 6 → 7 → 8

Host Lithology: N/A

Alteration: Gn may be altered to or replaced by Ang around the edges.

The earliest and most predominant mineral is Sd [<70 % overall], mostly cloudy, an- to subhedral [<125 μm], but some crystal edges may be clear and euhedral; most crystals have an undulatory extinction under XP. Fluid inclusions [<10 μm], 2-phase, appear to be common throughout Sd, which are at least partly responsible for the cloudy appearance, however few inclusions were optically usable, typically at crystal edges.

Minor Qz [<2% overall] may occur as discontinuous rims after Sd, but generally before Sp and Gn (below). Qz is an- to subhedral, and clear. There may be clusters of fluid inclusions within Qz, individual inclusions are generally <10 μm, and 2-phase.

Sp [<25 % overall] follows and is partly intergrown with Sd. Sp is internally zoned, defined by alternating growth layers of translucent light to dark brown and opaque; sub- to euhedral. The fringes of the Sp masses are generally pale brown and partly translucent. Sp appears to have nucleated in free space, where the hexagonal crystal colour bands radiate outwards, or in-filling voids after Sd (?). Within Sp there are clusters of fluid inclusions [<10 μm], 2-phase, however the dark brown colour generally obscures observations of fluid phase changes. Mineral inclusions of Po [Tr, mostly <250 μm] are commonly contained within Sp, many are elongate and appear to be parallel or formed along Sp crystal planes. Py [Tr] occurs as blebs [<60 μm], less common and more irregular than Po are also occur within Sp. Additional Py [<1 %] is mostly euhedral [<375 μm], and precipitated druing the transition from Sp to later Gn. Py may also occur as isolate grains within Sd.

Gn [5 % overall] is intergrown with or post-dates both Sd and Sp. Gn may be euhedral, or irregular infill around Sd and Sp, as discontinuous veinlets, or as

pockets/blebs suspended within Sd or Sp. Within some areas of Gn, there are irregular blebs of minor Ttr and Boul. Few irregular blebs of Ang are also present within Gn, which appears to be late and possibly alteration product after Gn. Cst and native tin [Tr] occur as blebs within Gn.

Try Again

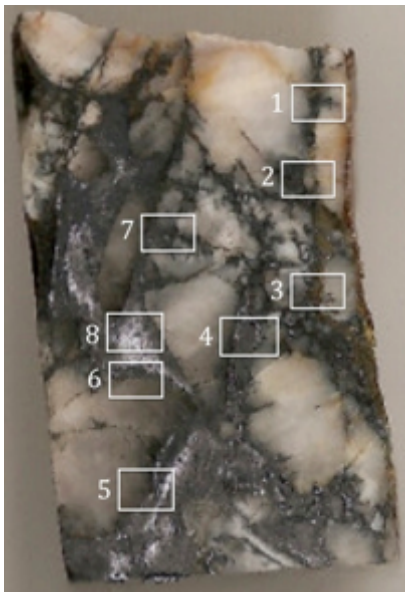

Location: Try Again; Surface

Rock Type: V: **Qz** → V/B: **Gn**(-Py-Ttr)-Pyr (→ Ang-Cer)

Stages: 1 → 8

Host Lithology: Irregular pockets and lenses of Pht/GSch are present around Qz. Few small and irregular fragments of Qtzt, comprised of anhedral, and cloudy Qz are incorporated into the later hydrothermal Qz vein/breccia-matrix.

Alteration: Pht/GSch may be partly altered to or replaced by Mica/Ms. Qtzt may be at least partly silicified or re-crystallization of Qz. Ang and Cer may be the alteration products or partly replace Gn.

The earliest hydrothermal phase is Qz [80 %], mostly anhedral and massive clusters [>2 mm], variably cloudy.

Gn [20 % overall] post-dates Qz as irregular infill and partly/locally brecciates the earlier Qz. Gn is euhedral, clustering as irregular masses [>2 mm]. The contact between Gn and Qz is generally irregular, and may reflect partial dissolution of Qz by the subsequent Gn-related mineralizing fluids. Locally derived Qtzt-clasts may be suspended within the Gn-matrix. Gn cleavage planes may irregular and curved, and may reflect post- or syn-depositional strain. Minor blebs of Ttr and Pyr are contained within and associated with Gn. Py [Tr] is contained within the Gn-matrix. Py is subhedral [mostly <1 mm], and is highly fractured. Some Py grains are contained within the earlier massive Qz, these are generally less fractured and more euhedral.

Ang and Cer occur late, after Gn, as thin irregular layers around and partly invasive into Gn.

SK_003

Location: Silver King; Surface

Rock Type: B: Qz

Stages: 1 (?)

Host Lithology: Qtzt and Pht clasts are abundant throughout, some may be >1cm.

Alteration: Silicification or recrystallization of Qz. Pht may be recrystallized as or replaced by Mica/Ms.

Hydrothermal Qz is mostly an- to subhedral [<500 μm]; cementing a clast-rich breccia. Abundant Mica/Ms is intergrown with Qz, as clusters, which appears to be recrystallized Pht clasts (?). There are few [<1%] pockets/blebs or grains of Py, Sp, and Gn within the Qtzt and the secondary Qz cement. These sulfides may originate within the sediments.

LQ_007

Location: Lucky Queen; Surface

Rock Type: B: (Qz-)**Sp**(-Sd) → **Gn** → B: **Qz**

Stages: (1 ?) 3 → 8 → 10

Host Lithology: Qtzt may be present; comprised of tightly packed Qz, anhedral [<250 μm].

Alteration: Silcification or re-crystallization of Qtzt. Oxidation, present as Fe-oxide lenses, irregular, and partly invasive along fractures, and between crystal boundaries.

The earliest hydrothermal phase is Sp, which has partly brecciated, and in-filling around Qtzt. Sp [10% overall, but locally abundant] is generally opaque, only faintly translucent deep reddish brown. There may be minor hydrothermal Qz nucleated on Qtzt clasts, and grown into the Sp-mztrix.

Following Sp there is an abrupt transition, but poorly preserved due to the invasive oxide material, to predominantly Gn. This Gn-rich stage may contain few Qtzt clasts. Gn forms a continuous, euhedral, intergrown masses; locally in some areas Gn may be almost completely replaced by translucent light brown Fe-oxide material (?).

Within the lower part of the TS, there is a Qz-cemented breccia. Suspended within Qz are abundant locally derived fragments of Gn and Qtzt – some clasts appear to be nearly in-situ.

Overall the Sp-Gn-Qz stages appear to define asymmetrical growth within a single vein structure.

WRN_008

Location: Wernecke; Surface

Rock Type: V: **Qz** →
V/B: **Sd**-Ttr(-Ccp-Gn-Sp-Cob/Ger)

Stages: 1 → 6-8

Host Lithology: Qtzt is comprised of tightly packed Qz, an- to subhedral grains [<125 μm]; intergrown with irregular pockets to undulatory foliated bands of Pht. Pht appears to be largely altered to Mica/Ms – clear to opaque and dark brown; crystal blades [<250 μm]. Foliated bands of Mica/Ms are mostly <500 μm wide, and may continue for mm's. There are a few Py grains, subhedral [<500 μm], contained within Qtzt.

Alteration: Silicification or re-crystallization of Qz. Pht may be re-crystallized as or replaced by Mica/Ms.

An early small vein(-breccia) in the lower part of the TS is cemented by predominantly Sd, mostly cloudy, sub- to euhedral, rhombohedral crystals [<1 mm], and commonly has undulatory or fanned extinction in XP. The cloudy texture in Sd is the result of abundant very fine fluid inclusions [<5 μm], 2-phase, and/or crystallographic impurities, microscopic opaque material (some sulfides), or patchy brown stain (Fe-oxide material). Fe-oxide generally follows crystal boundaries, cleavage planes, and fractures.

There is another and later stage of Sd, cementing a vein/breccia, cross-cutting the above earlier Sd. The later Sd vein-breccia stage in the upper part of the TS is texturally distinct from the earlier Sd type above, based on the more clear, sub- to euhedral, rhombohedral cleavage and also bladed crystals [<2 mm]. Small fluid inclusions [<10 μm], 2-phase, and/or crystallographic impurities (?) may be present within this later Sd phase, however no usable inclusions were located. Ttr [<1 % overall] occurs as an- to suhedral, as irregular pockets in-filling around Sd; one particular pocket is irregular and approximately 1 cm wide, with additional smaller blebs [<100 μm] commonly intergrown or contained within the surrounding Sd. Lesser Ccp, Gn, Sp, and Cob/Ger (?) may also be associated and intergrown with Ttr.

BRM_044

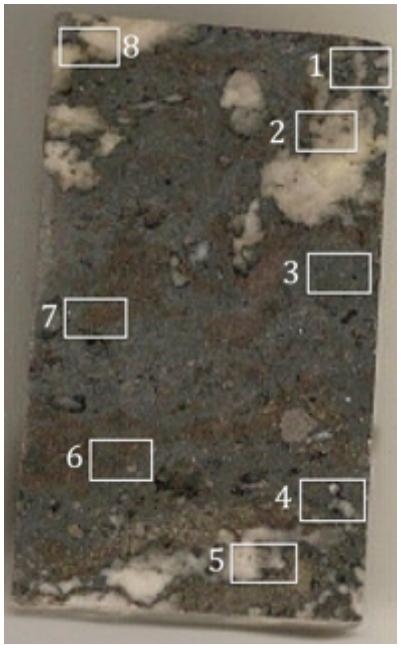

Location: Bermingham; Surface

Rock Type: V/B: **Qz** → **Sd**(-Py-Apy) → (Qz-)**Sp**-**Gn**-(Ttr)-Boul-Jam(-Val)

Stages: 1 → 6 → 7-8

Host Lithology: Possibly Qtzt clasts may be present, comprised of anhedral Qz; mostly dirty/cloudy, which appears to be a result of abundant fluid inclusions, as well as lesser fine opaque material. Remnants of Pht may be indicated by the presence of Mica/Ms.

Alteration: Silicification or re-crystallization of Qz. Pht may be altered to or replaced by Mica/Ms.

The earliest hydrothermal stage is Qz, partly intergrown with Sp and Gn (below). Qz has mostly nucleated on the existing Qtzt clasts. Qz is an- to subhedral, and clear [generally <250 μm], distinct from the Qtzt clasts.

Py and Apy appear to be the earliest sulfide minerals, and both are mostly spatially associated with each other. Both Py and Apy may be earlier phases, which appear to have been fractured and subsequently mobilized, forming 2 concentrated bands surrounded by and infilled by later Gn (and lesser Sp). Py is mostly anhedral [<500 μm], with frequently fuzzy grain boundaries that appears to be partly dissolved by fluid associated with later Gn and Sp. Apy is an- to subhedral, generally with sharp grain boundaries.

Sp and Gn both post-date the Qz, although in some areas Gn and Sp are partly intergrown with Qz. Sp is to be the principal sulfide after Qz, which then is followed by or partly intergrown with a more prominent Gn-rich phase. Sp is anhedral, translucent honey brown, as isolated pockets within Gn or as large irregular masses [>1 cm]. Gn is irregular in-filling masses, anhedral, surrounding or containing clasts/fragments of Py, Qz, and Sp. Gn is light grey, with a dull luster, which may be an effect of subsequent weathering or later stage alteration. Boul and Jam are commonly intergrown with Gn also as irregular, and anhedral masses or form sub- to euhedral tabular/elongate crystal clusters. Minor Ttr and Val are present as irregular blebs associated with Sp, Gn, Boul, and Jam.

EAG_047

Location: Eagle; Surface

Rock Type: V/B: (Qz-Py-Apy) → **Py-Sp**(-Py-Gn-Ang) (→ Sd)

Stages: (1 ? →) 4a(-5 ?) (→ 6)

Host Lithology: Qtzt [15 % overall] is comprised of compact Qz, anhedral [<250 μm], with minor disseminated Py and Apy.; some Qtzt is brecciated occuring as clasts contained within Py-Sp-cement (below). Minor Pht occurs as oriented/foliated pockets within Qtzt. Pht is altered to Mica/Ms, clear flakes to opaque dark brown.

Alteration: Silcification or re-crystallization of Qz. Qtzt may be partly dissolved. Pht has been altered to or replaced by Mica/Ms. Ang may be replacing or an alteration product after Gn.

The earliest hydrothermal phase is minor Qz, euhedral and prismatic, nucleating and grown out from the edge of Qtzt clasts. Py and Apy [5 % combined] may be the earliest sulfide phases, forming clusters around Qtzt edges, partly associated with Qz. Both Py and Apy are sub- to euhedral [generally <250 μm].

Another and more prominent generation of Py [20 % overall] is an- to euhedral, and massive, is partly intergrown or associated with the earlier Qz-Py-Apy and later Sp. After Py, there is a significant stage of predominantly Sp [50 % overall], generally dark to opaque, reddish brown in PPL, and massive infilling around Py-Apy and Qtzt clasts, and intergown with partly massive Py. Blebs [<100 μm] of Ccp (possibly Po) are common [<10 % within Sp] throughout Sp ("chalcopyrite disease").

Lesser Gn [5 %] is euhedral, as irregular masses associate with or infilling around Py, and follows Sp. The Py-Gn association may occur within irregular, partly discontinuous veinlets within Qtzt or as a more massive vein-filling stage [<1 cm wide]. Minor Ang may occur as thin rims around the edges of Gn. Sd [<5 % overall] is sub- to euhedral rhombs [<500 μm], and infills remnant vug space following, or partly intergrown with Py and Gn.

HOM_053-1

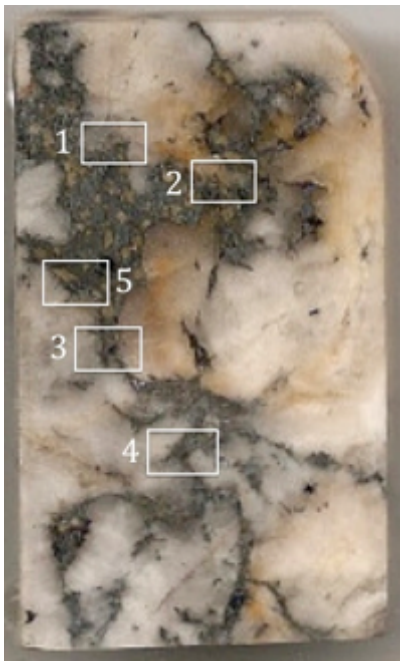

Location: Homestake; Surface

Rock Type: V/B: m**Qz → Gn-Boul**(-Sp-Sd)

Stages: 1 → 8 (?) (7-6 ?)

Host Lithology: N/A

Alteration: N/A

The earliest and principal hydrothermal phase is massive Qz [<90 %], mostly large crystals [may be >2 mm], anhedral. Qz is variable cloudy from abundant fluid inclusions, commonly in crystal core areas and contains blebs [<20 μm] of opaque material; and the crystal edges are comparatively more clear.

Gn and Boul post-date and infilling around Qz. Gn [<2 %] is an- to euhedral, as irregular in-filling masses. Boul [<10 %] is closely associated and intergrown with Gn. Boul is darker grey, and commonly forms elongate or needle-like crystal masses. Sp is minor [<1 %], present in a few pockets, partly intergrown with Gn and Boul, possibly post-genetic. Sp is translucent, pale to honey brown in PPL, an- to euhedral (?), as irregular pockets. There are minor Ccp (?) mineral inclusions [<10 μm] contained within Sp. Minor to trace Sd is intergrown with Gn, Boul, and Sp. Sd [<1 %] is sub- to euhedral [<1 mm], rhombs; crystals are partly dirty/cloudy in the crystal core, but becomes more clear around the edges. Sd may nucleate on Qz or be suspended within Gn and Boul.

HOM_053-2

Location: Homestake; Surface

Rock Type: V: (Qz-?)**Py**-Apy → **Py-Sp**(-Qz) → V: Qz

Stages: 1 → 4a → 4b or 10 ?

Host Lithology: Few Qtzt clasts remain; comprised of tightly packed Qz grains, anhedral [<250 μm]. The presence of Pht is apparent from Mica/Ms – clear to opaque dark brown, clusters of flakes.

Alteration: Silicification or re-crystallization of Qz. Pht may be altered to or replaced by pockets of Mica/Ms.

Py and Apy (?) are abundant in the upper part of the TS; they are closely associated with and/or surrounded by Mica/Ms clusters, and surrouned by Qz. Apy [15 % this unit] is anhedral to euhedral [<1 mm], however most crystals appear to be partly dissolved. Py [20 % this unit] is anhedral to euhedral [<1 mm]. Py and Apy may be early, associated with the original sediments; however some or most Py appears to be secondary growth – as most Py is not dissolved like Apy. The infilling Qz-cement (?) is anhedral [<1mm], mostly clear, but minor dirty/cloudy, due to the presence of common fluid inclusions – partly irregular [<30 μm], and generally 2-phase.

There is an undulatory contact, defined only by the abrupt presence/appearance of Sp. Minor Py, Apy, and Qz may scavenged from above (?) contained within Sp. Sp [50 % this unit] is translucent, pale to honey brown in PPL, anhedral (?), as irregular masses. There are very few mineral inclusions within Sp [<5 % contained within Sp]; these blebs [<10 μm], mostly Ccp (?), are generally located around the edges of Sp. Qz may continue during this stae partly intergrown with Sp; Qz is more and variably cloudy than above; however crystals are comparatively more clear where Qz comes in contact with Sp.

A later stage (?) Qz-vein is defined associated with the abrupt disappearance of Sp and Py. Here Qz [>99 % this unit] is an- to subhedral [mostly >1mm], variably cloudy – due to the presence of abundant fluid inclusions.

POR_056

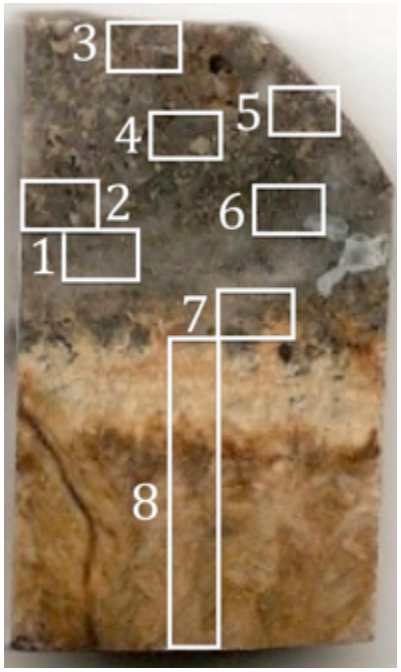

Location: Porcupine; Surface

Rock Type: V: **Qz**(-Sp-Py-Gn-Ang-Ttr) → (f,cld)**Sd** → (c,e)**Sd**

Stages: 10 → 11 (?)

Host Lithology: Few sporadic Qtzt clasts are present. Qtzt is comprised of Qz, tightly packed, anhedral [<1 mm].

Alteration: Silicification or re-crystallization of Qz. Pht may be recrystallized as or replaced by Mica/Ms.

The earliest hydrothermal phase is in the upper part of the TS and consists of mostly Qz is clear to cloudy; the result of abundant fluid inclsions, the clear crystals appear to be late, and may be partly intergrown with the subsequent sulfides. Fluid inclusions within Qz are common disseminated throughout or as clusters, individual inclusions are irregular [<25 μm].

Variable sulfides [>50 % combined within this unit] occur with, but appear to post-date Qz. Gn [<10 %] is an- to euhedral generally irregular intergrown with Py. Minor Ang and Ttr are also intergrown with each other and Gn. Sp [<40 %] is is translucent honey brown in PPL, an- to euhedral. Py [<5 % this unit] is an- to subhedral, commonly associated with Sp, but it's crystal structure is better developed within Qz. Py is commonly intergrown with the edges of Sp. Both Sp and Gn are irregular in-filling around Qz. The sulfide content decreases later in the paragenesis.

There is an abrupt transition from the predominantly Qz stage to a predominantly Sd stage. This contact is sharp, but irregular. This Sd unit is <1 cm wide; comprised an- to subhedral [<500 μm], and cloudy crystals – due to the abundance of fine fluid inclusions and/or crystallographic impurities, which renders the Sd almost opaque. Many crystals are fan or curve-shaped with undulatory extinction; overall the average crystal size decrease towards the upper boundary.

There is another transition from above to a texturally different Sd unit. Sd [>95 %] is irregularly shaped, clear, euhedral, rhombohedron, many crystals >2 mm; this stage occupies the lower 1/3 of the TS. The contact with the above unit is defined by an abrupt but partly intergrown transitioning over <2 mm from the cloudy Sd. There

may be usable fluid inclusions within this Sd, where crystals are clear, individual inclusions are mostly <10 μm, irregular to negative crystal vucuoles.

SP_069

(Image Not Available)

Location: Sign Post; Surface

Rock Type: V/B: (m)**Qz** → Sp-Py-**Gn**-<u>Ttr</u> → (B:)Sd

Stages: 1 → 7-8 → 11

Host Lithology: N/A

Alteration: Oxidation of sulfides.

There is an early Qz-cemented vein/breccia stage. Qz [40 % overall] is mostly anhedral [many >2 mm] and partly cloudy – due to abundant fluid inclusions and microscopic sulfides (possibly Py). Qz in some areas becomes clear may be sub- to euhedral during the wanning (?) of this stage.

Post-dating the above Qz there is a vein-filling to localized brecciation stage associated with (in paragenetic order) Sp, Py, Gn, then Sd. Sp [<10 % overall] is partly translucent honey to deep reddish brown, anhedral. Sp commonly contains clusters of Py blebs/pockets, anhedral; although Py may be remobilized from and earlier stage, which has been subsequently fractured and suspended within Sp. Alternatively some Py may have precipitated during the transition from Sp to Gn. Minor Ccp may be present within Sp as mineral inclusions – "chalcopyrite disease". Following Sp, the principal vein-breccia filling phase is Gn [35 % overall], as irregular masses, euhedral. Gn commonly contains Py [<10 % within Gn], an- to euhedral [<250 μm], which also tend to cluster. Minor Ttr as blebs [<250 μm], anhedral are contained within Gn, and often spatially associated with Py. A few pockets of Sp (similar as above) are also contained/intergrown with Gn.

After the sulfides, there is a later stage of Sd, associated with minor and localized brecciation. Sd [<5% overall] is an- to subhedral [<500 μm], as irregular vug-fill around Sp, Py, and Gn. Oxidation is apparent from translucent light brown material (Fe-oxide ?) altering or replacing many sulfides, and may be associated with the late/last hydrothermal Sd stage; or rather may only following the same path way.

K06-2: 167.2 m

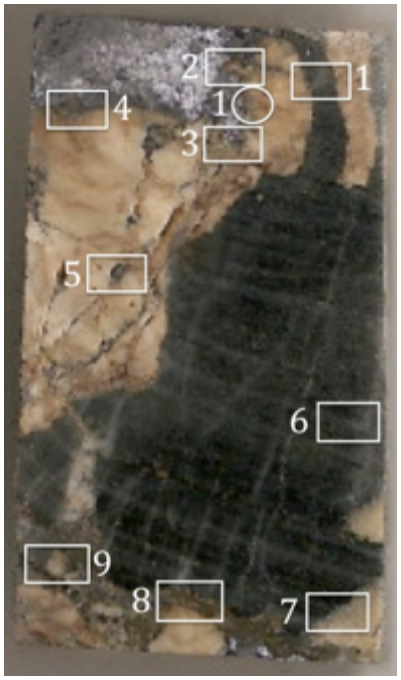

Location: Silver King

Rock Type: V/B: (Qz-)m**Sd** → **Gn**(-Sp-Py)-Ttr-Stn-Plb-Ag

Stages: 2 or 6 → 8

Host Lithology: Qtzt clasts [50 % overall] may be >2 cm, consiting of a mosaic of Qz grains, an- to subhedral [mostly <125 μm]; and contains wispy lenses of Pht, mostly altered to clusters of Mica/Ms flakes [<250 μm long and <20 μm wide]. Multiple lenses of Mica/Ms are generally oriented parallel, reflecting the pervasive F1 foliation. Qtzt clast boundaries may be sharp or irregular due to possible secondary growth of Qz from clast boundaries.

Alteration: Silicification and/or re-crystallization of Qtzt. Pht may be altered to or replaced by Mica/Ms.

The earliest hydrothermal phase is Sd [35 % overall, >95% this stage], generally sub- to euhedral [many >250 μm], mostly cloudy, but variably clear crystals may be late. The cloudy nature of Sd appears to be a result of abundand very fine fluid inclusions [mostly <5 mm], and crystallographic imperfections. Qtzt clasts may be suspended within Sd with sharp and straight to irregular boundaries. Minor hydrothermal Qz may nucleate on clast boundaries and grow into the Sd-matrix.

A Gn-rich stage with associated sulfosalts occurs after Sd. Gn occurs in vugs or fractures, and may form localized/micro-breccia, cross-cutting both Sd-matrix and Qtzt clasts. Gn [10 % overall] is mostly euhedral, irregular masses [>1 mm], but may be anhedral as smaller pockets. Gn and Py may be intergrown, where Py occurs along the edges between Sd and Gn, locally the Gn:Py ratio is 50:50. Py [5 % overall] is mostly an- to subhedral [250 μm to 1mm], and may be euhdral [<125 μm] mostly contained within Qtzt clasts. Minor Ttr, Stn, Plb, and native-Ag are partly intergrown with Gn as irregular pockets within fractures or they may be late associated with micro-brecciation.

K06-25: 44.8m

(No Image Available)

Location: K-Structure

Rock Type: V/B: **Gn**-Ang → B:Qz-Sd

Stages: 8 → 10-11

Host Lithology: N/A

Alteration: Oxidation and/or replacement of Gn by Ang around edges.

The earliest and most prominent hydrothermal phase is Gn [>90 % overall], euhedral; many crystal masses are >2mm. Gn has subsequently been brecciated and appears to be partly dissolved around some edges, as clast edges are typically highly irregular, and may appear diffuse. Ang may be present as irregular to discontinuous and 'fuzzy' rims as an alteration product or replacement around the edges of Gn.

Qz and Sd in-fills around the brecciated Gn. Qz may be earlier than Sd; however the two appear syn-genetic in areas. Qz [40 % this stage, 5 % overall] is an- to subhedral [mostly <50 μm]. Sd [60 % this stage, 5 % overall] is an- to subhedral [<250 μm], mostly irregular shaped intergrown around Qz and Gn.

K07-60: 121.8m

Location: Tick (Townsite)

Rock Type: V/B: (Qz-)**Sd**-Py

Stages: (1 ?)-2

Host Lithology: Qtzt [~50 % overall] is comprised of tightly packed Qz grains, an- to subhedral [<250 μm]; and occurs as brecciated clasts. Minor Pht, black, opaque, fine material, occurs as thin foliated, undulatory layers/bands [<100 μm wide] throughout Qtzt. Mica/Ms is clear to translucent brown, and may be an altered product from or replacing Pht within Qtzt.

Alteration: Silicification and/or recrystallization of Qz. Pht may be re-crystallized as Mica/Ms.

Qtzt clasts contain Py clusters in association with thin Pht (now Mica/Ms) layers; Py [<1 % overall] is an- to euhedral [<300 μm].

Minor hydrothermal Qz, sub- to euhedral [<250 μm] is common, nucleating on Qtzt clasts or clustering around Qtzt. Sd [~45 % overall; >90 % this stage] follows and is partly intergrown with Qz, and is an- to euhedral [<1.5 mm], variably clean to cloudy, many crystals are commonly twinned, or have a striated internal crystal structure. The presence of abundant very fine fluid inclusions [<5 μm] and/or crystallographic imperfections appears to be responsible for the cloudy appearance of Sd, which more commonly occurs near Qtzt clasts; also early Sd may be fine, nearly opaque, and brown. Qtzt clasts suspended within the Sd-cement, may be elongate fragements and are preferentially oriented. Py [<5 % with Sd stage] is anhedral, and in-filling vugs following Sd, and also appears to be partly replacing Sd, based on the highly irregular and partly invasive contact. Irregular and elongate masses/pockets of Py display the same preferential orientation as the Qtzt clasts. Remnant vugs occur after Sd and Py.

K07-66: 146.9 m

Location: Bellekeno East; ~980 masl

Rock Type: V: (cld)**Sd** → B: (Qz-)**Sp**(-Py) → V/B: (Qz-)**Sp**-Gn-<u>Ttr</u>(-Py-Ccp) → (V: Sd)

Stages: 2 → 3 → 7-8 → (11)

Host Lithology: Few Qtzt clasts may be present; however, re-cyrstallization of Qz appears to be pervasive, and secondary Qz growth results in irregular clasts of an- to euhedral Qz.

Alteration: Silicification or re-crystallization of Qtzt.

The earliest hydrothermal phase is Sd [<35 % overall], consisting of an- to subhedral [may be >2 mm], and variably cloudy. There appears to be subsequent brecciation of this earliest phase.

Clusters of Qz are commonly nucleate on and grow from the edges of the Sd. Qz [<2 % overall] is mostly sub- to euhedral [250 to 500 μm], in random orientations. Sp [<15 % overall] is the predominant breccia-matrix as irregular masses, an- to subhedral, light to dark brown. Note, there is a distinct lack of mineral inclusions within Sp. Qz crystals, sub- to euhedral [250 to 500 μm] may be suspended within the massive Sp or occur as irregular Qz veinlets, comprised of fine [<20 μm], anhedral. There is one partly irregular Sp veinlet [<500 μm wide] which cross-cuts the more massive Sp, and earlier Sd, but is mostly post-dated by additional Qz growth.

In the lower part of the TS, there is a zone of foliated mineralization, which cross-cuts the earlierst Sd stage. The foliation is defined by compositionally-rich bands and/or veins of either Py, Sp, Gn, and/or Sd. The earliest phase in this foliated zone is a band of Py, irregular, discontinuous [<250 μm wide]. Below this is a complex mix of predominantly Sp [<15 % overall], with Sd, Gn [<10 % overall] lesser Qz [<2 % overall], and Py [<2 % overall]. The Sd in this area may be remenants or clasts of the earliest Sd phase or possibly continuation of Sd mineralization. In one area Gn follows Sp, with minor Py between the two phases. Minor Ccp is intergrown with Sp spatially associated with Gn. Furtherdown and later still is another sub-stage (?) of Gn associated with more Sp, both following euhedral Qz. Some Qz-rich areas in this

foliated zone may be highly altered/re-crystallized remants of Qtzt clasts or possibly continuation of Qz precipitation.

There is one late stage veinlet of Sd [<750 μm wide], comprised of mostly clear, anhedral Sd. This vein may partly (micro-)brecciate the massive Sp, and contain suspended, small, angular fragments/clasts of Sp. Minor early Qz may be associated with this vein stage; however, some Qz crystals contained within the Sd veins.

K07-76: 115.3 m

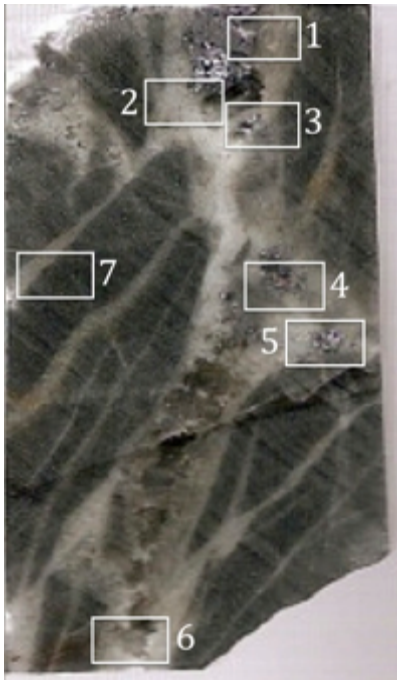

Location: Bellekeno East; ~965 masl

Rock Type: V/B: **Qz**(-Py) → (Sd-Apy-Sp-)**Gn**

Stages: 1 → (2-3) 5 or 8 (?)

Host Lithology: Host rock is Qtzt, comprised of anhedral Qz grains [<200 μm]. Thin lenses, and discontinuous layers of Mica/Ms [2 %] and Pht [2 %] define a pervasive foliation within the Qtzt. Mica/Ms lenses are generally <20 μm wide x <500 μm long, oriented, wavy, and discontinuous. Pht is fine grain material, black, and opaque.

Alteration: Silicification or re-crystallization of Qtzt.

Vein-filled fractures are comprised of most Qz, sub- to anhedral [<500 μm], however some larger Qz grains [<2 mm] are sub- to euhedral, cloudy - which appears to be the result of microscopic fluid/mineral inclusions and/or crystallographic imperfections. Minor Py may be intergrown with this stage of Qz.

After Qz there may be void space or partial infilling by Gn, sub- to euhedral, coarse [<2 mm], irregular infilling voids after Qz. Lesser Apy, and Sp are also associated with Gn. There is also minor Sd [<1 %], coarse [>500 μm] post-dating Qz, but pre-dates Gn.

K07-76: 125 m

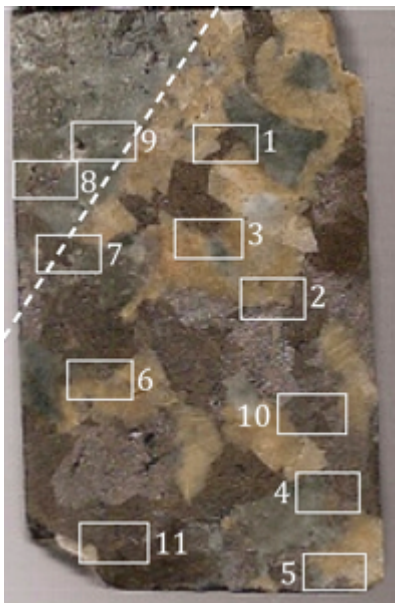

Location: Bellekeno East; ~965 masl

Rock Type: V/B: (Qz-)**Sd** → z**Sp**(-Apy-Cst-Cob/Ger-Boul-Gn-Ttr)

Stages: 6 → 7-8

Host Lithology: Qtzt [<20 % overall] occurs as brecciated clasts throughout, clast boundaries are sharp and straight to irregular. Qz grains are generally an- to subhedral [<200 μm]. Mica/Ms [<5 %], tan to clear, generally fine grain [<10 μm], forming clusters [<500 μm], intergrown with Qtzt (Qz). Pht is spatially associated with Ms, as clusters/pockets of opaque material.

Alteration: Silicification or re-crystallization of Qtzt.

The irregular borders are the result of secondary Qz growth from the edges of the Qz-clasts and growing into the breccia-matrix. Hydrothermal Qz is subhedral to euhedral [mostly <500 μm]. A cluster of Py (and possibly Apy) [2 % overall] is concentrated within a Qtzt clast. Py may form large [>2 mm] anhedral masses, or euhedral pockets [<500 μm]. There is a preferred orientation of the Py clusters, which spans the length of the clast, and is parallel the clast boundary.

The breccia-matrix is comprised of mostly Sd [30 %] and Sp [40 %]. After or syn-genetic with the earliest Qz-phase above is Sd, coarse [>1 mm], sub- to euhedral, with cloudy patches – which appears to be the result of common microscopic fluid/mineral inclusions and/or crystallographic imperfections. Following Sd and infilling around both Sd and the Qtzt clasts is Sp, coarse [>1 mm], subhedral to euhedral. The euhedral nature of Sp is defined by alternating colour zones of honey to dark brown bands/layers. Few fragments of Qz and Sd crystals are suspended or surrounded by Sp. Minor Gn [<1%] and Py [1 %] may infill after, or are intergrown with Sd and Sp. Py is subhedral, generally coarse [500 μm to >2 mm], and may contain inclusions of Ccp, anhedral [< 20 μm]. Gn is sub- to euhedral as pockets [<500 μm], and few coarse [>2 mm]. Additional mineral inclusions or blebs of commonly Ttr with lesser Boul, and trace Cob/Ger are associated and intergrown with Sp, Gn, and Sd. Minor [Tr] Cst, associated with Qz and Gn was identified near the wall-rock contact, which may be remnant from an earlier stage.

K07-86: 223.3 m

Location: Bellekeno – East; 940 masl

Rock Type: V/B: **Sd**(-Apy) → **Ccp**(-Sp)**-**Gn-Ttr-Plb

Stages: 6 → 8

Host Lithology: One Qtzt clast [>5 mm] is present, consisting of Qz grains, anhedral, [<125 μm]; the clast boundary is sharp, angular, and partly irregular.

Alteration: N/A

The earliest and most predominant hydrothermal phase is Sd [>90 % overall]; mostly sub- to euhedral [>500 μm, may be >2 mm]. Crystals are variably clean to cloudy patches – due to abundant fluid inclusions [many <10 μm] and/or crystallographic imperfections. Clusters of usable fluid inclusions [<20 μm], 2-phase are common in the more clear and euhedral crystals. Clear Sd crystals appear to form later commonly after or present around central cloudy areas. Minor Apy [<1 %] is sub- to euhedral, as individual crystals or clusters suspended within Sd, and may be spatially associated with the below sulfides and sulfosalts. In one fracture, still partly open, are small, euhedral, clear Sd crystals, as well as a few euhedral Qz crystals.

Ccp [<7 % overall] post-dates Sd, in-filling irregular voids, with lesser Sp, Gn and minor Ttr and Plb (possibly other sulfosalts). Some of the contacts between Ccp and Sd are very irregular, and may reflect dissolution of Sd. Ccp is anhedral, few pockets may be ~1 cm. Gn [<3 %] is generally an- to euhedral, as irregular pockets, present around the edges or intergrown with Ccp. Ttr and Plb [<1 % combined] are intergrown with or around the edges of Ccp as irregular pockets. Minor Sp [Tr] occurs as blebs suspended within Sd or partly intergrown with Ccp, and may be associated with the sulfosalts.

K07-86: 224 m

Location: Bellekeno – East; 940 masl

Rock Type: V: (Qz-)**Sd** → Sp → **Qz**

Stages: 6 (or 2?) → 7 (or 3?) → 10 ?

Host Lithology: Qtzt is comprised of a mosaic of Qz crystals, an- to subhedral [generally <200 μm]. A foliation fabric within Qtzt is defined by the orientation of Qz clusters and inter-layered Pht lenses.

Alteration: Silicification or re-crystallization of Qtzt.

Multiple veinlets of predominantly Sd [<60 % of vein-material], generally the earliest hydrothermal mineral, followed by Qz [<40 % of vein-material] cross-cut the Qtzt with overall sharp to partly undulatory vein edges. Sd is cloudy, coarse [mostly 500 μm to 2 mm], sub- to euhedral. Within Sd there are commonly fuzzy patches of orange to brown (possibly Fe-oxide staining?), which primarily follows crystal boundaries. Qz is sub- to euhedral [<500 μm] generally follows Sd, although minor Qz growth is minor early at the vein edges also common at the vein edges. Where Sd is absent along the vein walls, it is difficult to distinguish between the 2 phases of Qz. One pocket of Sp, an- to subhedral, coarse [>2 mm] occurs after Sd, partly intergrown with Qz.

K07-87: 106.7 m

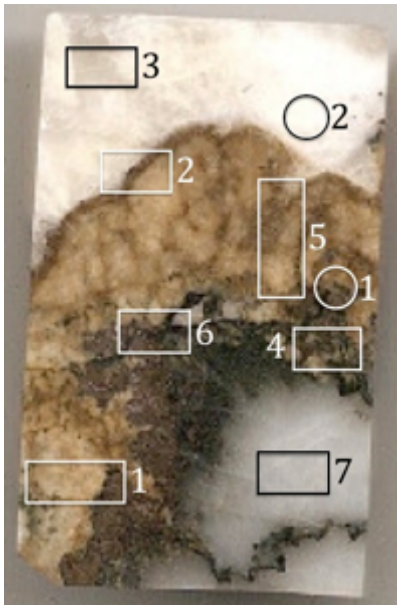

Location: Pool

Rock Type: V/B: **Sp**(-Py-Ccp-Gn?) → (cld)**Sd**(-Ank?) → m**Cal**

Stages: 7 (9?) → 9 → 12

Host Lithology: Qtzt (or massive Qz-vein) [40% overall]; also with irregular thin layers of GSch-PhSch (pressure dissolution ?). Qz is an- to subhedral [<300 μm].

Alteration: Silicification or re-crystallization of Qtzt.

The earliest hydrothermal phase is Sp [<10 % overall], translucent honey brown to deep red to opaque in PPL, an- to euhedral, partly banded; contains minor mineral inclusions of Ccp and Po [generally <20 μm]. Pockets of Py, and lesser Ccp (and Gn?) are spatially associated or partly intergrown around the edges of Sp masses. Py [<3 % overall] is mostly subhedral [<250 μm]. Ccp [<1 %] is irregular and anhedral [<50 μm].

Sd (possibly Ank?) [<30% overall], cloudy, and mostly sub- to euhedral [100 μm to 1mm], and generally follows and is also partly intergrown with Sp. More clear and euhedral Sd crystals are rhombohedral, some have an almost radiating-like crystal structure. The cloudy appearance is the result of abundant microscopic fluid inclusions, crystallographic imperfects, and other impurities (?); this texture renders Sd (Ank) essentially opaque in some areas and makes it difficult to identify and isolate usable fluid inclusions. Also associated with this stage are minor pockets of Ms/Mica, faint green in PPL, as radiating pockets [<200 μm].

The last stage is Cal [<25 % overall], massive, an- to euhedral [many >1mm], variably clear to cloudy, many display twinning; the smaller crystals [<125 μm] are generally anhedral. The cloudy nature of Cal is a result of microscopic fluid inclusions, crystallographic imperfections, and other impurities (?); in some patchy areas this texture renders Cal essentially opaque. Usable fluid inclusions in Cal are rare to non-existent.

K07-88: 59.6 m

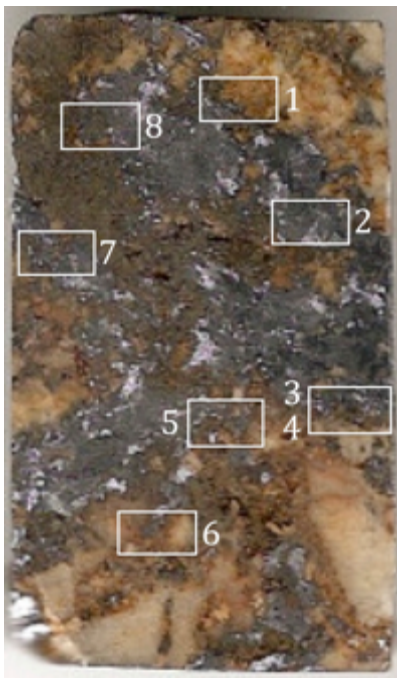

Location: Bermingham

Rock Type: V/B: Qz-**Sd** → **Sp**-**Gn**-Boul-Ttr-Stn-Plb

Stages: 1-2 → 7-8

Host Lithology: Qtzt clasts [5 % overall] are present, comprised of tightly packed Qz, an- to subhedral [<250 μm]. Minor Pht as thin foliated, undulatory layers/bands [<20 μm wide], now Mica/Ms, clear to translucent brown.

Alteration: Silicification or recrystallization of Qz. Pht may be recrystallized as or replaced by Mica/Ms. Minor oxidation of Gn rims.

The hydrothermal mineralization appears to be one single even that precipitated in sequence: Qz, Sd, Sp, and then Gn; with common intergrowth between all phases.

Hydrothermal Qz [5 % overall] is sub- to euhedral [<1 mm]; clear. Sd [30 % overall] is sub- to euhedral, but forms irregular crystal shapes [mostly <1.5 mm]. Some Sd masses become more clear around the edges where Sd comes in contact with Sp or Gn. Sp [20 % overall] is translucent pale to honey brown, an- to euhedral, as irregular masses generally following or in-filling around Qz and Sd, but intergrown with Gn. There are few Sp pockets that contain Ccp mineral inclusions ("chalcopyrite-disease"). Gn [40 % overall] is euhedral but forms irregular masses, partly intergrown but generally follows or infills around Qz and Sd. There are few Ccp blebs contained within and around the edges of Gn. Minor Boul, Ttr, Stn, and lesser Plb may be present as blebs/pockets [<250 μm] intergrown with Gn. There may be minor Pb-oxide around the edges of Gn, possibly due to the oxidation of Gn.

K07-95: 402.1 m

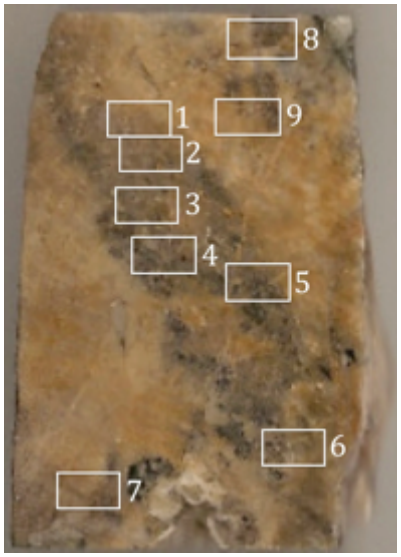

Location: Bellekeno – East; ~860 masl

Rock Type: V/B: **Sd**-Qz → Sp-Py(-Gn) → Sd

Stages: 2 → 3 → 6 ?

Host Lithology: Qtzt occurs as a few irregular angular clasts [<2 mm] suspended within a Sd-matrix. Qz is an- to euhedral [<500 μm]. 2 good or large clasts present, one is very irregular, the other is generally angular, with sharp to partly irregular edges.

Alteration: Silicification or re-crystallization of Qtzt.

The earliest hydrothermal phase is Sd [>80 % overall], an- to euhedral and cloudy to clear - there is no apparent spatial trend controlling the distribution of the cloudy or clear areas. This early Sd phase contains a few fragments of Qtzt as well as clusters of hydrothermal Qz [<1 % overall]. Minor Sp pockets/blebs [<250 μm], anhedral are contained within Sd; which post-dates Sd.

There is second stage of Sd precipitation that cross-cuts the first Sd-phase. This second Sd phase is mostly clear and euhedral [125 μm to 1 mm], although a few crystals may be subhedral and variably cloudy. There is a poorly defined, or is intergrown transition to coarse, sub- to euhedral Sd [many >5 mm], and clear. Irregular pockets [<1 mm] of Sp and Py [~5 % combined within this zone] are intergrown with Sd.

Locally there is a clast-rich breccia affecting the coarse, euhedral Sd. Sd-clasts [<500 μm] and contains irregular Sp-clasts [<250 μm]; both cemented within a Sd-matrix. This last Sd-phase is anhedral and dirty/cloudy.

There are minor remnant vugs after all the above phases.

K07-106: 402.2 m

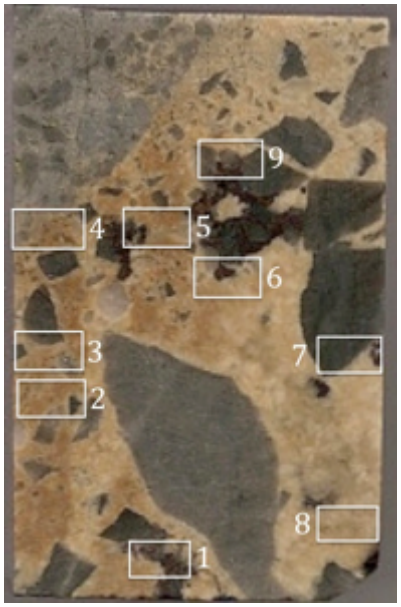

Location: Bellekeno – Southwest; ~985 masl

Rock Type: V/B: (Qz-)Sd → Sp(-Ttr-Apy)-Mica/Ms

Stages: 6 (or 2?) → 7

Host Lithology: Qtzt [35 % overall] are present as brecciated clasts suspended within a predominantly Sd-matrix. Qtzt consists of mostly an- to subhedral Qz grains [generally <200 μm]. Clast shapes and boundaries vary from angular, sharp and straight to undulatory, highly irregular and sub-rounded [from <500 μm to >2 cm]. Some irregularities may be due to minor secondary Qz growth.

Alteration: Silicification or re-crystallization of Qtzt.

Sd [<60 % overall] is the predominant matrix/cement of the hydrothermal breccia. There 2 textural types of Sd present: (1) mostly medium grain [<500 μm], an- to subhedral, and cloudy; and (2) clear, coarse [>500 μm], and sub- euhedral. The transition between these 2 types is gradational. In the coarse and lighter coloured Sd there occur within voids/pockets after the more fine and cloudy Sd-type. Sp [5 % overall] post-dates and follows both Sd and Qtzt-clasts. Sp is honey to dark brown, an- to euhedral [<500 μm], with alternating zones define by bands/layers of darker and lighter honey brown; coarse irregular masses may be >2 mm. Minor Mica/Ms [1 % overall] is intergrown with Sp and some nucleating from Qz fragments/ crystals or may in-fill discontinuous veins [<500 μm wide]. Minor blebs of Ttr may be associated or partly intergrown with Sp.

K07-122: 159.7 m

Location: Onek

Rock Type: V/B: m**Sd** → (Qz-)(m,z)**Sp**

Stages: 6 → 7

Host Lithology: N/A

Alteration: N/A

The earliest hydrothermal phase present is massive intergrown Sd [75 % overall] euhedral [commonly >2 mm]. Individual crystals appear variably cloudy – due to the presence of abundant very fine fluid/mineral inclusions and/or crystallographic imperfections. There is no apparent spatial control on the distribution of clear and cloudy areas, as both may be juxtaposed.

Sp [<25 % overall] post-dates, and is partly translucent, light to reddish brown, internally zoned – defined by bands/layers of alternating lighter and darker, and euhedral. Sp appears to be a large continuous mass around Sd. At the contact between Sd and Sp, and also intergrown with Sp there are few, minor pockets of Qz [<1 % overall], euhedral, prisms [<50 μm]. Minor Sd is also suspended within Sp. There are minor [<5 % overall] mineral inclusions [<10 μm] of Ccp within ("chalcopyrite-disease") within Sp – these inclusions are commonly located within the darker Sp bands.

K08-155: 132.5 m

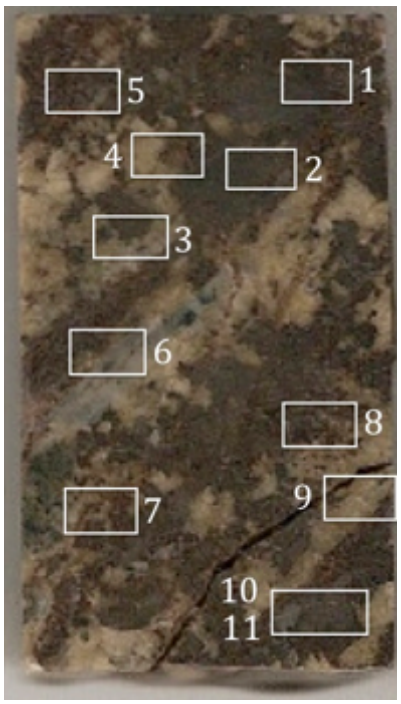

Location: Onek

Rock Type: B: (Qz-)**Sd** → (Qz-)**Sp**-Gn

Stages: (1-)2 → 3 (or 7 ?)

Host Lithology: Qtzt [15 % overall] occurs as clasts; comprised of predominantly tightly packet Qz, an- to subhedral [<250 μm]. Minor Pht is present as thin foliated, undulatory layers/bands [<100 μm wide]; commonly altered to Mica/Ms – clear to translucent brown or opaque material. There is minor Py present within Qtzt clasts, as fine, anhedral blebs; this Py may be of sedimentary origin.

Alteration: Silicification or re-crystallization of Qz. Pht may be recrystallized as or replaced by Mica/Ms.

The earliest hydrothermal phase is Qz [5 % overall] commonly nucleated on Qtzt clasts; but is partly continuous throughout, intergrown with Sd and Sp. Qz is mostly sub- to euhedral [<250 μm]; however there may be clusters of fine crystals [<50 μm].

Sd post-dates Qz and is the principal phase. Sd [35 % overall] is sub- to euhedral [generally between 100 μm to 2 mm], and mostly clear. Sd is intergrown with and generally followed by another (or continuous) Qz phase and subsequent Sp. A second hydrothermal Qz phase [10 % overall] is sub- to euhedral [<500 μm], and is closely associated with Sp; however some may occur as vein-fill. Sp [35 % overall] is translucent honey to reddish brown, with a banded texture defined by alternating lighter and darker layers, an- to euhedral, and appears to be a continuous vug in-filling mass. Ccp [<5 % within Sp] occurs as blebs/mineral inclusions [<10 μm] contained within Sp ("chalcopyrite disease"). The Ccp inclusions are located within the darker bands of Sp. Clusters of Qz and Sd are contained within the Sp mass. There may be few Gn and Py blebs [<20 μm] also contained within Sp.

K08-161: 229.8m

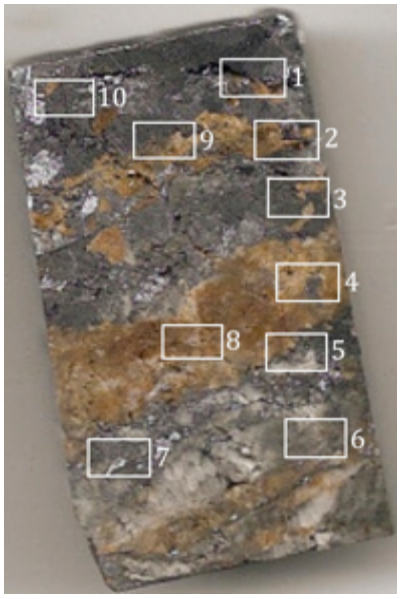

Location: Lucky Queen

Rock Type: B: Qz-Gn → Sd → Gn-Ttr-Pyr-Stn-Plb(-Cer)

Stages: 1(?)-5(?)→ 6 → 8

Host Lithology: Qtzt oocurs throughout as clasts; comprised of predominantly tightly packed Qz, an- to euhedral [<250 μm]. There may be minor pockets of Mica/Ms present within the Qtzt; also few areas with foliated undulatory, discontinuous lenese of opaque material.

Alteration: Silicification or re-crystallization of Qz. Pht may be altered to or replaced by Mica/Ms.

The earliest hydrothermal phase is Qz, most nucleated on Qtzt clasts, and intergrown with subsequent Gn and Sd. Hydrothermal Qz is difficult to distinguish from sedimentary Qz, only apparent from the euhedral Qz prisms. There is a Gn-rich phase after and partly intergrown with the above Qz. Gn is euhedral, but forms irregular, continuous masses or isolated pockets within Qtzt and/or seconday Qz. Areas of Gn appear to have locally brecciated Qtzt.

Sd post-dates the above Gn, and contains Qtzt clasts, there is again minor hydrothermal Qz commonly on Qtzt, prior to the surrounding Sd cement. Sd [20 % overall] is sub- to euhedral [<2 mm], and variably dirty/cloudy.

Following and partly intergrown with the above Sd unit, there is another phase of Gn; but this Gn stage is associated with minor brecciation affecting the above/previous stages. Minor Sp, pale to honey brown in PPL, present as a few pockets within Gn. Minor Stn, Plb, and lesser Plb [<1 % overall combined] are present as a pockets [<3 mm], contained within Gn. Minor Cer occurs as irregular pockets, intergrown with or replacing Gn.

K08-165: 174.8 m

Location: Keno 700

Rock Type: V: m**Qz**-m**Apy**(-Py) (→Sp)

Stages: 1 (→ 7?)

Host Lithology: An area of GSch-Pht, consisting of foliated Mica, clear to opaque/black, wavy with intergrown bands of Qz, anhedral [<100 μm] (from Qtzt).

Alteration: N/A

Most of the TS is comprised of massive Apy, contained within massive Qz. This early Qz is mostly anhedral [200 μm to 1 mm]. Some minor early Py [30 % within this zone] and Apy [5 % within this zone] is within GSch-Pht and intergrown with early Qz. Both Py and Apy are anhedral to euhedral, where the irregular/anhedral grains appear to have pitted or partly dissolved edges, and many of the grains are partly fractured.

Within the massive Qz there is a discontinuous layer [<500 μm] of Apy and Py. The more massive Apy is subhedral to euhedral, and is commonly fractured, and locally brecciated with a later phase of Qz, anhedral to subhedral. There are a few anhedral blebs [<20 μm] of Ccp contained within Py, as well as lesser anhedral Sp around Py. Minor Sp occurs throughout within fractures after massive Apy and Qz. Sp is anhedral, mostly translucent yellow. There are rare blebs [<100 μm] of Ccp associated with Sp.

K08-165: 176.5 m

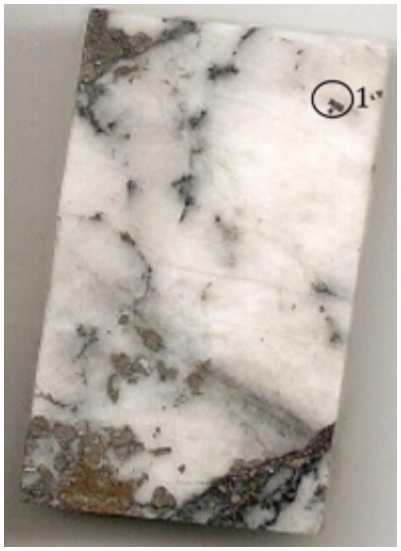

Location: Keno 700

Rock Type: V: m**Qz-Apy** → (-Sp-Gn) →
V/B: Qz(-Cal)

Stages: 1 (-7-8?) → (7-8) → 10(-12)

Host Lithology: Minor Qtzt may be intergrown with or contained within later hydrothermal Qz. Irregular zones of Pht/GSch are present, as fine grain opaque material.

Alteration: N/A

The predominant hydrothermal phase is Qz [>80 % overall], anhedral, coarse [<5 mm]; many crystals display progressive/undulatory extinction under XP. Apy [<10 %] is subhedral to euhedral [<1 mm], forming clusters, intergrown with Qz, and possibly minor in Qtzt. Lesser irregular pockets of Gn and Sp, may also be intergrown with Qz, or infilling crystal boundaries and within small irregular fractures. Gn may be anhedral to euhedral [<50 μm]; Sp is anhedral, and contains blebs of irregular Ccp, and euhedral Apy. Some earlier Apy appears to be brecciated/fractured clasts, with later anhedral Gn and Sp forming minor matrix.

There is a later stage vein/breccia structure [~3 mm wide], contains fragments of Apy, cemented by Qz and minor Cal. Qz is more abundant, anhedral [<500 μm]. Cal is an- to subhedral [<500 μm], with crystallographic twinning.

K09-185: 137 m

Location: Bellekeno – East, 980 masl

Rock Type: V/B: Sd(-Sp-Py) → Sd-Qz → Gn(-Py-zSp)

Stages: 2(-3) → 6 → 8(-7 or 9 ?)

Host Lithology: N/A

Alteration: N/A

The earliest hydrothermal phase is present in the lower portion of the TS, consisting of predominantly Sd, clean to variably cloudy, mostly sub- to euhedral, lesser anhedral [mostly >250 μm to >2 mm]. There are minor irregular pockets/blebs [<125 μm] of Sp and Py contained within this Sd; however some pockets of Sp may be introduced via fractures or within vugs from a later phase (below). There is a thin rim of Qz [<250 μm wide], anhedral, and discontinuous, post-dating the above earlier Sd.

The remainder of the TS is comprised of an irregular mix of intergrown Sd, Qz, Sp, Gn, and Py. Sd appears to be first in this sequence, with variable texture; from cloudy, an- to subhedral to subhedral blades and mostly clear, which may be zoned with cloudy bands commonly on the outer edges of the Sd blades. Qz is an- to euhedral; some Qz clusters may be the remnant Qtzt clasts. The sulfides are irregular pockets infilling after Sd and Qz. Gn [<5 % overall] is sub- to euhedral, as irregular pockets [mostly <500 μm], occurring around (after ?) Sp. Py is sub- to euhedral [<125 μm], and generally intergrown with Gn. Sp [<10 % overall] is an- to euhedral, as irregular pockets [<1 mm], partly intergrown with Gn, but generally as the last phase infilling vugs. Blebs of Gn [<50 μm] are common as mineral inclusions within Sp. The larger pockets of Sp [>1 mm] are internally zoned defined by alternating honey to dark brown bands/layers.

K09-187: 201.9 m

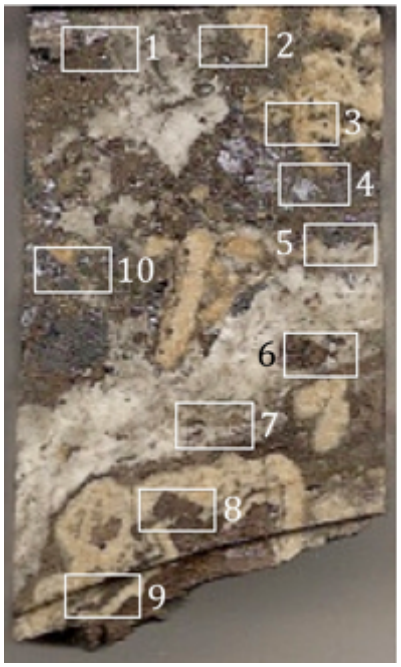

Location: Bellekeno East; ~950 masl

Rock Type: B: (m)**Sp**(-Qz-Sd) → **Gn**-Py →
V/B: b(cld)**Sd**-(Ank-) z**Sp**-Gn-Py →
V/B: **Qz**(-Sd?)

Stages: 7 → 8 → 9 → 10(-11 ?)

Host Lithology: N/A

Alteration: N/A

Sp [15 % overall] appears to be the earliest phase; as coarse, sub- to euhedral, irregular pockets; growth zones are defined by alternating bands of honey to dark brown layers [>4 mm thick]. Minor Qz and Sd are intergrown/contained within the Sp.

Following Sp, there is a stage of irregular and concentric banded Sd and minor Ank with lesser pockets of Sp; this unit is generally <1 cm wide. Sd [15 % overall] is medium [mostly <250 μm], an- to subhedral, and cloudy. There are discontinuous layers/bands of clear Sd, subhedral euhedral blades [<250 μm long, and <50 μm wide] intermittent within the predominantly cloudy Sd layers/bands. Sp may occur as irregular pockets, sub- euhedral [<2 mm] or at least one discontinuous layer [<2 mm wide] that generally follow after the clear Sd layers/bands, which is in-turn followed by bands of dirty Sd. Minor Gn as blebs, sub- to euhedral [<500 μm] may be contained within or associated with Sp. There is a large pocket/cluster [~2 mm] of Py, anhedral, or some euhedral as spherical growths [<250 μm] with an associated pocket [<250 μm] of Gn.

The last significant hydrothermal stage is predominantly Qz-cemented veins/breccia. Qz is anhedral to euhedral [<250 μm]; a zone ~1 cm thick, contains clasts and/or pockets of banded cloudy Sd and Sp, lesser Gn and minor Py. There is a small area of sulfide clast-rich breccia cemented by minor Sd, which appears to be a later breccia unit, post-dating the above Qz.

K09-199: 61.9 m

Location: Keno 700

Rock Type: V/B: mQz-Apy-Py → V: Sd(Apy-Qz-Sp-Ms)

Stages: 1 → 2/6?

Host Lithology: N/A

Alteration: Possible Fe-oxidation with/after and around the edges of Sd as ine grain creamy-orange (in TS) to red (in HS), follows grain boundaries, and is partly pervasive into Sd [<40 μm].

The earliest stage is massive Qz, intergrown with pockets or clusters of Apy, euhedral [<500 μm].

Multiple smaller veins containing Apy, Sp, Qz, Sd, and Mica/Ms cross-cut the Qz-Apy unit. Apy is the earliest in the veins, partly fractured and cemented and partly in-filled by the other vein-filling phases – possibly re-mobilized (?). Sd is the predominant vein-fill, cloudy, mostly anhedral to euhedral [<1 mm], the larger euhedral Sd displays crystallographic twinning. Sd appears clear under PPL, there is minor faint reddish to brownish red staining along crystal boundaries – possibly Fe-oxidation, with Apy and Mica/Ms. Qz is an- to subhedral, and may cluster, be suspended within the Sd-cement. Pockets of Sp are spatially associated with Apy. Mica/Ms is clear, with platy crystal habit.

K09-200: 85.7 m

Location: Keno 700

Rock Type: B: **Sd** (→ Ms-Qz)

Stages: 2 (6?)

Host Lithology: There are a few clasts of PhSch [<3 %] with minor Qz or Qtzt layers.

Alteration: Possible oxidation of Sd around the edges, forming Fe-oxide, fine grain creamy-orange (in TS) to red (in HS), follows grain boundaries, and is partly pervasive into Sd [<40 μm].

Essentially all Sd is coarse, mostly sub- to euhedral (many rhombohedral) crystals [100 μm to 1 mm], as an intergrown mosaic. Lenses or pockets of Qz, are comprised of fine [<50 μm], an- to subhedral grains. Flakes of Ms/Mica, fine grain [<50 μm] are associated and intergrown with Qz. Both Ms and Qz post-date Sd and precipitated within vugs and along fractures.

K09-200: 86.3 m

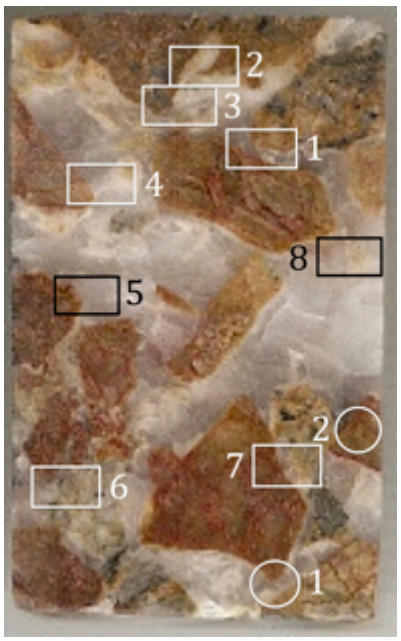

Location: Keno 700

Rock Type: V/B: (m)**Sd** → B: (Ank-)(m)**Cal**

Stages: 2/6 (?) → 12

Host Lithology: There are a few clasts of Qtzt with GSch-PhSch [overall <5 %]; irregular, angular to sub-rounded, contained within Sd. Qtzt – Qz is an- to euhedral [<50 μm].

Alteration: Possible oxidation of Sd around the edges, forming Fe-oxide, as fine grain creamy-orange (in TS) to red (in HS), follows grain boundaries, and is partly pervasive into Sd [<40 μm].

A remnant Qtzt clast has spatially associated Py and Apy [<50 μm] cemented within later Sd.

The earliest hydrothermal stage is predominantly Sd [>90 % this stage, <45 % overall] as massive, sub- to euhedral, rhombs [generally 100 μm to >1mm], mostly clear, with lesser cloudy. Clusters of fluid inclusions are common in coarse and euhedral Sd, they are irregular in shape [generally <20 μm], and contain 2-phases. There is a reddish stain (possibly Hem or Fe-oxide] concentrated within fractures in Sd; this occurred prior to the later Cal-cemented breccias (below).

The massive Sd stage has subsequently been brecciated and cemented by predominantly Cal. Minor Ank occurs as irregular and discontinuous rims on many Sd clasts prior to Cal. Ank [<5 % overall] is partly cloudy to clear, anhedral to euhedral, and forms bladed to radiating crystal masses. The cloudy appearance of Ank is the result of abundant crystallographic imperfections, and microscopic fluid inclusions; few usable fluid inclusions in Ank are two-phase, irregular to negative crystal shapes [<20 μm]. Cal [>95 % is stage, ~50 % overall] is massive, as intergrown irregular, sub- to euhedral crystals [mostly >2 mm], clear, and crystallographic twinning is common. Cal may appear milky white where irregular pockets of Ank are suspended within the Cal-matrix. No usable fluid inclusions were found within Cal.

K09-201: 236 m

(No Image Available)

Location: Keno 700

Rock Type: B: Sd(-Qz-Ms-Apy-Py)

Stages: 2

Host Lithology: N/A

Alteration: N/A

The earliest hydrothermal phase is Sd, occurring as a mosaic of intergrown cloudy and anhedral crystals [<500 μm]. Sd cements Qz, Mica/Ms, Py, and Apy. Qz may be isolated, an- to euhedral crystals [commonly <100 μm, up to 2 mm] or as conglomerates [may be >3 mm]. Qz may be intergrown with Mica/Ms, and less commonly with the sulfides. Mica is clear to creamy in PPL, in booklets of radiating crystals [<200 μm), some may be so fine grain that it appears opaque. Apy is an- to euhedral [<300 μm]. Py is mostly anhedral, lesser subhedral [<500 μm]. Some of the sulfides also appear to have crystallized around and on the edges of the Qz-Mica/Ms. Locally Apy, Py, Qz, and Mica/Ms are more abundant [~70 % combined], whereas within the Sd-cement, as follows: Apy 20 %, Py 20 %, Qz 20 %, and Mica 10 %.

There is a partly irregular veinlet [2 to 3 mm wide] cemented by Apy, Qz, Sd, Mica, and Py. Apy is the earliest mineral, along the vein edges, and constitutes ~5 % of the vein-fill; it borders or is partly intergrown with Mica/Ms, and lesser Qz. Mica/Ms [~5 % of the vein] occurs as flakes partly aligned to the vein edge. Qz is an- to subhedral [50 to 500 μm], partly intergrown with Mica and Apy; however most is main stage filling with Sd. The Qz:Sd ratio is 50:50 within the veinlet. Sd is partly cloudy, subhedral [generally ~500 μm]. Py more commonly within wall/host-rock; although also spatially associated and partly intergrown with Apy. The vein is asymmetrical and irregular, at least partly the result of subsequent deformation.

K09-201: 238 m

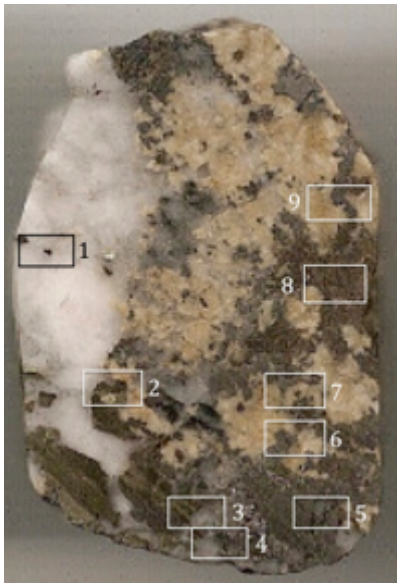

Location: Keno 700

Rock Type: V: (m)Qz(-Py-Apy) → V/B: Sd-Cal(-Py-Apy)-Sp → Gn(-Ttr-Pyr)

Stages: 1 → 6 (2 ?)-7 → 8

Host Lithology: N/A

Alteration: N/A

The earliest hydrothermal mineralization is massive Qz, an- to subhedral [10 μm up to 3 mm], partly intergrown with both Py and Apy. Py is an- to subhedral [10 μm up to 3mm]. Apy is similar to Py but generally more euhedral, both these sulfides commonly cluster together. Most of these sulfides appear to be introduced, or remobilized into the subsequent Sd-phase (below).

The Qz-Py-Apy assemblage has been partly brecciated and infilled by Sd [40 % overall, >90 % this stage], cloudy, an- to subhedral [generally 300 μm to 1 mm]. However further away from Qz-Py-Apy, Sd is more clear and euhedral, rhombohedral. There are minor fragments or individual crystals of Qz, Apy, and Py suspended within Sd. Apy and Py are also intergrown with Sd. Sp is associated and intergrown with Sd, Apy and Py. Sp is anhedral, translucent honey brown in PPL; yellowish around the edges, honey-brown in the center of masses. There are very few mineral inclusions/blebs of Ccp and Po within Sp. Minor Gn, anhedral, is intergrown with or around the edges of Sp, and lesser with Py and Apy. Gn could be a late stage vug filling after Sd and Sp. Minor Ttr and Pyr occur as blebs, associated with Gn.

K09-201: 239.1 m

Location: Keno 700

Rock Type: V: (m)Qz(-Apy) → Sp-Gn-Ttr-Pyr

Stages: 1 → 7-8

Host Lithology: N/A

Alteration: N/A

Massive Qz is the earliest and most predominant mineral, coarse [commonly >2 mm, to <10 μm], forming a mosaic of intergrown, anhedral crystals. Apy, Gn, and Sp are partly intergrown with Qz. These sulfides, particularly Gn and Sp have precipitated between Qz grains. There is one area where some Mica is associated with Apy, also having precipitated between Qz grains. Mica is fine [<100 μm], as sub- to euhedral radiating flakes; some of the Mica may be so fine grain that is appears opaque.

Sp is the most abundant sulfide, occuring as irregular and anhedral pockets (<1 cm to <200 μm). Gn is anhedral. Ttr is an- to euhedral [mostly 100 to 500 μm], and closely associated and/or intergrown with Gn. There is one inclusion of Pyr (?), translucent deep red in PPL, grey in RL (similar to Gn), anisotropic in XP, (~500 μm) contained within Gn, and associated with Ttr.

BKUD09-134: 39.5 m

Location: Bellekeno – Southwest

Rock Type: V/B: **Py**-**Sp**(-Mica-Apy-Cst-Gn) → V: **Qz**(-Py-Apy-Cst-Gn)

Stages: 4a → 4b

Host Lithology: Qtzt, is comprised of a mosaic of Qz grains [generally <100 μm].

Alteration: Silicification or re-crystallization of Qtzt.

Py [40 % overall] is sub- to euhedral, blebs of Sp occur within the larger Py crystals. Minor blebs of Gn also occur within Sp and Py. Sp [50 % overall] is honey brown and partly translucent around the edges, sub- euhedral [<200 μm wide x <300 μm long], occurs within aligned zones intergrown with, and post-dates Py. Py and Sp generally segregate into their own respective compositionally rich areas, as well as less commonly cross-cutting veinlets. Mineral inclusions of Ccp and lesser Po [< 10 μm] are common with Sp.

Later stage veinlets comprised of Qz, euhedral [200 μm x 300 μm] with pockets or clusters of Py and Apy, an- to euhedral [<100 μm]; may be present along the outer edges of the veinlets or within the middle, whereas the Qz appears to nucleate in the vein center and grow outward into Sp. Minor Cst occurs as clusters or isolated crystals, mostly subhedral, generally spatially associated or intergrown with Apy, as well as lesser Py. Veinlets also commonly contain pockets of minor micaceous mineral [needles ~ 100 μm long].

BKUD09-134: 41.35 m

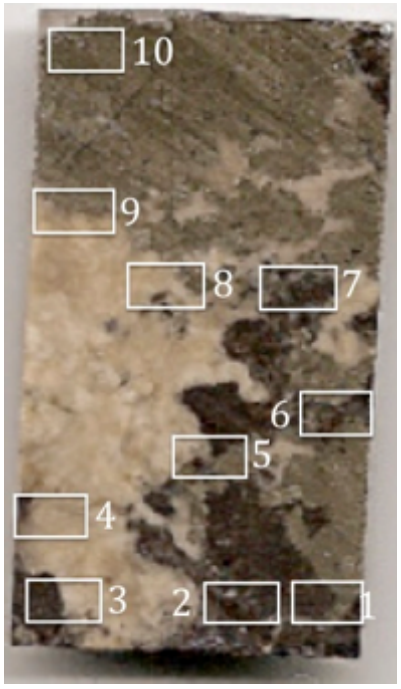

Location: Bellekeno – Southwest

Rock Type: V/B: (m,cld)**Sd** → **Py**-**Sp**(-Gn) → (m)Sd-Qz-Ank-Cal

Stages: 2 → 4a → 5 or 9-10-12 (?)

Host Lithology: N/A

Alteration: N/A

Sd [45 % overall] is massive, cloudy, euhedral rhombs, slightly pleochroic. Most of the Sd appears to be the earliest stage, which has been partially replaced by Py and Sp, where this occurs the boundaries between Py or Sp with Sd are highly irregular.

Sd is followed by a stage of predominantly Py [20 % overall] and Sp [25 % overall]. Py is generally earlier than Sp, and is mostly subhedral, lesser anhedral appears to nucleate on Sp. There are also a few irregular and discontinuous veinlets of Py cross-cutting zones of Sp. Sp is sub- to euhedral, commonly contains inclusions of Cpy [< 10 μm], and may be intergrown with Py (possibly replacement by Py ?). Apy [<1 %], an- to euhedral is associated with mostly Py and Sp. Gn [<1 %] is mostly anhedral as irregular blebs to mostly within Py and to a lesser extent within Sd and Sp. Minor Cpy and Sp is also present as irregular inclusions [50 μm] within Sd and Py.

There is a later stage of Sd, Ank, and Cal [<10 % overall, combined] with minor Qz. Qz [< 1 %], sub- to euhedral and prismatic [~200 μm wide x ~ 300 μm long], and is intergrown with Sd. Areas of micro-brecciated Sd, Py, and Sp from the earlier stages, with fragments nearly in-situ, are cemented by this later stage Sd and Qz.

BKUD09-134: 45 m

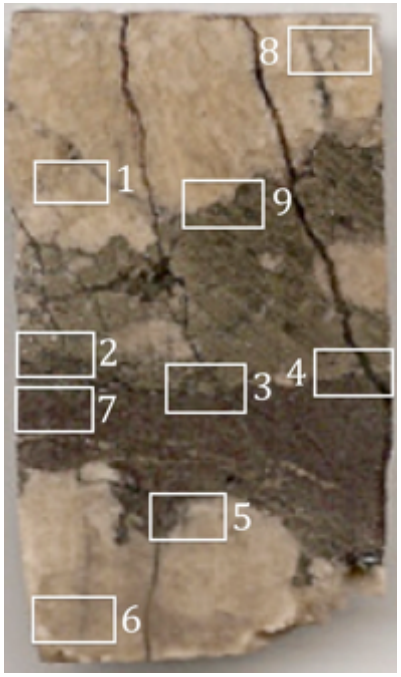

Location: Bellekeno – Southwest

Rock Type: V/B: m**Sd** → **Py**-**Sp**(-Apy-Cst-Gn) → Qz-Sd(-Ank)-Cal

Stages: 2 → 4a(-4b) → 9-10-12 (?)

Host Lithology: N/A

Alteration: N/A

Sd [>97 % overall, typical of this stage] is massive sub- to euhedral, some crystals display cleavage and lamellae twinning. Sd has an overall cloudy appearance, likely the result of abundant impurities, imperfections, and/or fluid inclusions – which may be concentrated along cleavage or crystal planes (?). There are minor pockets or blebs Py, Sp, Apy, and Gn contained within Sd. Py [<1 %] and Apy [<1 %], euhedral, light yellow, isotropic; these are possibly after Sd, but generally present along/between Sd crystal planes. There are also minor irregular pockets of Gn [<1 %], anhedral.

A Py- and Sp-rich vein cross-cuts massive Sd, is divided into distinct compositional zones, one area is Py-rich, the other Sp-rich. The Py-rich zone appears to be earlier, an- to euhedral [generally >1 mm], and commonly contains irregular blebs of Sp and Gn [<50 μm]. There is an irregular brecciated transition between the Py and Sp zones. The Sp-rich zone partly impedes into the Py-zone. Sp is massive and commonly contains inclusions [<50 μm] of Po and Ccp; the Po:Ccp ratio is 2:1. There are irregular pocketsor clasts (?) of Py contained within Sp. Along the edge of the Sp-zone edge and within Sd, there is an irregular and discontinuous layer/band of Py, Apy, Cst, with inclusions of Cpy and Gn within Py. Cst [<1 %] is an- to euhedral [mostly <100 μm] and is spatially associated with Apy, an- to euhedral [<300 μm], or rarely as inclusions within Py.

The last hydrothermal phase is a matrix-supported breccia between the Py and Sp vein zones. Brecciation predominantly occurs within the Sp-zone, cemented by Sd

with minor Ank and Qz, followed by Cal. The carbonates are an- to euhedral [<200 μm]. Qz is generally early, mostly nucleating from Py.

BKUD09-139: 8.3 m

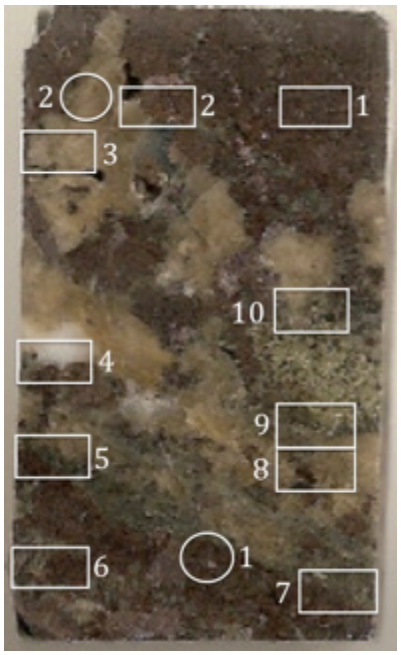

Location: Bellekeno – Southwest; ~965 masl

Rock Type: V/B: **Sd**(-Qz) → Py-**Ccp**-(z)**Sp**-Gn-Ttr(-Qz-Sd?)→ V/B: Qz-Sd → V/B: Cal

Stages: 6 → 7-8 → 10-11 → 12

Host Lithology: At least one Qtzt clast [500 μm wide x 2 mm long] is present within the Sd-matrix. Qz is mostly anhedral [<125 mm], may be re-crystallized and euhedral. Lenses of Mica are also associated with the clast. The clast boundary is irregular, possibily partly dissolved.

Alteration: Silicification and/or re-crystallization of Qtzt.

The earliest hydrothermal phase is Sd [25 % overall], sub- to euhedral [some crystals may be >2 mm]; smaller euhedral to anhedral Sd grains appear to form later during this stage and are intergrown with later Sp, Py, Ccp, and Ttr. Py may be early partly integrown with or contained within Sd. Qz is an- to euhedral, and is partly intergrown with or post-dates Sd(-Py).

After Sd, Sp [40 % overall] is translucent honey to dark brown, as sub- to euhedral, with alternating colour bands, as irregular masses [>2 cm]. Note that there is a lack of mineral inclusions within this Sp. Fluid inclusions may be present within this phase, irregular to oval shaped; few <40 μm, most <10 μm. Qz [<5 %], subhedral to euhedral, prismatic crystals [<500 μm] are commonly intergrown with Sp and also follows Sd (above) – this may be a later stage (see below) of Qz preferentially growing within 'soft' Sp or be contemporaneous with this stage. Py and Ccp are commonly associated and intergrown with each other, as well as with Sp; they occur as suhedral, irregular pockets or clusters, aound the edges of Qz and Sd; suggesting that some Py and Ccp may be earlier than Sp; or mostly later in the stage as irregular pockets infilling after and around Sp.

A later stage breccia [<2 mm wide] approximately follows the contact trend of the earlier Sd and Sp stages. This breccia is clast-rich [>80 % clasts], cemented by Sd [<10 % this stage] and Qz [<10% this stage], an- to subhedral. These clasts [<500 μm] appear to be locally derived Sd and Sp, angular (some still euhedral Sd) to irregular.

Minor late stage Cal fills voids/vugs after Sp and Sd; Cal is euhedral as irregular masses.

BKUD09-139: 8.4 m

Location: Bellekeno – Southwest; ~965 masl

Rock Type: V/B: **Sd**(-Qz-Sp) → (V:) Qz-Sd → **Sp**(-Py-Ccp-Qz-Sd) → V/B: **Cal**

Stages: 6 → (6 ?) → 7 → 12

Host Lithology: N/A

Alteration: N/A

Early Sd is subhedral to euhedral [generally >500 μm, many >2 mm], and may also be partly intergrown with later Sp and Qz. Qz is subhedral to euhedral [<500 μm], post-dates the earlier Sd, but may also be intergrown with a later phase of Sd [generally <500 μm].

A Sp-rich phase, comprised of mostly euhedral, alternating lighter honey and darker brown bands/layers, as irregular masses infilling vugs, and is partly intergrown with the Sd-rich stage. Note that there is a lack of mineral inclusions within this Sp. In some areas Sp is coarse and predominant, other areas Sp is intergrown with abundant Qz and Sd. Minor Py is anhedral to subhedral [mostly <100 μm, up to 500 μm], with lesser Ccp intergrown within the areas of mixed Sp, Qz, and Sd.

In the upper corner of the TS there is another generation of Qz after both the coarse euhedral Sd, and Sp-rich phases. Qz is anhedral to euhedral [<1 mm]; intergrown with lesser Sd and Sp, and then followed by more abundant Sd and Sp. This Qz-Sd-Sp

association may also occur as irregular veinlets [<500 μm wide] cross-cutting the earlier coarse, euhedral Sd.

There is an abrupt transition to late stage Cal as vein and breccia fill. Cal is anhedral to subhedral [mostly <1 mm]; some crystals are variably cloudy, but mostly clear.

BKUD09-140: 9.9 m

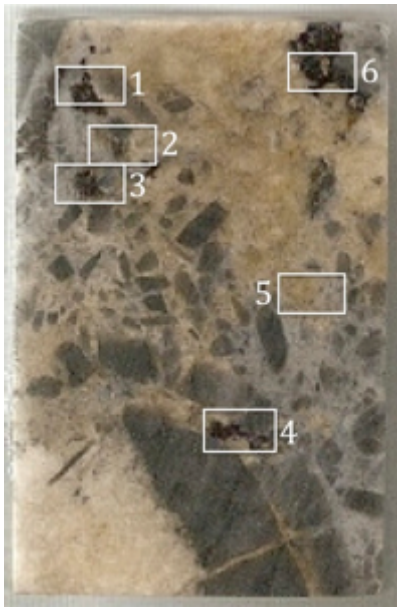

Location: Bellekeno – Southwest

Rock Type: B: Qz → V/B: (cld/c,clr)**Sd** → Sp(-Py-Gn)

Stages: 1 (?) → 2 → 3

Host Lithology: Qtzt is comprised of a mosaic of anhedral Qz [<100 μm]. The Qtzt has been brecciated and cemented by 2 types of Sd, based on texture. Qtzt fragments are angular to subrounded suspended in a cement of hydrothermal Qz and Sd.

Alteration: Silicification or re-crystallization of Qtzt.

Qz appears to be the earliest hydrothermal phase, nucleating/precipitating on, and locally cementing Qtzt clasts. Minor Mica/Ms is clear, as radiating crystals [<100 μm] associated with early Qz and to a lesser extent with subsequent Sd and Sp.

Sd is the most prominent breccia fill/matrix/cement. There are 2 texturally distinct types of Sd: (1) at one end of the TS there is cloudy, anhedral to subhedral, [generally <1 mm], the crystals are partly radiating (apparent from extinction under XP); (2) at the opposite side of the TS, Sd is more clear/translucent, mostly subhedral to euhedral, with common rhombohedal crystal structure. Both types of Sd are partly intergrown.

Following Sd are irregular pockets of in-filling Sp; deep red to brown, almost opaque grading to partly translucent in PPL, anhedral, and contains few blebs/inclusions of Ccp or lesser Gn. Locally, a pocket of Sp [<1 mm] is intergrown with irregular Ccp, Gn, and Py.

BKUD09-143: 51.2 m

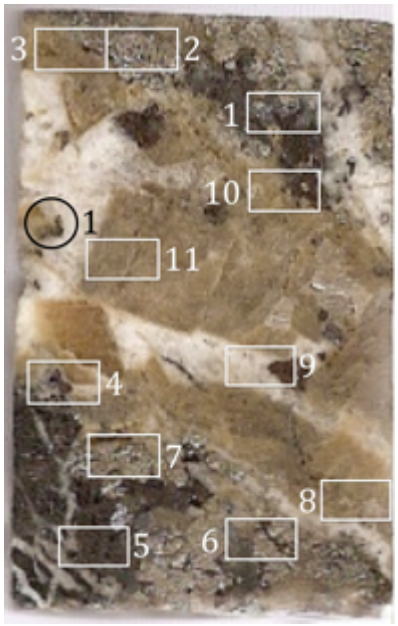

Location: Bellekeno – Southwest; ~950 masl

Rock Type: V/B: **Py**-(m)**Sp**(-Gn) → V/B: **Sd**(-Ank) → (z)Sp → **Qz**

Stages: 3/4a → 6 → 9 → 10

Host Lithology: N/A

Alteration: N/A

The earliest hydrothermal mineral assemblage present is comprised of Py and Sp. Py [10 % overall] is generally the earliest, an- to subhedral [mostly <4 mm]. Sp [10 % overall] may be coarse [mostly <4 mm], anhedral, dark purple in HS, and generally opaque to deep red in TS; and partly intergrown with Py.

A stage of predominantly Sd cross-cuts the earlier Py-Sp stage. Sd [50 % overall] is an- to mostly euhedral [generally <2 mm] some may be coarse [>4 mm]; and partly intergrown and brecciating the earlier sulfides at contact.

There is another later stage of Sp post-dating the above Sd stage. Here Sp [<5 % overall, this stage only] occurs as irregular pockets, and is sub- to euhedral, internally zoned, - defined by alternating parlty translucent honey to reddish brown layer/bands.

Lastly, Qz [10 % overall] is mostly irregular, an- to subhedral [<2 mm], infilling around/post-dating Sd and Sp. Some Qz has precipitated as irregular rims around Sd and Sp; this may be a sub-stage, partly syn-genetic with Sd.

BKUD09-143: 52.7 m

Location: Bellekeno – Southwest; ~965 masl

Rock Type: V: (Sp) → b(cld)**Sd**-z**Sp**(-Py-Gn) → V/B: **Qz**(-Sd?)

Stages: (7) → 9 → 10

Host Lithology: N/A

Alteration: N/A

The earliest hydrothermal mineral assemblage consists of mostly Sd and Sp. Sd occurs as 2 texturally distinct types: (1) the most common Sd phase occurs as layers of very cloudy, an- to subhedral [mostly <125 μm], and (2) less common layers [generally <500 μm thick] of more coarse [<500 μm, mostly <250 μm] and clear Sd. The 2 types of Sd form concentric, alternating, and repeating banded seuquences, where the cloudy Sd appears to be the earliest phase. In some areas the bands may close-in/meet each other (mirror image); this suggests that the precipitated in open space. There are clusters of Sp blebs [<20 μm] are intergrown with the above Sd but commonly follow the clear Sd layers. Sp is sub- to euhedral, and internally zoned - defined by alternating honey to dark brown bands/layers. Note that there is a distinct lack of mineral inclusions within this Sp. Minor pockets or blebs of Py and Gn may be intergrown with Sp.

Following the banded Sd and Sp stage, there is stage of brecciation and irregular veining, associated with in-filling Qz. Qz is an- to euhedral [<1 mm], and appears variably cloudy. The transition to the Qz-cemented breccia may be conformable or insequence after the banded Sd and Sp, based on areas where Qz crystals have nucleated and grown perpendicular from band Sd or Sp. However there are also areas where this Qz-cemented breccia affects and cross-cuts the above stage.

BKUD09-143: 52.8 m

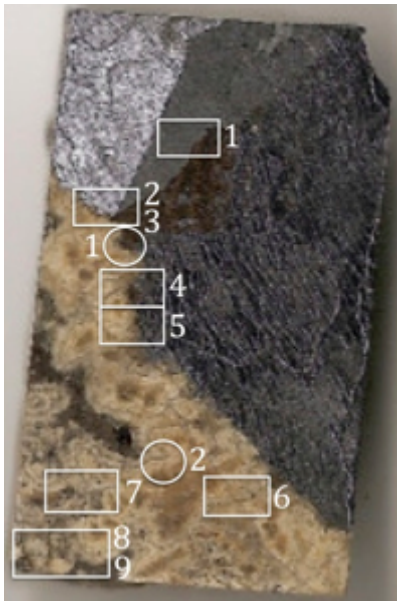

Location: Bellekeno – Southwest; ~965 masl

Rock Type: V/B: m**Gn**-<u>Ttr</u>(-Ccp)-Py-zSp → b**Sd**(-Ank ?)-z**Sp**-Py

Stages: 8(-7 ?) → 9

Host Lithology: N/A

Alteration: N/A

The earliest hydrothermal phase is massive Gn [60 % overall, >95 % this stage], euhedral. Gn contains pockets or blebs [<1 mm] of Ttr [<2 % overall], anhedral; and spatially associated or intergrown Ccp mineral inclusions [<20 μm].

Sp generally follows and is also partly intergrown with Gn, but may also define a later in-filling stage. Sp is euhedral, and internally zoned - defined by alternating translucent pale to reddish brown layers/bands; there are few [<5 %] Ccp mineral inclusions [<10 μm] within Sp. Very few usable fluid inclusions are present within this banded Sp stage [<20 μm, most <5 μm]. Ttr is also located near the upper boundary and may precipitate during the transitions from Gn to the subsequent Sp stage.

After the Gn-Sp there is an abrupt transition to a banded Sd(-Ank?) [<30 % overall]. Sd is mostly comprised of fine to medium crystals [<125 μm], cloudy, sub- to euhedral layers; intergrown with Sd layers of clear, sub- to euhedral [<250 μm], some radiating or bladed crystals,. The cloudy Sd texture is a result of abundant fluid inclusions and/or crystallographic imperfects, which may render the Sd essentially opaque. There are few usable fluid inclusions [generally <20 μm], as negative crystal vacuoles within this banded stage, but only observed within the layers of clear Sd phase. This banded texture forms concentric, alternating and repetitive layers of the 2 Sd types. At the Gn-Sd boundary there are clusters of Py, subhedral to euhedral [<1 mm] intergrown with both Gn and Sd. Pockets of Sp and lesser Py are also intergrown with the banded Sd; which generally follows or are intergrown with the clear, euhedral Sd phase (layers).

BKUD09-143: 53.5 m

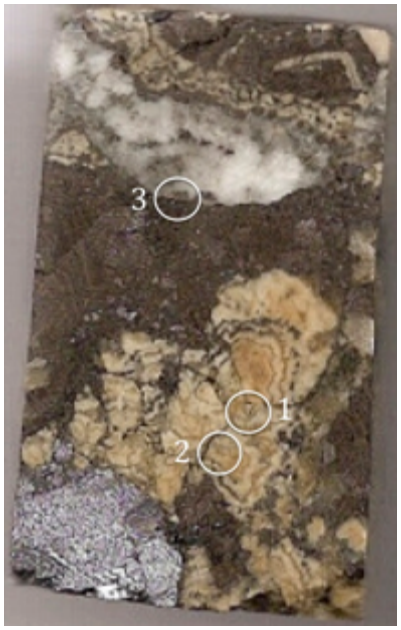

Location: Bellekeno – Southwest: ~965 masl

Rock Type: V/B: (Sp-)(m)**Gn** → b**Sd**-z**Sp**(-Py-Gn) → V/B: **Qz** → (B: Sd)

Stages: (7) 8 → 9 → 10 → 11

Host Lithology: N/A

Alteration: N/A

The earliest hydrothermal phase is Gn [<10% overall], occurs as a large pockets/clusters [>1 cm] of euhedral crystals [generally >1 mm], and may be massive. Most of the Gn has been lost during the thin section preparation.

Following Gn there is a stage of Sd and Sp which are partly intergrown with the earlier Gn. Sd [15 % overall] occurs as irregular concentric bands/layers of variable thickness [generally <500 μm]; texturally Sd varies from cloudy and fine [<250 μm] to more clear [<500 μm]. Irregular pockets of Sp [5 % this stage] are partly translucent honey to brown, an- to subhedral [mostly <500 μm]; generally follow or are associated with the more coarse and clear bands. The banded Sd stage terminates with a coarse clear Sd [<1 mm, up to 4 mm]. The repetitive bands of Sd is followed by another more prominent phase of Sp [30 % overall], coarse, sub- to euhedral, as alternating bands/zones [<1 mm thick] of honey to brown. There may be pockets of Gn [<500 μm] intergrown or associated with the banded Sd and Sp.

The banded Sd and Sp stage is followed by an irregular Qz-cemented vein. Qz [10 % overall] is partly cloudy, an- to subhedral [<1 mm].

A weak brecciation event post-dates the Qz stage, but does not largely affect it; rather the banded Sd and Sp phases are highly brecciated. Some clasts appear to be nearly in-situ and are generally larger [>1 mm], whereas many smaller, angular clasts [<500 μm] are concentrated into clast-rich/supported channels or zones [80 % clasts]. Sp fragments makes up ~60 to 70 % of the clasts, and Sd 10 to 20 %. There is generally no matrix/cement, only vug space; however minor Sd-matrix may be present. This breccia affects ~30 % of the central area of the thin section.

BKUD09-143: 54 m

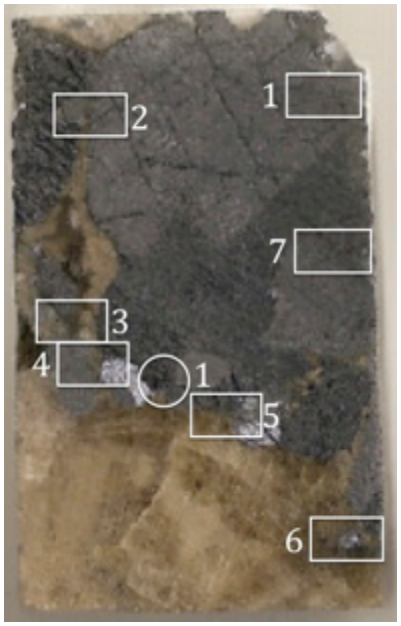

Location: Bellekeno – Southwest; ~965masl

Rock Type: V/B: m**Sd** (→ Sd-Ank-Ccp-Qz) → m**Gn**(-Ccp-Ttr-Stn-Plb)

Stages: 6 → 8

Host Lithology: N/A

Alteration: N/A

The earliest hydrothermal phase is massive Sd [<40 % overall; >90 % this stage], subhedral to mostly euhedral and coarse [generally >500 μm, many >2 mm]; with variably cloudy patches (present in all crystal sizes) - a result of abundant fluid inclusions and/or crystallographic imperfections. Usable 2-phase fluid inclusions [generally <30 μm] are common in this phase, either irregular or as negative vacuoles.

Following the above Sd stage or at later part of this stage, there is an abrupt transition to smaller Sd [<1 mm], subhedral to euhedral; intergrown with Ank (?), clear, subhedral, bladed crystals. Fluid inclusions are similar as in the above Sd stage. Blebs [<250 μm] of Ccp are anhedral and contained within this transitional stage of carbonates. Qz, an- to euhedral [<1 mm], is partly intergrown with Ank, and also occurs at the contact between the earlier coarse Sd and later Gn.

Massive Gn [<60 % overall; >90 % this stage], mostly euhedral, follows the above stages, as irregular masses in-filling around euhedral Sd; or partly intergrown with the transitional Sd and Ank. Minor Ttr, Stn [<2 % combined within this stage], and lesser Plb are present as blebs [<125 μm], anhedral, contained within, or occur as discontinuous pockets infilling fractures within Gn.

BKUD09-144: 36.6 m

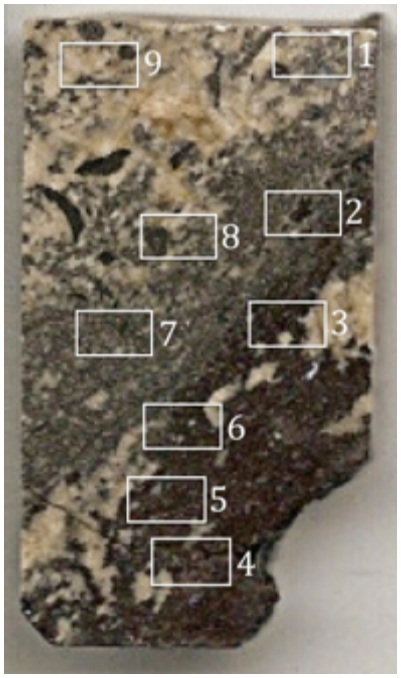

Location: Bellekeno – Southwest; 980 masl

Rock Type: V/B: **Sd-**(Qz-Sp-Py-Cst-)**Apy** →
V/B: Qz-Sd-d**Sp**(-Py-Apy)-<u>Gn</u> →
V: Qz-Apy

Stages: 1 → 3 (4a?) → 4b

Host Lithology: Qtzt clasts [5 %], are irregular and suspended within a Sd-matrix; comprised of white to clear-grey Qz.

Alteration: Qtzt clasts appear to be partially dissolved.

The earliest mineral phase is predominant Sd, an- to euhedral, cloudy to clear, some crystals display twinning, extinction under XP may be undulatory to radiating, most crystals are 500 μm to 1 mm or less. There are suspended clasts/grains of Apy intergrown with lesser Qz and minor Mica/Ms. These clasts are angular to subrounded. Mica/Ms where present is generally <50 μm, clear, and may be so fine grain that it appears opaque. Qz is mostly anhedral [<100 μm]; one clast is essentially all Qz, with individual crystals <1 mm. Apy is an- to euhedral, forming clusters [mostly <300 μm; few may be >500 μm]. At the lower boundary of this unit there is an Apy-rich area/zone.

There is a sharp transition to a Sp-rich zone. From this boundary there are a few coarse, euhedral Qz prisms that have grown into and/or are surrounded by mostly Sp and lesser Sd. Sp is deep red to brown, and only partly translucent, as irregular, an- to euhedral (?) masses, intergrown with lesser Sd. Blebs or inclusions of Ccp, Po, and Gn within Sp are common [total <10 % within Sp, ~3 % each]. Ccp and Po inclusions are mostly smaller [<50 μm] and concentrate along possible Sp crystallographic planes. Gn inclusions are generally larger [<100 μm] but more sporadic and always irregular. Gn from this stage is Ag-bearing (around 1 wt %). Apy is mostly subhedral to euhedral, and continues sporadically throughout the Sp-rich zone.

There is a discontinuous, undulatory vein cross-cutting Sp. The vein is <500 μm wide, the inner part of the vein is mostly Qz and Sd [<100 μm] intergrown with Apy [mostly <20 μm], subhedral to euhedral. The outer edges of the vein are lined within

discontinuous pockets of Apy [20 to 100 μm] and coarse, euhedral Qz prisms [<500 μm] extend outward from the vein margin into the surround Sp.

BKUD09-146: 46.5 m

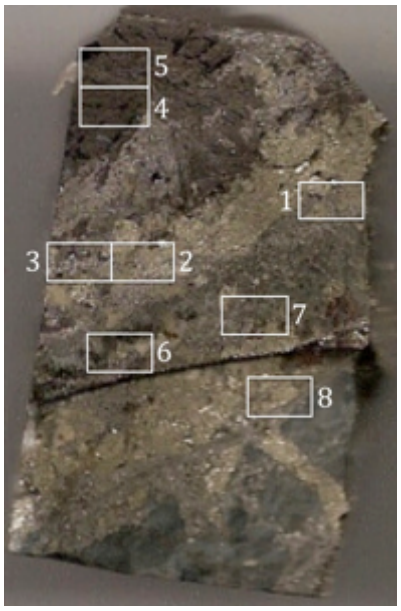

Location: Bellekeno – Southwest; ~970 masl

Rock Type: V/B: **Sd** →
V/B: **Py**-(m,d)**Sp**(-Apy-Cst-Gn)
(→ V: Qz-Apy-Py-Cst)

Stages: 2 → 4a (→ 4b)

Host Lithology: Qtzt clasts are present at the lower part of the TS; comprised of Qz grains [20 % overall], anhedral to subhedral [<250 μm] and cloudy.

Alteration: Silicification or re-crystallization of Qtzt.

The earliest stage of mineralization is Sd [10 % overall], subhedral to euhedral, <1 cm, and cloudy; in-filling veinlets or clast-rich breccia cement.

A stage of predominantly Py cross-cuts Qtzt and the first Sd stage above. Py [70 % this zone; 40 % overall], some Qtzt clasts are cemented within Py near the vein edge;. Py is mostly subhedral to euhedral [<500 μm], forming clusters larger and irregular clusters [<5 mm], locally continuous and massive; intergrown with lesser Apy, Sd, later Sp and Gn (below), and minor Cst (?). Apy [<15 % overall] is anhedral to euhedral [<500 μm], forming clusters, closely associated with Py. Cst [Tr] is subhedral to euhedral, intergrown and spatially associated with Apy, Py, and Qz. Minor Mica/Ms [Tr] is associated and intergrown with Py, within Qtzt clasts.

Following Py, there is an abrupt and partly intergrown transition to predominantly Sp [30 % overall]. Sp is anhedral to subhedral, deep red to brown in PPL, forming irregular partly continuous masses <4 mm wide. There are discontinuous layers of Py [<10 % this zone] and Apy [<10 % this zone], anhedral to euhedral around the Sp edges and intergrown with Sd [<10 % this zone]. Apy is generally more euhedral than above. Sd is texturally similar as above, subhedral to euhedral [<1 cm]. Minor Gn [<5 %] occurs as irregular pockets associated and intergrown with Apy and Sp. Vug space [<5 % overall] may be present in any of the above stages.

Lesser Sd may be continuous throughout partly intergrown with Qz, Sp and Py (above). Sd is subhedral to euhedral, [250 μm to 2 mm].

A Qz-cemented vein structure that parallels the Py-Sp vein structure, and is contained within the central area of the predominantly Py stage. Qz is anhedral to euhedral [<1 mm], partly cloudy.

BKUD09-148: 29.5 m

Location: Bellekeno – 99; 1025 masl

Rock Type: V/B: **Sd**-Py (→ (f,b,cldSd) → **Sp**(-Py-Po-Gn-Ttr) → b**Sd**(-Sp)-**Qz**

Stages: 2 → 7-8 → 9-10

Host Lithology: Qtzt

Alteration: Silicification or re-crystallization of Qtzt. Fe-oxidation associated with late stage Sd.

The earliest hydrothermal phase is predominantly Sd within Qtzt as irregular veinlets and micro breccias. Sd is comprised of both cloudy and clear grains, sub- to euhedral [generally >500 μm, many >1 mm]. Later during the transitional end of this stage, Sd grains generally become smaller [<500 μm], an- to subhedral. Py is intergrown with this transitional/later Sd. Py occurs as clusters, an- to euhedral, [<125 μm, many <20 μm].

A vein-structure in-filled by predominantly Sp occurs at the outer edges of the vein, as an irregular and generally continuous horizon [<5 mm wide]. Sp is sub- to euhedral, internally zoned defined by alternating honey to dark brown layers/bands. Within Sp there are few mineral inclusion/blebs [<50 μm] of Po and Gn, which generally occur within the darker bands. Py also occurs as pockets within micro-fractures within Sp. Within the cental part of the vein, after Sp, there are irregular layers of Sd grading from cloudy and anhedral [<125 μm] to clear, sub- to euhedral [<125 μm]. Intergrown with the clear Sd are pockets [<125 μm] of Sp, anhedral. Fe-oxide may stain this late stage Sd. The last vein-filling phase is Qz, an- to subhedral.

BKUD09-148: 33.5 m

Location: Bellekeno – 99; ~1025 masl

Rock Type: V/B: (Qz-)**Sd** → (Qz-)**Sp**-(Ccp-Py-Po-)**Gn**-Ttr-Sd

Stages: 6 → 7-8

Host Lithology: N/A

Alteration: N/A

The earliest and most prominant mineral is Sd [<65 % overall], sub- to euhedral [mostly >500 μm, few >1 cm], crystals are variably cloudy, there is no obvious distribution pattern of cloudy and clear crystals. Sd is intergrown with Sp, lesser Gn, and minor Ccp, Py and Qz [<2 %]. Gn [<1 %] is an- to euhedral [<500 μm], irregularly shaped, and contained within both textural-type of Sd.

Sp [<35 %] post-dates, and infilling irregular or negative crystal voids around Sd. Sp is partly translucent honey to brown in PPL, an- to euhedral, mostly coarse [>500 μm]; small pockets [<500 μm] may be contained within Sd. Minor anhedral blebs [<1 %] of Ccp [<250 μm] and Po [<750 μm] are contained within Sp. Py [<1 %], an- to euhedral [<500 μm] is spatially associated with Sp. Minor Ttr (Fah) occurs as irregular pockets/blebs associated and/or intergrown with Sp and Gn.

BKUD09-149: 38.3 m

Location: Bellekeno – Southwest; ~1055 masl

Rock Type: V/B: (Qz-)Sd → (Qz-)bSd-zSp-Py → V: Sp

Stages: 2 or 6 (?) → 9 → ?

Host Lithology: Qtzt [<40 % overall] occurs as brecciated clasts, predominantly cemented by Sd; locally areas vary from clast- to matrix-rich.

Alteration: Minor Fe-oxide (?) is present as fine, translucent brown material between or following crystal boundaries.

The earliest hydrothermal phase is Sd [<50 % overall], predominantly fine [<250 μm] and cloudy, with lesser clear and more coarse [250 to 500 μm]. These 2 texturally distinct types of Sd form irregular to partly concentric bands, intergrown with pockets of Sp and clusters of Py. Qz [<10 % overall] is sub- to euhedral [<500 μm]. and is commonly intergrown with Sd.

Sp [<25 % overall] is partly intergrown Sd and Qz, and post-dates infilling vugs. Sp may be euhedral [<1 cm], partly translucent honey to brown in PPL, and may form alterating zones of light and darker growth bands/layers. Py [1 %], an- to subhedral, occurs as isolated crystals [<250 μm] or as clusters [<2 mm], spatially associated with Sp.

A late stage (?) veinlet [<1 mm wide] of Sp cross-cuts all the above phases.

BKUD09-150: 63.2 m

Location: Bellekeno – Southwest; ~975 masl

Rock Type: V/B: (Qz-)Sd (?) → **Py**-Sd-(m)**Sp**(-Gn) → V: Qz(-Sd)

Stages: 2 → 4a → 4b

Host Lithology: N/A

Alteration: N/A

Sp, Py, Sd, and lesser Qz are intergrown/syn-genetic. Minor Qz may be earlier than, or partly intergrown with Sd and Sp; however it is also more abundant as a later stage/phase (see below). Py [15 % overall] may be the earliest mineral crystallized, or possibly appears as such due to the textural effects of the euhedral crystal growth; an- to subhedral [mostly <2 mm] and may form clusters [>1 cm]. Sp [50 % overall] is almost opaque to deep red, an- to subhedral, forming irregular masses around Py and also after Sd, and lesser Qz. There are minor pockets of Py and Gn contained within or around the edges of Sp and Sd. Gn [<1 %] is an- to euhedral, and forms irregular pockets [<500 μm]. Sd [30 % overall] is sub- to euhedral [mostly 500 μm to 2 mm], and variably cloudy to clear/translucent. Some Sd becomes increasingly cloudy – due to abundant fluid inclusions and/or crystallographic imperfections – towards the outer rim of the crystal.

Most of the Qz present [15 % overall] generally post-dates the above mineral phases, occuring as an irregular veinlet [<6 mm wide] with lesser Sd, which cross-cuts through the middle of the TS. Qz is sub- to euhedral [mostly 500 μm to 2 mm], generally cloudy around the outer edges of the crystal – due to abundant microscopic fluid inclusions, and/or crystallographic imperfections.

BKUD09-150: 64.1 m

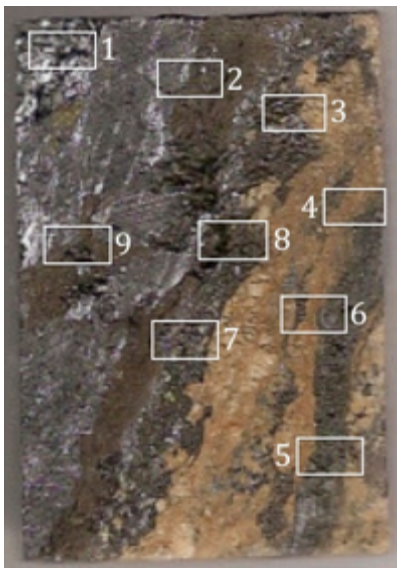

Location: Bellekeno – Southwest; ~975 masl

Rock Type: V/B: **Sd**(-Sp-Gn) → **Sp**(-Py-Gn-Ccp) → (m)**Gn**(-Sp)

Stages: 2 → 3 → 5

Host Lithology: N/A

Alteration: N/A

This sample appears to be comprised of multiple stages that may have been sheared, and mechanically mixed. Layers are highly strained and defined by compositionally/mineral-rich phases.

The earliest stage is comprised of mostly Sd [75 % in this zone] irregularly layered, with fine [<125 μm], anhedral, and cloudy grains; with fewer discontinuous layers of more clear, coarse [>125 μm to <1mm], an- to euhedral. Within this predominantly Sd-rich zone there are irregular pockets/layers of Sp [15 % this zone], an- to subhedral, partly translucent honey to brown in PPL, generally infilling around the clear Sd. There are also multiple irregular and discontinuous layers [<5 mm wide] comprised of predominantly Gn and/or Sp (see below for textural descriptions). Gn [locally 5 % this zone], an- to euhedral [mostly <1 mm] may occur as pockets, clusters, or discontinuous layers parallel the pervasive shear-planes/foliation.

Following the mechanically layered/mixed Sd and Sp zone, there is an abrupt and irregular transition to layers of either predominantly Gn or Sp [<2.5 cm wide, this zone]. The contact between these 2 zone is highly irregular, partly brecciated/faulted. Gn is mostly fine, anhedral, as irregular and foliated masses [<1 mm]; few Gn masses are sub- to euhedral and show deformation fabric; also Gn appears to be the last mineral phase. Sp is mostly dark, partly translucent deep red to partly translucent honey brown in PPL, irregular anhedral masses to euhedral [<2 mm] intergrown with and around Gn. Minor Ccp occurs as irregular pockets [<125 μm] contained within this Sp. Ccp [<2 %] occurs as irregular pockets [<500 μm] are commonly around the edges of Gn or within Sp; there are a few larger pockets [>1 cm] in Gn. There is also minor Sd [<1 %] and Qz [<1 %] intergrown with both Py and Sp.

BKUD09-151: 33.3m

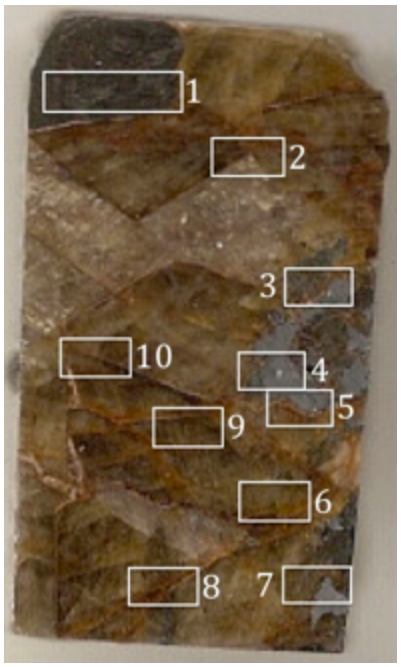

Location: Bellekeno – 99: ~1045 masl

Rock Type: V/B: (m,c,clr)Sd → (Qz-)Sp-Gn(-Ccp-Ttr)

Stages: 6 → 7-8

Host Lithology: N/A

Alteration: N/A

The earliest and most prominent mineral is Sd [<80 % overall], partly massive, euhedral [commonly >2mm]. Qz follows Sd, either as conformable thin layers [generally <250 μm] on Sd grains or filling veinlets cross-cutting and partly micro-brecciating Sd. Qz [<1 % overall] is an- to euhedral [<500 μm]. There is an unknown/unidentified mineral (?) associated with Qz, partly intergrown, but more commonly follows, in-filling the veins or vugs after and around Qz.

Sp [15 % overall] post-dates Qz and Sd, forming large, continuous, irregular masses [>2 mm], euhedral, translucent honey to reddish brown in PPL, with an internal zoned texture due to alternating light and dark growth layers/bands. There are few mineral inclusions (minor Py, Ccp and Po) contained within Sp ("chalcopyrite disease"). There is one pocket of Gn associated with Sp, and a few smaller isolated pockets within Sd, Qz, and/or Py. Gn [5 % overall] is euhedral, occuring as irregular masses in-filling after/around Sp, Qz, and Sd. Ttr (?) occurs as blebs/pockets around the edge or partly intergrown with Gn.

BKUD09-153: 63.4 m

Location: Bellekeno – Southwest; ~940 masl

Rock Type: V: (Qz-)(clr)**Sd** → b**Sd-Ank-Sp**(-Gn) → **Cal**

Stages: 6 (2?) → 9 → 12

Host Lithology: Qtzt is comprised of Qz grains [<100 μm], anhedral. Minor Apy [<250 μm], euhedral, disseminated within the Qtzt. Pht occurs as thin irregular and discontinuous stringers and may be disseminated throughout the Qtzt.

Alteration: Silicification or re-crystallization of Qtzt.

There are a couple early Qz-veinlets cross-cutting the Qtzt. One Qz-vein [~1 mm wide] consists of comb-texture, subhedral Qz growth perpendicular from the vein walls.

A vein-structure 14 mm wide cross-cuts the Qtzt and the earlier Qz-veinlets; comprised of minor early Qz, followed by Sd, Sp, then Cal. Early Qz are euhedral prisms [<1 mm], some perpendicular to vein wall. Following and partly intergrown with the earlier Qz is Sd, mostly clear, an- to euhedral, many with a 'tooth' crystal shape. This Sd stage is generally 500 μm to 1 mm thick, but may be discontinuous.

Post-dating the clear Sd there is a banded/layered unit [<1 mm wide] comprised of Sd and Ank, fine grain [<100 μm], cloudy an- to subhedral; grains generally have a bladed to feathery habit, and become clear and more coarse crystal [<300 μm] closer to the vein-center. There are at least 3 series of bands, the sequence generally evolves from fine and cloudy to clear and more coarse towards the vein-center.

After the Sd-Ank stage there are discontinuous pockets of Sp [<5 mm] with lesser Gn. Sp is translucent brown to yellow in PPL, an- to euhedral, and free of mineral inclusions, internal zoned defined by alternating lighter and darker colour growth bands/layers. Anhedral blebs of Gn are partly intergrown with, but generally appear to post-date Sp, precipitating closer to the vein center. There is a separate pocket of foliated or aligned Mica/Ms partly intergrown with Sp also contained within the transitional zone from the earlier Sd-Ank. Mica/Ms flakes are clear to translucent and tan, generally parallel the vein-wall orientation.

The last stage of hydrothermal mineralization is Cal, coarse [mostly >500 μm], an- to subhedral, filling the vein-center [<8 mm wide]. Many of the coarse clear Cal crystals display crystallographic twinning.

BKUD09-153: 84 m

Location: Bellekeno – Southwest; ~940 masl

Rock Type: V/B: m**Sd** →
Ank-Sd(-Qz)-zSp(-Apy-Gn)→
B:m**Cal**

Stages: 6 (2?) → 9 → 12

Host Lithology: N/A

Alteration: N/A

The earliest stage is predominantly Sd [<30 % overall; >90 % this stage], translucent light brown in PPL, sub- to euhedral, rhombohedrons [mostly 500 μm to >2mm]. Late in this stage Sd displays internal crystallographic banding/zonation near the edges, defined by thin layers with darker grey or very fine material [<10 μm], and/or due to abundant microscopic fluid inclusions, crystallographic imperfections.

There is an abrupt transition after the above Sd to mostly Ank, intergrown with Sd and lesser Sp. Ank is anhedral, fine [<100 μm], cloudy, with feathery crystal habit/texture. Sd is translucent light brown, an- to subhedral [<300 μm] (similar to BKUD09-153: 63.4m). Sp pockets are irregular, yellow to brown in PPL, and contains few mineral inclusions/blebs of Gn [<100 μm], and intergrown with Ank-Sd. Minor blebs of Apy, an- to euhedral, as isolated grains [<100 μm] or clusters have precipitated on the outer edge of Sp. Minor Qz, anhedral is also intergrown with Ank and Sd.

The last stage of hydrothermal mineralization consists of massive Cal, clear, coarse [mostly >1 mm], an- to subhedral; many coarse crystals display crystallographic twinning. There are a few clasts of Sd from the earliest stage suspended within the

massive Cal, and may occur in clusters. These clasts are rimmed by the same intermediate stage of Ank-Sd. There are also many isolated Sd crystals [<100 μm], sub- to euhedral within the Cal-matrix/cement. One Sd clast appears to show an earlier stage of Cal mineralization prior to the Ank-Sd stage (?).

BKUD09-153: 86.1 m

Location: Bellekeno – Southwest; ~940 masl

Rock Type: V: **Sd**(-Qz-Sp-Py-Apy)

Stages: 2

Host Lithology: Qtzt is comprised of Qz grains, anhedral [<300 μm]. Pht and GSch are very fine dark grey to black impurities disseminated or as discontinuous lenses throughout the Qtzt.

Alteration: Pht may be re-crystallized as or replaced by Mica/Ms.

Within the Qtzt, Apy [<1 %], mostly anhedral, maybe subhedral or euhedral [<50 μm] is disseminated throughout Qtzt. There is a fracture partially in-filled by Sd, Mica/Ms, and Qz cross-cutting the Qtzt. Sd is sub- to euhedral; Mica/Ms is clear to tan in PPL, as radiating flakes; Qz is an- to euhedral. Most of the fracture is vug space. There is minor Sd and Mica that has infiltrated and precipitated within the surrounding wall-rock.

There is a very sharp and straight contact between Qtzt and a predominantly Sd-filled vein-structure. Sd is variably cloudy to clear, an- to euhedral (<500 μm) and contains lesser Qz and minor Apy. Further into vein-center Sd transition to mostly clear, sub- to euhedral [>500 μm] grains. At vein-wallrock contact Apy is partly intergrown with Sd, as individual crystals or clusters, sub- to euhedral [<500 μm]. Qz is an- to euhedral. Minor Sp is translucent brown to yellow, anhedral [<100 μm] is spatially associated with Apy, but precipitated around or after Sd.

BKUD09-153: 87.5 m

(No Image Available)

Location: Bellekeno – Southwest; ~940 masl

Rock Type: V/B: Sd(-Ank-Sp) → m**Sp**(-Qz-Ms)-Py → V: b**Sd(**-Py)**-**z**Sp**(-Gn)**-Sd-Ank**

Stages: 2 → 3 → 9

Host Lithology: N/A

Alteration: N/A

The earliest hydrothermal stage consists Sd with lesser Ank. Sd is sub- to euhedral, [mostly >500 μm; <5 mm], and variably cloudy. Sp an- to subhedral, translucent brown to yellow in PPL is disseminated within Ank and Sd, also as pockets [<5 mm] infilling vugs; many are highly irregular and appear to be partly dissolving Ank and Sd. Minor Qz is euhedral [<600 μm] and is intergrown with Sp. Minor Mica/Ms is faint yellow, as radiating fibrous crystals [<200 μm] with Qz and Sp.

The above mineral assemblage is inferred to transitions to mostly massive Sp, sub- to euhedral crystals [<1 mm], partly translucent reddish to honey brown around the crystal edges. Mineral inclusions of Py [5 %] and lesser Po [1 %], and minor Ccp [Tr] are contained within Sp. Py is an- to euhedral [<100 μm], more commonly located along grain boundaries, and mostly appears to be precipitated after and on Sp. Po and Ccp are anhedral blebs [<10 μm] may be contained within Sp grains with minor anhedral Py.

The transition between the above 2 units (Sd-Ank and Sp) is not apparet because it is occupied by a later vein (below).

A later stage vein [4 mm wide] is comprised of predominantly banded Sd-Ank, with lesser Sp. Sd is sub- to euhedral [mostly <500 μm, to <2 mm]. The Ank unit [<1 mm wide] is typically cloudy [<200 μm], partly intergrown in the last/edge of the Sd. Within the Sd layer there are at least 2 discontinuous lenses [<20 μm wide x <500 μm long] of clustered Py, an- to euhedral [<10 μm]. There are also irregular pockets or fragments of Sp, which are likely sourced from the unit above.

Following the banded Sd-Ank units there is a layer [<4 mm] of Sp, euhedral, banded alternating layers of brown to yellow in PPL. There are a few irregular pockets [<500 μm] of Gn contained within Sp. At the lower boundary of this unit there are clusters of Py, sub- to euhedral [<50 μm].

The last phase of hydrothermal mineralization in the vein-center o is 3 to 10 mm wide; comprised of banded Sd-Ank and Cal. Sd is an- to subhedral [<500 μm] and appears to form radiating masses. Cal is clear, an- to subhedral [<300 μm], near the end it may be coarse and euhedral [500 μm to 2 mm].

BKUD09-157: 93.8 m

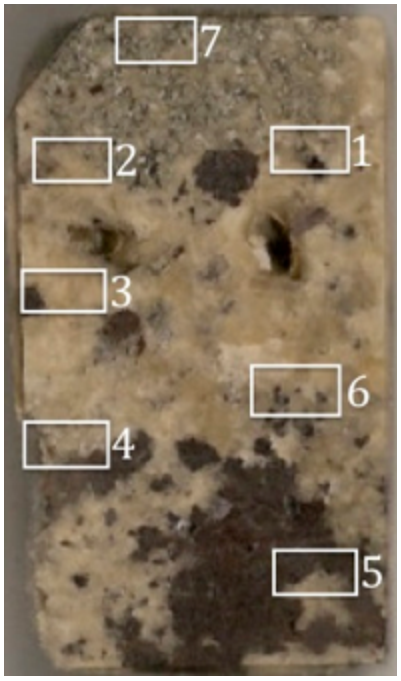

Location: Bellekeno – Southwest; ~930 masl

Rock Type: V/B: **Sd** → **Sp**-Py(-Sn)-Gn.

Stages: 2 → 3

Host Lithology: Qtzt clast (?) with abundant Py intergrown.

Alteration: Qtzt clasts appear to be almost completely dissolved and/or replaced by Sd.

The earliest hydrothermal phase is Sd [80 % overall], mostly cloudy, anhedral to lesser euhedral [generally <1 mm]. Sd post-dates and cements grains of Py, lesser Apy, and trace native tin. Py [<5 % overall] is an- to subhedral [mostly <1 mm], with lesser pockets of Qz around the edges. Qz is anhedral [<500 μm] and may represent the remnants of a Qtzt clast now mostly dissolved and/or replaced by Sd, with only Py and Apy remaining.

There is a transition from the above Sd unit, to Sd that is generally more clear, less cloudy, sub- to euhedral, as well as more coarse [many >2 mm], compared to above. Sd still contains minor clasts and/or pockets (?) of Qz, an- to euhedral [mostly <500 μm, few may be >1 mm.

Sp generally post-dates the above Sd infilling vugs, or may be partly intergrown with the previous Sd. Where Sp pockets are present Sd is generally smaller – possibly representing the waining of Sd precipitation. Sp is irregular and anhedral [many small pockets <1 mm, only one >1 cm], dark reddish brown to almost opaque. There are few Ccp and Po mineral inclusions within Sp (weak 'Chalcopyrite-disease'). The Ccp blebs are more common around the edges of Sp, or possibly along growth

planes. Pockets [<500 μm] of Py may be intergrown with or around the edges of Sp; smaller pockets [<50 μm] are also common within the predominant Sd-matrix. There may be remnant vugs after both Sd and Sp.

BKUD09-157: 100.5 m

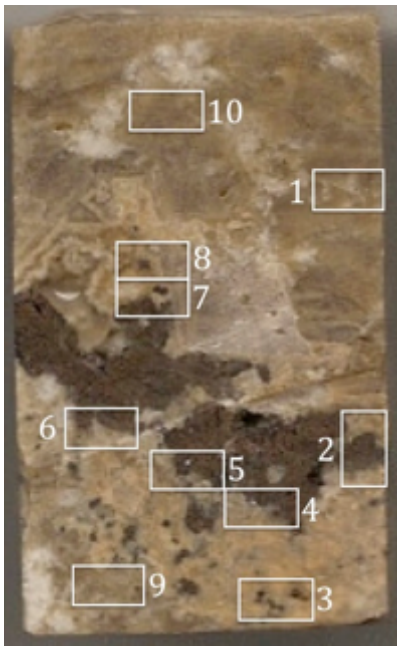

Location: Bellekeno – Southwest; ~930 masl

Rock Type: V/B: (m)**Sd**-**Qz** → b**Sd**-Ank-z**Sp**(-Gn) → Cal

Stages: 2 or 6 (?) → 9 → 12

Host Lithology: N/A

Alteration: N/A

The earliest phase is Sd [35 % overall], coarse [>500 μm, few >2 mm], sub- to euhedral, cloudy. Qz [20 % overall] is sub- to euhedral [mostly 125 μm to 1 mm], and intergrown with Sd. There is a transition to a texturally different and later Sd [25 % overall], which varies from fine [<125 μm] and cloudy, to clear and more coarse [<500 μm], both are anhedral. The cloudy, fine Sd-type may be intergrown of occur as thin rims [<250 μm wide] on and around the edges of the clear and euhedral Sd-type. Qz content decreases to <1 % within the later variable Sd type.

Sp [20 % overall] post-dates the above Sd, and is mostly coarse [>1 cm], euhedral, partly translucent honey to brown in PPL; a zoned texture is defined by alternating light to darker growth bands/layers. Smaller pockets of Sp [generally 125 μm to 1 mm] are intergrown within the fine, cloudy Sd. Minor Py and Gn occurs as pockets or blebs [<125 μm] within Sp.

Minor late stage Cal is partly associated with Sp or filling vugs.

BKUD09-157: 101.5 m

Location: Bellekeno - Southwest; 930 masl

Rock Type: B: (Qz)-**Sd**(-Sp-Py) → Qz

Stages: 2(-3) → 10 (or 4b ?)

Host Lithology: Qtzt is comprised of Qz, anhedral to lesser subhedral grains [<250 μm]; present as irregular clasts, angular to sub-rounded. Pht is very fine, opaque black material commonly occurs throughout the Qtzt.

Alteration: Possible silicification and/or re-crystallization of Qtzt. Pht may be re-crystallized as or replaced by Mica/Ms.

Within the Qtzt clasts, Py grains, an- to euhedral [generally <500 μm], and minor Sp are disseminated.

Mica/Ms as translucent, clear to pale green and blue, and occur as clusters of flakes or irregular pockets around many Qtzt clasts, and is partly intergrown or possibly re-mobilized into later Sd.

The earliest hydrothermal mineral is minor Qz, sub- to euhedral [<1 mm], which has mostly nucleated on the edges of Qtzt clasts. The most prominant hydrothermal phase is Sd [>90 % this stage], an- to euhedral [generally >500 μm], with both clear and cloudy crystals; appears orange in HS. There may be remnant vug space after Sd and Qz.

Following after Sd, there is minor Qz, an- to euhedral [<2 mm], in-filling around/after Sd. Minor Sp, anhedral [generally <500 μm] is intergrown with Sd and the later Qz. There are few grains of Py and Sp contained within the Sd-matrix; however, these may have only been remobilized from Qtzt (?).

BKUD09-157: 101.9 m

Location: Bellekeno - Southwest; 930 masl

Rock Type: V/B: m**Qz-Apy** →
V/B: m**Sd**(-Cpy-Py)

Stages: 1 → 2

Host Lithology: Qtzt, consisting of Qz grains [<300 μm], anhedral; occur as clasts within a predominantly Sd-matrix/cement.

Alteration: Silicification or re-crystallization of Qtzt.

Within Qtzt, there is minor Mica/Ms occuring as disseminated pockets/books of flakes [<200 μm]. Minor Apy is an- to euhedral [<200 μm] and Sp is an- to subhedral [<300 μm] are also disseminated within Qtzt clasts.

The earliest hydrothermal phase is a Qz-cemented breccia containing Qtzt clasts. Qz is an- to euhedral [mostly <200 μm, some >1 mm). There is a large cluster [>2 mm] of Apy [individual crystals are mostly <500 μm], an- to euhedral intergrown with the Qz-matrix.

Sd post-dates the above Qz-Apy stage, but may be partly invasive in some areas. There is also an earlier phase of Qz during this predoiminantly Sd-rich stage; this Qz is distinct from the earliest Qz-Apy stage (above). Sd is sub- to euhedral [mostly >500 μm; but generally <1 mm]. After or intergrown with Sd are pockets of Ccp, anhedral [<100 μm], and Py, an- to subhedral [<300 μm]. Less common are small pockets [<100 μm] of anhedral Apy within Sd.

A late fracture cross-cuts all the above hydrothermal phases, however, where it crosses a Qtzt clast, Apy clusters within the fracture which is otherwise void.

BKUD09-158: 35.9 m

Location: Bellekeno – Southwest; 1030 masl

Rock Type: B: (Qz-)**Sd**(-Py)

Stages: (1-)2

Host Lithology: Qtzt [<20 % overall] is comprised of Qz grains, anhedral to lesser subhedral grains [<250 μm]; occuring as clasts, irregular, angular to sub-rounded. Pht is very fine, opaque black foliated material to clear clusters of flakes, and may be altered to Mica/Ms (?); and occurs throughout the Qtzt. A pervasive foliation is apparent from the oriented and wavy layers of Pht/Mica/Ms.

Alteration: Possible silicification or re-crystallization of Qtzt; also Qtzt may be dissolved and/or replaced by Sd. Pht may be re-crystallized as or replaced by Ms/Mica.

Within Qtzt there are disseminated Py grains or clusters, an- to euhedral [generally <125 μm]. Py appears to be associated with Pht/Ms/Mica-rich areas, based on the relative concentrated and intergrown nature.

The earliest hydrothermal phase is minor Qz, sub- to euheral [<1 mm], which have mostly nucleated on the edges of Qtzt clasts. The most prominant hydrothermal phase is Sd [>90 % this stage, >80 % overall], an- to euhedral, mostly subhedral [>125 μm, many >2 mm], variably clean to cloudy, which cements and contains suspended Qtzt clasts. There are some areas of clustered Py grains, which appears to have originally been contained within a Qtzt clast, whereby the Qz-grains may have been dissolved and/or replaced by Sd. Here Py is sub- to euhedral [<50 μm], and may occur as bands less than a few Py crystals wide – possibly a relic texture of the thin Pht bands/layers.

BKUD09-158: 36 m

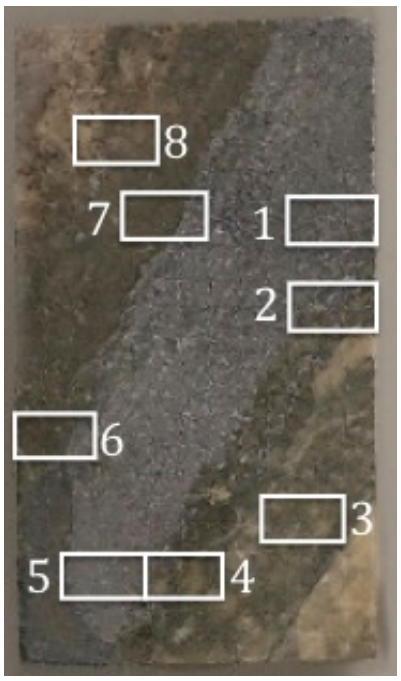

Location: Bellekeno – Southwest; 1030 masl

Rock Type: V/B: **Sd**(-Py) →
{**Sd**-Gn-Py-Ttr (B: Qz) →
Sd(-**Py**-**Gn**-Ttr-Sp-Qz)} →
Gn(-Ttr-Sp-Qz).

Stages: 2/6(?)→{mechanically mixed}→ 8

Host Lithology: N/A

Alteration: N/A

The earliest phase is Sd, an- to euhedral [generally 125 μm to <2 mm], variably cloudy to clear. There is disseminated Py, an- to euhedral [<125 μm] either contained within Sd or along crystal boundaries – some of this Py may define a transition to a later stage (below).

A vein-structure cross-cuts the above stage, comprised of 3 distinct units (below), the earliest/outer 2 units appear to be mechanical mixtures related to shearing.

The earliest unit of the vein-structure has a sharp, straight contact and is associated with a Sd-rich unit [90 % within this unit], intergrown with pockets of Gn [8 % this unit], lesser Py [2 %] and Ttr [Tr]. Sd is mostly an- to subhedral [generally between 50 μm and 1 mm], variably cloudy to clear. Gn is anhedral [<500 μm], and is commonly intergrown with or rimmed by few Py grains [<20 μm], an- to euhedral. Ttr occurs as irregular blebs [<60 μm] contained within Sd. A small Qz-cemented vein/breccia occupies the lower contact of this unit [<1mm wide or may pinch-out]. Here Qz is an- to euhedral, the euhedral prisms appear to be oriented parallel the vein/breccia. Minor Py, an- to euhedral [<20 μm] may cluster along this vein/breccia edge. Mechanical brecciation of the surrounding Sd (on both sides of the the V/B: Qz) is common.

Toward the center of vein structure, the subsequent unit is defined by an abrupt increase in sulfides, within this zone: Py [10 % this unit], Gn [10 %], Sp [5 %], and Ttr [5 %]; the remainder of this unit is Sd [65 %] and Qz [5 %]. Sd is mostly sub- to euhedral [generally <1 mm]. Py is larger [<250 μm], sub- to euhedral. Sp is anhedral

[generally <250 μm], irregular, translucent honey to dark brown in PPL, contains blebs [<10 μm] of Ccp disseminated – 'chalcopyrite-disease", and may be intergrown with Gn, Py, and Ttr. Gn although is internally euhedral, occurs as irregular pockets, and is also intergrown with Py and lesser Sp. Qz is an- to euhedral [<250 μm] and generally intergrown with the sulfide pockets.

The last stage and inner most zone of the vein-structure is dominated by Gn, anhedral, fine grain, continuous mass, within a zone <1 cm wide. Discontinuous bands and anhedral blebs of Py and Ttr [<5 % combined this unit] occur throughout Gn.

BKUD09-158: 36.5 m

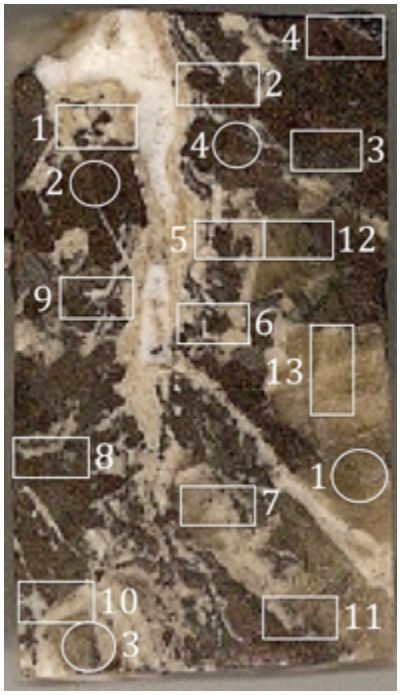

Location: Bellekeno – Southwest; ~1030 masl

Rock Type: V/B: **Sd-**z**Sp**(-Py-Gn-Ttr-Plb-Aca) → B: b**Sd**(**-**zSp) → **Qz** (→ Cal)

Stage: 6-7(-8) → 9 → 10 (→ 12)

Host Lithology: N/A

Alteration: N/A

The earliest phase is Sd, clear to partly cloudy, sub- to euhedral [mostly >1 mm]. Fluid inclusions may be present within Sd, either isolated or as clusters; areas of abundant microscopic fluid inclusions and/or crystallographic imperfections are the norm. Within Sd microscopic opaque and Sp mineral inclusions, dark grey to black, as anhedral blebs are common. There are also some localized areas with inclusions of Apy, sub- to euhedral [<100 μm] and blebs of Gn, anhedral [<300 μm]. Gn here is generally spatially associated or partly intergrown with Sp pockets.

Sp is partly intergrown with, but generally follows Sd, as translucent brown to yellow under PPL, euhedral, and texturally zoned – defined by alternating lighter and darker colour bands/layers. There are few fine mineral inclusions of Ccp [<5 μm] and lesseer Gn [<10 μm] closer to the edge of the Sp mass, and concentrated

along a crystallographic plane. Fluid inclusions may be present within Sp, usually as clusters, some appear to be primary, and 2-phase. Py is partly intergrown with, but more commonly follows Sp and Sd, precipitated around the edges as an- to subhedral [<200 μm] individual crystals; and may be associated with the banded Sd (below). Minor Gn, Ttr, Plb, and Aca [<1% combined] occur as irregularly shaped blebs, and are intergrown or contained within Sp.

A later irregular veinlet-filling stage is comprised of predominantly banded Sd, mostly fine [<200 μm], an- to subhedral, and cloudy – due to abundant microscopic fluid inclusions and/or crystallographic imperfections. There are fewer bands of comprised of more clear, sub- to euhedral Sd. Minor pockets of Sp (similar as described above) are intergrown with or after the clear and euhedral Sd-type bands.

Lastly, following the banded Sd in some areas there is a Qz veinlet-fill. Early Qz around the edges is anhedral [<200 μm], with relatively later Qz in the veinlet-center is more sub- to euhedral [<600 μm], and cloudy – due to abundant fluid inclusions.

The presence of later stage Cal after Qz is apparent in the HS.

BKUD09-158: 37 m

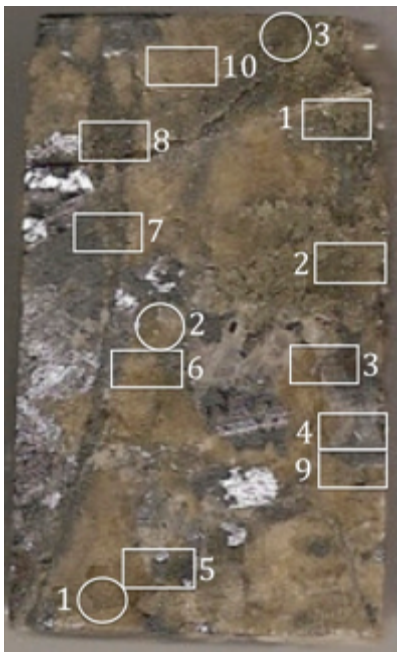

Location: Bellekeno – Southwest; ~1030 masl

Rock Type: V/B: (Py-)m**Sd**-(Ank-)**Qz** → (B:) (Sp-)**Gn**-Py-Ttr

Stages: 2 or 6 (?) → (7-)8

Host Lithology: Qtzt [<2 % overall], comprised of mostly Qz, fine [<125 μm], anhedral grains; occurs as clasts [>1 cm], angular, with irregular boundaries. There may be minor secondary or re-growth of Qz.

Alteration: Silicification or re-crystallization of Qtzt. Qtzt clasts may be dissolved and/or replaced by Sd.

Within Qtzt, Py [<3 % overall] is anhedral to subhedral [<250 μm], forming clusters [<5 mm], and may be early around/neucleating on Qtzt clasts, or intergrown with later Sd and Gn. Where Qtzt – Qz has been mostly removed/dissolved, only minor Py as irregular pockets remains.

The earliest hydrothermal phase is Sd [25 % overall], coarse [mostly >500 μm], sub- to euhedral, and cloudy – due to abundant microscopic mineral and/or fluid inclusions, as well as crystallographic impurities; and occurs as a breccia-matrix/cement. Following the coarse, euhedral Sd-type, there is a continuation of a texturally different type of Sd [25 % overall], more fine [mostly <500 μm] and an- to subhedral. This later Sd is also intergrown with Qz [20 % overall], sub- to euhedral [<1 mm].

Gn [25 % overall] generally post-dates and is partly intergrown with the above Sd-Qz. Gn is mostly euhedral, as large and continuous, irregular infilling masses. Additional Py (similar as described above) is also spatially associated with and partly intergrown with Gn. Minor Ttr as irregular blebs may be contained within Py and Gn. There is an area of inter-fingering micro-breccia [<5 mm wide] with clasts of Sd and infilling Sp and Gn matrix. This breccia phase appears to be syn-genetic and related to the massive Gn mineralization phase, which has generally not affected most of the earlier Sd.

BKUD09-160: 29.6 m

Location: Bellekeno – Southwest; ~950 masl

Rock Type: V: Py(-Mica/Ms)-Sp(-Qz) → Sd

Stage: 4a(-4b ?) → (6 ?)

Host Lithology: Qz-vein, massive, Qz is anhedral [mostly >60 μm, few >2 mm]. A foliation is apparent, where planes are occupied by Mica/Ms, black and opaque, or clear to faint green, occuring as clusters of flakes.

Alteration: Silicification or re-crystallization of Qz. Pht may be re-crystallized as or replaced by Mica/Ms.

Within the Qz-vein, blebs [<20 μm] of Py and Gn are spatially associated with the Mica areas.

A vein [<1 cm wide] cross-cuts the Qz-vein, infilled with pockets of mostly Py, Sp, and lesser Sd. Py is an- to subhedral, predominant in one area and absent in the remainder of the vein. After Py, Mica/Ms occurs as euhedral books and/or clusters [<250 μm]. Sp is partly translucent reddish brown to dark brown, anhedral to euhedral. Mineral inclusions/ blebs [<20 μm] of Py, Po, and lesser Ccp are disseminated throughout Sp, or clustering along growth planes. Sp may be partly intergrown with the earlier Mica/Ms (above).

Sd is the last vein-filling phase, but may also be intergrown with Mica, and Sp. Sd is euhedral [<2 mm], infilling irregular vugs. There is minor Qz, euhedral [<500 μm] suspended within Sp and Sd.

BKUD09-160: 56.5 m

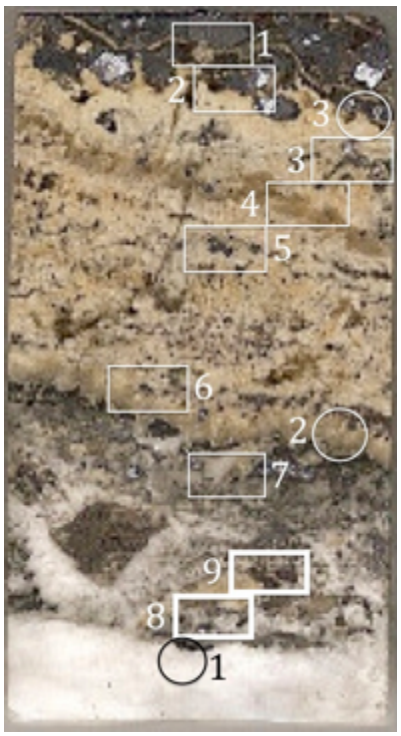

Location: Bellekeno – Southwest; ~950 masl

Rock Type: V: **Gn**-Sp(-Py) → b**Sd**-Gn-Py-Sp → V/B: (Gn-Sp-Py-Sd-)Ank-**Qz** → **Cal**

Stages: 8 → 9 → 10 → 12

Host Lithology: Fragments/clasts of thinly bedded PhSch-GSch with V_QzF1, possible Qtzt as a few irregular clasts [>6 cm].

Alteration: Silicification or re-crystallization of Qtzt.

The earliest mineral phase is a band of predominantly Gn, coarse [<1 mm], euhedral crystal clusters at the bottom of the TS. Gn in followed by and partly intergrown with Sp, which forms a discontinuous band [<150 μm thick] bordering Gn. Sp is translucent brown to honey in PPL, internally sub- to euhedral as irregular masses, and containing inclusions [<10 μm] of Py and Gn; these inclusions appear to cluster along crystallographic planes. Py is an- to euhedral [<500 μm], partly intergrown with, but mostly appears to follow Sp.

Then there is a stage of predominantly banded Sd; cloudy, fine (<50 μm), anhedral, and intergrown with irregular pockets/blebs of Sp, Py, and lesser Gn – similar textures and order of sulfides are consistent throughout this stage. Py is euhedral [mostly <50 μm], again partly intergrown with, but generally follows Sp. The fine and cloudy Sd-type forms repetitive bands/layers [1 to 2 mm wide] with fewer and multiple bands/layers [<100 μm wide] of the clear, sub- to euhedral Sd-type. There are multiple clusters of sulfides (as above), which mostly appear after or with the bands of clear, sub- to euhedral Sd. There is a discontinuous band/layer [~500 μm to 1 mm wide] of mostly Gn within this stage, which is otherwise predominantly Sd.

Following the last band of clear, euhedral Sd from the above stage there is a zone [approximately 7 mm wide] of intergrown Qz and Ank, cementing fragments of the above units. Qz is an- to euhedral [mostly <100 μm, lesser <1 mm]. Ank is fine [<50 μm], and cloudy, but may locally grade to sub- to euhedral [mostly <500 μm] and

disseminated, irregular pockets of sulfides. This stage is clast-supported, and the fragments [<2mm] have irregular orientations.

Following the above clast-supported breccia, there is an abrupt transition [over <50 μm] to a stage of predominantly Cal, an- to subhedral [100 μm to 2 mm].

BKUD09-161: 20 m

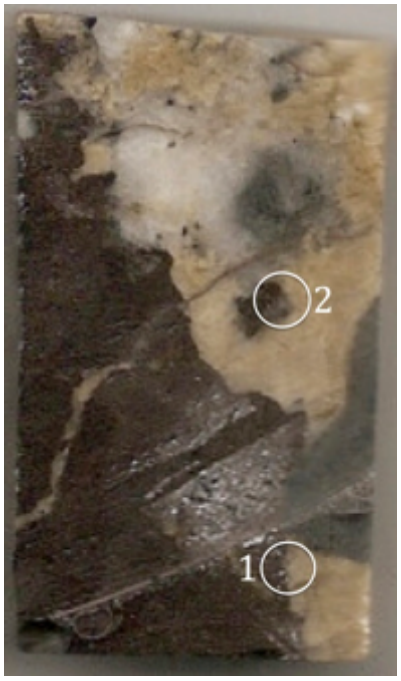

Location: Bellekeno – Southwest; ~990 masl

Rock Type: B: (Qz-)m**Sd** → (Qz-)m**Sp**(-Py-Gn)

Stage: 2 → 3

Host Lithology: Qtzt [<20 % overall] is comprised of a mosaic of Qz grains [<125 μm], anhedral; and occurs as clasts suspended within a mostly Sd and lesser Sp cemented breccia (below). The Qtzt clast boundaries are generally sharp, and irregular.

Alteration: Silicification of re-crystallization of Qtzt. Pht may be altered to or replaced by Mica/Ms (above).

The earliest hydrothermal phase is Qz growth may occur around the clast edge into the Sd-matrix (below). There may be minor Mica/Ms precipitating from the clast edges and intergrown with Sd.

After and partly intergrown with Qz and Mica/Ms is a Sd-cemented vein/breccia; which contains suspended Qtzt clasts. Sd [<30 % overall] is sub- to euhedral, coarse [>0.5 mm to >2 cm]; mostly cloudy, the result of abundant fluid inclusions and microscopic crystal imperfections, which results in a creamy and opaque appearance. Fluid inclusions [<15 μm] in Sd are variably present, most are very fine [<5 μm]; the cloudy texture precludes the unobstructed observation of any one inclusion effectively; only in later stages of mineralization (ie. at the edge of crystals) are relatively clear areas present. Minor irregular pockets of Gn [<1 mm], and lesser Py [<500 μm] [<2% combined] are suspended/contained within the Sd. Furthermore, there is minor Gn [<125 μm], an- to euhedral, occurring within open fracture or in-filling vug space after Sd. Also irregular and anhedral blebs of Gn [<50 μm] and Cpy [<50 μm] are disseminated within a Qtzt clasts [<1% combined] may be from an earlier stage (?).

Lesser Qz [<5%], sub- to euhedral [mostly 250 μm to 1 cm], is intergrown with/suspended within Sd or Sp, or more commonly as clusters between Sd and Sp. There are sporadic fluid inclusions [<30 μm] within Qz.

Sp [<55 % overall, >95 % this stage] post-dates Sd and Qz. Sp is massive opaque to deep red, an- to euhedral (?); there may be minor partly translucent areas in Sp, commonly around the edges. The transition from the earlier Sd and Qz is sharp to highly irregular – Sp may be partly invasive (replacing) or intergrown with the earlier phases. The euhedral nature of Sp is apparent from a series of parallel imperfections or oriented vugs (?). Ccp [<5 % within Sp] occurs as anhedral blebs [<100 μm] disseminated within Sp. There is one area of Py clustering, coarse [~1 cm], sub- to euhedral; intergrown with Sd and Sp. Minor Gn similar as decribed above also occurs within Sp.

BKUD09-161: 20.4 m

Location: Bellekeno – Southwest; ~990 masl

Rock Type: B: (Qz?)-Py(-Apy) → (Sd-Gn-Cal)

Stages: 1 (?) → (2-8-12 ?)

Host Lithology: Qtzt clasts [<10 %] within massive Qz-cemented breccia. Qtzt is comprised of fine Qz [mostly <100 mm] anhedral grains; in HS Qtzt appears grey, and hydrothermal Qz is white. Minor Pht may be present, which appears black and opaque. Mica/Ms is intergrown with the Qtzt.

Alteration: Silicification or partial re-crystallization of Qz. Pht may be re-crystalized as or replaced by Mica/Ms.

The distinction between hydrothermal Qz-matrix and Qtzt clasts is difficult; the 2 appear to be highly mixed, and re-crystallization of Qtzt may also be a factor. Hydrothermal Qz in HS is, milky white with abundant micorscopic fluid inclusions and crystallographic imperfections, more coarse [mostly >250 μm], an- to subhedral. Minor Mica/Ms is intergrown and disseminated within Qtzt [<1 %] and also as minor matrix-fill [<1 %]. Hydrothermal Mica/Ms may be coarse, clear, and form radiating clusters. Py [15 % overall, locally abundant] is an- to subhedral, mostly coarse [>1 cm], and forms a large cluster, partly intergrown with Qz-matrix. Py [15 % overall, >60 % locally] is an- to subhedral., mostly coarse [>1 cm]. This area is also has abundant vug space. There are few individual pockets/crystals of Apy [Tr] disseminated within Qtzt or lesser in the Qz-matrix.

Following Qz is minor Sd [<3 % overall], sub- to euhedral [<2 cm] with lesser Cal [Tr] infilling remnant vugs and partly intergrown with Qz.

BKUD09-163: 14.8 m

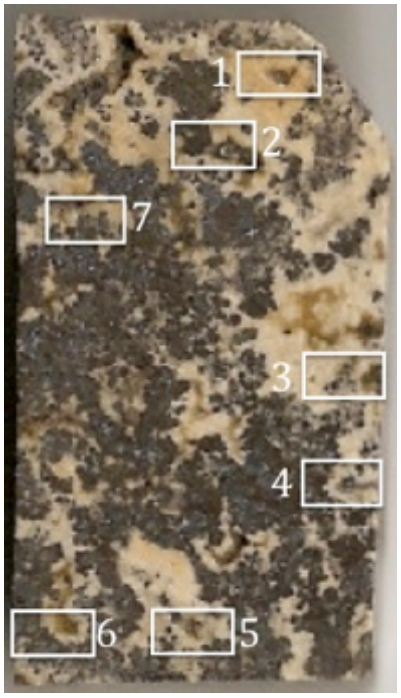

Location: Bellekeno – Southwest; 980 masl

Rock Type: V(/B): **Sd-Py-Gn-z*Sp*** (→ bSd-Cal)

Stages: 9 (→ 12)

Host Lithology: N/A

Alteration: N/A

The dominant mineral phase is Sd [60 % overall], occurs as repetitive sequences of alternating layers/bands of 2 textureally distinct types: cloudy, anhedral, and sub- to euhedral blades [<250 μm]; or clear, and generally more coarse [<500 μm]. Pockets of sulfides (Py, Gn, and Sp), where present, commonly occur with or follow the more clear and euhedral Sd bands.

Py [10 % overall] is generally the earliest sulfide, an- to euhedral [mostly >125 μm, to <2 mm], forming clusters [few ~1 cm]. Gn [10 % overall], may be euhedral internally, but mostly is irregularly shaped, and forms discontinuous rims around Py or more commonly as irregular pockets intergrown with or around Sd. Sp [20 % overall] follows Sd, Py, and Gn. Sp is euhedral, as irregular pockets, internally banded/zoned, defined by alternating layers of translucent honey to dark brown in PPL. Minor Ccp mineral inclusions occur within the dark brown bands of Sp, and to a lesser extent disseminated ("chalcopyrite disease").

There is an undertermined number of the above mineral sequence. The presence of late Cal was determined from HS observations.

BKUD09-163: 31.8 m

Location: Bellekeno – Southwest; ~980 masl

Rock Type: V/B: (Qz-)m**Sd-**(Apy-Py-Sp)
(→ V: Qz-Cal)

Stages: 2 (-3/4a?) (→ 10-12)

Host Lithology: Qtzt [15 %] is grey, fine, and massive, comprised of anhedral [<200 μm] Qz grains. At one end of the TS, brecciated Qtzt clasts, nearly in-situ, angular, elongate, and generally aligned parallel are present. Minor Apy and Sp [both <1 % each] are disseminated within the Qtzt. Apy is an- to euhedral (mostly anhedral <40 μm, one euhedral <400 μm); and Sp is anhedral [<60 μm].

Alteration: Silicification or recrystallization of Qtzt. Some of the clasts appear to have dissolved or been replaced by later Sd.

Early Qz is euhedral, prismatic crystals have nucleated on Qtzt clast edges. Following Qz, Sd [>80 %] is mostly cloudy, anhedral [<500 μm], with many of the crystals have an undulatory or radiating extinction pattern under XP, and occurs as a breccia cement. The cloudy appearance appears to be a result of abundant mineral and fluid inclusions [<10 μm] and/or crystallographic imperfections, many of which appear to be aligned parallel internal crystallographic planes. Cloudy Sd may be more common as an early phase as it appears to be most abundant around the brecciated Qtzt clasts, and extends into the vein/breccia center for approximate 15 mm, then transitions to more coarse and clear Sd, sub- to euhedral [generally >500 μm, some >3 mm]. Fluid inclusions [<10 μm] are also common [<5 %] within the more coarse and clear Sd. Apy [<1 %] is sub- to euhedral [<600 μm] and commonly occurs as clusters [generally <2 mm], intergrown with the cloudy Sd. There may be a genetic relationship between Apy and Qtzt, based on a frequent spatial associatation. Minor Sp is present within one area contained within Sd, as irregular pockets [~2 mm], translucent brown to yellow, anhedral, and contains mineral inclusions (mostly <20 μm, <5 % within Sp] of Ccp and Po. Minor blebs of anhedral Ccp, Po, and Apy also occur within the surrounding Sd.

The last phases of mineralization in the sample are Qz followed by Cal - not present in the thin section, but apparent from the hand sample description.

BKUD09-166: 16 m

Location: Bellekeno – Southwest; ~975 masl

Rock Type: V/B: (m)**Sd** → (cldSd-Cal) → B: Sp(-Gn-Py) → V: (m)**Gn**

Stages: 2 (or 6 ?) → 3 (or 7 ?) → 5 (or 8 ?)

Host Lithology: N/A

Alteration: N/A

The earliest mineral phase is Sd [<80 % overall], mostly clear to lesser cloudy, some crystals are euhedral and coarse [>2 cm]. However due to abundant brecciation much of the Sd has been broken and reduced to fine grain material [<10 μm]. The later breccia-zone [50 % overall] is localized between larger Sd crystal masses with Sd crystals [>250 μm], which make-up the clasts [>70 %], and finer Sd material [<10 μm] as the matrix [<30 %].

Sp with lesser Gn, and Py appears to be syngenetic with the above brecciation. These sulfides form irregular anhedral masses, as wispy layers or lenses, within the fine grain matrix, and around the more coarse Sd clasts. Sp [5 % of breccia unit] is dark to partly translucent honey brown in PPL, associated with or contains pockets of Py [Tr], and lesser Gn [Tr]. Gn may be associated with Py or isolated.

There is an abrupt transition after the coarse and euhdral Sd followed by a layer [<1 cm] of Sd, with cloudy and bladed crystals [<250 μm]; which is inturn followed by a layer [<500 μm wide] of Cal, clear, curved to bladed crystals [<250 μm]. Minor Gn is partly intergrown with Cal, but there is an abrupt transition a Gn-rich stage. Gn [>80 % locally, <20 % overall] is coarse, euhedral [>2 cm], the cleavage shows strain/deformation as triangular pits and planes are curved. Gn is more anhedral along the contact with Cal. Sd [<20 % locally with Gn] is coarse, euhedral, clear to slightly cloudy. Much of the Gn and Sd has been lost during sample preparation. The brecciation event (above) only partly affects the V/B: Gn stage, this may be an effect of rock mechanics; furthermore, this brecciation event may also be responsible for transporting Sd within the V/B: Gn stage.

BKUD09-166: 18.6 m

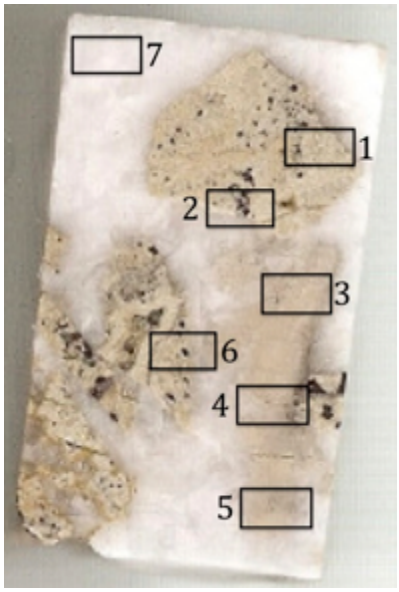

Location: Bellekeno – Southwest; ~975 masl

Rock Type: V/B: (b,cld)**Sd**-zSp(-Apy)
→ B: (Ank-)m**Cal**

Stages: 9 → 12

Host Lithology: N/A

Alteration: Some Sd clasts appear to be altered or replaced by green-grey Ms (?), which is then being preferentially removed – weak, weathers or mobilized easily.

An earlier phase of Sd, an- to subhedral [<200 μm], cloudy, and banded, with thin layers of clear, sub- to euhedral Sd [<100 μm]. Intergrown with the banded dirty and clear Sd and pockets of Sp, mostly anhedral [mostly <1 mm], which contains variable inclusions [<10 μm] of Ccp and Po (?). Apy, an- to subhedral [<60 μm], lesser euhedral, are spatially associated with and partly intergrown with Sp.

The clasts edges are mostly sharp, rounded, to irregular, and cemented within an essentially pure Cal-matrix/cement. Cal is mostly irregular, intergrown euhedral crystals [commonly >1 mm]; crystallographic twinning is common. Irregular and anhedral Cal [<200 μm] has been precipitated in pockets around the Sd clasts. Sp and Apy anhedral blebs [<50 μm] may be contained within the anhedral Cal-matrix, rarely present within the Cal-matrix.

BKUD09-171: 32.8 m

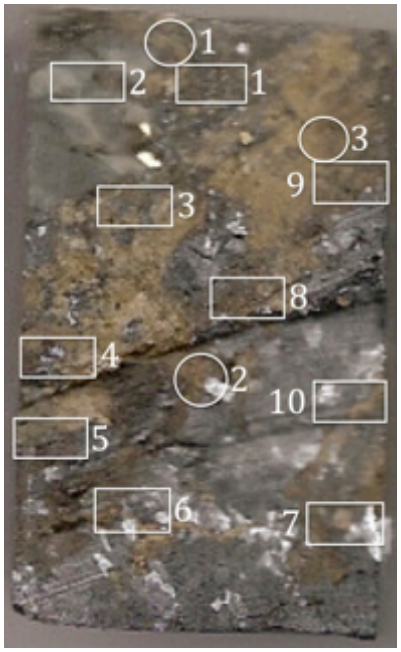

Location: Bellekeno – 99; ~990 masl

Rock Type: V/B: **Sd** → Sd/Ank (?) →
(B:) (Qz-)Sp-Py-**Gn**-<u>Ttr</u>

Stages: 6 → (?) → 7-8

Host Lithology: A few Qtzt clasts are present, mostly comprised of a mosaic of irregular Qz grains [<125 mm], anhedral. There are minor pockets or clusters of Mica/Ms flakes, clear.

Alteration: Possible re-crystallization of Qtzt. Pht may be re-crystallized as or replaced by Mica/Ms.

With Qtzt clasts there are minor disseminated blebs of Sp. Sp [1 % within Qtzt] is irregular and anhedral [<125 μm]. Immediately infilling around Qtzt is mostly Sd, with lesser Sp and Gn. Sd [60 % this unit, <25 % overall] is cloudy, sub- to euhedral [generally <500 μm] near the Qtzt clasts; some Sd crystals are >2 mm, and more clear; this type of Sd appears to be later as these crystals are further away from clast contacts. In some areas, there are irregular layers [<500 μm] of Sd and/or Ank, cloudy and anhedral, following clear, euhedral Sd.

Sp and Gn may be intergrown with Sd, however generally post-dates infilling around euhedral Sd grains, or as irregular pockets. Sp [20 % overall] is partly translucent honey to light brown in PPL; an- to euhedral [most pockets <1 cm]; alternating colour bands, defines crystallographic growth zones. Sp contains few irregular pockets [<500 μm] of Gn and Py. Gn [20 % overall] is intergrown with or post-dates Sd and Sp, mostly as irregular pockets, or euhedral clusters [<1 cm]. Minor Py [<5 % overall], as irregular pockets [<500 μm] are also intergrown with Gn. Minor Qz [<10 % within this unit; <500 μm] is intergrown with the Sd-Sp-Gn unit. There are localized zones of brecciation, which appears to be syn-genetic or associated with the Sp-Gn mineralization; the minor matrix is fine grain Sd, possibly only re-mobilized from the earlier Sd mineralization.

BKUD09-171: 43.5 m

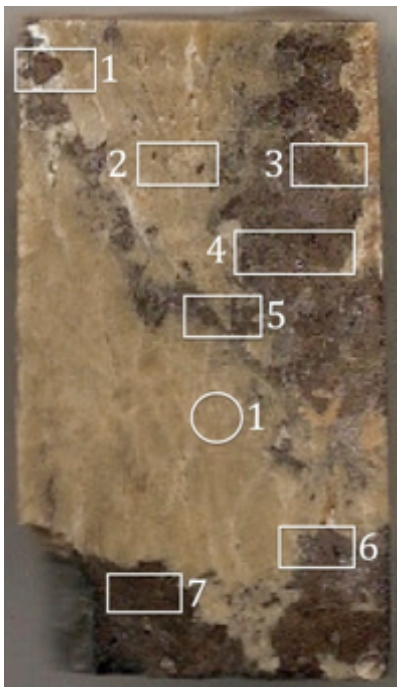

Location: Bellekeno – 99; ~990 masl

Rock Type: V/B: m**Sd** → (Qz-Py-Apy)z**Sp**(-Gn) → (cld)**Sd**

Stages: 2 → 3 → 9

Host Lithology: N/A

Alteration: N/A

The earliest hydrothermal phase is mostly massive Sd [<70% overall], clear to cloudy, sub- to euhedral [many >2 mm]. The cloudy Sd crystals are typically <1 mm, and generally follows, precipitating on or after the more coarse and clear Sd crystals, and may be more spatially associated with later Sp and lesser Qz.

Sp [<25% overall] is partly intergrown with, but generally post-dates Sd, as partly translucent honey to red-brown in PPL, an- to euhedral, irregular masses [mostly >2 mm], with alternating colour bands defining growth zones. Qz is commonly intergrown with or spatially associated with Sp. Qz [<5% overall] is sub- to euhedral [mostly <500 μm, few >2 mm], variably cloudy - commonly the crystal core is cloudy and abruptly transitions to a more clear outer layer/zone - in some crystals defining a banded texture. Py and Apy [combined <1% overall] are an- to euhedral [typically <125 μm] occurs around the edges of the larger Sp masses, and also partly intergrown with Qz and Sd.

Minor late stage Sd is cloudy to clear, fine, an- to subhedral [mostly <125 to <250 μm]; post-dating or partly intergrown with Sp.

BKUD09-173: 31.2 m

Location: Bellekeno – 99

Rock Type: V/B: (cld)Sd → (V/B:) Sp-Py(-Apy-Sd) → Qz

Stages: 2 → 3 or 4a → 4b

Host Lithology: Qtzt as clasts, mostly comprised of irregular anhedral Qz grains [<125 μm]. A pervasive foliation is apparent, defined by numerous wavy thin layers [<125 μm wide] comprised of discontinuous very fine grain material (Mica/Ms ?) – opaque in PPL.

Alteration: Possible silicification or re-crystallization of Qtzt.

The principal and earliest hydrothermal phase is Sd [<70 % overall, >95 % locally], an- to euhedral [mostly <1 cm], mostly cloudy, but may also be clear. There is no obvious spatial pattern for the distribution of the cloudy and clear Sd crystals.

Then there is a stage of Sp-Py mineralization, as irregular vein-fill post-dating Sd. Sp [15 % overall, >80 % locally] occurs as irregular masses, dark purple to faint translucent brown in areas. Py [15 % overall, >90 % locally] occurs as irregular clusters of an- to subhedral crystals [<2 mm], and may form around the edges of larger Sp masses. Apy may be associated with Py and also intergrown with Sp. Apy [<5 % overall] is an- to subhedral, as irregular pockets [mostly <250 μm]. There may be clusters of brecciated Sd contained within the Sp-Py unit. There is also minor Sd associated with the Sp-Py stage; this Sd is similarly cloudy to clear, an- to euhedral [mostly <1 mm], and intergrown with lesser Sp and Py. Minor Qz is associated with the Sp-Py stage, but appears to be a later stage.

Appendix III

A. Electron Microprobe Data: Carbonates

A total of 475 data points analysed carbonate mineral chemistry. Equipment specifications are documented in Section 3.1.

B. Electron Microprobe Data: Sulfides, Oxides, and Sulfates

A total of 1,377 data points analysed sulfide, oxide, and sulfate mineral chemistry. Equipment specifications are documented in Section 3.1.

A. Electron Microprobe Data: Carbonates

Sample	Location	Description	Stages	Total	CO_2	MgO	CaO	MnO	FeO	SrO
Bellekeno										
Siderite: stage 2										
BKUD09-134-39.5-2-1	BK_SW, 965 masl	With Sp, Py	2, 4a	99.976	38.605	0.796	0.364	17.800	42.374	0.027
BKUD09-134-39.5-3-1	BK_SW, 965 masl	With Sp, Py	2, 4a	99.984	38.445	0.770	0.322	17.005	43.423	0.010
BKUD09-134-39.5-3-2	BK_SW, 965 masl	With Sp, Py	2, 4a	99.867	39.095	0.558	0.147	13.285	46.199	0.000
BKUD09-134-39.5-5-1	BK_SW, 965 masl	With Sp, Py	2, 4a	99.992	38.595	1.264	0.205	14.362	45.514	0.031
BKUD09-134-39.5-5-2	BK_SW, 965 masl	With Sp, Py	2, 4a	99.990	38.306	0.799	0.154	11.952	48.707	0.009
BKUD09-134-39.5-6-3	BK_SW, 965 masl	With Sp, Py, Qz	2, 4a	99.943	39.045	0.861	0.281	17.019	42.689	0.031
BKUD09-134-39.5-6-3	BK_SW, 965 masl	With Sp, Py, Qz	2, 4a	99.963	39.512	1.583	0.567	15.095	43.183	0.000
BKUD09-134-39.5-7-1	BK_SW, 965 masl	With Sp, Py	2, 4a	99.963	39.385	1.586	0.547	15.133	43.282	0.000
BKUD09-134-41.35-1-2	BK_SW, 965 masl	With Cal, Sp	2, 4a	99.978	38.257	0.651	0.448	12.490	48.091	0.000
BKUD09-134-41.35-2-1	BK_SW, 965 masl	Sequence	2, 4a	99.970	38.136	1.481	0.481	14.815	45.023	0.009
BKUD09-134-41.35-2-2	BK_SW, 965 masl	Sequence	2, 4a	100.000	38.466	1.606	0.509	14.696	44.671	0.009
BKUD09-134-41.35-2-3	BK_SW, 965 masl	Sequence	2, 4a	99.989	38.359	1.379	0.633	15.440	44.151	0.017
BKUD09-134-41.35-2-4	BK_SW, 965 masl	Sequence	2, 4a	99.962	38.419	1.532	0.936	16.364	42.682	0.005
BKUD09-134-41.35-2-5	BK_SW, 965 masl	Sequence	2, 4a	99.979	38.107	1.830	0.739	14.775	44.468	0.026
BKUD09-134-41.35-2-6	BK_SW, 965 masl	Sequence	2, 4a	99.978	38.677	1.543	0.664	15.241	43.760	0.000
BKUD09-134-41.35-2-7	BK_SW, 965 masl	Sequence	2, 4a	99.965	38.110	1.122	0.224	17.517	42.950	0.034
BKUD09-134-41.35-3-1	BK_SW, 965 masl	With Ank, Sp, Py	2, 4a	99.929	38.669	0.899	0.428	17.858	42.025	0.000
BKUD09-134-41.35-3-4	BK_SW, 965 masl	With Ank, Sp, Py	2, 4a	99.958	40.914	0.905	0.693	13.739	43.687	0.000
BKUD09-134-41.35-4-1	BK_SW, 965 masl	With Sp, Py	2, 4a	99.981	38.463	0.617	0.190	14.572	46.106	0.031
BKUD09-134-41.35-5-1	BK_SW, 965 masl	With Sp, Py, Qz, Cal	2, 4a	99.981	38.537	1.230	0.205	16.969	43.006	0.005
BKUD09-134-41.35-5-3	BK_SW, 965 masl	With Sp, Py, Qz, Cal	2, 4a	99.985	38.518	0.631	0.101	13.017	47.710	0.000
BKUD09-134-41.35-6-1	BK_SW, 965 masl	With Sp, Py	2, 4a	99.981	37.663	0.766	0.112	13.953	47.437	0.019

A. Electron Microprobe Data: Carbonates

BKUD09-134-41.35m-2-1-3	BK_SW, 965 masl	With Cal, Sp	2, 4a	99.997	38.253	0.785	0.357	15.316	45.234	0.015
BKUD09-134-41.35m-2-2-1	BK_SW, 965 masl	With Ank, Sp, Py	2, 4a	99.992	38.225	0.695	0.096	13.799	47.138	0.000
BKUD09-134-41.35m-2-3-1	BK_SW, 965 masl	With Sp	2, 4a	99.985	38.634	1.764	0.528	15.164	43.856	0.000
BKUD09-134-41.35m-2-3-2	BK_SW, 965 masl	With Sp	2, 4a	99.982	38.477	1.170	0.229	16.251	43.800	0.011
BKUD09-134-41.35m-2-4-1	BK_SW, 965 masl	With Cal, Sp	2, 4a	99.979	38.024	0.556	0.180	13.715	47.455	0.021
BKUD09-134-41.35m-2-5-1	BK_SW, 965 masl	With Sp, Py	2, 4a	99.995	38.255	0.693	0.126	13.821	47.023	0.003
BKUD09-134-41.35m-2-5-2	BK_SW, 965 masl	With Sp, Py	2, 4a	99.970	38.660	1.439	1.085	17.167	41.540	0.040
BKUD09-134-41.35m-2-6-1	BK_SW, 965 masl	With Sp, Py	2, 4a	100.000	38.606	1.996	0.663	14.392	44.312	0.011
BKUD09-134-41.35m-2-8-1	BK_SW, 965 masl	(cld)	2, 4a	99.950	39.492	1.911	0.843	14.773	42.890	0.004
BKUD09-134-41.35m-2-9-1	BK_SW, 965 masl	With Cal, Py	2, 4a	99.992	38.468	0.931	0.329	14.680	45.499	0.027
BKUD09-134-41.35m-2-10-1	BK_SW, 965 masl	With Cal, Py	2, 4a	99.950	38.706	1.009	0.141	14.377	45.701	0.000
BKUD09-134-41.35m-2-10-3	BK_SW, 965 masl	With Cal, Py	2, 4a	100.000	38.605	1.071	0.185	16.295	43.749	0.035
BKUD09-134-45m-2-1-1	BK_SW, 965 masl	With Py	2, 4a	99.979	38.004	0.756	0.202	12.705	48.261	0.028
BKUD09-134-45m-2-2-1	BK_SW, 965 masl	With Py, Sp, Ank	2, 4a	99.982	38.263	0.665	0.207	12.587	48.242	0.009
BKUD09-134-45m-2-3-1	BK_SW, 965 masl	With Py, Sp, Cal	2, 4a	99.976	38.134	0.668	0.177	13.486	47.474	0.000
BKUD09-134-45m-2-4-1	BK_SW, 965 masl	Within Sp	2, 4a	99.981	38.219	0.749	0.156	13.425	47.383	0.034
BKUD09-134-45m-2-4-2	BK_SW, 965 masl	Within Sp	2, 4a	99.991	38.220	0.809	0.404	15.613	44.889	0.000
BKUD09-134-45m-2-5-1	BK_SW, 965 masl	With Sp	2, 4a	99.974	39.108	2.680	0.776	14.531	42.878	0.000
BKUD09-134-45m-2-6-1	BK_SW, 965 masl	(cld)	2, 4a	99.979	38.723	1.121	0.346	16.196	43.563	0.012
BKUD09-134-45m-2-7-1	BK_SW, 965 masl	With Sp, Ank	2, 4a	99.984	38.352	0.865	0.202	13.919	46.606	0.021
BKUD09-134-45m-2-8-1	BK_SW, 965 masl	(cld)	2, 4a	99.932	38.540	1.642	0.251	13.783	45.714	0.000
BKUD09-134-45m-2-9-1	BK_SW, 965 masl	Outer, with Py	2, 4a	99.983	38.557	0.836	0.251	13.877	46.446	0.004
BKUD09-134-45m-2-9-2	BK_SW, 965 masl	Inner, with Py	2, 4a	99.981	39.107	1.422	0.189	14.678	44.518	0.025
BKUD09-140-9-9m-1-4	BK_SW	With Qz, Sp	1, 2	99.995	38.773	1.625	1.662	14.837	43.021	0.059
BKUD09-140-9-9m-1-5	BK_SW	With Qz, Sp	1, 2	99.975	38.311	1.139	0.563	18.905	40.982	0.035
BKUD09-140-9-9m-1-6	BK_SW	With Qz, Sp	1, 2	99.998	38.583	2.219	0.953	16.948	41.243	0.032

A. Electron Microprobe Data: Carbonates

BKUD09-140-9-9m-2-4	BK_SW	With Qz, Ms, Sp	1, 2	99.988	37.884	1.681	1.206	16.316	42.858	0.041
BKUD09-140-9-9m-2-5	BK_SW	With Qz, Ms, Sp	1, 2	99.976	38.178	1.197	0.631	20.029	39.917	0.014
BKUD09-140-9-9m-2-6	BK_SW	With Qz, Ms, Sp	1, 2	99.987	37.853	1.013	0.434	15.423	45.188	0.062
BKUD09-140-9-9m-2-7	BK_SW	With Qz, Ms, Sp	1, 2	99.977	37.908	1.491	2.191	15.750	42.564	0.031
BKUD09-140-9-9m-3-3	BK_SW	With Qz, Sp	1, 2	99.985	38.200	0.792	0.309	15.811	44.783	0.063
BKUD09-140-9-9m-3-4	BK_SW	With Qz, Sp	1, 2	99.962	37.858	1.472	1.288	15.888	43.387	0.064
BKUD09-140-9-9m-4-3	BK_SW	With Qz, Sp	1, 2	99.972	38.269	1.492	1.111	15.800	43.265	0.035
BKUD09-140-9-9m-4-4	BK_SW	With Qz, Sp	1, 2	99.989	38.716	0.999	0.487	19.559	40.190	0.000
BKUD09-140-9-9m-4-5	BK_SW	With Qz, Sp	1, 2	100.000	37.909	0.910	0.286	16.242	44.549	0.045
BKUD09-140-9-9m-5-4	BK_SW	With Qz, Sp	1, 2	99.982	38.131	1.714	1.323	16.108	42.642	0.032
BKUD09-140-9-9m-5-5	BK_SW	With Qz, Sp	1, 2	99.962	38.037	1.072	0.545	19.277	40.968	0.063
BKUD09-140-9-9m-6-4	BK_SW	With Qz, Sp	1, 2	99.951	38.086	1.564	0.555	16.833	42.886	0.026
BKUD09-140-9-9m-6-5	BK_SW	With Qz, Sp	1, 2	100.000	38.023	0.772	0.146	12.747	48.233	0.054
BKUD09-140-9-9m-6-6	BK_SW	With Qz, Sp	1, 2	99.986	38.318	0.961	0.408	13.327	46.923	0.044
BKUD09-140-9-9m-6-7	BK_SW	With Qz, Sp	1, 2	100.000	37.787	0.953	0.092	12.504	48.572	0.066
BKUD09-144-36-6m_1-3	BK_SW, SW-end, 980 masl	With WR	2, 3	99.974	37.873	1.960	1.149	14.841	44.088	0.053
BKUD09-144-36-6m_2-5	BK_SW, SW-end, 980 masl	With Py, WR	2, 3	100.000	38.450	2.336	1.145	15.079	42.918	0.041
BKUD09-144-36-6m_3-4	BK_SW, SW-end, 980 masl	With Sp	2, 3	99.930	37.878	2.506	0.710	16.095	42.703	0.012
BKUD09-144-36-6m_4-14	BK_SW, SW-end, 980 masl	With Sp	2, 3	99.956	38.221	1.447	0.934	18.314	41.022	0.000
BKUD09-144-36-6m_5-4	BK_SW, SW-end, 980 masl	With Sp	2, 3	99.959	38.186	1.700	1.349	17.182	41.498	0.039
BKUD09-144-36-6m_5-5	BK_SW, SW-end, 980 masl	With Sp	2, 3	99.994	38.045	1.476	1.008	16.634	42.770	0.010
BKUD09-144-36-6m_6-8	BK_SW, SW-end, 980 masl	With Sp	2, 3	99.967	38.043	1.243	0.449	15.400	44.753	0.042
BKUD09-144-36-6m_7-6	BK_SW, SW-end,	With Py, WR	2, 3	100.000	38.014	2.093	1.201	15.672	42.961	0.031

A. Electron Microprobe Data: Carbonates

	980 masl									
BKUD09-144-36-6m_8-1	BK_SW, SW-end, 980 masl	With Py, WR	2, 3	99.999	37.935	1.246	0.331	16.686	43.738	0.041
BKUD09-144-36-6m_9-1	BK_SW, SW-end, 980 masl	With WR	2, 3	100.000	38.158	1.466	0.494	12.712	47.129	0.022
BKUD09-148-33-5m-1-4	BK_99, 1025 masl	Inner, with Sp	2/6 ?, 7	99.967	37.632	0.999	0.300	17.420	43.568	0.000
BKUD09-148-33-5m-1-5	BK_99, 1025 masl	Outer, with Sp	2/6 ?, 7	99.970	37.233	1.082	0.180	14.139	47.279	0.033
BKUD09-148-33-5m-3-4	BK_99, 1025 masl	Inner, with Sp	2/6 ?, 7	99.970	36.906	0.806	0.134	14.775	47.293	0.024
BKUD09-148-33-5m-3-5	BK_99, 1025 masl	Outer, with Sp	2/6 ?, 7	100.000	37.277	0.902	0.137	13.246	48.315	0.054
BKUD09-148-33-5m-4-6	BK_99, 1025 masl	Inner, with Sp	2/6 ?, 7	100.000	37.584	1.288	0.510	18.506	42.033	0.045
BKUD09-148-33-5m-4-7	BK_99, 1025 masl	Outer, with Sp	2/6 ?, 7	99.977	39.364	1.873	0.973	18.083	39.413	0.055
BKUD09-148-33-5m-5-3	BK_99, 1025 masl	With Gn	2/6 ?, 7	99.963	37.513	0.857	0.073	14.432	47.030	0.053
BKUD09-148-33-5m-5-4	BK_99, 1025 masl	With Sp	2/6 ?, 7	99.995	38.136	1.328	0.481	16.891	43.087	0.058
BKUD09-148-33-5m-6-4	BK_99, 1025 masl	With Qz, Sp	2/6 ?, 7	100.000	37.051	1.281	0.468	18.037	43.033	0.048
BKUD09-148-33-5m-7-4	BK_99, 1025 masl	With Qz, Sp, Ttr	2/6 ?, 7	99.949	37.609	1.004	0.097	16.417	44.763	0.034
BKUD09-148-33-5m-7-6	BK_99, 1025 masl	With Sp	2/6 ?, 7	99.977	37.846	2.394	1.151	21.232	37.310	0.024
BKUD09-148-33-5m-8-4	BK_99, 1025 masl	With Qz, Sp	2/6 ?, 7	99.996	37.022	1.473	0.625	17.155	43.625	0.066
BKUD09-148-33-5m-10-1	BK_99, 1025 masl	With Sp	2/6 ?, 7	99.996	37.720	1.103	0.340	17.443	43.361	0.025
BKUD09-153-84m-1-1	BK_SW, SW-end, 940 masl	With Cal	2/6 ?	99.958	37.778	0.729	0.258	13.519	47.592	0.062
BKUD09-153-84m-2-3	BK_SW, SW-end, 940 masl	With Cal	2/6 ?	99.963	37.541	0.908	0.467	13.800	47.157	0.074
BKUD09-153-84m-5-1	BK_SW, SW-end, 940 masl	(clr)	2/6 ?	99.928	38.784	1.125	0.274	12.944	46.725	0.076
BKUD09-153-87-5m-4-3	BK_SW, SW-end, 940 masl	With Sp	2, 3	99.982	38.383	1.090	0.597	20.267	39.584	0.022
BKUD09-153-87-5m-5-3	BK_SW, SW-end, 940 masl	With Sp	2, 3	99.943	38.272	1.284	0.661	18.273	41.393	0.037
BKUD09-153-87-5m-5-4	BK_SW, SW-end, 940 masl	With Sp	2, 3	100.000	38.221	0.912	0.251	18.316	42.143	0.065

A. Electron Microprobe Data: Carbonates

BKUD09-153-87-5m-10-3	BK_SW, SW-end, 940 masl	With Sp	2, 3	99.978	37.150	0.494	0.097	14.042	48.065	0.049
BKUD09-153-87-5m-10-4	BK_SW, SW-end, 940 masl	With Sp	2, 3	99.994	37.360	0.648	0.133	15.327	46.404	0.098
BKUD09-153-87-5m-11-1	BK_SW, SW-end, 940 masl	With Sp	2	99.988	37.950	1.028	0.589	18.192	42.171	0.028
BKUD09-153-87-5m-12-2	BK_SW, SW-end, 940 masl	With Sp	2	99.985	38.167	1.128	0.580	19.858	40.167	0.050
BKUD09-157-100-5m-1-2	BK_SW, SW-end, 930 masl	With Sp	2/6 ?, 9, 12	99.975	37.815	1.126	0.416	15.862	44.506	0.024
BKUD09-157-100-5m-2-7	BK_SW, SW-end, 930 masl	Sequence	2/6 ?, 9, 12	99.993	37.714	1.710	0.602	17.091	42.735	0.078
BKUD09-157-100-5m-3-3	BK_SW, SW-end, 930 masl	With Sp	2/6 ?, 9, 12	99.988	38.184	1.515	0.474	16.500	43.082	0.030
BKUD09-157-100-5m-4-4	BK_SW, SW-end, 930 masl	With Sp	2/6 ?, 9, 12	100.000	37.530	1.147	0.249	16.091	44.944	0.008
BKUD09-157-100-5m-5-3	BK_SW, SW-end, 930 masl	With Sp	2/6 ?, 9, 12	100.000	38.202	1.299	0.602	16.842	42.990	0.042
BKUD09-157-100-5m-6-3	BK_SW, SW-end, 930 masl	With Sp	2/6 ?, 9, 12	99.964	37.719	0.953	0.353	16.842	43.994	0.045
BKUD09-157-100-5m-8-5	BK_SW, SW-end, 930 masl	With Ank, Sp	2/6 ?, 9, 12	99.978	38.506	1.251	1.034	15.720	43.385	0.049
BKUD09-157-100-5m-9-1	BK_SW, SW-end, 930 masl	(clr)	2/6 ?, 9, 12	99.988	37.394	1.051	0.246	15.235	46.030	0.009
BKUD09-157-100-5m-10-1	BK_SW, SW-end, 930 masl	(clr)	2/6 ?, 9, 12	99.989	38.067	1.370	0.691	17.141	42.645	0.043
BKUD09-163-31.8m-1-3	BK_SW, 980 masl	(cld), With WR	2	99.987	40.261	1.459	1.694	14.601	41.885	0.084
BKUD09-163-31-8m-1-4	BK_SW, 980 masl	With WR	2	100.000	39.128	1.902	0.791	14.754	43.395	0.030
BKUD09-163-31.8m-2-4	BK_SW, 980 masl	(cld), With Py, Apy	2	100.000	38.571	2.060	0.662	13.377	45.198	0.093
BKUD09-163-31-8m-2-5	BK_SW, 980 masl	With Py, Apy	2	100.000	38.349	1.288	0.707	16.108	43.531	0.017

A. Electron Microprobe Data: Carbonates

BKUD09-163-31.8m-3-4	BK_SW, 980 masl	(cld), Inner, With Apy	2	99.993	37.752	0.935	0.292	15.518	45.391	0.069
BKUD09-163-31-8m-3-5	BK_SW, 980 masl	(cld), Outer, with Apy	2	100.000	38.196	1.810	1.257	16.021	42.635	0.082
BKUD09-163-31-8m-3-6	BK_SW, 980 masl	(cld), Inner, With Apy	2	100.000	38.074	0.883	0.358	16.525	44.131	0.030
BKUD09-163-31-8m-4-6	BK_SW, 980 masl	Outer	2	100.000	38.204	1.572	0.861	18.103	41.189	0.070
BKUD09-163-31-8m-4-7	BK_SW, 980 masl	With Apy	2	100.000	38.548	0.982	0.637	19.965	39.829	0.038
BKUD09-163-31.8m-5-1	BK_SW, 980 masl	(cld), With WR	2	99.979	38.765	2.605	1.400	14.625	42.500	0.060
BKUD09-163-31.8m-7-1	BK_SW, 980 masl	(clr)	2	99.984	37.327	1.500	0.701	15.948	44.365	0.093
BKUD09-163-31-8m-7-3	BK_SW, 980 masl	Sequence, from below	2	100.000	38.098	1.431	0.750	16.818	42.846	0.058
BKUD09-163-31-8m-7-4	BK_SW, 980 masl	Sequence	2	100.000	38.274	1.501	0.767	15.054	44.343	0.061
BKUD09-163-31-8m-7-5	BK_SW, 980 masl	Sequence	2	100.000	38.631	2.855	0.783	13.937	43.753	0.042
BKUD09-163-31-8m-7-6	BK_SW, 980 masl	Sequence	2	100.000	38.235	2.275	0.754	16.024	42.648	0.065
BKUD09-163-31-8m-7-7	BK_SW, 980 masl	Sequence, near 7-3	2	100.000	38.974	2.374	0.772	14.631	43.240	0.009
	n =	121	AVERAGE	99.980	38.253	1.287	0.554	15.704	44.114	0.032
			MINIMUM	99.867	36.906	0.494	0.073	11.952	37.310	0.000
			MAXIMUM	100.000	40.914	2.855	2.191	21.232	48.707	0.098
Siderite: stage 6										
K07-76-125m-1-1	BK_E, 965 masl	Outer, with Sp	2/6 ?, 7, 8	99.979	38.641	0.612	0.090	14.270	46.238	0.095
K07-76-125m-1-2	BK_E, 965 masl	Inner, with Sp	2/6 ?, 7, 8	99.996	38.902	0.635	0.393	15.347	44.524	0.077
K07-76-125m-2-1	BK_E, 965 masl	Inner, with Sp, Ttr	2/6 ?, 7, 8	99.974	40.074	0.518	0.083	13.723	45.454	0.086
K07-76-125m-2-2	BK_E, 965 masl	Outer, with Sp, Ttr	2/6 ?, 7, 8	100.000	40.186	0.648	0.315	15.021	43.633	0.099
K07-76-125m-3-1	BK_E, 965 masl	Inner	2/6 ?, 7, 8	99.967	40.754	0.925	0.330	14.174	43.641	0.095
K07-76-125m-3-2	BK_E, 965 masl	Outer, near Gn	2/6 ?, 7, 8	99.997	39.841	0.599	0.156	13.115	46.155	0.104

A. Electron Microprobe Data: Carbonates

K07-76-125m-4-1	BK_E, 965 masl	After Qz, before Sp	2/6 ?, 7, 8	100.000	41.847	0.579	0.144	13.085	44.215	0.073
K07-76-125m-4-2	BK_E, 965 masl	After Qz, before Sp	2/6 ?, 7, 8	99.999	41.719	0.599	0.122	12.704	44.743	0.083
K07-76-125m-5-1	BK_E, 965 masl	With Sp	2/6 ?, 7, 8	100.000	43.125	0.458	0.153	13.249	42.864	0.062
K07-76-125m-5-2	BK_E, 965 masl	With Gn	2/6 ?, 7, 8	99.994	43.225	0.447	0.241	12.958	43.002	0.090
K07-76-125m-6-1	BK_E, 965 masl	Outer, with Sp, Gn, Ttr	2/6 ?, 7, 8	100.000	41.212	0.444	0.060	13.301	44.874	0.067
K07-76-125m-6-2	BK_E, 965 masl	Inner	2/6 ?, 7, 8	99.980	41.330	0.564	0.092	11.841	46.099	0.044
K07-76-125m-6-3	BK_E, 965 masl	With Qz	2/6 ?, 7, 8	99.997	41.403	0.569	0.314	14.515	43.106	0.081
K07-76-125m-7-1	BK_E, 965 masl	With Boul, Sp, Gn	2/6 ?, 7, 8	99.965	40.304	0.645	0.204	14.162	44.583	0.057
K07-76-125m-9-1	BK_E, 965 masl	With Sp, Ttr	2/6 ?, 7, 8	99.971	38.704	0.682	0.345	15.571	44.557	0.104
K07-106-402-2m-1-3	BK_SW, NE-end, 985 masl	With Sp	6, 7	100.000	38.341	1.063	0.618	14.111	45.853	0.016
K07-106-402-2m-2-5	BK_SW, NE-end, 985 masl	With Sp	6, 7	100.000	39.095	3.296	1.160	14.443	41.988	0.017
K07-106-402-2m-2-6	BK_SW, NE-end, 985 masl	Inner	6, 7	100.000	39.411	3.302	1.075	13.888	42.255	0.069
K07-106-402-2m-5-4	BK_SW, NE-end, 985 masl	Within Sp	6, 7	100.000	39.137	1.650	0.909	14.972	43.281	0.051
K07-106-402-2m-5-5	BK_SW, NE-end, 985 masl	With Qz	6, 7	100.000	39.362	2.951	1.292	15.477	40.907	0.011
K07-106-402-2m-6-4	BK_SW, NE-end, 985 masl	With Sp	6, 7	100.000	39.193	2.081	0.764	15.321	42.593	0.047
K07-106-402-2m-7-5	BK_SW, NE-end, 985 masl	With Sp	6, 7	100.000	39.852	2.000	0.692	14.351	43.094	0.011
K07-106-402-2m-7-6	BK_SW, NE-end, 985 masl	Inner	6, 7	100.000	39.919	2.183	0.893	15.190	41.793	0.022
K07-106-402-2m-9-7	BK_SW, NE-end, 985 masl	With Sp, Apy, Ttr	6, 7, 8	100.000	40.025	2.363	0.726	13.455	43.388	0.043

A. Electron Microprobe Data: Carbonates

BKUD09-143-51-2m-1-8	BK_SW, NE-end, 1000 masl	With Sp, Py, before Ank	2, 4a	100.000	40.642	0.999	0.423	17.177	40.705	0.054
BKUD09-143-51-2m-2-8	BK_SW, NE-end, 1000 masl	With Sp, Py	2, 4a	100.000	39.949	0.797	0.172	14.821	44.200	0.062
BKUD09-143-51-2m-2-9	BK_SW, NE-end, 1000 masl	Inner	2, 4a, 6/11?	100.000	39.966	0.800	0.219	13.879	45.067	0.070
BKUD09-143-51-2m-3-5	BK_SW, NE-end, 1000 masl	Inner	2, 4a, 6/11?	100.000	41.739	2.316	3.466	16.791	35.645	0.043
BKUD09-143-51-2m-4-8	BK_SW, NE-end, 1000 masl	With Sp	2, 4a, 6/11?	100.000	41.557	1.213	0.475	16.068	40.685	0.003
BKUD09-143-51-2m-5-7	BK_SW, NE-end, 1000 masl	With Sp, Py	2, 4a	100.000	40.889	0.854	0.165	13.153	44.885	0.055
BKUD09-143-51-2m-6-6	BK_SW, NE-end, 1000 masl	With Sp, Py	2, 4a	100.000	41.821	1.023	0.322	13.158	43.615	0.060
BKUD09-143-51-2m-6-7	BK_SW, NE-end, 1000 masl	With Sp, Py	2, 4a	100.000	42.080	1.028	0.562	13.973	42.327	0.030
BKUD09-143-51-2m-7-4	BK_SW, NE-end, 1000 masl	With Py	2, 4a	100.000	41.771	0.961	0.563	14.517	42.166	0.023
BKUD09-143-51-2m-8-7	BK_SW, NE-end, 1000 masl	With Py	2, 4a, 6/11?	100.000	41.580	0.979	0.222	13.208	43.965	0.046
BKUD09-143-51-2m-9-5	BK_SW, NE-end, 1000 masl	With Sp	10 , 6/11?	100.000	41.539	0.657	0.247	9.915	47.631	0.012
BKUD09-143-51-2m-10-6	BK_SW, NE-end, 1000 masl	With Sp	10 , 6/11?	100.000	41.223	0.661	0.271	9.498	48.300	0.047
BKUD09-143-51-2m-11-3	BK_SW, NE-end, 1000 masl	Inner	10 , 6/11?	100.000	42.319	0.762	0.311	12.364	44.203	0.042
BKUD09-158-36-5m-3-6	BK_SW, NE-end, 1030 masl	With Sp	6, 7	100.000	38.352	0.721	0.313	16.004	44.561	0.049
BKUD09-158-36-5m-4-7	BK_SW, NE-end, 1030 masl	With Sp, Ttr	6, 7, 8	100.000	38.256	0.874	0.542	16.278	44.047	0.003
BKUD09-158-36-5m-8-6	BK_SW, NE-end, 1030 masl	With Sp	6, 7	100.000	38.979	0.799	0.387	15.065	44.709	0.061

A. Electron Microprobe Data: Carbonates

BKUD09-158-36-5m-9-10	BK_SW, NE-end, 1030 masl	With Sp	6, 7	100.000	38.689	0.613	0.259	14.321	46.062	0.056
BKUD09-158-36-5m-10-8	BK_SW, NE-end, 1030 masl	With Sp, Ttr	6, 7, 8	100.000	38.694	0.776	0.181	13.119	47.199	0.031
BKUD09-158-36-5m-11-10	BK_SW, NE-end, 1030 masl	With Sp, Gn, Ttr	6, 7, 8	100.000	39.098	0.711	0.061	12.546	47.554	0.030
BKUD09-158-36-5m-13-9	BK_SW, NE-end, 1030 masl	Sequence	6 ?	100.000	39.706	0.979	0.623	14.122	44.518	0.052
BKUD09-158-36-5m-13-10	BK_SW, NE-end, 1030 masl	Sequence	6 ?	100.000	39.693	0.572	0.183	13.237	46.295	0.020
BKUD09-158-36-5m-13-11	BK_SW, NE-end, 1030 masl	Sequence	6 ?	100.000	40.234	1.345	1.132	13.641	43.637	0.011
BKUD09-158-37m-1-5	BK_SW, NE-end, 1030 masl	With Py, Qz, Gn	2/6 ?, 8	99.996	37.408	0.802	0.104	12.746	48.904	0.017
BKUD09-158-37m-2-6	BK_SW, NE-end, 1030 masl	With Gn, Ttr, Py, Cal	2/6 ?, 8	99.979	37.485	0.745	0.157	14.296	47.228	0.033
BKUD09-158-37m-2-7	BK_SW, NE-end, 1030 masl	With Gn, Ttr, Py, Cal	2/6 ?, 8	99.974	37.710	0.820	0.165	14.256	46.949	0.034
BKUD09-158-37m-5-5	BK_SW, NE-end, 1030 masl	With Gn, Sp, Ttr, Qz	2/6 ?, 8	99.985	38.125	0.660	0.241	14.831	46.085	0.004
BKUD09-158-37m-6-4	BK_SW, NE-end, 1030 masl	With Ank, Gn, Sp	2/6 ?, 8	100.000	38.167	0.957	0.378	16.644	43.801	0.013
BKUD09-158-37m-6-7	BK_SW, NE-end, 1030 masl	With Ank, Gn, Sp	2/6 ?, 8	99.985	38.066	0.748	0.175	13.561	47.367	0.057
BKUD09-158-37m-7-7	BK_SW, NE-end, 1030 masl	With Gn, Sp, Ttr, Qz	2/6 ?, 8	99.976	38.137	1.099	0.773	19.396	40.508	0.031
BKUD09-158-37m-8-4	BK_SW, NE-end, 1030 masl	With Py	2/6 ?, 8	99.963	37.523	2.577	0.393	18.470	40.942	0.033
BKUD09-158-37m-9-2	BK_SW, NE-end, 1030 masl	With Gn, Py	2/6 ?, 8	99.983	37.771	0.768	0.182	15.320	45.886	0.000
BKUD09-158-37m-10-1	BK_SW, NE-end, 1030 masl	(clr)	2/6 ?, 8	100.000	37.608	1.338	0.652	18.466	41.847	0.040

A. Electron Microprobe Data: Carbonates

BKUD09-158-37m-11-1	BK_SW, NE-end, 1030 masl	(clr)	2/6 ?, 8	100.000	37.813	1.219	0.598	17.601	42.713	0.010
BKUD09-171-32-8m-1-4	BK_99, 990 masl	With Gn, Sp, Py,Qz	2/6 ?, 7, 8	99.968	37.253	1.287	0.317	15.546	45.515	0.035
BKUD09-171-32-8m-2-6	BK_99, 990 masl	With Gn, Apy, WR	2/6 ?, 7, 8	99.996	37.622	0.937	0.274	16.564	44.542	0.001
BKUD09-171-32-8m-3-5	BK_99, 990 masl	With Gn, Py, WR	2/6 ?, 7, 8	99.980	37.740	0.851	0.144	14.916	46.222	0.032
BKUD09-171-32-8m-4-4	BK_99, 990 masl	With Gn, Sp, Py	2/6 ?, 7, 8	100.000	37.358	0.884	0.204	14.609	46.858	0.046
BKUD09-171-32-8m-5-6	BK_99, 990 masl	With Gn, Sp, Py	2/6 ?, 7, 8	99.988	37.728	0.719	0.443	17.877	43.163	0.027
BKUD09-171-32-8m-6-5	BK_99, 990 masl	With Gn, Sp, Py	2/6 ?, 7, 8	100.000	37.688	0.718	0.291	16.771	44.451	0.032
BKUD09-171-32-8m-7-4	BK_99, 990 masl	With Gn, Sp	2/6 ?, 7, 8	99.958	37.654	1.091	0.252	14.700	46.168	0.055
BKUD09-171-32-8m-7-6	BK_99, 990 masl	With Gn, Sp	2/6 ?, 7, 8	100.000	37.922	0.847	0.310	14.759	46.068	0.047
BKUD09-171-32-8m-8-5	BK_99, 990 masl	With Gn, Sp, Ttr, Qz	2/6 ?, 7, 8	99.978	37.723	0.662	0.239	16.979	44.299	0.005
BKUD09-171-32-8m-9-4	BK_99, 990 masl	With Gn, Sp, Ttr, Qz	2/6 ?, 7, 8	99.996	37.271	0.649	0.272	17.247	44.511	0.022
BKUD09-171-32-8m-10-1	BK_99, 990 masl	With Ank, Qz	2/6 ?, 7, 8	100.000	37.662	0.880	0.302	15.114	45.948	0.061
	n =	68	AVERAGE	99.993	39.468	1.052	0.428	14.644	44.335	0.044
			MINIMUM	99.958	37.253	0.444	0.060	9.498	35.645	0.000
			MAXIMUM	100.000	43.225	3.302	3.466	19.396	48.904	0.104
Siderite: stage 9										
BKUD09-153-84m-3-2	BK_SW, SW-end, 940 masl	(cld), with Cal	9, 12	100.000	37.656	0.787	0.475	13.891	47.079	0.078
BKUD09-153-84m-4-1	BK_SW, SW-end, 940 masl	(cld), with Sp, Cal	2/9 ?, 12	99.974	38.090	0.765	0.385	15.976	44.689	0.046
BKUD09-153-84m-4-3	BK_SW, SW-end, 940 masl	(cld), with Sp, Cal	9, 11	99.974	37.871	1.065	0.743	15.845	44.320	0.100
BKUD09-153-84m-4-4	BK_SW, SW-end, 940 masl	(cld), with Sp, Cal	2/9 ?, 12	99.955	37.746	0.890	0.381	15.838	45.009	0.070
BKUD09-153-84m-6-1	BK_SW, SW-end,	(cld), with Cal	2/9 ?, 12	99.978	37.636	0.934	0.229	13.769	47.324	0.087

A. Electron Microprobe Data: Carbonates

	940 masl									
BKUD09-153-84m-6-2	BK_SW, SW-end, 940 masl	(cld), with Cal	2/9 ?, 12	99.980	38.338	0.970	0.973	18.545	41.067	0.069
BKUD09-153-87-5m-1-14	BK_SW, SW-end, 940 masl	(cld), with Sp	9	99.994	37.502	1.171	0.498	16.474	44.290	0.024
BKUD09-153-87-5m-2-8	BK_SW, SW-end, 940 masl	Sequence	9	99.995	37.532	0.866	0.286	13.236	48.009	0.008
BKUD09-153-87-5m-2-9	BK_SW, SW-end, 940 masl	Sequence	9	99.941	38.048	1.142	0.094	10.343	50.288	0.000
BKUD09-153-87-5m-2-10	BK_SW, SW-end, 940 masl	Sequence	9	99.973	37.852	0.699	0.111	14.800	46.448	0.048
BKUD09-153-87-5m-2-11	BK_SW, SW-end, 940 masl	Sequence	9	99.995	37.794	0.623	0.171	15.163	46.172	0.039
BKUD09-153-87-5m-2-12	BK_SW, SW-end, 940 masl	Sequence	9	99.964	37.997	0.654	0.226	14.149	46.841	0.030
BKUD09-153-87-5m-6-12	BK_SW, SW-end, 940 masl	With Sp	9	100.000	38.132	1.075	0.933	16.992	42.716	0.083
BKUD09-153-87-5m-7-3	BK_SW, SW-end, 940 masl	With Sp	9	99.937	37.832	0.821	0.589	15.693	44.960	0.033
BKUD09-153-87-5m-8-4	BK_SW, SW-end, 940 masl	Sequence	9	99.998	38.021	1.011	0.460	15.876	44.543	0.048
BKUD09-153-87-5m-8-5	BK_SW, SW-end, 940 masl	Sequence	9	100.000	38.259	0.838	0.547	15.538	44.686	0.068
BKUD09-153-87-5m-8-6	BK_SW, SW-end, 940 masl	Sequence	9	99.975	37.903	0.923	0.416	14.384	46.293	0.038
BKUD09-153-87-5m-8-7	BK_SW, SW-end, 940 masl	Sequence	9	99.980	38.282	0.998	0.735	17.193	42.695	0.045
BKUD09-153-87-5m-8-8	BK_SW, SW-end, 940 masl	Sequence	9	99.987	37.801	1.057	0.581	15.599	44.865	0.072
BKUD09-153-87-5m-9-8	BK_SW, SW-end, 940 masl	Sequence	9	99.991	37.837	0.673	0.104	14.565	46.749	0.019
BKUD09-153-87-5m-9-9	BK_SW, SW-end,	Sequence	9	99.996	37.564	0.825	0.071	16.175	45.290	0.044

A. Electron Microprobe Data: Carbonates

	940 masl									
BKUD09-153-87-5m-9-10	BK_SW, SW-end, 940 masl	Sequence	9	99.965	37.508	0.739	0.079	10.734	50.839	0.047
BKUD09-153-87-5m-9-11	BK_SW, SW-end, 940 masl	Sequence	9	99.977	37.890	0.834	0.307	13.288	47.623	0.023
BKUD09-153-87-5m-9-12	BK_SW, SW-end, 940 masl	Sequence	9	99.971	37.552	0.951	0.477	17.091	43.841	0.051
BKUD09-153-87-5m-9-13	BK_SW, SW-end, 940 masl	Sequence	9	99.953	37.812	0.667	0.097	14.687	46.639	0.013
BKUD09-153-87-5m-9-14	BK_SW, SW-end, 940 masl	Sequence	9	100.000	37.576	0.602	0.168	15.113	46.400	0.060
BKUD09-153-87-5m-13-3	BK_SW, SW-end, 940 masl	With Sp	9	99.984	38.075	1.178	0.863	16.447	43.322	0.045
BKUD09-153-87-5m-13-5	BK_SW, SW-end, 940 masl	With Sp	9	99.941	38.113	1.087	0.968	16.252	43.460	0.043
BKUD09-153-87-5m-14-2	BK_SW, SW-end, 940 masl	With Sp	9	99.976	37.934	1.051	0.583	16.397	43.945	0.044
BKUD09-158-36-5m-1-7	BK_SW, NE-end, 1030 masl	With Sp	7, 9	100.000	38.058	0.971	0.911	16.012	44.038	0.010
BKUD09-158-36-5m-1-8	BK_SW, NE-end, 1030 masl	With Qz	9, 10	100.000	38.383	1.031	0.668	16.632	43.273	0.013
BKUD09-158-36-5m-2-10	BK_SW, NE-end, 1030 masl	With Qz	9, 10	100.000	38.402	1.547	1.517	18.161	40.370	0.003
BKUD09-158-36-5m-2-11	BK_SW, NE-end, 1030 masl	With Sp	7, 9	100.000	38.557	1.010	0.539	15.891	43.938	0.065
BKUD09-158-36-5m-5-8	BK_SW, NE-end, 1030 masl	With Sp, Ank	9	100.000	38.674	1.017	1.398	14.742	44.139	0.031
BKUD09-158-36-5m-6-9	BK_SW, NE-end, 1030 masl	With Sp	9	100.000	38.571	0.581	0.355	17.225	43.256	0.013
BKUD09-158-36-5m-7-7	BK_SW, NE-end, 1030 masl	With Sp, Ank	9	100.000	38.934	0.959	0.777	15.400	43.876	0.054
BKUD09-160-56-5m-1-7	BK_SW, SW-end,	(cld), with Gn	8, 9	100.000	38.438	1.135	1.172	15.563	43.598	0.046

A. Electron Microprobe Data: Carbonates

	950 masl									
BKUD09-160-56-5m-1-8	BK_SW, SW-end, 950 masl	(cld), with Gn	8, 9	100.000	38.350	1.116	1.001	14.620	44.837	0.026
BKUD09-160-56-5m-1-9	BK_SW, SW-end, 950 masl	(cld), with Gn	8, 9	99.974	38.074	1.046	1.309	15.852	43.587	0.043
BKUD09-160-56-5m-2-4	BK_SW, SW-end, 950 masl	(cld), with Sp	9	99.970	38.074	1.139	0.916	14.319	45.414	0.056
BKUD09-160-56-5m-2-5	BK_SW, SW-end, 950 masl	(cld), with Sp	9	100.000	38.233	0.902	1.134	17.381	42.313	0.022
BKUD09-160-56-5m-3-8	BK_SW, SW-end, 950 masl	(cld), with Gn	9	99.971	37.888	0.959	0.752	16.397	43.888	0.012
BKUD09-160-56-5m-3-9	BK_SW, SW-end, 950 masl	(cld), with Gn	9	100.000	38.447	1.302	0.816	14.837	44.466	0.059
BKUD09-160-56-5m-4-5	BK_SW, SW-end, 950 masl	(clr), with Gn, Sp	9	100.000	38.473	0.889	0.700	16.569	43.240	0.042
BKUD09-160-56-5m-5-3	BK_SW, SW-end, 950 masl	(cld), with Gn, Sp	9	100.000	37.956	1.104	1.180	15.084	44.563	0.062
BKUD09-160-56-5m-6-7	BK_SW, SW-end, 950 masl	(cld), with Gn, Sp	9	99.997	38.510	1.281	0.934	18.055	41.177	0.032
BKUD09-160-56-5m-6-8	BK_SW, SW-end, 950 masl	(cld), with Gn, Sp	9	100.000	38.364	1.548	3.387	17.658	38.943	0.056
BKUD09-160-56-5m-7-11	BK_SW, SW-end, 950 masl	(cld), with Qz	9, 10	99.972	38.142	1.447	0.952	16.751	42.604	0.056
BKUD09-160-56-5m-9-4	BK_SW, SW-end, 950 masl	(cld), with Qz	9, 10	99.997	37.875	0.967	0.732	14.559	45.767	0.068
BKUD09-160-56-5m-9-5	BK_SW, SW-end, 950 masl	(cld), with Qz	9, 10	99.976	38.149	0.951	1.057	18.046	41.717	0.035
BKUD09-163-14-8m-1-4	BK_SW, 980 masl	With Ttr	9	99.995	39.023	1.459	1.761	16.186	41.566	0.000
BKUD09-163-14-8m-1-5	BK_SW, 980 masl	With Sp	9	100.000	38.144	0.991	1.211	15.675	43.941	0.038
BKUD09-163-14-8m-2-10	BK_SW, 980 masl	With Sp	9	100.000	38.908	0.977	0.925	17.034	42.142	0.014
BKUD09-163-14-8m-2-11	BK_SW, 980 masl	With Py	9	100.000	39.006	1.391	1.076	16.296	42.203	0.029

A. Electron Microprobe Data: Carbonates

BKUD09-163-14-8m-3-7	BK_SW, 980 masl	With Sp	9	100.000	38.584	1.101	1.044	16.119	43.101	0.053
BKUD09-163-14-8m-3-8	BK_SW, 980 masl	With Gn	9	100.000	38.081	0.850	0.858	13.728	46.452	0.031
BKUD09-163-14-8m-4-5	BK_SW, 980 masl	With Sp, Py, Gn	9	99.988	38.559	1.090	1.300	15.635	43.406	0.000
BKUD09-163-14-8m-6-5	BK_SW, 980 masl	With Sp	9	100.000	38.124	1.045	0.747	14.964	45.060	0.061
BKUD09-163-14-8m-7-5	BK_SW, 980 masl	Late, with Ank	9	100.000	38.713	1.168	0.591	16.497	43.013	0.018
BKUD09-163-14-8m-7-8	BK_SW, 980 masl	With Gn	9	100.000	38.309	1.073	1.219	15.954	43.420	0.026
BKUD09-166-18.6m-1-2	BK_SW, 975 masl	With Cal	9, 12	99.964	38.676	1.475	1.488	17.388	40.852	0.069
BKUD09-166-18.6m-2-1	BK_SW, 975 masl	With Cal	9, 12	99.963	38.861	1.100	0.794	14.154	44.774	0.075
BKUD09-166-18.6m-3-1	BK_SW, 975 masl	With Cal	9, 12	99.985	38.492	1.046	1.206	15.367	43.736	0.097
BKUD09-166-18.6m-3-4	BK_SW, 975 masl	Outer, With Cal	9, 12	99.972	39.161	1.481	5.670	16.835	36.658	0.133
BKUD09-166-18.6m-4-1	BK_SW, 975 masl	Inner, With Cal	9, 12	99.965	37.802	1.264	1.147	15.513	43.334	0.061
BKUD09-166-18.6m-4-2	BK_SW, 975 masl	Outer, With Cal	9, 12	99.952	38.468	1.239	0.969	14.617	44.510	0.085
BKUD09-166-18.6m-5-1	BK_SW, 975 masl	With Cal	9, 12	99.975	38.617	1.359	1.524	16.951	41.391	0.115
BKUD09-166-18.6m-5-3	BK_SW, 975 masl	Inner, With Cal	9, 12	99.998	38.915	1.290	0.971	16.392	42.299	0.082
BKUD09-166-18.6m-5-5	BK_SW, 975 masl	Outer, With Cal	9, 12	99.940	38.106	1.211	1.296	16.851	42.388	0.088
BKUD09-166-18.6m-6-1	BK_SW, 975 masl	Rim, With Cal	9, 12	99.969	38.614	0.927	0.553	14.173	45.599	0.089
	n =	70	AVERAGE	99.984	38.198	1.033	0.873	15.659	44.132	0.048
			MINIMUM	99.937	37.502	0.581	0.071	10.343	36.658	0.000
			MAXIMUM	100.000	39.161	1.548	5.670	18.545	50.839	0.133
Ankerite: mostly stages 9 to 12 and/or 4a (?)										
BKUD09-134-41.35-3-3	BK_SW, 965 masl	After Sp, with Sd	4a, 9, 12	99.989	49.490	10.003	29.940	2.941	7.501	0.027
BKUD09-134-41.35m-2-2-2	BK_SW, 965 masl	After Sp, Py	4a, 9, 12	99.994	45.836	8.473	30.544	4.596	10.380	0.075
BKUD09-134-45m-2-2-2	BK_SW, 965 masl	After Sp, Py	4a, 9, 12	100.000	46.887	10.844	30.961	2.779	8.377	0.058
BKUD09-134-45m-2-3-2	BK_SW, 965 masl	After Sp, Py, with Gn	4a, 9, 12	99.995	47.525	12.159	31.385	1.886	6.882	0.042
BKUD09-134-45m-2-3-3	BK_SW, 965 masl	After Sp, Py, with Gn	4a, 9, 12	100.000	44.947	7.309	28.064	5.125	14.483	0.012

A. Electron Microprobe Data: Carbonates

BKUD09-134-45m-2-7-2	BK_SW, 965 masl	After Sp	4a, 9, 12	100.000	45.507	8.450	29.428	4.212	12.303	0.060
BKUD09-134-45m-2-7-3	BK_SW, 965 masl	After Sp	4a, 9, 12	100.000	46.103	9.754	29.987	3.365	10.610	0.066
BKUD09-143-51-2m-1-7	BK_SW, NE-end, 1000 masl	With Sp, Py, after Sd	2, 4a	100.000	44.752	9.527	32.633	2.994	10.041	
BKUD09-143-51-2m-3-4	BK_SW, NE-end, 1000 masl	After Sd, with Qz	2, 4a	99.988	44.425	9.057	32.621	3.316	10.570	
BKUD09-143-51-2m-3-6	BK_SW, NE-end, 1000 masl	After Sd, with Qz	2, 4a	100.000	44.174	9.009	33.432	3.177	10.190	
BKUD09-143-51-2m-3-7	BK_SW, NE-end, 1000 masl	After Sd, with Qz	2, 4a	100.000	45.405	11.782	33.666	1.466	7.652	
BKUD09-143-51-2m-4-9	BK_SW, NE-end, 1000 masl	After Sd, with Qz	2, 4a	100.000	44.181	8.957	33.419	2.640	10.782	
BKUD09-143-51-2m-5-8	BK_SW, NE-end, 1000 masl	After Sd, before Sp	2, 4a	100.000	45.259	5.864	28.970	9.076	10.738	
BKUD09-143-51-2m-7-5	BK_SW, NE-end, 1000 masl	After Py, Sd	2, 4a	100.000	44.767	9.375	33.146	2.457	10.176	
BKUD09-143-51-2m-8-8	BK_SW, NE-end, 1000 masl	After Py, Sd	2, 4a	100.000	44.844	11.924	34.766	1.130	7.324	
BKUD09-153-84m-1-2	BK_SW, SW-end, 940 masl	Before Cal	12	99.987	43.528	4.503	28.076	9.531	14.229	0.085
BKUD09-153-84m-2-4	BK_SW, SW-end, 940 masl	Before Cal	12	99.990	43.900	5.078	28.165	8.422	14.261	0.104
BKUD09-153-84m-3-3	BK_SW, SW-end, 940 masl	Before Cal	9	99.971	45.842	8.763	31.033	3.437	10.714	0.104
BKUD09-153-84m-4-2	BK_SW, SW-end, 940 masl	With Sp	9	100.000	43.473	3.799	27.631	10.815	14.170	0.081
BKUD09-153-84m-6-3	BK_SW, SW-end, 940 masl	Darker	9	99.969	45.156	8.791	31.445	3.523	10.863	0.098
BKUD09-153-84m-6-6	BK_SW, SW-end, 940 masl	Lighter	9	99.967	44.398	5.529	28.743	7.233	13.933	0.101
BKUD09-153-87-5m-12-1	BK_SW, SW-end, 940 masl	After Sd	3, 9	100.000	44.999	12.172	33.041	2.910	6.682	0.071

A. Electron Microprobe Data: Carbonates

BKUD09-153-87-5m-13-1	BK_SW, SW-end, 940 masl	After Sp	9	99.985	44.693	11.060	33.983	3.168	6.945	0.084
BKUD09-153-87-5m-13-2	BK_SW, SW-end, 940 masl	After above	9	99.996	43.580	8.594	32.623	4.063	10.975	0.073
BKUD09-153-87-5m-13-4	BK_SW, SW-end, 940 masl	Later	9	100.000	42.713	5.673	29.626	9.172	12.672	0.049
BKUD09-153-87-5m-14-1	BK_SW, SW-end, 940 masl	After Sp	9	99.984	43.596	8.523	32.746	4.336	10.641	0.077
BKUD09-153-87-5m-14-3	BK_SW, SW-end, 940 masl	Later	9	100.000	44.875	11.424	33.573	3.303	6.680	0.083
BKUD09-153-87-5m-6-11	BK_SW, SW-end, 940 masl	Before Sp	9	99.973	44.052	8.753	31.937	4.453	10.605	0.057
BKUD09-153-87-5m-8-9	BK_SW, SW-end, 940 masl	Before Sp	9	99.975	45.115	11.819	33.438	3.159	6.280	0.078
BKUD09-157-100-5m-2-4	BK_SW, SW-end, 930 masl	Sequence, near Cal	9/12 ?	99.988	41.508	15.730	32.590	2.662	7.388	0.024
BKUD09-157-100-5m-2-5	BK_SW, SW-end, 930 masl	Banded sequence	9/12 ?	99.980	42.541	10.949	30.553	5.411	10.403	0.036
BKUD09-157-100-5m-2-6	BK_SW, SW-end, 930 masl	Sequence, near Sd	9/12 ?	99.990	42.941	4.538	26.915	12.314	13.210	0.056
BKUD09-157-100-5m-8-2	BK_SW, SW-end, 930 masl	Sequence, near Cal	9/12 ?	99.984	41.414	15.418	32.888	2.952	7.182	0.024
BKUD09-157-100-5m-8-3	BK_SW, SW-end, 930 masl	Banded sequence	9/12 ?	99.987	43.235	11.904	30.664	3.177	10.880	0.049
BKUD09-157-100-5m-8-4	BK_SW, SW-end, 930 masl	Sequence, near Sd	9/12 ?	99.984	42.856	4.256	26.981	13.579	12.258	0.016
BKUD09-158-36-5m-5-9	BK_SW, NE-end, 1030 masl	After Sd, before Qz	6, 7, 9	100.000	43.692	10.062	33.055	4.365	8.766	
BKUD09-158-36-5m-7-8	BK_SW, NE-end, 1030 masl	After Sd, before Qz	6, 7, 9	100.000	45.006	10.120	32.324	4.435	8.073	
BKUD09-158-37m-5-6	BK_SW, NE-end, 1030 masl	Darker, after Py	6, 8, 12	100.000	39.555	13.531	32.670	3.884	10.116	0.124

A. Electron Microprobe Data: Carbonates

BKUD09-158-37m-5-7	BK_SW, NE-end, 1030 masl	Lighter, after Py	6, 8, 12	99.983	43.493	12.325	30.971	2.823	10.035	0.061
BKUD09-158-37m-6-5	BK_SW, NE-end, 1030 masl	Lighter, after Sd	6, 8, 12	100.000	44.091	12.230	30.950	2.751	9.799	0.073
BKUD09-158-37m-6-6	BK_SW, NE-end, 1030 masl	Darker, after Sd	6, 8, 12	100.000	39.621	15.136	32.003	3.756	9.338	0.053
BKUD09-158-37m-6-8	BK_SW, NE-end, 1030 masl	With Gn, Ttr	6, 8, 12	99.994	41.329	15.777	32.292	3.582	6.850	0.037
BKUD09-158-37m-7-9	BK_SW, NE-end, 1030 masl	After Sd, with Gn, Ttr	6, 8, 12	100.000	40.654	14.002	31.876	3.719	9.603	0.063
BKUD09-160-56-5m-7-12	BK_SW, SW-end, 950 masl	With Py, Sp, Gn, Qz	9, 10	100.000	44.061	9.067	32.834	5.360	8.012	0.573
BKUD09-160-56-5m-7-13	BK_SW, SW-end, 950 masl	With Py, Sp, Gn, Qz	9, 10	100.000	43.920	8.980	32.762	5.487	8.131	0.672
BKUD09-160-56-5m-8-10	BK_SW, SW-end, 950 masl	With Py, Sp, Gn, Qz	9, 10	99.990	43.785	8.276	30.576	6.283	10.635	0.416
BKUD09-160-56-5m-8-11	BK_SW, SW-end, 950 masl	With Py, Sp, Gn, Qz	9, 10	100.000	44.139	9.575	31.110	5.237	9.113	0.709
BKUD09-163-14-8m-7-6	BK_SW, 980 masl	Inner, darker	9	100.000	43.893	10.150	33.852	3.536	8.478	0.092
BKUD09-163-14-8m-7-7	BK_SW, 980 masl	Outer, lighter	9	99.979	43.550	7.751	32.537	4.523	11.618	0.000
BKUD09-166-18.6m-5-4	BK_SW, 980 masl	Before Cal	12	99.981	45.325	8.381	31.791	4.127	10.152	0.092
BKUD09-171-32-8m-6-7	BK_99, 990 masl	Brx-cement	6, 8, 10, 12	99.968	45.898	9.782	27.490	7.036	9.498	0.167
BKUD09-171-32-8m-7-5	BK_99, 990 masl	After Sd, with Gn	6, 8, 10, 12	99.976	43.268	11.607	26.422	6.190	12.364	0.069
BKUD09-171-32-8m-10-2	BK_99, 990 masl	After Sd, with Gn	6, 8, 10, 12	99.981	43.868	11.728	30.690	3.976	9.442	0.238
	n =	53	AVERAGE	99.991	44.107	9.778	31.242	4.714	9.981	0.119
			MINIMUM	99.967	39.555	3.799	26.422	1.130	6.280	0.000
			MAXIMUM	100.000	49.490	15.777	34.766	13.579	14.483	0.709
Calcite: stage 12										

A. Electron Microprobe Data: Carbonates

K07-106-402-2m-1-4	BK_SW, NE-end, 985 masl	With Sd	6, 7, 12	100.000	42.929	0.253	51.858	3.036	1.901	
BKUD09-134-41.35-1-1	BK_SW, 965 masl	After Sp	4a, 9, 12	99.952	37.805	0.163	58.725	2.165	1.000	0.054
BKUD09-134-41.35-5-2	BK_SW, 965 masl	After Sp, Py	4a, 9, 12	99.992	43.605	0.125	51.790	2.679	1.691	0.081
BKUD09-134-41.35m-2-1-1	BK_SW, 965 masl	After Sp, Py	4a, 9, 12	99.971	39.878	0.129	57.414	1.626	0.843	0.026
BKUD09-134-41.35m-2-1-2	BK_SW, 965 masl	After Sp, Py	4a, 9, 12	100.000	44.138	0.479	52.169	1.075	1.609	0.038
BKUD09-134-41.35m-2-4-2	BK_SW, 965 masl	After Sp	4a, 9, 12	99.993	43.456	0.492	52.046	1.874	1.976	0.141
BKUD09-134-41.35m-2-6-2	BK_SW, 965 masl	After Sp, Py	4a, 9, 12	99.966	44.994	0.171	51.119	2.128	1.475	0.075
BKUD09-134-41.35m-2-7-2	BK_SW, 965 masl	After Sp, Py	4a, 9, 12	99.962	44.349	0.164	50.903	3.766	0.709	0.060
BKUD09-134-41.35m-2-9-2	BK_SW, 965 masl	After Sp, Py	4a, 9, 12	99.959	43.782	0.165	54.004	1.122	0.801	0.066
BKUD09-134-41.35m-2-10-2	BK_SW, 965 masl	After Sp, Py	4a, 9, 12	100.000	39.858	0.170	56.456	2.060	1.351	0.080
BKUD09-134-41.35m-2-10-4	BK_SW, 965 masl	After Sp, Py	4a, 9, 12	99.954	41.703	0.243	55.042	1.518	1.354	0.095
BKUD09-153-84m-1-3	BK_SW, SW-end, 940 masl	Brx-cement	12	99.983	43.679	0.312	52.006	1.940	1.936	0.096
BKUD09-153-84m-2-1	BK_SW, SW-end, 940 masl	Brx-cement	12	99.992	43.461	0.187	52.473	2.090	1.660	0.096
BKUD09-153-84m-2-2	BK_SW, SW-end, 940 masl	Brx-cement	12	99.971	44.113	0.300	52.752	2.159	0.558	0.064
BKUD09-153-84m-3-1	BK_SW, SW-end, 940 masl	Brx-cement	12	99.975	44.688	0.197	51.533	2.169	1.342	0.030
BKUD09-153-84m-6-4	BK_SW, SW-end, 940 masl	Brx-cement	12	99.969	45.260	0.285	49.032	4.376	0.889	0.112
BKUD09-153-84m-6-5	BK_SW, SW-end, 940 masl	Brx-cement	12	99.980	44.663	0.204	50.722	2.374	1.883	0.105
BKUD09-153-84m-7-1	BK_SW, SW-end, 940 masl	Brx-cement	12	99.980	44.868	0.159	51.299	2.191	1.363	0.076
BKUD09-153-84m-7-2	BK_SW, SW-end, 940 masl	Brx-cement	12	99.982	45.513	0.211	49.786	2.388	1.977	0.090
BKUD09-157-100-5m-2-3	BK_SW, SW-end,	After Sp, Ank	9/12 ?	99.970	41.328	0.466	55.970	1.312	0.779	0.115

A. Electron Microprobe Data: Carbonates

	930 masl									
BKUD09-158-37m-2-8	BK_SW, NE-end, 1030 masl	After Sd, Py, Ttr	8/12?	100.000	40.151	0.145	55.685	2.437	1.415	0.088
BKUD09-158-37m-3-4	BK_SW, NE-end, 1030 masl	After, Sd, Gn, Ttr	8/12?	99.992	43.833	0.334	53.279	1.419	1.046	0.077
BKUD09-158-37m-4-5	BK_SW, NE-end, 1030 masl	After Sd, with Py, Ttr	8/12?	100.000	40.713	0.389	56.139	1.831	0.821	0.039
BKUD09-158-37m-9-1	BK_SW, NE-end, 1030 masl	After Sd, with Py, Ttr	8/12?	99.979	39.457	0.429	57.655	1.448	0.867	0.069
BKUD09-166-18.6m-1-1	BK_SW, 975 masl	Brx-cement	12	99.980	43.965	0.090	49.912	4.398	1.476	0.118
BKUD09-166-18.6m-1-3	BK_SW, 975 masl	Brx-cement	12	99.948	45.165	0.081	48.976	4.304	1.352	0.061
BKUD09-166-18.6m-1-4	BK_SW, 975 masl	Brx-cement	12	99.978	44.365	0.097	49.890	4.211	1.297	0.107
BKUD09-166-18.6m-2-2	BK_SW, 975 masl	Brx-cement	12	99.981	44.584	0.412	51.792	2.241	0.842	0.100
BKUD09-166-18.6m-3-5	BK_SW, 975 masl	Brx-cement	12	99.985	44.317	0.119	50.089	3.948	1.438	0.068
BKUD09-166-18.6m-3-6	BK_SW, 975 masl	Brx-cement	12	99.958	43.687	0.083	50.588	4.112	1.329	0.159
BKUD09-166-18.6m-5-2	BK_SW, 975 masl	Brx-cement	12	99.956	44.752	0.122	49.562	3.868	1.562	0.091
BKUD09-166-18.6m-6-3	BK_SW, 975 masl	Brx-cement	12	99.988	45.186	0.385	50.786	1.437	2.089	0.085
	n =	32	AVERAGE	99.978	43.258	0.236	52.545	2.491	1.332	0.083
			MINIMUM	99.948	37.805	0.081	48.976	1.075	0.558	0.026
			MAXIMUM	100.000	45.513	0.492	58.725	4.398	2.089	0.159
Alice										
Siderite: stage 6										
Alice_1-1	Alice, surface	Outer, near Gn	6, 7, 8/9 ?	99.992	39.022	2.704	0.185	23.457	34.535	0.054
Alice_1-2	Alice, surface	Inner, darker	6, 7, 8/9 ?	99.989	38.565	6.762	0.861	24.588	29.130	0.029
Alice_1-3	Alice, surface	Inner, lighter	6, 7, 8/9 ?	99.990	37.844	2.024	0.327	27.296	32.391	0.048
Alice_2-1	Alice, surface	Lighter	6, 7, 8/9 ?	99.982	38.225	2.316	0.349	27.010	32.040	0.016
Alice_2-2	Alice, surface	Darker	6, 7, 8/9 ?	99.974	38.417	6.850	1.006	24.082	29.549	0.032
Alice_3-1	Alice, surface	Inner, lighter	6, 7, 8/9 ?	99.983	38.564	1.267	0.225	25.971	33.922	0.006

A. Electron Microprobe Data: Carbonates

Alice_3-2	Alice, surface	Outer, darker	6, 7, 8/9 ?	99.993	38.604	6.025	0.927	24.749	29.681	0.000
Alice_4-1	Alice, surface	Darker	6, 7, 8/9 ?	99.985	38.447	7.285	0.786	24.073	29.352	0.019
Alice_4-2	Alice, surface	Lighter	6, 7, 8/9 ?	99.988	38.025	1.371	0.147	24.516	35.893	0.014
Alice_5-1	Alice, surface	Outer	6, 7, 8/9 ?	99.989	38.468	1.291	0.139	24.092	35.965	0.023
Alice_5-2	Alice, surface	Inner	6, 7, 8/9 ?	99.981	38.495	4.290	0.467	24.590	32.100	0.033
Alice_6-1	Alice, surface	Lighter	6, 7, 8/9 ?	100.000	38.162	1.597	0.255	25.164	34.729	0.031
Alice_6-2	Alice, surface	Darker	6, 7, 8/9 ?	99.991	39.019	6.034	0.772	24.769	29.262	0.049
	n =	13	AVERAGE	99.987	38.450	3.832	0.496	24.950	32.196	0.027
			MINIMUM	99.974	37.844	1.267	0.139	23.457	29.130	0.000
			MAXIMUM	100.000	39.022	7.285	1.006	27.296	35.965	0.054
Wernecke										
Siderite: stage 6										
WRN-008-1-6	Wernecke, surface	Late, edge	6, 8	100.000	39.438	4.155	0.505	13.321	42.574	0.007
WRN-008-1-7	Wernecke, surface	With Fah	6, 8	100.000	39.116	5.213	0.551	8.758	46.327	0.035
WRN-008-2-3	Wernecke, surface	With Fah	6, 8	100.000	39.048	5.459	0.459	10.960	44.049	0.026
WRN-008-2-4	Wernecke, surface	Edge, with Ttr	6, 8	100.000	39.805	4.177	0.774	9.404	45.799	0.042
WRN-008-3-17	Wernecke, surface	With Ccp, Ttr	6, 8	100.000	39.184	4.764	1.282	9.341	45.345	0.084
WRN-008-3-18	Wernecke, surface	With Ccp, Ttr	6, 8	100.000	39.631	4.819	2.174	8.275	45.051	0.051
WRN-008-4-3	Wernecke, surface	With Py	6, 8	99.997	39.063	5.678	0.338	10.800	44.118	0.000
WRN-008-7-4	Wernecke, surface	With Ccp, Gn	6, 8	100.000	39.858	4.984	2.035	7.232	45.848	0.043
WRN-008-8-1	Wernecke, surface	Upper vein edge	6, 8	100.000	39.654	5.648	0.704	12.338	41.614	0.043
WRN-008-8-2	Wernecke, surface	Sequence	6, 8	100.000	39.522	5.552	0.841	12.633	41.406	0.047
WRN-008-8-3	Wernecke, surface	Sequence	6, 8	100.000	39.736	5.138	0.919	13.181	41.014	0.012
WRN-008-8-4	Wernecke, surface	Lower vein edge	6, 8	100.000	39.664	5.561	0.434	12.123	42.179	0.039
	n =	12	AVERAGE	100.000	39.477	5.096	0.918	10.697	43.777	0.036
			MINIMUM	99.997	39.048	4.155	0.338	7.232	41.014	0.000
			MAXIMUM	100.000	39.858	5.678	2.174	13.321	46.327	0.084

A. Electron Microprobe Data: Carbonates

Silver King										
Siderite: stage 6										
K06-2-167-2m_1-1	Silver King	With Qz, Gn	2/6 ?	99.999	38.019	3.575	1.661	22.063	34.572	0.023
K06-2-167-2m_2-1	Silver King	Earlier, with Gn, Py	2/6 ?	99.983	38.034	2.294	0.964	19.578	39.082	0.011
K06-2-167-2m_2-2	Silver King	Later, with Gn, Py	2/6 ?	99.994	38.789	2.097	1.083	21.504	36.491	0.017
K06-2-167-2m_3-1	Silver King	With Gn, Py	2/6 ?	99.988	38.509	2.822	1.277	21.974	35.358	0.000
K06-2-167-2m_3-2	Silver King	Within Py	2/6 ?	99.978	38.244	2.561	0.839	24.672	33.605	0.007
K06-2-167-2m_4-1	Silver King	Before Gn	2/6 ?	99.973	38.817	2.298	1.343	20.372	37.105	0.000
K06-2-167-2m_5-1	Silver King	With Ttr, Gn	2/6 ?	99.985	37.851	3.150	0.688	19.406	38.830	0.011
K06-2-167-2m_6-1	Silver King	With Plb	2/6 ?	100.000	38.531	3.155	0.660	20.690	36.880	0.017
K06-2-167-2m_7-1	Silver King	Outer, with Ttr, Gn	2/6 ?	100.000	38.307	3.267	0.785	22.171	35.362	0.061
K06-2-167-2m_7-2	Silver King	Inner, with Ttr, Gn	2/6 ?	99.968	38.430	2.746	0.790	22.617	35.295	0.052
K06-2-167-2m_8-1	Silver King	With Ttr, Gn	2/6 ?	99.973	37.993	2.831	0.538	18.527	40.020	0.045
K06-2-167-2m_9-1	Silver King	With Ttr, Gn	2/6 ?	99.971	38.331	2.468	0.658	18.224	40.243	0.027
	n =	12	AVERAGE	99.984	38.321	2.772	0.941	20.983	36.903	0.022
			MINIMUM	99.968	37.851	2.097	0.538	18.224	33.605	0.000
			MAXIMUM	100.000	38.817	3.575	1.661	24.672	40.243	0.061
Pool										
Siderite: stage 9										
K07-87-106-7m_1-1	Pool	With Ank, Ms, Sp	9, 12	99.990	38.263	4.903	3.643	17.649	35.475	0.024
K07-87-106-7m_1-7	Pool	Outer, with Cal	9, 12	99.973	37.809	4.973	2.519	16.402	38.206	0.029
K07-87-106-7m-1-13	Pool	With Ms, Sp	9	100.000	39.058	3.622	2.858	18.328	36.096	0.037

A. Electron Microprobe Data: Carbonates

K07-87-106-7m_2-1	Pool		inner, with Cal	9, 12	99.988	38.562	5.521	2.644	16.403	36.809	0.009
K07-87-106-7m-2-8	Pool		Before Ank, Cal	9	100.000	39.542	4.671	3.002	16.254	36.505	0.026
K07-87-106-7m_4-1	Pool		Outer, with Cal, Sp	9, 12	99.999	37.849	5.088	2.386	16.904	37.730	0.016
K07-87-106-7m_5-1	Pool		inne, with Cal	9, 12	99.997	37.892	5.957	2.818	16.533	36.752	0.013
K07-87-106-7m_6-4	Pool		With Ank, Ms, Sp	9, 12	99.992	38.698	5.086	2.598	16.175	37.407	0.025
		n =	8	AVERAGE	99.992	38.459	4.978	2.808	16.831	36.872	0.022
				MINIMUM	99.973	37.809	3.622	2.386	16.175	35.475	0.009
				MAXIMUM	100.000	39.542	5.957	3.643	18.328	38.206	0.037
Ankerite: stage 9											
K07-87-106-7m_1-3	Pool		With Ms, before Cal	9	99.957	43.592	13.968	32.195	2.880	7.187	0.109
K07-87-106-7m_1-4	Pool		Lighter	9	100.000	43.876	9.641	30.408	4.420	11.574	0.023
K07-87-106-7m_1-5	Pool		Darker	9	99.963	43.670	12.766	31.790	5.449	6.227	0.054
K07-87-106-7m_2-4	Pool		Before Cal	9	99.982	44.394	15.693	32.113	3.392	4.351	0.024
K07-87-106-7m-2-6	Pool		With Sp	9, 12	100.000	44.945	12.345	34.968	3.267	4.421	
K07-87-106-7m_4-2	Pool		Darker	9	100.000	44.124	12.593	31.509	2.810	8.864	0.029
K07-87-106-7m_4-3	Pool		Darker	9	99.942	43.675	13.804	31.566	4.312	6.535	0.032
K07-87-106-7m_4-4	Pool		Lighter	9	99.978	43.198	9.486	29.923	4.966	12.332	0.027
K07-87-106-7m_5-3	Pool		Inner, with Ms	9	99.985	43.369	12.576	31.769	3.900	8.264	0.073
K07-87-106-7m_5-4	Pool		Middle, lighter	9	99.992	43.550	9.463	29.651	4.985	12.238	0.058
K07-87-106-7m_5-5	Pool		Outer, darker	9	99.984	43.387	13.447	31.976	4.632	6.446	0.055
K07-87-106-7m_6-3	Pool		With Sp	9	99.979	43.592	10.527	28.874	4.375	12.512	0.028
K07-87-106-7m_6-5	Pool		With Sp	9	99.994	43.252	3.810	26.346	12.430	14.096	0.032
K07-87-106-7m_7-1	Pool		Lighter	9	100.000	44.003	5.233	29.364	11.203	10.140	0.017
K07-87-106-7m_7-2	Pool		Darker	9	99.989	43.802	13.454	31.582	2.511	8.502	0.086
		n =	15	AVERAGE	99.983	43.762	11.254	30.936	5.035	8.912	0.046

A. Electron Microprobe Data: Carbonates

			MINIMUM	99.942	43.198	3.810	26.346	2.511	4.351	0.017
			MAXIMUM	100.000	44.945	15.693	34.968	12.430	14.096	0.109
Calcite: stage 12										
K07-87-106-7m_1-8	Pool	After Ank	12	99.988	43.939	0.301	52.581	1.494	1.620	0.024
K07-87-106-7m_2-2	Pool	After Ank	12	99.976	43.589	0.141	52.122	3.145	0.944	0.017
K07-87-106-7m_2-3	Pool	Later	12	99.966	43.802	0.195	53.130	1.256	1.541	0.026
K07-87-106-7m-2-5	Pool	With Sp	9, 12	100.000	42.083	0.283	54.354	2.253	1.024	
K07-87-106-7m-2-7	Pool	Transition	9, 12	100.000	42.456	0.273	53.771	2.499	0.962	
K07-87-106-7m_3-1	Pool	Later	12	99.990	43.779	0.308	53.055	1.320	1.503	0.001
K07-87-106-7m_5-6	Pool	After Ank	12	99.982	44.193	0.111	51.782	2.460	1.387	0.034
	n =	7	AVERAGE	99.986	43.406	0.230	52.971	2.061	1.283	0.020
			MINIMUM	99.966	42.083	0.111	51.782	1.256	0.944	0.001
			MAXIMUM	100.000	44.193	0.308	54.354	3.145	1.620	0.034
Porcupine Siderite: stage 11 (?)										
POR-056-7-6	Porcupine, surface	Inner, darker	11	100.000	39.388	3.415	0.517	19.287	37.329	0.065
POR-056-7-7	Porcupine, surface	Outer, lighter	11	100.000	39.211	1.844	0.202	17.238	41.475	0.031
POR-056-8-2	Porcupine, surface	After Qz	11	100.000	39.236	3.363	0.458	17.123	39.751	0.071
POR-056-8-3	Porcupine, surface	With Qz	11	100.000	39.415	3.440	0.965	18.196	37.954	0.030
POR-056-8-4	Porcupine, surface	Begin coarse, lower	11	100.000	39.585	3.916	1.835	16.704	37.934	0.026
POR-056-8-5	Porcupine, surface	Sequence	11	100.000	39.935	4.277	1.349	15.353	39.050	0.037
POR-056-8-6	Porcupine, surface	Sequence	11	100.000	39.849	3.526	1.108	16.727	38.789	0.002
	n =	7	AVERAGE	100.000	39.517	3.397	0.919	17.233	38.897	0.037
			MINIMUM	100.000	39.211	1.844	0.202	15.353	37.329	0.002

A. Electron Microprobe Data: Carbonates

			MAXIMUM	100.000	39.935	4.277	1.835	19.287	41.475	0.071
Keno 700										
Siderite: stage 6 (?)										
K09-200-86.3m-1-1	Keno 700	With Qz	2/6?, 12	99.973	38.151	1.575	0.179	11.786	48.195	0.061
K09-200-86.3m-1-2	Keno 700	With Qz, Py	2/6?, 12	99.951	38.432	1.474	0.194	11.916	47.805	0.078
K09-200-86.3m-1-3	Keno 700	With Qz, Py	2/6?, 12	99.999	38.283	1.712	0.217	12.340	47.341	0.070
K09-200-86.3m-1-5	Keno 700	With Qz, Py	2/6?, 12	99.972	39.684	4.980	1.953	14.876	38.395	0.059
K09-200-86.3m-1-6	Keno 700	With Qz, Py	2/6?, 12	99.975	39.126	3.352	0.749	16.959	39.630	0.128
K09-200-86.3m-2-2	Keno 700	With Cal, Ank	2/6?, 12	99.956	39.022	4.010	1.188	19.331	36.314	0.059
K09-200-86.3m-3-1	Keno 700	With Cal, Ank	2/6?, 12	100.000	39.253	3.781	0.534	17.233	39.065	0.072
K09-200-86.3m-3-4	Keno 700	Inner, with Cal, Ank	2/6?, 12	99.984	37.717	0.761	0.145	10.782	50.459	0.068
K09-200-86.3m-3-5	Keno 700	Outer, with Cal, Ank	2/6?, 12	100.000	39.872	6.101	1.682	11.621	40.619	0.053
K09-200-86.3m-4-1	Keno 700	Inner, with Cal	2/6?, 12	99.989	39.112	2.872	0.339	16.569	41.074	0.016
K09-200-86.3m-4-2	Keno 700	Middle, with Cal	2/6?, 12	99.971	38.108	0.770	0.114	10.383	50.502	0.079
K09-200-86.3m-4-3	Keno 700	Rim, with Cal	2/6?, 12	100.000	39.386	6.173	1.275	8.522	44.500	0.105
K09-200-86.3m-5-1	Keno 700	With Cal, Ank	2/6?, 12	100.000	38.002	1.096	0.144	13.963	46.661	0.095
K09-200-86.3m-5-2	Keno 700	With Cal, Ank	2/6?, 12	99.957	39.876	6.158	1.331	10.272	42.227	0.057
K09-200-86.3m-5-3	Keno 700	With Cal, Ank	2/6?, 12	99.957	37.710	1.278	0.139	10.543	50.183	0.083
K09-200-86.3m-6-1	Keno 700	Inner, with Cal	2/6?, 12	99.985	50.220	1.449	0.278	13.831	34.088	0.119
K09-200-86.3m-6-2	Keno 700	Outer, with Cal	2/6?, 12	99.990	39.280	3.351	0.577	16.291	40.349	0.110
K09-200-86.3m-6-4	Keno 700	With Cal	2/6?, 12	99.995	38.852	4.172	0.595	16.329	39.946	0.093
K09-200-86.3m-7-1	Keno 700	Inner, with Cal, Ank	2/6?, 12	99.995	39.748	5.801	1.901	9.969	42.429	0.094
K09-200-86.3m-7-2	Keno 700	Outer, with Cal, Ank	2/6?, 12	99.971	38.474	1.249	0.374	19.057	40.664	0.104
K09-200-86.3m-7-4	Keno 700	Outer, with Cal,	2/6?, 12	99.996	38.062	1.940	0.164	17.864	41.798	0.131

A. Electron Microprobe Data: Carbonates

K09-200-86.3m-7-5	Keno 700	Ank Inner, with Cal, Ank	2/6?, 12	99.991	38.323	1.802	0.380	18.557	40.811	0.108
K09-201-238m-2-7	Keno 700	Sequence	2/6 ?	99.975	39.028	1.801	0.413	19.475	38.949	0.058
K09-201-238m-2-8	Keno 700	Sequence	2/6 ?	100.000	38.609	1.542	0.274	20.226	39.199	0.036
K09-201-238m-2-9	Keno 700	Sequence	2/6 ?	100.000	38.442	2.021	0.271	19.919	39.252	0.062
K09-201-238m-2-10	Keno 700	Sequence	2/6 ?	99.959	38.515	1.958	0.912	20.103	38.407	0.036
K09-201-238m-2-11	Keno 700	Sequence	2/6 ?	100.000	38.682	2.112	0.669	20.746	37.699	0.038
K09-201-238m-3-12	Keno 700	With Py, Apy	2/6 ?	99.993	38.532	1.803	0.558	22.402	36.673	0.003
K09-201-238m-3-13	Keno 700	With Py, Apy	2/6 ?	99.993	38.238	2.596	0.298	16.081	42.685	0.056
K09-201-238m-4-12	Keno 700	With Py, Apy	2/6 ?	99.960	38.462	1.376	0.326	20.213	39.526	0.023
K09-201-238m-5-10	Keno 700	With Py, Apy, Sp	2/6 ?	99.977	38.151	1.441	0.227	20.684	39.427	0.048
K09-201-238m-5-11	Keno 700	With Py, Apy, Sp	2/6 ?	99.999	38.561	1.779	0.448	20.911	38.229	0.038
K09-201-238m-5-12	Keno 700	With Py, Apy, Sp	2/6 ?	99.956	39.146	1.550	0.282	20.415	38.495	0.025
K09-201-238m-6-8	Keno 700	With Py, Apy, Sp	2/6 ?	99.973	38.366	2.998	0.631	18.578	39.303	0.054
K09-201-238m-6-9	Keno 700	With Py, Apy, Sp	2/6 ?	99.984	37.817	1.400	0.400	19.514	40.797	0.020
K09-201-238m-7-11	Keno 700	With Py, Apy, Sp	2/6 ?	99.980	38.471	2.003	0.203	17.372	41.846	0.041
K09-201-238m-7-12	Keno 700	With Py, Apy, Sp	2/6 ?	99.953	38.010	1.490	0.453	22.458	37.491	0.045
K09-201-238m-7-13	Keno 700	With Py, Apy, Sp	2/6 ?	100.000	39.576	2.401	0.481	18.250	39.215	0.045
K09-201-238m-7-14	Keno 700	With Py, Apy, Sp	2/6 ?	100.000	38.444	1.473	0.340	20.872	38.783	0.049
K09-201-238m-7-15	Keno 700	With Py, Apy, Sp	2/6 ?	100.000	38.870	1.924	0.440	20.835	37.832	0.044
K09-201-238m-7-16	Keno 700	With Py, Apy, Sp	2/6 ?	99.976	38.826	2.897	0.608	20.826	36.699	0.067
K09-201-238m-7-17	Keno 700	With Py, Apy, Sp	2/6 ?	99.989	38.278	1.484	0.449	21.097	38.631	0.046
K09-201-238m-8-14	Keno 700	With Sp, Gn, Ttr, Pyr	2/6 ?	100.000	38.277	1.709	0.247	21.217	38.471	0.024
K09-201-238m-8-15	Keno 700	With Sp, Gn, Ttr, Pyr	2/6 ?	99.965	38.639	2.341	0.368	20.120	38.423	0.042
K09-201-238m-9-6	Keno 700	With Py, Apy, Gn	2/6 ?	99.941	38.278	1.955	0.422	20.829	38.432	0.000

A. Electron Microprobe Data: Carbonates

K09-201-238m-9-7	Keno 700		With Py, Apy, Gn	2/6 ?	99.979	38.817	4.106	0.566	16.359	40.043	0.044
		n =	46	AVERAGE	99.982	38.907	2.479	0.538	17.141	40.816	0.060
				MINIMUM	99.941	37.710	0.761	0.114	8.522	34.088	0.000
				MAXIMUM	100.000	50.220	6.173	1.953	22.458	50.502	0.131
Ankerite: stage 11 to 12 (?)											
K09-200-86.3m-2-3	Keno 700		Early, before Cal	<11	99.991	44.563	8.363	30.389	4.157	11.530	0.173
K09-200-86.3m-3-3	Keno 700		Early, before Cal	<11	99.964	46.362	10.866	31.807	1.806	8.892	0.100
K09-200-86.3m-3-7	Keno 700		With Qz	10 ?	99.980	46.801	9.706	32.148	2.374	8.735	0.182
K09-200-86.3m-5-5	Keno 700		Early, before Cal	<11	99.957	46.256	10.870	32.223	1.699	8.694	0.142
K09-200-86.3m-8-1	Keno 700		Early, before Cal	<11	99.981	45.842	10.607	32.238	1.347	9.775	0.115
		n =	5	AVERAGE	99.975	45.964	10.082	31.761	2.277	9.525	0.142
				MINIMUM	99.957	44.563	8.363	30.389	1.347	8.694	0.100
				MAXIMUM	99.991	46.801	10.870	32.238	4.157	11.530	0.182
Calcite: stage 12											
K09-200-86.3m-2-1	Keno 700		Brx-cement	12	99.943	44.485	0.180	54.064	0.088	1.033	0.083
K09-200-86.3m-3-2	Keno 700		Brx-cement	12	99.980	45.477	0.651	51.234	0.451	2.085	0.075
K09-200-86.3m-3-6	Keno 700		Brx-cement	12	99.969	44.075	0.204	54.337	0.090	1.173	0.072
K09-200-86.3m-4-4	Keno 700		Brx-cement	12	99.971	44.521	0.301	54.073	0.166	0.812	0.081
K09-200-86.3m-5-4	Keno 700		Brx-cement	12	99.997	44.487	0.170	54.172	0.299	0.686	0.149
K09-200-86.3m-8-2	Keno 700		Brx-cement	12	100.000	45.008	0.258	53.176	0.088	1.294	0.115
		n =	6	AVERAGE	99.977	44.675	0.294	53.509	0.197	1.180	0.096
				MINIMUM	99.943	44.075	0.170	51.234	0.088	0.686	0.072
				MAXIMUM	100.000	45.477	0.651	54.337	0.451	2.085	0.149

B. Electron Microprobe Data: Sulfides, Oxides, and Sulfates

Sample	Location	Stages	Total	S	Fe	Cu	Zn	As	Ag	Cd	Sn	Sb	Pb	Bi	Ni	Co	Mo
Arsenopyrite: various stages																	
BRM_044_1-3	Bermingham, surface	6, 7, 8	99.373	23.492	35.879	0.000	0.007	39.815	0.022	0.032	0.000	0.050	0.000	0.000	0.004	0.021	0.000
BRM_044_4-3	Bermingham, surface	6, 7, 8, 9	99.204	22.672	35.774	0.000	0.000	40.835	0.000	0.000	0.000	0.054	0.000	0.000	0.000	0.024	0.000
BRM_044_4-5	Bermingham, surface	6, 7, 8, 10	98.927	22.413	35.623	0.000	0.000	41.002	0.000	0.000	0.000	0.015	0.000	0.000	0.000	0.018	0.000
BRM_044_5-3	Bermingham, surface	6, 7, 8, 11	99.067	22.505	35.840	0.003	0.013	40.733	0.009	0.000	0.000	0.058	0.000	0.000	0.001	0.024	0.000
BRM_044_6-4	Bermingham, surface	7, 8	99.454	22.042	35.132	0.007	0.261	42.075	0.000	0.038	0.000	0.063	0.000	0.000	0.009	0.026	0.000
BRM-044-6-10	Bermingham, surface	7, 8	99.477	22.561	35.866	0.018	0.232	41.100	0.000	0.094	0.000	0.059	0.177	0.000		0.000	0.000
BRM_044_7-5	Bermingham, surface	6, 7, later?	99.119	21.067	35.000	0.006	0.165	43.026	0.026	0.014	0.000	0.056	0.000	0.000	0.008	0.027	0.000
BRM_044_8-3	Bermingham, surface	6, 7, later?	99.115	21.148	35.386	0.000	0.000	42.519	0.000	0.108	0.000	0.014	0.000	0.000	0.011	0.028	0.000
EAG_047_1-2	Eagle, surface	4a	99.218	21.324	35.067	0.000	0.082	42.567	0.019	0.028	0.000	0.114	0.000	0.000	0.065	0.104	0.000
EAG_047_3-5	Eagle, surface	4a	99.335	21.109	35.021	0.014	0.000	42.744	0.000	0.024	0.009	0.123	0.000	0.000	0.128	0.094	0.000
EAG_047_5-4	Eagle, surface	4a	98.805	21.403	35.291	0.000	0.006	42.094	0.000	0.000	0.000	0.078	0.000	0.000	0.025	0.109	0.000
EAG_047_7-3	Eagle, surface	4a	99.408	21.204	35.348	0.003	0.017	42.754	0.019	0.035	0.000	0.218	0.000	0.000	0.009	0.023	0.000
POR_056_6-1	Porcupine, surface	7, 8, 10	98.854	21.537	35.490	0.008	0.025	41.819	0.015	0.002	0.008	0.014	0.000	0.000	0.002	0.013	0.000
K07-76-115-3m-3-3	BK_E, 965 masl	1, 5, 8	99.978	21.012	35.136	0.000	0.000	43.235	0.040	0.040	0.000	0.054	0.000	0.000	0.040	0.326	0.000
K07-76-125m-3-7	BK_E, 965 masl	6	100.775	22.693	35.615	0.000	0.000	42.112	0.009	0.000	0.000	0.445	0.000	0.000	0.001	0.058	0.000
K07-76-125m-4-6	BK_E, 965 masl	6, 7, 8?	98.557	23.329	35.408	0.000	0.000	39.346	0.000	0.019	0.000	0.492	0.000	0.000	0.001	0.048	0.000
K07-76-125m-8-3	BK_E, 965 masl	1, 4b?	99.369	20.802	35.137	0.000	0.024	43.246	0.010	0.060	0.003	0.014	0.000	0.000	0.000	0.357	0.000
K07-76-125m-8-4	BK_E, 965 masl	1, 4b?	100.836	20.811	34.614	0.000	0.014	44.667	0.013	0.016	0.000	0.040	0.000	0.000	0.000	0.585	0.000
K07-106-402-2m_9-3	BK_SW, NE-end, 985 masl	2/6?, 7	99.540	20.699	35.277	0.005	0.083	43.726	0.000	0.046	0.000	0.027	0.000	0.000	0.000	0.034	0.000
K09-201-238m-1-2	Keno 700	1, 6, 7, 8	100.745	23.229	35.622	0.000	0.015	41.772	0.017	0.035	0.000	0.046	0.000	0.000	0.006	0.000	0.111
K09-201-238m-2-3	Keno 700	1, 6, 7, 8	101.218	22.965	35.402	0.005	0.004	43.125	0.014	0.007	0.000	0.017	0.000	0.000	0.000	0.000	0.000
K09-201-238m-3-2	Keno 700	1, 6,	101.411	22.357	35.651	0.000	0.000	43.407	0.008	0.023	0.000	0.095	0.000	0.000	0.000	0.000	0.089

B. Electron Microprobe Data: Sulfides, Oxides, and Sulfates

		7, 8															
K09-201-238m-3-5	Keno 700	1, 6, 7, 8	101.394	23.564	36.124	0.001	0.007	41.791	0.015	0.000	0.000	0.057	0.000	0.000	0.006	0.000	0.042
K09-201-238m-3-8	Keno 700	1, 6, 7, 8	101.161	23.902	35.851	0.007	0.000	41.430	0.025	0.019	0.000	0.021	0.000	0.050	0.023	0.000	0.000
K09-201-238m-4-1	Keno 700	1, 6, 7, 8	101.715	22.158	35.592	0.000	0.000	43.995	0.011	0.000	0.007	0.086	0.000	0.000	0.002	0.000	0.013
K09-201-238m-4-10	Keno 700	1, 6, 7, 8	101.262	22.952	35.664	0.000	0.015	42.511	0.019	0.045	0.000	0.135	0.000	0.000	0.000	0.000	0.000
K09-201-238m-5-1	Keno 700	1, 6, 7, 8	101.332	23.537	35.861	0.000	0.004	42.110	0.025	0.026	0.000	0.027	0.000	0.000	0.010	0.000	0.005
K09-201-238m-5-8	Keno 700	1, 6, 7, 8	101.452	23.616	35.786	0.010	0.000	42.206	0.000	0.000	0.010	0.031	0.000	0.000	0.007	0.000	0.017
K09-201-238m-6-1	Keno 700	1, 6, 7, 8	100.962	22.148	35.553	0.015	0.014	43.554	0.023	0.000	0.000	0.009	0.000	0.000	0.000	0.000	0.021
K09-201-238m-7-1	Keno 700	1, 6, 7, 8	101.092	22.609	35.539	0.015	0.000	43.028	0.017	0.000	0.000	0.033	0.000	0.000	0.013	0.000	0.026
K09-201-238m-7-5	Keno 700	1, 6, 7, 8	100.157	22.313	35.469	0.000	0.000	42.621	0.018	0.002	0.000	0.000	0.000	0.000	0.008	0.000	0.036
K09-201-238m-9-3	Keno 700	1, 6, 7, 8	101.120	23.192	35.897	0.000	0.004	42.060	0.023	0.031	0.000	0.000	0.000	0.000	0.000	0.000	0.000
BKUD09-134-39-5m-2-4	BK_SW, NE-end, 1015 masl	4a	101.035	21.936	36.101	0.000	0.765	42.293	0.020	0.039	0.000	0.103	0.000	0.000	0.000	0.000	0.000
BKUD09-134-39-5m-4-6	BK_SW, NE-end, 1015 masl	4a	100.104	21.511	35.238	0.000	0.103	43.301	0.027	0.000	0.000	0.000	0.000	0.000	0.000	0.172	0.000
BKUD09-134-39-5m-6-7	BK_SW, NE-end, 1015 masl	4a	99.140	22.073	35.742	0.005	0.027	41.569	0.017	0.000	0.000	0.059	0.000	0.000	0.000	0.000	0.000
BKUD09-134-39-5m-7-4	BK_SW, NE-end, 1015 masl	4a	99.190	20.542	35.179	0.000	0.000	43.739	0.013	0.000	0.000	0.012	0.000	0.000	0.000	0.000	0.000
BKUD09-134-39-5m-10-4	BK_SW, NE-end, 1015 masl	4a	99.870	21.215	35.394	0.000	0.076	43.483	0.000	0.000	0.000	0.000	0.000	0.000	0.000	0.007	0.000
BKUD09-134-39-5m-10-9	BK_SW, NE-end, 1015 masl	4a	100.574	20.895	34.976	0.010	1.090	43.946	0.000	0.000	0.000	0.000	0.000	0.000	0.000	0.000	0.000
BKUD09-134-41-35m-2-1-5	BK_SW, NE-end, 1015 masl	2, 4a	100.135	22.410	35.839	0.000	0.000	41.784	0.027	0.044	0.000	0.126	0.000	0.000	0.000	0.000	0.000
BKUD09-134-41-35m-2-7-4	BK_SW, NE-end, 1015 masl	2, 4a	100.804	22.919	36.135	0.026	0.626	41.148	0.008	0.000	0.000	0.317	0.000	0.000	0.000	0.000	0.000
BKUD09-134-41-35m-2-9-6	BK_SW, NE-end, 1015 masl	2, 4a	100.453	22.562	36.378	0.000	0.009	41.718	0.014	0.000	0.000	0.059	0.000	0.000	0.000	0.000	0.000
BKUD09-134-41-35m-2-10-5	BK_SW, NE-end, 1015 masl	2, 4a	99.899	21.893	35.615	0.000	0.000	41.711	0.024	0.026	0.000	0.646	0.000	0.033	0.000	0.002	0.000
BKUD09-134-45m-2-1-2	BK_SW, NE-end, 1015 masl	2, 4a	100.115	21.632	35.682	0.009	0.000	42.835	0.000	0.000	0.000	0.114	0.000	0.000	0.000	0.000	0.000
BKUD09-134-45m-2-3-10	BK_SW, NE-end, 1015 masl	2, 4a	99.771	21.029	34.583	0.000	0.000	43.503	0.002	0.023	0.000	0.112	0.000	0.000	0.000	0.586	0.000

B. Electron Microprobe Data: Sulfides, Oxides, and Sulfates

BKUD09-134-45m-2-5-5	BK_SW, NE-end, 1015 masl	2, 3, 4a	100.106	21.447	35.633	0.014	0.008	43.110	0.015	0.054	0.000	0.059	0.000	0.000	0.000	0.000	0.000
BKUD09-143-51-2m-2-3	BK_SW, NE-end, 1000 masl	4a	97.672	20.540	34.866	0.000	0.000	42.187	0.012	0.026	0.000	0.183	0.000	0.000	0.000	0.042	0.000
BKUD09-143-51-2m-2-4	BK_SW, NE-end, 1000 masl	4a	98.528	20.946	35.137	0.012	0.000	42.260	0.000	0.009	0.000	0.025	0.000	0.000	0.019	0.011	0.000
BKUD09-143-52-8m_4-2	BK_SW, NE-end, 1000 masl	8, 9	99.214	18.648	33.546	0.000	0.000	43.584	0.002	0.036	0.030	2.729	0.000	0.000	0.037	0.556	0.000
BKUD09-143-52-8m_4-3	BK_SW, NE-end, 1000 masl	8, 9	99.255	22.714	35.578	0.000	0.000	40.487	0.002	0.019	0.000	0.571	0.000	0.000	0.018	0.030	0.000
BKUD09-144-36-6m-1-1	BK_SW, SW-end, 980 masl	2	101.392	22.470	35.393	0.000	0.005	43.397	0.021	0.087	0.000	0.048	0.000	0.000	0.057	0.017	0.000
BKUD09-144-36-6m-2-2	BK_SW, SW-end, 980 masl	2	100.820	21.817	35.388	0.005	0.000	43.781	0.022	0.038	0.000	0.032	0.000	0.000	0.005	0.000	0.044
BKUD09-144-36-6m-4-4	BK_SW, SW-end, 980 masl	3	100.973	23.111	35.336	0.000	0.430	42.143	0.004	0.049	0.000	0.186	0.000	0.000	0.047	0.000	0.036
BKUD09-144-36-6m-4-13	BK_SW, SW-end, 980 masl	3	101.050	22.401	35.505	0.000	0.361	42.954	0.018	0.000	0.008	0.000	0.000	0.000	0.096	0.078	0.000
BKUD09-144-36-6m-6-3	BK_SW, SW-end, 980 masl	3	100.766	21.809	35.049	0.192	0.048	43.695	0.023	0.012	0.000	0.052	0.000	0.000	0.149	0.108	0.000
BKUD09-144-36-6m-6-4	BK_SW, SW-end, 980 masl	3	101.151	21.635	34.438	0.007	0.010	44.011	0.014	0.068	0.000	0.056	0.000	0.010	0.318	0.497	0.020
BKUD09-144-36-6m-7-3	BK_SW, SW-end, 980 masl	2	101.012	21.415	35.090	0.011	0.002	44.121	0.023	0.056	0.017	0.049	0.000	0.041	0.029	0.051	0.109
BKUD09-144-36-6m-7-4	BK_SW, SW-end, 980 masl	2	100.700	21.567	35.405	0.004	0.000	43.880	0.020	0.000	0.000	0.000	0.000	0.000	0.005	0.000	0.000
BKUD09-146-46-5m-1-2	BK_SW, SW-end, 970 masl	4a	99.245	19.780	34.738	0.000	0.000	44.807	0.000	0.000	0.000	0.127	0.000	0.000	0.000	0.039	0.000
BKUD09-146-46-5m-2-1	BK_SW, SW-end, 970 masl	4a	97.944	19.878	34.785	0.000	0.000	43.227	0.000	0.070	0.011	0.077	0.000	0.000	0.000	0.032	0.000
BKUD09-146-46-5m-3-2	BK_SW, SW-end, 970 masl	4a	97.820	19.762	34.653	0.014	0.002	43.328	0.002	0.072	0.000	0.093	0.000	0.000	0.007	0.014	0.000
BKUD09-146-46-5m-3-8	BK_SW, SW-end, 970 masl	4a	97.375	20.420	34.699	0.019	0.010	42.022	0.008	0.045	0.000	0.063	0.000	0.000	0.000	0.037	0.000
BKUD09-146-46-5m-4-3	BK_SW, SW-end, 970 masl	4a	100.175	19.739	34.642	0.019	0.007	45.699	0.000	0.000	0.000	0.119	0.000	0.000	0.000	0.112	0.000
BKUD09-146-46-5m-6-2	BK_SW, SW-end, 970 masl	4a	99.559	20.022	34.694	0.000	0.006	44.875	0.022	0.044	0.000	0.053	0.000	0.000	0.007	0.045	0.000
BKUD09-146-46-5m-7-2	BK_SW, SW-end, 970 masl	4a	99.311	21.188	35.114	0.014	0.000	42.855	0.023	0.019	0.000	0.000	0.000	0.000	0.161	0.020	0.000
BKUD09-146-46-5m-8-2	BK_SW, SW-end, 970 masl	4a	98.396	21.697	35.455	0.000	0.000	41.056	0.000	0.112	0.000	0.111	0.000	0.000	0.000	0.030	0.000
BKUD09-146-46-5m-8-5	BK_SW, SW-end, 970 masl	4a	98.939	19.946	34.343	0.000	0.000	44.520	0.015	0.066	0.000	0.038	0.000	0.000	0.005	0.049	0.000
BKUD09-148-29-5m_7-2	BK_99, 1025 masl	2	99.091	22.914	35.515	0.000	0.000	40.098	0.013	0.000	0.000	0.448	0.000	0.000	0.009	0.102	0.000

B. Electron Microprobe Data: Sulfides, Oxides, and Sulfates

BKUD09-148-29-5m_7-3	BK_99, 1025 masl	2	99.043	23.534	35.750	0.023	0.000	39.152	0.000	0.036	0.005	0.525	0.000	0.000	0.014	0.042	0.000
BKUD09-153-87-5m-3-3	BK_SW, SW-end, 940 masl	3	100.392	24.271	34.969	0.022	0.423	40.046	0.011	0.000	0.000	0.914	0.000	0.000	0.000	0.000	0.026
BKUD09-157-93-8m_2-2	BK_SW, SW-end, 930 masl	2, 3	99.380	20.670	34.675	0.009	0.016	43.609	0.011	0.000	0.000	0.271	0.000	0.000	0.030	0.187	0.000
BKUD09-157-93-8m_7-2	BK_SW, SW-end, 930 masl	2, 3	99.420	21.535	35.155	0.000	0.000	42.264	0.017	0.000	0.000	0.042	0.000	0.000	0.617	0.054	0.000
BKUD09-158-36m_8-1	BK_SW, NE-end, 1030 masl	2/6?, 8	99.184	22.895	35.500	0.007	0.022	40.078	0.000	0.024	0.000	0.778	0.000	0.000	0.036	0.149	0.000
BKUD09-158-37m-1-4	BK_SW, NE-end, 1030 masl	2/6?, 8	99.368	20.697	35.111	0.000	0.000	43.701	0.028	0.000	0.000	0.061	0.000	0.000	0.010	0.032	0.000
BKUD09-158-37m-2-4	BK_SW, NE-end, 1030 masl	2/6?, 8	99.310	20.844	34.929	0.000	0.014	43.370	0.000	0.000	0.000	0.221	0.000	0.000	0.064	0.107	0.000
BKUD09-163-31-8m-1-1	BK_SW, 980 masl	2	101.209	23.927	35.928	0.010	0.003	41.384	0.011	0.000	0.000	0.036	0.000	0.000	0.010	0.000	0.000
BKUD09-163-31-8m-2-1	BK_SW, 980 masl	2	100.907	22.160	35.201	0.000	0.008	43.601	0.011	0.002	0.000	0.058	0.000	0.000	0.090	0.013	0.000
BKUD09-163-31-8m-3-1	BK_SW, 980 masl	2	100.762	23.510	35.530	0.003	0.010	42.036	0.038	0.000	0.000	0.000	0.000	0.000	0.000	0.000	0.000
BKUD09-163-31-8m-3-2	BK_SW, 980 masl	2	100.968	23.572	35.626	0.013	0.007	41.715	0.021	0.000	0.000	0.096	0.000	0.000	0.014	0.000	0.004
BKUD09-171-32-8m-2-4	BK_99, 990 masl	2/6?, 8	98.024	20.379	35.241	0.008	0.000	42.566	0.000	0.056	0.000	0.119	0.000	0.000	0.000	0.014	0.000
n = 79	AVERAGE		99.911	21.859	35.334	0.007	0.064	42.527	0.012	0.024	0.001	0.156	0.002	0.002	0.029	0.065	0.008
	MINIMUM		97.375	18.648	33.546	0.000	0.000	39.152	0.000	0.000	0.000	0.000	0.000	0.000	0.000	0.000	0.000
	MAXIMUM		101.715	24.271	36.378	0.192	1.090	45.699	0.040	0.112	0.030	2.729	0.177	0.050	0.617	0.586	0.111
Pyrite: various stages																	
Alice_3-7	Alice, surface	6, 7, 8	99.773	51.089	45.832	0.000	0.034	3.209	0.000	0.034	0.000	0.000	0.000	0.000	0.010	0.025	0.000
Alice_5-6	Alice, surface	6, 7, 9	98.918	50.261	45.289	0.000	0.031	3.755	0.000	0.000	0.000	0.000	0.000	0.000	0.005	0.022	0.000
Alice_8-6	Alice, surface	6, 7, 10	99.400	52.240	46.013	0.016	0.022	1.175	0.014	0.074	0.000	0.000	0.000	0.000	0.014	0.039	0.000
TryAgain_1-3	Try Again, surface	8?	99.343	52.785	46.079	0.001	0.016	0.457	0.016	0.013	0.000	0.000	0.000	0.000	0.052	0.025	0.000
TryAgain-1-5	Try Again, surface	8?	100.826	53.414	46.841	0.000	0.030	0.540	0.000	0.057	0.000	0.019	0.277	0.000		0.000	0.000
TryAgain_2-4	Try Again, surface	8?	99.329	53.217	46.353	0.009	0.019	0.030	0.010	0.000	0.023	0.000	0.000	0.000	0.002	0.023	0.000
TryAgain-2-7	Try Again, surface	8?	100.704	53.661	46.923	0.009	0.008	0.099	0.007	0.000	0.000	0.000	0.212	0.000		0.005	0.078
TryAgain-2-8	Try Again, surface	8?	101.064	53.623	47.273	0.001	0.000	0.376	0.000	0.000	0.003	0.000	0.110	0.000		0.003	0.000
TryAgain_3-4	Try Again, surface	8?	99.305	53.141	46.487	0.010	0.008	0.013	0.000	0.000	0.000	0.021	0.000	0.000	0.000	0.047	0.000
TryAgain_3-5	Try Again, surface	8?	99.258	53.021	46.381	0.009	0.030	0.035	0.002	0.044	0.000	0.000	0.000	0.000	0.000	0.035	0.000

B. Electron Microprobe Data: Sulfides, Oxides, and Sulfates

TryAgain-3-8	Try Again, surface	8?	101.152	53.888	47.263	0.018	0.000	0.023	0.000	0.003	0.000	0.000	0.212	0.000		0.000	0.000
WRN_008_4-1	Wernecke, surface	6, 8	99.960	53.373	46.605	0.000	0.000	0.225	0.000	0.000	0.000	0.001	0.000	0.000	0.000	0.026	0.000
WRN_008_5-1	Wernecke, surface	6, 8	99.736	53.186	46.217	0.004	0.010	0.774	0.001	0.000	0.000	0.000	0.000	0.000	0.009	0.072	0.000
WRN_008_6-1	Wernecke, surface	6, 8	99.981	52.903	46.505	0.000	0.000	0.603	0.007	0.053	0.000	0.000	0.000	0.000	0.174	0.040	0.000
WRN-008-6-4	Wernecke, surface		101.032	53.679	47.283	0.000	0.000	0.274	0.001	0.060	0.000	0.000	0.121	0.000		0.010	0.000
BRM_044_4-6	Bermingham, surface	6, 7, 8	99.666	52.257	46.372	0.013	0.000	1.205	0.000	0.120	0.000	0.000	0.000	0.000	0.005	0.032	0.000
BRM_044_5-5	Bermingham, surface	6, 7, 8	100.155	52.848	46.443	0.000	0.000	0.925	0.008	0.046	0.009	0.011	0.000	0.000	0.000	0.028	0.000
EAG_047_1-3	Eagle, surface	4a	100.060	53.302	47.072	0.000	0.000	0.025	0.000	0.000	0.000	0.000	0.000	0.000	0.015	0.034	0.000
EAG_047_2-4	Eagle, surface	4a	100.322	53.553	46.995	0.000	0.000	0.031	0.001	0.081	0.000	0.000	0.000	0.000	0.000	0.029	0.000
EAG_047_3-2	Eagle, surface	4a	100.125	53.089	46.678	0.000	0.002	0.636	0.000	0.010	0.000	0.000	0.000	0.000	0.000	0.023	0.000
EAG_047_3-6	Eagle, surface	4a	99.900	53.369	46.712	0.011	0.000	0.034	0.000	0.046	0.000	0.000	0.000	0.000	0.011	0.044	0.000
EAG_047_4-3	Eagle, surface	4a	99.969	53.598	46.656	0.012	0.009	0.019	0.000	0.010	0.000	0.000	0.000	0.000	0.003	0.031	0.000
EAG_047_6-1	Eagle, surface	4a	100.093	53.561	46.908	0.002	0.006	0.000	0.010	0.000	0.000	0.000	0.000	0.000	0.000	0.035	0.000
EAG_047_7-1	Eagle, surface	4a	100.155	53.344	46.658	0.009	0.000	0.511	0.000	0.000	0.000	0.000	0.000	0.000	0.012	0.035	0.000
POR_056_1-2	Porcupine, surface	7, 8, 10	99.532	52.602	46.332	0.006	0.000	0.848	0.000	0.000	0.000	0.000	0.000	0.000	0.007	0.007	0.000
POR_056_2-6	Porcupine, surface	7, 8, 10	100.058	53.193	46.874	0.008	0.018	0.019	0.010	0.065	0.000	0.000	0.000	0.000	0.003	0.034	0.000
POR_056_2-7	Porcupine, surface	7, 8, 10	99.910	51.760	46.160	0.005	0.166	2.126	0.019	0.000	0.000	0.000	0.000	0.000	0.020	0.033	0.000
POR_056_3-2	Porcupine, surface	7, 8, 10	99.094	51.689	46.296	0.000	0.010	1.654	0.009	0.000	0.000	0.000	0.000	0.000	0.003	0.018	0.000
POR_056_3-4	Porcupine, surface	7, 8, 10	99.949	53.078	46.805	0.000	0.051	0.235	0.007	0.000	0.000	0.000	0.000	0.000	0.000	0.028	0.000
POR_056_4-1	Porcupine, surface	7, 8, 10	100.332	53.206	47.267	0.016	0.000	0.057	0.016	0.029	0.000	0.019	0.000	0.000	0.000	0.047	0.000
POR_056_4-2	Porcupine, surface	7, 8, 10	100.151	52.582	46.579	0.000	0.105	1.027	0.014	0.000	0.000	0.000	0.000	0.000	0.000	0.017	0.000
POR_056_5-3	Porcupine, surface	7, 8, 10	100.181	52.772	46.547	0.004	0.054	1.050	0.005	0.000	0.000	0.000	0.000	0.000	0.000	0.028	0.000
POR_056_5-4	Porcupine, surface	7, 8, 10	99.932	53.287	46.852	0.000	0.013	0.041	0.027	0.060	0.000	0.000	0.000	0.000	0.000	0.038	0.000
POR_056_6-3	Porcupine, surface	7, 8, 10	100.951	51.875	46.454	0.000	0.277	2.725	0.000	0.026	0.000	0.000	0.000	0.000	0.000	0.033	0.000

B. Electron Microprobe Data: Sulfides, Oxides, and Sulfates

POR_056_6-4	Porcupine, surface	7, 8, 10	99.609	51.398	45.935	0.000	0.018	2.531	0.000	0.029	0.000	0.000	0.000	0.000	0.017	0.044	0.000
POR_056_7-3	Porcupine, surface	7, 8, 10	99.348	51.471	45.981	0.000	0.004	2.242	0.005	0.000	0.000	0.000	0.000	0.000	0.000	0.038	0.000
POR_056_8-1	Porcupine, surface	7, 8, 10	99.363	53.082	46.517	0.000	0.000	0.063	0.000	0.000	0.000	0.000	0.000	0.000	0.000	0.037	0.000
K06-2-167-2m_2-4	Silver King	6, 8	100.175	53.318	46.835	0.007	0.000	0.232	0.027	0.013	0.000	0.000	0.000	0.000	0.000	0.030	0.000
K06-2-167-2m_3-4	Silver King	6, 8	100.033	53.167	46.769	0.000	0.000	0.396	0.000	0.000	0.021	0.000	0.000	0.000	0.006	0.024	0.000
K06-2-167-2m_4-3	Silver King	6, 8	100.228	53.592	46.733	0.000	0.000	0.143	0.001	0.000	0.000	0.001	0.000	0.000	0.008	0.021	0.000
K06-2-167-2m_5-4	Silver King	6, 8	99.611	53.224	46.429	0.014	0.006	0.129	0.009	0.046	0.000	0.000	0.000	0.000	0.000	0.018	0.000
K06-2-167-2m_8-3	Silver King	6, 8	100.180	53.367	46.811	0.000	0.021	0.366	0.000	0.005	0.000	0.000	0.000	0.000	0.001	0.031	0.000
K06-2-167-2m_9-3	Silver King	6, 8	99.812	53.610	46.477	0.000	0.002	0.029	0.006	0.016	0.000	0.006	0.000	0.000	0.003	0.024	0.000
K07-76-115-3m-5-2	BK_E, 965 masl	1, 5, 8	100.031	53.207	46.757	0.002	0.005	0.198	0.025	0.010	0.000	0.000	0.000	0.000	0.007	0.042	0.000
K07-76-125m-4-7	BK_E, 965 masl	6	99.747	52.586	46.001	0.004	0.029	1.128	0.008	0.000	0.000	0.015	0.000	0.000	0.067	0.156	0.000
K07-87-106-7m-1-12	Pool	9	101.247	52.963	47.254	0.010	0.017	1.219	0.011	0.060	0.000	0.010	0.088	0.000		0.000	0.000
K07-87-106-7m-4-6	Pool	9	101.175	51.792	47.123	0.019	0.038	2.388	0.000	0.000	0.000	0.015	0.240	0.000		0.000	0.000
K07-87-106-7m-6-7	Pool	9	101.564	53.334	47.649	0.044	0.129	0.414	0.013	0.070	0.000	0.000	0.366	0.000		0.000	0.000
K07-87-106-7m-6-8	Pool	9	101.227	53.637	47.472	0.000	0.000	0.370	0.016	0.065	0.000	0.000	0.165	0.000		0.022	0.000
K07-88-59-6m_3-3	Bermingham	2/6 ?, 8	100.257	53.497	46.122	0.000	0.000	0.300	0.025	0.000	0.015	0.000	0.000	0.000	0.270	0.443	0.000
K07-88-59-6m_6-3	Bermingham	2/6 ?, 8	99.809	53.196	46.653	0.014	0.000	0.045	0.012	0.000	0.000	0.000	0.000	0.000	0.070	0.029	0.000
K07-95-402-1m_1-2	BK_E, 860 masl	2, 3	100.489	53.997	46.119	0.014	0.011	0.035	0.005	0.000	0.000	0.000	0.000	0.000	0.000	0.572	0.000
K07-95-402-1m_2-2	BK_E, 860 masl	2, 3	100.353	53.837	45.922	0.018	0.002	0.019	0.000	0.058	0.000	0.000	0.000	0.000	0.026	0.901	0.000
K07-95-402-1m_3-1	BK_E, 860 masl	2, 3	99.889	53.689	46.502	0.000	0.000	0.020	0.011	0.000	0.000	0.000	0.000	0.000	0.086	0.040	0.000
K07-95-402-1m_4-1	BK_E, 860 masl	2, 3	99.557	53.496	46.142	0.014	0.000	0.060	0.004	0.000	0.000	0.000	0.000	0.000	0.087	0.032	0.000
K07-95-402-1m_5-1	BK_E, 860 masl	2, 3	99.947	53.888	46.150	0.002	0.000	0.014	0.000	0.011	0.000	0.000	0.000	0.000	0.083	0.094	0.000
K07-95-402-1m_5-3	BK_E, 860 masl	2, 3	100.143	52.857	46.124	0.018	0.280	1.176	0.000	0.042	0.000	0.000	0.000	0.000	0.017	0.032	0.000
K07-95-402-1m_9-2	BK_E, 860 masl	2, 3	99.524	52.989	45.755	0.000	1.002	0.254	0.005	0.000	0.000	0.000	0.000	0.000	0.000	0.043	0.000
K09-187-201-9m-1-4	BK_E, 950 masl	6, 7, 8, 9, 10	99.759	51.241	45.945	0.153	0.094	2.346	0.040	0.000	0.000	0.011	0.000	0.000	0.010	0.022	0.000
K09-187-201-9m-1-5	BK_E, 950 masl	6, 7, 8, 9,	99.648	52.451	46.715	0.110	0.000	0.594	0.015	0.000	0.000	0.000	0.000	0.000	0.000	0.033	0.000

B. Electron Microprobe Data: Sulfides, Oxides, and Sulfates

		10														
K09-187-201-9m-3-4	BK_E, 950 masl	6, 7, 8, 9, 10	99.906	52.794	47.014	0.045	0.091	0.128	0.031	0.045	0.000	0.022	0.000	0.000	0.014	0.041	0.000
K09-187-201-9m-4-4	BK_E, 950 masl	6, 7, 8, 9, 10	100.401	52.738	47.020	0.090	0.000	0.542	0.022	0.008	0.000	0.000	0.000	0.000	0.015	0.025	0.000
K09-187-201-9m-5-3	BK_E, 950 masl	6, 7, 8, 9, 10	99.656	52.781	47.045	0.008	0.082	0.061	0.051	0.065	0.000	0.010	0.000	0.000	0.003	0.017	0.000
K09-187-201-9m-7-1	BK_E, 950 masl	6, 7, 8, 9, 10	97.029	51.015	44.082	0.005	0.009	0.141	0.087	0.000	0.000	2.022	0.000	0.000	0.017	0.029	0.000
K09-187-201-9m-7-2	BK_E, 950 masl	6, 7, 8, 9, 10	99.890	53.273	46.736	0.003	0.000	0.013	0.019	0.000	0.000	0.144	0.000	0.000	0.000	0.039	0.000
K09-187-201-9m-10-2	BK_E, 950 masl	6, 7, 8, 9, 10	100.530	52.686	46.615	0.089	0.153	1.088	0.061	0.030	0.000	0.000	0.000	0.000	0.060	0.029	0.000
K09-187-201-9m-10-4	BK_E, 950 masl	6, 7, 8, 9, 10	99.347	52.176	46.780	0.113	0.007	0.490	0.038	0.000	0.000	0.095	0.000	0.000	0.000	0.021	0.000
BKUD09-134-39-5m-10-1	BK_SW, 965 masl	4a	100.473	53.080	47.278	0.000	0.000	0.519	0.000	0.000	0.000	0.000	0.000	0.000	0.000	0.000	0.000
BKUD09-134-39-5m-1-5	BK_SW, 965 masl	4a	100.663	53.625	47.118	0.000	0.078	0.473	0.019	0.000	0.000	0.000	0.000	0.000	0.000	0.000	0.000
BKUD09-134-39-5m-2-5	BK_SW, 965 masl	4a	100.626	52.814	46.852	0.000	0.247	1.126	0.027	0.000	0.000	0.000	0.000	0.000	0.000	0.000	0.000
BKUD09-134-39-5m-2-7	BK_SW, 965 masl	4a	100.658	53.090	47.120	0.000	0.000	0.983	0.030	0.000	0.000	0.000	0.000	0.000	0.000	0.000	0.000
BKUD09-134-39-5m-3-3	BK_SW, 965 masl	4a	100.435	53.769	47.235	0.001	0.000	0.007	0.008	0.000	0.000	0.000	0.000	0.000	0.000	0.000	0.000
BKUD09-134-39-5m-4-4	BK_SW, 965 masl	4a	100.602	53.391	46.901	0.000	0.013	0.860	0.000	0.017	0.000	0.000	0.000	0.000	0.000	0.000	0.000
BKUD09-134-39-5m-5-5	BK_SW, 965 masl	4a	100.551	53.611	46.780	0.000	0.001	0.624	0.017	0.002	0.000	0.000	0.000	0.000	0.000	0.000	0.000
BKUD09-134-39-5m-6-10	BK_SW, 965 masl	4a	100.584	53.504	46.898	0.000	0.651	0.036	0.015	0.000	0.000	0.000	0.000	0.000	0.000	0.000	0.000
BKUD09-134-39-5m-6-8	BK_SW, 965 masl	4a	100.336	52.887	46.517	0.004	0.309	0.943	0.028	0.017	0.000	0.000	0.000	0.000	0.000	0.000	0.000
BKUD09-134-39-5m-6-9	BK_SW, 965 masl	4a	100.923	53.667	47.162	0.007	0.114	0.303	0.027	0.000	0.000	0.000	0.000	0.000	0.000	0.000	0.000
BKUD09-134-39-5m-7-3	BK_SW, 965 masl	4a	100.390	53.727	47.134	0.014	0.030	0.049	0.018	0.000	0.000	0.000	0.000	0.000	0.000	0.000	0.000
BKUD09-134-39-5m-9-5	BK_SW, 965 masl	4a	102.161	54.981	47.080	0.020	0.333	0.021	0.015	0.069	0.000	0.000	0.000	0.000	0.000	0.000	0.000
BKUD09-134-41-35m-1-1-3	BK_SW, NE-end, 1015 masl	4a	100.501	52.767	47.017	0.003	0.000	1.178	0.023	0.000	0.000	0.000	0.000	0.000	0.000	0.000	0.000
BKUD09-134-41-35m-1-3-5	BK_SW, NE-end, 1015 masl	4a	100.820	53.189	46.942	0.004	0.000	1.094	0.043	0.000	0.000	0.000	0.000	0.000	0.000	0.000	0.000

B. Electron Microprobe Data: Sulfides, Oxides, and Sulfates

BKUD09-134-41-35m-1-4-3	BK_SW, NE-end, 1015 masl	4a	100.557	52.726	46.864	0.004	0.000	1.114	0.002	0.000	0.000	0.000	0.000	0.000	0.000	0.031	0.000
BKUD09-134-41-35m-1-5-7	BK_SW, NE-end, 1015 masl	4a	100.792	52.986	47.036	0.000	0.000	1.185	0.022	0.059	0.000	0.000	0.000	0.000	0.000	0.000	0.000
BKUD09-134-41-35m-1-6-4	BK_SW, NE-end, 1015 masl	4a	100.507	53.491	47.406	0.000	0.000	0.025	0.012	0.002	0.000	0.000	0.000	0.000	0.000	0.000	0.000
BKUD09-134-41-35m-1-7-2	BK_SW, NE-end, 1015 masl	4a	99.794	53.215	47.204	0.002	0.000	0.013	0.013	0.003	0.000	0.000	0.000	0.000	0.000	0.000	0.000
BKUD09-134-41-35m-1-7-4	BK_SW, NE-end, 1015 masl	4a	100.335	53.981	46.793	0.000	0.008	0.022	0.026	0.025	0.000	0.000	0.000	0.000	0.000	0.000	0.000
BKUD09-134-41-35m-1-7-5	BK_SW, NE-end, 1015 masl	4a	99.819	52.902	47.422	0.009	0.000	0.033	0.034	0.000	0.000	0.000	0.000	0.000	0.000	0.000	0.000
BKUD09-134-41-35m-2-10-6	BK_SW, NE-end, 1015 masl	2, 4a	100.858	53.689	46.882	0.000	0.000	0.732	0.000	0.042	0.000	0.000	0.000	0.000	0.000	0.000	0.000
BKUD09-134-41-35m-2-1-6	BK_SW, NE-end, 1015 masl	2, 4a	100.893	54.139	47.269	0.000	0.000	0.013	0.021	0.000	0.000	0.000	0.000	0.000	0.000	0.000	0.000
BKUD09-134-41-35m-2-2-4	BK_SW, NE-end, 1015 masl	2, 4a	101.235	53.055	46.531	0.015	0.127	1.819	0.000	0.017	0.000	0.000	0.000	0.000	0.000	0.000	0.000
BKUD09-134-41-35m-2-5-3	BK_SW, NE-end, 1015 masl	2, 4a	99.913	52.818	46.443	0.009	0.022	1.012	0.024	0.055	0.000	0.000	0.000	0.000	0.000	0.000	0.000
BKUD09-134-41-35m-2-5-4	BK_SW, NE-end, 1015 masl	2, 4a	101.037	53.214	46.926	0.000	0.037	1.141	0.037	0.054	0.000	0.000	0.000	0.000	0.000	0.000	0.000
BKUD09-134-41-35m-2-5-7	BK_SW, NE-end, 1015 masl	2, 4a	101.515	53.391	46.895	0.000	0.538	1.051	0.000	0.045	0.000	0.000	0.000	0.000	0.000	0.000	0.000
BKUD09-134-41-35m-2-6-3	BK_SW, NE-end, 1015 masl	2, 4a	100.775	53.449	47.196	0.008	0.032	0.619	0.006	0.000	0.000	0.000	0.000	0.000	0.000	0.000	0.000
BKUD09-134-41-35m-2-9-3	BK_SW, NE-end, 1015 masl	2, 4a	101.392	53.419	47.125	0.000	0.000	1.074	0.034	0.075	0.000	0.000	0.000	0.000	0.000	0.000	0.000
BKUD09-134-45m-2-2-3	BK_SW, NE-end, 1015 masl	2, 4a	100.563	53.175	46.998	0.000	0.040	0.807	0.005	0.000	0.000	0.000	0.000	0.000	0.000	0.000	0.000
BKUD09-134-45m-2-3-4	BK_SW, NE-end, 1015 masl	2, 4a	101.114	54.114	47.129	0.025	0.140	0.029	0.015	0.000	0.000	0.000	0.000	0.000	0.000	0.000	0.000
BKUD09-134-45m-2-5-3	BK_SW, NE-end, 1015 masl	2, 4a	100.648	53.634	46.999	0.000	0.021	0.525	0.040	0.024	0.000	0.000	0.000	0.000	0.000	0.000	0.000
BKUD09-134-45m-2-9-3	BK_SW, NE-end, 1015 masl	2, 4a	100.341	52.789	46.907	0.000	0.018	1.047	0.027	0.079	0.000	0.000	0.000	0.000	0.000	0.000	0.000
BKUD09-139-8-3m_10-3	BK_SW, 965 masl		99.679	53.292	46.627	0.000	0.008	0.035	0.000	0.063	0.000	0.000	0.000	0.000	0.008	0.051	0.000
BKUD09-139-8-3m_3-4	BK_SW, 965 masl		100.311	53.646	46.741	0.002	0.000	0.068	0.000	0.042	0.016	0.000	0.000	0.000	0.002	0.019	0.000
BKUD09-139-8-3m_5-3	BK_SW, 965 masl		100.664	54.146	46.801	0.005	0.055	0.008	0.000	0.000	0.000	0.000	0.000	0.000	0.000	0.025	0.000
BKUD09-139-8-3m_6-2	BK_SW, 965 masl		100.143	53.531	46.188	0.034	0.010	0.652	0.015	0.031	0.000	0.000	0.000	0.000	0.000	0.038	0.000
BKUD09-139-8-3m_7-3	BK_SW, 965 masl		100.370	53.662	46.732	0.033	0.054	0.027	0.022	0.031	0.010	0.009	0.000	0.000	0.005	0.030	0.000
BKUD09-139-8-3m_8-6	BK_SW, 965 masl		99.513	53.262	46.296	0.017	0.010	0.023	0.002	0.055	0.000	0.000	0.000	0.000	0.018	0.033	0.000

B. Electron Microprobe Data: Sulfides, Oxides, and Sulfates

BKUD09-139-8-3m_9-5	BK_SW, 965 masl		99.329	53.135	46.447	0.048	0.008	0.026	0.013	0.000	0.000	0.006	0.000	0.000	0.020	0.024	0.000
BKUD09-140-9-9m-2-3	BK_SW	2, 3	101.729	55.356	46.952	0.002	0.000	0.015	0.018	0.051	0.000	0.000	0.000	0.000	0.005	0.000	0.000
BKUD09-140-9-9m-6-3	BK_SW	2, 3	102.387	54.641	46.649	0.002	0.012	1.404	0.005	0.010	0.000	0.000	0.000	0.000	0.001	0.000	0.044
BKUD09-143-51-2m-1-6	BK_SW, NE-end, 1000 masl	4a	98.210	51.795	46.571	0.009	0.045	0.037	0.014	0.005	0.000	0.000	0.000	0.000	0.000	0.045	0.000
BKUD09-143-51-2m-2-6	BK_SW, NE-end, 1000 masl	4a, 6	97.587	51.154	46.426	0.000	0.000	0.092	0.013	0.000	0.000	0.000	0.000	0.000	0.004	0.036	0.000
BKUD09-143-51-2m-2-7	BK_SW, NE-end, 1000 masl	4a, 6	97.966	50.952	45.978	0.022	0.025	1.397	0.006	0.015	0.000	0.017	0.000	0.000	0.000	0.036	0.000
BKUD09-143-51-2m-3-3	BK_SW, NE-end, 1000 masl	4a, 6	97.859	51.398	46.388	0.012	0.000	0.437	0.009	0.000	0.000	0.000	0.000	0.000	0.000	0.033	0.000
BKUD09-143-51-2m-4-3	BK_SW, NE-end, 1000 masl	4a	97.884	50.823	46.344	0.015	0.000	1.026	0.017	0.055	0.000	0.000	0.000	0.000	0.010	0.038	0.000
BKUD09-143-51-2m-6-3	BK_SW, NE-end, 1000 masl	4a	97.731	51.469	46.660	0.000	0.000	0.072	0.008	0.000	0.000	0.002	0.000	0.000	0.000	0.035	0.000
BKUD09-143-51-2m-7-1	BK_SW, NE-end, 1000 masl	4a	98.242	51.787	46.567	0.015	0.002	0.030	0.034	0.010	0.000	0.000	0.000	0.000	0.000	0.038	0.000
BKUD09-143-51-2m-7-2	BK_SW, NE-end, 1000 masl	4a	97.983	51.306	46.122	0.000	0.000	0.824	0.006	0.000	0.000	0.003	0.000	0.000	0.009	0.029	0.000
BKUD09-143-51-2m-8-4	BK_SW, NE-end, 1000 masl	4a	97.787	51.134	46.929	0.000	0.000	0.054	0.027	0.038	0.000	0.000	0.000	0.000	0.000	0.035	0.000
BKUD09-143-51-2m-8-5	BK_SW, NE-end, 1000 masl	4a	97.781	51.213	46.853	0.000	0.000	0.057	0.023	0.000	0.000	0.000	0.000	0.000	0.000	0.044	0.000
BKUD09-143-52-8m_3-7	BK_SW, NE-end, 1000 masl		100.550	53.809	47.001	0.000	0.000	0.025	0.000	0.000	0.000	0.000	0.000	0.000	0.009	0.041	0.000
BKUD09-143-52-8m_3-9	BK_SW, NE-end, 1000 masl		100.527	53.607	46.878	0.043	0.014	0.171	0.000	0.076	0.000	0.000	0.000	0.000	0.004	0.028	0.000
BKUD09-143-52-8m_4-8	BK_SW, NE-end, 1000 masl		100.219	53.531	46.817	0.007	0.017	0.082	0.015	0.048	0.000	0.000	0.000	0.000	0.002	0.036	0.000
BKUD09-143-52-8m_5-5	BK_SW, NE-end, 1000 masl		100.301	52.140	46.239	0.014	0.006	2.161	0.020	0.000	0.000	0.000	0.000	0.000	0.001	0.032	0.000
BKUD09-144-36-6m-4-6	BK_SW, SW-end, 980 masl	3	102.175	54.934	46.832	0.005	0.000	0.907	0.007	0.000	0.000	0.000	0.000	0.000	0.012	0.000	0.131
BKUD09-144-36-6m-5-3	BK_SW, SW-end, 980 masl	3	102.751	55.681	46.350	0.031	1.226	0.028	0.042	0.028	0.000	0.047	0.000	0.000	0.000	0.000	0.014
BKUD09-146-46-5m-1-3	BK_SW, SW-end, 970 masl	4a	97.714	50.589	46.240	0.000	0.001	0.885	0.000	0.008	0.000	0.000	0.000	0.000	0.004	0.032	0.000
BKUD09-146-46-5m-2-3	BK_SW, SW-end, 970 masl	4a	97.725	50.778	46.466	0.000	0.000	0.856	0.002	0.005	0.000	0.000	0.000	0.000	0.000	0.026	0.000
BKUD09-146-46-5m-3-1	BK_SW, SW-end, 970 masl	4a	98.132	50.780	46.400	0.000	0.002	1.226	0.020	0.028	0.000	0.000	0.000	0.000	0.007	0.027	0.000
BKUD09-146-46-5m-6-1	BK_SW, SW-end, 970 masl	4a	97.830	50.960	46.151	0.000	0.007	0.978	0.014	0.000	0.000	0.000	0.000	0.000	0.017	0.044	0.000

B. Electron Microprobe Data: Sulfides, Oxides, and Sulfates

BKUD09-146-46-5m-7-3	BK_SW, SW-end, 970 masl	4a	98.002	51.331	45.995	0.000	0.000	0.975	0.031	0.013	0.000	0.000	0.000	0.000	0.000	0.032	0.000
BKUD09-146-46-5m-8-4	BK_SW, SW-end, 970 masl	4a	97.367	50.839	45.813	0.000	0.002	1.231	0.008	0.013	0.000	0.000	0.000	0.000	0.000	0.048	0.000
BKUD09-148-29-5m_2-2	BK_99, 1025 masl		100.136	52.479	46.217	0.114	0.027	1.624	0.000	0.000	0.000	0.000	0.000	0.000	0.008	0.017	0.000
BKUD09-148-29-5m_7-1	BK_99, 1025 masl		100.244	53.775	46.640	0.009	0.000	0.021	0.000	0.045	0.000	0.000	0.000	0.000	0.007	0.044	0.000
BKUD09-148-29-5m_8-1	BK_99, 1025 masl		100.160	53.693	46.475	0.007	0.000	0.016	0.000	0.068	0.000	0.000	0.000	0.000	0.010	0.042	0.000
BKUD09-148-33-5m-4-4	BK_99, 1025 masl	2/6? 7, 8	98.881	51.183	45.942	0.059	0.000	1.875	0.030	0.000	0.005	0.000	0.000	0.000	0.000	0.043	0.000
BKUD09-150-64-1m-3-5	BK_SW, SW-end, 975 masl	2, 3, 5?	100.083	52.502	46.693	0.008	0.047	0.926	0.027	0.020	0.011	0.000	0.000	0.000	0.026	0.048	0.000
BKUD09-150-64-1m-4-3	BK_SW, SW-end, 975 masl	2, 3, 5?	100.081	52.629	46.676	0.003	0.037	0.908	0.025	0.093	0.000	0.042	0.000	0.000	0.000	0.031	0.000
BKUD09-150-64-1m-6-3	BK_SW, SW-end, 975 masl	2, 3, 5?	99.789	53.116	46.629	0.001	0.003	0.308	0.008	0.046	0.000	0.000	0.000	0.000	0.008	0.042	0.000
BKUD09-157-93-8m_1-1	BK_SW, SW-end, 930 masl		99.962	53.646	46.516	0.005	0.000	0.028	0.015	0.052	0.000	0.000	0.000	0.000	0.001	0.037	0.000
BKUD09-157-93-8m_2-1	BK_SW, SW-end, 930 masl		100.077	53.035	46.441	0.023	0.026	0.831	0.007	0.000	0.032	0.000	0.000	0.000	0.000	0.024	0.000
BKUD09-157-93-8m_4-2	BK_SW, SW-end, 930 masl		100.195	53.754	46.487	0.028	0.035	0.072	0.000	0.034	0.000	0.000	0.000	0.000	0.001	0.040	0.000
BKUD09-157-93-8m_4-5	BK_SW, SW-end, 930 masl		100.365	53.582	46.065	0.038	0.639	0.066	0.016	0.018	0.000	0.000	0.000	0.000	0.054	0.030	0.000
BKUD09-157-93-8m_6-2	BK_SW, SW-end, 930 masl		99.815	53.487	46.268	0.000	0.033	0.042	0.000	0.058	0.000	0.025	0.000	0.000	0.000	0.103	0.000
BKUD09-157-93-8m_7-1	BK_SW, SW-end, 930 masl		100.286	53.775	46.652	0.000	0.000	0.018	0.011	0.018	0.000	0.000	0.000	0.000	0.010	0.029	0.000
BKUD09-158-36m_2-3	BK_SW, NE-end, 1030 masl		100.139	52.900	46.658	0.002	0.025	0.892	0.012	0.000	0.000	0.000	0.000	0.000	0.000	0.028	0.000
BKUD09-158-36m_4-2	BK_SW, NE-end, 1030 masl		100.105	53.349	46.710	0.011	0.071	0.442	0.002	0.000	0.000	0.000	0.000	0.000	0.000	0.032	0.000
BKUD09-158-36m_6-4	BK_SW, NE-end, 1030 masl		100.422	53.312	46.417	0.185	0.041	0.345	0.022	0.094	0.000	0.049	0.000	0.000	0.069	0.080	0.000
BKUD09-158-36m_6-5	BK_SW, NE-end, 1030 masl		100.348	53.621	46.717	0.012	0.015	0.151	0.000	0.000	0.026	0.000	0.000	0.000	0.000	0.029	0.000
BKUD09-158-36-5m-1-3	BK_SW, NE-end, 1030 masl	6, 7	102.854	55.084	46.836	0.009	0.236	0.977	0.016	0.036	0.000	0.000	0.000	0.000	0.043	0.000	0.000
BKUD09-158-36-5m-3-1	BK_SW, NE-end, 1030 masl	6, 7	102.960	55.201	46.777	0.038	0.012	1.372	0.021	0.000	0.000	0.000	0.000	0.000	0.000	0.000	0.052
BKUD09-158-36-5m-9-5	BK_SW, NE-end, 1030 masl	6, 7	99.923	54.679	45.436	0.016	0.441	0.393	0.020	0.051	0.000	0.000	0.000	0.000	0.000	0.000	0.000
BKUD09-158-37m-1-2	BK_SW, NE-end, 1030 masl	2/6?, 8, 11	97.950	50.286	45.928	0.039	0.008	2.070	0.003	0.096	0.000	0.000	0.000	0.000	0.000	0.016	0.000

B. Electron Microprobe Data: Sulfides, Oxides, and Sulfates

BKUD09-158-37m-2-3	BK_SW, NE-end, 1030 masl	2/6?, 8, 11	96.702	49.377	44.674	0.004	0.002	2.449	0.008	0.000	0.000	0.000	0.000	0.000	0.738	0.000
BKUD09-158-37m-2-5	BK_SW, NE-end, 1030 masl	2/6?, 8, 11	98.440	51.672	46.517	0.028	0.000	0.209	0.018	0.099	0.000	0.000	0.000	0.000	0.029	0.000
BKUD09-158-37m-4-1	BK_SW, NE-end, 1030 masl	2/6?, 8, 11	97.948	51.168	46.185	0.031	0.000	0.979	0.017	0.000	0.000	0.000	0.000	0.000	0.023	0.000
BKUD09-158-37m-8-1	BK_SW, NE-end, 1030 masl	2/6?, 8, 11	98.450	49.947	45.989	0.000	0.000	2.418	0.000	0.046	0.000	0.000	0.000	0.000	0.010	0.284	0.000
BKUD09-160-56-5m-4-3	BK_SW, SW-end, 950 masl	8, 9, 10, 11	102.638	55.715	46.849	0.000	0.008	0.352	0.015	0.074	0.000	0.031	0.000	0.000	0.000	0.000	0.000
BKUD09-160-56-5m-7-1	BK_SW, SW-end, 950 masl	8, 9, 10, 11	102.460	54.587	46.694	0.200	0.000	1.287	0.025	0.000	0.000	0.000	0.000	0.000	0.007	0.000	0.104
BKUD09-160-56-5m-7-6	BK_SW, SW-end, 950 masl	8, 9, 10, 11	102.741	55.067	47.056	0.018	0.179	0.912	0.022	0.061	0.000	0.000	0.000	0.000	0.009	0.000	0.000
BKUD09-160-56-5m-7-8	BK_SW, SW-end, 950 masl	8, 9, 10, 11	102.993	55.935	46.659	0.009	0.136	0.643	0.027	0.000	0.000	0.000	0.000	0.000	0.016	0.000	0.014
BKUD09-160-56-5m-8-2	BK_SW, SW-end, 950 masl	8, 9, 10, 11	102.625	55.287	46.761	0.009	0.060	0.686	0.037	0.061	0.000	0.011	0.000	0.000	0.002	0.000	0.082
BKUD09-160-56-5m-8-4	BK_SW, SW-end, 950 masl	8, 9, 10, 11	102.880	55.088	46.543	0.000	0.030	1.671	0.022	0.000	0.000	0.000	0.000	0.000	0.000	0.000	0.005
BKUD09-160-56-5m-9-2	BK_SW, SW-end, 950 masl	8, 9, 10, 11	102.700	54.518	46.692	0.046	0.031	1.686	0.020	0.114	0.000	0.000	0.000	0.000	0.000	0.000	0.000
BKUD09-163-14-8m_1-3	BK_SW, 980 masl	9	100.020	53.253	46.471	0.027	0.037	0.380	0.008	0.005	0.000	0.000	0.000	0.000	0.000	0.045	0.000
BKUD09-163-14-8m_2-4	BK_SW, 980 masl	9	99.859	53.655	46.386	0.019	0.001	0.076	0.017	0.000	0.000	0.000	0.000	0.000	0.000	0.025	0.000
BKUD09-163-14-8m_2-8	BK_SW, 980 masl	9	100.001	53.254	46.556	0.142	0.000	0.315	0.009	0.017	0.000	0.000	0.000	0.000	0.000	0.034	0.000
BKUD09-163-14-8m_3-5	BK_SW, 980 masl	9	100.017	52.984	46.624	0.036	0.033	0.686	0.000	0.000	0.000	0.000	0.000	0.000	0.000	0.033	0.000
BKUD09-163-14-8m_4-3	BK_SW, 980 masl	9	100.010	53.038	46.710	0.001	0.059	0.537	0.000	0.000	0.000	0.000	0.000	0.000	0.000	0.031	0.000
BKUD09-163-14-8m_5-1	BK_SW, 980 masl	9	100.269	53.161	46.855	0.000	0.010	0.342	0.019	0.103	0.000	0.000	0.000	0.000	0.045	0.047	0.000
BKUD09-163-14-8m_5-2	BK_SW, 980 masl	9	100.149	53.550	46.929	0.012	0.002	0.031	0.014	0.031	0.000	0.000	0.000	0.000	0.000	0.029	0.000
BKUD09-163-14-8m_6-3	BK_SW, 980 masl	9	100.682	53.034	47.087	0.000	0.024	0.776	0.007	0.039	0.000	0.000	0.000	0.000	0.000	0.027	0.000
BKUD09-163-14-8m_7-2	BK_SW, 980 masl	9	100.411	53.342	47.028	0.033	0.021	0.256	0.019	0.000	0.000	0.000	0.000	0.000	0.000	0.033	0.000
BKUD09-171-32-8m-1-3	BK_99, 990 masl	2/6?, 7, 8	98.975	50.802	46.352	0.000	0.136	1.851	0.006	0.112	0.000	0.000	0.000	0.000	0.008	0.042	0.000
BKUD09-171-32-8m-3-3	BK_99, 990 masl	2/6?, 7, 8	98.423	51.405	46.365	0.000	0.000	0.983	0.000	0.000	0.000	0.014	0.000	0.000	0.002	0.030	0.000
BKUD09-171-32-8m-4-1	BK_99, 990 masl	2/6?, 7, 8	98.426	51.819	46.733	0.023	0.000	0.036	0.009	0.000	0.012	0.000	0.000	0.000	0.002	0.021	0.000
BKUD09-171-32-8m-5-1	BK_99, 990 masl	2/6?, 7, 8	98.047	50.437	46.185	0.000	0.139	1.439	0.003	0.061	0.018	0.017	0.000	0.000	0.013	0.020	0.000
BKUD09-171-32-8m-6-4	BK_99, 990 masl	2/6?,	98.463	52.258	46.140	0.016	0.051	0.061	0.000	0.000	0.000	0.000	0.000	0.000	0.000	0.029	0.000

B. Electron Microprobe Data: Sulfides, Oxides, and Sulfates

		7, 8															
BKUD09-173-31-2m_2-2	BK_99, 990 masl	2, 3?	100.047	52.825	46.254	0.000	0.078	0.982	0.000	0.024	0.000	0.003	0.000	0.000	0.028	0.066	0.000
BKUD09-173-43-5m_3-2	BK_99, 990 masl	2, 3?	99.889	52.211	45.979	0.018	0.027	1.854	0.003	0.026	0.000	0.000	0.000	0.000	0.000	0.033	0.000
BKUD09-173-43-5m_3-3	BK_99, 990 masl	2, 3?	99.266	51.674	45.942	0.030	0.000	1.923	0.022	0.000	0.000	0.000	0.000	0.000	0.004	0.043	0.000
BKUD09-173-43-5m_4-1	BK_99, 990 masl	2, 3?	99.956	52.263	45.971	0.000	0.229	1.839	0.010	0.000	0.000	0.000	0.000	0.000	0.005	0.034	0.000
BKUD09-173-43-5m_5-3	BK_99, 990 masl	2, 3?	100.669	52.797	45.738	0.000	0.727	1.235	0.032	0.039	0.000	0.001	0.000	0.000	0.223	0.105	0.000
BKUD09-173-43-5m_7-2	BK_99, 990 masl	2, 3?	100.801	54.181	46.531	0.010	0.306	0.013	0.013	0.000	0.000	0.000	0.000	0.000	0.000	0.038	0.000
n = 182	AVERAGE		100.043	52.962	46.584	0.015	0.062	0.673	0.013	0.023	0.001	0.015	0.010	0.000	0.011	0.041	0.003
	MINIMUM		96.702	49.377	44.082	0.000	0.000	0.000	0.000	0.000	0.000	0.000	0.000	0.000	0.000	0.000	0.000
	MAXIMUM		102.993	55.935	47.649	0.200	1.226	3.755	0.087	0.120	0.032	2.022	0.366	0.000	0.270	0.901	0.131
Pyrrhotite: various stages																	
BKUD09-134-45m-2-4-3	BK_SW, NE-end, 1015 masl	4a	98.322	38.794	58.837	0.048	0.930	0.029	0.022	0.036	0.000	0.000	0.000	0.000		0.000	
BKUD09-134-45m-2-7-5	BK_SW, NE-end, 1015 masl	4a	99.583	39.238	58.724	0.015	1.685	0.011	0.036	0.016	0.000	0.000	0.000	0.004		0.000	
BKUD09-144-36-6m-3-3	BK_SW, SW-end, 980 masl	3, 4a ?	101.058	41.580	58.742	0.023	1.145	0.020	0.027	0.014	0.000	0.000	0.000	0.000	0.005	0.000	0.030
BKUD09-163-31-8m-2-2	BK_SW, 980 masl	2	100.514	41.126	59.627	0.024	0.000	0.032	0.019	0.000	0.000	0.000	0.000	0.000	0.012	0.000	0.018
BKUD09-163-31-8m-4-3	BK_SW, 980 masl	2, 3	100.797	41.448	59.297	0.021	0.316	0.030	0.010	0.000	0.000	0.000	0.000	0.000	0.000	0.000	0.115
BKUD09-163-31-8m-4-4	BK_SW, 980 masl	2, 3	100.223	41.127	59.014	0.023	0.326	0.026	0.028	0.019	0.000	0.000	0.000	0.000	0.000	0.000	0.160
WRN_008_4-2	Wernecke, surface	6	98.264	38.856	58.834	0.000	0.003	0.027	0.000	0.012	0.000	0.000	0.000	0.000	0.625	0.033	
WRN-008-6-5	Wernecke, surface	6	98.314	38.855	59.471	0.000	0.000	0.022	0.011	0.054	0.000	0.000	0.105	0.000		0.000	0.000
n = 8	AVERAGE		99.634	40.128	59.068	0.019	0.550	0.025	0.019	0.019	0.000	0.000	0.013	0.001	0.128	0.004	0.064
	MINIMUM		98.264	38.794	58.724	0.000	0.000	0.011	0.000	0.000	0.000	0.000	0.000	0.000	0.000	0.000	0.000
	MAXIMUM		101.058	41.580	59.627	0.048	1.685	0.032	0.036	0.054	0.000	0.000	0.105	0.004	0.625	0.033	0.160
Cassiterite: mostly stages 2 to 4a																	
Alice-3-8	Alice, surface	6, 7, 8	80.354	0.016	0.121	0.017	0.083	0.010	0.000	0.035	80.13	0.000	0.000	0.066		0.010	0.000
K07-76-125m-7-3	BK_E, 965 masl	7, 8 ?	78.274	0.020	0.128	0.019	0.000	0.055	0.000	0.012	78.16	0.000	0.000	0.000	0.000	0.001	0.000
K07-76-125m-7-4	BK_E, 965 masl	7, 8 ?	78.021	0.007	0.590	0.000	0.013	0.005	0.000	0.000	77.92	0.000	0.011	0.000	0.008	0.000	0.000

B. Electron Microprobe Data: Sulfides, Oxides, and Sulfates

K07-76-125m-7-7	BK_E, 965 masl	7, 8 ?	78.590	0.006	0.307	0.000	0.000	0.090	0.000	0.003	78.30	0.000	0.000	0.000	0.005	0.000	0.000
K07-76-125m-8-2	BK_E, 965 masl	7, 8 ?	78.687	0.001	0.069	0.001	0.004	0.065	0.000	0.000	78.53	0.000	0.000	0.000	0.000	0.000	0.000
BKUD09-134-39-5m-1-7	BK_SW, NE-end, 1015 masl	4a	80.445	0.026	0.143	0.000	0.064	0.000	0.000	0.000	80.67	0.000	0.000	0.035	0.000	0.000	0.000
BKUD09-134-39-5m-2-9	BK_SW, NE-end, 1015 masl	4a	79.822	0.024	0.240	0.021	0.079	0.009	0.000	0.000	79.81	0.000	0.019	0.000	0.000	0.001	0.000
BKUD09-134-39-5m-3-6	BK_SW, NE-end, 1015 masl	4a	79.249	0.022	0.166	0.001	0.015	0.000	0.000	0.000	79.42	0.000	0.000	0.054	0.000	0.002	0.000
BKUD09-134-39-5m-3-7	BK_SW, NE-end, 1015 masl	4a	79.367	0.000	0.129	0.007	0.060	0.000	0.000	0.000	79.56	0.000	0.000	0.000	0.000	0.000	0.000
BKUD09-134-39-5m-3-8	BK_SW, NE-end, 1015 masl	4a	79.395	0.024	0.079	0.000	0.005	0.000	0.000	0.000	79.56	0.000	0.068	0.023	0.000	0.000	0.000
BKUD09-134-39-5m-3-9	BK_SW, NE-end, 1015 masl	4a	79.670	0.000	0.187	0.011	0.010	0.000	0.000	0.000	79.97	0.000	0.000	0.000	0.000	0.006	0.000
BKUD09-134-39-5m-3-10	BK_SW, NE-end, 1015 masl	4a	79.746	0.022	0.288	0.001	0.001	0.011	0.000	0.000	79.76	0.000	0.000	0.042	0.000	0.003	0.000
BKUD09-134-39-5m-5-3	BK_SW, NE-end, 1015 masl	4a	80.157	0.017	0.237	0.007	0.044	0.000	0.000	0.000	80.11	0.000	0.000	0.097	0.000	0.011	0.000
BKUD09-134--5m-10-3	BK_SW, NE-end, 1015 masl	4a	79.629	0.017	0.096	0.003	0.000	0.000	0.000	0.000	79.89	0.000	0.000	0.031	0.000	0.000	0.000
BKUD09-134-39-5m-10-10	BK_SW, NE-end, 1015 masl	4a	80.526	0.041	0.035	0.012	0.316	0.000	0.000	0.012	80.48	0.000	0.000	0.000	0.000	0.000	0.000
BKUD09-134-45m-2-3-5	BK_SW, NE-end, 1015 masl	2, 4a	83.289	3.143	4.679	0.000	0.155	0.015	0.000	0.000	75.69	0.000	0.000	0.000	0.000	0.000	0.000
BKUD09-134-45m-2-3-7	BK_SW, NE-end, 1015 masl	2, 4a	79.640	0.015	0.993	0.007	0.481	0.000	0.000	0.000	78.43	0.000	0.026	0.000	0.000	0.000	0.000
BKUD09-134-45m-2-5-6	BK_SW, NE-end, 1015 masl	2, 4a	80.157	0.020	0.190	0.013	0.000	0.000	0.000	0.000	80.27	0.000	0.000	0.069	0.000	0.016	0.000
BKUD09-144-36-6m-1-2	BK_SW, 980 masl	2, 4a	81.020	0.008	0.062	0.008	0.008	0.003	0.000	0.000	81.04	0.000	0.000	0.008	0.000	0.006	0.000
BKUD09-144-36-6m-2-1	BK_SW, 980 masl	2, 4a	81.195	0.000	0.097	0.009	0.001	0.036	0.000	0.000	81.31	0.000	0.000	0.029	0.000	0.002	0.000
BKUD09-144-36-6m-2-3	BK_SW, 980 masl	2, 4a	81.093	0.014	0.093	0.004	0.003	0.026	0.000	0.000	81.36	0.000	0.000	0.000	0.000	0.000	0.000
BKUD09-144-36-6m-4-11	BK_SW, 980 masl	2, 4a	80.899	0.007	0.097	0.000	0.292	0.022	0.000	0.054	80.31	0.000	0.021	0.000	0.003	0.008	0.016
BKUD09-144-36-6m-6-1	BK_SW, 980 masl	2, 4a	80.171	0.018	0.133	0.044	0.007	0.035	0.000	0.000	80.17	0.000	0.016	0.086	0.007	0.009	0.000
BKUD09-144-36-6m-6-2	BK_SW, 980 masl	2, 4a	81.639	0.011	0.190	0.031	0.010	0.018	0.000	0.000	81.43	0.000	0.000	0.000	0.000	0.003	0.006
BKUD09-144-36-6m-7-1	BK_SW, 980 masl	2, 4a	80.385	0.008	0.169	0.000	0.001	0.028	0.000	0.000	80.44	0.000	0.062	0.000	0.005	0.007	0.000
BKUD09-144-36-6m-7-2	BK_SW, 980 masl	2, 4a	81.130	0.000	0.164	0.002	0.000	0.000	0.000	0.000	81.06	0.000	0.035	0.033	0.000	0.010	0.014
BKUD09-146-46-5m-3-7	BK_SW, SW-end, 970 masl	4a	75.678	0.033	1.556	0.007	0.005	0.076	0.000	0.000	74.68	0.000	0.000	0.008	0.000	0.007	0.000
BKUD09-146-46-5m-4-2	BK_SW, SW-end, 970 masl	4a	77.009	0.000	0.102	0.000	0.000	0.044	0.000	0.000	77.18	0.000	0.000	0.025	0.002	0.012	0.000

B. Electron Microprobe Data: Sulfides, Oxides, and Sulfates

BKUD09-146-46-5m-8-3	BK_SW, SW-end, 970 masl	4a	76.318	0.018	0.108	0.000	0.000	0.081	0.000	0.000	75.64	0.000	0.024	0.022	0.000	0.000	0.000
n = 29	AVERAGE		79.709	0.122	0.395	0.008	0.057	0.022	0.000	0.004	79.35	0.000	0.010	0.022	0.001	0.004	0.001
	MINIMUM		75.678	0.000	0.035	0.000	0.000	0.000	0.000	0.000	74.68	0.000	0.000	0.000	0.000	0.000	0.000
	MAXIMUM		83.289	3.143	4.679	0.044	0.481	0.090	0.000	0.054	81.43	0.000	0.068	0.097	0.008	0.016	0.016
Native Tin: mostly stages 2 to 4a																	
Alice_3-4	Alice, surface	6, 7, 8	98.011	0.089	0.886	0.000	0.000	0.000	0.000	0.044	97.50	0.000	0.000	0.000	0.000	0.005	0.000
BKUD09-157-93-8m_2-3	BK_SW, SW-end, 970 masl	2 - 4a	100.899	0.017	0.313	0.000	0.005	0.014	0.000	0.000	100.6	0.000	0.000	0.003	0.000	0.000	0.000
BKUD09-157-93-8m_4-4	BK_SW, SW-end, 970 masl	2 - 4a	99.509	0.006	0.234	0.006	0.047	0.000	0.000	0.000	99.25	0.000	0.068	0.000	0.000	0.000	0.000
n = 3	AVERAGE		99.473	0.038	0.477	0.002	0.017	0.005	0.000	0.015	99.11	0.000	0.023	0.001	0.000	0.002	0.000
	MINIMUM		98.011	0.006	0.234	0.000	0.000	0.000	0.000	0.000	97.50	0.000	0.000	0.000	0.000	0.000	0.000
	MAXIMUM		100.899	0.089	0.886	0.006	0.047	0.014	0.000	0.044	100.6	0.000	0.068	0.003	0.000	0.005	0.000
Sphalerite: stage 3																	
K07-76-115-3m-7-2	BK_E, 965 masl	3?	98.694	32.175	6.996	0.000	58.927	0.070	0.014	0.683	0.000	0.000	0.000	0.000	0.003	0.000	0.000
K07-95-402-1m_1-1	BK_E, 860 masl	3	99.348	33.184	10.182	0.035	55.053	0.024	0.001	1.098	0.000	0.000	0.000	0.000	0.011	0.002	0.000
K07-95-402-1m_2-1	BK_E, 860 masl	3	100.132	33.135	4.243	0.014	62.133	0.018	0.017	0.658	0.000	0.000	0.000	0.000	0.013	0.015	0.000
K07-95-402-1m_3-2	BK_E, 860 masl	3	99.722	33.242	8.270	0.040	57.377	0.037	0.000	0.841	0.000	0.000	0.000	0.000	0.000	0.003	0.000
K07-95-402-1m_4-3	BK_E, 860 masl	3	99.320	33.717	9.945	0.034	55.122	0.053	0.029	0.818	0.000	0.000	0.000	0.000	0.009	0.000	0.000
K07-95-402-1m_5-2	BK_E, 860 masl	3	99.601	33.701	9.596	0.018	55.640	0.033	0.001	0.715	0.000	0.015	0.000	0.000	0.004	0.013	0.000
K07-95-402-1m_5-5	BK_E, 860 masl	3	98.708	33.187	9.535	0.009	55.408	0.052	0.000	0.938	0.000	0.000	0.000	0.000	0.006	0.017	0.000
K07-95-402-1m_6-1	BK_E, 860 masl	3	98.963	33.572	9.913	0.001	54.912	0.024	0.000	0.745	0.000	0.000	0.000	0.000	0.013	0.000	0.000
K07-95-402-1m_7-1	BK_E, 860 masl	3	99.073	33.212	8.073	0.003	57.133	0.033	0.020	0.815	0.000	0.000	0.000	0.000	0.000	0.004	0.000
K07-95-402-1m_8-1	BK_E, 860 masl	3	99.366	33.342	9.580	0.011	55.816	0.017	0.015	0.882	0.000	0.000	0.000	0.000	0.000	0.000	0.000
K07-95-402-1m_9-1	BK_E, 860 masl	3	99.529	33.528	10.813	0.014	54.382	0.035	0.000	0.963	0.000	0.000	0.000	0.000	0.000	0.000	0.000
K08-155-132-5m_1-1	Onek	3	96.413	31.769	6.484	0.027	58.046	0.022	0.000	0.025	0.000	0.008	0.000	0.000	0.004	0.007	0.000
K08-155-132-5m_2-1	Onek	3	97.639	32.467	7.041	0.149	57.982	0.016	0.006	0.023	0.110	0.000	0.000	0.000	0.000	0.011	0.000
K08-155-132-5m_2-2	Onek	3	97.156	32.503	6.738	0.030	57.929	0.035	0.013	0.000	0.000	0.000	0.000	0.000	0.008	0.002	0.000

B. Electron Microprobe Data: Sulfides, Oxides, and Sulfates

K08-155-132-5m_3-1	Onek	3	97.812	32.678	5.753	0.102	59.215	0.024	0.008	0.008	0.092	0.000	0.000	0.000	0.000	0.000	0.000
K08-155-132-5m_4-1	Onek	3	96.743	32.467	6.491	0.065	57.825	0.030	0.004	0.000	0.000	0.000	0.000	0.000	0.000	0.011	0.000
K08-155-132-5m_5-1	Onek	3	96.792	32.838	6.321	0.055	57.569	0.000	0.010	0.000	0.000	0.000	0.000	0.000	0.006	0.000	0.000
K08-155-132-5m_6-1	Onek	3	97.558	32.251	4.913	0.020	60.307	0.010	0.000	0.086	0.000	0.000	0.000	0.000	0.003	0.003	0.000
K08-155-132-5m_7-1	Onek	3	98.788	33.271	5.844	0.025	59.582	0.041	0.000	0.144	0.000	0.000	0.000	0.000	0.000	0.000	0.000
K08-155-132-5m_7-2	Onek	3	97.621	32.629	6.931	0.232	57.640	0.032	0.000	0.055	0.106	0.000	0.000	0.000	0.021	0.005	0.000
K08-155-132-5m_8-1	Onek	3	98.095	32.919	7.625	0.109	57.689	0.029	0.025	0.000	0.031	0.000	0.000	0.000	0.000	0.001	0.000
K08-155-132-5m_9-1	Onek	3	98.865	33.004	5.318	0.019	60.591	0.063	0.000	0.000	0.000	0.000	0.000	0.000	0.000	0.015	0.000
K08-155-132-5m_10-1	Onek	3	98.840	33.001	5.425	0.034	60.587	0.028	0.000	0.000	0.000	0.000	0.000	0.000	0.002	0.009	0.000
K08-155-132-5m_11-1	Onek	3	98.746	32.727	5.835	0.036	60.189	0.004	0.000	0.061	0.000	0.000	0.000	0.000	0.001	0.007	0.000
BKUD09-140-9-9m-1-2	BK_99	2, 3	100.887	34.391	9.746	0.065	55.806	0.036	0.006	0.758	0.000	0.000	0.000	0.000	0.000	0.000	0.167
BKUD09-140-9-9m-2-1	BK_99	2, 3	100.724	34.511	6.887	0.055	58.771	0.023	0.000	0.674	0.000	0.000	0.000	0.000	0.005	0.000	0.038
BKUD09-140-9-9m-3-2	BK_99	2, 3	100.633	34.593	8.421	0.000	56.888	0.022	0.000	0.794	0.000	0.000	0.000	0.000	0.005	0.000	0.012
BKUD09-140-9-9m-4-1	BK_99	2, 3	101.453	35.015	9.256	0.011	56.404	0.023	0.015	0.827	0.000	0.001	0.000	0.000	0.006	0.000	0.046
BKUD09-140-9-9m-5-1	BK_99	2, 3	101.030	34.696	9.845	0.010	55.723	0.028	0.008	0.777	0.000	0.000	0.000	0.000	0.000	0.000	0.185
BKUD09-140-9-9m-6-1	BK_99	2, 3	100.830	34.690	10.917	0.059	54.210	0.038	0.005	0.963	0.000	0.014	0.000	0.000	0.000	0.000	0.000
BKUD09-144-36-6m-3-2	BK_SW, SW-end, 980 masl	3	101.611	34.903	5.080	0.000	61.216	0.023	0.005	0.579	0.000	0.000	0.000	0.000	0.009	0.000	0.103
BKUD09-144-36-6m-4-2	BK_SW, SW-end, 980 masl	3	100.641	34.746	10.871	0.044	54.316	0.029	0.021	0.905	0.000	0.000	0.000	0.000	0.000	0.000	0.056
BKUD09-144-36-6m-4-3	BK_SW, SW-end, 980 masl	3	100.407	34.621	6.594	0.053	58.453	0.046	0.019	0.868	0.000	0.000	0.000	0.000	0.000	0.004	0.015
BKUD09-144-36-6m-4-9	BK_SW, SW-end, 980 masl	3	100.973	34.995	9.336	0.053	55.971	0.036	0.002	0.907	0.000	0.026	0.000	0.000	0.005	0.000	0.029
BKUD09-144-36-6m-4-10	BK_SW, SW-end, 980 masl	3	101.413	34.783	7.671	0.063	58.257	0.023	0.000	0.669	0.000	0.000	0.000	0.000	0.000	0.000	0.095
BKUD09-144-36-6m-4-12	BK_SW, SW-end, 980 masl	3	101.001	34.579	9.431	0.616	55.801	0.027	0.000	0.782	0.000	0.009	0.000	0.000	0.007	0.000	0.000
BKUD09-144-36-6m-5-2	BK_SW, SW-end, 980 masl	3	101.014	34.594	8.345	0.384	57.035	0.030	0.010	0.886	0.000	0.000	0.000	0.000	0.000	0.003	0.000
BKUD09-148-33-5m-1-1	BK_99, 1025 masl	3	97.786	31.589	7.267	0.044	58.095	0.073	0.009	0.819	0.000	0.000	0.000	0.000	0.000	0.002	0.000
BKUD09-148-33-5m-1-3	BK_99, 1025 masl	3	97.130	31.335	7.004	0.000	58.049	0.024	0.004	0.676	0.000	0.025	0.000	0.000	0.002	0.000	0.000
BKUD09-148-33-5m-2-1	BK_99, 1025 masl	3	97.716	31.846	7.756	0.019	57.197	0.046	0.016	0.907	0.000	0.006	0.000	0.000	0.003	0.026	0.000

B. Electron Microprobe Data: Sulfides, Oxides, and Sulfates

BKUD09-148-33-5m-3-1	BK_99, 1025 masl	3	98.170	31.744	7.037	0.028	58.783	0.069	0.012	0.791	0.000	0.000	0.000	0.000	0.000	0.000	0.000
BKUD09-148-33-5m-3-2	BK_99, 1025 masl	3	97.798	31.431	5.801	0.008	60.086	0.090	0.011	0.658	0.000	0.000	0.000	0.000	0.000	0.010	0.000
BKUD09-148-33-5m-4-1	BK_99, 1025 masl	3	97.073	31.357	7.363	0.049	57.602	0.025	0.021	0.822	0.000	0.000	0.000	0.000	0.000	0.018	0.000
BKUD09-148-33-5m-4-5	BK_99, 1025 masl	3	97.619	31.714	7.221	0.010	58.018	0.000	0.006	0.755	0.000	0.000	0.000	0.000	0.008	0.006	0.000
BKUD09-148-33-5m-5-1	BK_99, 1025 masl	3	97.099	31.377	7.211	0.060	57.869	0.035	0.000	0.823	0.000	0.000	0.000	0.000	0.003	0.017	0.000
BKUD09-148-33-5m-6-1	BK_99, 1025 masl	3	96.405	31.079	6.847	0.000	57.875	0.000	0.000	0.832	0.000	0.000	0.000	0.000	0.000	0.000	0.000
BKUD09-148-33-5m-6-2	BK_99, 1025 masl	3	97.285	31.340	4.255	0.000	61.426	0.065	0.000	0.520	0.000	0.000	0.000	0.000	0.000	0.009	0.000
BKUD09-148-33-5m-7-1	BK_99, 1025 masl	3	97.857	31.567	7.275	0.024	58.356	0.056	0.000	0.631	0.000	0.000	0.000	0.057	0.000	0.000	0.000
BKUD09-148-33-5m-8-1	BK_99, 1025 masl	3	97.429	31.542	6.850	0.035	58.504	0.000	0.000	0.635	0.000	0.000	0.000	0.000	0.009	0.007	0.000
BKUD09-148-33-5m-9-1	BK_99, 1025 masl	3	97.342	31.466	9.260	0.136	55.532	0.084	0.008	0.836	0.000	0.000	0.000	0.000	0.001	0.011	0.000
BKUD09-148-33-5m-9-2	BK_99, 1025 masl	3	97.724	31.442	8.043	0.026	57.564	0.053	0.001	0.892	0.000	0.000	0.000	0.000	0.009	0.012	0.000
BKUD09-150-64-1m-1-1	BK_SW, 975 masl	3, 7	97.980	33.143	4.760	0.083	59.408	0.012	0.005	0.562	0.029	0.000	0.000	0.000	0.000	0.000	0.000
BKUD09-150-64-1m-2-2	BK_SW, 975 masl	3, 7	98.648	32.203	5.722	0.183	59.952	0.064	0.013	0.567	0.129	0.000	0.000	0.000	0.000	0.001	0.000
BKUD09-150-64-1m-2-3	BK_SW, 975 masl	3, 7	99.397	32.390	5.587	0.230	60.268	0.000	0.013	0.628	0.225	0.000	0.000	0.000	0.000	0.009	0.000
BKUD09-150-64-1m-3-1	BK_SW, 975 masl	3, 7	99.076	32.275	7.653	0.240	57.983	0.157	0.016	0.824	0.092	0.000	0.000	0.000	0.000	0.013	0.000
BKUD09-150-64-1m-3-6	BK_SW, 975 masl	3, 7	98.251	31.913	6.681	0.388	58.383	0.096	0.009	0.658	0.337	0.000	0.000	0.000	0.000	0.010	0.000
BKUD09-150-64-1m-4-1	BK_SW, 975 masl	3, 7	99.786	31.865	3.177	0.255	63.412	0.065	0.003	0.815	0.186	0.000	0.000	0.017	0.007	0.001	0.000
BKUD09-150-64-1m-5-2	BK_SW, 975 masl	3, 7	98.497	32.098	6.746	0.398	58.308	0.000	0.039	0.699	0.306	0.000	0.000	0.000	0.004	0.005	0.000
BKUD09-150-64-1m-6-1	BK_SW, 975 masl	3, 7	99.373	32.655	6.629	0.231	58.977	0.070	0.002	0.865	0.131	0.000	0.000	0.000	0.000	0.015	0.000
BKUD09-150-64-1m-7-1	BK_SW, 975 masl	3, 7	98.096	32.061	6.573	0.578	57.681	0.035	0.036	0.764	0.488	0.000	0.000	0.000	0.008	0.018	0.000
BKUD09-150-64-1m-8-4	BK_SW, 975 masl	3, 7	98.585	31.999	3.678	0.065	62.336	0.052	0.011	0.674	0.000	0.000	0.000	0.000	0.002	0.007	0.000
BKUD09-150-64-1m-9-2	BK_SW, 975 masl	3, 7	97.555	32.252	5.906	0.313	58.034	0.045	0.004	0.692	0.251	0.000	0.000	0.000	0.000	0.021	0.000
BKUD09-153-87-5m-2-1	BK_SW, 940 masl	3	100.983	35.882	5.920	0.037	58.448	0.027	0.019	0.571	0.000	0.000	0.000	0.015	0.000	0.000	0.139
BKUD09-153-87-5m-2-4	BK_SW, 940 masl	3	100.444	35.483	9.776	0.019	54.445	0.000	0.000	0.883	0.000	0.000	0.000	0.000	0.000	0.000	0.157
BKUD09-153-87-5m-2-6	BK_SW, 940 masl	3	100.955	35.800	7.664	0.088	56.517	0.039	0.003	0.913	0.000	0.000	0.000	0.000	0.003	0.000	0.119
BKUD09-153-87-5m-3-1	BK_SW, 940 masl	3	100.461	36.202	10.233	0.013	53.202	0.010	0.004	0.795	0.000	0.001	0.000	0.000	0.000	0.000	0.237
BKUD09-153-87-5m-3-2	BK_SW, 940 masl	3	100.397	35.910	10.075	0.023	53.605	0.037	0.004	0.734	0.000	0.000	0.000	0.000	0.000	0.000	0.108
BKUD09-153-87-5m-3-4	BK_SW, 940 masl	3	99.823	35.646	10.135	0.038	53.088	0.045	0.013	1.032	0.000	0.000	0.000	0.000	0.013	0.000	0.090

B. Electron Microprobe Data: Sulfides, Oxides, and Sulfates

BKUD09-153-87-5m-4-1	BK_SW, 940 masl	3	101.123	35.012	10.337	0.034	54.890	0.019	0.002	0.905	0.000	0.045	0.000	0.000	0.009	0.000	0.048
BKUD09-153-87-5m-4-2	BK_SW, 940 masl	3	101.534	34.944	3.643	0.000	62.569	0.019	0.012	0.627	0.000	0.021	0.000	0.000	0.000	0.000	0.023
BKUD09-153-87-5m-5-1	BK_SW, 940 masl	3	101.039	35.346	10.223	0.027	54.608	0.026	0.014	0.916	0.000	0.000	0.000	0.000	0.000	0.000	0.123
BKUD09-153-87-5m-5-2	BK_SW, 940 masl	3	100.949	35.058	10.249	0.015	55.063	0.027	0.024	0.704	0.000	0.000	0.000	0.000	0.004	0.000	0.058
BKUD09-153-87-5m-9-1	BK_SW, 940 masl	3	101.127	35.195	7.630	0.119	57.262	0.036	0.010	0.918	0.000	0.026	0.000	0.000	0.005	0.000	0.042
BKUD09-153-87-5m-9-4	BK_SW, 940 masl	3	101.912	35.302	6.533	0.107	59.363	0.025	0.005	0.646	0.000	0.000	0.000	0.000	0.001	0.000	0.210
BKUD09-153-87-5m-10-1	BK_SW, 940 masl	3	102.052	35.379	6.280	0.000	59.586	0.029	0.011	0.764	0.000	0.000	0.000	0.000	0.007	0.009	0.147
BKUD09-153-87-5m-10-2	BK_SW, 940 masl	3	101.658	36.149	10.479	0.060	54.295	0.015	0.000	0.654	0.000	0.000	0.000	0.067	0.006	0.000	0.018
BKUD09-157-93-8m_1-2	BK_SW, 930 masl	3	98.163	32.850	10.919	0.039	53.647	0.043	0.000	0.846	0.000	0.000	0.000	0.000	0.009	0.015	0.000
BKUD09-157-93-8m_3-1	BK_SW, 930 masl	3	99.188	33.472	10.272	0.038	54.695	0.008	0.000	0.951	0.000	0.000	0.000	0.000	0.000	0.009	0.000
BKUD09-157-93-8m_4-1	BK_SW, 930 masl	3	100.007	33.403	5.767	0.111	60.243	0.040	0.001	0.527	0.007	0.000	0.000	0.000	0.003	0.003	0.000
BKUD09-157-93-8m_5-1	BK_SW, 930 masl	3	98.825	33.276	8.605	0.024	56.353	0.031	0.010	0.822	0.000	0.000	0.000	0.000	0.000	0.002	0.000
BKUD09-157-93-8m_5-2	BK_SW, 930 masl	3	98.702	33.561	8.718	0.086	55.724	0.039	0.000	0.836	0.000	0.006	0.000	0.000	0.000	0.006	0.000
BKUD09-157-93-8m_6-1	BK_SW, 930 masl	3	98.727	33.489	10.068	0.042	54.537	0.041	0.001	0.846	0.000	0.000	0.000	0.000	0.000	0.000	0.000
BKUD09-157-93-8m_4-6	BK_SW, 930 masl	3	99.904	33.472	5.383	0.009	60.384	0.033	0.005	0.681	0.000	0.000	0.000	0.000	0.005	0.005	0.000
BKUD09-163-31-8m-4-1	BK_SW, 980 masl	2, 3	100.723	35.136	9.675	0.030	55.022	0.024	0.011	0.778	0.000	0.005	0.000	0.015	0.000	0.000	0.084
BKUD09-163-31-8m-4-2	BK_SW, 980 masl	2, 3	100.766	34.983	9.818	0.015	55.218	0.042	0.018	0.819	0.000	0.000	0.000	0.000	0.000	0.000	0.153
BKUD09-171-43-5m_1-1	BK_99, 990 masl	2, 3	98.249	33.288	4.867	0.020	60.375	0.053	0.000	0.060	0.000	0.000	0.000	0.000	0.002	0.000	0.000
BKUD09-171-43-5m_1-2	BK_99, 990 masl	2, 3	98.627	33.173	4.189	0.034	61.352	0.035	0.007	0.033	0.000	0.000	0.000	0.000	0.000	0.010	0.000
BKUD09-171-43-5m_2-1	BK_99, 990 masl	2, 3	98.508	33.607	8.429	0.021	56.622	0.032	0.021	0.151	0.000	0.021	0.000	0.000	0.000	0.000	0.000
BKUD09-171-43-5m_3-1	BK_99, 990 masl	2, 3	99.438	33.424	4.041	0.016	62.172	0.005	0.000	0.000	0.000	0.049	0.000	0.000	0.000	0.001	0.000
BKUD09-171-43-5m_3-4	BK_99, 990 masl	2, 3	98.914	33.366	6.892	0.036	58.462	0.017	0.015	0.033	0.000	0.000	0.000	0.013	0.000	0.017	0.000
BKUD09-171-43-5m_4-2	BK_99, 990 masl	2, 3	99.612	33.061	3.524	0.037	62.857	0.030	0.019	0.015	0.000	0.000	0.000	0.000	0.010	0.000	0.000
BKUD09-171-43-5m_4-3	BK_99, 990 masl	2, 3	99.258	32.836	3.862	0.012	62.556	0.015	0.021	0.025	0.000	0.002	0.000	0.000	0.005	0.000	0.000
BKUD09-171-43-5m_4-4	BK_99, 990 masl	2, 3	99.384	33.423	6.666	0.038	59.448	0.024	0.014	0.003	0.000	0.000	0.000	0.000	0.000	0.005	0.000
BKUD09-171-43-5m_5-1	BK_99, 990 masl	2, 3	99.578	33.641	6.970	0.031	58.863	0.018	0.028	0.056	0.000	0.000	0.000	0.000	0.000	0.014	0.000
BKUD09-171-43-5m_6-1	BK_99, 990 masl	2, 3	99.503	33.409	6.861	0.019	59.137	0.053	0.015	0.003	0.000	0.000	0.000	0.000	0.001	0.003	0.000
BKUD09-171-43-5m_6-2	BK_99, 990 masl	2, 3	99.758	33.682	7.733	0.003	58.455	0.011	0.006	0.015	0.000	0.000	0.000	0.010	0.002	0.000	0.000

B. Electron Microprobe Data: Sulfides, Oxides, and Sulfates

BKUD09-171-43-5m_6-3	BK_99, 990 masl	2, 3	99.000	33.379	7.363	0.036	58.369	0.075	0.027	0.000	0.000	0.000	0.000	0.000	0.000	0.008	0.000
BKUD09-171-43-5m_6-4	BK_99, 990 masl	2, 3	98.899	33.806	8.167	0.025	56.997	0.044	0.023	0.000	0.000	0.000	0.000	0.038	0.007	0.008	0.000
BKUD09-171-43-5m_7-1	BK_99, 990 masl	2, 3	98.752	33.596	9.484	0.004	55.671	0.000	0.001	0.068	0.000	0.000	0.000	0.000	0.006	0.000	0.000
n = 99	AVERAGE		99.220	33.394	7.475	0.073	57.775	0.034	0.009	0.575	0.025	0.003	0.000	0.002	0.003	0.005	0.025
	MINIMUM		96.405	31.079	3.177	0.000	53.088	0.000	0.000	0.000	0.000	0.000	0.000	0.000	0.000	0.000	0.000
	MAXIMUM		102.052	36.202	10.919	0.616	63.412	0.157	0.039	1.098	0.488	0.049	0.000	0.067	0.021	0.026	0.237
Galena: Stage 3 (and/or 2)																	
K08-155-132-5m_7-3	Onek	2, 3	100.851	13.854	0.226	0.006	2.524	0.024	1.083	0.000	0.000	0.006	84.94	0.000	0.016	0.000	0.000
BKUD09-140-9-9m-1-1	BK_SW	2, 3	102.753	14.024	0.037	0.075	0.036	0.012	0.046	0.000	0.000	0.161	88.56	0.000	0.000	0.010	0.000
BKUD09-140-9-9m-3-1	BK_SW	2, 3	100.561	14.097	0.023	0.007	0.000	0.023	0.576	0.061	0.000	0.676	85.16	0.000	0.000	0.000	0.000
BKUD09-140-9-9m-2-2	BK_SW	2, 3	101.046	14.562	0.086	0.014	0.507	0.023	0.501	0.000	0.000	0.062	85.48	0.000	0.000	0.007	0.000
BKUD09-140-9-9m-5-2	BK_SW	2, 3	100.767	14.134	0.082	0.006	0.626	0.012	0.345	0.082	0.000	0.130	85.60	0.000	0.010	0.000	0.000
BKUD09-140-9-9m-5-3	BK_SW	2, 3	101.582	14.150	0.033	0.000	0.256	0.015	0.100	0.000	0.008	0.205	87.06	0.000	0.014	0.000	0.000
BKUD09-144-36-6m-3-1	BK_SW, SW-end, 980 masl	2, 3/4a ?	101.287	14.355	0.315	0.013	0.607	0.020	0.369	0.000	0.000	0.000	85.91	0.000	0.007	0.013	0.000
BKUD09-144-36-6m-4-1	BK_SW, SW-end, 980 masl	2, 3/4a ?	100.637	14.398	0.037	0.010	0.000	0.028	0.706	0.082	0.000	0.083	85.41	0.000	0.006	0.000	0.000
BKUD09-144-36-6m-4-7	BK_SW, SW-end, 980 masl	2, 3/4a ?	99.380	14.159	0.008	0.000	0.000	0.031	0.721	0.000	0.000	0.085	84.44	0.000	0.000	0.000	0.000
BKUD09-144-36-6m-5-1	BK_SW, SW-end, 980 masl	2, 3/4a ?	99.658	14.291	0.022	0.015	0.007	0.019	0.785	0.009	0.000	0.042	84.57	0.000	0.000	0.000	0.000
BKUD09-144-36-6m-6-6	BK_SW, SW-end, 980 masl	2, 3/4a ?	102.161	14.549	0.193	0.210	2.534	0.018	0.842	0.000	0.000	0.000	83.93	0.000	0.000	0.013	0.000
BKUD09-144-36-6m-7-5	BK_SW, SW-end, 980 masl	2, 3/4a ?	99.253	14.123	0.487	0.021	0.012	0.046	0.748	0.076	0.073	0.000	83.727	0.000	0.000	0.010	0.000
BKUD09-157-93-8m_4-3	BK_SW, SW-end, 930 masl	2, 3	97.371	13.539	2.197	0.002	0.045	0.000	0.605	0.000	0.000	0.042	81.851	0.000	0.003	0.006	0.000
BKUD09-157-93-8m_6-3	BK_SW, SW-end, 930 masl	2, 3	99.823	13.560	1.672	0.000	0.000	0.024	0.355	0.000	0.014	0.020	85.159	0.000	0.000	0.001	0.000
BKUD09-157-93-8m_7-3	BK_SW, SW-end, 930 masl	2, 3	98.201	13.686	0.035	0.000	0.000	0.053	0.023	0.027	0.000	0.246	85.246	0.000	0.010	0.003	0.000

B. Electron Microprobe Data: Sulfides, Oxides, and Sulfates

n = 15	AVERAGE		100.355	14.099	0.364	0.025	0.477	0.023	0.520	0.022	0.006	0.117	85.137	0.000	0.004	0.004	0.000
	MINIMUM		97.371	13.539	0.008	0.000	0.000	0.000	0.023	0.000	0.000	0.000	81.851	0.000	0.000	0.000	0.000
	MAXIMUM		102.753	14.562	2.197	0.210	2.534	0.053	1.083	0.082	0.073	0.676	88.561	0.000	0.016	0.013	0.000
Sphalerite: stage 4a																	
BKUD09-134-41-35m-2-1-4	BK_SW, 1015 masl	4a	99.168	33.114	9.841	0.015	55.565	0.011	0.009	0.733	0.000	0.000	0.000	0.050	0.000	0.000	0.000
BKUD09-134-41-35m-2-2-3	BK_SW, 1015 masl	4a	99.238	33.268	9.907	0.095	55.392	0.017	0.007	0.940	0.000	0.000	0.000	0.000	0.000	0.005	0.000
BKUD09-134-41-35m-2-5-6	BK_SW, 1015 masl	4a	99.332	33.159	11.197	0.016	54.213	0.035	0.018	0.833	0.000	0.000	0.000	0.000	0.000	0.000	0.000
BKUD09-134-41-35m-2-6-5	BK_SW, 1015 masl	4a	99.978	33.540	9.848	0.022	55.832	0.025	0.000	0.876	0.000	0.000	0.000	0.000	0.000	0.000	0.000
BKUD09-134-41-35m-2-7-3	BK_SW, 1015 masl	4a	99.829	33.376	9.360	0.098	56.275	0.030	0.004	0.901	0.000	0.000	0.000	0.000	0.000	0.000	0.000
BKUD09-134-45m-2-2-4	BK_SW, 1015 masl	4a	99.701	32.633	5.255	0.062	61.279	0.011	0.018	0.492	0.000	0.000	0.000	0.070	0.000	0.006	0.000
BKUD09-134-45m-2-2-6	BK_SW, 1015 masl	4a	99.367	32.834	8.981	0.067	56.891	0.024	0.000	0.789	0.000	0.000	0.000	0.000	0.000	0.007	0.000
BKUD09-134-45m-2-3-6	BK_SW, 1015 masl	4a	99.551	32.877	8.120	0.068	58.028	0.002	0.011	0.740	0.000	0.000	0.000	0.000	0.000	0.000	0.000
BKUD09-134-45m-2-4-4	BK_SW, 1015 masl	4a	99.816	33.251	9.111	0.040	56.794	0.040	0.000	0.828	0.000	0.000	0.000	0.000	0.000	0.003	0.000
BKUD09-134-45m-2-5-2	BK_SW, 1015 masl	4a	99.573	32.569	8.409	0.142	57.777	0.028	0.005	0.897	0.000	0.000	0.000	0.000	0.000	0.000	0.000
BKUD09-134-45m-2-7-4	BK_SW, 1015 masl	4a	99.774	32.759	9.264	0.032	56.845	0.030	0.004	0.873	0.000	0.000	0.000	0.028	0.000	0.000	0.000
BKUD09-134-45m-2-9-4	BK_SW, 1015 masl	4a	99.373	32.950	7.251	0.017	58.587	0.027	0.000	0.625	0.000	0.000	0.000	0.014	0.000	0.000	0.000
BKUD09-134-45m-2-9-6	BK_SW, 1015 masl	4a	100.239	32.918	8.129	0.024	58.515	0.010	0.004	0.822	0.000	0.000	0.000	0.000	0.000	0.000	0.000
BKUD09-134-39-5m-1-3	BK_SW, 1015 masl	4a	100.311	33.303	7.845	0.104	58.259	0.004	0.035	0.814	0.000	0.000	0.000	0.041	0.000	0.000	0.000
BKUD09-134-39-5m-2-2	BK_SW, 1015 masl	4a	99.472	32.703	8.252	0.154	57.536	0.007	0.015	0.843	0.000	0.000	0.000	0.055	0.000	0.005	0.000
BKUD09-134-39-5m-3-5	BK_SW, 1015 masl	4a	100.379	32.948	5.067	0.088	61.756	0.026	0.000	0.615	0.000	0.000	0.000	0.000	0.000	0.000	0.000
BKUD09-134-39-5m-4-2	BK_SW, 1015 masl	4a	98.841	32.928	10.280	0.086	54.980	0.026	0.000	0.921	0.000	0.000	0.000	0.000	0.000	0.000	0.000
BKUD09-134-39-5m-5-4	BK_SW, 1015 masl	4a	99.130	32.366	8.276	1.607	55.941	0.043	0.034	0.905	0.000	0.000	0.000	0.000	0.000	0.004	0.000
BKUD09-134-39-5m-5-7	BK_SW, 1015 masl	4a	99.229	32.782	9.412	0.081	55.974	0.025	0.017	1.003	0.000	0.000	0.000	0.032	0.000	0.000	0.000
BKUD09-134-39-5m-6-5	BK_SW, 1015 masl	4a	98.963	32.786	11.114	0.158	54.241	0.020	0.027	0.756	0.000	0.031	0.000	0.000	0.000	0.000	0.000
BKUD09-134-39-5m-6-6	BK_SW, 1015 masl	4a	98.178	32.620	8.125	0.136	56.708	0.014	0.020	0.840	0.000	0.000	0.000	0.000	0.000	0.009	0.000
BKUD09-134-39-5m-9-3	BK_SW, 1015 masl	4a	98.789	32.644	10.751	0.082	54.593	0.038	0.002	0.952	0.000	0.000	0.000	0.000	0.000	0.000	0.000

B. Electron Microprobe Data: Sulfides, Oxides, and Sulfates

BKUD09-134-39-5m-10-5	BK_SW, 1015 masl	4a	99.172	32.557	7.712	0.122	58.236	0.021	0.000	0.824	0.000	0.000	0.000	0.000	0.000	0.000	0.000
BKUD09-134-39-5m-10-7	BK_SW, 1015 masl	4a	98.721	32.155	8.499	0.050	57.072	0.032	0.000	0.971	0.000	0.000	0.000	0.000	0.000	0.000	0.000
BKUD09-134-41-35m-1-1-5	BK_SW, 1015 masl	4a	99.423	32.862	9.895	0.088	55.934	0.018	0.000	1.023	0.000	0.000	0.000	0.000	0.000	0.001	0.000
BKUD09-134-41-35m-1-2-8	BK_SW, 1015 masl	4a	99.340	32.968	11.290	0.026	54.268	0.035	0.000	0.903	0.000	0.027	0.000	0.000	0.000	0.000	0.000
BKUD09-134-41-35m-1-4-5	BK_SW, 1015 masl	4a	99.239	33.009	11.430	0.067	53.923	0.028	0.000	0.985	0.000	0.000	0.000	0.000	0.000	0.000	0.000
BKUD09-134-41-35m-1-5-5	BK_SW, 1015 masl	4a	99.596	32.896	9.402	0.027	56.653	0.009	0.000	0.859	0.000	0.021	0.000	0.000	0.000	0.000	0.000
BKUD09-134-41-35m-1-6-2	BK_SW, 1015 masl	4a	99.109	32.766	10.243	0.036	55.406	0.033	0.002	0.923	0.000	0.000	0.000	0.000	0.000	0.000	0.000
BKUD09-134-41-35m-1-7-1	BK_SW, 1015 masl	4a	98.859	32.893	11.548	0.068	53.744	0.014	0.029	0.811	0.000	0.000	0.000	0.000	0.000	0.004	0.000
BKUD09-143-51-2m-1-4	BK_SW, 1005 masl	4a	96.603	31.490	10.111	0.009	54.537	0.002	0.011	0.822	0.000	0.000	0.000	0.000	0.004	0.006	0.000
BKUD09-143-51-2m-1-5	BK_SW, 1005 masl	4a	97.725	31.610	9.202	0.011	55.989	0.010	0.000	0.867	0.000	0.001	0.000	0.020	0.000	0.017	0.000
BKUD09-143-51-2m-4-4	BK_SW, 1005 masl	4a	96.588	30.667	7.756	0.090	57.221	0.136	0.011	0.660	0.000	0.000	0.000	0.000	0.008	0.018	0.000
BKUD09-143-51-2m-4-6	BK_SW, 1005 masl	4a	97.319	30.984	8.071	0.006	57.411	0.027	0.001	0.807	0.000	0.015	0.000	0.046	0.000	0.000	0.000
BKUD09-143-51-2m-5-2	BK_SW, 1005 masl	4a	96.925	31.317	9.460	0.039	55.397	0.000	0.000	0.855	0.000	0.000	0.000	0.000	0.000	0.011	0.000
BKUD09-143-51-2m-5-4	BK_SW, 1005 masl	4a	97.220	31.119	9.991	0.003	55.366	0.033	0.009	0.820	0.000	0.000	0.000	0.000	0.000	0.007	0.000
BKUD09-143-51-2m-5-5	BK_SW, 1005 masl	4a	96.592	31.534	8.303	0.031	56.074	0.084	0.000	0.882	0.000	0.000	0.000	0.000	0.016	0.000	0.000
BKUD09-143-51-2m-6-4	BK_SW, 1005 masl	4a	97.322	30.916	8.070	0.015	57.770	0.105	0.007	0.690	0.000	0.000	0.000	0.000	0.010	0.006	0.000
BKUD09-143-51-2m-8-3	BK_SW, 1005 masl	4a	97.316	31.186	6.875	0.000	58.848	0.072	0.000	0.610	0.000	0.000	0.000	0.000	0.000	0.006	0.000
BKUD09-143-51-2m-11-2	BK_SW, 1005 masl	4a	97.141	31.319	7.986	0.022	57.063	0.070	0.000	0.778	0.000	0.038	0.000	0.000	0.000	0.013	0.000
BKUD09-146-46-5m-2-2	BK_SW, 970 masl	4a	97.490	31.606	8.997	0.046	55.992	0.092	0.009	0.829	0.000	0.000	0.000	0.000	0.013	0.002	0.000
BKUD09-146-46-5m-3-3	BK_SW, 970 masl	4a	97.514	31.693	9.280	0.061	55.728	0.000	0.000	0.905	0.000	0.000	0.000	0.000	0.000	0.000	0.000
BKUD09-146-46-5m-4-4	BK_SW, 970 masl	4a	95.981	31.427	8.332	0.155	55.483	0.076	0.000	0.892	0.000	0.000	0.000	0.000	0.013	0.009	0.000
BKUD09-146-46-5m-5-1	BK_SW, 970 masl	4a	96.221	31.277	10.416	0.036	53.774	0.055	0.000	0.892	0.000	0.000	0.000	0.000	0.001	0.000	0.000
EAG_047_1-1	Eagle, surface	4a	99.287	33.399	9.388	0.046	56.498	0.068	0.001	0.065	0.000	0.000	0.000	0.000	0.005	0.006	0.000
EAG_047_2-1	Eagle, surface	4a	97.196	33.017	8.643	0.913	54.920	0.059	0.007	0.003	0.000	0.000	0.000	0.000	0.000	0.001	0.000
EAG_047_2-2	Eagle, surface	4a	99.605	33.336	8.166	0.012	58.018	0.000	0.001	0.037	0.000	0.000	0.000	0.000	0.000	0.009	0.000
EAG_047_3-1	Eagle, surface	4a	98.893	33.076	8.934	0.011	56.983	0.027	0.000	0.028	0.000	0.021	0.000	0.000	0.000	0.013	0.000

B. Electron Microprobe Data: Sulfides, Oxides, and Sulfates

EAG_047_3-3	Eagle, surface	4a	98.810	32.899	5.524	0.047	60.545	0.024	0.002	0.000	0.000	0.017	0.000	0.000	0.002	0.000	0.000
EAG_047_4-1	Eagle, surface	4a	98.618	32.963	9.254	0.019	56.651	0.025	0.005	0.000	0.000	0.000	0.000	0.000	0.007	0.008	0.000
EAG_047_4-2	Eagle, surface	4a	98.531	33.051	8.226	0.023	57.349	0.020	0.022	0.000	0.000	0.000	0.000	0.000	0.000	0.002	0.000
EAG_047_5-1	Eagle, surface	4a	98.621	33.423	7.831	0.085	57.247	0.037	0.001	0.000	0.000	0.036	0.000	0.031	0.007	0.008	0.000
n = 52	AVERAGE		98.639	32.495	8.897	0.103	56.578	0.033	0.007	0.706	0.000	0.004	0.000	0.007	0.002	0.004	0.000
	MINIMUM		95.981	30.667	5.067	0.000	53.744	0.000	0.000	0.000	0.000	0.000	0.000	0.000	0.000	0.000	0.000
	MAXIMUM		100.379	33.540	11.548	1.607	61.756	0.136	0.035	1.023	0.000	0.038	0.000	0.070	0.016	0.018	0.000
Galena: stage 4a																	
EAG_047_1-4	Eagle, surface	4a	101.615	13.570	0.040	0.000	0.023	0.009	0.799	0.000	0.012	0.682	87.776	0.000	0.011	0.000	0.000
EAG_047_2-3	Eagle, surface	4a	100.263	13.311	0.053	0.000	0.055	0.055	0.260	0.000	0.000	0.369	87.600	0.000	0.000	0.000	0.000
EAG_047_2-5	Eagle, surface	4a	101.468	13.589	0.567	0.000	0.064	0.039	0.140	0.000	0.000	0.273	88.240	0.000	0.000	0.000	0.000
EAG_047_2-6	Eagle, surface	4a	101.443	13.219	0.029	0.002	0.000	0.054	0.243	0.000	0.042	0.410	88.638	0.000	0.000	0.004	0.000
EAG_047_3-4	Eagle, surface	4a	100.173	13.284	0.035	0.000	0.029	0.034	0.000	0.000	0.000	0.168	88.068	0.000	0.014	0.000	0.000
EAG_047_4-4	Eagle, surface	4a	102.012	13.741	0.052	0.000	0.025	0.013	0.036	0.000	0.000	0.125	89.276	0.000	0.016	0.006	0.000
EAG_047_5-2	Eagle, surface	4a	99.594	13.568	0.087	0.018	0.186	0.027	0.070	0.000	0.000	0.179	86.897	0.000	0.007	0.000	0.000
EAG_047_6-2	Eagle, surface	4a	101.162	13.439	0.062	0.000	0.000	0.042	0.414	0.000	0.000	0.688	87.474	0.000	0.003	0.000	0.000
EAG_047_7-2	Eagle, surface	4a	101.535	13.452	0.304	0.024	0.018	0.057	0.070	0.000	0.000	0.209	88.447	0.000	0.000	0.000	0.000
EAG_047_7-4	Eagle, surface	4a	101.378	13.527	0.968	0.017	0.125	0.092	0.103	0.000	0.000	0.208	87.788	0.000	0.000	0.000	0.000
K07-95-402-1m_4-2	BK_E, 860 masl	4a?	96.419	13.742	0.669	0.001	0.000	0.045	1.727	0.117	0.000	0.000	80.195	0.908	0.001	0.003	0.000
K07-95-402-1m_5-4	BK_E, 860 masl	4a?	100.723	13.639	1.566	0.000	0.290	0.000	0.043	0.000	0.000	0.081	86.084	0.000	0.000	0.011	0.000
BKUD09-134-41-35m-2-1-7	BK_SW, Mid, 965 masl	4a	98.386	13.850	0.709	0.008	0.000	0.000	0.547	0.077	0.000	0.115	84.012	0.000	0.000	0.000	0.000
BKUD09-134-41-35m-2-2-5	BK_SW, Mid, 965 masl	4a	100.933	13.679	1.848	0.003	0.035	0.011	0.801	0.000	0.000	0.043	85.484	0.000	0.000	0.005	0.000
BKUD09-134-41-35m-2-3-3	BK_SW, Mid, 965 masl	4a	96.392	13.771	0.093	0.001	0.001	0.005	1.967	0.094	0.000	0.126	79.911	1.262	0.000	0.000	0.000
BKUD09-134-41-35m-2-6-4	BK_SW, Mid, 965 masl	4a	98.941	13.781	0.546	0.004	0.074	0.016	0.766	0.000	0.000	0.212	84.402	0.000	0.000	0.007	0.000
BKUD09-134-41-35m-2-6-6	BK_SW, Mid, 965 masl	4a	98.149	13.776	0.841	0.000	0.139	0.000	2.083	0.117	0.000	0.000	80.322	1.708	0.000	0.000	0.000
BKUD09-134-41-35m-2-9-4	BK_SW, Mid, 965 masl	4a	99.269	13.439	2.356	0.000	0.010	0.007	0.996	0.035	0.000	0.000	83.405	0.000	0.000	0.000	0.000

B. Electron Microprobe Data: Sulfides, Oxides, and Sulfates

BKUD09-134-41-35m-2-9-5	BK_SW, Mid, 965 masl	4a	101.902	13.540	0.277	0.195	0.182	0.003	0.025	0.000	0.002	0.105	88.487	0.000	0.000	0.006	0.000
BKUD09-134-41-35m-2-10-7	BK_SW, Mid, 965 masl	4a	99.105	13.448	2.141	0.000	0.000	0.000	1.033	0.000	0.000	0.000	83.821	0.000	0.000	0.000	0.000
BKUD09-134-45m-2-1-3	BK_SW, Mid, 965 masl	4a	98.128	13.056	2.089	0.000	0.000	0.081	0.657	0.183	0.000	0.000	82.956	0.000	0.000	0.016	0.000
BKUD09-134-45m-2-1-4	BK_SW, Mid, 965 masl	4a	96.439	13.544	0.093	0.000	0.000	0.000	2.191	0.000	0.000	0.025	79.341	2.067	0.000	0.000	0.000
BKUD09-134-45m-2-2-5	BK_SW, Mid, 965 masl	4a	98.424	13.751	1.311	0.009	0.034	0.000	2.584	0.202	0.000	0.000	78.517	2.998	0.000	0.002	0.000
BKUD09-134-45m-2-2-7	BK_SW, Mid, 965 masl	4a	100.967	13.402	0.568	0.015	0.102	0.019	0.244	0.029	0.006	0.340	86.981	0.000	0.000	0.017	0.000
BKUD09-134-45m-2-3-9	BK_SW, Mid, 965 masl	4a	100.091	13.395	0.081	0.024	0.406	0.000	0.268	0.000	0.000	0.386	86.288	0.000	0.000	0.012	0.000
BKUD09-134-45m-2-4-5	BK_SW, Mid, 965 masl	4a	101.308	13.549	0.599	0.009	0.358	0.000	0.296	0.000	0.027	0.319	87.096	0.000	0.000	0.000	0.000
BKUD09-134-45m-2-5-4	BK_SW, Mid, 965 masl	4a	98.077	13.651	0.349	0.032	0.004	0.000	2.869	0.082	0.000	0.006	78.344	3.504	0.000	0.000	0.000
BKUD09-134-45m-2-9-5	BK_SW, Mid, 965 masl	4a	98.216	13.486	0.408	0.006	0.002	0.000	1.943	0.000	0.000	0.000	81.945	1.394	0.000	0.012	0.000
BKUD09-134-39-5m-1-6	BK_SW, Mid, 965 masl	4a	99.761	13.759	0.254	0.000	0.940	0.000	1.623	0.044	0.000	0.042	83.257	0.690	0.000	0.026	0.000
BKUD09-134-39-5m-2-6	BK_SW, Mid, 965 masl	4a	98.486	13.116	2.617	0.000	0.412	0.784	2.399	0.000	0.000	0.000	78.381	1.656	0.000	0.000	0.000
BKUD09-134-39-5m-2-8	BK_SW, Mid, 965 masl	4a	100.322	13.390	0.076	0.006	0.043	0.000	0.857	0.000	0.000	0.086	86.827	0.000	0.000	0.011	0.000
BKUD09-134-39-5m-3-4	BK_SW, Mid, 965 masl	4a	100.284	13.429	0.680	0.000	0.013	0.000	0.706	0.021	0.000	0.149	86.055	0.000	0.000	0.001	0.000
BKUD09-134-39-5m-4-3	BK_SW, Mid, 965 masl	4a	101.303	13.036	0.227	0.028	2.657	0.000	2.076	0.000	0.000	0.004	81.889	1.998	0.000	0.033	0.000
BKUD09-134-39-5m-4-5	BK_SW, Mid, 965 masl	4a	100.562	13.465	1.466	0.000	0.011	0.007	0.624	0.000	0.000	0.039	85.796	0.000	0.000	0.000	0.000
BKUD09-134-39-5m-5-6	BK_SW, Mid, 965 masl	4a	100.620	13.471	0.271	0.000	0.000	0.005	0.784	0.000	0.000	0.063	86.962	0.000	0.000	0.000	0.000
BKUD09-134-39-5m-7-5	BK_SW, Mid, 965 masl	4a	98.210	13.281	0.375	0.016	0.000	0.004	1.957	0.033	0.000	0.000	81.792	1.636	0.000	0.002	0.000
BKUD09-134-39-5m-10-2	BK_SW, Mid, 965 masl	4a	98.526	13.318	0.231	0.012	0.001	0.000	0.647	0.000	0.003	0.087	84.990	0.000	0.000	0.000	0.000
BKUD09-134-41-35m-1-1-4	BK_SW, Mid, 965 masl	4a	100.753	13.246	0.386	0.000	0.001	0.000	0.807	0.000	0.000	0.036	87.111	0.000	0.000	0.000	0.000
BKUD09-134-41-35m-1-1-6	BK_SW, Mid, 965 masl	4a	100.021	13.334	0.153	0.008	1.255	0.000	0.981	0.000	0.000	0.071	85.512	0.000	0.000	0.006	0.000
BKUD09-134-41-35m-1-3-6	BK_SW, Mid, 965 masl	4a	99.553	13.295	0.393	0.000	0.008	0.000	1.053	0.000	0.000	0.008	85.683	0.000	0.000	0.005	0.000
BKUD09-134-41-35m-1-4-4	BK_SW, Mid, 965 masl	4a	98.688	13.050	1.141	0.000	0.000	0.000	2.052	0.069	0.000	0.000	81.665	1.491	0.000	0.000	0.000

B. Electron Microprobe Data: Sulfides, Oxides, and Sulfates

BKUD09-134-41-35m-1-5-8	BK_SW, Mid, 965 masl	4a	97.407	13.458	0.044	0.010	0.000	0.000	2.127	0.062	0.000	0.079	80.380	2.084	0.000	0.000	0.000
BKUD09-134-41-35m-1-5-9	BK_SW, Mid, 965 masl	4a	97.235	13.442	0.036	0.001	0.109	0.001	2.051	0.075	0.000	0.106	80.378	1.845	0.000	0.004	0.000
BKUD09-134-41-35m-1-5-10	BK_SW, Mid, 965 masl	4a	97.248	13.610	0.380	0.000	0.011	0.000	2.037	0.063	0.000	0.086	80.514	1.341	0.000	0.000	0.000
BKUD09-134-41-35m-1-5-11	BK_SW, Mid, 965 masl	4a	97.693	13.206	0.123	0.007	0.000	0.002	1.175	0.000	0.000	0.000	84.313	0.000	0.000	0.000	0.000
BKUD09-134-41-35m-1-6-5	BK_SW, Mid, 965 masl	4a	97.449	13.245	0.010	0.004	0.000	0.015	2.049	0.133	0.000	0.062	80.824	1.955	0.000	0.005	0.000
BKUD09-134-41-35m-1-6-6	BK_SW, Mid, 965 masl	4a	96.582	13.351	0.042	0.001	0.000	0.000	2.209	0.000	0.000	0.000	79.583	2.332	0.000	0.000	0.000
BKUD09-134-41-35m-1-6-7	BK_SW, Mid, 965 masl	4a	98.301	13.218	0.129	0.009	0.019	0.000	1.675	0.112	0.000	0.030	82.823	1.182	0.000	0.000	0.000
BKUD09-134-41-35m-1-7-3	BK_SW, Mid, 965 masl	4a	99.269	13.249	1.039	0.007	0.954	0.000	2.889	0.154	0.000	0.000	78.294	3.542	0.000	0.004	0.000
BKUD09-143-51-2m-1-3	BK_SW, NE-end, 1000 masl	4a	99.383	13.011	0.008	0.012	0.027	0.061	0.229	0.000	0.000	0.150	86.798	0.000	0.003	0.000	0.000
BKUD09-143-51-2m-2-5	BK_SW, NE-end, 1000 masl	4a	98.974	12.847	1.979	0.013	0.000	0.756	0.600	0.000	0.000	0.074	83.687	0.000	0.000	0.000	0.000
BKUD09-143-51-2m-4-5	BK_SW, NE-end, 1000 masl	4a	100.735	12.709	1.021	0.008	0.010	0.054	0.364	0.102	0.000	0.000	87.435	0.000	0.000	0.001	0.000
BKUD09-143-51-2m-4-7	BK_SW, NE-end, 1000 masl	4a	99.251	13.221	0.581	0.016	0.891	0.027	0.876	0.000	0.000	0.443	84.579	0.000	0.009	0.006	0.000
BKUD09-143-51-2m-7-3	BK_SW, NE-end, 1000 masl	4a	97.292	12.730	0.346	0.003	0.002	0.090	1.114	0.035	0.022	0.045	83.910	0.000	0.000	0.001	0.000
BKUD09-143-51-2m-8-6	BK_SW, NE-end, 1000 masl	4a	101.166	12.612	0.133	0.000	0.000	0.081	0.879	0.000	0.000	0.894	87.470	0.000	0.000	0.000	0.000
BKUD09-146-46-5m-1-1	BK_SW, SW-end, 970 masl	4a	97.586	12.919	0.088	0.020	0.007	0.119	0.613	0.168	0.007	0.004	84.572	0.000	0.000	0.000	0.000
BKUD09-146-46-5m-1-4	BK_SW, SW-end, 970 masl	4a	98.900	12.650	0.177	0.009	0.000	0.100	0.494	0.026	0.000	0.090	86.524	0.000	0.007	0.006	0.000
BKUD09-146-46-5m-3-5	BK_SW, SW-end, 970 masl	4a	98.230	12.897	0.465	0.002	0.000	0.121	0.667	0.000	0.006	0.056	84.995	0.000	0.002	0.000	0.000
BKUD09-146-46-5m-3-6	BK_SW, SW-end, 970 masl	4a	100.251	12.435	0.042	0.000	0.000	0.077	0.611	0.000	0.000	0.075	88.204	0.000	0.000	0.018	0.000
BKUD09-146-46-5m-4-1	BK_SW, SW-end, 970 masl	4a	96.340	12.963	0.043	0.003	0.007	0.052	1.193	0.076	0.000	0.093	82.669	0.156	0.013	0.002	0.000
BKUD09-146-46-5m-7-1	BK_SW, SW-end, 970 masl	4a	96.890	12.908	0.104	0.000	0.006	0.050	1.075	0.058	0.000	0.511	83.164	0.000	0.000	0.011	0.000
BKUD09-146-46-5m-8-1	BK_SW, SW-end, 970 masl	4a	97.626	12.716	0.066	0.000	0.000	0.047	1.245	0.047	0.000	0.058	84.337	0.153	0.008	0.000	0.000
n = 62	AVERAGE		99.249	13.319	0.546	0.009	0.154	0.049	1.063	0.036	0.002	0.137	84.341	0.579	0.001	0.004	0.000
	MINIMUM		96.340	12.435	0.008	0.000	0.000	0.000	0.000	0.000	0.000	0.000	78.294	0.000	0.000	0.000	0.000

B. Electron Microprobe Data: Sulfides, Oxides, and Sulfates

	MAXIMUM		102.012	13.850	2.617	0.195	2.657	0.784	2.889	0.202	0.042	0.894	89.276	3.542	0.016	0.033	0.000
Sphalerite: stage 7																	
Alice_1-7	Alice, surface	6, 7, 8	98.643	32.936	1.719	0.001	64.014	0.030	0.000	0.010	0.000	0.000	0.000	0.042	0.012	0.000	0.000
Alice_2-4	Alice, surface	6, 7, 8	99.096	32.850	0.733	0.000	65.772	0.029	0.010	0.000	0.000	0.000	0.000	0.000	0.001	0.000	0.000
Alice_2-7	Alice, surface	6, 7, 8	97.738	32.945	2.907	0.038	61.878	0.048	0.012	0.099	0.000	0.000	0.000	0.000	0.013	0.014	0.000
Alice_3-6	Alice, surface	6, 7, 8	98.465	33.096	1.862	0.413	62.623	0.011	0.000	0.053	0.452	0.006	0.000	0.000	0.006	0.000	0.000
Alice_4-3	Alice, surface	6, 7, 8	97.900	32.999	3.277	0.044	61.808	0.066	0.000	0.000	0.000	0.002	0.000	0.000	0.000	0.001	0.000
Alice_5-3	Alice, surface	6, 7, 8	97.875	32.974	3.515	0.034	61.436	0.014	0.000	0.033	0.000	0.000	0.000	0.010	0.005	0.005	0.000
Alice-5-10	Alice, surface	6, 7, 8	98.491	32.928	3.562	0.081	60.692	0.031	0.001	0.857	0.000	0.000	0.000	0.000		0.000	0.032
Alice_6-3	Alice, surface	6, 7, 8	98.506	33.191	1.588	0.000	63.901	0.013	0.000	0.036	0.000	0.011	0.000	0.000	0.001	0.000	0.000
Alice_7-1	Alice, surface	6, 7, 8	97.663	32.646	1.204	0.010	63.839	0.039	0.020	0.056	0.000	0.011	0.000	0.016	0.000	0.000	0.000
Alice_8-3	Alice, surface	6, 7, 8	97.763	33.221	2.224	0.256	61.956	0.023	0.024	0.000	0.314	0.000	0.000	0.000	0.000	0.005	0.000
Alice_8-10	Alice, surface	6, 7, 8	97.420	32.885	1.789	0.077	62.349	0.041	0.061	0.000	0.050	0.054	0.000	0.000	0.000	0.000	0.000
WRN_008_3-7	Wernecke, surface	6, 7, 8	98.413	32.773	4.112	1.716	59.872	0.022	0.014	0.017	0.000	0.002	0.000	0.000	0.001	0.007	0.000
WRN-008-3-9	Wernecke, surface	6, 7, 8	98.638	32.684	3.493	0.557	60.796	0.070	0.028	1.204	0.000	0.028	0.000	0.000		0.000	0.060
WRN-008-3-15	Wernecke, surface	6, 7, 8	99.707	31.848	3.482	3.265	54.308	0.060	2.329	1.143	0.000	2.865	0.629	0.000		0.000	0.000
BRM_044_1-4	Bermingham, surface	6, 7, 8, 10	99.604	33.210	3.346	0.009	62.842	0.051	0.000	0.032	0.000	0.023	0.000	0.000	0.006	0.000	0.000
BRM_044_3-3	Bermingham, surface	6, 7, 8, 10	99.243	33.331	3.646	0.000	62.585	0.008	0.000	0.000	0.000	0.003	0.000	0.000	0.000	0.000	0.000
BRM-044-3-8	Bermingham, surface	6, 7, 8, 10	98.887	32.955	3.694	0.000	61.830	0.038	0.000	0.518	0.000	0.000	0.000	0.000		0.009	0.009
BRM_044_4-4	Bermingham, surface	6, 7, 8, 10	99.199	32.774	3.771	0.000	62.722	0.059	0.016	0.068	0.000	0.000	0.000	0.000	0.000	0.001	0.000
BRM_044_5-4	Bermingham, surface	6, 7, 8, 10	98.862	32.881	4.268	0.002	61.911	0.021	0.000	0.010	0.000	0.000	0.000	0.000	0.000	0.008	0.000
BRM_044_6-3	Bermingham, surface	6, 7, 8, 10	99.101	32.873	3.443	0.004	62.787	0.059	0.000	0.012	0.000	0.000	0.000	0.000	0.003	0.001	0.000
BRM_044_7-4	Bermingham, surface	6, 7, 8, 10	99.302	33.026	3.473	0.000	62.806	0.050	0.020	0.077	0.000	0.000	0.000	0.000	0.004	0.000	0.000
HOM_053-1_3-1	Homestake, surface	1, 7, 8	98.778	32.345	3.874	0.010	62.659	0.022	0.000	0.098	0.000	0.000	0.000	0.000	0.008	0.000	0.000
HOM_053-1_3-2	Homestake, surface	1, 7, 8	98.973	32.832	1.650	0.251	64.156	0.056	0.010	0.000	0.125	0.016	0.000	0.000	0.000	0.000	0.000

B. Electron Microprobe Data: Sulfides, Oxides, and Sulfates

HOM_053-1_5-1	Homestake, surface	1, 7, 8	98.666	33.064	1.388	0.048	64.450	0.040	0.000	0.010	0.000	0.000	0.000	0.000	0.000	0.007	0.000
HOM-053-1-5-7	Homestake, surface	1, 7, 8	100.230	33.474	0.745	0.055	64.902	0.030	0.000	1.010	0.000	0.009	0.077	0.000		0.005	0.042
POR_056_1-1	Porcupine, surface	7	98.086	32.880	1.335	0.000	63.955	0.020	0.026	0.005	0.000	0.002	0.000	0.000	0.002	0.000	0.000
POR_056_1-5	Porcupine, surface	7	98.967	32.910	5.006	0.000	60.850	0.052	0.000	0.096	0.000	0.000	0.000	0.000	0.003	0.008	0.000
POR_056_2-1	Porcupine, surface	7	98.263	32.736	4.337	0.018	61.252	0.054	0.000	0.101	0.000	0.018	0.000	0.000	0.000	0.000	0.000
POR_056_3-1	Porcupine, surface	7	99.189	32.942	4.117	0.004	62.266	0.066	0.000	0.048	0.008	0.000	0.000	0.000	0.005	0.002	0.000
POR_056_4-5	Porcupine, surface	7	99.420	32.996	4.416	0.013	62.190	0.080	0.000	0.000	0.000	0.000	0.000	0.000	0.000	0.000	0.000
POR_056_5-5	Porcupine, surface	7	99.043	32.907	4.432	0.000	61.946	0.022	0.005	0.043	0.000	0.014	0.000	0.000	0.000	0.007	0.000
POR_056_6-2	Porcupine, surface	7	99.516	32.583	1.336	0.222	64.924	0.049	0.000	0.071	0.267	0.000	0.000	0.000	0.000	0.008	0.000
POR_056_7-1	Porcupine, surface	7	98.743	32.682	0.833	0.014	65.364	0.033	0.000	0.010	0.000	0.000	0.000	0.000	0.000	0.004	0.000
K07-76-125m-1-3	BK_E, 965 masl	7	99.466	32.587	4.587	0.117	61.544	0.000	0.006	0.706	0.024	0.000	0.000	0.000	0.000	0.014	0.000
K07-76-125m-1-4	BK_E, 965 masl	7	98.452	32.101	3.242	0.078	62.474	0.112	0.032	0.496	0.012	0.053	0.000	0.000	0.004	0.000	0.000
K07-76-125m-2-3	BK_E, 965 masl	7	99.579	32.443	4.726	0.200	61.270	0.075	0.020	0.743	0.199	0.000	0.000	0.000	0.007	0.010	0.000
K07-76-125m-2-4	BK_E, 965 masl	7	99.714	32.418	4.923	0.170	61.348	0.064	0.000	0.698	0.101	0.000	0.000	0.000	0.000	0.004	0.000
K07-76-125m-3-3	BK_E, 965 masl	7	99.270	32.624	4.259	0.064	61.878	0.006	0.029	0.571	0.017	0.000	0.000	0.000	0.004	0.000	0.000
K07-76-125m-3-4	BK_E, 965 masl	7	98.938	32.258	4.530	0.007	61.669	0.093	0.000	0.659	0.000	0.000	0.000	0.000	0.000	0.001	0.000
K07-76-125m-3-5	BK_E, 965 masl	7	99.327	32.366	4.046	0.002	62.495	0.060	0.008	0.667	0.000	0.000	0.000	0.000	0.000	0.016	0.000
K07-76-125m-4-3	BK_E, 965 masl	7	99.427	32.240	4.227	0.014	62.401	0.087	0.000	0.597	0.000	0.000	0.000	0.000	0.000	0.000	0.000
K07-76-125m-4-4	BK_E, 965 masl	7	99.255	32.099	4.741	0.075	61.689	0.081	0.011	0.619	0.010	0.000	0.000	0.000	0.003	0.000	0.000
K07-76-125m-5-4	BK_E, 965 masl	7	99.632	32.869	5.447	0.281	59.841	0.055	0.009	0.718	0.221	0.000	0.000	0.000	0.002	0.005	0.000
K07-76-125m-5-5	BK_E, 965 masl	7	98.810	32.263	5.724	0.442	59.374	0.004	0.012	0.740	0.313	0.000	0.000	0.000	0.000	0.011	0.000
K07-76-125m-6-4	BK_E, 965 masl	7	99.044	32.187	5.643	0.287	59.790	0.092	0.028	0.738	0.159	0.000	0.000	0.000	0.003	0.009	0.000
K07-76-125m-6-5	BK_E, 965 masl	7	98.947	32.359	5.562	0.527	59.467	0.000	0.031	0.702	0.428	0.000	0.000	0.000	0.000	0.000	0.000
K07-76-125m-7-5	BK_E, 965 masl	7	99.570	32.457	4.669	0.086	61.607	0.058	0.015	0.723	0.020	0.000	0.000	0.000	0.000	0.000	0.000
K07-76-125m-7-6	BK_E, 965 masl	7	99.358	32.138	5.307	0.496	60.511	0.080	0.004	0.675	0.353	0.000	0.000	0.000	0.005	0.000	0.000
K07-76-125m-9-2	BK_E, 965 masl	7	99.580	32.266	4.745	0.191	61.563	0.099	0.001	0.531	0.177	0.000	0.000	0.000	0.000	0.006	0.000
K07-76-125m-10-1	BK_E, 965 masl	7	99.305	32.357	4.729	0.235	61.215	0.039	0.000	0.754	0.128	0.008	0.000	0.000	0.000	0.002	0.000

B. Electron Microprobe Data: Sulfides, Oxides, and Sulfates

K07-76-125m-10-2	BK_E, 965 masl	7	99.154	32.910	5.398	0.192	60.026	0.041	0.026	0.773	0.000	0.000	0.000	0.000	0.004	0.020	0.000
K07-76-125m-10-6	BK_E, 965 masl	7	98.112	31.959	5.455	0.521	58.773	0.129	0.035	0.766	0.317	0.000	0.000	0.000	0.007	0.000	0.000
K07-76-125m-10-7	BK_E, 965 masl	7	99.315	32.456	4.753	0.191	61.306	0.085	0.013	0.603	0.118	0.000	0.000	0.000	0.015	0.000	0.000
K07-76-125m-11-2	BK_E, 965 masl	7	98.814	32.138	4.907	0.276	60.514	0.114	0.000	0.646	0.164	0.000	0.000	0.000	0.003	0.007	0.000
K07-86-223-3m_1-4	BK_E, 940 masl	7	100.070	32.891	4.731	0.753	61.070	0.071	0.000	0.675	0.000	0.022	0.000	0.000	0.000	0.002	0.000
K07-86-223-3m_3-4	BK_E, 940 masl	7	100.336	33.364	8.957	0.106	57.198	0.063	0.000	0.783	0.000	0.000	0.000	0.000	0.005	0.010	0.000
K07-88-59-6m_1-5	Bermingham	7	99.369	32.997	2.930	0.000	63.295	0.014	0.020	0.063	0.000	0.000	0.000	0.000	0.000	0.000	0.000
K07-88-59-6m_2-3	Bermingham	7	99.590	32.979	3.382	0.000	63.376	0.044	0.014	0.000	0.000	0.011	0.000	0.000	0.002	0.003	0.000
K07-88-59-6m_4-5	Bermingham	7	99.480	32.736	1.570	0.000	65.351	0.038	0.000	0.003	0.000	0.000	0.000	0.000	0.000	0.000	0.000
K07-88-59-6m_4-6	Bermingham	7	99.202	32.683	2.531	0.000	64.290	0.068	0.000	0.000	0.000	0.000	0.000	0.000	0.003	0.006	0.000
K07-88-59-6m_5-4	Bermingham	7	99.430	32.841	3.100	0.019	63.464	0.061	0.004	0.067	0.000	0.000	0.000	0.000	0.006	0.011	0.000
K07-88-59-6m_7-2	Bermingham	7	98.723	32.806	2.903	0.058	63.259	0.007	0.000	0.000	0.000	0.000	0.000	0.000	0.011	0.000	0.000
K07-88-59-6m_7-3	Bermingham	7	99.151	33.027	3.293	0.039	62.890	0.026	0.004	0.015	0.000	0.000	0.000	0.000	0.011	0.000	0.000
K07-88-59-6m_8-1	Bermingham	7	99.022	32.748	2.454	0.000	63.968	0.020	0.000	0.061	0.000	0.017	0.000	0.000	0.000	0.010	0.000
K07-106-402-2m_1-2	BK_SW, NE-end, 985 masl	7	99.842	33.125	2.670	0.000	64.117	0.000	0.000	0.018	0.000	0.000	0.000	0.042	0.000	0.000	0.000
K07-106-402-2m_2-3	BK_SW, NE-end, 985 masl	7	99.952	33.132	3.273	0.009	63.398	0.047	0.000	0.091	0.000	0.000	0.000	0.000	0.005	0.012	0.000
K07-106-402-2m_6-3	BK_SW, NE-end, 985 masl	7	99.323	33.364	5.075	0.011	60.971	0.043	0.006	0.005	0.000	0.000	0.000	0.000	0.000	0.007	0.000
K07-106-402-2m_9-1	BK_SW, NE-end, 985 masl	7	99.562	33.205	2.936	0.000	63.613	0.029	0.000	0.008	0.000	0.026	0.000	0.000	0.000	0.004	0.000
K07-106-402-2m_9-6	BK_SW, NE-end, 985 masl	7	99.630	32.968	5.361	0.017	61.479	0.021	0.000	0.010	0.000	0.033	0.000	0.000	0.000	0.015	0.000
K07-106-402-2m_7-3	BK_SW, NE-end, 985 masl	7	99.878	33.316	2.522	0.000	64.113	0.034	0.012	0.000	0.000	0.000	0.000	0.000	0.000	0.000	0.000
K07-106-402-2m_7-4	BK_SW, NE-end, 985 masl	7	99.159	33.338	3.999	0.017	62.128	0.009	0.017	0.021	0.000	0.000	0.000	0.000	0.004	0.000	0.000
K09-187-201-9m-1-2	BK_E, 950 masl	7, 8, 9, 10	99.114	31.471	1.338	0.045	65.634	0.032	0.000	0.558	0.000	0.004	0.000	0.000	0.000	0.008	0.000
K09-187-201-9m-2-1	BK_E, 950 masl	7, 8, 9, 10	99.525	32.171	2.641	0.168	63.863	0.063	0.028	0.602	0.079	0.001	0.000	0.000	0.000	0.000	0.000
K09-187-201-9m-3-2	BK_E, 950 masl	7, 8, 9, 10	99.599	32.177	2.363	0.145	64.404	0.063	0.013	0.599	0.035	0.000	0.000	0.000	0.007	0.000	0.000
K09-187-201-9m-3-5	BK_E, 950 masl	7, 8, 9, 10	99.936	32.840	3.791	0.186	62.184	0.093	0.014	0.811	0.083	0.000	0.000	0.000	0.000	0.001	0.000

B. Electron Microprobe Data: Sulfides, Oxides, and Sulfates

K09-187-201-9m-4-2	BK_E, 950 masl	7, 8, 9, 10	99.274	32.001	3.994	0.268	62.383	0.000	0.014	0.690	0.178	0.000	0.000	0.000	0.014	0.000	0.000
K09-187-201-9m-4-3	BK_E, 950 masl	7, 8, 9, 10	98.972	32.049	3.627	0.019	62.713	0.053	0.009	0.602	0.000	0.000	0.000	0.000	0.005	0.001	0.000
K09-187-201-9m-5-2	BK_E, 950 masl	7, 8, 9, 10	99.078	31.925	3.130	0.647	61.380	0.079	0.596	0.547	0.267	0.659	0.000	0.000	0.000	0.019	0.000
K09-187-201-9m-6-1	BK_E, 950 masl	7, 8, 9, 10	99.247	31.891	1.925	0.097	64.716	0.141	0.000	0.442	0.068	0.000	0.000	0.086	0.000	0.000	0.000
K09-187-201-9m-6-2	BK_E, 950 masl	7, 8, 9, 10	98.960	31.731	1.941	0.134	64.760	0.036	0.022	0.478	0.140	0.000	0.000	0.000	0.000	0.009	0.000
K09-187-201-9m-7-4	BK_E, 950 masl	7, 8, 9, 10	99.318	32.192	2.499	0.180	64.010	0.136	0.011	0.510	0.110	0.004	0.000	0.000	0.008	0.003	0.000
K09-187-201-9m-8-1	BK_E, 950 masl	7, 8, 9, 10	98.807	32.005	4.187	0.365	60.609	0.056	0.496	0.635	0.145	0.325	0.000	0.023	0.000	0.000	0.000
K09-187-201-9m-9-1	BK_E, 950 masl	7, 8, 9, 10	99.462	32.188	3.192	0.167	63.178	0.040	0.000	0.640	0.072	0.005	0.000	0.000	0.000	0.005	0.000
K09-187-201-9m-9-2	BK_E, 950 masl	7, 8, 9, 10	98.838	32.112	3.772	0.043	62.485	0.132	0.000	0.501	0.000	0.000	0.000	0.000	0.009	0.000	0.000
K09-187-201-9m-10-3	BK_E, 950 masl	7, 8, 9, 10	98.734	31.630	2.473	0.345	63.848	0.054	0.001	0.552	0.173	0.000	0.000	0.000	0.015	0.007	0.000
K09-201-238m-3-3	Keno 700	7	101.544	34.532	2.274	0.010	64.162	0.039	0.000	0.810	0.000	0.000	0.000	0.000	0.014	0.000	0.000
K09-201-238m-4-3	Keno 700	7	101.103	34.531	3.702	0.000	62.137	0.028	0.004	0.730	0.000	0.000	0.000	0.000	0.000	0.000	0.188
K09-201-238m-4-6	Keno 700	7	101.973	34.712	1.786	0.000	64.756	0.041	0.000	0.763	0.000	0.000	0.000	0.000	0.001	0.000	0.179
K09-201-238m-5-3	Keno 700	7	102.792	35.027	2.323	0.011	64.635	0.031	0.018	0.718	0.000	0.000	0.000	0.000	0.000	0.000	0.152
K09-201-238m-5-5	Keno 700	7	102.559	35.068	2.287	0.023	64.261	0.028	0.000	0.847	0.000	0.000	0.000	0.000	0.000	0.001	0.234
K09-201-238m-6-6	Keno 700	7	101.368	34.677	3.194	0.000	62.965	0.026	0.000	0.662	0.000	0.000	0.000	0.000	0.000	0.002	0.059
K09-201-238m-7-2	Keno 700	7	101.338	34.348	3.982	0.000	62.515	0.043	0.004	0.644	0.000	0.000	0.000	0.000	0.000	0.006	0.092
K09-201-238m-7-3	Keno 700	7	101.410	34.292	2.748	0.259	63.266	0.024	0.001	0.723	0.188	0.000	0.000	0.000	0.000	0.000	0.010
K09-201-238m-7-7	Keno 700	7	101.552	34.403	2.615	0.007	63.846	0.025	0.000	0.743	0.000	0.000	0.000	0.000	0.000	0.010	0.089
K09-201-238m-7-8	Keno 700	7	100.501	34.185	3.888	0.022	61.807	0.020	0.002	0.723	0.000	0.000	0.000	0.000	0.003	0.011	0.096
K09-201-238m-8-1	Keno 700	7	102.046	35.377	3.781	0.000	62.344	0.032	0.001	0.547	0.000	0.000	0.000	0.000	0.002	0.000	0.142
BKUD09-139-8-3m_1-1	BK_SW, 965 masl	7	99.712	32.947	7.540	0.039	58.785	0.075	0.000	0.720	0.000	0.000	0.000	0.000	0.000	0.001	0.000
BKUD09-139-8-3m_2-2	BK_SW, 965 masl	7	100.431	32.878	3.424	0.029	63.810	0.037	0.012	0.552	0.000	0.003	0.000	0.000	0.000	0.005	0.000
BKUD09-139-8-3m_2-3	BK_SW, 965 masl	7	100.494	33.119	4.998	0.004	62.212	0.046	0.000	0.514	0.000	0.000	0.000	0.000	0.008	0.000	0.000
BKUD09-139-8-3m_2-4	BK_SW, 965 masl	7	100.324	33.189	5.946	0.042	60.657	0.060	0.022	0.624	0.042	0.000	0.000	0.000	0.000	0.011	0.000
BKUD09-139-8-3m_2-5	BK_SW, 965 masl	7	100.482	33.211	6.165	0.001	60.620	0.039	0.025	0.523	0.000	0.000	0.000	0.000	0.000	0.010	0.000

B. Electron Microprobe Data: Sulfides, Oxides, and Sulfates

BKUD09-139-8-3m_2-6	BK_SW, 965 masl	7	100.280	32.886	4.912	0.014	62.187	0.007	0.006	0.575	0.000	0.000	0.000	0.000	0.008	0.001	0.000
BKUD09-139-8-3m_3-1	BK_SW, 965 masl	7	100.166	33.018	3.637	0.000	63.191	0.023	0.000	0.538	0.000	0.000	0.000	0.000	0.000	0.014	0.000
BKUD09-139-8-3m_3-2	BK_SW, 965 masl	7	100.535	32.932	4.159	0.010	62.873	0.012	0.002	0.534	0.000	0.020	0.000	0.000	0.002	0.001	0.000
BKUD09-139-8-3m_3-3	BK_SW, 965 masl	7	100.027	33.316	5.249	0.003	61.233	0.029	0.003	0.576	0.000	0.000	0.000	0.000	0.000	0.000	0.000
BKUD09-139-8-3m_4-1	BK_SW, 965 masl	7	99.474	32.949	4.612	0.019	61.678	0.000	0.002	0.498	0.000	0.000	0.000	0.000	0.001	0.005	0.000
BKUD09-139-8-3m_5-1	BK_SW, 965 masl	7	99.524	32.921	6.655	0.077	59.067	0.045	0.000	0.731	0.086	0.000	0.000	0.000	0.016	0.006	0.000
BKUD09-139-8-3m_5-2	BK_SW, 965 masl	7	100.204	33.203	6.312	0.052	59.819	0.013	0.006	0.542	0.025	0.015	0.000	0.006	0.004	0.012	0.000
BKUD09-139-8-3m_6-1	BK_SW, 965 masl	7	99.311	33.331	7.541	0.057	57.760	0.032	0.006	0.758	0.002	0.000	0.000	0.000	0.000	0.008	0.000
BKUD09-139-8-3m_7-1	BK_SW, 965 masl	7	99.022	32.970	7.136	0.103	58.211	0.041	0.000	0.718	0.071	0.000	0.000	0.000	0.000	0.016	0.000
BKUD09-139-8-3m_7-2	BK_SW, 965 masl	7	99.674	33.180	6.347	0.020	59.502	0.038	0.007	0.703	0.000	0.000	0.000	0.000	0.000	0.006	0.000
BKUD09-139-8-3m_7-6	BK_SW, 965 masl	7	98.085	32.905	5.761	0.109	58.690	0.035	0.004	0.662	0.001	0.000	0.000	0.000	0.010	0.011	0.000
BKUD09-139-8-3m_7-7	BK_SW, 965 masl	7	99.276	33.087	4.345	0.113	61.297	0.014	0.014	0.566	0.044	0.000	0.000	0.000	0.007	0.008	0.000
BKUD09-139-8-3m_8-1	BK_SW, 965 masl	7	99.004	33.102	4.556	0.000	61.142	0.007	0.000	0.452	0.013	0.021	0.000	0.000	0.014	0.006	0.000
BKUD09-139-8-3m_8-4	BK_SW, 965 masl	7	98.467	33.160	6.793	3.375	54.680	0.048	0.000	0.618	0.000	0.000	0.000	0.054	0.017	0.004	0.000
BKUD09-139-8-3m_9-1	BK_SW, 965 masl	7	99.098	33.363	4.897	0.000	60.526	0.000	0.019	0.528	0.000	0.000	0.000	0.000	0.000	0.002	0.000
BKUD09-139-8-3m_10-1	BK_SW, 965 masl	7	99.286	33.218	7.672	0.007	57.906	0.013	0.000	0.690	0.000	0.000	0.000	0.000	0.002	0.005	0.000
BKUD09-143-51-2m-9-3	BK_SW, 1005 masl	7	96.541	30.791	3.346	0.003	61.797	0.063	0.008	0.639	0.000	0.000	0.000	0.000	0.000	0.014	0.000
BKUD09-143-51-2m-9-4	BK_SW, 1005 masl	7	96.692	30.943	6.599	0.012	58.615	0.099	0.005	0.679	0.000	0.000	0.000	0.000	0.000	0.014	0.000
BKUD09-143-51-2m-10-3	BK_SW, 1005 masl	7	97.419	31.005	5.453	0.008	60.394	0.000	0.000	0.662	0.000	0.000	0.000	0.000	0.003	0.000	0.000
BKUD09-143-51-2m-10-4	BK_SW, 1005 masl	7	96.948	30.854	5.592	0.000	60.022	0.013	0.000	0.660	0.000	0.000	0.000	0.000	0.004	0.005	0.000
BKUD09-143-51-2m-10-5	BK_SW, 1005 masl	7	97.025	31.030	7.627	0.017	57.688	0.060	0.000	0.817	0.000	0.000	0.000	0.000	0.005	0.009	0.000
BKUD09-148-29-5m_1-1	BK_99, 1025 masl	7	101.042	33.142	4.865	0.148	62.129	0.053	0.000	0.602	0.072	0.000	0.000	0.000	0.001	0.008	0.000
BKUD09-148-29-5m_2-1	BK_99, 1025 masl	7	100.774	32.897	2.459	0.108	64.912	0.024	0.000	0.605	0.022	0.015	0.000	0.000	0.000	0.000	0.000
BKUD09-148-29-5m_2-3	BK_99, 1025 masl	7	100.160	33.004	3.328	0.059	63.389	0.057	0.091	0.520	0.000	0.026	0.000	0.000	0.000	0.007	0.000
BKUD09-148-29-5m_3-1	BK_99, 1025 masl	7	100.395	33.090	3.314	0.045	63.398	0.022	0.029	0.581	0.000	0.000	0.000	0.000	0.007	0.007	0.000
BKUD09-148-29-5m_4-1	BK_99, 1025 masl	7	99.579	32.889	5.281	0.258	60.085	0.015	0.015	0.693	0.299	0.000	0.000	0.000	0.002	0.000	0.000
BKUD09-148-29-5m_4-2	BK_99, 1025 masl	7	99.790	33.096	4.252	0.020	61.846	0.035	0.003	0.713	0.014	0.000	0.000	0.000	0.002	0.000	0.000
BKUD09-148-29-5m_5-1	BK_99, 1025 masl	7	99.330	32.522	4.625	0.165	61.425	0.012	0.000	0.672	0.145	0.000	0.000	0.000	0.000	0.015	0.000

B. Electron Microprobe Data: Sulfides, Oxides, and Sulfates

BKUD09-148-29-5m_6-2	BK_99, 1025 masl	7	100.065	33.161	3.554	0.111	62.732	0.031	0.007	0.595	0.014	0.000	0.000	0.000	0.003	0.003	0.000
BKUD09-148-29-5m_9-1	BK_99, 1025 masl	7	99.843	33.023	3.613	0.000	62.841	0.047	0.000	0.478	0.000	0.000	0.000	0.000	0.000	0.003	0.000
BKUD09-151-33-3m_1-1	BK_99, 1045 masl	7	98.979	33.034	4.561	0.070	61.280	0.008	0.001	0.058	0.000	0.000	0.000	0.000	0.000	0.012	0.000
BKUD09-151-33-3m_1-2	BK_99, 1045 masl	7	98.555	33.097	5.317	0.322	59.583	0.040	0.001	0.020	0.286	0.000	0.000	0.000	0.000	0.000	0.000
BKUD09-151-33-3m_1-3	BK_99, 1045 masl	7	98.551	32.915	5.609	0.344	59.278	0.039	0.016	0.013	0.448	0.000	0.000	0.000	0.001	0.006	0.000
BKUD09-151-33-3m_1-4	BK_99, 1045 masl	7	99.182	33.386	5.165	0.233	60.087	0.044	0.000	0.023	0.224	0.000	0.000	0.000	0.005	0.002	0.000
BKUD09-151-33-3m_1-5	BK_99, 1045 masl	7	98.953	32.982	4.839	0.222	60.740	0.011	0.005	0.000	0.261	0.000	0.000	0.000	0.000	0.009	0.000
BKUD09-151-33-3m_1-6	BK_99, 1045 masl	7	98.829	33.038	4.726	0.156	60.894	0.005	0.005	0.000	0.087	0.000	0.000	0.000	0.000	0.021	0.000
BKUD09-151-33-3m_2-1	BK_99, 1045 masl	7	98.868	33.135	5.627	0.460	59.214	0.040	0.023	0.000	0.522	0.000	0.000	0.000	0.000	0.001	0.000
BKUD09-151-33-3m_3-2	BK_99, 1045 masl	7	98.168	33.099	4.718	0.135	60.311	0.027	0.002	0.000	0.021	0.000	0.000	0.000	0.000	0.001	0.000
BKUD09-151-33-3m_3-3	BK_99, 1045 masl	7	97.830	32.768	4.524	0.079	60.392	0.048	0.008	0.038	0.000	0.000	0.000	0.000	0.008	0.011	0.000
BKUD09-151-33-3m_4-3	BK_99, 1045 masl	7	98.849	33.653	4.780	0.104	60.449	0.012	0.000	0.000	0.000	0.000	0.000	0.000	0.003	0.013	0.000
BKUD09-151-33-3m_7-1	BK_99, 1045 masl	7	99.197	33.293	5.359	0.080	60.385	0.039	0.000	0.023	0.035	0.000	0.000	0.022	0.002	0.000	0.000
BKUD09-151-33-3m_7-2	BK_99, 1045 masl	7	98.546	32.957	5.516	0.264	59.585	0.009	0.005	0.025	0.260	0.000	0.000	0.000	0.000	0.000	0.000
BKUD09-151-33-3m_9-1	BK_99, 1045 masl	7	99.251	33.209	5.259	0.162	60.514	0.012	0.011	0.000	0.150	0.000	0.000	0.000	0.000	0.013	0.000
BKUD09-151-33-3m_10-1	BK_99, 1045 masl	7	98.776	33.061	4.422	0.082	61.181	0.064	0.002	0.078	0.092	0.000	0.000	0.000	0.000	0.014	0.000
BKUD09-153-87-5m-1-2	BK_SW, 940 masl	7	101.132	35.869	5.635	0.000	58.908	0.042	0.000	0.618	0.000	0.000	0.000	0.048	0.000	0.000	0.076
BKUD09-153-87-5m-1-3	BK_SW, 940 masl	7	100.886	35.476	5.374	0.000	59.275	0.026	0.015	0.560	0.000	0.000	0.000	0.063	0.003	0.008	0.101
BKUD09-153-87-5m-1-4	BK_SW, 940 masl	7	100.562	35.728	5.243	0.071	58.742	0.014	0.000	0.884	0.000	0.000	0.000	0.000	0.000	0.000	0.091
BKUD09-153-87-5m-1-5	BK_SW, 940 masl	7	100.464	35.895	5.004	0.055	58.822	0.024	0.010	0.569	0.017	0.000	0.000	0.000	0.000	0.001	0.144
BKUD09-153-87-5m-1-6	BK_SW, 940 masl	7	99.959	35.580	5.502	0.192	58.178	0.007	0.009	0.534	0.126	0.000	0.000	0.000	0.000	0.010	0.156
BKUD09-153-87-5m-1-7	BK_SW, 940 masl	7	100.243	35.603	6.341	0.382	57.028	0.052	0.008	0.601	0.281	0.000	0.000	0.000	0.000	0.014	0.142
BKUD09-153-87-5m-1-8	BK_SW, 940 masl	7	100.379	35.458	5.132	0.095	59.138	0.024	0.003	0.513	0.027	0.000	0.000	0.000	0.004	0.000	0.107
BKUD09-153-87-5m-1-9	BK_SW, 940 masl	7	100.271	35.121	4.954	0.066	59.471	0.029	0.000	0.575	0.000	0.000	0.000	0.000	0.000	0.001	0.198
BKUD09-153-87-5m-1-10	BK_SW, 940 masl	7	100.575	35.791	4.139	0.019	60.151	0.047	0.000	0.463	0.000	0.000	0.000	0.029	0.001	0.000	0.037
BKUD09-153-87-5m-1-11	BK_SW, 940 masl	7	100.792	35.353	3.655	0.021	61.053	0.051	0.000	0.667	0.000	0.000	0.000	0.000	0.000	0.000	0.213
BKUD09-153-87-5m-1-12	BK_SW, 940 masl	7	100.536	35.656	4.353	0.000	60.168	0.043	0.000	0.441	0.025	0.000	0.000	0.000	0.002	0.000	0.000
BKUD09-153-87-5m-6-1	BK_SW, 940 masl	7	101.594	34.762	3.557	0.017	62.572	0.029	0.018	0.558	0.012	0.000	0.000	0.000	0.000	0.000	0.100

B. Electron Microprobe Data: Sulfides, Oxides, and Sulfates

BKUD09-153-87-5m-6-2	BK_SW, 940 masl	7	101.896	34.994	5.642	0.006	60.590	0.031	0.000	0.644	0.000	0.012	0.000	0.000	0.000	0.000	0.129
BKUD09-153-87-5m-6-3	BK_SW, 940 masl	7	101.951	34.870	4.578	0.035	61.612	0.035	0.009	0.566	0.051	0.000	0.000	0.029	0.008	0.006	0.192
BKUD09-153-87-5m-6-3	BK_SW, 940 masl	7	101.822	35.047	4.715	0.026	61.316	0.018	0.001	0.635	0.000	0.000	0.000	0.000	0.000	0.005	0.215
BKUD09-153-87-5m-6-4	BK_SW, 940 masl	7	102.025	34.898	4.725	0.023	61.614	0.015	0.006	0.705	0.006	0.007	0.000	0.000	0.016	0.000	0.131
BKUD09-153-87-5m-6-5	BK_SW, 940 masl	7	101.793	35.103	4.240	0.024	62.048	0.039	0.002	0.522	0.000	0.000	0.000	0.000	0.002	0.000	0.005
BKUD09-153-87-5m-6-6	BK_SW, 940 masl	7	101.967	34.992	4.820	0.062	61.382	0.032	0.000	0.551	0.017	0.000	0.000	0.000	0.000	0.000	0.160
BKUD09-153-87-5m-6-7	BK_SW, 940 masl	7	101.856	35.125	6.934	0.407	58.219	0.038	0.010	0.785	0.350	0.000	0.000	0.015	0.000	0.004	0.035
BKUD09-153-87-5m-6-8	BK_SW, 940 masl	7	101.562	35.251	6.425	0.040	59.287	0.035	0.009	0.666	0.000	0.000	0.000	0.000	0.000	0.000	0.067
BKUD09-153-87-5m-6-9	BK_SW, 940 masl	7	101.986	34.839	5.570	0.109	60.656	0.031	0.000	0.619	0.065	0.000	0.000	0.082	0.006	0.009	0.066
BKUD09-153-87-5m-6-10	BK_SW, 940 masl	7	101.325	34.833	5.790	0.133	60.206	0.020	0.013	0.541	0.000	0.007	0.000	0.000	0.000	0.016	0.070
BKUD09-153-87-5m-7-1	BK_SW, 940 masl	7	101.034	34.920	5.811	0.235	59.428	0.026	0.011	0.673	0.141	0.000	0.000	0.000	0.004	0.000	0.000
BKUD09-153-87-5m-8-1	BK_SW, 940 masl	7	100.122	35.671	4.242	0.032	59.784	0.013	0.010	0.532	0.000	0.008	0.000	0.000	0.007	0.000	0.086
BKUD09-157-100-5m-1-1	BK_SW, 930 masl	7	97.996	31.695	4.454	0.035	61.329	0.000	0.000	0.523	0.026	0.000	0.000	0.000	0.004	0.012	0.000
BKUD09-157-100-5m-2-1	BK_SW, 930 masl	7	97.738	31.455	3.528	0.032	62.221	0.095	0.014	0.641	0.000	0.000	0.000	0.000	0.001	0.014	0.000
BKUD09-157-100-5m-2-2	BK_SW, 930 masl	7	96.469	30.946	3.890	0.005	60.900	0.017	0.001	0.505	0.000	0.021	0.000	0.003	0.003	0.007	0.000
BKUD09-157-100-5m-3-1	BK_SW, 930 masl	7	97.600	30.990	2.192	0.010	63.889	0.042	0.015	0.581	0.013	0.000	0.000	0.000	0.014	0.000	0.000
BKUD09-157-100-5m-3-2	BK_SW, 930 masl	7	98.248	31.649	3.403	0.040	62.573	0.032	0.039	0.558	0.007	0.000	0.000	0.000	0.000	0.006	0.000
BKUD09-157-100-5m-4-1	BK_SW, 930 masl	7	97.584	31.426	4.815	0.141	60.783	0.036	0.000	0.460	0.107	0.000	0.000	0.000	0.000	0.001	0.000
BKUD09-157-100-5m-4-2	BK_SW, 930 masl	7	97.689	31.457	5.117	0.000	60.697	0.004	0.000	0.596	0.000	0.000	0.000	0.000	0.005	0.011	0.000
BKUD09-157-100-5m-4-3	BK_SW, 930 masl	7	97.550	31.188	4.568	0.066	60.874	0.108	0.005	0.661	0.023	0.000	0.000	0.000	0.000	0.001	0.000
BKUD09-157-100-5m-5-1	BK_SW, 930 masl	7	96.932	31.352	4.712	0.141	60.333	0.040	0.010	0.466	0.135	0.000	0.000	0.000	0.001	0.001	0.000
BKUD09-157-100-5m-6-1	BK_SW, 930 masl	7	97.438	31.470	4.920	0.039	60.084	0.084	0.000	0.678	0.008	0.000	0.000	0.080	0.000	0.025	0.000
BKUD09-157-100-5m-7-1	BK_SW, 930 masl	7	97.304	31.461	5.217	0.016	60.019	0.080	0.010	0.640	0.000	0.000	0.000	0.000	0.000	0.013	0.000
BKUD09-157-100-5m-7-2	BK_SW, 930 masl	7	97.881	31.393	2.478	0.000	63.422	0.000	0.003	0.617	0.000	0.000	0.000	0.041	0.000	0.000	0.000
BKUD09-157-100-5m-8-1	BK_SW, 930 masl	7	97.552	31.660	4.248	0.010	61.172	0.036	0.022	0.587	0.000	0.000	0.000	0.000	0.000	0.000	0.000
BKUD09-158-36m_1-2	BK_SW, 1030 masl	7	100.048	33.009	4.623	1.142	61.001	0.039	0.009	0.536	0.000	0.000	0.000	0.000	0.000	0.001	0.000
BKUD09-158-36m_2-4	BK_SW, 1030 masl	7	100.037	33.349	5.795	0.087	60.370	0.048	0.000	0.598	0.000	0.000	0.000	0.000	0.000	0.004	0.000
BKUD09-158-36m_6-2	BK_SW, 1030 masl	7	100.275	32.885	4.376	1.486	61.034	0.036	0.037	0.554	0.000	0.000	0.000	0.000	0.000	0.000	0.000

B. Electron Microprobe Data: Sulfides, Oxides, and Sulfates

BKUD09-158-36m_6-6	BK_SW, 1030 masl	7	102.977	33.184	6.111	3.112	59.911	0.010	0.015	0.702	0.129	0.038	0.000	0.000	0.006	0.000	0.000
BKUD09-158-36m_7-3	BK_SW, 1030 masl	7	99.974	33.381	3.690	0.212	61.794	0.061	0.033	0.650	0.167	0.000	0.000	0.010	0.013	0.010	0.000
BKUD09-158-36m_8-2	BK_SW, 1030 masl	7	99.522	33.157	5.317	0.045	60.580	0.000	0.000	0.553	0.000	0.000	0.000	0.000	0.000	0.004	0.000
BKUD09-158-36m_8-3	BK_SW, 1030 masl	7	99.764	32.821	4.734	0.010	61.439	0.053	0.000	0.592	0.000	0.000	0.000	0.000	0.000	0.001	0.000
BKUD09-158-36-5m-1-1	BK_SW, 1030 masl	7	100.962	34.420	3.875	0.229	61.566	0.055	0.017	0.643	0.182	0.010	0.000	0.000	0.002	0.006	0.025
BKUD09-158-36-5m-1-2	BK_SW, 1030 masl	7	101.202	34.422	3.621	0.043	62.399	0.015	0.004	0.722	0.000	0.000	0.000	0.015	0.010	0.010	0.055
BKUD09-158-36-5m-1-4	BK_SW, 1030 masl	7	101.571	34.699	1.978	0.224	63.605	0.037	0.041	0.893	0.206	0.000	0.000	0.000	0.000	0.000	0.029
BKUD09-158-36-5m-2-1	BK_SW, 1030 masl	7	101.349	34.757	4.340	0.225	61.177	0.035	0.021	0.654	0.118	0.007	0.000	0.000	0.000	0.000	0.128
BKUD09-158-36-5m-2-6	BK_SW, 1030 masl	7	101.480	34.769	4.469	0.048	61.493	0.014	0.010	0.737	0.000	0.005	0.000	0.000	0.000	0.000	0.060
BKUD09-158-36-5m-3-2	BK_SW, 1030 masl	7	101.418	34.328	4.061	0.054	62.215	0.051	0.015	0.564	0.000	0.000	0.000	0.151	0.000	0.000	0.050
BKUD09-158-36-5m-4-3	BK_SW, 1030 masl	7	101.045	34.527	5.522	0.120	60.140	0.002	0.000	0.573	0.071	0.000	0.000	0.000	0.004	0.000	0.096
BKUD09-158-36-5m-4-4	BK_SW, 1030 masl	7	101.177	34.744	5.903	0.315	59.385	0.028	0.006	0.760	0.211	0.000	0.000	0.000	0.000	0.000	0.032
BKUD09-158-36-5m-5-1	BK_SW, 1030 masl	7	101.379	34.506	3.644	0.046	62.672	0.006	0.000	0.638	0.000	0.009	0.000	0.000	0.010	0.000	0.049
BKUD09-158-36-5m-5-3	BK_SW, 1030 masl	7	101.003	33.946	2.503	0.045	64.034	0.028	0.001	0.545	0.000	0.021	0.000	0.000	0.006	0.000	0.095
BKUD09-158-36-5m-5-5	BK_SW, 1030 masl	7	100.764	34.056	4.258	0.261	61.302	0.022	0.013	0.668	0.246	0.000	0.000	0.000	0.006	0.001	0.054
BKUD09-158-36-5m-6-1	BK_SW, 1030 masl	7	101.634	34.873	5.451	0.107	60.422	0.036	0.002	0.642	0.047	0.000	0.000	0.000	0.009	0.000	0.178
BKUD09-158-36-5m-6-2	BK_SW, 1030 masl	7	101.571	34.729	5.502	0.073	60.584	0.025	0.000	0.543	0.038	0.008	0.000	0.000	0.004	0.010	0.077
BKUD09-158-36-5m-6-3	BK_SW, 1030 masl	7	101.730	34.858	5.205	0.052	60.829	0.028	0.006	0.590	0.000	0.000	0.000	0.107	0.015	0.000	0.102
BKUD09-158-36-5m-6-4	BK_SW, 1030 masl	7	101.809	34.688	4.125	0.009	62.329	0.023	0.009	0.563	0.000	0.007	0.000	0.000	0.000	0.000	0.147
BKUD09-158-36-5m-6-5	BK_SW, 1030 masl	7	101.987	35.223	5.037	0.209	60.690	0.003	0.002	0.641	0.128	0.007	0.000	0.000	0.000	0.000	0.185
BKUD09-158-36-5m-7-1	BK_SW, 1030 masl	7	101.599	34.562	2.118	0.124	63.975	0.028	0.013	0.627	0.040	0.032	0.000	0.020	0.010	0.004	0.128
BKUD09-158-36-5m-7-3	BK_SW, 1030 masl	7	101.835	34.361	2.111	0.171	64.505	0.019	0.007	0.578	0.161	0.000	0.000	0.000	0.011	0.003	0.093
BKUD09-158-36-5m-8-2	BK_SW, 1030 masl	7	101.241	34.274	4.442	0.023	61.879	0.024	0.000	0.624	0.000	0.000	0.000	0.000	0.004	0.000	0.115
BKUD09-158-36-5m-9-1	BK_SW, 1030 masl	7	101.292	34.374	5.148	0.080	61.053	0.036	0.005	0.623	0.045	0.025	0.000	0.000	0.004	0.000	0.119
BKUD09-158-36-5m-9-2	BK_SW, 1030 masl	7	101.055	34.700	5.885	0.292	59.477	0.000	0.016	0.702	0.103	0.000	0.000	0.000	0.011	0.000	0.085
BKUD09-158-36-5m-9-3	BK_SW, 1030 masl	7	101.105	34.189	5.172	0.170	60.840	0.033	0.006	0.581	0.125	0.000	0.000	0.000	0.000	0.010	0.170
BKUD09-158-36-5m-9-4	BK_SW, 1030 masl	7	101.917	34.627	4.235	0.003	62.512	0.027	0.000	0.638	0.008	0.000	0.000	0.000	0.016	0.000	0.049
BKUD09-158-36-5m-10-5	BK_SW, 1030 masl	7	100.897	34.315	4.575	0.000	61.572	0.049	0.000	0.556	0.000	0.000	0.000	0.000	0.011	0.005	0.096

B. Electron Microprobe Data: Sulfides, Oxides, and Sulfates

BKUD09-158-36-5m-11-5	BK_SW, 1030 masl	7	101.241	34.305	4.918	0.015	61.417	0.027	0.000	0.743	0.000	0.000	0.000	0.000	0.000	0.000	0.083
BKUD09-158-36-5m-11-6	BK_SW, 1030 masl	7	101.066	34.222	5.825	0.187	59.852	0.043	0.012	0.739	0.170	0.013	0.000	0.000	0.000	0.006	0.135
BKUD09-158-37m-5-2	BK_SW, 1030 masl	7	97.025	32.037	5.861	0.099	58.454	0.121	0.022	0.615	0.000	0.016	0.000	0.000	0.014	0.005	0.000
BKUD09-158-37m-6-3	BK_SW, 1030 masl	7	97.909	32.316	2.422	0.002	62.275	0.099	0.000	0.688	0.000	0.000	0.000	0.000	0.014	0.004	0.000
BKUD09-158-37m-7-2	BK_SW, 1030 masl	7	98.080	31.722	6.366	0.158	58.957	0.031	0.018	0.827	0.176	0.000	0.000	0.000	0.000	0.016	0.000
BKUD09-171-32-8m-1-2	BK_99, 990 masl	7	98.519	31.526	5.406	0.067	60.791	0.038	0.000	0.748	0.000	0.026	0.000	0.000	0.017	0.000	0.000
BKUD09-171-32-8m-3-4	BK_99, 990 masl	7	97.242	31.411	6.179	0.035	59.185	0.023	0.000	0.701	0.000	0.000	0.000	0.000	0.001	0.019	0.000
BKUD09-171-32-8m-4-2	BK_99, 990 masl	7	97.704	31.427	6.258	0.023	59.563	0.000	0.001	0.575	0.000	0.000	0.000	0.000	0.000	0.007	0.000
BKUD09-171-32-8m-5-2	BK_99, 990 masl	7	96.965	31.124	6.243	0.045	59.055	0.000	0.000	0.605	0.000	0.000	0.000	0.000	0.007	0.002	0.000
BKUD09-171-32-8m-5-4	BK_99, 990 masl	7	96.635	31.244	5.820	0.170	58.852	0.025	0.002	0.533	0.060	0.000	0.000	0.023	0.000	0.007	0.000
BKUD09-171-32-8m-5-5	BK_99, 990 masl	7	97.625	31.513	5.447	0.314	59.566	0.000	0.010	0.740	0.233	0.000	0.000	0.000	0.000	0.009	0.000
BKUD09-171-32-8m-6-1	BK_99, 990 masl	7	97.410	31.411	4.545	0.035	60.820	0.011	0.000	0.579	0.000	0.000	0.000	0.000	0.015	0.000	0.000
BKUD09-171-32-8m-6-2	BK_99, 990 masl	7	96.760	31.412	5.725	0.206	58.802	0.031	0.018	0.521	0.102	0.000	0.000	0.000	0.002	0.007	0.000
BKUD09-171-32-8m-7-3	BK_99, 990 masl	7	96.258	31.652	4.582	0.137	59.603	0.000	0.011	0.501	0.033	0.000	0.000	0.000	0.003	0.000	0.000
BKUD09-171-32-8m-8-4	BK_99, 990 masl	7	97.475	31.301	4.392	0.000	60.993	0.074	0.003	0.628	0.000	0.000	0.000	0.000	0.000	0.000	0.000
BKUD09-171-32-8m-9-3	BK_99, 990 masl	7	97.733	31.390	4.414	0.184	60.943	0.040	0.000	0.623	0.079	0.000	0.000	0.000	0.000	0.008	0.000
n = 229	AVERAGE		99.551	33.151	4.290	0.161	61.433	0.039	0.023	0.486	0.057	0.020	0.003	0.004	0.003	0.004	0.028
	MINIMUM		96.258	30.791	0.733	0.000	54.308	0.000	0.000	0.000	0.000	0.000	0.000	0.000	0.000	0.000	0.000
	MAXIMUM		102.977	35.895	8.957	3.375	65.772	0.141	2.329	1.204	0.522	2.865	0.629	0.151	0.017	0.025	0.234
Chalcopyrite: mostly stages 6 to 8																	
WRN_008_1-3	Wernecke, surface	6, 8	96.929	34.202	28.128	33.189	0.000	0.007	0.641	0.156	0.003	0.899	0.000	0.000	0.000	0.002	
WRN_008_1-4	Wernecke, surface	6, 8	97.542	32.883	26.093	32.030	0.000	0.041	3.416	0.444	0.000	2.902	0.000	0.000	0.000	0.029	
WRN_008_1-5	Wernecke, surface	6, 8	98.029	32.795	25.371	31.419	0.000	0.054	4.368	0.504	0.000	3.791	0.000	0.000	0.000	0.019	
WRN_008_3-2	Wernecke, surface	6, 8	97.670	34.553	29.237	33.839	0.000	0.021	0.142	0.051	0.036	0.267	0.000	0.000	0.000	0.017	
WRN_008_3-3	Wernecke, surface	6, 8	97.266	30.835	24.219	29.378	0.000	0.022	10.532	1.276	0.000	1.304	0.000	0.000	0.015	0.026	
WRN-008-3-8	Wernecke, surface	6, 8	100.153	34.767	29.504	34.661	0.269	0.030	0.321	0.081	0.000	0.480	0.214	0.000		0.008	0.000

B. Electron Microprobe Data: Sulfides, Oxides, and Sulfates

WRN-008-3-16	Wernecke, surface	6, 8	99.196	34.899	29.550	34.590	0.000	0.021	0.204	0.000	0.000	0.405	0.012	0.000		0.008	0.000
WRN_008_7-2	Wernecke, surface	6, 8	95.892	34.485	28.382	33.390	0.000	0.043	0.130	0.073	0.000	0.000	0.000	0.000	0.014	0.011	
K07-86-223-3m_1-1	BK_E, 940 masl	6, 8	98.655	34.701	29.800	34.348	0.000	0.030	0.004	0.000	0.118	0.006	0.000	0.000	0.000	0.015	
K07-86-223-3m_2-1	BK_E, 940 masl	6, 8	98.615	34.915	29.742	34.349	0.000	0.004	0.015	0.000	0.218	0.000	0.000	0.000	0.000	0.011	
K07-86-223-3m_3-1	BK_E, 940 masl	6, 8	98.650	34.903	29.776	34.218	0.000	0.029	0.000	0.076	0.188	0.000	0.000	0.000	0.000	0.017	
K07-86-223-3m_3-5	BK_E, 940 masl	6, 8	97.045	34.389	28.677	34.134	0.000	0.032	0.000	0.003	0.175	0.000	0.000	0.000	0.000	0.015	
K07-86-223-3m_4-1	BK_E, 940 masl	6, 8	99.073	35.209	29.844	34.318	0.000	0.053	0.000	0.015	0.150	0.000	0.000	0.000	0.000	0.019	
K07-86-223-3m_5-1	BK_E, 940 masl	6, 8	98.856	34.811	29.674	34.423	0.000	0.054	0.000	0.032	0.086	0.000	0.000	0.027	0.000	0.015	
K07-86-223-3m_6-1	BK_E, 940 masl	6, 8	98.648	34.684	29.976	34.361	0.000	0.035	0.008	0.000	0.201	0.000	0.000	0.000	0.013	0.017	
BKUD09-139-8-3m_2-1	BK_SW, 965 masl	6, 7, 8	98.297	34.674	29.602	34.369	0.000	0.039	0.000	0.000	0.100	0.000	0.000	0.000	0.000	0.001	
BKUD09-139-8-3m_7-4	BK_SW, 965 masl	6, 7, 8	98.017	34.593	29.693	33.892	0.000	0.028	0.019	0.000	0.125	0.000	0.000	0.000	0.004	0.028	
BKUD09-139-8-3m_7-5	BK_SW, 965 masl	6, 7, 8	98.550	34.920	29.382	33.816	0.361	0.030	0.017	0.000	0.120	0.000	0.000	0.000	0.007	0.013	
BKUD09-139-8-3m_8-3	BK_SW, 965 masl	6, 7, 8	97.160	34.685	28.460	33.484	0.300	0.049	0.033	0.025	0.124	0.038	0.000	0.000	0.004	0.009	
BKUD09-139-8-3m_8-5	BK_SW, 965 masl	6, 7, 8	98.294	34.910	29.488	33.974	0.000	0.012	0.013	0.074	0.078	0.000	0.000	0.000	0.005	0.021	
BKUD09-139-8-3m_9-2	BK_SW, 965 masl	6, 7, 8	97.958	34.697	29.562	33.909	0.000	0.034	0.011	0.000	0.053	0.000	0.000	0.000	0.002	0.022	
BKUD09-139-8-3m_9-4	BK_SW, 965 masl	6, 7, 8	98.254	34.961	29.463	34.056	0.000	0.042	0.000	0.000	0.000	0.000	0.000	0.000	0.003	0.015	
BKUD09-139-8-3m_9-6	BK_SW, 965 masl	6, 7, 8	97.757	34.682	29.636	33.984	0.000	0.028	0.010	0.000	0.071	0.000	0.000	0.000	0.000	0.015	
BKUD09-139-8-3m_10-2	BK_SW, 965 masl	6, 7, 8	98.282	34.960	29.567	34.220	0.000	0.037	0.004	0.072	0.018	0.000	0.000	0.000	0.000	0.024	
BKUD09-140-9-9m-1-3	BK_SW	1, 2, 3 ?	99.847	36.389	30.122	33.777	0.000	0.051	0.028	0.000	0.009	0.000	0.000	0.000	0.006	0.000	0.067
BKUD09-143-52-8m_2-3	BK_SW, NE-end, 1000 masl	8, 9	94.288	34.792	27.182	30.498	0.000	0.058	0.513	0.139	0.027	1.447	0.000	0.000	0.000	0.022	
BKUD09-143--54m_3-3	BK_SW, NE-end, 1000 masl	6, 8	98.595	35.295	29.641	34.129	0.000	0.000	0.093	0.007	0.058	0.000	0.000	0.000	0.000	0.018	
BKUD09-143--54m_4-3	BK_SW, NE-end, 1000 masl	6, 8	98.627	34.819	29.604	33.987	0.000	0.031	0.618	0.096	0.083	0.008	0.000	0.000	0.000	0.017	
BKUD09-143--54m_4-4	BK_SW, NE-end, 1000 masl	6, 8	97.831	33.838	28.645	32.904	0.000	0.045	2.518	0.039	0.035	0.000	0.000	0.000	0.000	0.017	
BKUD09-143--54m_8-3	BK_SW, NE-end, 1000 masl	6, 8	98.788	34.922	29.705	34.415	0.000	0.033	0.000	0.000	0.165	0.000	0.000	0.000	0.000	0.018	
BKUD09-144-36-6m-6-7	BK_SW, SW-end, 980 masl	2, 3	99.919	36.780	29.116	32.945	1.722	0.021	0.025	0.000	0.000	0.000	0.000	0.009	0.000	0.000	0.000
BKUD09-150-64-1m-2-4	BK_SW, SW-end, 975 masl	3, 5 ?	97.816	34.088	29.684	34.016	0.000	0.078	0.050	0.005	0.126	0.034	0.000	0.006	0.000	0.022	

B. Electron Microprobe Data: Sulfides, Oxides, and Sulfates

BKUD09-150-64-1m-3-2	BK_SW, SW-end, 975 masl	3, 5 ?	97.434	34.037	29.610	34.098	0.000	0.037	0.017	0.000	0.200	0.000	0.000	0.000	0.000	0.020	
BKUD09-150-64-1m-7-3	BK_SW, SW-end, 975 masl	3, 5 ?	96.219	33.804	29.086	33.697	0.000	0.000	0.015	0.017	0.141	0.000	0.000	0.000	0.000	0.019	
BKUD09-150-64-1m-8-3	BK_SW, SW-end, 975 masl	3, 5 ?	97.540	34.061	29.450	34.055	0.000	0.167	0.020	0.000	0.195	0.000	0.000	0.000	0.000	0.021	
BKUD09-151-33-3m_3-5	BK_99, 1045 masl	6, 7, 8	97.947	34.817	29.031	34.040	0.000	0.029	0.048	0.030	0.151	0.056	0.000	0.006	0.004	0.018	
BKUD09-153-87-5m-3-5	BK_SW, SW-end, 940 masl	3	100.261	37.831	29.041	32.571	1.154	0.027	0.170	0.070	0.000	0.018	0.000	0.000	0.009	0.000	0.012
BKUD09-153-87-5m-9-2	BK_SW, SW-end, 940 masl	3	101.449	37.181	29.546	32.638	1.971	0.016	0.106	0.027	0.018	0.000	0.000	0.000	0.000	0.000	0.021
n = 38	AVERAGE		98.193	34.704	29.008	33.582	0.152	0.036	0.634	0.087	0.081	0.307	0.006	0.001	0.002	0.015	0.017
	MINIMUM		94.288	30.835	24.219	29.378	0.000	0.000	0.000	0.000	0.000	0.000	0.000	0.000	0.000	0.000	0.000
	MAXIMUM		101.449	37.831	30.122	34.661	1.971	0.167	10.532	1.276	0.218	3.791	0.214	0.027	0.015	0.029	0.067
Galena: stage 8 (and/or 5?)																	
Alice_1-4	Alice, surface	6, 7, 8	98.307	13.643	0.036	0.018	0.000	0.055	**0.798**	0.000	0.000	**0.424**	84.399	0.000	0.000	0.000	0.000
Alice_2-3	Alice, surface	6, 7, 8	100.355	13.435	0.049	0.019	0.020	0.035	0.053	0.000	0.000	0.183	87.954	0.000	0.000	0.000	0.000
Alice_3-3	Alice, surface	6, 7, 8	100.232	13.611	0.051	0.006	0.005	0.022	0.052	0.000	0.000	0.180	87.651	0.000	0.001	0.005	0.000
Alice_4-6	Alice, surface	6, 7, 8	100.682	13.529	0.065	0.012	0.076	0.037	0.000	0.000	0.000	0.103	88.259	0.000	0.001	0.004	0.000
Alice_5-7	Alice, surface	6, 7, 8	100.061	13.606	0.063	0.000	0.000	0.034	0.000	0.000	0.000	0.165	87.624	0.000	0.002	0.006	0.000
Alice_5-8	Alice, surface	6, 7, 8	100.365	13.490	0.037	0.001	0.013	0.051	0.007	0.000	0.000	0.139	87.833	0.000	0.000	0.000	0.000
Alice-5-13	Alice, surface	6, 7, 8	100.050	13.767	0.055	0.000	0.020	0.036	0.029	0.000	0.000	0.144	86.081	0.000		0.000	0.024
Alice_6-6	Alice, surface	6, 7, 8	101.901	13.440	0.049	0.008	0.077	0.010	0.003	0.000	0.000	0.148	89.418	0.000	0.000	0.000	0.000
Alice_7-2	Alice, surface	6, 7, 8	100.771	13.571	0.029	0.001	0.008	0.038	0.000	0.000	0.000	0.102	88.410	0.000	0.000	0.005	0.000
Alice_8-1	Alice, surface	6, 7, 8	100.200	13.596	0.037	0.000	0.008	0.062	0.013	0.000	0.000	0.118	87.529	0.000	0.000	0.000	0.000
Alice_8-7	Alice, surface	6, 7, 8	99.701	13.592	0.256	0.000	0.040	0.046	0.102	0.000	0.000	0.132	86.908	0.000	0.001	0.000	0.000
TryAgain_1-1	Try Again, surface	8 ?	99.206	13.404	0.031	0.000	0.000	0.044	0.000	0.000	0.000	0.079	87.108	0.000	0.000	0.010	0.000
TryAgain_2-1	Try Again, surface	8 ?	98.434	13.571	0.013	0.018	0.000	0.046	0.135	0.000	0.038	0.277	85.639	0.000	0.010	0.005	0.000
TryAgain_3-1	Try Again, surface	8 ?	99.196	13.377	0.032	0.002	0.000	0.018	0.054	0.000	0.000	0.187	86.871	0.000	0.000	0.005	0.000
TryAgain_4-1	Try Again, surface	8 ?	101.095	13.402	0.019	0.024	0.029	0.046	0.065	0.000	0.030	0.298	88.345	0.000	0.011	0.000	0.000
TryAgain_5-1	Try Again, surface	8 ?	100.382	13.498	0.006	0.000	0.026	0.025	0.111	0.000	0.000	0.300	87.936	0.000	0.004	0.004	0.000

B. Electron Microprobe Data: Sulfides, Oxides, and Sulfates

TryAgain_6-1	Try Again, surface	8 ?	99.919	13.539	0.020	0.003	0.001	0.027	0.065	0.000	0.000	0.240	87.350	0.000	0.000	0.000	0.000
TryAgain_6-3	Try Again, surface	8 ?	100.115	13.595	0.025	0.012	0.003	0.033	0.078	0.000	0.000	0.185	87.563	0.000	0.000	0.007	0.000
TryAgain_7-1	Try Again, surface	8 ?	99.419	13.636	0.033	0.000	0.002	0.042	0.057	0.000	0.000	0.220	86.700	0.000	0.000	0.015	0.000
TryAgain_8-1	Try Again, surface	8 ?	99.818	13.373	0.043	0.008	0.004	0.040	0.055	0.000	0.000	0.187	87.344	0.000	0.000	0.022	0.000
WRN_008_7-1	Wernecke, surface	6, 8	99.996	13.537	0.019	0.000	0.000	0.050	0.166	0.000	0.000	0.231	87.075	0.000	0.011	0.000	0.000
HOM_053-1_1-1	Homestake, surface	1, 7, 8	100.702	13.619	0.016	0.000	0.000	0.044	0.129	0.000	0.000	0.214	88.117	0.000	0.022	0.000	0.000
HOM-053-1-1-4	Homestake, surface	1, 7, 8	100.444	13.654	0.026	0.022	0.006	0.029	0.101	0.000	0.000	0.292	86.281	0.000		0.000	0.041
HOM_053-1_2-1	Homestake, surface	1, 7, 8	99.724	13.581	0.025	0.002	0.000	0.053	0.100	0.000	0.000	0.319	87.034	0.000	0.000	0.000	0.000
HOM-053-1-2-3	Homestake, surface	1, 7, 8	100.592	13.668	0.013	0.000	0.020	0.029	0.125	0.021	0.000	0.301	86.390	0.000		0.000	0.000
HOM_053-1_3-4	Homestake, surface	1, 7, 8	99.520	13.260	0.041	0.020	0.023	0.035	0.025	0.000	0.000	0.187	87.116	0.000	0.000	0.000	0.000
HOM-053-1-3-6	Homestake, surface	1, 7, 8	99.918	13.475	0.027	0.015	0.000	0.018	0.074	0.021	0.000	0.200	86.074	0.000		0.000	0.000
HOM_053-1_4-2	Homestake, surface	1, 7, 8	99.957	13.755	0.034	0.000	0.000	0.025	0.053	0.000	0.000	0.183	87.334	0.000	0.000	0.007	0.000
HOM-053-1-4-4	Homestake, surface	1, 7, 8	99.870	13.895	0.030	0.000	0.000	0.042	0.000	0.012	0.000	0.219	85.683	0.000		0.000	0.012
HOM-053-1-4-5	Homestake, surface	1, 7, 8	99.065	13.621	0.039	0.000	0.000	0.000	0.069	0.000	0.000	0.174	85.209	0.000		0.000	0.097
HOM_053-1_5-2	Homestake, surface	1, 7, 8	101.643	13.475	0.047	0.012	0.143	0.029	0.036	0.000	0.000	0.127	89.213	0.000	0.000	0.000	0.000
HOM-053-1-5-5	Homestake, surface	1, 7, 8	100.672	13.508	0.071	0.000	0.019	0.002	0.005	0.075	0.000	0.178	86.711	0.000		0.005	0.044
POR_056_1-3	Porcupine, surface	8	99.549	13.141	0.781	0.000	0.127	0.000	0.000	0.000	0.000	0.037	86.185	0.000	0.021	0.000	0.000
POR_056_1-4	Porcupine, surface	8	99.527	13.595	0.058	0.015	0.000	0.051	0.000	0.000	0.000	0.070	87.223	0.000	0.000	0.000	0.000
POR_056_1-6	Porcupine, surface	8	102.818	13.705	0.141	0.028	2.023	0.051	0.000	0.000	0.042	0.026	88.101	0.000	0.000	0.000	0.000
POR_056_2-3	Porcupine, surface	8	99.874	13.404	0.040	0.000	0.025	0.030	0.043	0.000	0.000	0.099	87.731	0.000	0.000	0.000	0.000
POR_056_3-6	Porcupine, surface	8	100.862	13.502	0.060	0.048	0.392	0.023	0.000	0.000	0.000	0.123	87.917	0.000	0.000	0.011	0.000
POR_056_4-3	Porcupine, surface	8	100.144	13.568	0.058	0.004	0.000	0.003	0.000	0.000	0.000	0.037	87.947	0.000	0.000	0.000	0.000
POR_056_5-1	Porcupine, surface	8	100.310	13.415	0.025	0.000	0.008	0.042	0.000	0.000	0.000	0.032	88.163	0.000	0.001	0.017	0.000
POR_056_6-5	Porcupine, surface	8	100.490	13.578	0.036	0.000	0.033	0.066	0.000	0.000	0.000	0.016	88.194	0.000	0.000	0.011	0.000
POR_056_7-2	Porcupine, surface	8	100.846	13.307	0.038	0.004	0.009	0.051	0.000	0.000	0.000	0.104	88.529	0.000	0.011	0.002	0.000

B. Electron Microprobe Data: Sulfides, Oxides, and Sulfates

POR_056_7-4	Porcupine, surface	8	99.887	13.680	0.364	0.012	0.000	0.005	0.000	0.000	0.000	0.117	87.118	0.000	0.000	0.000	0.000
POR_056_7-5	Porcupine, surface	8	100.068	13.394	0.257	0.004	0.016	0.032	0.006	0.000	0.000	0.115	87.645	0.000	0.005	0.000	0.000
K06-2-167-2m_2-3	Silver King	8	99.659	13.387	0.026	0.004	0.034	0.000	0.093	0.000	0.000	0.179	87.276	0.000	0.012	0.000	0.000
K06-2-167-2m_3-3	Silver King	8	100.376	13.576	0.036	0.006	0.009	0.044	0.000	0.000	0.000	0.077	87.896	0.000	0.004	0.001	0.000
K06-2-167-2m_3-6	Silver King	8	101.068	13.557	0.086	0.177	0.000	0.055	0.000	0.000	0.000	0.131	88.345	0.000	0.009	0.007	0.000
K06-2-167-2m_4-2	Silver King	8	100.814	13.515	0.027	0.000	0.006	0.040	0.046	0.000	0.000	0.245	88.246	0.000	0.014	0.000	0.000
K06-2-167-2m_5-3	Silver King	8	100.995	13.479	0.062	0.226	0.050	0.007	0.000	0.000	0.000	0.123	88.381	0.000	0.009	0.020	0.000
K06-2-167-2m_8-4	Silver King	8	100.924	13.550	0.384	0.311	0.027	0.032	0.000	0.000	0.000	0.079	87.857	0.000	0.000	0.000	0.000
K06-2-167-2m_9-2	Silver King	8	100.331	13.498	0.044	0.001	0.022	0.038	0.000	0.000	0.000	0.105	87.982	0.000	0.010	0.000	0.000
K06-25-44-8m_1-1	K-structure	8	99.362	13.463	0.025	0.000	0.003	0.019	**0.499**	0.000	0.005	**0.485**	86.188	0.000	0.033	0.000	0.000
K06-25-44-8m_1-2	K-structure	8	100.660	13.576	0.044	0.010	0.010	0.038	0.173	0.000	0.000	0.303	87.769	0.000	0.015	0.000	0.000
K06-25-44-8m_2-1	K-structure	8	100.290	13.472	0.046	0.013	0.007	0.023	0.060	0.000	0.017	0.190	87.776	0.000	0.000	0.000	0.000
K06-25-44-8m_3-1	K-structure	8	100.987	13.556	0.005	0.015	0.022	0.058	0.090	0.000	0.014	0.221	88.121	0.000	0.008	0.000	0.000
K06-25-44-8m_4-1	K-structure	8	100.182	13.434	0.032	0.000	0.000	0.020	0.066	0.000	0.000	0.227	87.758	0.000	0.007	0.000	0.000
K06-25-44-8m_5-1	K-structure	8	100.264	13.560	0.025	0.009	0.000	0.016	0.156	0.000	0.000	0.409	87.208	0.000	0.000	0.004	0.000
K07-76-115-3m-1-1	BK_E, 965 masl	8 ?	102.561	12.046	0.031	0.000	0.000	0.052	**0.749**	0.000	0.000	**0.766**	89.595	0.000	0.000	0.013	0.000
K07-76-115-3m-2-1	BK_E, 965 masl	8 ?	100.161	13.126	0.029	0.000	0.000	0.058	**0.698**	0.128	0.000	0.097	86.955	0.000	0.011	0.003	0.000
K07-76-115-3m-3-1	BK_E, 965 masl	8 ?	99.584	13.339	0.015	0.016	0.008	0.043	**0.942**	0.000	0.049	0.017	86.181	0.000	0.000	0.014	0.000
K07-76-115-3m-3-2	BK_E, 965 masl	8 ?	98.887	13.326	0.016	0.026	0.001	0.078	**0.956**	0.000	0.000	0.053	85.904	0.000	0.000	0.007	0.000
K07-76-115-3m-4-1	BK_E, 965 masl	8 ?	101.800	13.081	0.007	0.000	0.019	0.092	0.054	0.000	0.000	0.159	89.508	0.000	0.001	0.021	0.000
K07-76-115-3m-5-1	BK_E, 965 masl	8 ?	100.061	13.259	0.038	0.000	0.000	0.090	0.403	0.000	0.000	0.136	87.228	0.000	0.000	0.000	0.000
K07-76-115-3m-6-1	BK_E, 965 masl	8 ?	98.351	13.253	0.001	0.000	0.000	0.060	**0.577**	0.000	0.000	0.109	85.295	0.000	0.001	0.022	0.000
K07-76-125m-3-6	BK_E, 965 masl	6, 7, 8	101.924	13.151	0.123	0.000	0.000	0.085	0.017	0.000	0.000	0.106	89.463	0.000	0.002	0.002	0.000
K07-76-125m-5-3	BK_E, 965 masl	6, 7, 8	102.691	13.293	0.055	0.006	0.549	0.038	0.012	0.000	0.000	0.188	89.816	0.000	0.001	0.000	0.000
K07-76-125m-5-6	BK_E, 965 masl	3, 4?	98.081	13.975	0.052	0.000	0.009	0.071	0.171	0.093	0.000	0.358	84.450	0.000	0.000	0.000	0.000
K07-76-125m-5-7	BK_E, 965 masl	6, 7, 8	100.101	13.207	0.037	0.005	0.000	0.116	0.015	0.099	0.000	0.174	87.500	0.000	0.000	0.007	0.000
K07-76-125m-5-8	BK_E, 965 masl	6, 7, 8	101.869	13.336	0.014	0.000	0.013	0.079	0.049	0.023	0.000	0.229	89.105	0.000	0.008	0.006	0.000
K07-76-125m-6-6	BK_E, 965 masl	6, 7, 8	100.975	12.941	0.028	0.000	0.000	0.000	0.000	0.000	0.000	0.104	89.394	0.000	0.000	0.000	0.000

B. Electron Microprobe Data: Sulfides, Oxides, and Sulfates

K07-76-125m-6-9	BK_E, 965 masl	6, 7, 8	102.680	13.201	0.018	0.000	0.003	0.099	0.049	0.000	0.000	0.224	90.088	0.000	0.000	0.000	0.000
K07-76-125m-6-10	BK_E, 965 masl	6, 7, 8	101.866	13.170	0.023	0.000	0.008	0.091	0.000	0.061	0.000	0.086	89.446	0.000	0.001	0.009	0.000
K07-76-125m-7-8	BK_E, 965 masl	3, 4?	101.974	13.295	0.097	0.009	0.019	0.072	0.033	0.000	0.000	0.139	89.410	0.000	0.000	0.008	0.000
K07-76-125m-8-5	BK_E, 965 masl	3, 4?	99.429	13.476	0.135	0.017	0.018	0.032	0.135	0.035	0.043	**0.432**	84.893	0.000	0.000	0.015	0.000
K07-86-223-3m_2-4	BK_E, 940 masl	8?	98.390	13.762	0.024	0.023	0.003	0.026	**0.516**	0.000	0.000	0.028	84.798	0.000	0.000	0.000	0.000
K07-86-223-3m_3-3	BK_E, 940 masl	6, 8?	97.543	13.644	0.012	0.007	0.019	0.031	**0.821**	0.094	0.000	**0.428**	83.518	0.000	0.018	0.000	0.000
K07-86-223-3m_4-3	BK_E, 940 masl	8?	98.977	13.389	0.074	0.088	0.000	0.007	0.253	0.000	0.000	0.000	86.143	0.000	0.005	0.000	0.000
K07-86-223-3m_5-3	BK_E, 940 masl	8?	99.785	13.630	0.043	0.020	0.010	0.034	**0.494**	0.000	0.000	0.167	86.578	0.000	0.000	0.000	0.000
K07-86-223-3m_6-3	BK_E, 940 masl	8?	99.954	13.419	0.552	**0.577**	0.053	0.033	0.382	0.000	0.000	0.049	86.109	0.000	0.000	0.002	0.000
K07-88-59-6m_1-1	Bermingham	8	100.419	13.492	0.026	0.000	0.005	0.018	0.013	0.000	0.000	0.101	88.155	0.000	0.005	0.000	0.000
K07-88-59-6m_1-2	Bermingham	8	100.136	13.738	0.052	0.000	0.040	0.013	0.071	0.000	0.000	0.147	87.592	0.000	0.000	0.000	0.000
K07-88-59-6m_1-4	Bermingham	8	99.899	13.615	0.041	0.015	0.007	0.031	0.000	0.000	0.000	0.125	87.405	0.000	0.000	0.013	0.000
K07-88-59-6m_2-1	Bermingham	8	100.069	13.622	0.037	0.000	0.000	0.011	0.163	0.000	0.000	0.303	87.411	0.000	0.000	0.000	0.000
K07-88-59-6m_3-1	Bermingham	8	100.266	13.505	0.050	0.007	0.000	0.050	0.121	0.000	0.000	0.248	87.824	0.000	0.000	0.000	0.000
K07-88-59-6m_4-1	Bermingham	8	102.836	13.420	0.034	0.012	0.000	0.040	0.415	0.000	0.000	0.525	89.525	0.000	0.000	0.015	0.000
K07-88-59-6m_5-1	Bermingham	8	102.111	13.345	0.024	0.029	0.016	0.044	0.120	0.000	0.000	0.243	89.694	0.000	0.014	0.000	0.000
K07-88-59-6m_6-1	Bermingham	8	101.311	13.352	0.040	0.000	0.000	0.039	0.103	0.000	0.000	0.220	88.857	0.000	0.002	0.000	0.000
K07-88-59-6m_7-1	Bermingham	8	100.888	13.459	0.020	0.009	0.000	0.041	0.076	0.000	0.017	0.135	88.526	0.000	0.007	0.000	0.000
K07-88-59-6m_8-2	Bermingham	8	102.068	13.462	0.009	0.003	0.027	0.033	0.130	0.000	0.000	0.257	89.834	0.000	0.000	0.000	0.000
K07-88-59-6m_8-3	Bermingham	8	102.607	14.054	0.032	0.000	0.054	0.040	0.000	0.000	0.000	0.915	88.947	0.000	0.000	0.006	0.000
K08-161-229-8m_1-1	Lucky Queen	8	100.525	13.436	0.041	0.012	0.016	0.015	0.072	0.000	0.000	0.227	87.939	0.000	0.000	0.000	0.000
K08-161-229-8m_1-4	Lucky Queen	8	100.171	13.498	0.043	0.015	0.000	0.021	0.096	0.000	0.000	0.185	87.801	0.000	0.000	0.000	0.000
K08-161-229-8m_2-1	Lucky Queen	8	100.238	13.482	0.039	0.000	0.000	0.033	0.064	0.000	0.000	0.122	87.921	0.000	0.000	0.000	0.000
K08-161-229-8m_2-2	Lucky Queen	8	100.295	13.624	0.010	0.012	0.000	0.027	0.144	0.000	0.011	0.354	87.337	0.000	0.012	0.006	0.000
K08-161-229-8m_2-3	Lucky Queen	8	100.745	13.614	0.022	0.000	0.015	0.027	0.096	0.000	0.000	0.268	88.029	0.000	0.002	0.000	0.000
K08-161-229-8m_3-1	Lucky Queen	8	99.512	13.469	0.008	0.000	0.001	0.022	0.068	0.000	0.000	0.178	87.190	0.000	0.000	0.000	0.000
K08-161-229-8m_3-3	Lucky Queen	8	100.498	13.678	0.013	0.000	0.000	0.006	0.127	0.000	0.000	0.242	87.856	0.000	0.001	0.000	0.000
K08-161-229-8m_4-1	Lucky Queen	8	99.550	13.543	0.034	0.004	0.000	0.034	0.123	0.000	0.000	0.241	87.118	0.000	0.000	0.000	0.000

B. Electron Microprobe Data: Sulfides, Oxides, and Sulfates

K08-161-229-8m_5-1	Lucky Queen	8	100.310	13.417	0.014	0.011	0.023	0.051	0.115	0.000	0.033	0.239	87.675	0.000	0.003	0.015	0.000
K08-161-229-8m_6-1	Lucky Queen	8	100.582	13.479	0.032	0.000	0.019	0.032	0.136	0.000	0.000	0.258	87.912	0.000	0.000	0.012	0.000
K08-161-229-8m_7-1	Lucky Queen	8	101.904	13.628	0.019	0.000	0.002	0.047	0.127	0.000	0.000	0.330	89.082	0.000	0.004	0.001	0.000
K08-161-229-8m_8-1	Lucky Queen	8	101.856	13.578	0.025	0.000	0.000	0.035	**0.454**	0.000	0.000	**0.619**	88.575	0.000	0.000	0.000	0.000
K08-161-229-8m_9-1	Lucky Queen	8	100.693	13.469	0.029	0.000	0.003	0.028	0.073	0.000	0.014	0.137	88.409	0.000	0.000	0.000	0.000
K08-161-229-8m_10-1	Lucky Queen	8	101.668	13.628	0.066	0.015	0.006	0.045	0.090	0.000	0.023	0.209	88.920	0.000	0.000	0.000	0.000
K09-187-201-9m-1-1	BK_E, 950 masl	7, 8, 9, 10	102.777	13.089	0.053	0.000	0.018	0.119	0.059	0.000	0.000	0.226	90.273	0.000	0.000	0.000	0.000
K09-187-201-9m-2-2	BK_E, 950 masl	7, 8, 9, 10	101.486	13.262	0.020	0.000	0.008	0.037	0.009	0.065	0.000	0.164	89.021	0.000	0.000	0.000	0.000
K09-187-201-9m-2-3	BK_E, 950 masl	7, 8, 9, 10	102.183	13.119	0.006	0.000	0.000	0.087	0.107	0.000	0.000	0.199	89.714	0.000	0.000	0.000	0.000
K09-187-201-9m-3-1	BK_E, 950 masl	7, 8, 9, 10	101.580	13.001	0.008	0.009	0.000	0.094	0.135	0.000	0.000	0.311	89.038	0.000	0.000	0.002	0.000
K09-187-201-9m-3-3	BK_E, 950 masl	7, 8, 9, 10	101.677	12.998	0.002	0.000	0.027	0.009	0.000	0.029	0.000	0.144	89.528	0.000	0.004	0.003	0.000
K09-187-201-9m-4-1	BK_E, 950 masl	7, 8, 9, 10	102.746	13.109	0.002	0.011	0.000	0.146	0.177	0.000	0.000	0.408	89.980	0.000	0.011	0.016	0.000
K09-187-201-9m-4-5	BK_E, 950 masl	8	100.441	13.317	0.030	0.011	0.000	0.032	**1.673**	0.014	0.000	**1.516**	84.852	0.000	0.000	0.000	0.000
K09-187-201-9m-5-1	BK_E, 950 masl	7, 8, 9, 10	102.762	12.938	0.000	0.005	0.000	0.080	0.000	0.000	0.000	0.131	90.776	0.000	0.000	0.007	0.000
K09-187-201-9m-8-2	BK_E, 950 masl	7, 8, 9, 10	101.392	13.235	0.013	0.000	0.075	0.099	0.086	0.009	0.005	0.275	88.536	0.000	0.000	0.000	0.000
K09-187-201-9m-10-1	BK_E, 950 masl	7, 8, 9, 10	101.980	13.175	0.000	0.010	0.000	0.089	0.035	0.105	0.000	0.159	89.512	0.000	0.000	0.000	0.000
K09-187-201-9m-10-5	BK_E, 950 masl	7, 8, 9, 10	102.625	13.077	0.184	0.002	0.000	0.048	0.084	0.000	0.004	0.104	90.103	0.000	0.000	0.024	0.000
K09-201-238m-1-5	Keno 700	8	100.575	14.415	0.520	0.021	0.005	0.039	0.026	0.000	0.000	0.070	85.572	0.000	0.009	0.012	0.000
K09-201-238m-2-2	Keno 700	8	101.523	14.640	0.045	0.007	0.000	0.020	0.000	0.000	0.039	0.082	86.778	0.000	0.000	0.000	0.000
K09-201-238m-2-4	Keno 700	8	101.460	13.345	0.513	0.000	0.024	0.077	0.004	0.000	0.006	0.113	87.417	0.000	0.000	0.000	0.000
K09-201-238m-2-6	Keno 700	8	100.825	14.346	0.209	0.000	0.000	0.030	0.000	0.000	0.000	0.000	86.552	0.000	0.000	0.001	0.000
K09-201-238m-3-4	Keno 700	8	102.484	14.373	0.348	0.000	0.000	0.021	0.015	0.065	0.000	0.094	87.642	0.000	0.019	0.000	0.000
K09-201-238m-3-6	Keno 700	8	102.459	14.346	0.960	0.010	0.007	0.080	0.000	0.003	0.001	0.125	87.129	0.000	0.003	0.000	0.000
K09-201-238m-4-2	Keno 700	8	101.569	14.307	0.974	0.009	0.000	0.098	0.000	0.006	0.000	0.147	86.060	0.000	0.006	0.000	0.000
K09-201-238m-4-5	Keno 700	8	102.374	14.492	0.227	0.011	0.432	0.038	0.000	0.029	0.000	0.029	87.147	0.000	0.000	0.007	0.000
K09-201-238m-4-11	Keno 700	8	102.916	14.101	0.197	0.000	0.002	0.059	0.095	0.094	0.000	0.180	88.192	0.000	0.001	0.007	0.000

B. Electron Microprobe Data: Sulfides, Oxides, and Sulfates

K09-201-238m-5-2	Keno 700	8	102.024	14.204	0.070	0.013	0.266	0.043	0.002	0.000	0.000	0.098	87.505	0.000	0.000	0.003	0.000
K09-201-238m-5-7	Keno 700	8	101.211	14.274	0.041	0.012	0.000	0.048	0.000	0.106	0.000	0.081	86.761	0.000	0.000	0.000	0.000
K09-201-238m-6-3	Keno 700	8	101.147	14.396	0.188	0.000	0.003	0.039	0.003	0.000	0.000	0.101	86.629	0.000	0.004	0.000	0.000
K09-201-238m-6-4	Keno 700	8	101.634	14.406	0.032	0.000	0.003	0.039	0.005	0.000	0.000	0.108	87.226	0.000	0.008	0.000	0.000
K09-201-238m-6-7	Keno 700	8	102.587	14.251	0.004	0.008	0.065	0.002	0.000	0.000	0.000	0.056	88.409	0.000	0.000	0.000	0.000
K09-201-238m-7-4	Keno 700	8	101.833	14.411	0.046	0.000	0.391	0.048	0.000	0.000	0.000	0.060	87.186	0.000	0.000	0.000	0.000
K09-201-238m-7-6	Keno 700	8	100.712	14.464	0.024	0.025	0.000	0.034	0.064	0.000	0.000	0.135	86.172	0.000	0.000	0.000	0.000
K09-201-238m-7-10	Keno 700	8	101.383	14.174	0.033	0.007	0.000	0.058	0.036	0.097	0.000	0.102	87.014	0.000	0.000	0.000	0.000
K09-201-238m-8-9	Keno 700	8	101.336	14.459	0.064	0.197	0.303	0.019	0.078	0.041	0.000	0.155	86.298	0.000	0.000	0.000	0.000
K09-201-238m-9-2	Keno 700	8	101.207	14.134	0.447	0.005	0.000	0.035	0.000	0.012	0.000	0.000	86.796	0.000	0.005	0.000	0.000
K09-201-238m-9-4	Keno 700	8	101.128	14.199	0.077	0.000	0.000	0.030	0.000	0.105	0.000	0.092	86.868	0.000	0.012	0.003	0.000
BKUD09-139-8-3m_5-4	BK_SW, 965 masl	8	100.297	13.588	0.444	0.017	0.000	0.021	0.154	0.000	0.000	0.276	86.941	0.000	0.000	0.000	0.000
BKUD09-139-8-3m_5-5	BK_SW, 965 masl	8	102.158	13.684	0.088	0.000	1.455	0.000	0.000	0.033	0.000	0.154	87.656	0.000	0.000	0.001	0.000
BKUD09-143-51-2m-5-3	BK_SW, NE-end, 1000 masl	8	99.442	12.690	0.032	0.004	0.088	0.093	0.389	0.050	0.000	0.032	87.085	0.000	0.001	0.012	0.000
BKUD09-143-51-2m-5-6	BK_SW, NE-end, 1000 masl	8	100.215	12.690	0.038	0.001	0.000	0.112	0.663	0.023	0.000	0.290	87.437	0.000	0.000	0.003	0.000
BKUD09-143-51-2m-6-5	BK_SW, NE-end, 1000 masl	8	98.725	12.828	0.020	0.000	0.000	0.000	**0.500**	0.052	0.000	0.073	86.290	0.000	0.006	0.000	0.000
BKUD09-143-52-8m_1-1	BK_SW, NE-end, 1000 masl	8	101.309	13.588	0.017	0.008	0.010	0.031	0.051	0.000	0.061	0.261	88.589	0.000	0.012	0.000	0.000
BKUD09-143-52-8m_1-2	BK_SW, NE-end, 1000 masl	8	101.116	13.683	0.042	0.000	0.038	0.024	0.085	0.000	0.016	0.251	88.412	0.000	0.000	0.000	0.000
BKUD09-143-52-8m_2-1	BK_SW, NE-end, 1000 masl	8	102.517	13.645	0.031	0.005	0.000	0.058	0.089	0.000	0.028	0.187	89.704	0.000	0.000	0.000	0.000
BKUD09-143-52-8m_3-1	BK_SW, NE-end, 1000 masl	8	101.099	13.526	0.038	0.000	0.029	0.022	0.119	0.000	0.000	0.291	88.551	0.000	0.000	0.000	0.000
BKUD09-143-52-8m_4-6	BK_SW, NE-end, 1000 masl	8	102.401	13.576	0.011	0.000	0.004	0.041	0.113	0.000	0.000	0.215	89.762	0.000	0.005	0.000	0.000
BKUD09-143-52-8m_5-1	BK_SW, NE-end, 1000 masl	8	100.494	13.554	0.029	0.004	0.000	0.006	0.031	0.000	0.000	0.179	88.048	0.000	0.000	0.000	0.000
BKUD09-143--54m_1-1	BK_SW, NE-end, 1000 masl	8	99.720	13.789	0.031	0.000	0.017	0.023	0.077	0.033	0.008	0.206	86.443	0.000	0.017	0.000	0.000
BKUD09-143--54m_2-1	BK_SW, NE-end, 1000 masl	8	98.981	13.470	0.038	0.000	0.000	0.008	0.008	0.000	0.000	0.092	86.445	0.000	0.013	0.000	0.000
BKUD09-143--54m_2-2	BK_SW, NE-end, 1000 masl	8	99.240	13.559	0.038	0.000	0.000	0.009	0.000	0.000	0.000	0.071	86.551	0.000	0.000	0.001	0.000

B. Electron Microprobe Data: Sulfides, Oxides, and Sulfates

BKUD09-143--54m_3-1	BK_SW, NE-end, 1000 masl	8	100.357	13.782	0.012	0.013	0.001	0.053	0.021	0.160	0.000	0.155	87.189	0.000	0.000	0.000	0.000
BKUD09-143--54m_3-6	BK_SW, NE-end, 1000 masl	8	97.856	13.688	0.035	0.005	0.023	0.051	0.106	0.000	0.000	0.163	84.737	0.000	0.013	0.007	0.000
BKUD09-143--54m_4-1	BK_SW, NE-end, 1000 masl	8	98.432	13.431	0.043	0.003	0.000	0.022	0.004	0.027	0.000	0.177	85.867	0.000	0.000	0.003	0.000
BKUD09-143--54m_4-2	BK_SW, NE-end, 1000 masl	8	100.007	13.482	0.014	0.000	0.000	0.006	0.000	0.042	0.000	0.021	87.351	0.000	0.008	0.003	0.000
BKUD09-143--54m_5-1	BK_SW, NE-end, 1000 masl	8	100.881	13.582	0.030	0.000	0.000	0.005	0.059	0.000	0.010	0.190	88.025	0.000	0.000	0.000	0.000
BKUD09-143--54m_5-3	BK_SW, NE-end, 1000 masl	8	99.932	13.658	0.022	0.005	0.005	0.010	0.273	0.039	0.038	**0.549**	86.242	0.000	0.000	0.000	0.000
BKUD09-143--54m_6-1	BK_SW, NE-end, 1000 masl	8	100.637	13.417	0.027	0.008	0.000	0.007	0.132	0.000	0.000	0.252	87.762	0.000	0.000	0.000	0.000
BKUD09-143--54m_7-1	BK_SW, NE-end, 1000 masl	8	100.455	13.615	0.013	0.000	0.000	0.000	0.177	0.048	0.000	**0.430**	87.147	0.000	0.000	0.000	0.000
BKUD09-143--54m_8-1	BK_SW, NE-end, 1000 masl	8	99.614	13.664	0.361	0.047	1.483	0.045	**0.517**	0.000	0.028	**0.620**	83.771	0.000	0.000	0.000	0.000
BKUD09-148-33-5m-1-2	BK_99, 1025 masl	5/8?	101.010	12.782	0.057	0.041	0.531	0.055	0.043	0.000	0.000	0.212	88.140	0.000	0.001	0.008	0.000
BKUD09-148-33-5m-3-3	BK_99, 1025 masl	5/8?	98.378	12.984	0.339	0.016	2.280	0.137	0.115	0.064	0.000	0.344	82.946	0.000	0.000	0.004	0.000
BKUD09-148-33-5m-4-2	BK_99, 1025 masl	5/8?	100.587	12.698	0.193	0.232	0.042	0.097	0.019	0.061	0.029	0.166	87.791	0.000	0.008	0.000	0.000
BKUD09-148-33-5m-5-2	BK_99, 1025 masl	5/8?	99.526	12.798	0.091	0.000	0.000	0.000	0.074	0.086	0.001	0.231	87.113	0.000	0.000	0.011	0.000
BKUD09-148-33-5m-6-3	BK_99, 1025 masl	5/8?	98.804	12.724	0.055	0.000	0.002	0.068	0.135	0.000	0.000	0.190	86.638	0.000	0.000	0.014	0.000
BKUD09-148-33-5m-7-3	BK_99, 1025 masl	5/8?	101.339	13.084	0.217	0.036	3.242	0.060	0.044	0.038	0.000	0.165	85.736	0.000	0.000	0.008	0.000
BKUD09-148-33-5m-8-3	BK_99, 1025 masl	5/8?	98.650	12.776	0.084	0.000	0.031	0.021	0.118	0.000	0.000	0.262	86.351	0.000	0.007	0.000	0.000
BKUD09-150-64-1m-1-2	BK_SW, SW-end, 975 masl	8	101.931	13.264	0.000	0.015	0.000	0.036	0.133	0.000	0.000	0.232	89.196	0.000	0.009	0.000	0.000
BKUD09-150-64-1m-2-1	BK_SW, SW-end, 975 masl	8	102.943	13.346	0.015	0.015	0.000	0.090	0.042	0.000	0.000	0.000	90.378	0.000	0.008	0.000	0.000
BKUD09-150-64-1m-3-3	BK_SW, SW-end, 975 masl	8	101.491	13.216	0.025	0.000	0.000	0.055	0.011	0.055	0.010	0.175	88.928	0.000	0.020	0.007	0.000
BKUD09-150-64-1m-3-4	BK_SW, SW-end, 975 masl	8	102.242	13.160	0.030	0.020	0.000	0.115	0.066	0.000	0.000	0.235	89.642	0.000	0.000	0.000	0.000
BKUD09-150-64-1m-4-4	BK_SW, SW-end, 975 masl	8	102.379	13.169	0.022	0.006	0.009	0.044	0.040	0.023	0.002	0.084	89.804	0.000	0.012	0.017	0.000
BKUD09-150-64-1m-5-1	BK_SW, SW-end, 975 masl	8	102.787	13.295	0.028	0.000	0.292	0.050	0.000	0.035	0.000	0.080	90.011	0.000	0.000	0.000	0.000
BKUD09-150-64-1m-5-3	BK_SW, SW-end, 975 masl	8	102.185	12.982	0.044	0.000	0.029	0.035	0.000	0.050	0.016	0.000	90.207	0.000	0.008	0.000	0.000
BKUD09-150-64-1m-6-2	BK_SW, SW-end, 975 masl	8	101.767	13.172	0.003	0.014	0.000	0.120	0.009	0.000	0.000	0.138	89.375	0.000	0.000	0.001	0.000

B. Electron Microprobe Data: Sulfides, Oxides, and Sulfates

BKUD09-150-64-1m-7-2	BK_SW, SW-end, 975 masl	8	102.579	13.215	0.020	0.000	0.036	0.077	0.012	0.000	0.000	0.174	90.194	0.000	0.000	0.005	0.000
BKUD09-150-64-1m-8-1	BK_SW, SW-end, 975 masl	8	100.517	13.273	0.039	0.000	0.009	0.008	0.096	0.000	0.000	0.269	87.647	0.000	0.000	0.000	0.000
BKUD09-150-64-1m-9-1	BK_SW, SW-end, 975 masl	8	102.629	13.166	0.000	0.033	0.000	0.068	0.103	0.009	0.028	0.143	89.938	0.000	0.000	0.000	0.000
BKUD09-151-33-3m_3-1	BK_99, 1045 masl	8	101.030	13.619	0.029	0.000	0.008	0.005	0.266	0.000	0.000	0.546	88.108	0.000	0.000	0.013	0.000
BKUD09-151-33-3m_4-1	BK_99, 1045 masl	8	101.167	13.430	0.039	0.000	0.000	0.016	0.105	0.000	0.000	0.172	88.884	0.000	0.000	0.000	0.000
BKUD09-151-33-3m_6-1	BK_99, 1045 masl	8	101.274	13.527	0.025	0.004	0.032	0.034	0.081	0.000	0.000	0.199	89.008	0.000	0.000	0.000	0.000
BKUD09-151-33-3m_8-1	BK_99, 1045 masl	8	101.304	13.637	0.433	0.000	0.011	0.027	0.142	0.000	0.000	0.226	88.150	0.000	0.000	0.001	0.000
BKUD09-157-100-5m-5-2	BK_SW, SW-end, 930 masl	8	101.800	12.852	0.059	0.061	0.930	0.075	0.076	0.000	0.015	0.248	88.407	0.000	0.000	0.019	0.000
BKUD09-157-100-5m-6-2	BK_SW, SW-end, 930 masl	8	99.267	12.919	0.018	0.000	0.142	0.126	0.050	0.000	0.000	0.230	86.922	0.000	0.000	0.010	0.000
BKUD09-158-36m_1-1	BK_SW, NE-end, 1030 masl	5/8?	97.041	13.590	0.061	0.014	0.000	0.032	0.081	0.054	0.000	0.231	83.958	0.000	0.001	0.000	0.000
BKUD09-158-36m_2-1	BK_SW, NE-end, 1030 masl	5/8?	99.446	13.660	0.011	0.000	0.014	0.044	0.017	0.009	0.000	0.210	86.410	0.000	0.002	0.007	0.000
BKUD09-158-36m_3-2	BK_SW, NE-end, 1030 masl	5/8?	100.516	13.720	0.630	0.000	0.000	0.013	0.095	0.000	0.000	0.232	86.914	0.000	0.003	0.000	0.000
BKUD09-158-36m_4-1	BK_SW, NE-end, 1030 masl	5/8?	99.914	13.743	0.031	0.024	0.002	0.031	0.006	0.000	0.015	0.107	86.986	0.000	0.000	0.004	0.000
BKUD09-158-36m_5-2	BK_SW, NE-end, 1030 masl	5/8?	99.456	13.493	0.021	0.014	0.000	0.025	0.068	0.000	0.000	0.136	86.772	0.000	0.015	0.000	0.000
BKUD09-158-36m_5-3	BK_SW, NE-end, 1030 masl	5/8?	99.914	13.469	0.027	0.000	0.009	0.000	0.024	0.000	0.000	0.231	87.255	0.000	0.000	0.000	0.000
BKUD09-158-36m_6-1	BK_SW, NE-end, 1030 masl	5/8?	99.871	13.587	0.025	0.000	0.007	0.036	0.087	0.052	0.000	0.278	86.885	0.000	0.000	0.018	0.000
BKUD09-158-36m_6-7	BK_SW, NE-end, 1030 masl	5/8?	98.920	13.457	0.394	0.006	0.242	0.033	0.010	0.000	0.000	0.146	85.683	0.000	0.000	0.013	0.000
BKUD09-158-36m_7-1	BK_SW, NE-end, 1030 masl	5/8?	99.455	13.662	0.032	0.000	0.000	0.023	0.029	0.057	0.036	0.236	86.368	0.000	0.000	0.003	0.000
BKUD09-158-36-5m-4-1	BK_SW, NE-end, 1030 masl	8	101.539	14.318	0.040	0.007	0.000	0.011	0.010	0.000	0.000	0.089	87.319	0.000	0.000	0.000	0.000
BKUD09-158-36-5m-4-2	BK_SW, NE-end, 1030 masl	8	102.353	14.336	0.035	0.007	0.000	0.015	0.060	0.035	0.000	0.349	87.517	0.000	0.021	0.000	0.000
BKUD09-158-36-5m-6-7	BK_SW, NE-end, 1030 masl	8	102.869	14.351	0.058	0.020	0.691	0.036	0.037	0.000	0.000	0.178	87.648	0.000	0.002	0.006	0.000
BKUD09-158-36-5m-7-2	BK_SW, NE-end, 1030 masl	8	101.631	14.235	0.025	0.014	0.000	0.027	0.052	0.000	0.012	0.175	87.109	0.000	0.004	0.000	0.000
BKUD09-158-36-5m-8-1	BK_SW, NE-end, 1030 masl	8	101.337	14.259	0.137	0.007	0.005	0.003	0.148	0.000	0.000	0.202	86.824	0.000	0.000	0.000	0.000
BKUD09-158-36-5m-10-4	BK_SW, NE-end,	8	101.275	14.130	0.037	0.024	0.024	0.028	0.000	0.000	0.000	0.044	87.124	0.000	0.001	0.006	0.000

B. Electron Microprobe Data: Sulfides, Oxides, and Sulfates

	1030 masl																
BKUD09-158-36-5m-11-3	BK_SW, NE-end, 1030 masl	8	102.373	14.293	0.026	0.000	0.028	0.015	0.044	0.000	0.000	0.243	87.927	0.000	0.000	0.000	0.000
BKUD09-158-37m-1-3	BK_SW, NE-end, 1030 masl	5/8?	101.081	12.850	0.512	0.080	0.021	0.060	0.116	0.032	0.000	0.113	88.215	0.000	0.000	0.027	0.000
BKUD09-158-37m-2-1	BK_SW, NE-end, 1030 masl	5/8?	100.048	12.840	0.029	0.030	0.000	0.043	0.068	0.000	0.000	0.187	87.731	0.000	0.011	0.006	0.000
BKUD09-158-37m-3-1	BK_SW, NE-end, 1030 masl	5/8?	99.126	12.841	0.008	0.007	0.000	0.148	**0.444**	0.076	0.000	**0.591**	85.927	0.000	0.008	0.000	0.000
BKUD09-158-37m-3-3	BK_SW, NE-end, 1030 masl	5/8?	97.186	12.646	0.020	0.000	0.000	0.059	0.088	0.079	0.000	0.192	84.961	0.000	0.002	0.016	0.000
BKUD09-158-37m-4-4	BK_SW, NE-end, 1030 masl	5/8?	99.245	12.768	0.033	0.000	0.008	0.161	0.054	0.000	0.000	0.133	87.025	0.000	0.000	0.010	0.000
BKUD09-158-37m-5-1	BK_SW, NE-end, 1030 masl	5/8?	99.865	12.777	0.067	0.015	0.000	0.157	0.160	0.000	0.000	0.297	87.297	0.000	0.015	0.008	0.000
BKUD09-158-37m-5-4	BK_SW, NE-end, 1030 masl	5/8?	99.901	12.873	0.004	0.019	0.007	0.034	0.009	0.000	0.000	0.097	87.909	0.000	0.000	0.000	0.000
BKUD09-158-37m-6-2	BK_SW, NE-end, 1030 masl	5/8?	99.250	12.655	0.033	0.085	0.000	0.062	0.091	0.000	0.000	0.170	87.258	0.000	0.030	0.015	0.000
BKUD09-158-37m-7-1	BK_SW, NE-end, 1030 masl	5/8?	98.440	12.863	0.013	0.006	0.000	0.082	0.019	0.000	0.000	0.110	86.453	0.000	0.000	0.000	0.000
BKUD09-158-37m-7-6	BK_SW, NE-end, 1030 masl	5/8?	98.275	12.773	0.015	0.022	0.008	0.048	0.027	0.036	0.000	0.197	86.036	0.000	0.003	0.014	0.000
BKUD09-160-56-5m-1-1	BK_SW, SW-end, 950 masl	8	101.646	14.240	0.009	0.000	0.009	0.031	0.540	0.012	0.000	0.660	86.190	0.000	0.000	0.000	0.000
BKUD09-160-56-5m-1-6	BK_SW, SW-end, 950 masl	8	102.349	14.068	0.186	0.012	0.311	0.037	0.027	0.026	0.000	0.152	87.687	0.000	0.000	0.000	0.000
BKUD09-160-56-5m-2-3	BK_SW, SW-end, 950 masl	8	101.235	14.210	0.000	0.003	0.004	0.042	0.055	0.000	0.000	0.112	87.039	0.000	0.000	0.000	0.000
BKUD09-160-56-5m-3-1	BK_SW, SW-end, 950 masl	8	102.003	14.234	0.020	0.000	0.000	0.012	0.148	0.029	0.000	0.342	87.196	0.000	0.000	0.000	0.000
BKUD09-160-56-5m-3-6	BK_SW, SW-end, 950 masl	8	101.744	14.006	0.018	0.000	0.000	0.033	0.036	0.009	0.000	0.139	87.610	0.000	0.006	0.000	0.000
BKUD09-160-56-5m-4-1	BK_SW, SW-end, 950 masl	8	101.348	14.246	0.000	0.003	0.000	0.031	0.026	0.000	0.000	0.139	87.037	0.000	0.002	0.013	0.000
BKUD09-160-56-5m-5-2	BK_SW, SW-end, 950 masl	8	101.415	14.359	0.015	0.000	0.013	0.034	0.050	0.000	0.041	0.139	87.015	0.000	0.000	0.000	0.000
BKUD09-160-56-5m-6-4	BK_SW, SW-end, 950 masl	8	101.142	13.967	0.178	0.011	0.036	0.022	0.023	0.000	0.000	0.188	86.864	0.000	0.002	0.000	0.000
BKUD09-160-56-5m-6-6	BK_SW, SW-end, 950 masl	8	102.035	13.988	0.009	0.000	0.000	0.043	0.066	0.112	0.000	0.215	87.722	0.000	0.006	0.000	0.000
BKUD09-160-56-5m-7-5	BK_SW, SW-end, 950 masl	8	102.011	14.039	0.032	0.000	0.000	0.016	0.000	0.000	0.000	0.124	88.044	0.000	0.013	0.000	0.000
BKUD09-160-56-5m-8-1	BK_SW, SW-end, 950 masl	8	101.419	14.275	0.021	0.011	0.033	0.023	0.000	0.135	0.014	0.139	86.693	0.000	0.000	0.015	0.000

B. Electron Microprobe Data: Sulfides, Oxides, and Sulfates

BKUD09-160-56-5m-8-6	BK_SW, SW-end, 950 masl	8	102.350	14.185	0.075	0.000	0.148	0.028	0.023	0.000	0.000	0.157	88.076	0.000	0.000	0.010	0.000
BKUD09-160-56-5m-9-1	BK_SW, SW-end, 950 masl	8	102.220	14.211	0.042	0.000	0.000	0.011	0.000	0.000	0.000	0.082	88.129	0.000	0.000	0.004	0.000
BKUD09-171-32-8m-1-1	BK_99, 990 masl	2	97.027	12.754	0.000	0.022	0.002	0.122	**0.721**	0.000	0.000	0.260	84.271	0.000	0.011	0.001	0.000
BKUD09-171-32-8m-2-5	BK_99, 990 masl	2	99.260	12.491	0.100	0.033	0.001	0.026	0.102	0.024	0.050	0.172	86.964	0.000	0.014	0.000	0.000
BKUD09-171-32-8m-3-1	BK_99, 990 masl	2	99.310	12.731	0.026	0.000	0.013	0.100	0.431	0.000	0.000	0.280	86.592	0.000	0.000	0.009	0.000
BKUD09-171-32-8m-3-2	BK_99, 990 masl	2	99.670	12.697	0.000	0.000	0.020	0.074	0.249	0.000	0.000	0.255	87.358	0.000	0.000	0.007	0.000
BKUD09-171-32-8m-4-3	BK_99, 990 masl	2	98.833	13.015	0.000	0.000	0.000	0.130	0.305	0.041	0.000	0.068	86.157	0.000	0.000	0.022	0.000
BKUD09-171-32-8m-5-3	BK_99, 990 masl	8	96.891	12.933	0.009	0.004	0.000	0.019	**1.242**	0.006	0.000	**1.414**	82.180	0.000	0.007	0.000	0.000
BKUD09-171-32-8m-6-3	BK_99, 990 masl	5/8?	100.162	12.779	0.012	0.000	0.116	0.072	0.089	0.059	0.018	0.232	87.778	0.000	0.000	0.007	0.000
BKUD09-171-32-8m-7-1	BK_99, 990 masl	5/8?	98.184	13.105	0.003	0.005	0.002	0.128	0.088	0.000	0.002	0.192	85.580	0.000	0.001	0.000	0.000
BKUD09-171-32-8m-7-2	BK_99, 990 masl	5/8?	98.020	12.724	0.024	0.000	0.138	0.064	0.361	0.000	0.018	0.000	85.594	0.000	0.012	0.000	0.000
BKUD09-171-32-8m-8-1	BK_99, 990 masl	5/8?	99.430	12.867	0.000	0.108	0.000	0.050	0.067	0.006	0.000	0.193	86.994	0.000	0.000	0.000	0.000
BKUD09-171-32-8m-8-3	BK_99, 990 masl	5/8?	98.422	12.874	0.000	0.000	0.000	0.096	0.114	0.000	0.000	0.288	86.040	0.000	0.004	0.000	0.000
BKUD09-171-32-8m-9-1	BK_99, 990 masl	5/8?	99.746	12.577	0.006	0.000	0.063	0.059	0.000	0.024	0.000	0.156	87.763	0.000	0.009	0.000	0.000
n = 232	AVERAGE		100.591	13.498	0.077	0.016	0.081	0.044	0.124	0.014	0.004	0.205	87.474	0.000	0.003	0.004	0.001
	MINIMUM		96.891	12.046	0.000	0.000	0.000	0.000	0.000	0.000	0.000	0.000	82.180	0.000	0.000	0.000	0.000
	MAXIMUM		102.943	14.640	0.974	0.577	3.242	0.161	1.673	0.160	0.061	1.516	90.776	0.000	0.033	0.027	0.097
Boulangerite: stage 8																	
Alice-3-10	Alice, surface	6, 7, 8	100.164	18.568	0.026	0.016	0.019	0.170	0.000	0.000	0.138	25.64	55.735	0.000		0.000	0.000
Alice-5-14	Alice, surface	6, 7, 8	100.010	18.451	0.031	0.000	0.000	0.128	0.450	0.109	0.092	25.99	54.737	0.000		0.000	0.000
Alice-5-16	Alice, surface	6, 7, 8	101.736	18.750	0.044	0.051	0.847	0.394	0.000	0.043	0.109	25.48	55.977	0.000		0.011	0.041
Alice-7-6	Alice, surface	6, 7, 8	99.984	18.257	0.033	0.001	0.000	0.271	0.000	0.053	0.108	24.29	56.961	0.000		0.000	0.001
Alice-7-7	Alice, surface	6, 7, 8	99.536	18.101	0.018	0.031	0.026	0.318	0.000	0.000	0.096	25.42	55.763	0.000		0.000	0.000
Alice-8-11	Alice, surface	6, 7, 8	100.395	18.740	0.019	0.022	0.005	0.141	0.000	0.000	0.067	26.02	55.599	0.000		0.000	0.020
BRM-044-1-6	Bermingham, surface	6, 7, 8	99.310	18.644	0.021	0.000	0.005	0.151	0.000	0.000	0.124	26.50	53.963	0.000		0.000	0.015
BRM-044-2-5	Bermingham, surface	6, 7, 8	100.638	18.643	0.040	0.000	0.020	0.121	0.000	0.000	0.062	26.05	55.734	0.000		0.000	0.046
BRM-044-2-6	Bermingham,	6, 7, 8	100.178	18.586	0.028	0.005	0.000	0.101	0.000	0.030	0.135	26.25	55.116	0.000		0.000	0.000

B. Electron Microprobe Data: Sulfides, Oxides, and Sulfates

	surface															
BRM-044-3-7	Bermingham, surface	6, 7, 8	100.860	18.785	0.046	0.000	0.008	0.131	0.000	0.000	0.111	26.15	55.593	0.000	0.000	0.056
BRM-044-4-7	Bermingham, surface	6, 7, 8	100.177	18.659	0.019	0.014	0.006	0.127	0.000	0.000	0.078	26.30	54.978	0.000	0.000	0.000
BRM-044-6-6	Bermingham, surface	6, 7, 8	99.519	18.549	0.020	0.000	0.054	0.129	0.000	0.000	0.050	26.07	54.821	0.000	0.022	0.041
BRM-044-7-6	Bermingham, surface	6, 7, 8	100.899	18.767	0.045	0.009	0.000	0.169	0.000	0.000	0.123	26.25	55.448	0.000	0.007	0.002
BRM-044-7-8	Bermingham, surface	6, 7, 8	99.232	17.901	0.029	0.018	0.000	0.095	0.000	0.021	0.153	26.48	54.440	0.000	0.004	0.018
BRM-044-8-5	Bermingham, surface	6, 7, 8	100.690	18.868	0.019	0.004	0.002	0.133	0.000	0.000	0.113	26.49	55.062	0.000	0.000	0.039
HOM-053-1-1-5	Homestake, surface	1, 7, 8	100.477	18.853	0.046	0.028	0.000	0.108	0.000	0.000	0.048	26.40	55.236	0.000	0.000	0.000
HOM-053-1-1-6	Homestake, surface	1, 7, 8	100.057	18.799	0.027	0.033	0.009	0.105	0.000	0.000	0.099	26.05	54.968	0.000	0.000	0.047
HOM-053-1-2-4	Homestake, surface	1, 7, 8	99.049	18.850	0.000	0.023	0.020	0.124	0.000	0.000	0.094	26.00	54.104	0.000	0.011	0.012
HOM-053-1-3-5	Homestake, surface	1, 7, 8	100.789	18.676	0.011	0.027	0.004	0.111	0.000	0.022	0.076	26.29	55.538	0.000	0.022	0.035
HOM-053-1-4-6	Homestake, surface	1, 7, 8	101.200	18.795	0.046	0.056	0.000	0.111	0.000	0.000	0.032	26.37	55.870	0.000	0.008	0.000
HOM-053-1-5-6	Homestake, surface	1, 7, 8	100.604	18.634	0.054	0.046	0.000	0.119	0.000	0.000	0.053	26.16	55.663	0.000	0.000	0.040
n = 21	AVERAGE		100.262	18.613	0.030	0.018	0.049	0.155	0.021	0.013	0.093	26.03	55.300	0.000	0.004	0.020
	MINIMUM		99.049	17.901	0.000	0.000	0.000	0.095	0.000	0.000	0.032	24.29	53.963	0.000	0.000	0.000
	MAXIMUM		101.736	18.868	0.054	0.056	0.847	0.394	0.450	0.109	0.153	26.50	56.961	0.000	0.022	0.056
Jamesonite: stage 8																
BRM-044-1-7	Bermingham, surface	6, 7, 8	100.349	21.548	2.574	0.000	0.027	0.117	0.000	0.074	0.116	35.78	40.002	0.000	0.005	0.037
BRM-044-2-4	Bermingham, surface	6, 7, 8	99.724	21.343	2.641	0.003	0.097	0.114	0.000	0.000	0.162	35.77	39.733	0.000	0.000	0.036
BRM-044-3-6	Bermingham, surface	6, 7, 8	99.309	21.661	2.530	0.024	0.045	0.142	0.000	0.000	0.114	35.39	39.432	0.000	0.009	0.004
BRM-044-4-8	Bermingham, surface	6, 7, 8	99.931	21.636	2.524	0.000	0.052	0.099	0.000	0.000	0.115	35.96	39.651	0.000	0.000	0.044
BRM-044-4-9	Bermingham, surface	6, 7, 8	97.977	20.261	2.437	0.000	0.047	0.121	0.000	0.046	0.143	35.72	39.156	0.000	0.005	0.000
BRM-044-6-7	Bermingham, surface	6, 7, 8	99.928	21.333	2.570	0.003	0.107	0.091	0.000	0.151	0.080	35.32	40.420	0.000	0.000	0.000

B. Electron Microprobe Data: Sulfides, Oxides, and Sulfates

BRM-044-6-8		Bermingham, surface	6, 7, 8	99.767	21.218	2.540	0.001	0.069	0.105	0.000	0.000	0.098	35.51	40.215	0.000		0.000	0.055
BRM-044-7-7		Bermingham, surface	6, 7, 8	100.944	21.551	2.608	0.018	0.072	0.130	0.000	0.000	0.163	35.53	41.012	0.000		0.000	0.000
BRM-044-8-4		Bermingham, surface	6, 7, 8	100.587	21.518	2.568	0.011	0.020	0.121	0.000	0.000	0.086	35.68	40.673	0.000		0.000	0.000
	n = 9	AVERAGE		99.835	21.341	2.554	0.007	0.060	0.116	0.000	0.030	0.119	35.63	40.033	0.000		0.002	0.020
		MINIMUM		97.977	20.261	2.437	0.000	0.020	0.091	0.000	0.000	0.080	35.32	39.156	0.000		0.000	0.000
		MAXIMUM		100.944	21.661	2.641	0.024	0.107	0.142	0.000	0.151	0.163	35.96	41.012	0.000		0.009	0.055
Tetrahedrite: stages 7 and 8																		
Alice_1-5		Alice, surface	6, 7, 8	99.109	20.830	0.397	16.041	6.095	0.103	29.826	0.030	0.000	26.521	0.000	0.000	0.000	0.000	0.000
Alice-1-8		Alice, surface	6, 7, 8	101.101	20.657	0.352	15.932	6.174	0.146	31.110	0.983	0.000	26.252	0.085	0.000		0.003	0.000
Alice-1-9		Alice, surface	6, 7, 8	100.621	22.277	2.996	21.140	3.411	0.144	23.145	1.021	0.000	26.960	0.030	0.000		0.000	0.025
Alice_2-6		Alice, surface	6, 7, 8	102.008	22.131	4.407	21.108	2.094	0.300	22.899	2.541	0.000	27.024	0.000	0.000	0.000	0.000	0.000
Alice_4-4		Alice, surface	6, 7, 8	101.818	22.673	3.734	20.852	2.513	0.184	22.733	2.583	0.000	27.203	0.000	0.000	0.001	0.011	0.000
Alice_4-5		Alice, surface	6, 7, 8	102.031	22.181	3.764	20.490	2.766	0.289	23.270	2.936	0.000	26.830	0.000	0.000	0.004	0.010	0.000
Alice_5-5		Alice, surface	6, 7, 8	101.806	22.185	3.430	20.643	3.254	0.334	22.798	2.704	0.000	27.015	0.000	0.000	0.007	0.000	0.000
Alice-5-11		Alice, surface	6, 7, 8	100.834	21.616	3.147	19.392	3.688	0.191	25.863	0.800	0.000	26.690	0.000	0.000		0.018	0.007
Alice_6-4		Alice, surface	6, 7, 8	101.907	22.285	4.196	20.679	3.062	0.515	22.321	2.960	0.000	26.210	0.000	0.000	0.001	0.000	0.000
Alice-6-8		Alice, surface	6, 7, 8	101.880	22.428	4.270	21.702	3.054	0.512	22.757	0.828	0.000	26.560	0.079	0.031		0.000	0.069
Alice_7-4		Alice, surface	6, 7, 8	101.368	22.139	3.071	21.297	2.939	0.226	22.374	2.815	0.000	26.939	0.000	0.000	0.007	0.011	0.000
Alice_7-5		Alice, surface	6, 7, 8	102.271	20.916	2.679	17.359	3.328	0.192	28.318	3.487	0.000	26.717	0.000	0.000	0.000	0.004	0.000
Alice_8-4		Alice, surface	6, 7, 8	102.246	20.271	2.783	14.889	3.395	0.182	31.549	3.716	0.000	26.176	0.000	0.019	0.000	0.000	0.000
Alice_8-5		Alice, surface	6, 7, 8	101.404	22.181	3.649	21.506	2.584	0.183	21.964	2.694	0.000	27.248	0.000	0.000	0.000	0.000	0.000
Alice-8-12		Alice, surface	6, 7, 8	101.343	22.543	3.357	21.719	3.534	0.280	22.642	0.644	0.000	26.999	0.068	0.000		0.000	0.000
TryAgain_4-2		Try Again, surface	8 ?	102.083	20.604	5.237	14.459	0.139	0.086	32.075	3.888	0.000	26.219	0.000	0.000	0.000	0.017	0.000
TryAgain-4-4		Try Again, surface	8 ?	100.668	20.811	5.327	14.815	0.169	0.118	32.886	1.054	0.000	26.185	0.000	0.000		0.001	0.016
TryAgain-4-5		Try Again, surface	8 ?	100.969	20.564	4.785	9.305	0.413	0.083	39.184	1.715	0.000	25.671	0.230	0.000		0.003	0.000
WRN_008_1-1		Wernecke, surface	6, 8	101.522	22.137	4.291	21.018	1.615	0.235	22.818	2.732	0.000	27.003	0.000	0.000	0.000	0.017	0.000
WRN_008_1-2		Wernecke,	6, 8	101.874	22.105	3.350	20.414	2.742	0.273	23.780	2.875	0.000	26.862	0.000	0.014	0.005	0.007	0.000

B. Electron Microprobe Data: Sulfides, Oxides, and Sulfates

	surface															
WRN_008_2-1	Wernecke, surface	6, 8	100.908	22.177	4.181	21.269	1.725	0.205	22.485	2.490	0.000	26.991	0.000	0.000	0.000	0.000	0.000
WRN_008_2-2	Wernecke, surface	6, 8	100.781	21.664	4.384	20.540	1.777	0.255	24.535	3.013	0.000	25.283	0.000	0.000	0.000	0.000	0.000
WRN_008_3-4	Wernecke, surface	6, 8	101.751	20.685	3.478	17.465	1.517	0.205	33.085	3.780	0.000	22.197	0.000	0.000	0.000	0.000	0.000
WRN-008-3-10	Wernecke, surface	6, 8	100.021	21.154	3.650	18.051	1.923	0.316	32.956	0.748	0.000	21.904	0.104	0.000		0.007	0.000
WRN-008-3-14	Wernecke, surface	6, 8	99.873	21.183	3.599	17.829	1.660	0.177	32.630	0.690	0.000	22.816	0.000	0.000		0.001	0.000
POR_056_1-7	Porcupine, surface	7, 8, 10	102.585	21.010	4.833	18.542	2.903	0.138	25.878	3.036	0.000	26.769	0.000	0.000	0.000	0.003	0.000
POR_056_2-5	Porcupine, surface	7, 8, 10	101.355	22.546	2.993	23.481	3.467	0.375	19.418	2.254	0.000	27.053	0.000	0.000	0.012	0.000	0.000
POR-056-2-8	Porcupine, surface	7, 8, 10, 11	100.545	23.045	2.878	24.290	3.508	0.345	19.064	0.661	0.000	27.161	0.023	0.000		0.000	0.045
POR_056_3-5	Porcupine, surface	7, 8, 10, 11	99.069	22.408	2.052	22.808	4.176	0.244	18.111	2.206	0.000	27.376	0.000	0.000	0.000	0.000	0.000
POR-056-4-7	Porcupine, surface	7, 8, 10, 11	100.077	22.778	3.671	22.520	2.603	0.314	21.038	0.744	0.000	26.897	0.152	0.000		0.000	0.000
POR-056-4-8	Porcupine, surface	7, 8, 10, 11	100.383	22.975	2.421	24.034	3.969	0.557	19.519	0.637	0.000	26.855	0.000	0.000		0.000	0.000
POR-056-5-7	Porcupine, surface	7, 8, 10, 11	100.681	22.534	2.224	23.498	4.263	0.271	20.627	0.635	0.000	26.986	0.088	0.000		0.020	0.000
K09-201-238m-8-7	Keno 700	1, 6, 7, 8	100.044	19.841	3.194	12.729	3.245	0.168	40.869	0.808	0.000	19.317	0.000	0.000	0.000	0.000	0.022
K09-201-238m-8-3	Keno 700	1, 6, 7, 8	102.166	21.510	2.470	14.465	4.777	0.144	32.014	0.606	0.000	26.507	0.000	0.093	0.002	0.000	0.024
K09-201-238m-8-4	Keno 700	1, 6, 7, 8	102.346	23.902	2.733	20.848	5.167	0.158	21.451	0.787	0.000	27.638	0.000	0.000	0.000	0.000	0.000
K09-201-238m-8-8	Keno 700	1, 6, 7, 8	102.399	22.859	1.345	18.754	5.542	0.191	26.733	0.586	0.000	26.822	0.000	0.000	0.012	0.009	0.067
K09-201-238m-8-10	Keno 700	1, 6, 7, 8	102.659	22.947	3.111	18.724	3.414	0.358	26.667	0.697	0.000	27.291	0.000	0.000	0.008	0.000	0.057
K06-2-167-2m_3-5	Silver King	6, 8	102.628	21.197	5.407	18.222	0.404	0.103	27.460	3.365	0.000	26.760	0.000	0.000	0.000	0.002	0.000
K06-2-167-2m_5-2	Silver King	6, 8	101.587	20.757	5.124	17.784	0.562	0.257	28.200	3.117	0.000	26.343	0.000	0.000	0.000	0.002	0.000
K06-2-167-2m_7-5	Silver King	6, 8	101.429	19.899	4.997	14.346	0.448	0.186	32.685	3.687	0.000	25.760	0.000	0.000	0.009	0.007	0.000
K06-2-167-2m_7-6	Silver King	6, 8	101.695	19.089	3.975	16.174	1.405	0.171	34.464	3.744	0.000	23.206	0.000	0.000	0.000	0.001	0.000
K06-2-167-2m_8-6	Silver King	6, 8	98.545	20.600	4.738	16.066	0.755	0.135	31.586	3.804	0.000	21.641	0.000	0.000	0.000	0.000	0.000
BRM_044_1-5	Bermingham, surface	7, 8	101.738	23.133	3.590	26.497	2.783	0.146	15.609	1.787	0.000	28.146	0.000	0.000	0.000	0.022	0.000

B. Electron Microprobe Data: Sulfides, Oxides, and Sulfates

BRM_044_3-4	Bermingham, surface	7, 8	100.942	23.331	3.753	27.030	2.500	0.400	14.972	1.679	0.000	27.617	0.000	0.000	0.007	0.005	0.000
K07-88-59-6m_1-6	Bermingham	2/6, 8	99.732	22.809	3.445	21.207	2.406	0.275	20.607	2.272	0.000	27.265	0.000	0.000	0.009	0.009	0.000
K07-88-59-6m_2-4	Bermingham	2/6, 8	101.664	22.479	3.533	22.357	2.591	0.262	21.140	2.301	0.000	27.171	0.000	0.034	0.000	0.000	0.000
K07-88-59-6m_2-5	Bermingham	2/6, 8	102.507	21.201	3.353	18.677	2.809	0.255	26.828	3.077	0.000	26.521	0.000	0.025	0.001	0.000	0.000
K07-88-59-6m_4-3	Bermingham	2/6, 8	101.189	22.382	4.047	22.895	2.011	0.194	20.320	2.201	0.000	27.498	0.000	0.000	0.000	0.005	0.000
K07-88-59-6m_4-4	Bermingham	2/6, 8	100.191	22.328	3.800	21.902	2.093	0.196	20.817	2.091	0.000	27.323	0.000	0.000	0.000	0.009	0.000
K07-88-59-6m_5-3	Bermingham	2/6, 8	100.466	22.549	3.934	23.127	2.181	0.199	19.709	2.070	0.000	27.134	0.000	0.000	0.000	0.003	0.000
K07-88-59-6m_8-4	Bermingham	2/6, 8	100.961	22.532	3.635	21.374	2.776	0.236	21.588	2.235	0.000	26.919	0.000	0.000	0.000	0.006	0.000
K08-161-229-8m_3-6	Lucky Queen	6, 8	101.573	21.686	4.496	18.813	0.992	0.250	26.065	3.173	0.000	26.646	0.000	0.000	0.013	0.000	0.000
K08-161-229-8m_5-2	Lucky Queen	6, 8	102.149	20.586	3.142	16.165	2.637	0.130	30.305	3.407	0.000	26.345	0.000	0.000	0.020	0.000	0.000
K08-161-229-8m_5-3	Lucky Queen	6, 8	101.166	21.815	3.066	19.387	2.555	0.145	25.025	3.128	0.000	26.622	0.000	0.000	0.000	0.006	0.000
K08-161-229-8m_7-3	Lucky Queen	6, 8	102.717	20.442	2.415	15.773	3.627	0.124	31.031	3.669	0.000	26.266	0.000	0.000	0.000	0.000	0.000
K08-161-229-8m_7-4	Lucky Queen	6, 8	101.601	21.889	4.218	19.043	1.128	0.177	26.132	2.831	0.000	26.724	0.000	0.000	0.000	0.004	0.000
K08-161-229-8m_7-6	Lucky Queen	6, 8	102.739	20.893	4.167	16.031	1.382	0.094	30.490	3.544	0.000	26.621	0.000	0.000	0.000	0.000	0.000
K08-161-229-8m_9-2	Lucky Queen	6, 8	101.906	21.235	2.620	18.411	3.513	0.180	26.647	3.148	0.000	26.599	0.000	0.000	0.000	0.004	0.000
K07-106-402-2m_9-2	BK_SW, NE-end, 985 masl	6, 7	102.578	22.292	5.159	20.446	1.118	0.351	23.978	3.011	0.000	26.377	0.000	0.008	0.000	0.020	0.000
K07-76-125m-2-5	BK_E, 965 masl	6, 7, 8	99.317	22.317	4.624	22.228	1.340	0.333	20.527	0.507	0.000	27.187	0.000	0.000	0.000	0.001	0.000
K07-76-125m-2-6	BK_E, 965 masl	6, 7, 8	100.064	22.235	4.554	22.039	1.497	0.267	21.323	0.617	0.000	26.918	0.000	0.000	0.000	0.000	0.000
K07-76-125m-10-3	BK_E, 965 masl	6, 7, 8	99.866	22.328	4.748	22.053	1.297	0.286	21.015	0.476	0.000	27.154	0.000	0.079	0.001	0.006	0.000
K07-76-125m-10-4	BK_E, 965 masl	6, 7, 8	99.507	22.183	4.712	22.673	1.322	0.270	20.253	0.484	0.000	27.016	0.000	0.000	0.000	0.004	0.000
K07-76-125m-10-5	BK_E, 965 masl	6, 7, 8	100.387	22.539	4.668	22.295	1.753	0.395	20.721	0.452	0.000	27.193	0.000	0.000	0.009	0.012	0.000
K07-76-125m-11-1	BK_E, 965 masl	6, 7, 8	99.255	22.417	4.603	21.943	1.258	0.389	20.936	0.427	0.000	26.892	0.000	0.000	0.000	0.020	0.000
K07-76-125m-6-7	BK_E, 965 masl	6, 7, 8	99.851	22.344	4.703	22.236	1.338	0.298	20.897	0.531	0.000	27.357	0.000	0.000	0.009	0.007	0.000
K07-76-125m-6-8	BK_E, 965 masl	6, 7, 8	99.926	22.161	4.403	22.269	1.600	0.221	20.854	0.530	0.000	27.333	0.000	0.000	0.002	0.012	0.000
K07-86-223-3m_1-2	BK_E, 940 masl	6, 8	100.459	22.703	4.457	22.742	1.591	0.234	21.121	0.566	0.000	27.317	0.000	0.000	0.000	0.009	0.000
K07-86-223-3m_2-2	BK_E, 940 masl	6, 8	100.472	23.062	4.333	24.322	1.761	0.231	19.023	0.517	0.000	27.654	0.000	0.000	0.000	0.000	0.000
K07-86-223-3m_2-5	BK_E, 940 masl	6, 8	100.745	23.091	4.306	24.725	2.038	0.219	18.260	0.437	0.000	27.781	0.000	0.000	0.000	0.009	0.000

B. Electron Microprobe Data: Sulfides, Oxides, and Sulfates

K07-86-223-3m_3-2	BK_E, 940 masl	6, 8	99.890	22.760	4.348	23.204	1.638	0.184	20.113	0.448	0.000	27.254	0.000	0.000	0.011	0.003	0.000
K07-86-223-3m_4-2	BK_E, 940 masl	6, 8	100.596	22.963	4.331	23.421	1.665	0.323	20.393	0.505	0.000	27.333	0.000	0.000	0.000	0.002	0.000
K07-86-223-3m_5-2	BK_E, 940 masl	6, 8	100.506	23.064	4.564	24.130	1.461	0.249	19.255	0.539	0.000	27.506	0.000	0.000	0.000	0.007	0.000
K07-86-223-3m_6-2	BK_E, 940 masl	6, 8	100.541	22.810	4.503	24.329	1.539	0.226	18.998	0.430	0.000	27.772	0.000	0.000	0.016	0.004	0.000
BKUD09-139-8-3m_6-3	BK_SW, 965 masl	6, 7, 8	100.849	22.886	5.701	24.446	1.856	0.137	17.550	0.524	0.000	27.829	0.000	0.000	0.016	0.002	0.000
BKUD09-139-8-3m_8-2	BK_SW, 965 masl	6, 7, 9	100.374	23.245	3.292	25.977	3.239	0.108	16.080	0.547	0.000	28.016	0.000	0.003	0.001	0.013	0.000
BKUD09-139-8-3m_9-3	BK_SW, 965 masl	6, 7, 10	100.027	22.703	3.851	23.698	2.717	0.107	19.588	0.385	0.000	27.176	0.000	0.000	0.001	0.005	0.000
BKUD09-139-8-3m_10-4	BK_SW, 965 masl	6, 7, 11	100.509	23.809	3.963	29.496	2.612	0.130	11.539	0.317	0.070	28.521	0.000	0.000	0.018	0.000	0.000
BKUD09-143-52-8m_2-2	BK_SW, NE-end, 1000 masl	7, 8, 9	101.949	22.684	4.769	22.406	1.206	0.282	21.260	2.274	0.000	27.221	0.000	0.000	0.000	0.000	0.000
BKUD09-143-52-8m_3-2	BK_SW, NE-end, 1000 masl	7, 8, 9	102.222	22.623	4.455	22.414	1.527	0.175	21.182	2.545	0.000	27.506	0.000	0.000	0.000	0.000	0.000
BKUD09-143-52-8m_3-3	BK_SW, NE-end, 1000 masl	7, 8, 9	102.397	20.768	3.824	16.359	2.102	0.117	29.826	3.261	0.000	26.697	0.000	0.000	0.001	0.000	0.000
BKUD09-143-52-8m_3-8	BK_SW, NE-end, 1000 masl	7, 8, 9	101.788	22.412	4.638	22.174	1.407	0.301	21.618	2.465	0.000	27.079	0.000	0.000	0.000	0.006	0.000
BKUD09-143-52-8m_4-7	BK_SW, NE-end, 1000 masl	7, 8, 9	100.958	22.573	4.587	22.145	1.268	0.279	21.098	2.329	0.000	27.163	0.000	0.000	0.000	0.011	0.000
BKUD09-143-52-8m_5-2	BK_SW, NE-end, 1000 masl	7, 8, 9	101.448	22.385	4.297	20.718	1.628	0.115	23.133	2.323	0.000	27.175	0.000	0.000	0.000	0.001	0.000
BKUD09-143-52-8m_5-3	BK_SW, NE-end, 1000 masl	7, 8, 9	102.011	22.519	4.312	22.387	1.701	0.224	21.135	2.524	0.000	27.385	0.000	0.006	0.000	0.003	0.000
BKUD09-143-52-8m_5-7	BK_SW, NE-end, 1000 masl	7, 8, 9	100.950	22.247	5.191	21.998	0.901	0.120	21.230	2.465	0.000	27.120	0.000	0.000	0.006	0.007	0.000
BKUD09-143-52-8m_6-2	BK_SW, NE-end, 1000 masl	7, 8, 9	101.584	22.608	4.473	22.233	1.594	0.261	21.257	2.259	0.000	27.091	0.000	0.000	0.009	0.000	0.000
BKUD09-143-54m_3-4	BK_SW, NE-end, 1000 masl	6, 8	100.530	22.481	4.633	21.184	1.236	0.130	23.074	0.690	0.000	27.050	0.000	0.000	0.000	0.010	0.000
BKUD09-143-54m_3-5	BK_SW, NE-end, 1000 masl	6, 8	99.984	21.974	3.830	20.311	2.065	0.172	24.319	0.700	0.000	26.878	0.000	0.000	0.000	0.010	0.000
BKUD09-143-54m_4-5	BK_SW, NE-end, 1000 masl	6, 8	100.075	21.925	4.105	20.628	1.797	0.164	24.106	0.678	0.000	26.944	0.000	0.000	0.000	0.012	0.000
BKUD09-143-54m_6-2	BK_SW, NE-end, 1000 masl	6, 8	99.639	22.153	4.373	21.108	1.494	0.214	23.438	0.715	0.000	26.453	0.000	0.000	0.009	0.004	0.000
BKUD09-143-54m_6-3	BK_SW, NE-end, 1000 masl	6, 8	100.211	20.771	4.064	16.169	1.750	0.404	30.576	0.854	0.000	26.091	0.000	0.000	0.000	0.000	0.000
BKUD09-143-54m_7-2	BK_SW, NE-end, 1000 masl	6, 8	100.403	21.227	5.527	17.669	0.000	0.089	28.659	0.817	0.000	26.777	0.000	0.000	0.000	0.003	0.000
BKUD09-143--54m_8-2	BK_SW, NE-end, 1000 masl	6, 8	100.516	22.678	4.846	21.708	0.709	0.237	22.735	0.762	0.000	26.948	0.000	0.000	0.000	0.005	

B. Electron Microprobe Data: Sulfides, Oxides, and Sulfates

BKUD09-148-29-5m_3-2	BK_99, 1025 masl	2, 7, 9	101.444	22.849	4.751	22.206	2.539	0.223	21.359	0.557	0.000	27.060	0.000	0.000	0.000	0.013	0.000
BKUD09-148-29-5m_6-1	BK_99, 1025 masl	2, 7, 9	100.718	22.409	4.772	20.650	2.410	0.211	23.230	0.623	0.000	26.771	0.000	0.000	0.000	0.000	0.000
BKUD09-148-33-5m-4-3	BK_99, 1025 masl	2/6 3/7	94.113	21.712	4.369	19.114	3.857	0.192	17.450	0.637	0.000	23.440	0.000	0.000	0.000	0.006	0.000
BKUD09-148-33-5m-7-2	BK_99, 1025 masl	2/6? 3/7?	98.179	21.473	4.695	21.095	1.158	0.209	22.242	0.509	0.000	26.508	0.000	0.000	0.000	0.009	0.000
BKUD09-148-33-5m-8-2	BK_99, 1025 masl	2/6? 3/7?	98.712	21.554	4.301	21.500	1.838	0.227	21.547	0.572	0.000	27.043	0.000	0.000	0.000	0.020	0.000
BKUD09-151-33-3m_3-4	BK_99, 1045 masl	6, 7, 8	102.019	22.444	4.550	21.776	1.325	0.247	21.968	2.653	0.000	27.378	0.000	0.000	0.000	0.004	0.000
BKUD09-151-33-3m_3-6	BK_99, 1045 masl	6, 7, 8	100.759	22.857	3.442	22.477	2.567	0.201	20.199	2.245	0.000	27.248	0.000	0.000	0.003	0.005	0.000
BKUD09-151-33-3m_3-7	BK_99, 1045 masl	6, 7, 8	101.034	22.290	4.749	21.272	1.148	0.258	22.462	2.448	0.000	26.962	0.000	0.000	0.000	0.004	0.000
BKUD09-151-33-3m_4-2	BK_99, 1045 masl	6, 7, 8	101.410	22.502	4.660	21.556	1.240	0.274	21.900	2.504	0.000	27.031	0.000	0.000	0.000	0.010	0.000
BKUD09-151-33-3m_5-1	BK_99, 1045 masl	6, 7, 8	101.059	22.414	4.813	21.170	1.002	0.265	22.122	2.386	0.000	26.988	0.000	0.000	0.004	0.000	0.000
BKUD09-151-33-3m_8-2	BK_99, 1045 masl	6, 7, 8	101.145	22.688	4.663	22.895	1.217	0.287	20.787	2.397	0.000	26.759	0.000	0.000	0.000	0.015	0.000
BKUD09-151-33-3m_8-3	BK_99, 1045 masl	6, 7, 8	100.276	21.983	4.422	21.914	1.216	0.204	23.424	2.629	0.000	24.867	0.000	0.000	0.004	0.002	0.000
BKUD09-151-33-3m_9-2	BK_99, 1045 masl	6, 7, 8	102.057	22.528	5.060	21.104	1.833	0.224	22.347	2.463	0.000	26.970	0.000	0.000	0.000	0.000	0.000
BKUD09-158-36m_2-2	BK_SW, NE-end, 1030 masl	2/6, 8	100.143	22.488	4.034	21.832	2.024	0.257	22.211	0.570	0.000	26.930	0.000	0.000	0.009	0.005	0.000
BKUD09-158-36m_3-1	BK_SW, NE-end, 1030 masl	2/6, 8	100.718	22.623	4.469	22.778	1.586	0.253	21.207	0.532	0.000	27.479	0.000	0.000	0.001	0.000	0.000
BKUD09-158-36m_4-4	BK_SW, NE-end, 1030 masl	2/6, 8	99.986	22.445	4.668	21.544	1.233	0.300	22.674	0.597	0.000	26.797	0.000	0.000	0.000	0.000	0.000
BKUD09-158-36m_5-1	BK_SW, NE-end, 1030 masl	2/6, 8	100.080	22.553	4.108	21.892	1.831	0.226	22.029	0.603	0.000	27.134	0.000	0.000	0.000	0.000	0.000
BKUD09-158-36m_6-3	BK_SW, NE-end, 1030 masl	2/6, 8	99.629	22.239	4.007	21.633	2.021	0.239	22.284	0.474	0.000	27.113	0.000	0.000	0.000	0.005	0.000
BKUD09-158-36m_7-2	BK_SW, NE-end, 1030 masl	2/6, 8	98.314	22.355	4.018	20.438	1.872	0.469	21.699	0.512	0.000	27.100	0.000	0.000	0.002	0.010	0.000
BKUD09-158-36-5m-2-2	BK_SW, NE-end, 1030 masl	6, 7, 9, 10	102.826	23.261	5.205	18.099	2.446	0.230	26.551	0.585	0.000	26.620	0.000	0.013	0.000	0.002	0.066
BKUD09-158-36-5m-2-3	BK_SW, NE-end, 1030 masl	6, 7, 9, 10	101.893	23.827	4.538	22.368	1.765	0.243	22.499	0.564	0.000	27.000	0.000	0.000	0.000	0.000	0.000
BKUD09-158-36-5m-2-4	BK_SW, NE-end, 1030 masl	6, 7, 9, 10	101.297	23.607	4.635	22.518	1.571	0.283	21.252	0.625	0.000	27.551	0.000	0.004	0.005	0.000	0.066
BKUD09-158-36-5m-5-2	BK_SW, NE-end, 1030 masl	6, 7, 9, 10	102.235	23.481	5.276	17.854	1.599	0.258	27.415	0.630	0.000	26.485	0.000	0.000	0.000	0.000	0.016
BKUD09-158-36-5m-10-1	BK_SW, NE-end, 1030 masl	6, 7, 9, 10	101.365	22.390	4.260	19.173	2.062	0.183	25.737	0.621	0.000	27.172	0.000	0.004	0.000	0.000	0.096
BKUD09-158-36-5m-10-2	BK_SW, NE-end, 1030 masl	6, 7, 9, 10	101.967	22.867	4.415	19.778	1.948	0.181	24.979	0.784	0.000	27.254	0.000	0.000	0.000	0.000	0.113

B. Electron Microprobe Data: Sulfides, Oxides, and Sulfates

BKUD09-158-36-5m-11-1	BK_SW, NE-end, 1030 masl	6, 7, 9, 10	101.269	23.494	5.016	21.557	1.547	0.310	22.304	0.622	0.000	27.239	0.000	0.000	0.011	0.000	0.078
BKUD09-158-36-5m-11-2	BK_SW, NE-end, 1030 masl	6, 7, 9, 10	101.898	23.836	5.035	21.599	1.646	0.322	22.336	0.541	0.000	27.235	0.000	0.043	0.000	0.000	0.075
BKUD09-158-37m-1-1	BK_SW, NE-end, 1030 masl	6, 8, 11, 12	98.371	21.449	4.626	21.516	1.193	0.257	21.308	0.483	0.000	26.976	0.000	0.071	0.000	0.012	0.000
BKUD09-158-37m-2-2	BK_SW, NE-end, 1030 masl	6, 8, 11, 12	98.385	21.622	4.575	21.659	1.145	0.301	21.241	0.626	0.000	26.750	0.000	0.074	0.000	0.000	0.000
BKUD09-158-37m-3-2	BK_SW, NE-end, 1030 masl	6, 8, 11, 12	98.210	21.325	4.790	21.597	1.054	0.228	21.332	0.602	0.000	26.887	0.000	0.000	0.000	0.002	0.000
BKUD09-158-37m-4-2	BK_SW, NE-end, 1030 masl	6, 8, 11, 12	97.765	21.252	4.536	21.569	1.404	0.274	21.173	0.636	0.000	26.529	0.000	0.000	0.000	0.000	0.000
BKUD09-158-37m-4-3	BK_SW, NE-end, 1030 masl	6, 8, 11, 12	97.929	21.439	4.308	22.045	1.570	0.238	20.923	0.464	0.000	26.702	0.000	0.003	0.000	0.013	0.000
BKUD09-158-37m-5-3	BK_SW, NE-end, 1030 masl	6, 8, 11, 12	98.447	21.475	4.217	20.807	1.735	0.212	22.365	0.525	0.000	26.566	0.000	0.050	0.000	0.015	0.000
BKUD09-158-37m-6-1	BK_SW, NE-end, 1030 masl	6, 8, 11, 12	97.737	21.386	3.773	22.236	2.175	0.432	20.078	0.565	0.000	26.633	0.000	0.000	0.000	0.017	0.000
BKUD09-158-37m-7-3	BK_SW, NE-end, 1030 masl	6, 8, 11, 12	98.533	21.595	4.327	21.989	1.682	0.312	21.086	0.501	0.000	26.863	0.000	0.000	0.015	0.000	0.000
BKUD09-158-37m-7-4	BK_SW, NE-end, 1030 masl	6, 8, 11, 12	98.204	21.345	4.284	22.054	1.767	0.254	20.949	0.436	0.000	26.823	0.000	0.000	0.000	0.000	0.000
BKUD09-158-37m-7-5	BK_SW, NE-end, 1030 masl	6, 8, 11, 12	98.636	21.539	4.279	22.200	1.707	0.147	21.222	0.531	0.000	26.750	0.000	0.000	0.000	0.000	0.000
BKUD09-158-37m-8-2	BK_SW, NE-end, 1030 masl	6, 8, 11, 12	98.403	21.508	4.064	21.706	1.970	0.207	20.983	0.626	0.000	27.014	0.000	0.000	0.002	0.000	0.000
BKUD09-158-37m-8-3	BK_SW, NE-end, 1030 masl	6, 8, 11, 12	99.751	21.685	4.559	21.734	1.613	0.175	22.089	0.483	0.000	27.020	0.000	0.000	0.000	0.010	0.000
BKUD09-171-32-8m-8-2	BK_99, 990 masl	6, 7, 8	98.548	21.750	4.648	22.550	1.204	0.249	20.082	0.464	0.000	27.311	0.000	0.000	0.000	0.000	0.000
BKUD09-171-32-8m-9-2	BK_99, 990 masl	6, 7, 8	98.591	21.598	4.712	22.756	1.156	0.228	20.205	0.532	0.000	26.902	0.000	0.000	0.011	0.018	0.000
n = 135	AVERAGE		100.682	22.086	4.076	20.773	2.082	0.234	23.447	1.526	0.001	26.691	0.006	0.004	0.002	0.005	0.006
	MINIMUM		94.113	19.089	0.352	9.305	0.000	0.083	11.539	0.030	0.000	19.317	0.000	0.000	0.000	0.000	0.000
	MAXIMUM		102.826	23.902	5.701	29.496	6.174	0.557	40.869	3.888	0.070	28.521	0.230	0.093	0.020	0.022	0.113
Pyrargyrite: stages 7 to 8																	
K08-161-229-8m_3-5	Lucky Queen	6, 7, 8, 10	101.260	16.376	0.020	0.402	0.000	0.180	54.904	6.590	0.000	22.933	0.000	0.000	0.003	0.000	
K09-201-238m-8-11	Keno 700	1, 6, 7, 8	102.235	17.265	0.064	0.959	0.203	0.125	60.332	1.119	0.000	22.137	0.000	0.020	0.000	0.000	0.078
K09-201-238m-8-12	Keno 700	1, 6, 7, 8	102.005	17.630	0.012	0.844	0.222	0.104	59.868	1.364	0.000	21.999	0.000	0.000	0.005	0.017	0.039
n = 3	AVERAGE		101.834	17.090	0.032	0.735	0.142	0.136	58.368	3.024	0.000	22.357	0.000	0.007	0.003	0.006	0.058

B. Electron Microprobe Data: Sulfides, Oxides, and Sulfates

	MINIMUM		101.260	16.376	0.012	0.402	0.000	0.104	54.904	1.119	0.000	21.999	0.000	0.000	0.000	0.000	0.039
	MAXIMUM		102.235	17.630	0.064	0.959	0.222	0.180	60.332	6.590	0.000	22.933	0.000	0.020	0.005	0.017	0.078
Stephanite: stages 7 to 8																	
K08-161-229-8m_3-4	Lucky Queen		102.752	13.233	0.033	0.221	0.006	0.073	68.148	8.740	0.000	12.518	0.000	0.000	0.004	0.000	0.000
BKUD09-143-54m_3-2	BK_SW, NE-end, 1000 masl		101.349	16.075	0.026	0.049	0.002	0.033	68.798	1.388	0.000	14.950	0.000	0.000	0.000	0.001	0.000
BKUD09-143-54m_5-2	BK_SW, NE-end, 1000 masl		97.961	15.465	0.022	0.039	0.008	0.067	66.841	1.369	0.000	14.263	0.000	0.000	0.007	0.000	0.000
K06-2-167-2m_6-3	Silver King	6, 8	97.718	12.831	0.032	0.369	0.034	0.024	74.719	9.880	0.000	0.094	0.000	0.000	0.000	0.001	0.000
K07-88-59-6m_2-2	Bermingham		97.953	14.099	0.097	0.126	0.487	0.045	74.840	8.263	0.000	0.000	0.000	0.000	0.017	0.000	0.000
n = 5	AVERAGE		99.547	14.341	0.042	0.161	0.107	0.048	70.669	5.928	0.000	8.365	0.000	0.000	0.006	0.000	0.000
	MINIMUM		97.718	12.831	0.022	0.039	0.002	0.024	66.841	1.369	0.000	0.000	0.000	0.000	0.000	0.000	0.000
	MAXIMUM		102.752	16.075	0.097	0.369	0.487	0.073	74.840	9.880	0.000	14.950	0.000	0.000	0.017	0.001	0.000
Polybasite: stages 7 to 8																	
K07-86-223-3m_1-3	BK_E, 940 masl	6, 8	102.575	13.526	0.120	4.355	0.000	0.088	71.851	1.369	0.000	11.386	0.000	0.023	0.000	0.000	0.000
K07-86-223-3m_1-5	BK_E, 940 masl	6, 8	101.772	13.738	0.204	3.937	0.000	0.063	71.310	1.428	0.000	11.203	0.000	0.000	0.000	0.000	0.000
K07-86-223-3m_2-3	BK_E, 940 masl	6, 8	101.787	12.682	0.022	2.485	0.001	0.040	74.259	1.389	0.000	10.878	0.000	0.000	0.016	0.018	0.000
n = 3	AVERAGE		102.044	13.315	0.115	3.592	0.000	0.064	72.473	1.396	0.000	11.156	0.000	0.008	0.005	0.006	0.000
	MINIMUM		101.772	12.682	0.022	2.485	0.000	0.040	71.310	1.369	0.000	10.878	0.000	0.000	0.000	0.000	0.000
	MAXIMUM		102.575	13.738	0.204	4.355	0.001	0.088	74.259	1.428	0.000	11.386	0.000	0.023	0.016	0.018	0.000
Andorite (?): stages 7 to 8																	
Alice-5-15	Alice, surface	6, 7, 8	99.923	18.796	0.023	0.044	0.000	0.102	24.410	0.741	0.000	27.269	29.037	0.000		0.002	0.000
Unknown mineral: stages 6 to 8																	
WRN_008_3-3	Wernecke, surface	6, 7, 8	97.266	30.835	24.219	29.378	0.000	0.022	10.532	1.276	0.000	1.304	0.000	0.000	0.015	0.026	
Valentinite: stages 6 to 8																	
BRM_044_3-5	Bermingham, surface	6, 7, 8	84.162	0.207	0.103	0.018	0.182	1.764	0.000	0.093	0.444	80.160	0.528	0.000	0.000	0.000	

B. Electron Microprobe Data: Sulfides, Oxides, and Sulfates

BRM_044_5-6		Bermingham, surface	6, 7, 8	84.477	0.020	0.173	0.008	0.668	4.718	0.010	0.055	0.424	77.280	0.173	0.000	0.000	0.000	
BRM_044_6-5		Bermingham, surface	6, 7, 8	85.286	0.136	0.066	0.018	0.225	3.185	0.006	0.039	0.391	80.578	0.334	0.006	0.000	0.000	
BRM-044-6-9		Bermingham, surface	6, 7, 8	82.911	0.153	0.106	0.010	0.174	1.912	0.012	0.036	0.323	79.863	0.188	0.098		0.011	0.000
BRM-044-6-11		Bermingham, surface	6, 7, 8	81.431	0.079	0.082	0.009	0.156	2.416	0.000	0.011	0.319	77.752	0.326	0.080		0.000	0.021
	n = 5	AVERAGE		83.653	0.119	0.106	0.013	0.281	2.799	0.006	0.047	0.380	79.127	0.310	0.037	0.000	0.002	0.010
		MINIMUM		81.431	0.020	0.066	0.008	0.156	1.764	0.000	0.011	0.319	77.280	0.173	0.000	0.000	0.000	0.000
		MAXIMUM		85.286	0.207	0.173	0.018	0.668	4.718	0.012	0.093	0.444	80.578	0.528	0.098	0.000	0.011	0.021
Cobaltite-Gersdorffite: stages 6 to 8																		
K07-76-125m-4-8		BK_E, 965 masl	6 - 8?	99.002	19.326	9.540	0.000	0.000	44.659	0.011	0.000	0.031	0.151	0.000	0.000	23.49	1.772	0.000
WRN_008_6-3		Wernecke, surface	6, 8	98.393	19.325	5.164	0.000	0.000	43.623	0.000	0.007	0.018	0.261	0.000	0.000	17.34	12.73	0.000
WRN_008_7-3		Wernecke, surface	6, 8	97.545	19.639	8.768	0.000	0.016	43.763	0.023	0.000	0.000	0.083	0.000	0.000	15.85	9.450	0.000
	n = 3	AVERAGE		98.314	19.430	7.824	0.000	0.005	44.015	0.012	0.002	0.016	0.165	0.000	0.000	18.89	7.986	0.000
		MINIMUM		97.545	19.325	5.164	0.000	0.000	43.623	0.000	0.000	0.000	0.083	0.000	0.000	15.85	1.772	0.000
		MAXIMUM		99.002	19.639	9.540	0.000	0.016	44.659	0.023	0.007	0.031	0.261	0.000	0.000	23.49	12.73	0.000
Anglesite: stage 8 or later																		
Alice-3-9		Alice, surface	6, 7, 8	75.452	7.795	0.037	0.000	0.000	0.024	0.000	0.000	0.000	0.000	67.810	0.000		0.010	0.068
Alice-3-11		Alice, surface	6, 7, 8	75.063	7.855	0.028	0.021	0.087	0.050	0.000	0.000	0.000	0.000	67.109	0.000		0.000	0.110
Alice-6-7		Alice, surface	6, 7, 8	77.468	7.961	0.037	0.030	1.483	0.041	0.000	0.000	0.000	0.000	68.078	0.000		0.000	0.056
Alice-6-9		Alice, surface	6, 7, 8	78.890	8.115	0.059	0.000	1.857	0.045	0.000	0.092	0.000	0.000	68.657	0.000		0.008	0.137
Alice-7-8		Alice, surface	6, 7, 8	73.691	7.871	0.029	0.010	0.010	0.036	0.000	0.000	0.027	0.000	65.950	0.000		0.000	0.086
Alice-8-13		Alice, surface	6, 7, 8	79.496	7.900	0.301	0.069	2.158	0.061	0.000	0.036	0.000	0.000	68.983	0.000		0.005	0.129
POR-056-2-9		Porcupine, surface	7 - 11	75.746	7.757	0.184	0.049	0.299	0.018	0.000	0.000	0.000	0.000	67.507	0.000		0.014	0.037
POR-056-2-10		Porcupine, surface	7 - 11	75.016	7.950	0.140	0.014	0.157	0.053	0.000	0.000	0.000	0.016	66.749	0.000		0.000	0.094
POR-056-4-6		Porcupine, surface	7 - 11	74.507	7.906	0.056	0.000	0.000	0.156	0.000	0.000	0.000	0.000	66.552	0.000		0.003	0.085
POR-056-5-6		Porcupine, surface	7 - 11	74.910	7.926	0.053	0.006	0.001	0.240	0.000	0.000	0.042	0.000	66.762	0.000		0.008	0.030

B. Electron Microprobe Data: Sulfides, Oxides, and Sulfates

TryAgain-1-4	Try Again, surface	8 ?	73.506	7.753	0.008	0.009	0.000	0.089	0.000	0.000	0.000	0.000	65.833	0.000		0.000	0.028
TryAgain-2-5	Try Again, surface	8 ?	74.447	7.887	0.033	0.000	0.000	0.058	0.000	0.000	0.000	0.000	66.559	0.000		0.000	0.132
TryAgain-2-6	Try Again, surface	8 ?	74.564	7.524	0.066	0.000	0.004	0.061	0.000	0.000	0.000	0.000	67.019	0.000		0.000	0.103
TryAgain-5-4	Try Again, surface	8 ?	75.101	7.413	0.030	0.000	0.019	0.380	0.000	0.000	0.000	0.091	67.274	0.000		0.000	0.078
TryAgain-6-4	Try Again, surface	8 ?	73.001	7.889	0.031	0.000	0.000	0.217	0.000	0.000	0.000	0.000	65.135	0.000		0.000	0.075
n = 15	AVERAGE		75.390	7.834	0.073	0.014	0.405	0.102	0.000	0.009	0.005	0.007	67.065	0.000		0.002	0.083
	MINIMUM		73.001	7.413	0.008	0.000	0.000	0.018	0.000	0.000	0.000	0.000	65.135	0.000		-0.010	0.028
	MAXIMUM		79.496	8.115	0.301	0.069	2.158	0.380	0.000	0.092	0.042	0.091	68.983	0.000		0.014	0.137
Cerussite: stage 8 or later																	
TryAgain-3-6	Try Again, surface	8 ?	77.317	0.043	0.083	0.000	0.000	0.053	0.000	0.024	0.000	0.000	77.225	0.000		0.000	0.035
TryAgain-3-7	Try Again, surface	8 ?	77.893	0.051	0.280	0.000	0.004	0.066	0.000	0.000	0.003	0.000	77.645	0.000		0.006	0.048
TryAgain-5-5	Try Again, surface	8 ?	86.226	0.538	0.114	0.010	0.031	***13.887***	0.000	0.006	0.000	0.144	71.483	0.000		0.005	0.077
WRN-008-3-13	Wernecke, surface	6, 8	78.825	0.098	0.470	0.504	0.181	0.016	0.000	0.000	0.007	0.000	77.624	0.000		0.000	0.000
n = 4	AVERAGE		80.065	0.182	0.237	0.129	0.054	3.506	0.000	0.007	0.003	0.036	75.994	0.000		0.003	0.040
	MINIMUM		77.317	0.043	0.083	0.000	0.000	0.016	0.000	0.000	0.000	0.000	71.483	0.000		0.000	0.000
	MAXIMUM		86.226	0.538	0.470	0.504	0.181	13.887	0.000	0.024	0.007	0.144	77.645	0.000		0.006	0.077
Sphalerite: stage 9																	
K07-87-106-7m-1-9	Pool	9	99.718	32.872	3.959	0.036	61.948	0.033	0.017	0.841	0.000	0.000	0.094	0.000		0.010	0.057
K07-87-106-7m-1-10	Pool	9	100.345	33.162	5.129	0.043	60.645	0.041	0.038	1.212	0.000	0.000	0.103	0.000		0.008	0.101
K07-87-106-7m-2-5	Pool	9	100.818	33.668	3.082	0.038	63.676	0.057	0.000	0.186	0.000	0.000	0.186	0.000		0.002	0.012
K07-87-106-7m-4-5	Pool	9	99.997	32.786	4.177	0.000	62.056	0.051	0.000	0.880	0.000	0.000	0.167	0.000		0.005	0.000
K07-87-106-7m-6-6	Pool	9	100.312	33.115	3.762	0.006	62.318	0.079	0.001	0.890	0.000	0.003	0.228	0.000		0.000	0.000
BKUD09-143-52-8m_1-3	BK_SW, 1000 masl	7, 8, 9	98.804	33.296	6.481	0.362	58.462	0.014	0.000	0.000	0.373	0.000	0.000	0.000	0.004	0.021	0.000
BKUD09-143-52-8m_3-4	BK_SW, 1000 masl	9	99.932	33.067	4.310	0.039	62.450	0.039	0.001	0.065	0.000	0.025	0.000	0.000	0.001	0.014	0.000
BKUD09-143-52-8m_4-1	BK_SW, 1000 masl	9	99.177	33.060	4.083	0.120	62.222	0.032	0.013	0.000	0.078	0.000	0.000	0.000	0.007	0.000	0.000
BKUD09-143-52-8m_4-5	BK_SW, 1000 masl	9	99.173	32.924	4.411	0.472	61.393	0.036	0.013	0.000	0.020	0.000	0.000	0.000	0.000	0.016	0.000
BKUD09-143-52-8m_5-4	BK_SW, 1000 masl	9	99.011	32.954	5.643	0.358	59.697	0.003	0.002	0.013	0.455	0.000	0.000	0.000	0.000	0.007	0.000

B. Electron Microprobe Data: Sulfides, Oxides, and Sulfates

BKUD09-143-52-8m_5-6	BK_SW, 1000 masl	9	99.535	33.395	4.354	0.095	61.800	0.006	0.014	0.000	0.017	0.000	0.000	0.000	0.000	0.017	0.000
BKUD09-143-52-8m_6-1	BK_SW, 1000 masl	9	99.376	33.336	4.731	0.010	61.427	0.045	0.003	0.010	0.047	0.000	0.000	0.000	0.000	0.000	0.000
BKUD09-143-52-8m_7-1	BK_SW, 1000 masl	9	99.099	33.164	4.661	0.175	60.889	0.013	0.005	0.013	0.179	0.000	0.000	0.000	0.000	0.000	0.000
BKUD09-143-52-8m_8-1	BK_SW, 1000 masl	9	98.574	33.055	4.141	0.236	61.005	0.045	0.027	0.043	0.245	0.000	0.000	0.000	0.000	0.000	0.000
BKUD09-143-52-8m_9-1	BK_SW, 1000 masl	9	98.698	32.991	4.803	0.273	60.305	0.045	0.000	0.068	0.334	0.012	0.000	0.000	0.011	0.002	0.000
BKUD09-160-56-5m-1-2	BK_SW, 950 masl	9	101.160	34.367	5.748	0.676	59.267	0.019	0.013	0.843	0.394	0.000	0.000	0.000	0.000	0.000	0.065
BKUD09-160-56-5m-1-3	BK_SW, 950 masl	9	102.170	35.091	5.516	0.120	60.751	0.020	0.000	0.672	0.018	0.000	0.000	0.000	0.003	0.003	0.082
BKUD09-160-56-5m-1-5	BK_SW, 950 masl	9	101.331	34.940	7.468	5.705	52.615	0.018	0.119	0.635	0.009	0.000	0.000	0.000	0.000	0.000	0.023
BKUD09-160-56-5m-2-1	BK_SW, 950 masl	9	100.848	34.085	4.410	0.265	61.405	0.033	0.006	0.662	0.191	0.000	0.000	0.000	0.001	0.000	0.077
BKUD09-160-56-5m-3-2	BK_SW, 950 masl	9	101.569	34.460	4.138	0.080	62.024	0.059	0.043	0.629	0.080	0.000	0.000	0.005	0.000	0.000	0.137
BKUD09-160-56-5m-3-5	BK_SW, 950 masl	9	101.702	34.173	4.906	2.780	55.901	0.029	0.275	0.963	2.517	0.119	0.000	0.000	0.000	0.000	0.110
BKUD09-160-56-5m-3-7	BK_SW, 950 masl	9	101.174	34.505	4.611	2.387	58.948	0.062	0.042	0.646	0.000	0.032	0.000	0.000	0.000	0.000	0.057
BKUD09-160-56-5m-4-2	BK_SW, 950 masl	9	101.437	34.586	2.533	0.652	62.748	0.024	0.053	0.592	0.437	0.000	0.000	0.000	0.000	0.000	0.017
BKUD09-160-56-5m-4-4	BK_SW, 950 masl	9	101.127	34.020	2.377	0.875	61.976	0.038	0.332	0.705	0.844	0.005	0.000	0.000	0.001	0.000	0.160
BKUD09-160-56-5m-5-1	BK_SW, 950 masl	9	101.309	34.226	6.429	0.241	58.912	0.033	0.268	0.976	0.117	0.150	0.000	0.000	0.000	0.000	0.131
BKUD09-160-56-5m-6-1	BK_SW, 950 masl	9	101.506	34.383	3.399	0.615	61.846	0.030	0.086	0.712	0.441	0.000	0.000	0.000	0.000	0.000	0.000
BKUD09-160-56-5m-6-5	BK_SW, 950 masl	9	100.661	33.830	4.075	0.796	60.995	0.047	0.100	0.606	0.079	0.087	0.000	0.015	0.000	0.000	0.097
BKUD09-160-56-5m-7-2	BK_SW, 950 masl	9	100.668	33.887	4.694	1.274	59.195	0.075	0.263	0.588	0.575	0.051	0.000	0.000	0.003	0.000	0.210
BKUD09-160-56-5m-7-3	BK_SW, 950 masl	9	100.850	32.933	2.876	1.689	57.630	0.048	2.499	0.622	0.878	1.634	0.000	0.000	0.000	0.016	0.148
BKUD09-160-56-5m-7-4	BK_SW, 950 masl	9	100.111	34.012	4.664	1.024	59.854	0.009	0.032	0.521	0.000	0.023	0.000	0.000	0.006	0.000	0.042
BKUD09-160-56-5m-7-9	BK_SW, 950 masl	9	101.307	34.167	3.990	1.644	60.317	0.018	0.290	0.613	0.093	0.000	0.000	0.049	0.000	0.000	0.118
BKUD09-160-56-5m-7-10	BK_SW, 950 masl	9	100.854	33.607	2.442	1.579	58.975	0.043	1.846	0.651	0.644	1.161	0.000	0.000	0.003	0.000	0.058
BKUD09-160-56-5m-8-5	BK_SW, 950 masl	9	101.549	34.205	4.027	2.764	57.132	0.036	1.329	0.481	0.593	1.046	0.000	0.000	0.002	0.000	0.000
BKUD09-160-56-5m-9-3	BK_SW, 950 masl	9	100.939	33.899	4.163	0.260	61.968	0.049	0.024	0.596	0.009	0.003	0.000	0.000	0.000	0.000	0.114
BKUD09-163-14-8m_1-2	BK_SW, Mid, 980 masl	9	100.832	32.989	2.749	0.392	63.396	0.021	0.045	0.702	0.471	0.000	0.000	0.019	0.001	0.018	0.000
BKUD09-163-14-8m_2-1	BK_SW, Mid, 980 masl	9	99.759	32.828	2.498	0.013	63.662	0.068	0.047	0.630	0.000	0.041	0.000	0.000	0.000	0.014	0.000
BKUD09-163-14-8m_2-2	BK_SW, Mid, 980 masl	9	99.512	32.210	5.608	1.410	53.053	0.054	3.623	0.626	0.169	2.835	0.000	0.000	0.000	0.012	0.000

B. Electron Microprobe Data: Sulfides, Oxides, and Sulfates

BKUD09-163-14-8m_2-3	BK_SW, Mid, 980 masl	9	99.580	33.117	4.616	0.089	61.150	0.049	0.007	0.664	0.000	0.002	0.000	0.000	0.003	0.000	0.000
BKUD09-163-14-8m_3-1	BK_SW, Mid, 980 masl	9	99.507	33.098	2.128	0.019	63.935	0.021	0.010	0.575	0.000	0.000	0.000	0.000	0.004	0.003	0.000
BKUD09-163-14-8m_3-2	BK_SW, Mid, 980 masl	9	100.528	33.511	1.999	0.004	64.610	0.012	0.000	0.606	0.000	0.000	0.000	0.000	0.000	0.000	0.000
BKUD09-163-14-8m_3-3	BK_SW, Mid, 980 masl	9	99.979	32.453	5.914	0.817	56.384	0.046	2.021	0.576	0.418	1.313	0.000	0.000	0.002	0.000	0.000
BKUD09-163-14-8m_3-4	BK_SW, Mid, 980 masl	9	99.570	32.902	3.919	0.297	61.454	0.031	0.052	0.667	0.327	0.051	0.000	0.000	0.000	0.010	0.000
BKUD09-163-14-8m_3-6	BK_SW, Mid, 980 masl	9	99.760	32.996	5.500	0.137	60.517	0.060	0.024	0.469	0.102	0.034	0.000	0.000	0.000	0.008	0.000
BKUD09-163-14-8m_4-1	BK_SW, Mid, 980 masl	9	99.836	32.852	2.875	0.119	63.306	0.034	0.005	0.690	0.066	0.000	0.000	0.000	0.000	0.016	0.000
BKUD09-163-14-8m_4-4	BK_SW, Mid, 980 masl	9	99.954	33.008	4.898	0.242	60.988	0.030	0.012	0.608	0.250	0.020	0.000	0.000	0.002	0.007	0.000
BKUD09-163-14-8m_5-4	BK_SW, Mid, 980 masl	9	100.666	33.258	5.352	0.436	60.543	0.023	0.048	0.689	0.439	0.000	0.000	0.000	0.000	0.015	0.000
BKUD09-163-14-8m_6-2	BK_SW, Mid, 980 masl	9	100.722	33.000	2.824	0.104	64.081	0.051	0.000	0.688	0.103	0.031	0.000	0.000	0.000	0.006	0.000
BKUD09-163-14-8m_7-3	BK_SW, Mid, 980 masl	9	100.938	33.118	4.014	0.121	63.079	0.028	0.012	0.562	0.075	0.000	0.000	0.000	0.000	0.012	0.000
BKUD09-163-14-8m_7-4	BK_SW, Mid, 980 masl	9	100.327	33.424	7.635	0.927	57.665	0.030	0.122	0.622	0.086	0.000	0.000	0.000	0.000	0.005	0.000
n = 49	AVERAGE		100.333	33.489	4.341	0.670	60.624	0.036	0.281	0.537	0.248	0.177	0.016	0.002	0.001	0.005	0.037
	MINIMUM		98.574	32.210	1.999	0.000	52.615	0.003	0.000	0.000	0.000	0.000	0.000	0.000	0.000	0.000	0.000
	MAXIMUM		102.170	35.091	7.635	5.705	64.610	0.079	3.623	1.212	2.517	2.835	0.228	0.049	0.011	0.021	0.210
Galena: stage 9																	
K07-87-106-7m-1-11	Pool	9	100.780	13.648	0.009	0.000	0.013	0.055	0.000	0.000	0.000	0.000	87.196	0.000		0.015	0.000
K07-87-106-7m-2-6	Pool	9	99.280	13.466	0.032	0.032	0.054	0.014	0.000	0.000	0.000	0.000	85.807	0.000		0.006	0.083
BKUD09-153-87-5m-7-2	BK_SW, 940 masl	9 ?	101.941	14.735	0.012	0.015	0.035	0.017	**1.557**	0.000	0.000	**1.999**	83.642	0.000	0.013	0.000	0.000
BKUD09-163-14-8m_1-1	BK_SW, Mid, 980 masl	9	99.074	13.443	0.036	0.003	0.117	0.034	0.048	0.000	0.024	0.191	86.113	0.000	0.001	0.000	0.000
BKUD09-163-14-8m_2-5	BK_SW, Mid, 980 masl	9	98.019	13.576	0.056	0.002	0.004	0.009	0.084	0.000	0.000	0.246	85.061	0.000	0.002	0.000	0.000
BKUD09-163-14-8m_2-6	BK_SW, Mid, 980 masl	9	98.331	13.683	0.140	0.000	0.011	0.050	0.047	0.042	0.000	0.100	85.222	0.000	0.017	0.006	0.000
BKUD09-163-14-8m_4-2	BK_SW, Mid, 980 masl	9	98.507	13.529	0.020	0.000	0.000	0.020	0.032	0.094	0.000	0.095	85.627	0.000	0.005	0.000	0.000
BKUD09-163-14-8m_5-3	BK_SW, Mid, 980 masl	9	97.707	13.554	0.057	0.000	0.000	0.056	0.014	0.000	0.000	0.128	85.014	0.000	0.007	0.004	0.000

B. Electron Microprobe Data: Sulfides, Oxides, and Sulfates

BKUD09-163-14-8m_6-1	BK_SW, Mid, 980 masl	9	96.964	13.449	0.050	0.006	0.013	0.036	0.075	0.000	0.000	0.165	84.305	0.000	0.007	0.000	0.000
BKUD09-163-14-8m_6-4	BK_SW, Mid, 980 masl	9	100.223	13.771	0.040	0.010	0.030	0.030	0.138	0.000	0.000	0.278	86.847	0.000	0.000	0.000	0.000
BKUD09-163-14-8m_7-1	BK_SW, Mid, 980 masl	9	98.226	13.566	0.052	0.012	0.000	0.015	0.105	0.000	0.000	0.142	85.480	0.000	0.000	0.000	0.000
n = 11	AVERAGE		99.005	13.675	0.046	0.007	0.025	0.031	0.191	0.012	0.002	0.304	85.483	0.000	0.006	0.003	0.008
	MINIMUM		96.964	13.443	0.009	0.000	0.000	0.009	0.000	0.000	0.000	0.000	83.642	0.000	0.000	0.000	0.000
	MAXIMUM		101.941	14.735	0.140	0.032	0.117	0.056	1.557	0.094	0.024	1.999	87.196	0.000	0.017	0.015	0.083

Appendix IV

Fluid Inclusion Data

A total of 288 fluid inclusions were analyzed. Equipment specifications are documented in Section 3.3. The fluid inclusion data is grouped according to vein location, host mineral, and paragenetic stages. Fluid salinity was calculated from either T_m (Bodnar, 1993) or T_{mCl} (Diamon, 1992). Where both T_m and T_{mCl} measurements were acquired from a single fluid inclusion, T_{mCl} was given preference, and listed in the 'Salinity (Final)' column.

Sample	FI No.	Chip No.	FI Type	T_h (°C)	T_e (°C)	T_m (°C)	T_{mCl} (°C)	T_{hCO2} (°C)	T_{mCO2} (°C)	Salinity (Final) (wt % NaCl equiv.)	Salinity (T_m) (wt % NaCl equiv.)	Salinity (T_{mCl}) (wt % NaCl equiv.)	Date
Bellekeno													
Siderite: stage 2													
BKUD09-158: 37m	40	1	P	270.0	-42.0	-10.0				13.9	13.9		15-Mar-11
BKUD09-158: 37m	41	1	P	260.0									15-Mar-11
BKUD09-158: 37m	42	1	PS	253.0	-41.4	-5.0				7.9	7.9		15-Mar-11
BKUD09-158: 37m	62	3	P	268.0	-44.0	-9.6				13.5	13.5		15-Mar-11
BKUD09-158: 37m	63	3	P	280.1	-45.3	-8.4				12.2	12.2		15-Mar-11
BKUD09-158: 37m	64	3	P	273.7	-47.9	-8.4				12.2	12.2		15-Mar-11
BKUD09-158: 37m	65	3	P	274.0	-43.9	-8.4				12.2	12.2		15-Mar-11
BKUD09-158: 37m	66	3	P	261.5		-9.6				13.5	13.5		15-Mar-11
BKUD09-158: 37m	68	3	P	258.8	-47.0	-8.4				12.2	12.2		15-Mar-11
BKUD09-158: 37m	69	3	P	252.1	-31.0	-9.6				13.5	13.5		15-Mar-11

BKUD09-163: 31.8m	180	1	P	285.0	-23.0		3.5			11.2		11.2	30-Mar-11
BKUD09-163: 31.8m	181	1	PS	285.0	-23.0		3.5			11.2		11.2	30-Mar-11
BKUD09-163: 31.8m	182	1	P	276.0	-23.0	-9.0				12.8	12.8		30-Mar-11
BKUD09-163: 31.8m	183	1	P	277.0	-26.0	-9.0				12.8	12.8		30-Mar-11
BKUD09-163: 31.8m	184	1	PS	292.5	-28.0		3.5			11.2		11.2	30-Mar-11
BKUD09-161: 20m	248	2	P	261.0	-28.0	-9.2				13.1	13.1		07-Apr-11
BKUD09-161: 20m	249	2	P	249.0	-28.0								07-Apr-11
BKUD09-161: 20m	250	2	P	276.0	-37.0	-6.9				10.4	10.4		07-Apr-11
BKUD09-161: 20m	251	2	P	277.0	-22.0								07-Apr-11
BKUD09-161: 20m	252	2	P	275.0									07-Apr-11
n =	20	AVERAGE		270.2	-34.1	-8.6	3.5			12.1	12.3	11.2	
		MINIMUM		249.0	-47.9	-10.0	3.5			7.9	7.9	11.2	
		MAXIMUM		292.5	-22.0	-5.0	3.5			13.9	13.9	11.2	
Quartz: stage 2-3													
BKUD09-161: 20m	240	1	P	281.0	-28.0	-10.0	4.8			9.3	13.9	9.3	06-Apr-11
BKUD09-161: 20m	241	1	P	265.0	-28.0		5.0			9.0		9.0	06-Apr-11
BKUD09-161: 20m	242	1	P	291.0	-39.0	-8.0				11.7	11.7		06-Apr-11
BKUD09-161: 20m	243	1	P	275.0	-28.0	-8.1				11.8	11.8		06-Apr-11
BKUD09-161: 20m	244	1	P	298.0	-22.0								06-Apr-11
BKUD09-161: 20m	245	1	P	293.0	-22.0								06-Apr-11
BKUD09-161: 20m	246	2	P	266.3	-38.0	-9.4				13.3	13.3		06-Apr-11
BKUD09-161: 20m	247	2	P	267.8	-32.0	-9.6				13.5	13.5		06-Apr-11
N =	8	AVERAGE		279.6	-29.6	-9.0	4.9			11.4	12.8	9.1	
		MINIMUM		265.0	-39.0	-10.0	4.8			9.0	11.7	9.0	
		MAXIMUM		298.0	-22.0	-8.0	5.0			13.5	13.9	9.3	
Siderite: stage 6													
BKUD09-148: 33.5m	1	1	P	267.0									09-Mar-11

BKUD09-148: 33.5m	2	1	PS	263.0									09-Mar-11
BKUD09-148: 33.5m	3	1	PS	268.5	-28.0	-7.6				11.2	11.2		09-Mar-11
BKUD09-158: 36.5m	23	1	P	231.4	-48.0	-7.7				11.3	11.3		14-Mar-11
BKUD09-158: 36.5m	24	1	PS	223.0									14-Mar-11
BKUD09-158: 36.5m	32	3		250.0	-43.0	-7.5				11.1	11.1		14-Mar-11
BKUD09-158: 36.5m	33	3		238.5		-8.5				12.3	12.3		14-Mar-11
BKUD09-171: 32.8m	91	3	P	256.0	-31.0		-5.0			19.7		19.7	22-Mar-11
BKUD09-171: 32.8m	92	3	P	250.0	-30.0								22-Mar-11
BKUD09-171: 32.8m	93	3	P	251.0									22-Mar-11
BKUD09-171: 32.8m	94	3	P	251.0									22-Mar-11
BKUD09-171: 32.8m	95	3	P	258.0									22-Mar-11
BKUD09-171: 32.8m	96	3	P	254.2									22-Mar-11
BKUD09-171: 32.8m	97	3	P	256.0									22-Mar-11
BKUD09-171: 32.8m	98	3	P	251.0	-21.0								22-Mar-11
BKUD09-171: 32.8m	99	3	P	262.0									22-Mar-11
BKUD09-171: 32.8m	100	3	P	252.0									22-Mar-11
BKUD09-171: 32.8m	101	3	P	243.3	-30.0		-2.0			17.5		17.5	22-Mar-11
BKUD09-171: 32.8m	102	3	P	250.2	-21.0								22-Mar-11
BKUD09-171: 32.8m	103	3	P	250.0									22-Mar-11
BKUD09-171: 32.8m	104	3	P	254.2									22-Mar-11
K07-86: 223.3m	112	1	P	250.5									23-Mar-11
K07-86: 223.3m	113	1	P	251.5			-3.5			18.7		18.7	23-Mar-11
K07-86: 223.3m	115	1	P	253.0			-3.0			18.3		18.3	23-Mar-11
K07-86: 223.3m	116	1	P		-37.0								23-Mar-11
K07-86: 223.3m	117	1	P	250.0									23-Mar-11
K07-86: 223.3m	118	1	P	253.0									23-Mar-11
K07-86: 223.3m	119	1	P	**269.0**	-30.0	**-8.5**				12.3	12.3		23-Mar-11
K07-86: 223.3m	120	1	P	258.0	-28.0		-3.0			18.3		18.3	23-Mar-11

BKUD09-143: 51.2m	130	1	P	257.0		-11.5				15.5	15.5		24-Mar-11
BKUD09-143: 51.2m	131	1	P	261.0	-32.0	-12.0				16.0	16.0		24-Mar-11
BKUD09-143: 51.2m	132	1	P	258.0	-32.0	-11.5				15.5	15.5		24-Mar-11
BKUD09-143: 51.2m	133	1	P	255.5	-32.0	-11.3				15.3	15.3		24-Mar-11
BKUD09-143: 51.2m	134	1	P	256.0	-32.0	-6.1	1.8			13.4	9.3	13.4	24-Mar-11
BKUD09-143: 51.2m	135	1	P	257.0	-12.0								24-Mar-11
BKUD09-143: 51.2m	136	1	P	256.5	-32.0	-11.0	2.0			13.2	15.0	13.2	24-Mar-11
BKUD09-143: 51.2m	137	1	P	256.0	-28.0	-9.7	3.0			11.9	13.6	11.9	24-Mar-11
BKUD09-143: 54m	185	1	P	243.0	-33.0		-3.0			18.3		18.3	31-Mar-11
BKUD09-143: 54m	186	1	P	243.0									31-Mar-11
BKUD09-143: 54m	187	1	P	261.3									31-Mar-11
BKUD09-143: 54m	188	1	P	265.0									31-Mar-11
BKUD09-143: 54m	189	1	P	247.0		-6.0				9.2	9.2		31-Mar-11
BKUD09-143: 54m	190	1	P	255.0	-24.0	-11.0				15.0	15.0		31-Mar-11
BKUD09-143: 54m	191	1	P	235.5	-33.0	-7.0				10.5	10.5		31-Mar-11
BKUD09-143: 54m	192	1	P	258.0	-24.0	-12.0				16.0	16.0		31-Mar-11
BKUD09-143: 54m	193	1	P	214.0									31-Mar-11
BKUD09-143: 54m	194	1	P		-25.0	-11.0				15.0	15.0		31-Mar-11
BKUD09-143: 54m	195	1	P	255.0	-32.0	-15.6				19.1	19.1		31-Mar-11
BKUD09-143: 54m	196	1	P	255.0	-25.0	-11.5				15.5	15.5		31-Mar-11
BKUD09-143: 54m	197	1	P	258.0	-25.0	-11.5				15.5	15.5		31-Mar-11
BKUD09-143: 54m	198	1	P	257.0	-25.0	-11.0				15.0	15.0		31-Mar-11
BKUD09-143: 54m	199	1	P	256.0	-25.0								31-Mar-11
BKUD09-143: 54m	200	1	P	251.0	-25.0								31-Mar-11
BKUD09-143: 54m	201	1	P		-25.0	-11.5				15.5	15.5		31-Mar-11
BKUD09-143: 54m	202	1	P	260.0		-11.5				15.5	15.5		31-Mar-11
BKUD09-143: 54m	203	1	P	258.0	-32.0	-16.5	-4.0			19.0	19.8	19.0	31-Mar-11
BKUD09-143: 54m	204	1	P	249.0	-43.0	-12.4				16.3	16.3		31-Mar-11

BKUD09-171: 43.5m	269	1	P	269.0									08-Apr-11
BKUD09-171: 43.5m	270	1	P	251.0									08-Apr-11
BKUD09-171: 43.5m	271	1	P	255.0	-22.0								08-Apr-11
BKUD09-171: 43.5m	272	1	P	253.0	-42.0		-5.0			19.7		19.7	08-Apr-11
BKUD09-171: 43.5m	273	1	P	268.0									08-Apr-11
BKUD09-171: 43.5m	274	1	P	266.0									08-Apr-11
BKUD09-171: 43.5m	275	1	P	253.0	-30.0		-5.0			19.7		19.7	08-Apr-11
BKUD09-148: 33.5m	276	1	P	253.0	-34.0	-11.0	0.0			15.6	15.0	15.5	06-Apr-11
BKUD09-148: 33.5m	277	1	PS		-29.0								06-Apr-11
BKUD09-171: 32.8m	278	2	P	281.7	-32.0	-10.7	-3.0			18.3	14.7	18.3	04-Apr-11
BKUD09-171: 32.8m	279	2	PS	254.0									04-Apr-11
BKUD09-171: 32.8m	280	2	PS	256.5									04-Apr-11
BKUD09-171: 32.8m	281	2	P	254.0		-12.6	-1.0			16.6	16.5	16.6	04-Apr-11
BKUD09-171: 32.8m	282	2	P	256.5									04-Apr-11
BKUD09-171: 32.8m	283	2	PS	257.0									04-Apr-11
BKUD09-171: 32.8m	284	2	P	261.0	-32.0		2.0			13.2		13.2	04-Apr-11
BKUD09-171: 32.8m	285	2	P	261.5	-37.0		1.0			14.4		14.4	04-Apr-11
BKUD09-171: 32.8m	286	2	PS	256.0	-47.0	-9.9	-2.7			18.1	13.8	18.1	04-Apr-11
BKUD09-171: 32.8m	287	2	PS	254.0	-35.0	-9.5				13.4	13.4		04-Apr-11
BKUD09-171: 32.8m	288	2	PS	258.5									04-Apr-11
n =	8	AVERAGE		257.3	-37.8	-10.7	-0.2			15.1	14.6	15.6	
		MINIMUM		254.0	-47.0	-12.6	-2.7			13.2	13.4	13.2	
		MAXIMUM		261.5	-32.0	-9.5	2.0			18.1	16.5	18.1	
Sphalerite: stage 7													
BKUD09-148: 33.5m	4	2	P	223.6									09-Mar-11
BKUD09-148: 33.5m	5	2	P	221.5		-8.3				12.0	12.0		09-Mar-11
BKUD09-148: 33.5m	6	2	P	222.0									09-Mar-11

BKUD09-148: 33.5m	7	2	P	228.1	-38.0	-8.1				11.8	11.8		09-Mar-11
BKUD09-148: 33.5m	8	2	P	225.7									09-Mar-11
BKUD09-158: 36.5m	25	2	P	228.0	-33.0		-3.8			18.9		18.9	14-Mar-11
BKUD09-158: 36.5m	26	2	P	225.0									14-Mar-11
BKUD09-158: 36.5m	27	2	PS	227.0									14-Mar-11
BKUD09-158: 36.5m	28	2	P	225.0									14-Mar-11
BKUD09-158: 36.5m	29	2	P	223.0			-4.0			19.0		19.0	14-Mar-11
BKUD09-158: 36.5m	30	2	PS	229.0	-46.0	-8.0				11.7	11.7		14-Mar-11
BKUD09-158: 36.5m	34	4	P	232.5	-27.0	-7.2				10.7	10.7		14-Mar-11
BKUD09-158: 36.5m	35	4	P	223.5	-46.0	-7.4				11.0	11.0		14-Mar-11
BKUD09-158: 36.5m	36	4	PS	223.0	-46.0	-7.2				10.7	10.7		14-Mar-11
BKUD09-158: 36.5m	37	4	PS	223.5									14-Mar-11
BKUD09-158: 36.5m	38	4	PS	223.0		-7.2				10.7	10.7		14-Mar-11
BKUD09-158: 36.5m	39	4	PS	223.0									14-Mar-11
BKUD09-139: 8.3m	205	1	P	243.5	-40.0	-13.8	-2.0			17.5	17.6	17.5	01-Apr-11
BKUD09-139: 8.3m	206	1	P	248.5									01-Apr-11
BKUD09-139: 8.3m	207	1	P	246.0									01-Apr-11
BKUD09-139: 8.3m	208	1	P	245.0	-44.0	-16.0	-2.3			17.7	19.4	17.7	01-Apr-11
BKUD09-139: 8.3m	209	1	P	244.5	-40.0	-14.1	-4.0			19.0	17.9	19.0	01-Apr-11
BKUD09-139: 8.3m	210	1	P	238.5									01-Apr-11
BKUD09-139: 8.3m	211	1	P	238.5	-51.0	-14.2	-0.5			16.1	18.0	16.1	01-Apr-11
BKUD09-139: 8.3m	212	1	P	246.5		-14.3				18.0	18.0		01-Apr-11
BKUD09-139: 8.3m	213	1	P	238.0	-40.0	-14.3				18.0	18.0		01-Apr-11
BKUD09-139: 8.3m	214	1	P	252.5	-27.0		-4.5			19.4		19.4	01-Apr-11
BKUD09-139: 8.3m	215	1	P	248.0	-27.0	-14.3				18.0	18.0		01-Apr-11
BKUD09-139: 8.3m	216	1	P	253.0									01-Apr-11
BKUD09-139: 8.3m	217	1	P	246.5	-27.0	-14.1				17.9	17.9		01-Apr-11
BKUD09-139: 8.3m	218	1	P	260.5									01-Apr-11

BKUD09-139: 8.3m	219	1	P	257.5	-40.0	-14.1	-4.0			19.0	17.9	19.0	01-Apr-11
K09-187: 201.9m	253	1	P	213.5	-47.0	-7.5				11.1	11.1		08-Apr-11
K09-187: 201.9m	254	1	P	225.0		-6.0	4.0			10.5	9.2	10.5	08-Apr-11
K09-187: 201.9m	255	1	P	232.0		-7.0	3.0			11.9	10.5	11.9	08-Apr-11
K09-187: 201.9m	256	1	P	230.0	-25.0	-7.5				11.1	11.1		08-Apr-11
K09-187: 201.9m	257	1	P	226.0	-41.0	-8.0	5.0			9.0	11.7	9.0	08-Apr-11
K09-187: 201.9m	258	1	P	229.0	-37.0	-8.0	4.0			10.5	11.7	10.5	08-Apr-11
BKUD09-171: 43.5m	259	1	P	232.0	-28.0	-11.2				15.2	15.2		08-Apr-11
BKUD09-171: 43.5m	260	1	P	227.0	-43.0	-8.1				11.8	11.8		08-Apr-11
BKUD09-171: 43.5m	261	1	P	256.0	-28.0								08-Apr-11
BKUD09-171: 43.5m	262	1	P	226.0	-24.0								08-Apr-11
BKUD09-171: 43.5m	263	1	P	231.0	-35.0	-9.5	2.5			12.6	13.4	12.6	08-Apr-11
BKUD09-171: 43.5m	264	1	P	244.0		-15.4				19.0	19.0		08-Apr-11
BKUD09-171: 43.5m	265	1	P	235.0		-11.0				15.0	15.0		08-Apr-11
BKUD09-171: 43.5m	266	1	P	230.0	-24.0	-10.6				14.6	14.6		08-Apr-11
BKUD09-171: 43.5m	267	1	P	210.0	-28.0	-11.0				15.0	15.0		08-Apr-11
BKUD09-171: 43.5m	268	1	P	218.0									08-Apr-11
n =	48	AVERAGE		233.3	-35.8	-10.5	-0.5			14.5	14.2	15.5	
		MINIMUM		210.0	-51.0	-16.0	-4.5			9.0	9.2	9.0	
		MAXIMUM		260.5	-24.0	-6.0	5.0			19.4	19.4	19.4	
Siderite: stage 9													
BKUD09-143: 53.5m	10	1	PS	240.0									10-Mar-11
BKUD09-143: 53.5m	11	1	S	242.0									10-Mar-11
BKUD09-143: 53.5m	12	1	S	242.0									10-Mar-11
BKUD09-143: 53.5m	13	1	S	237.0									10-Mar-11
BKUD09-143: 53.5m	14	2	S	238.0									10-Mar-11
BKUD09-143: 53.5m	15	2	S	239.0	-47.0	-1.4				2.4	2.4		10-Mar-11

BKUD09-158: 36.5m	31	3	P	235.5		-5.1				8.0	8.0		14-Mar-11
BKUD09-160: 56.5m	84	2	P	232.6	-28.0	-3.2				5.3	5.3		21-Mar-11
BKUD09-160: 56.5m	85	2	P	222.5		-6.2				9.5	9.5		21-Mar-11
BKUD09-160: 56.5m	86	2	P	225.4		-6.5				9.9	9.9		21-Mar-11
BKUD09-160: 56.5m	87	3	P	240.0	-16.0	-7.0				10.5	10.5		21-Mar-11
BKUD09-160: 56.5m	88	3	P	229.7		-4.0				6.4	6.4		21-Mar-11
BKUD09-160: 56.5m	89	3	PS	248.8		-7.2				10.7	10.7		21-Mar-11
BKUD09-160: 56.5m	90	3	P	276.3	-28.0	-7.6				11.2	11.2		21-Mar-11
BKUD09-143: 52.8m	223	2	P	190.0		-4.0				6.4	6.4		04-Apr-11
BKUD09-143: 52.8m	224	2	P	248.0									04-Apr-11
BKUD09-143: 52.8m	225	2	P	244.0	-21.0	-5.0				7.9	7.9		04-Apr-11
BKUD09-143: 52.8m	226	2	P	243.0	-21.0	-5.0				7.9	7.9		04-Apr-11
BKUD09-143: 52.8m	227	2	P	242.0		-8.0				11.7	11.7		04-Apr-11
BKUD09-143: 52.8m	228	2	P	245.0	-22.0	-6.0				9.2	9.2		04-Apr-11
n =	20	AVERAGE		238.0	-26.1	-5.4				8.4	8.4		
		MINIMUM		190.0	-47.0	-8.0				2.4	2.4		
		MAXIMUM		276.3	-16.0	-1.4				11.7	11.7		
Sphalerite: stage 9													
BKUD09-143: 53.5m	16	3		160.0	-23.0	-1.7				2.9	2.9		10-Mar-11
BKUD09-143: 51.2m	121	1	PS	164.0	-28.0	-5.0				7.9	7.9		24-Mar-11
BKUD09-143: 51.2m	123	1	P	195.5	-28.0	-4.0				6.4	6.4		24-Mar-11
BKUD09-143: 51.2m	124	1	P	171.0		-4.0				6.4	6.4		24-Mar-11
BKUD09-143: 51.2m	125	1	PS	145.0	-28.0								24-Mar-11
BKUD09-143: 51.2m	126	1	PS	163.0									24-Mar-11
BKUD09-143: 51.2m	127	1	P	171.0		-5.0				7.9	7.9		24-Mar-11
BKUD09-143: 51.2m	128	1	P	171.0	-26.0	-5.0				7.9	7.9		24-Mar-11
BKUD09-143: 51.2m	129	1	P	177.5	-46.0	-5.0				7.9	7.9		24-Mar-11

BKUD09-143: 52.8m	221	1	P	172.5	-35.0	-1.8				3.1	3.1		01-Apr-11
BKUD09-143: 52.8m	222	1	P		-24.0	-1.8				3.1	3.1		01-Apr-11
n =	11	AVERAGE		169.1	-29.8	-3.7				5.9	5.9		
		MINIMUM		145.0	-46.0	-5.0				2.9	2.9		
		MAXIMUM		195.5	-23.0	-1.7				7.9	7.9		
Quartz: stage 8													
BKUD09-158: 37m	43	2	S	200.0		-2.3				3.9	3.9		15-Mar-11
BKUD09-158: 37m	44	2	S	222.5	-48.8	-1.6				2.7	2.7		15-Mar-11
BKUD09-158: 37m	45	2	S	222.5		-1.6				2.7	2.7		15-Mar-11
BKUD09-158: 37m	46	2	S	224.5									15-Mar-11
BKUD09-158: 37m	47	2	S	221.0									15-Mar-11
BKUD09-158: 37m	48	2	S	217.0									15-Mar-11
BKUD09-158: 37m	49	2	S			-2.1				3.5	3.5		15-Mar-11
BKUD09-158: 37m	50	2	S	229.0	-30.0	-1.9				3.2	3.2		15-Mar-11
BKUD09-158: 37m	51	2	S			-2.1				3.5	3.5		15-Mar-11
BKUD09-158: 37m	52	2	S	213.0		-2.1				3.5	3.5		15-Mar-11
BKUD09-158: 37m	53	2	S	226.0	-36.0	-2.0				3.4	3.4		15-Mar-11
BKUD09-158: 37m	54	2	S			-2.0				3.4	3.4		15-Mar-11
BKUD09-158: 37m	55	2	S	248.5	-48.0	-2.2				3.7	3.7		15-Mar-11
BKUD09-158: 37m	56	2	S	247.5	-46.0	-2.2				3.7	3.7		15-Mar-11
BKUD09-158: 37m	57	2	S	235.0	-35.0	-1.8				3.1	3.1		15-Mar-11
BKUD09-158: 37m	58	2	S	219.0	-35.0	-1.8				3.1	3.1		15-Mar-11
BKUD09-158: 37m	59	2	S	263.0	-31.0	-1.9				3.2	3.2		15-Mar-11
BKUD09-158: 37m	60	2	S	229.0	-43.0	-1.7				2.9	2.9		15-Mar-11
BKUD09-158: 37m	61	2	S	229.0	-44.0	-1.9				3.2	3.2		15-Mar-11
n =	19	AVERAGE		227.9	-39.7	-2.0				3.3	3.3		
		MINIMUM		200.0	-48.8	-2.3				2.7	2.7		
		MAXIMUM		263.0	-30.0	-1.6				3.9	3.9		

Calcite: stage 12													
BKUD09-160: 56.5m	77	1	P	175.4	-36.0								18-Mar-11
BKUD09-160: 56.5m	78	1	PS	173.1		-3.9				6.3	6.3		18-Mar-11
BKUD09-160: 56.5m	79	1	PS	172.9		-3.9				6.3	6.3		18-Mar-11
BKUD09-160: 56.5m	80	1	PS			-3.0				5.0	5.0		18-Mar-11
BKUD09-160: 56.5m	81	1	PS	171.9		-3.9				6.3	6.3		18-Mar-11
BKUD09-160: 56.5m	82	1	PS	186.0		-3.1				5.1	5.1		18-Mar-11
BKUD09-160: 56.5m	83	1	P	164.0		-3.9				6.3	6.3		18-Mar-11
n =	7	AVERAGE		173.9	-36.0	-3.6				5.9	5.9		
		MINIMUM		164.0	-36.0	-3.9				5.0	5.0		
		MAXIMUM		186.0	-36.0	-3.0				6.3	6.3		
Keno 700 Quartz: stage 1													
K08-165: 176.5m	146	1	S	257.5		-10.0				13.9	13.9		25-Mar-11
K08-165: 176.5m	147	1	S	274.0	-47.0	-10.0				13.9	13.9		25-Mar-11
K08-165: 176.5m	148	1	S	252.5							0.0		25-Mar-11
K08-165: 176.5m	149	1	S	254.0	-22.0	-7.8				11.5	11.5		25-Mar-11
K08-165: 176.5m	150	1	S		-25.0	-6.3				9.6	9.6		25-Mar-11
K08-165: 176.5m	151	1	S	257.5	-28.0	-7.5				11.1	11.1		25-Mar-11
K08-165: 176.5m	152	1	S	243.5	-22.0	-8.0				11.7	11.7		25-Mar-11
K08-165: 176.5m	153	1	S	243.5	-22.0	-10.0				13.9	13.9		25-Mar-11
K08-165: 176.5m	154	1	S	267.5	-32.0	-7.8				11.5	11.5		25-Mar-11
K08-165: 176.5m	155	1	S	262.0	-32.0	-7.8				11.5	11.5		25-Mar-11
K08-165: 176.5m	156	1	S	262.5		-6.7				10.1	10.1		25-Mar-11
K08-165: 176.5m	157	1	S	253.5	-22.0	-7.8				11.5	11.5		25-Mar-11
n =	12	AVERAGE		257.1	-28.0	-8.2				11.8	10.8		

		MINIMUM		243.5	-47.0	-10.0				9.6	0.0		
		MAXIMUM		274.0	-22.0	-6.3				13.9	13.9		
Homestake													
Quartz: stage 1													
HOM-053	158	1	P	295.1	-52.0	-4.5		24	-57	7.2	7.2		28-Mar-11
HOM-053	159	1	P	290.2	-47.0			24.7	-56.9				28-Mar-11
HOM-053	160	1	P	298.7	-28.0		10.0	24.7	-56.9	0.0		0.0	28-Mar-11
HOM-053	161	1	P	290.5			10.0	24.6	-56.9	0.0		0.0	28-Mar-11
HOM-053	162	1	P	288.3			10.2	24.5	-56.9	0.0		-0.4	28-Mar-11
HOM-053	163	1	P	289.5			10.2	24.6	-56.9	0.0		-0.4	28-Mar-11
HOM-053	164	1	P	289.0	-21.0		10.2	24.7	-57	0.0		-0.4	28-Mar-11
HOM-053	165	1	P		-32.0		10.2		-56.8	0.0		-0.4	28-Mar-11
HOM-053	166	1	P	299.4			10.2	24.9	-56.8	0.0		-0.4	28-Mar-11
HOM-053	167	1	P	290.8	-26.0		10.2	24.7	-56.9	0.0		-0.4	28-Mar-11
HOM-053	168	1	P	292.6				24.9	-56.8				28-Mar-11
HOM-053	169	1	P	293.0		-3.2	10.2		-56.8	5.3	5.3	-0.4	28-Mar-11
HOM-053	170	1	P	293.2			10.2	24.9	-56.8	0.0		-0.4	28-Mar-11
HOM-053	171	1	P	293.2			10.2	24.9	-56.8	0.0		-0.4	28-Mar-11
HOM-053	172	1	P	281.5			7.9	25.9	-56.8	4.1		4.1	28-Mar-11
HOM-053	173	1	P	303.5	-21.0	-6.0	10.0		-56.8	9.2		0.0	28-Mar-11
n =	16	AVERAGE		292.6	-32.4	-4.6	10.0	24.8	-56.9	1.8	6.2	0.0	
		MINIMUM		281.5	-52.0	-6.0	7.9	24.0	-57.0	0.0	5.3	-0.4	
		MAXIMUM		303.5	-21.0	-3.2	10.2	25.9	-56.8	9.2	7.2	4.1	
Silver King													
Siderite: stage (6 ?)													
K06-2: 167.2m	105	1	P	277.0	-26.0		-1.0			16.6		16.6	22-Mar-11

K06-2: 167.2m	106	1	P	276.0									22-Mar-11
K06-2: 167.2m	107	1	P	277.0									22-Mar-11
K06-2: 167.2m	108	1	P	276.0	-42.0		-2.0			17.5		17.5	22-Mar-11
K06-2: 167.2m	109	1	P	282.0	-42.0		-2.5			17.9		17.9	22-Mar-11
K06-2: 167.2m	110	1	P	273.5	-42.0	-10.0				13.9	13.9		22-Mar-11
K06-2: 167.2m	111	1	P	277.0									22-Mar-11
n =	7	AVERAGE		276.9	-38.0	-10.0	-1.8			16.5	13.9	17.3	
		MINIMUM		273.5	-42.0	-10.0	-2.5			13.9	13.9	16.6	
		MAXIMUM		282.0	-26.0	-10.0	-1.0			17.9	13.9	17.9	
Keno 700 Siderite: stage 6 (?)													
K09-200: 86.3m	71	2	P	254.0									18-Mar-11
K09-200: 86.3m	72	2	P	259.9									18-Mar-11
K09-200: 86.3m	73	2	P	260.5	-41.0		-2.5			17.9		17.9	18-Mar-11
K09-200: 86.3m	74	2	P	259.9									18-Mar-11
K09-200: 86.3m	75	2	P	260.2	-41.0	-10.5				14.5	14.5		18-Mar-11
K09-200: 86.3m	76	2	PS	259.2	-43.0		-4.8			19.6		19.6	18-Mar-11
n =	6	AVERAGE		259.0	-41.7	-10.5	-3.7			17.3	14.5	18.7	
		MINIMUM		254.0	-43.0	-10.5	-4.8			14.5	14.5	17.9	
		MAXIMUM		260.5	-41.0	-10.5	-2.5			19.6	14.5	19.6	
Alice Siderite: stage 6													
Alice	174	2	P	245.0		-10.0				13.9	13.9		29-Mar-11
Alice	175	2	P	248.0		-9.0				12.8	12.8		29-Mar-11
Alice	176	2	P	248.0		-10.0				13.9	13.9		29-Mar-11
Alice	177	2	P	232.0	-28.0	-9.0				12.8	12.8		29-Mar-11

Alice	178	2	P	233.2	-38.0	-10.0				13.9	13.9		29-Mar-11
Alice	179	2	P	238.0		-9.0				12.8	12.8		29-Mar-11
n =	6	AVERAGE		240.7	-33.0	-9.5				13.4	13.4		
		MINIMUM		232.0	-38.0	-10.0				12.8	12.8		
		MAXIMUM		248.0	-28.0	-9.0				13.9	13.9		
Sphalerite: stage 7													
Alice	138	1	P	246.0	-42.0	-5.5				8.5	8.5		25-Mar-11
Alice	139	1	P	248.0									25-Mar-11
Alice	140	1	P	248.0	-23.0	-5.0				7.9	7.9		25-Mar-11
Alice	141	1	P	246.0		-4.0				6.4	6.4		25-Mar-11
Alice	142	1	P	248.0		-4.0				6.4	6.4		25-Mar-11
Alice	143	1	P	239.0		-5.5				8.5	8.5		25-Mar-11
Alice	144	1	P	246.0	-31.0	-5.0				7.9	7.9		25-Mar-11
Alice	145	1	P	245.0	-26.0	-5.0				7.9	7.9		25-Mar-11
n =	8	AVERAGE		245.8	-30.5	-4.9				7.7	7.7		
		MINIMUM		239.0	-42.0	-5.5				6.4	6.4		
		MAXIMUM		248.0	-23.0	-4.0				8.5	8.5		
Pool Sphalerite: stage 9													
K07-87: 106.7m	229	1	PS	196.5	-45.0	-1.2				2.1	2.1		05-Apr-11
K07-87: 106.7m	230	1	PS	205.5	-22.0	-1.0				1.7	1.7		05-Apr-11
K07-87: 106.7m	231	1	PS	200.6	-35.0	-1.0				1.7	1.7		05-Apr-11
K07-87: 106.7m	232	1	PS	197.5	-22.0	-1.2				2.1	2.1		05-Apr-11
K07-87: 106.7m	233	1	PS	202.2	-22.0	-0.1				0.2	0.2		05-Apr-11
K07-87: 106.7m	234	1	PS	201.3		-0.3				0.5	0.5		05-Apr-11
K07-87: 106.7m	235	1	PS	200.5		0.0				0.0	0.0		05-Apr-11

K07-87: 106.7m	237	1	PS	169.5		-1.0				1.7	1.7		05-Apr-11
n =	8	AVERAGE		196.7	-29.2	-0.7				1.3	1.3		
		MINIMUM		169.5	-45.0	-1.2				0.0	0.0		
		MAXIMUM		205.5	-22.0	0.0				2.1	2.1		
Calcite: stage 12													
K07-87: 106.7m	238	2	S	252.0	-38.0	0.0				0.0	0.0		06-Apr-11

Appendix V

X-Ray Diffraction Plots

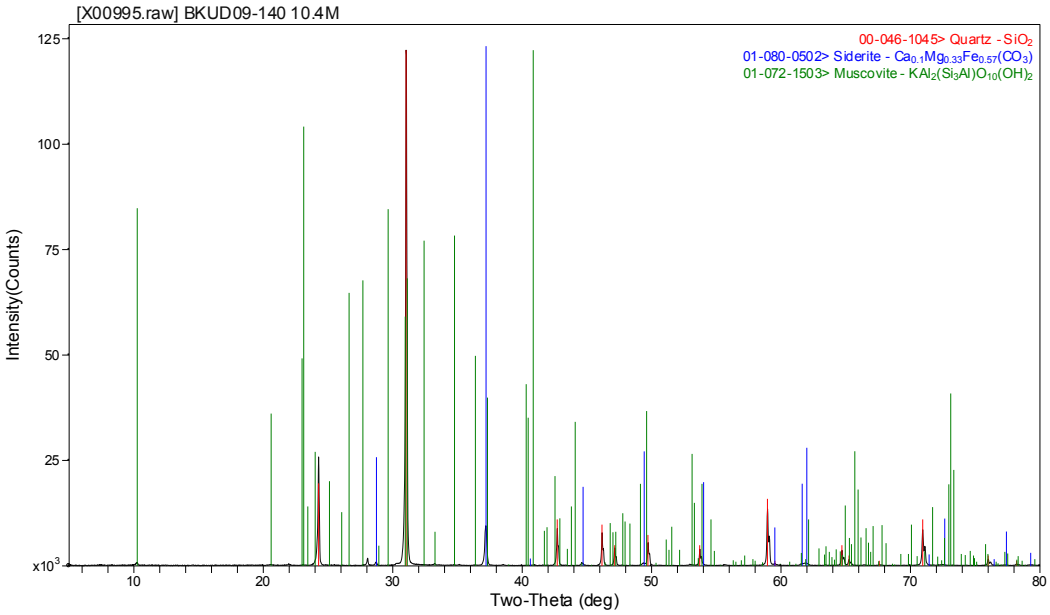

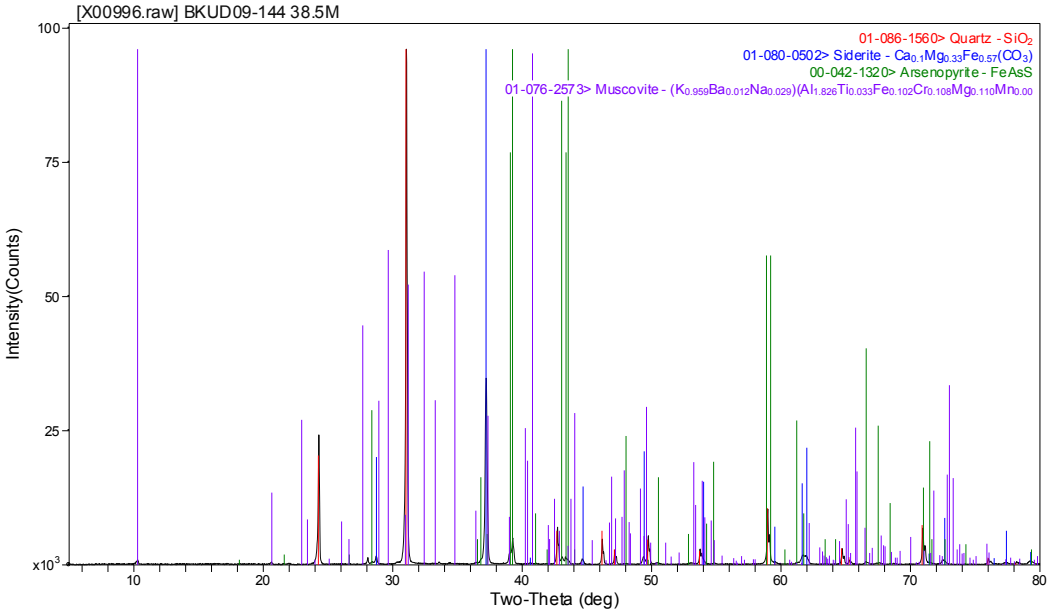

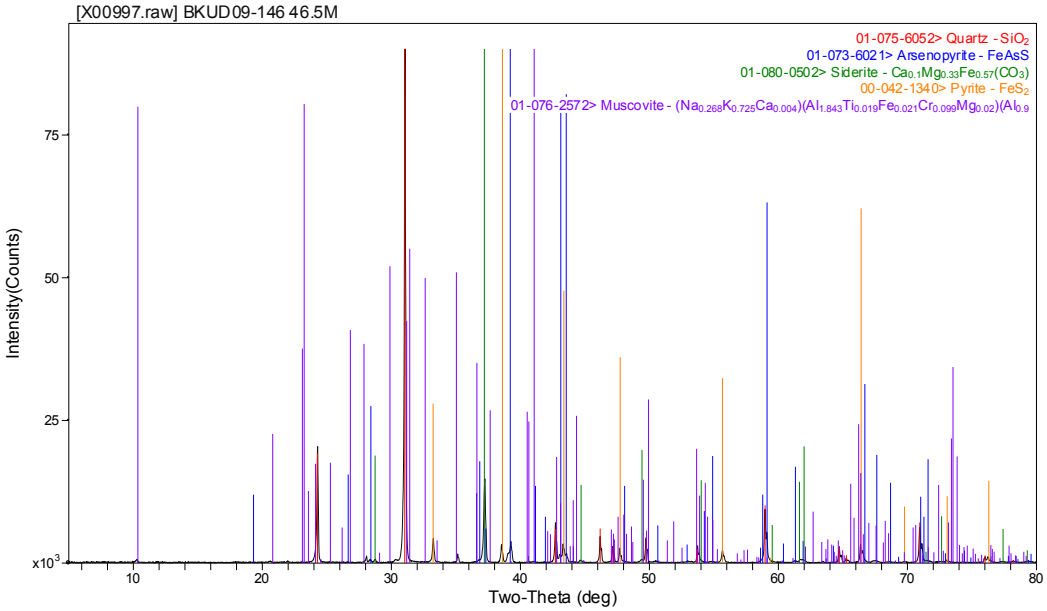
[X00997.raw] BKUD09-146 46.5M
01-075-6052> Quartz - SiO2
01-073-6021> Arsenopyrite - FeAsS
01-080-0502> Siderite - Ca0.1Mg0.33Fe0.57(CO3)
00-042-1340> Pyrite - FeS2
01-076-2572> Muscovite - (Na0.268K0.725Ca0.004)(Al1.843Ti0.019Fe0.021Cr0.099Mg0.02)(Al0.9
Intensity(Counts)
x10^3
75
50
25
10
20
30
40
50
60
70
80
Two-Theta (deg)

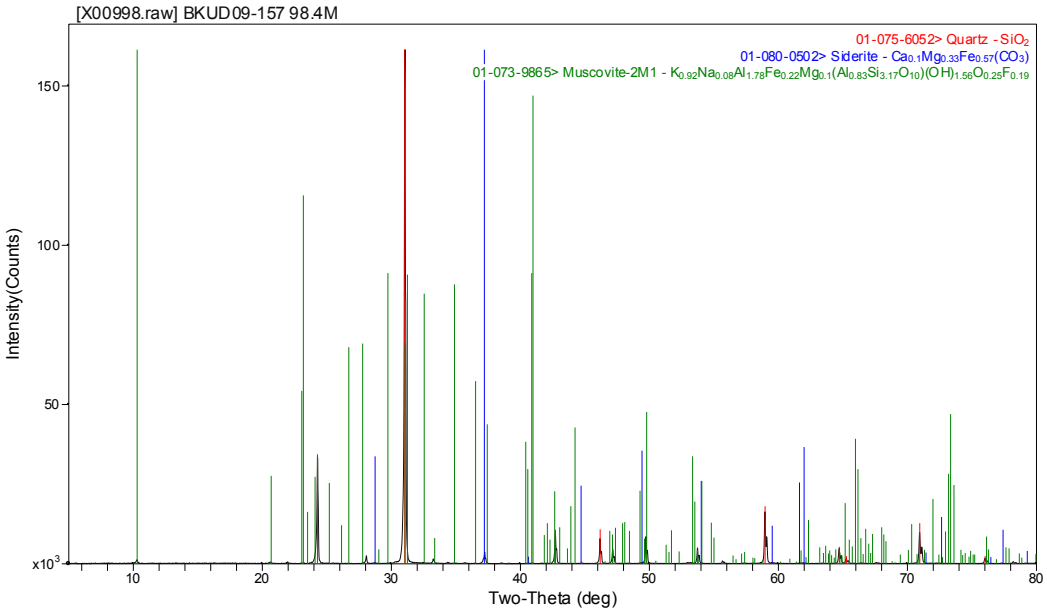
[X00998.raw] BKUD09-157 98.4M
01-075-6052> Quartz - SiO2
01-080-0502> Siderite - Ca0.1Mg0.33Fe0.57(CO3)
01-073-9865> Muscovite-2M1 - K0.92Na0.08Al1.78Fe0.22Mg0.1(Al0.83Si3.17O10)(OH)1.56O0.25F0.19
Intensity(Counts)
x10^3
150
100
50
10
20
30
40
50
60
70
80
Two-Theta (deg)

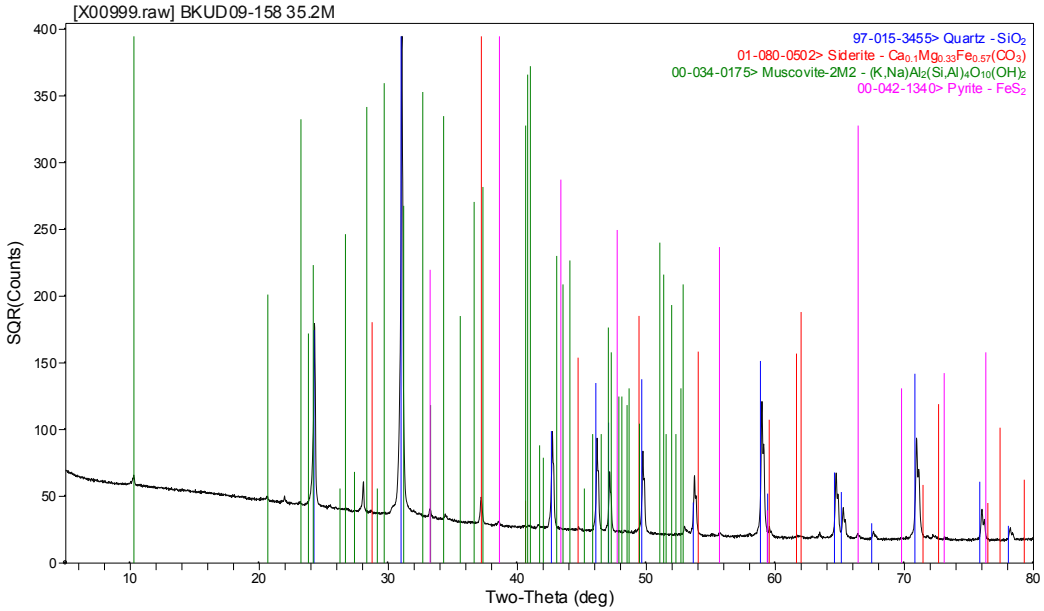
[X00999.raw] BKUD09-158 35.2M
97-015-3455> Quartz - SiO2
01-080-0502> Siderite - Ca0.1Mg0.33Fe0.57(CO3)
00-034-0175> Muscovite-2M2 - (K,Na)Al2(Si,Al)4O10(OH)2
00-042-1340> Pyrite - FeS2
SQR(Counts)
Two-Theta (deg)

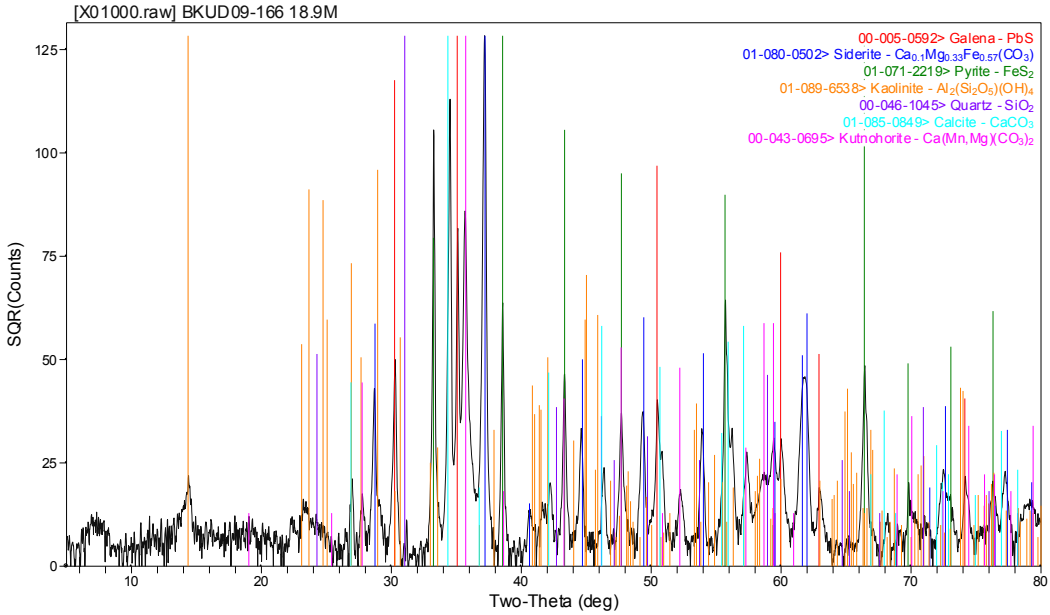
[X01000.raw] BKUD09-166 18.9M
00-005-0592> Galena - PbS
01-080-0502> Siderite - Ca0.1Mg0.33Fe0.57(CO3)
01-071-2219> Pyrite - FeS2
01-089-6538> Kaolinite - Al2(Si2O5)(OH)4
00-046-1045> Quartz - SiO2
01-085-0849> Calcite - CaCO3
00-043-0695> Kutnohorite - Ca(Mn,Mg)(CO3)2
SQR(Counts)
Two-Theta (deg)

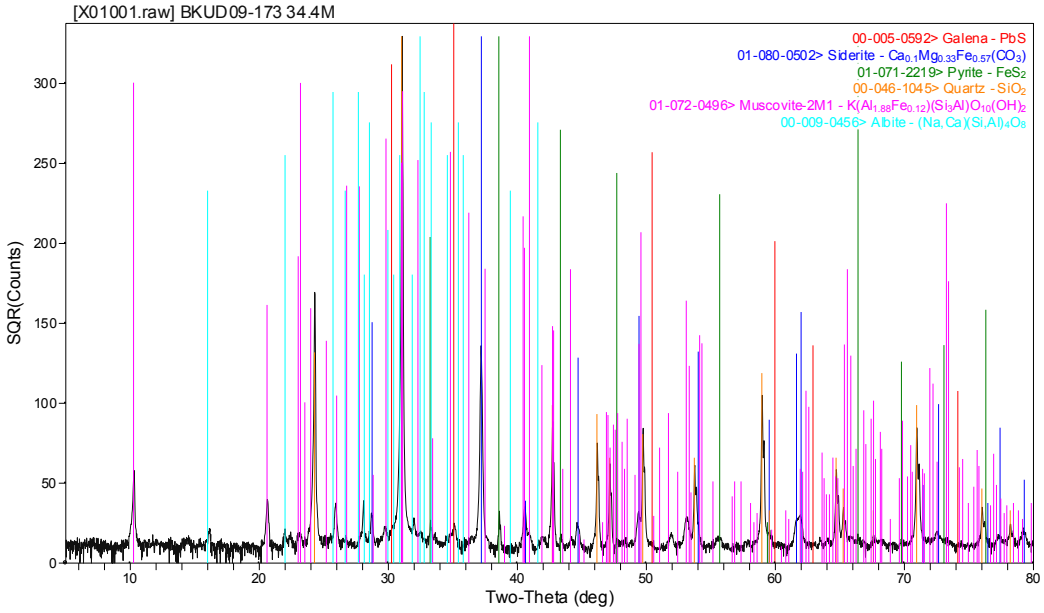
[X01001.raw] BKUD09-173 34.4M
00-005-0592> Galena - PbS
01-080-0502> Siderite - $Ca_{0.1}Mg_{0.33}Fe_{0.57}(CO_3)$
01-071-2219> Pyrite - FeS_2
00-046-1045> Quartz - SiO_2
01-072-0496> Muscovite-2M1 - $K(Al_{1.88}Fe_{0.12})(Si_3Al)O_{10}(OH)_2$
00-009-0456> Albite - $(Na,Ca)(Si,Al)_4O_8$
SQR(Counts)
Two-Theta (deg)

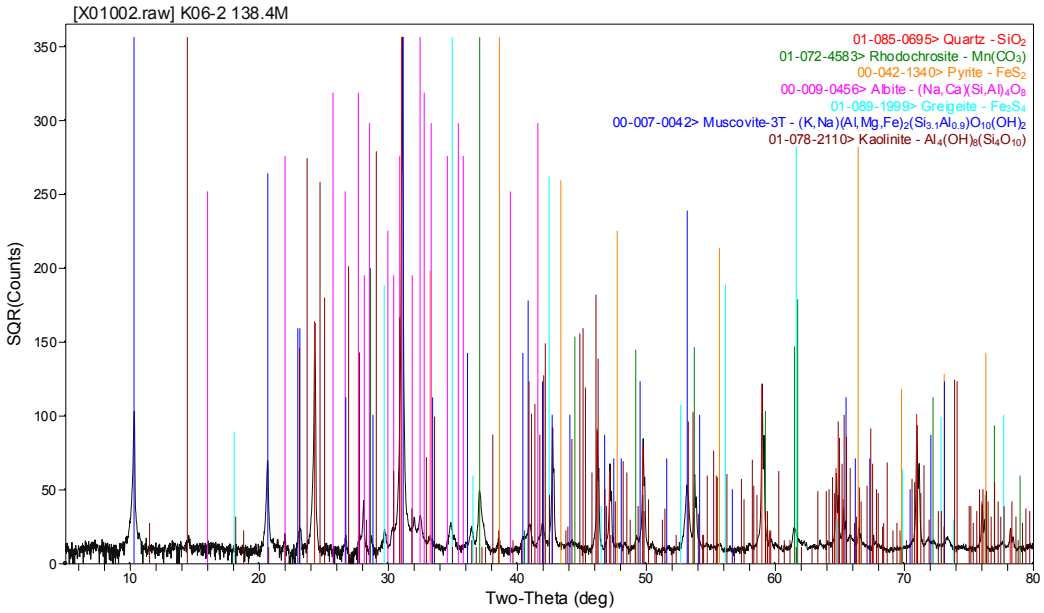
[X01002.raw] K06-2 138.4M
01-085-0695> Quartz - SiO_2
01-072-4583> Rhodochrosite - $Mn(CO_3)$
00-042-1340> Pyrite - FeS_2
00-009-0456> Albite - $(Na,Ca)(Si,Al)_4O_8$
01-089-1999> Greigeite - Fe_3S_4
00-007-0042> Muscovite-3T - $(K,Na)(Al,Mg,Fe)_2(Si_{3.1}Al_{0.9})O_{10}(OH)_2$
01-078-2110> Kaolinite - $Al_4(OH)_8(Si_4O_{10})$
SQR(Counts)
Two-Theta (deg)

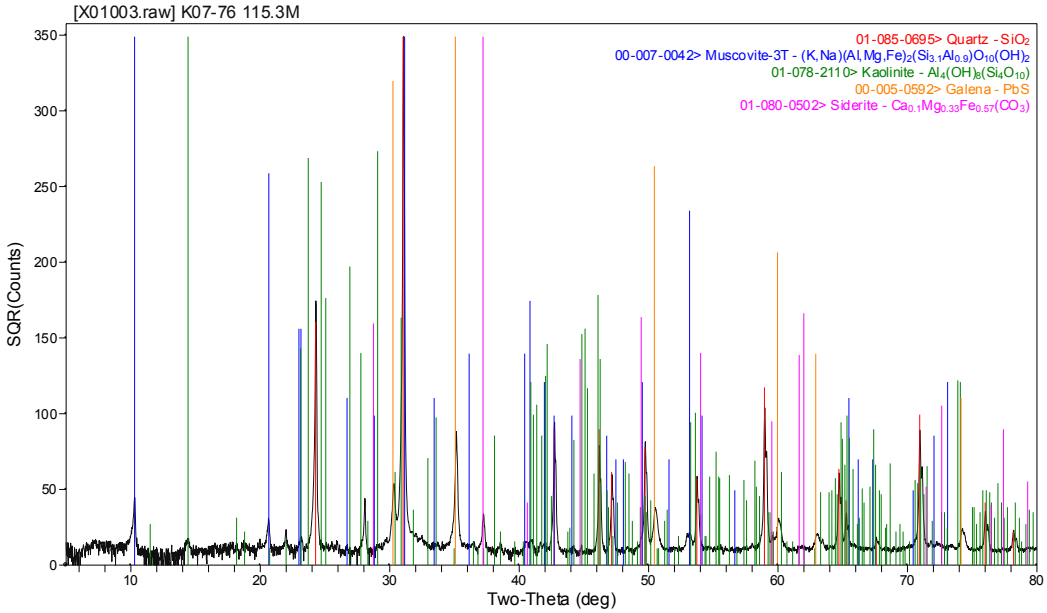
[X01003.raw] K07-76 115.3M
01-085-0695> Quartz - SiO2
00-007-0042> Muscovite-3T - (K,Na)(Al,Mg,Fe)2(Si3.1Al0.9)O10(OH)2
01-078-2110> Kaolinite - Al4(OH)8(Si4O10)
00-005-0592> Galena - PbS
01-080-0502> Siderite - Ca0.1Mg0.33Fe0.57(CO3)
SQR(Counts)
Two-Theta (deg)

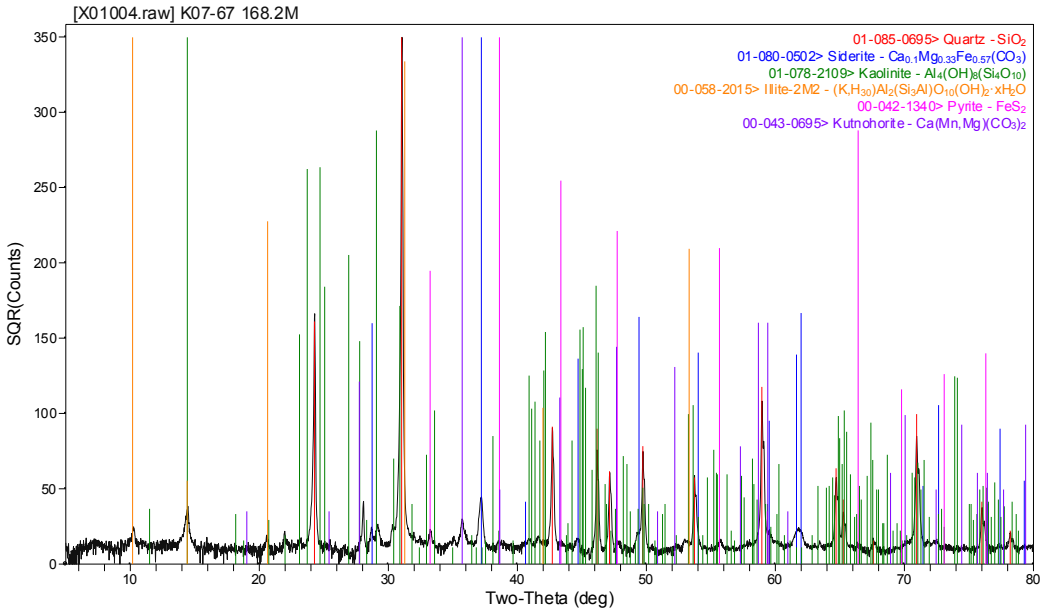
[X01004.raw] K07-67 168.2M
01-085-0695> Quartz - SiO2
01-080-0502> Siderite - Ca0.1Mg0.33Fe0.57(CO3)
01-078-2109> Kaolinite - Al4(OH)8(Si4O10)
00-058-2015> Illite-2M2 - (K,H30)Al2(Si3Al)O10(OH)2·xH2O
00-042-1340> Pyrite - FeS2
00-043-0695> Kutnohorite - Ca(Mn,Mg)(CO3)2
SQR(Counts)
Two-Theta (deg)

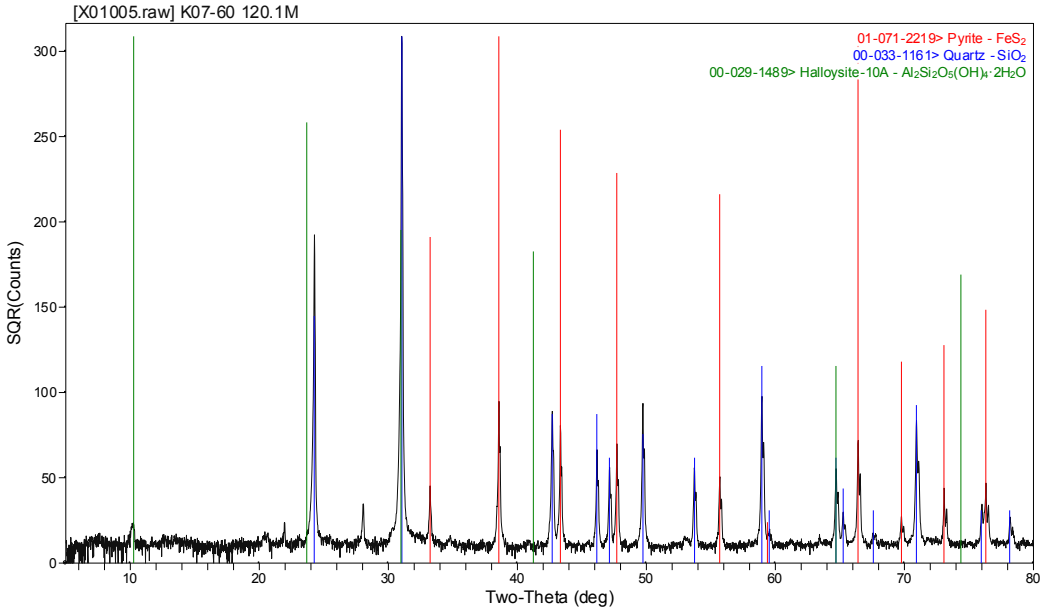
[X01005.raw] K07-60 120.1M
01-071-2219> Pyrite - FeS2
00-033-1161> Quartz - SiO2
00-029-1489> Halloysite-10A - Al2Si2O5(OH)4·2H2O
SQR(Counts)
Two-Theta (deg)

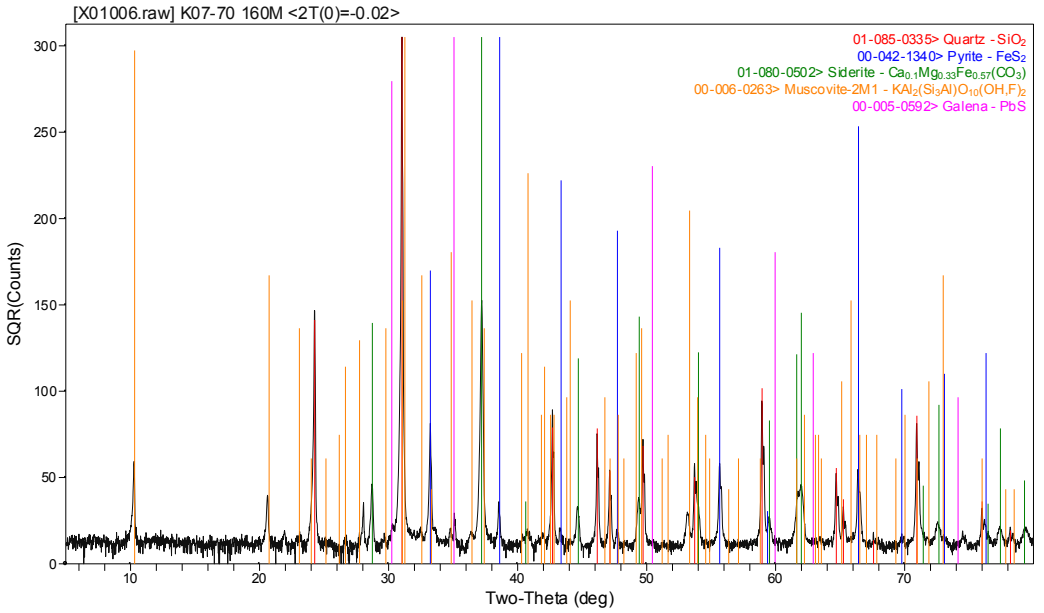
[X01006.raw] K07-70 160M <2T(0)=-0.02>
01-085-0335> Quartz - SiO2
00-042-1340> Pyrite - FeS2
01-080-0502> Siderite - Ca0.1Mg0.33Fe0.57(CO3)
00-006-0263> Muscovite-2M1 - KAl2(Si3Al)O10(OH,F)2
00-005-0592> Galena - PbS
SQR(Counts)
Two-Theta (deg)

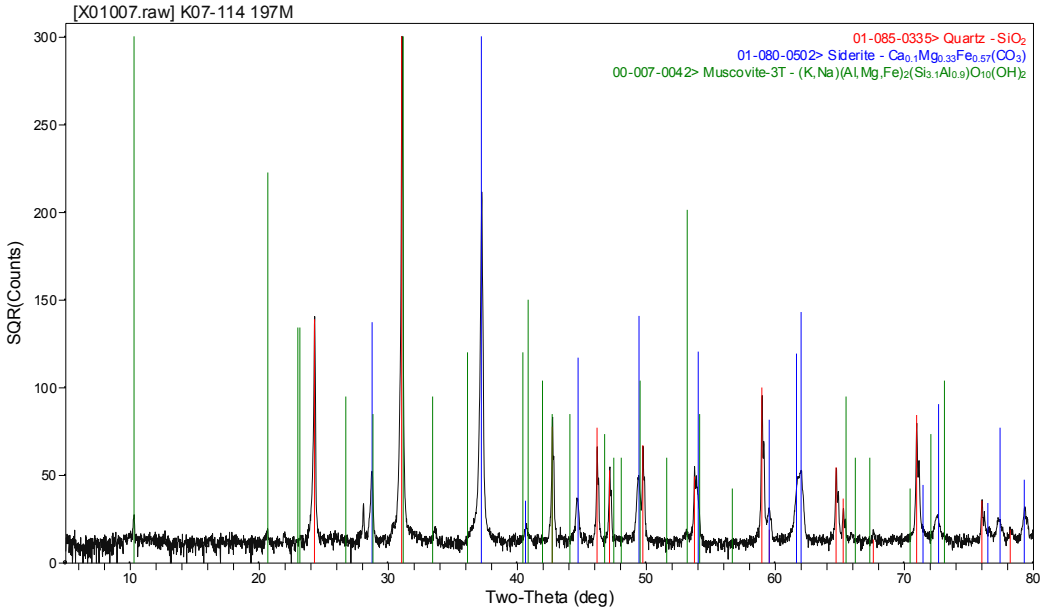
[X01007.raw] K07-114 197M
01-085-0335> Quartz - SiO2
01-080-0502> Siderite - Ca0.1Mg0.33Fe0.57(CO3)
00-007-0042> Muscovite-3T - (K,Na)(Al,Mg,Fe)2(Si3.1Al0.9)O10(OH)2
SQR(Counts)
Two-Theta (deg)

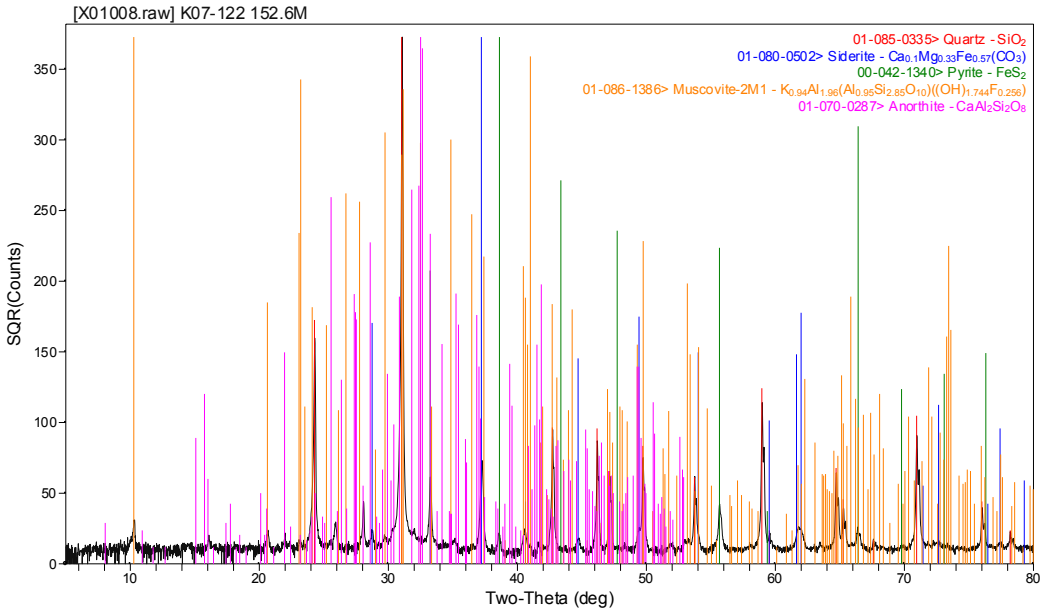
[X01008.raw] K07-122 152.6M
01-085-0335> Quartz - SiO2
01-080-0502> Siderite - Ca0.1Mg0.33Fe0.57(CO3)
00-042-1340> Pyrite - FeS2
01-086-1386> Muscovite-2M1 - K0.94Al1.96(Al0.95Si2.85O10)((OH)1.744F0.256)
01-070-0287> Anorthite - CaAl2Si2O8
SQR(Counts)
Two-Theta (deg)

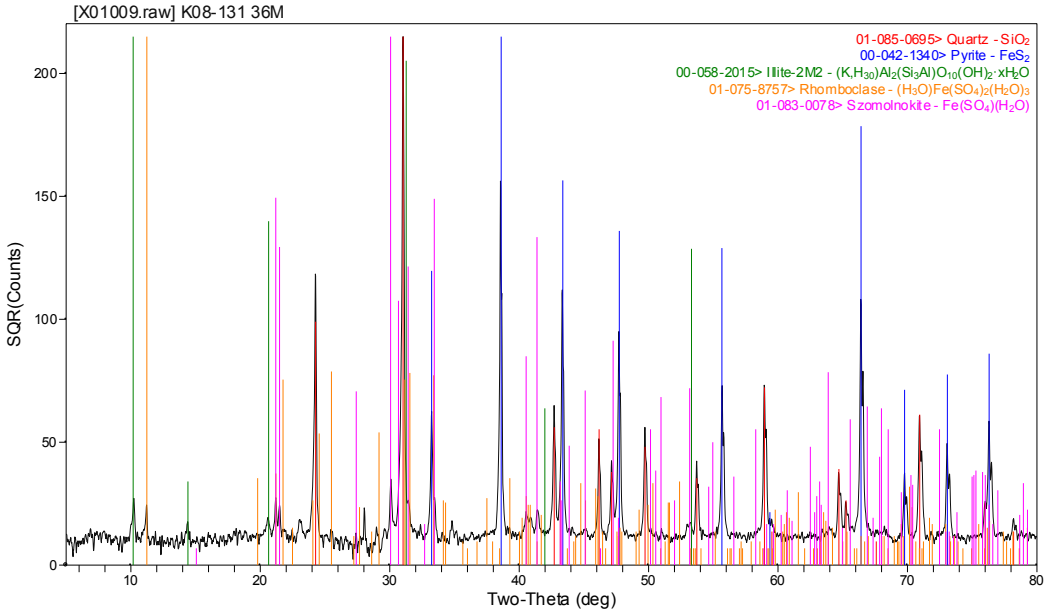
[X01009.raw] K08-131 36M
01-085-0695> Quartz - SiO2
00-042-1340> Pyrite - FeS2
00-058-2015> Illite-2M2 - (K,H30)Al2(Si3Al)O10(OH)2·xH2O
01-075-8757> Rhomboclase - (H3O)Fe(SO4)2(H2O)3
01-083-0078> Szomolnokite - Fe(SO4)(H2O)
SQR(Counts)
Two-Theta (deg)

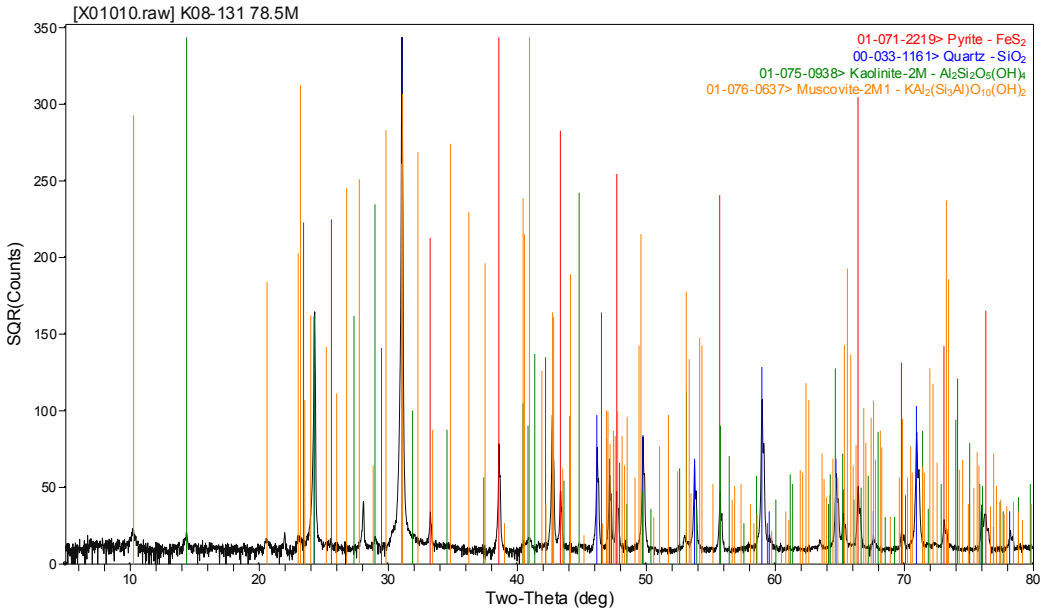
[X01010.raw] K08-131 78.5M
01-071-2219> Pyrite - FeS2
00-033-1161> Quartz - SiO2
01-075-0938> Kaolinite-2M - Al2Si2O5(OH)4
01-076-0637> Muscovite-2M1 - KAl2(Si3Al)O10(OH)2
SQR(Counts)
Two-Theta (deg)

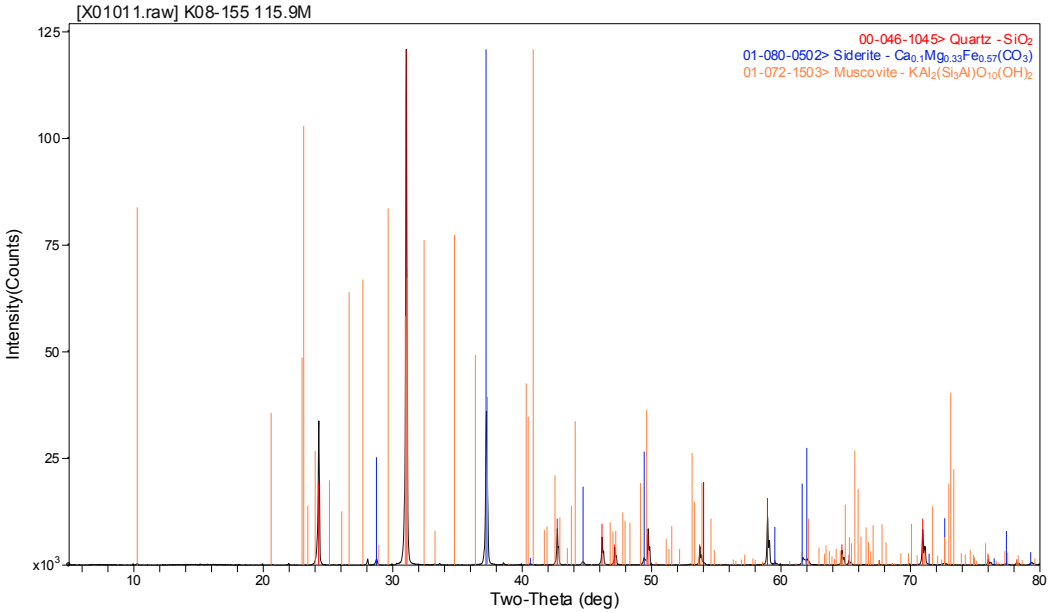
[X01011.raw] K08-155 115.9M
00-046-1045> Quartz - SiO2
01-080-0502> Siderite - Ca0.1Mg0.33Fe0.57(CO3)
01-072-1503> Muscovite - KAl2(Si3Al)O10(OH)2
Intensity(Counts)
x10^3
Two-Theta (deg)

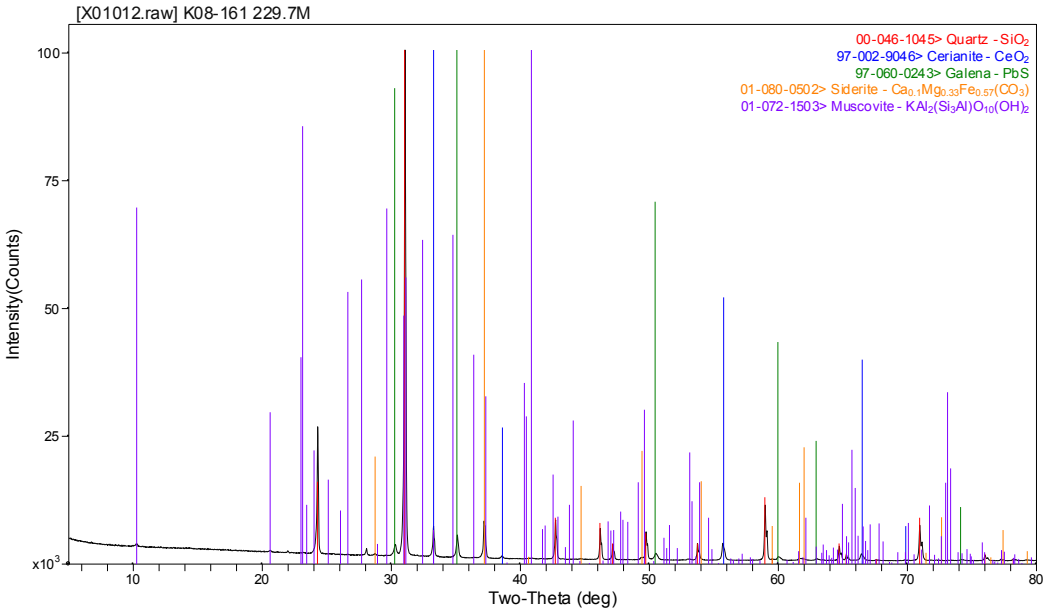
[X01012.raw] K08-161 229.7M
00-046-1045> Quartz - SiO2
97-002-9046> Cerianite - CeO2
97-060-0243> Galena - PbS
01-080-0502> Siderite - Ca0.1Mg0.33Fe0.57(CO3)
01-072-1503> Muscovite - KAl2(Si3Al)O10(OH)2
Intensity(Counts)
x10^3
Two-Theta (deg)

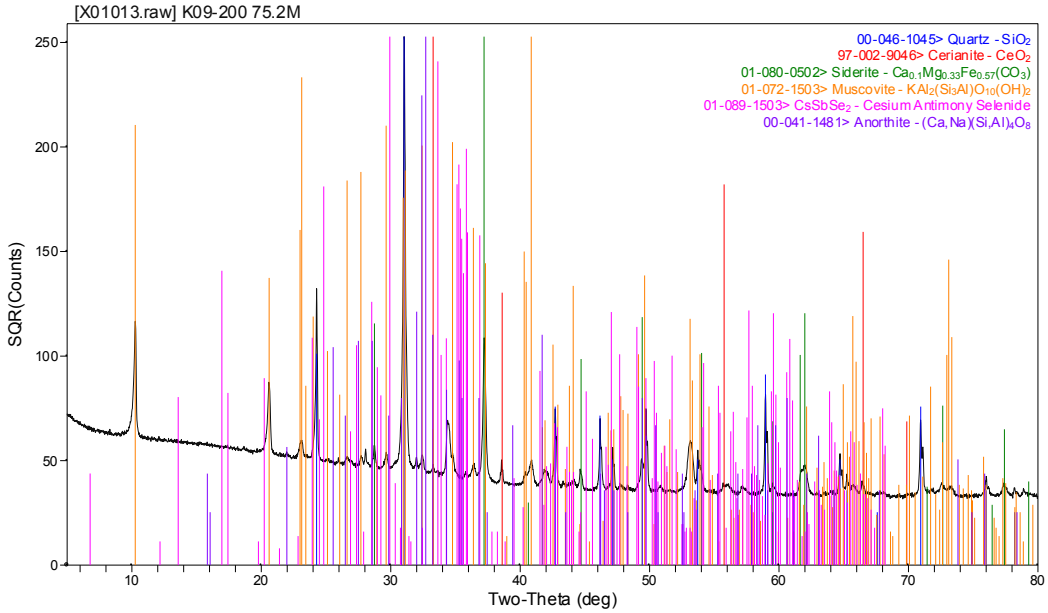
[X01013.raw] K09-200 75.2M
00-046-1045> Quartz - SiO2
97-002-9046> Cerianite - CeO2
01-080-0502> Siderite - Ca0.1Mg0.33Fe0.57(CO3)
01-072-1503> Muscovite - KAl2(Si3Al)O10(OH)2
01-089-1503> CsSbSe2 - Cesium Antimony Selenide
00-041-1481> Anorthite - (Ca,Na)(Si,Al)4O8
SQR(Counts)
Two-Theta (deg)

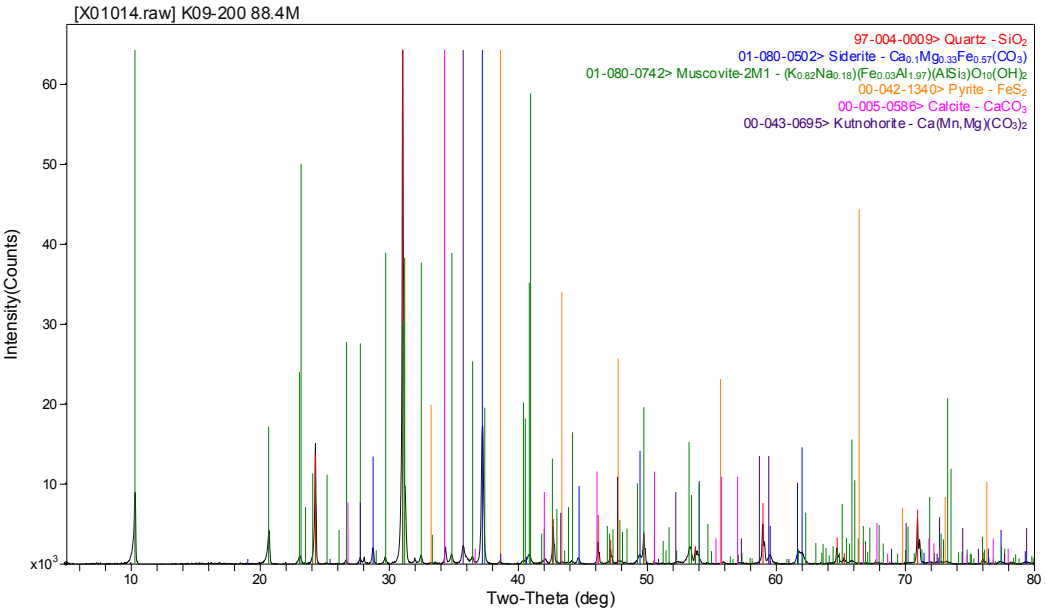
[X01014.raw] K09-200 88.4M
97-004-0009> Quartz - SiO2
01-080-0502> Siderite - Ca0.1Mg0.33Fe0.57(CO3)
01-080-0742> Muscovite-2M1 - (K0.82Na0.18)(Fe0.03Al1.97)(AlSi3)O10(OH)2
00-042-1340> Pyrite - FeS2
00-005-0586> Calcite - CaCO3
00-043-0695> Kutnohorite - Ca(Mn,Mg)(CO3)2
Intensity(Counts)
x10^3
Two-Theta (deg)

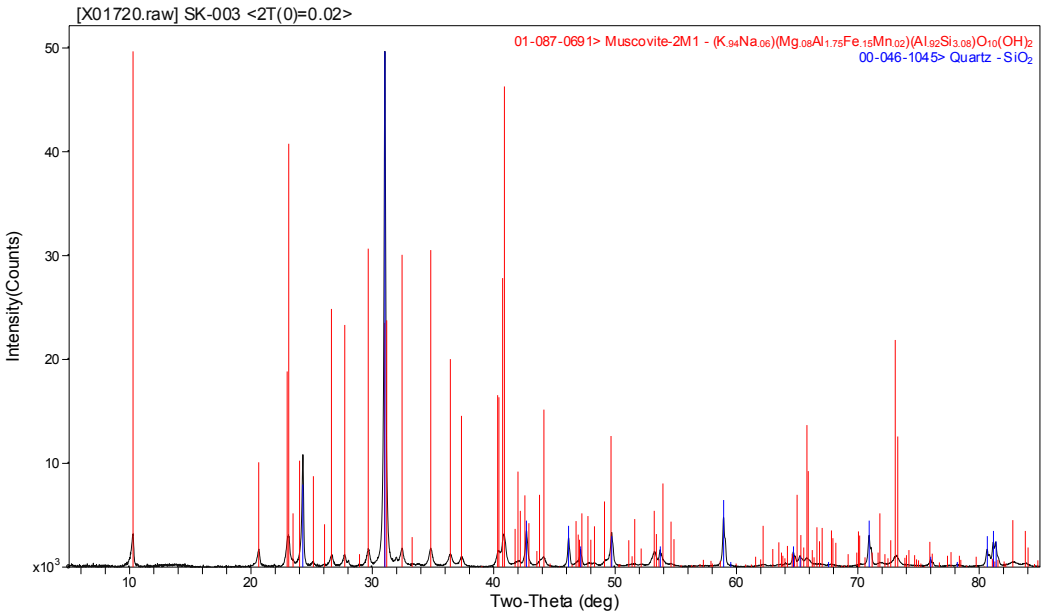
[X01720.raw] SK-003 <2T(0)=0.02>
01-087-0691> Muscovite-2M1 - (K.94Na.06)(Mg.08Al1.75Fe.15Mn.02)(Al.92Si3.08)O10(OH)2
00-046-1045> Quartz - SiO2
Intensity(Counts)
x10^3
Two-Theta (deg)

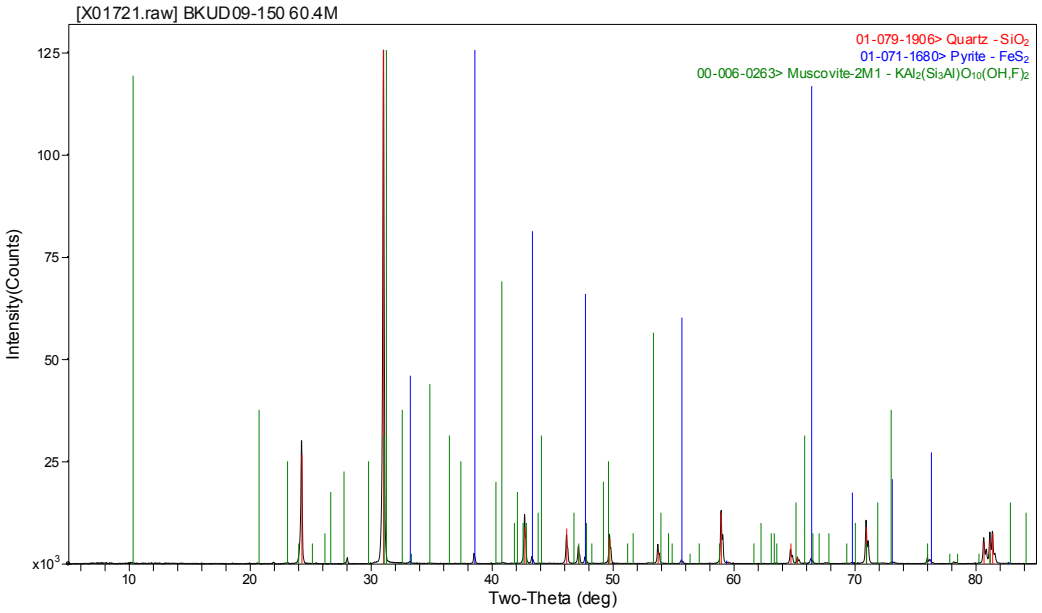
[X01721.raw] BKUD09-150 60.4M
01-079-1906> Quartz - SiO2
01-071-1680> Pyrite - FeS2
00-006-0263> Muscovite-2M1 - KAl2(Si3Al)O10(OH,F)2
Intensity(Counts)
x10^3
Two-Theta (deg)

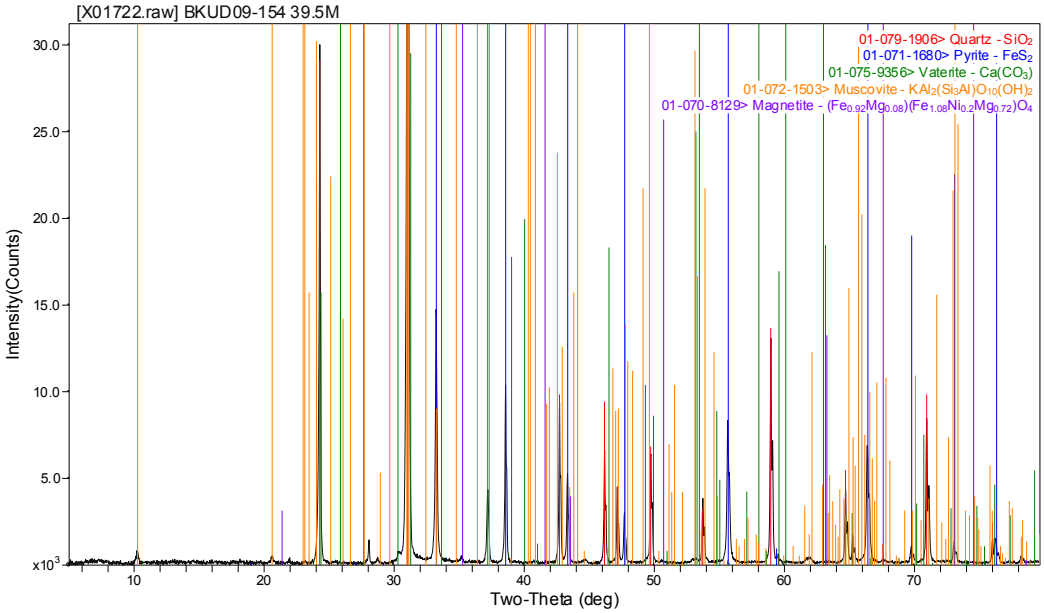
[X01722.raw] BKUD09-154 39.5M
01-079-1906> Quartz - SiO2
01-071-1680> Pyrite - FeS2
01-075-9356> Vaterite - Ca(CO3)
01-072-1503> Muscovite - KAl2(Si3Al)O10(OH)2
01-070-8129> Magnetite - (Fe0.92Mg0.08)(Fe1.08Ni0.2Mg0.72)O4
Intensity(Counts)
x10^3
Two-Theta (deg)

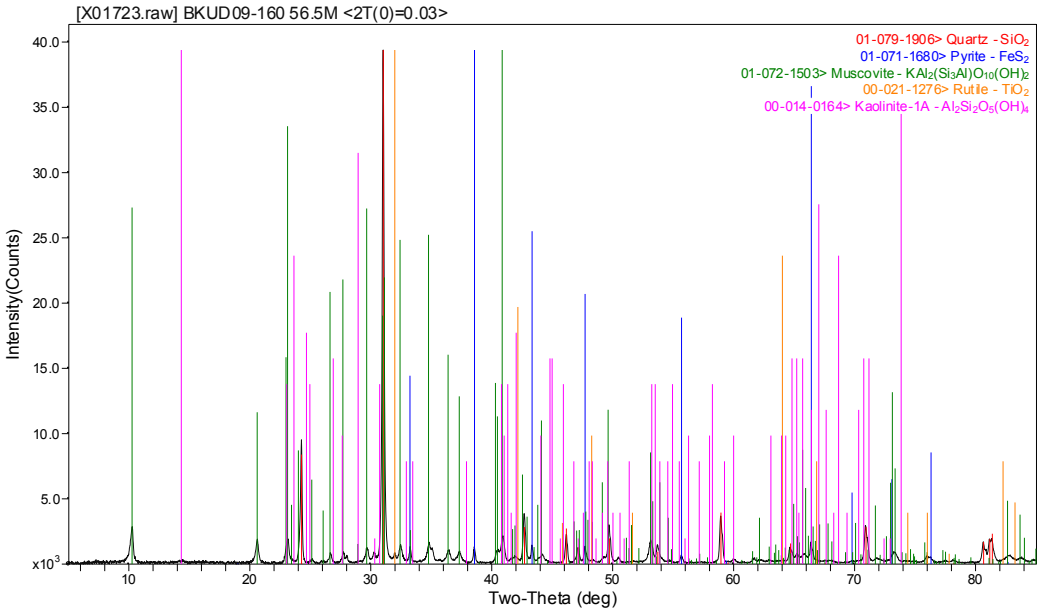
[X01723.raw] BKUD09-160 56.5M <2T(0)=0.03>
01-079-1906> Quartz - SiO2
01-071-1680> Pyrite - FeS2
01-072-1503> Muscovite - KAl2(Si3Al)O10(OH)2
00-021-1276> Rutile - TiO2
00-014-0164> Kaolinite-1A - Al2Si2O5(OH)4
Intensity(Counts)
x10^3
Two-Theta (deg)

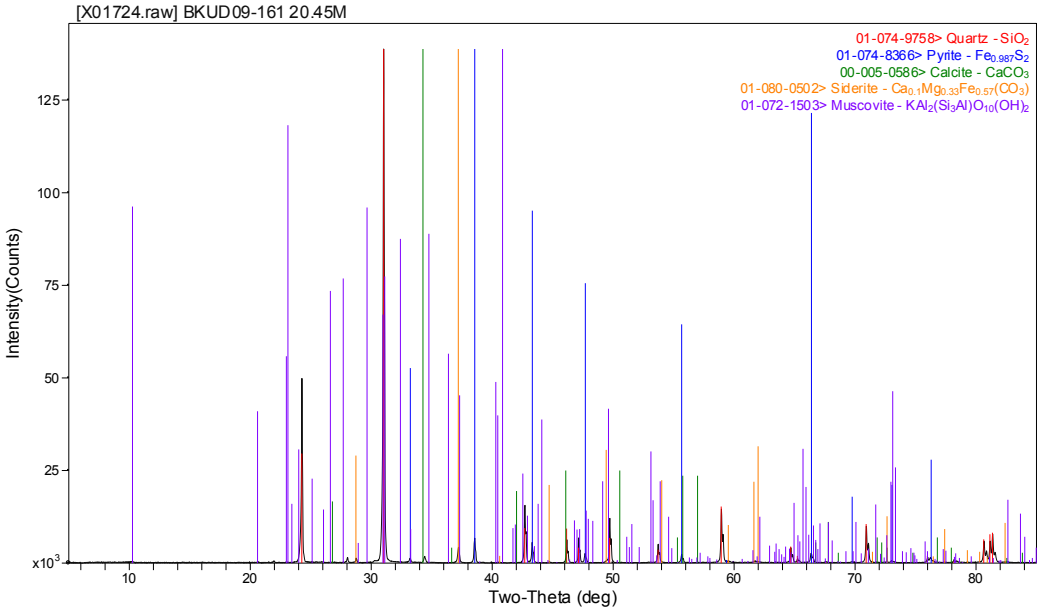
[X01724.raw] BKUD09-161 20.45M
01-074-9758> Quartz - SiO2
01-074-8366> Pyrite - Fe0.987S2
00-005-0586> Calcite - CaCO3
01-080-0502> Siderite - Ca0.1Mg0.33Fe0.57(CO3)
01-072-1503> Muscovite - KAl2(Si3Al)O10(OH)2
Intensity(Counts)
x10^3
125
100
75
50
25
10
20
30
40
50
60
70
80
Two-Theta (deg)

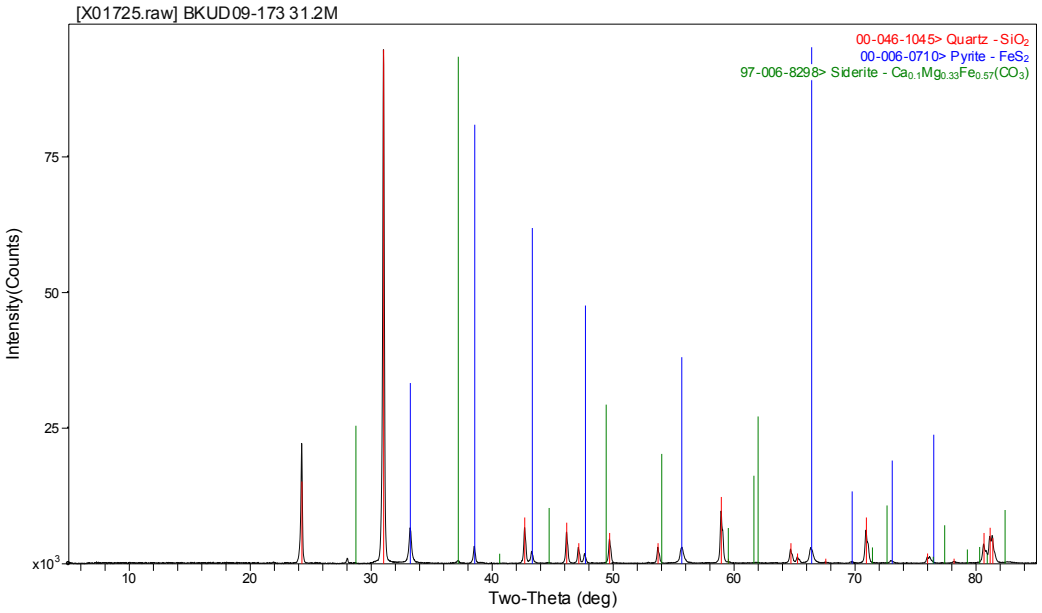
[X01725.raw] BKUD09-173 31.2M
00-046-1045> Quartz - SiO2
00-006-0710> Pyrite - FeS2
97-006-8298> Siderite - Ca0.1Mg0.33Fe0.57(CO3)
Intensity(Counts)
x10^3
75
50
25
10
20
30
40
50
60
70
80
Two-Theta (deg)

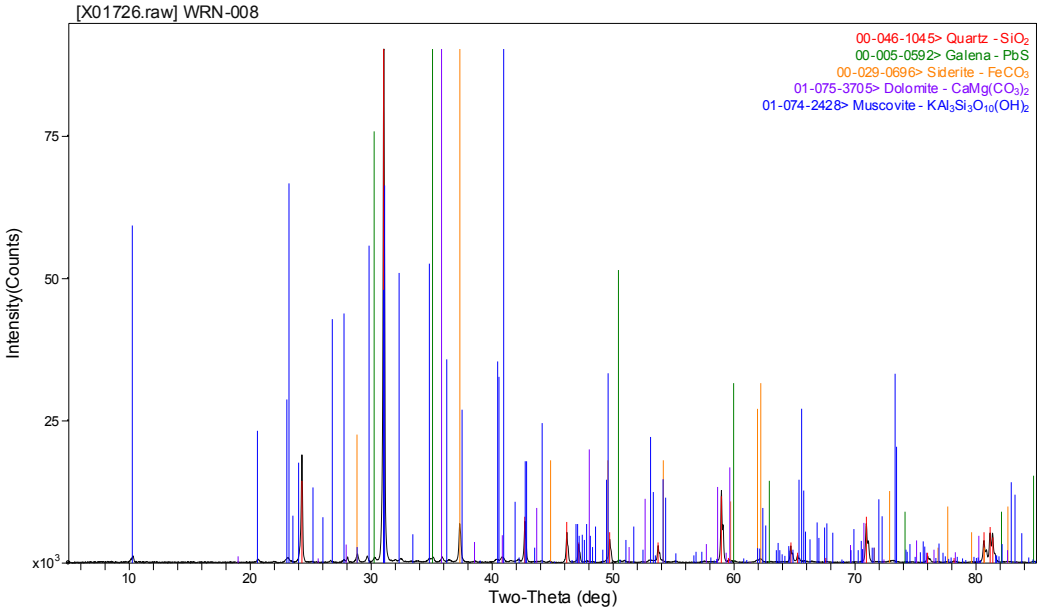
[X01726.raw] WRN-008
00-046-1045> Quartz - SiO2
00-005-0592> Galena - PbS
00-029-0696> Siderite - FeCO3
01-075-3705> Dolomite - CaMg(CO3)2
01-074-2428> Muscovite - KAl3Si3O10(OH)2
Intensity(Counts)
x10^3
Two-Theta (deg)

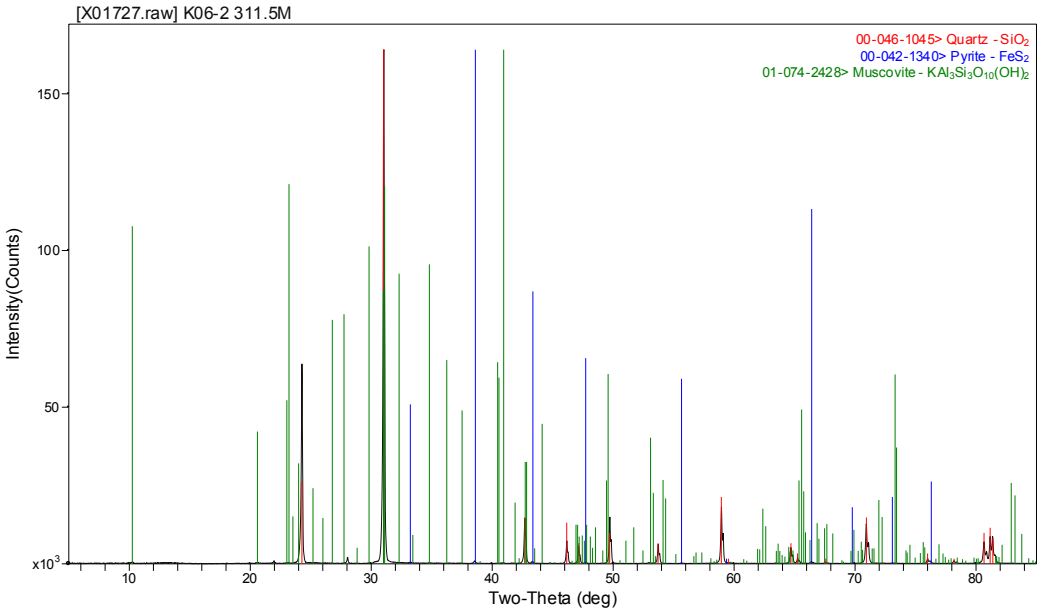
[X01727.raw] K06-2 311.5M
00-046-1045> Quartz - SiO2
00-042-1340> Pyrite - FeS2
01-074-2428> Muscovite - KAl3Si3O10(OH)2
Intensity(Counts)
x10^3
Two-Theta (deg)

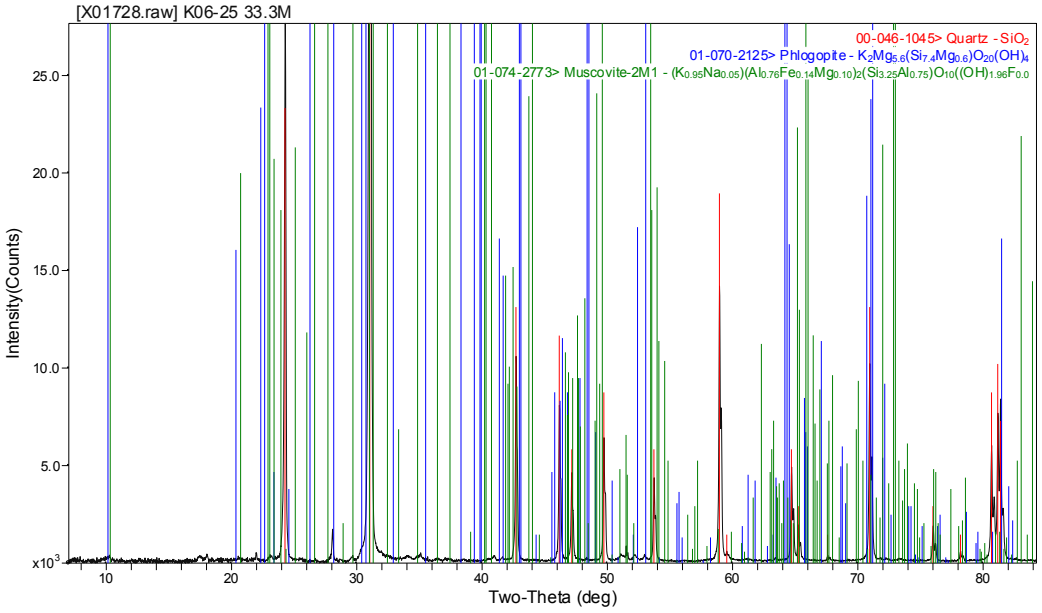
[X01728.raw] K06-25 33.3M
00-046-1045> Quartz - SiO2
01-070-2125> Phlogopite - K2Mg5.6(Si7.4Mg0.6)O20(OH)4
01-074-2773> Muscovite-2M1 - (K0.95Na0.05)(Al0.76Fe0.14Mg0.10)2(Si3.25Al0.75)O10((OH)1.96F0.0
Intensity(Counts)
x10^3
25.0
20.0
15.0
10.0
5.0
10
20
30
40
50
60
70
80
Two-Theta (deg)

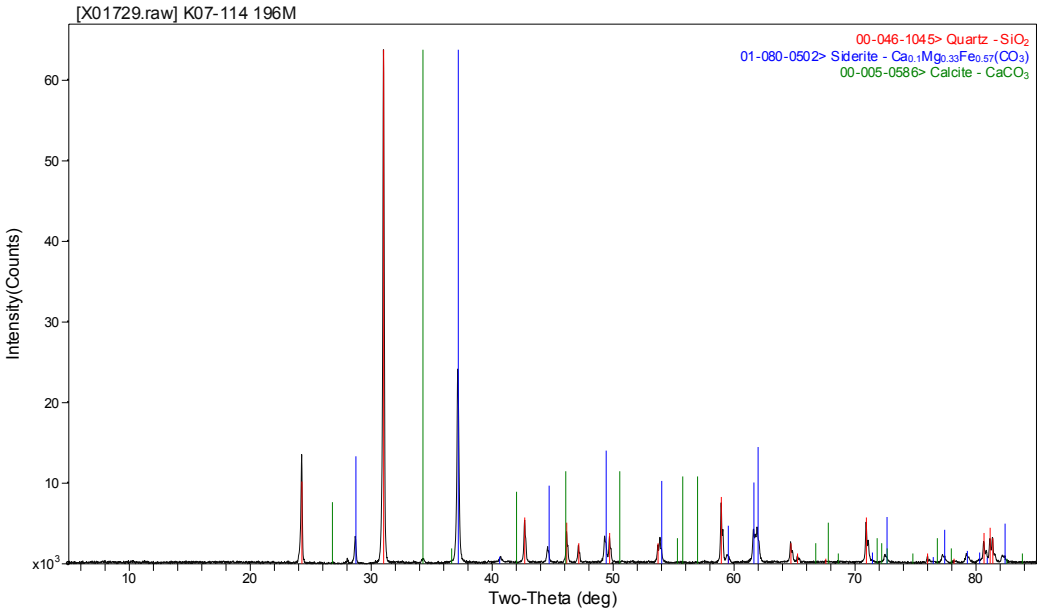
[X01729.raw] K07-114 196M
00-046-1045> Quartz - SiO2
01-080-0502> Siderite - Ca0.1Mg0.33Fe0.57(CO3)
00-005-0586> Calcite - CaCO3
Intensity(Counts)
x10^3
60
50
40
30
20
10
10
20
30
40
50
60
70
80
Two-Theta (deg)

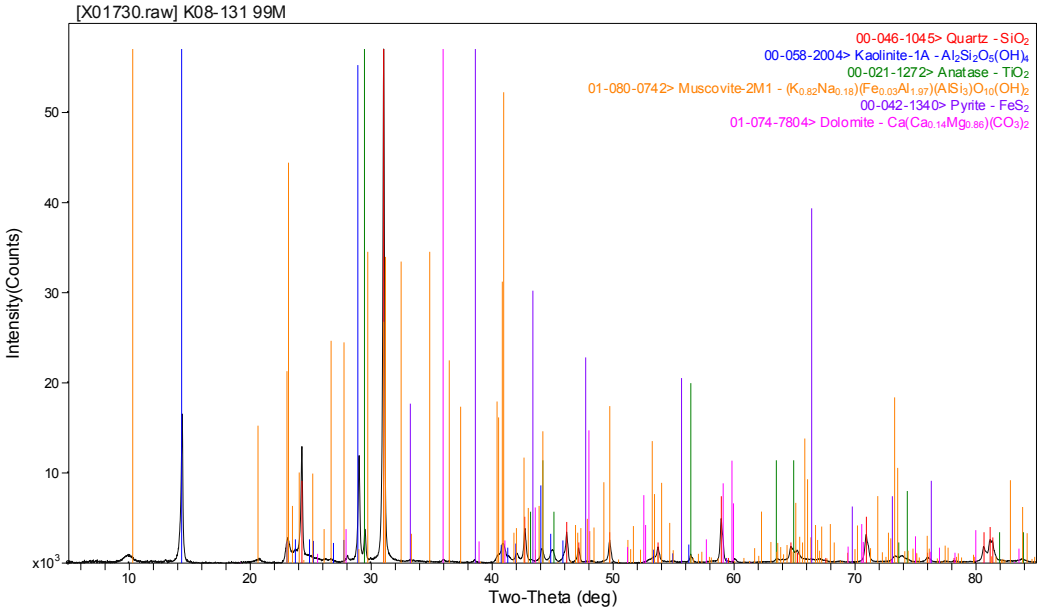
[X01730.raw] K08-131 99M
00-046-1045> Quartz - SiO2
00-058-2004> Kaolinite-1A - Al2Si2O5(OH)4
00-021-1272> Anatase - TiO2
01-080-0742> Muscovite-2M1 - (K0.82Na0.18)(Fe0.03Al1.97)(AlSi3)O10(OH)2
00-042-1340> Pyrite - FeS2
01-074-7804> Dolomite - Ca(Ca0.14Mg0.86)(CO3)2
Intensity(Counts)
x10^3
Two-Theta (deg)

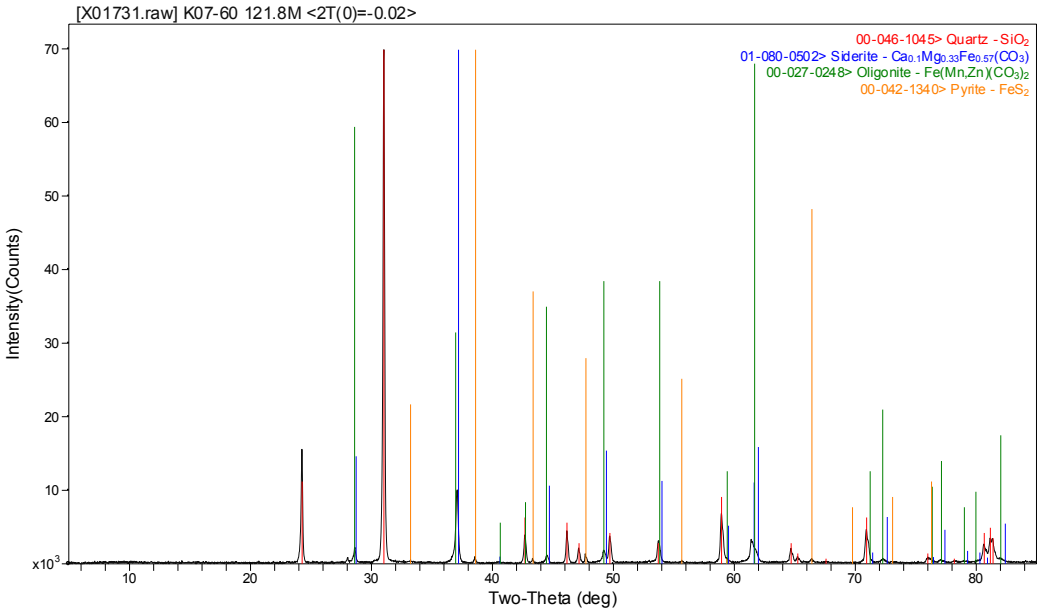
[X01731.raw] K07-60 121.8M <2T(0)=-0.02>
00-046-1045> Quartz - SiO2
01-080-0502> Siderite - Ca0.1Mg0.33Fe0.57(CO3)
00-027-0248> Oligonite - Fe(Mn,Zn)(CO3)2
00-042-1340> Pyrite - FeS2
Intensity(Counts)
x10^3
Two-Theta (deg)

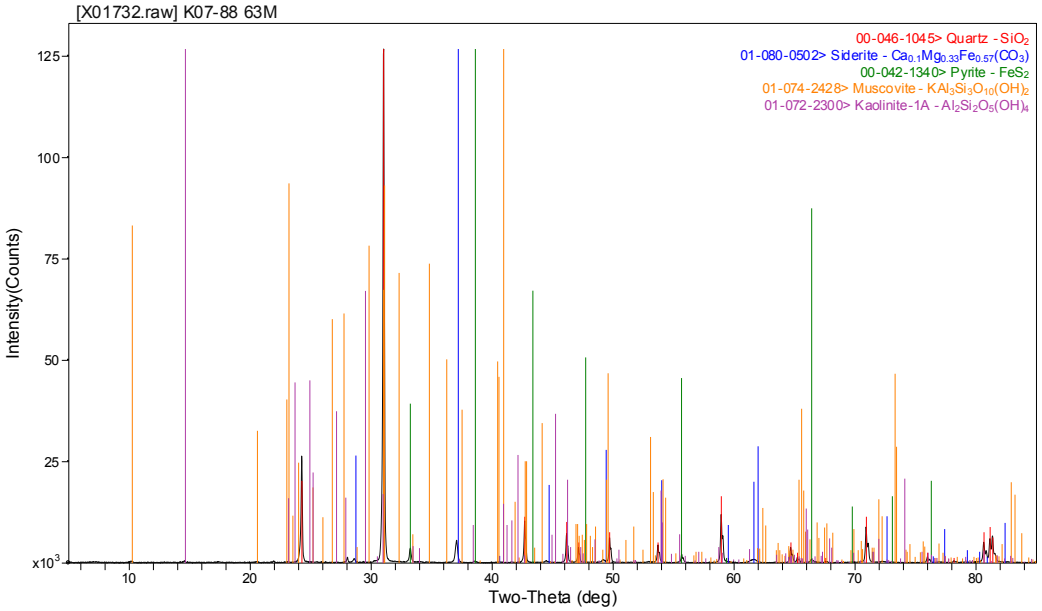
[X01732.raw] K07-88 63M
00-046-1045> Quartz - SiO2
01-080-0502> Siderite - Ca0.1Mg0.33Fe0.57(CO3)
00-042-1340> Pyrite - FeS2
01-074-2428> Muscovite - KAl3Si3O10(OH)2
01-072-2300> Kaolinite-1A - Al2Si2O5(OH)4
Intensity(Counts)
x10^3
125
100
75
50
25
10
20
30
40
50
60
70
80
Two-Theta (deg)

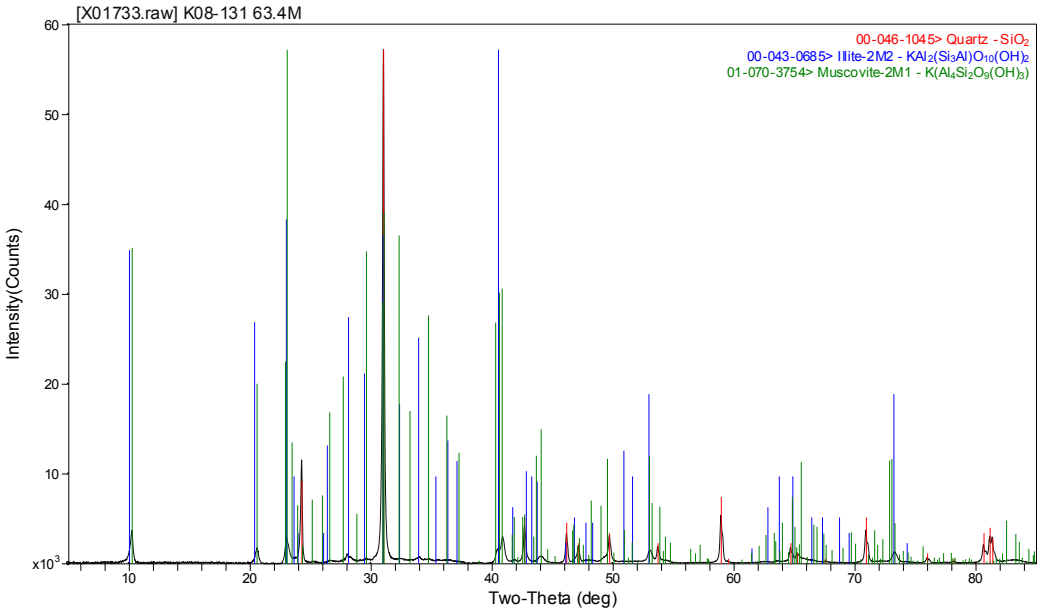
[X01733.raw] K08-131 63.4M
00-046-1045> Quartz - SiO2
00-043-0685> Illite-2M2 - KAl2(Si3Al)O10(OH)2
01-070-3754> Muscovite-2M1 - K(Al4Si2O9(OH)3)
Intensity(Counts)
x10^3
60
50
40
30
20
10
10
20
30
40
50
60
70
80
Two-Theta (deg)

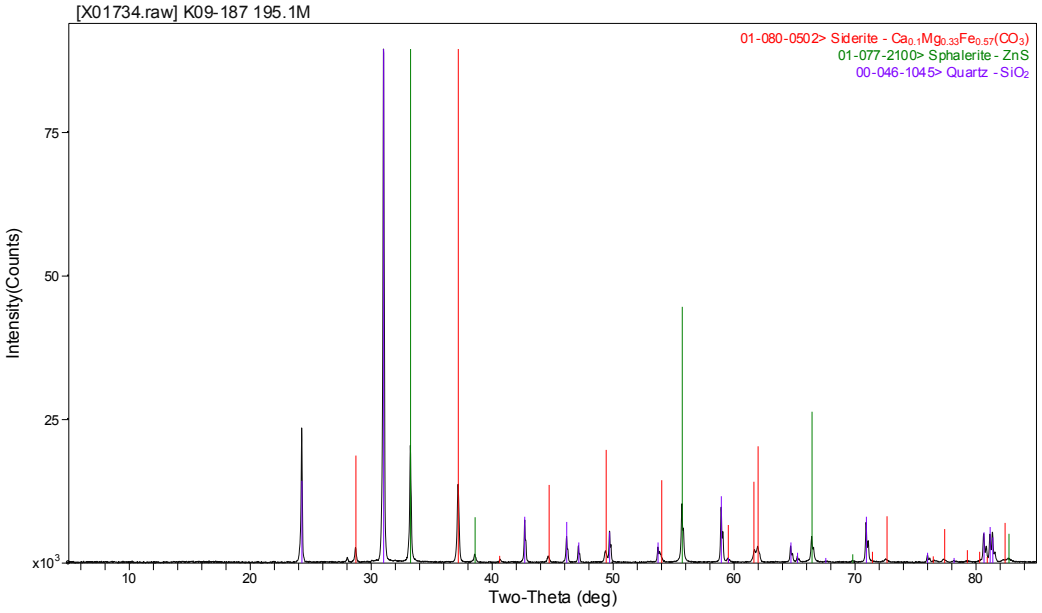
[X01734.raw] K09-187 195.1M
01-080-0502> Siderite - Ca0.1Mg0.33Fe0.57(CO3)
01-077-2100> Sphalerite - ZnS
00-046-1045> Quartz - SiO2
Intensity(Counts)
x10^3
75
50
25
10
20
30
40
50
60
70
80
Two-Theta (deg)

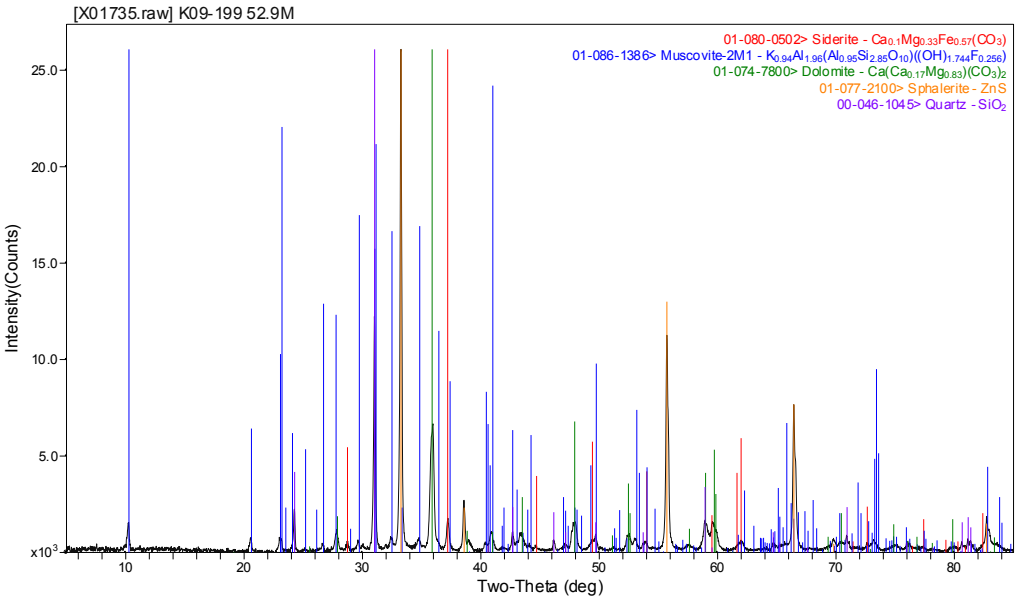
[X01735.raw] K09-199 52.9M
01-080-0502> Siderite - Ca0.1Mg0.33Fe0.57(CO3)
01-086-1386> Muscovite-2M1 - K0.94Al1.96(Al0.95Si2.85O10)((OH)1.744F0.256)
01-074-7800> Dolomite - Ca(Ca0.17Mg0.83)(CO3)2
01-077-2100> Sphalerite - ZnS
00-046-1045> Quartz - SiO2
Intensity(Counts)
x10^3
25.0
20.0
15.0
10.0
5.0
10
20
30
40
50
60
70
80
Two-Theta (deg)